DESIGN AND SYNTHESIS OF FLUORESCENT UNNATURAL TRIAZOLYL AMINO ACIDS AND CONSTRAINED MOLECULAR SCAFFOLD AND THEIR APPLICATIONS IN PEPTIDOMIMETICS

A Dissertation Submitted to the
Indian Institute of Technology Guwahati
As Partial Fulfillment for the Award of Degree of

Doctor of Philosophy
in Chemistry
by

Subhashis Jana
Roll No. 11612203

Department of Chemistry
Indian Institute of Technology Guwahati
Guwahati 781039
June 2016

Dedicated to

My
Parents
And
Those who have helped me

INDIAN INSTITUTE OF TECHNOLOGY, GUWAHATI
Department of Chemistry

DECLARATION

I do hereby declare that the research work embodied in this thesis entitled "***Design and Synthesis of Fluorescent Unnatural Triazolyl Amino Acids and Constrained Molecular Scaffold and Their Application In Peptidomimetics***" has been carried out by me under the supervision of **Dr. Subhendu Sekhar Bag** in the Department of Chemistry, Indian Institute of Technology Guwahati, India.

In keeping with the general practice of reporting scientific observations, due acknowledgements have been made wherever the work described is based on the findings of other investigators.

IIT Guwahati
June, 2016.

Subhashis Jana

Dr. Subhendu Sekhar Bag, Ph.D.
Associate Professor
Department of Chemistry
Indian Institute of Technology
Guwahati -781039
Assam, INDIA

Ph: +91-361-258-2324 (O)
Ph: +91-361-258-4324 (R)
Fax: +91-361-258-2349

E-mail: ssbag75@yahoo.co.in
ssbag75@iitg.ernet.in

CERTIFICATE

This is to certify that the research work presented in this thesis entitled "***Design and Synthesis of Fluorescent Unnatural Triazolyl Amino Acids and Constrained Molecular Scaffold and Their Application In Peptidomimetics***" is an authentic record of the results obtained from the research work carried out by **Mr. Subhashis Jana** under my supervision in the Department of Chemistry, Indian Institute of technology Guwahati, India. This work is original and has not been submitted elsewhere for a degree or award.

IIT Guwahati
June, 2016

Dr. Subhendu Sekhar Bag
(Thesis Supervisor)

ACKNOWLODGEMENT

It is with high regards and profound respect that I express a deep sense of sincere gratitude to my supervisor **Dr. Subhendu Sekhar Bag** for his stimulating guidance, precious constructive suggestions and decisive insights during the entire course of my research work.

I would like to thank my Doctoral Committee members, **Prof. Anil Kumar Saikia** (chairman), **Dr. Chandan Mukherjee** (member) and **Prof. Siddhartha Sankar Ghosh** (member) for their intellectual input, encouragement, valuable suggestions and comments during the entire course of my research work.

I wish to thank my lab mates Rajen da, Sangita Di, Afsana, Suman, Manoj, Suranjan, and Hiranya for their cooperation, support and pleasant company throughout my research work. Without their help it would have been impossible to complete my research work. I would also like to acknowledge summer trainee students Nitish, Mritunjoy, Dibbendu, Achinta, Raghu, Sunit, Sourav and Ashim for their help, support and pleasant company in the laboratory during their summer project work.

Sincere thanks go to my other lab mates Zia da, Dipankar, Momina, Tridip, Anindya for their cooperation and sharing some happy moments inside and outside the laboratory.

I would like to acknowledge my seniors Chaitanya da, Himansu da and Francis da who have indirectly helped me during the entire course of my research work. Special thanks to Babulal da for his help in collecting XRD data. Thanks to my batch mates Ashim, Arindam da, Dinabandhu, Sameer, Sougata and Nabajeet for their support and suggestions. Thanks to all of my friends, juniors and seniors whom I met during my past five years of life for their help.

My honest regards to all the faculty members of our department for their encouragement and help. I want to express my thanks to Kesho Singh and Chandan Borgohain for his help in collecting Mass Spectra data and our technical and official staffs for their help and support.

Finally, I owe success to my parents (Mr. Chitta Ranjan Jana and Mrs. Pranati Jana) who have been a constant source of inspiration to carry out my career. I wish to thank them for

giving me the freedom to pursue a career path of my choice and their constant support and encouragement in realizing my dreams.

I want to express my thanks to my brother and sister and all the family members for their support.

I would like to acknowledge the Department of Chemistry, IIT Guwahati for giving me the opportunity and fellowship to carry out my research work.

Subhashis Jana

Subhashis Jana

Present Address:

C/O: Dr. Subhendu Sekhar Bag
Department of Chemistry
Indian Institute of Technology Guwahati
Guwahati – 781039, Assam, India
Phone: +91 361 2582324
E mail: j.subhashis@iitg.ernet.in
sjana.chem@gmail.com

Permanent Address:

Vill – Chak Bahich Beria
P. O. – Uttar Soutan Chak
Dist. – Purba Medinipur
Pin – 721664
West Bengal, India
Mobile**:** +91 7896808732

Area of Interest

Design and synthesis of unnatural fluorescent amino acids for chemical and biochemical application.

Education:

2016 **Ph. D.** [Thesis submitted (June)] **Title:** "Design and Synthesis of Fluorescent Unnatural Triazolyl Amino Acids and Constrained Molecular Scaffold and Their Application In Peptidomimetics."

2010 **Master of Science** (*in Organic Chemistry*) **Title: "**Linkage Analysis of Polysaccharide Obtained From Edible Mushroom Using the Methylation Tool."
Vidyasagar University , West Bengal

2006 **Bachelor of Science** *(Chemistry Hons.)*
Tamralipta Mahavidyalaya
Vidyasagar University

Honors/Awards:

- Junior Research Fellowship and Eligibility for Lectureship (**CSIR-JRF-NET**), June– 2010, awarded by Council of Scientific & Industrial Research and University Grants Commission, India.

List of Publications

1. ● Synthesis, Photophysical Properties of Triazolyl-Donor/Acceptor Chomophores Decorated Unnatural Amino Acids: Incorporation of a Pair into Leu-Enkephalin Peptide and Application of Triazolylperylene Amino Acid in Sensing BSA ● Bag, S. S.; Jana, S.; Pradhan, M. K.● *Bioorg. Med. Chem.* **2016**, XX : Y.YY.1-YY.. (*In Press*)
2. ● Triazolo-β-aza-ε-amino acid and its aromatic analogue as novel scaffolds for β -turn peptidomimetics ● Bag, S. S.; Jana, S.; Yashmeen, A.; De, S. ● *Chem. Commun.* **2015**, *51*, 5242.
3. ● Triazolyl-donor–acceptor chromophore-decorated unnatural amino acids and peptides: FRET events in a β-turn conformation ● Bag, S. S.; Jana, S.; Yashmeen, A.; Senthilkumar, K.; Bag, R. ● *Chem. Commun.* **2014**, *50*, 433.
4. ● Dual door entry to exciplex emission in a chimeric DNA duplex containing non nucleoside–nucleoside pair ● Bag, S. S.; Talukdar, S.; Kundu, R.; Saito, I.; Jana, S. ● *Chem. Commun*. **2014**, *50*, 829.
5. ● Wavelength Shifting Oligonucleotide Probe for the Detection of Adenosine of a Target DNA with Enhanced Fluorescence Signal ● Bag, S. S.; Pradhan, M. K.; Das, S. K.; Jana, S.; Bag, R. ● *Bioorg. Med. Chem. Lett*. **2014**, *24*, 4678**.**
6. ● Sensing of biomolecules and label-free discrimination of DNA containing a triple T–C/T–G mismatch pair with a fluorescence light-up probe, triazolylpyrene (^{TNDMB}Py) ● Bag, S. S.; Kundu, R.; Jana, S. ● *Tetrahedron Lett***. 2013**, *54*, 2627.
7. ●Solvatochromic fluorescent cyanophenoxazine: design, synthesis, photophysical properties and fluorescence light-up sensing of ct-DNA ● Bag, S. S.; Ghorai, S.; Jana, S.; Mukherjee, C. ● *RSC Advances*, **2013**, *3*, 5374.
8. ●Highly solvatochromic fluorescent naphthalimides: Design, synthesis, photophysical properties and fluorescence switch-on sensing of ct-DNA ● Bag, S. S.; Pradhan, M. K.; Kundu, R.; Jana, S. ● *Bioorg. Med. Chem. Lett.* **2013**, *23*, 96.

Article 4, 5, 6, 7, 8 are not included in the thesis.

Communicated

1. Trichromophoric β-Sheet Pentapeptide as A Dual Door Entry System to Excimer Emission and Application in Sensing of BSA, Bag, S. S.; Jana, S.; Pradhan, M. K. submitted.
2. Axially chiral Aromatic Triazolyl Unnatural Amino Acid Scaffold and Its Pyrenyl Amides as Efficient Fluorescent Discriminator of Ethanol-Methanol, Bag, S. S.; Jana, S. submitted.

List of Conferences/Symposiums

1. FRET Event in a Conceptual Unnatural β-Turn Tripeptide, **NIICT-2014**, March 2-5, **2014**, CSIR-IICT Hyderabad, Hyderabad, India.
2. FRET Event in a Conceptual Unnatural β-Turn Tripeptide, **FICS-2014,** December 4-6, **2014**, IIT Guwahati, Assam, India
3. Triazolo-β-aza-ε-amino acid and its aromatic analogue as novel scaffolds for β -turn peptidomimetics, **ISBOC-2015**, January 11-15, 2015, IISER Pune, Pune, India.
4. Dual door entry to exciplex emission in a chimeric DNA duplex containing nonnucleoside–nucleoside pair **17 th CRSI National Symposium in Chemistry-2015,** February 5-8, 2015, CSIR-NCL, Pune, India.

ABSTRACT

Design and synthesis of unnatural amino acids towards expansion of genetic code is going at a fast space. At the same time various developments of chemistry, platform and protocols are going on for the genetic incorporation of such designer amino acids into a protein system of Eukaryotic cells. With the advent of sophisticated synthetic chemistry more complex amino acids are being designed the encoding of which need the evolution of new aaRS/tRNA pairs that may also allow the *in vivo* synthesis of biopolymers with unnatural backbones. The incorporation of unnatural amino acid into protein expectedly would generate protein-based therapeutics that would certainly have an impact on medicine. Furthermore, biomedical researchers are constantly engaged in the development of new peptides/proteins based therapeutics with high metabolic stability, much more selectivity, high efficiency and suitable pharmacokinetics by maintaining the features responsible for biological activity and introducing both structural and functional specific modifications. The challenges in this endeavor have opened a new field of mimicked research, called peptidomimetics. During recent decades the basic concepts and approaches to peptidomimetic constructs have evolved to cover diverse compounds and synthetic strategies such as 'click chemistry' to generate a diverse array of drug candidates. As for an example, while β-turn peptidomimetics is needed to target key protein–protein interactions in major diseases, β-hairpin/ β-sheet mimicking is promising for next-generation therapeutics in medicine. Thus, both the research with constrained small molecule scaffold attracted great interest during the last two decades. The peptidomimetic approach has thus been powerful in addressing the key recognition elements by scaffold-based peptidomimetic architectures that expectedly would afford a wide array of medicinally important molecules displaying different binding affinity and pharmacokinetic profile. On the other hand progress towards the design of fluorescent unnatural amino acids (FUAA) are not only restricted to monitor protein's microenvironment, study structure, conformation, function and dynamics of proteins, monitor protein-protein/protein-drug/ protein-DNA interactions but also extended to the cellular imaging with the help of integration of imaging techniques to observe dynamic yet delicate cellular functions in more complex systems through the ongoing advancement of protocols for multiple-FUAA incorporation into protein systems. Therefore, with the advancement of knowledge and strategies of chemistry and biology, FUAAs expectedly would continue to be at the forefront in aiding researchers to gain insights into fundamental questions concerning life's essential biological functions involving protein interactions, recognition, and synthesis.

Therefore, this thesis entitled **"DESIGN AND SYNTHESIS OF FLUORESCENT UNNATURAL TRIAZOLYL AMINO ACIDS AND CONSTRAINED MOLECULAR SCAFFOLD AND THEIR APPLICATIONS IN PEPTIDOMIMETICS"** is a manifestation of research work towards: the (a) synthesis and studies of photophysical properties of unnatural triazolyl donor/acceptor

aromatic amino acids, (b) synthesis of unnatural triazolyl-donor/acceptor amino acid decorated peptides and studies on their conformation and photophysical property, (c) design and synthesis of triazolo-β-aza-ε-amino acid as novel scaffold for β-turn peptidomimetics, (d) synthesis of an aromatic triazolo amino acid scaffolded trichromophoric β-sheet pentapeptide as a "Dual Door Entry System to Excimer" emission and its application in sensing of BSA, (e) studies on the fluorimetric discrimination of methanol from ethanol exploiting aromatic triazolo amino acid scaffold and its mono and bispyrenyl amides. Towards this journey, a variety of novel unnatural fluorescent triazolyl donor/acceptor chromophore decorated amino acids, peptides and fluorescent peptides based on conformationally constrained small molecule scaffold were synthesized and their conformation and photophysical properties were investigated.

The thesis contains a total of **6 Chapters** including one Introduction Chapter (**Chapter 1**). Each chapter contains their individual introduction, experimental and reference sections. In short, **Chapter 1** is a critical survey of applications of unnatural amino acids and conformationally constrained small, molecular scaffold/ non-peptide isostere in the context of peptidomimetics and generation of functional peptides with novel photophysical properties. **Chapter 2** elaborates the synthesis of trizolyl donor/acceptor chromophore decorated fluorescent unnatural amino acids *via* "click" chemistry and study of their photophysical properties. Our design concept based on the hypothesis that a the pseudoaromatic 1,2,3-triazole can modulate the electronic characteristics of the chromophores and endow new properties to the unnatural amino acids. Pair of such donor/acceptor fluorescent UNAAs if incorporated into two termini of a tripeptide separated by a natural amino acid might adopt a specific peptide secondary structure via backbone H-bonding and could get extra stabilization via hydrophobic, π-π stacking and van der Waals interactions in the side chain. **Chapter 3** describes the studies on the synthesis and π-stacking/photophysical interaction property between triazolyl donor/acceptor amino acid (^{TPhen}**Ala**^{Do}/^{TNB}**Ala**^{Ac}) which are separated by a single natural alanine in our synthesized tripeptide. FRET event and its solvent assisted amplification are presented in details. **Chapter 4** introduced triazolo-β-aza-ε-amino acid (^{Al}**TAA**) as a conformationally constrained molecular scaffold in a peptide backbone mark a novel class of unnatural peptide building blocks to induce desirable secondary structures in small linear peptides. The synthesis of aromatic triazolo amino acid scaffold which placed in a trichromophoric fluorescent pentapeptide backbone act as a turn mimetic β-sheet nucleator and its application in sensing BSA are discussed in **Chapter 5**. Finally, **Chapter 6** deals with fluorimetric discrimination of ethanol from methanol utilising axially chiral aromatic triazolo amino acid scaffold (^{Ar}**TAA**) and its mono- and bis-pyrenyl amides.

CHAPTER 1: APPLICATIONS OF UNNATURAL AMINO ACIDS AND CONFORMATIONALLY CONSTRAINED SMALL MOLECULE SCAFFOLD: A REVIEW

This chapter highlights some of the applications of unnatural amino acids and conformationally constrained small, molecular scaffold/ non-peptide isostere in the context of peptidomimetics to induce desirable secondary structures in small linear peptides and generation of functional peptides with novel photophysical properties, involvement in FRET or excimer emission events in the peptidomimetics (**Figure A1**). Thus, this chapter is a reflection/overview of all the chapters of the present dissertation.

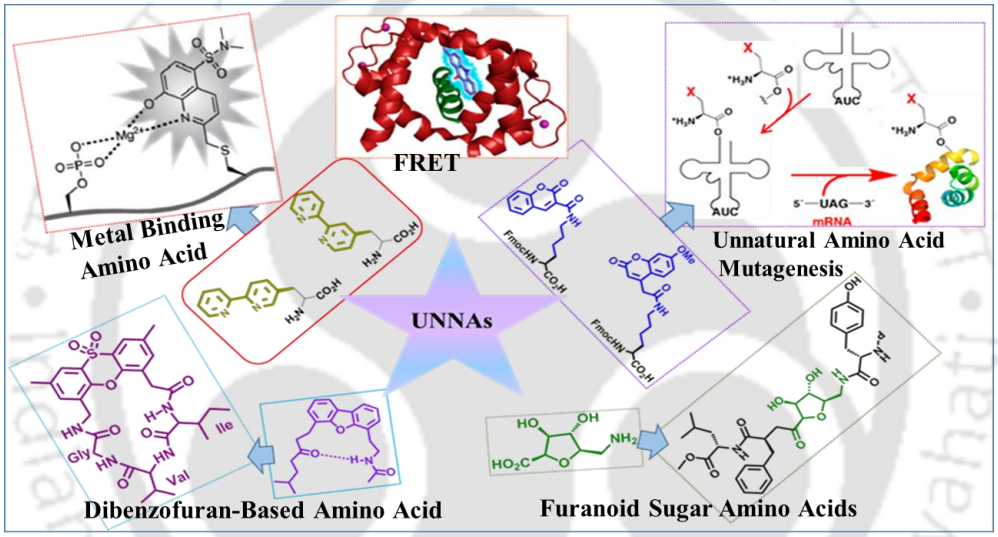

Figure A1: Schematic presentation of fluorescent unnatural amino acids and conformationally constraints small molecular scaffolds.

In Nature, only nine canonical amino acids with a limited number of functional groups available for protein modification. So, the lack of significant fluorescence in naturally occurring amino acids has prompted the design of fluorescent amino acids with improved photophysical properties for protein chemistry research. Thus, much effort has been devoted to developed stable non-natural fluorescent amino acids. Several multiple chromophore labeled peptides/proteins has been developed for investigating folding mechanism, detection of a target protein, enzyme activity detection and studying protein-protein/protein-drug interactions utilising various fluorescence phenomena such as FRET, excimer and exciplex emission. Furthermore, natural peptides/proteins are generally poor drug candidates due to their low oral bioavailability and unfavorable pharmacokinetics. Therefore, field of peptidomimetics is evolved to replace biologically active parts of peptides with non-peptide structures

to increase bioavailability of peptide-based drugs. Conformationally constrained amino acids/ scaffolds restrict the rotation of amide bond, side chain modified amino acids could restrict conformational flexibility via steric interactions and helps adopting a folded conformation without drastically changing the stereo-electronic properties. Towards this end several unnatural amino acids (UNAA)/amino acids scaffolds with novel functionalities have been designed and incorporated within a protein's framework aiming to expand the genetic code or to have enzymatically stable peptide-based drugs candidates.

CHAPTER 2: STUDIES ON THE SYNTHESIS AND PHOTOPHYSICAL PROPERTIES OF FLUORESCENT UNNATURAL TRIAZOLYL AMINO ACIDS

This chapter describes the design and synthesis of microenvironment sensitive fluorescent triazolyl unnatural amino acids (UNAA) decorated with donor and/or acceptor aromatic chromophores via click chemistry. As a part of our ongoing research efforts on the installation/modulation of emission response and the design of biomolecular building blocks via click chemistry, we thought that it would be worthwhile to synthesize triazolyl amino acids containing donor/acceptor aromatics to produce new and novel photophysical property. We envisioned that the fluorescent amino acids could also be useful in the study of interaction with target biomolecule such as BSA with the help of fluorescence spectroscopy.

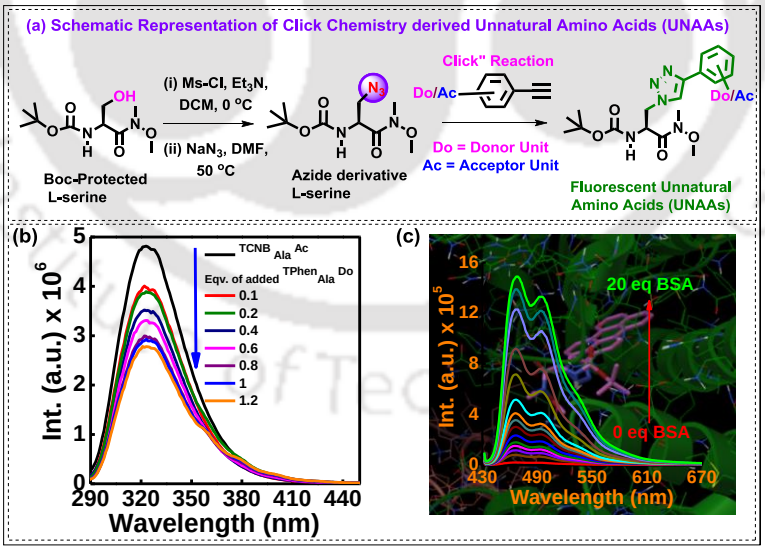

Figure A2: (a) Schematic presentation of synthesis of triazolyl unnatural amino acids (UNAA). (b) FRET quenching event of donor amino acid (^{TPhen}**Ala**^{Do}) in presence of acceptor amino acid (^{TCNB}**Ala**^{Ac}) in ACN solvent. (c) Fluorescence titration of triazolyl perylene amino acid (^{TPer}**Ala**^{Do}) with BSA protein in phosphate buffer pH ~ 7.

The synthesized fluorescent amino acids show interesting solvatochromic characteristic and/or intramolecular charge transfer (ICT) feature as is revealed from the UV-visible, fluorescence photophysical properties and DFT/TDDFT calculation. HOMO-LUMO distribution shows that the emissive states of some of the amino acids are characterized with more significant electron redistribution between the triazolyl moiety and the aromatic chromophores linked to it leading to modulated emission property. A pair of donor-acceptor amino acid ^{TPhen}**Ala**^{Do}/^{TCNB}**Ala**^{Ac} shows interesting photophysical interaction property indicating a FRET quenching event. Furthermore, one of the amino acid, triazolyl-perylene amino acid (^{Per}**Ala**^{Do}), has been exploited for studying interaction with BSA and found that it is able to sense BSA with an enhancement of fluorescence intensity. (**Figure A2**).

All experimental results are presented in this chapter.

CHAPTER 3: SYNTHESIS, CONFORMATION AND STUDY OF PHOTOPHYSICS OF TRIAZOLYL DONOR–ACCEPTOR UNNATURAL AMINO ACIDS DECORATED TRIPEPTIDES: A FRET EVENT IN β-TURN CONFORMATION

The Chapter **3** deals with the studies on the synthesis and π-stacking/photophysical interaction property between triazolyl donor/acceptor amino acid (^{TPhen}**Ala**^{Do}/^{TNB}**Ala**^{Ac}) which remained separated by a single natural alanine in our synthesized tripeptide. The synthesis and photophysical properties of the amino acids are previously described in **Chapter 2.** FRET event and its solvent assisted amplification are presented in details. A literature study revealed that there exist very limited no of fluorescent peptides which might adopt/mimic a particular secondary structure of protein and can show very interesting photophysical properties in a predefined manner. Moreover, a limited number of fluorescent amino acids have been incorporated into short peptides to study the protein–protien interaction. Therefore, designing fluorescent peptides is currently an attractive research area to study photophysics for various biophysical applications

With this background we envisioned that upon incorporation of two of such fluorescent UNAAs into two termini of a tripeptide separated by a natural alanine might adopt β-turn conformation via backbone H-bonding interaction (**Figure A3**). We also expected that the hydrophobic, π-π stacking and van der Waals interactions in the side chain would stabilize the conformation and allow the two terminal triazolyl aromatics to involve in dipolar photophysical interaction, most likely Förster resonance energy transfer (FRET) process. FRET being a distance dependent phenomenon is widely being utilized in elucidating structures, dynamics of proteins, in studying biomolecular interactions and conformational distribution of an

unstructured peptide and in many other sensory applications. Thus, we were interested in β-turn peptidomimetic capable of showing FRET interaction between two terminally placed fluorescent unnatural amino acids.

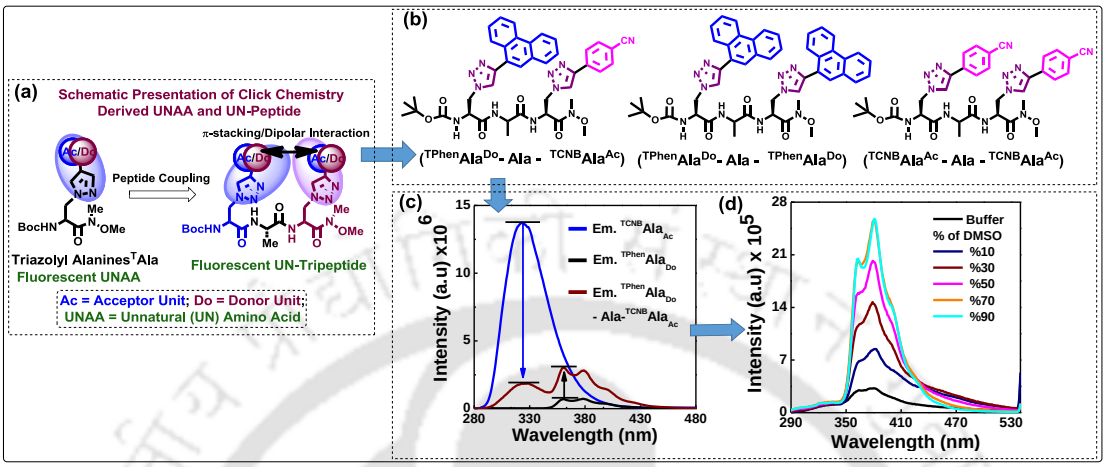

Figure A3: (a) Schematic presentation of synthesis of triazolyl **UNAAs** decorated tripeptides. (b) Structures of the peptides. (c) Fluorescence spectra of individual amino acids (Black for ^{TPhen}**Ala**^{Do} and Blue for ^{TCNB}**Ala**^{Ac}) and the tripeptide ^{TPhen}**Ala**^{Do}**-Ala-**^{TCNB}**Ala**^{Ac} (Red) containing these two amino acids in CH_3CN with 10 μM concentration. (d) Amplification of FRET signal in phosphate buffer (pH 7.0) upon addition of increasing % of DMSO (λ_{ex} = 272 nm).

The secondary structures of peptides were estimated by recording its CD spectrum in acetonitrile and methanol which showed a β-turn conformation and indicated a signature of aromatic absorption/π-π stacking interaction between two aromatic moieties of terminal amino acids in all three peptides. All the spectroscopic evidences (IR, NMR) and the molecular modelling study supported the β-turn conformation of peptides which was mostly originated from backbone H-bonding interaction and stabilized by other side chain interactions like hydrophobic, π-π stacking interactions between the terminal **TPhen** and **TCNB** moieties.

The Förster resonance energy transfer (FRET) was also established in the conceptually designed novel unnatural β-turn peptide containing a new class of fluorescent unnatural donor/acceptor amino acids. The FRET process occurred from **TCNB** moiety of ^{TCNB}**Ala**^{Ac} (FRET donor) to **TPhen** unit of ^{TPhen}**Ala**^{Do} (FRET acceptor). Our developed FRET pair, ^{TCNB}**Ala**^{Ac} - ^{TPhen}**Ala**^{Do}, wherein both the partners are unnatural amino acid, is new to the best of our knowledge. As FRET can provide information about peptide/protein conformation, our unnatural amino acid pair (FRET pair) and the FRET peptide might find application in studying solution conformational distribution of an unstructured peptide and FRET based bioassay. We also establish that the FRET-induced fluorescence could be modulated with a change

in solvent polarity and FRET signal could be optimized upon addition of DMSO to 296 % enhancement which possibly fine-tuned the donor/acceptor interaction to minimize the non-radiative deactivation process leading to increase in intensity.

All experimental results are presented in detail in this chapter.

CHAPTER 4: SYNTHESIS OF TRIAZOLO β - AZA - ε- AMINO ACID AS NOVEL SCAFFOLD FOR β -TURN PEPTIDOMIMETICS

This chapter describes the synthesis of β-aza-ε-amino acid as a conformationally constrained molecular scaffold. Readily accessible triazolo-β-aza-ε-amino acid (**^{Al}TAA**) in a peptide backbone mark a novel class of unnatural peptide building blocks to induce desirable secondary structures in small linear peptides. This is demonstrated in a Leu-enkephalin analogue with purely β-turn conformation wherein the scaffold replaces the original Gly-Gly dipeptide sequence. Interestingly, it also induces a β-turn structure in a pentapeptide wherein FRET is established between two novel fluorescent triazolyl unnatural amino acids in two termini.

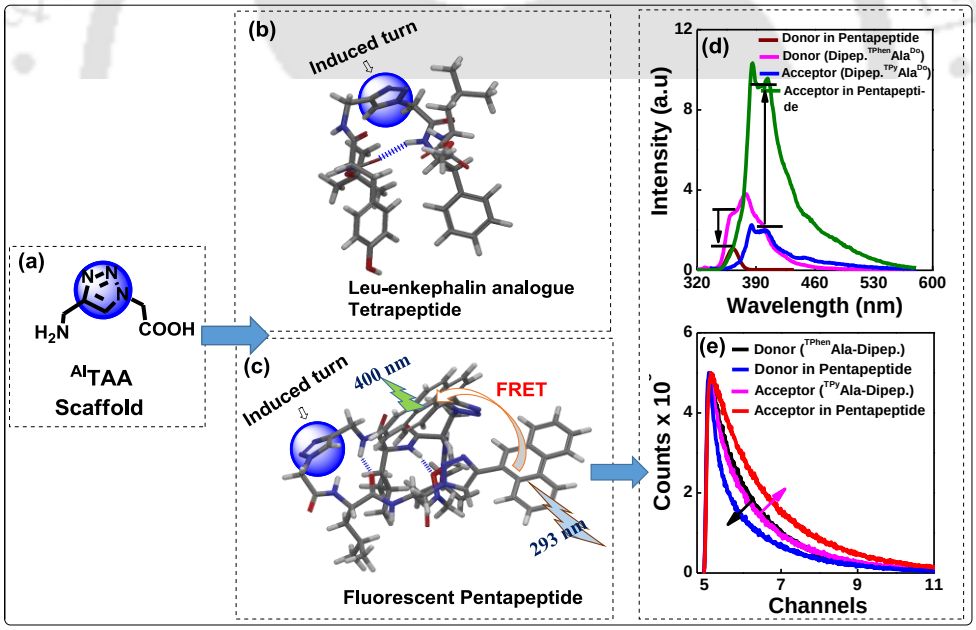

Figure A4: Graphical presentation of the (a) constrained molecular scaffold-triazolo amino acid (**^{Al}TAA)**, (b-c) peptidomimetics. (d) Steady state and (e) time resolved fluorescence spectra of triazolyl donor acceptor amino acids decorated fluorescent β-turn pentapeptide (peptidomimetics shown in **c**) showing a FRET process (Boc-**^{TPy}Ala^{Do}**-Leu-**^{Al}TAA**-Leu-**^{TPhen}Ala^{Do}**-CO_2Me).

The recent advancement on the design of conformationally constrained of small molecular scaffold for peptidomimetics prompted us to relook into the rigid framework of pseudo-aromatic triazole unit. We observed that a designed triazolo amino acid with constrained backbone angles ω(i) and ϕ(i+1), would expected to induce folded conformations in linear peptides. Moreover, the triazole unit is metabolically inert, can easily associate with biological targets, act as *trans*-amide mimetics and tolerate various reactions conditions used in peptide synthesis. Though the click chemistry has been utilised in mimicking protein's secondary structures, to the best of our knowledge, the triazolo amino acids as a scaffold has not been explored. We envisioned that upon incorporation into a backbone a linear peptide might adopt β-turn conformation. This is again obvious if we could incorporate ^{Al}**TAA** into Leu-enkephalin by replacing its Gly-Gly dipeptide segment that is known to be flexible and amenable to different conformations depending on the binding environment.

With this aim we have synthesis a triazolo-β-aza-ε-amino acid, ^{Al}**TAA** and studied its effect on the structural properties of linear peptide, a Leu-enkephalin analogue and of a model fluorescent pentapeptide (Boc-^{TPy}**Ala**^{Do}-Leu-^{Al}**TAA**-Leu-^{TPhen}**Ala**^{Do}-CO_2Me), wherein two fluorescent unnatural triazolo amino acids, (^{TPy}**Ala**^{Do} and ^{TPhen}**Ala**^{Do}), are embeded at the two arms of the scaffold via an intervening leucin in each arm. Furthermore, we were curious to know the impact of adopted conformation on the photophysical interaction property, if at all, among the terminal fluorescent amino acids.

The structural and conformational analysis of Leu-enkephalin analogue peptide and fluorescent peptide by various spectroscopic techniques, such as CD spectra, IR, VT-NMR and 2D NMR and molecular dynamics (MD) simulation studies established well-defined type II β-turn structure induced by the novel β-turn-mimetic constrained molecular scaffold, the triazolo amino acid ^{Al}**TAA**. An examination of the photophysical properties of fluorescent pentapeptide established the our concept of FRET in a β-turn conformation.

Exploration of turn mimetics and the sequence specific DNA binding event of tetra-amides of this molecular scaffold might lead to the generation of a new family of distamycin analogue.The easily accessible aliphatic triazolo amino acid ^{Al}**TAA** was introduced for the first time as a β-turn-mimetic constrained molecular scaffold (**Figure A4)**.

All experimental results are presented in this chapter.

CHAPTER 5: DESIGN AND SYNTHESIS OF AROMATIC TRIAZOLO AMINO ACID AS CONFORMATIONALLY CONSTRAINED MOLECULER SCAFFOLD AND ITS APPLICATION IN β –SHEET NEUCLEATING PEPTIDOMIMETICS AND SENSING BSA PROTEIN

In this chapter we describe the design and synthesis of aromatic triazolo amino acid scaffold which in a peptide backbone act as a turn mimetic β-sheet nucleator. The photophysical outcome from an aromatic triazolo amino acid scaffolded trichromophoric fluorescent pentapeptide and its application in sensing BSA are also described. Among the various bioactive conformations, the β-sheet structure is the second most common structural motif of protein. The β-sheet not only plays a scaffolding role, but also serves as a key recognition motif in many important biological processes involving protein-protein and protein-DNA interactions.

As a part of our ongoing research effort on the design of unnatural biomolecular building blocks via click chemistry and β-turn peptidomimetics with unnatural fluorescent amino acid (discussed in **chapter 3**) and aliphatic triazolo amino acid scaffolded β-turn peptidomimetics (designed in **chapter 4**) we thought that more rigid triazolo amino acid scaffold such as an aromatic analogue in the turn conformation might act as a "β-turn mimic as β-sheet folding nucleator". Moreover, design of a fluorescent peptide which in a folded β-sheet conformation might have impact on its photophysical outcome is fundamentally of great importance owing to their possible applications in gaining insight into the living cell *via* studying their inter-biomolecular interaction property.

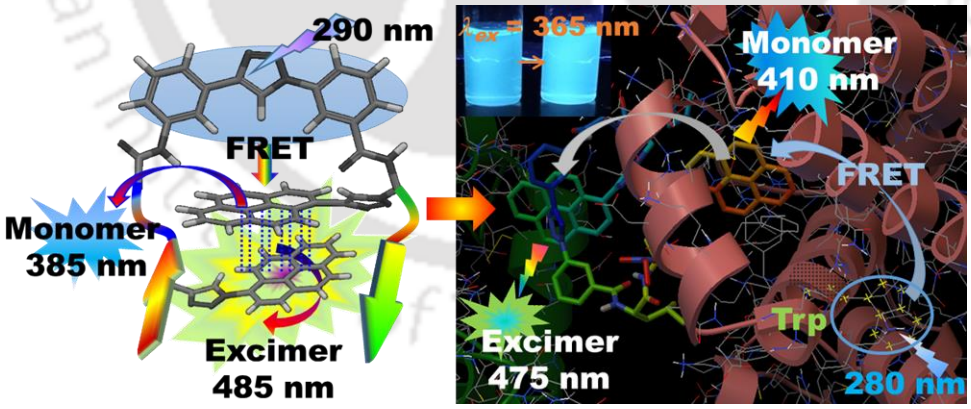

Figure A5: Schematic presentation of the aromatic triazolyl amino acid scaffold **^{Ar}TAA** based dual door entry system trichromophoric fluorescent pentaptide and protien-peptide interaction.

Therefore, with this background and concept we have successfully synthesised aromatic triazolo amino acid scaffold (**^{Ar}TAA**) and incorporated into a short linear

peptide/ trichromophoric fluorescent pentapeptide (Boc-^{TPy}**Ala**^{Do}-Leu-^{Ar}**TAA**-Leu-^{TPy}**Ala**^{Do}-CO_2Me) and studied of conformation and photophysics. The structural and conformational analysis of Leu-enkephalin analogue peptide and trichromophoric fluorescent pentapeptide by various spectroscopic techniques, such as CD spectra, IR, VT-NMR and 2D NMR and molecular dynamics (MD) simulation studies established predominant β-sheet like structure with some contribution from turn conformation nucleated by the novel β-turn-mimetic constrained molecular scaffold, the aromatic triazolo amino acid (^{Ar}**TAA**).

An examination of the photophysical properties of trichromophoric fluorescent pentapeptide established the fundamental concept of dual door entry to excimer emission. Both the processes of excitation of **TPy** of ^{TPy}**Ala**^{Do}-either energy transfer from excited scaffold amino acid, ^{Ar}**TAA** (FRET) to **TPy** or direct excitation of **TPy**-led to the excimer emission in pentapeptide. This study would provide fundamental guidelines to design such conceptual fluorescent probe of dual door entry system to excimer emission. To the best of our knowledge this is the start of a new generation of probes which would find wide applications in the field of chemical biology. Moreover, the novel probe of dual door entry to excimer emission system was found to be an effective fluorescence light-up probe for detecting and studying protein–peptide interactions in solution. Studying other specific protein–peptide interactions of significant clinical interest utilizing conceptual fluorescent peptide-probe is our current research focus.

All experimental results are presented in this chapter.

CHAPTER 6: APPLICATION OF AROMATIC TRIAZOLYL AMINO ACID SCAFFOLD AND ITS MONO- AND BIS-PYRENYL AMIDES AS FLUORESCENCE LIGHT-UP SENSORS OF ETHANOL

This chapter deals with the fluorimetric discrimination of ethanol from methanol utilising aromatic triazolo amino acid scaffold (^{Ar}**TAA**) and its mono- and bis-pyrenyl amides. Discrimination of methanol and ethanol with subtle differences in polarities is a difficult task and remains as a challenge. Therefore, design of robust fluorescence sensor of ethanol is highly demanding. In the previous chapter we observed the triazolyl amino acid scaffold which is in hairpin shape shows optical chirality. This scaffold was primarily designed as nucleator of peptide secondary structures. A study of photophysical property of the scaffold in various organic solvents left us a clue that it can be used for discrimination between methanol and ethanol. Moreover, the axial chirality of the probe scaffold lead us to envisioned that discrimination of methanol and ethanol with subtle differences in polarities could be achieved via differential H-bonding and hydrophobic interactions.

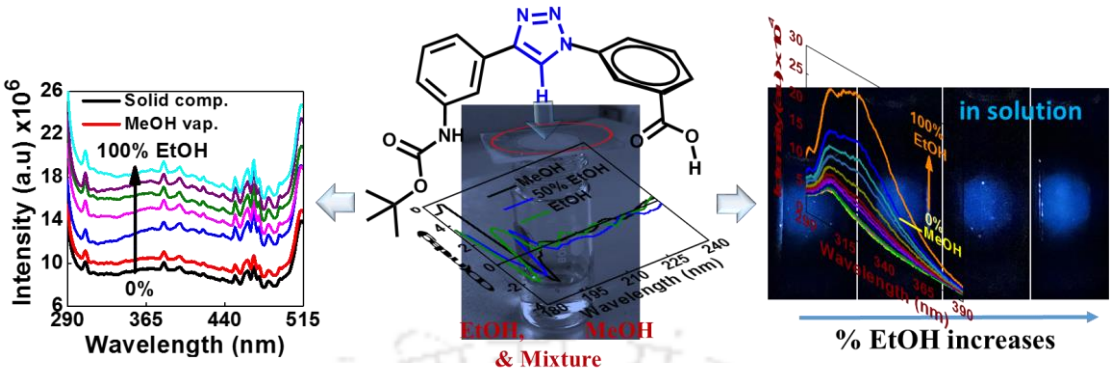

Figure A6: Graphical presentation of the fluorimetric discrimination of ethanol and methanol.

Therefore, we took the task for sensing ethanol with the help of aromatic triazolo amino acid scaffold **^{Ar}TAA**. As the wavelength of emission for the aromatic triazolo amino acid scaffold **^{Ar}TAA** lies in the UV-region, so we planned to modify the scaffold and hence, prepared its mono pyrenyl amide and bis-pyrenyl-bis-amide derivatives and to study of fluorescence photophysical properties toward discriminating ethanol and methanol both in liquid and vapour phase of all the sensors.

Our study revealed that all the three sensors, simple scaffold (**^{Ar}TAA**), mono- (**PyAm-^{Ar}TAA**) and bis-pyrenyl- (**Py$_2$Am-^{Ar}TAA**) amides, show similar sensitivity with detection limit of 2.2 v/v% of ethanol. The solid films of these sensors are also found to be effective in sensing ethanol vapor via generation of distinct and enhanced fluorescence signal (**Figure A6)**. All our experimental results suggest the role of axial chirality of the hairpin-shape scaffold in differential solvation guided H-bonding interaction in discriminating ethanol from methanol with a switch-on fluorescence response.

All experimental results are presented in this chapter.

List of Abbreviations

Aib	α-Amino isobutyric acid
Ac (Superscript)	Acceptor
Ala	Alanine
Arg	Arginine
^{Al}TAA	Triazolo-β-aza-ε-amino acid
^{Ar}TAA	Aromatic triazolo amino acid
Amber	Assisted model building with energy refinement
7AW	7-Azatryptophane
Ar	Aryl
Adk	Adenylate kinase
Abs	Absorbance
Bi_2O_3	Bismuth oxide
B3LYP	Becke, three-parameter, Lee-Yang-Parr
BSA	Bovin serum albumin
BTB	Bromo ethyl blue
Cu_2O	Cuprous oxide
CD	Circular dichroism
CT	Charge transfer
Cu	Copper
CuI	Copper iodide
Cyhex	Cyclohexane
$CHCl_3$	Chloroform
$CDCl_3$	Deuterated chloroform
$CuSO_4$	Copper sulfate
CR	Click reagent
CuAAC	Copper-catalysed azide-alkyne cycloaddition

CH_3CN	Acetonitrile
CLC	Cholesteric liquid crystal
Do (Superscript)	Donor
DHFR	Dihydrofolate reductase
Dtc	5,5-Dimethylthiazolidine-4-carboxylic acid
Diox/Dx	1,4-Dioxane
DMF	Dimethyl formamide
DMSO	Dimethyl sulfoxide
DMSO-d_6	Deuterated dimethyl sulfoxide
DCE	Dichloroethane
DNA	Deoxyribonucleic acid
DFT	Density functional theory
DCM	Dichloromethane
DIPEA	N,N-Diisopropyl ethyl amine
DMAP	N, N-Dimethylamino pyridine
4-DMAP	4-(*N*,*N*-Dimethylamino)-phthalimide
6-DMNA	6-*N*,*N*-Dimethylamino-2-3-naphthalimidoalanine
Dnp	2,4 Dinitrophenyl
Et_3N	Triethylamine
EtOAc	Ethylacetate
EtOH	Ethanol
eV	Electron volt
EDC.HCl	1-(3-Dimethylaminopropyl)-3-ethylcarbodiimide hydrochloride
Eqv.	Equivalent
Fl	Fluorescence
FSD	Fourier self-deconvolution

FRET	Förster resonance energy transfer
GPCRs	G-protein coupled receptors
GO	Graphene oxide
HOBT	1-Hydroxy-benzotriazole
HRMS	High resolution mass spectrometry
HOMO	Highest occupied molecular orbital
HIV	Human immunodeficiency virus
5HW	5-Hydroxytryptophane
ICT	Intramolecular charge transfer
ITC	Isothermal calorimetry
IR	Infrared spectroscopy
IL	Ionic liquid
In_2O_3	Indium oxide
KOH	Potassium hydroxide
KBr	Potassium bromide
K	Kelvin
Leu	Leucine
LiOH	Lithium hydroxide
LUMO	Lowest unoccupied molecular orbital
MCA	7-Methoxycoumerin-4-acetic acid
MD	Molecular dynamics
Max	Maxima
MeOH	Methanol
mM	Mili molar
m.p.	Melting point
NaN_3	Sodium azide
$NaHCO_3$	Sodium bicarbonate

Na_2SO_4	Sodium sulphate
NMR	Nuclear magnetic resonance
NOESY	Nuclear overhauser effect spectroscopy
mM	Milimolar
nm	Nanometer
ORTEP	Oak ridge thermal ellipsoid plot
OPLS	Optimized potentials for liquid simulations
O_2	Oxygen
Pro	Proline
Py	Pyrene
PyAm-ArTAA	Mono pyrenyl amide aromatic triazolo amino acid
Py_2Am-ArTAA	Bis-pyrenyl-bis-amide aromatic triazolo amino acid
Per	Perylene
PL	Photoluminescence
PNA	Protein nucleic acid
RuAAC	Ruthenium-catalysed azide-alkyne cycloaddition
PRODAN	6-Propionyl-2-dimethylaminonaphthalene
PPh_3	Triphenyl phosphine
Pd	Palladium
PET	Photoinduced electron transfer
Ph	Phenyl
Ppm	Parts per million
$PdCl_2(PPh_3)_2$	Bis(triphenylphosphine)palladium(II) dichloride
r.t.	Room temperature
RNA	Ribonucleic acid
ROSEY	Rotating frame nuclear overhauser effect spectroscopy
SPPS	Solid phase peptide synthesis

SAAs	Sugar amino acids
Ser	Serine
$SOCl_2$	Thionyl chloride
Trp	Tryptophan
Tyr	Tyrosine
$^{TNDMB}Ala^{Do}$	Triazolyl N,N-dimethylaminobenzene alanine amino acid
$^{TPyr}Ala^{Do}$	Triazolyl pyridine alanine amino acid
$^{TMNap}Ala^{Do}$	Triazolyl 6-methoxynaphthalene alanine amino acid
$^{TDMB}Ala^{Do}$	Triazolyl dimethoxybenzene alanine amino acid
$^{TPhen}Ala^{Do}$	Triazolyl phenanthrene alanine amino acid
$^{T4\text{-}DMAPNI}Ala^{Do}$	Triazolyl 4-(4-N,N-dimethylaminophenylethynyl)-N-(2-propynyl)-1,8 naphthalimide alanine amino acid
$^{TPy}Ala^{Do}$	Triazolyl pyrene alanine amino acid
$^{TBAPy}Ala^{Do}$	Triazolyl pyrenebutaramido alanine amino acid
$^{TPer}Ala^{Do}$	Triazolyl perylene alanine amino acid
$^{TCNB}Ala^{Ac}$	Triazolyl cyanobenzene alanine amino acid
$^{TNB}Ala^{Ac}$	Triazolyl nitrobenzene alanine amino acid
$^{TDTFMB}Ala^{Ac}$	Triazolyl 3,5-trifluoromethylphenyl alanine amino acid
$^{T4\text{-}CPNI}Ala^{Ac}$	Triazolyl 4-(2-(4-(cyano)phenyl)ethynyl)-1,8- naphthalimide alanine amino acid
TPhen	Triazolyl phenanthrene
TCNB	Triazolyl cyanobenzene
TPy	Triazolyl Pyrene
TBAF	Tetrabutylammonium fluoride
TLC	Thin layer chromatography
THF	Tetrahydrofuran
TDDFT	Time dependent density functional theory

TCSPC	Time correlated single photon counting
TEA	Triethyl amine
TFA	Trifluoroacetic Acid
TMS	Trimethylsilyl
UNAAs	Unnatural amino acids
UV	Ultra violate
μM	Micro molar
Val	Valine
VT	Variable temperature
Wt	Water
Φ	Quantum yield
ε	Molar extinction co-efficient
τ	Decay time
Å	Angstrom (10^{-8}cm)
$\tilde{\nu}$	Wave number
λ	Wave length
ϕ and ψ	Torsion angle
λ_{max}^{abs}	Absorption maxima
λ_{max}^{fl}	Fluorescence maxima
Δf	Solvent polarity parameter
μ_e	Excited state dipoemoment
μ_g	Ground state dipoemoment

NMR Data

δ	Chemical shift in NMR
s	singlet
d	doublet

t	triplet
q	quartet
m	multiplet
bs	broad singlet
dd	double doublet
dt	doublet of triplet
ddd	doublet of doublet of doublet
J	coupling constant in Hz

CONTENTS

Page No.

Chapter 1

APPLICATIONS OF UNNATURAL AMINO ACIDS AND CONFORMATIONALLY CONSTRAINED SMALL MOLECULE SCAFFOLD: A REVIEW

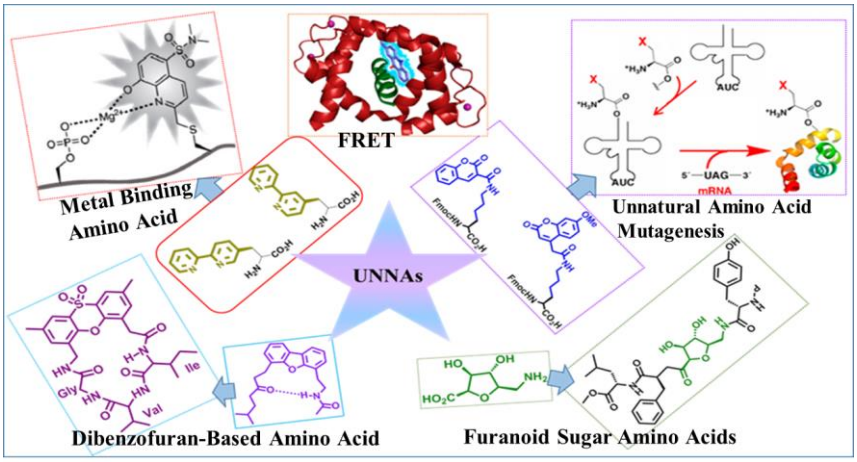

1.1. Introduction

Amino acids are indispensable ingredients of life system and protein function. Proteins play a vital role in all living organisms to maintain the cell structures, properties and functions. However, in all organisms, the building blocks of all the translated proteins are the same 20 natural amino acids. Moreover, natural selection/evolution has generated a large no of proteins with more or less common structures and functions in a population.[1] Therefore, these proteins are highly specialized for performing specific jobs and thus, are not suitable for a different function other than they use to do the specific job. To perform a complex additional function by a protein, it needs other functionalities within its framework.[1b] Post-translational modifications, cofactor-dependent catalysis, and pyrrolysine/selenocystein incorporation in bacteria proves that the natural evolutionary movement needs extra chemical functionalities other than those present within the 20 natural amino acids.[2]

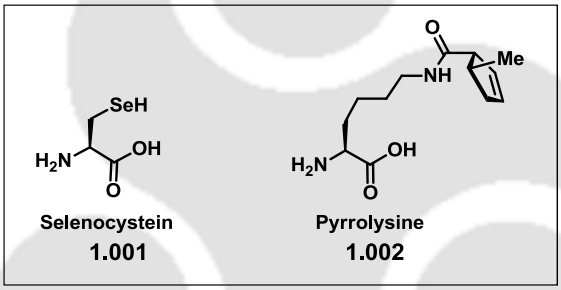

Figure 1.1. Presentation of naturally occurring 21st and 22nd amino acids.

Thus, the approach "directed evolution", have come up with proteins of altered structural and functional properties that do not occur in nature.[3] As for example, researchers are trying to generate new proteins to function as potent therapeutic with high oral viability or as a sensitive probe for visualizing intracellular events and understanding molecular interactions inside a cell. Now a day, scientists are involved in designing the proteins *via* rational approach of directed evolution to produce new proteins with desirable properties. Therefore, inspired by Natures' post-translational modification to include different functional units or molecules into the proteins, chemoselective conjugation methods have been developed to attach probe to proteins; thereby facilitating the study of structure and functions at molecular level.[4] However, conventional bioconjugation reaction has several drawbacks and mostly exploited the only nine canonical amino acids with limited functional groups and abundance for modification/ligation within a protein. Therefore, site-specific conjugation of an additional functionality/probe molecule to a desired canonical amino acid within a protein's framework is a challenging task.[5] To circumvent this problem, several chemical and biochemical methodology have been developed to site-specifically

incorporate "designer amino acids" (the unnatural amino acids) with desired functionalities to probe protein structure, conformation and function and to generate proteins/enzyme for several novel biochemical applications, such as for chemical synthesis, biomedical research or even as therapeutics.[6] Therefore, the research in the field of design and synthesis of non-natural amino acids with novel properties, to encode it genetically and to incorporate it site-specifically into a protein *via* bio-orthogonal strategy, is growing at a fast space for the growing demand of proteins of potential therapeutic and many other diversified novel biotechnological applications.[6, 7] Therefore, an expanded genetic code when site-specifically incorporated into protein would allow us to study proteins' physicochemical/biophysical properties which would otherwise be extremely difficult-(a) probing protein structure, conformation, function and interbiomolecular interaction, (b) regulating protein activity, (c) monitoring the mode of action, (d) improving immunogenicity, and (e) very recent development of a protein with a "chemical warhead" which target specific cellular components.[8, 9]

The historical development of synthesis or semisynthetic methods for introduction of unnatural amino acids into peptide and proteins by Offord and Kaiser has paved the way to develop methods for site specific incorporation of more unnatural amino acids into proteins by Schultz *et al.* towards expanding the genetic code and reaching the goal of semisynthetic organism.[10] Towards this end, an increasing amount of interest from various research groups has resulted in the acceleration of progress of design of unnatural amino acids for application in protein engineering. Several non-natural amino acids were reported looking after the steric and electronic properties and incorporated into proteins site specifically.[11] Moreover, for the growing demand of proteins of diverse and improved functionality, several unnatural amino acids (UNAA) with novel functionalities have been incorporated within a protein's framework via the developed strategies of bioconjugations like translational incorporation, semisynthetic incorporation, bio-orthogonal conjugation and most recently developed recombinant introduction of amino acids into protein.[12] Among the various examples of UNAAs, the work of Schultz *et al.* about the encoding an amino acid with a chemical warhead which target specific cellular components, is highly appreciable. Therefore, the synthesis of unnatural amino acids with novel functionality is highly demanding and is currently an emerging area of research because of the currently developed technology, "recombinant introduction" of amino acid into proteins.[13] However, many of the reported unnatural amino acids are not suitable for giving novel biological properties of the proteins or not containing functionality/signaling elements for labeling the proteins that can offer information about protein's structure, function and dynamics with a fast and easily detectable signal generation.

Sensing of proteins' microenvironment needs the help of highly sensitive fluorescence probe. Extremely sensitive fluorescence based detection techniques find widespread applications for probing of structure, function, dynamics of biomolecules,

for visualizing intracellular events, understanding molecular interactions inside a cell and for enabling experiments to be measured in solution.[14] Many such aspects have been studied either by exploiting intrinsic fluorescence of tryptophan amino acid in a protein or extrinsic fluorescent label. However, intrinsic fluorescence limits the interpretation of the results in presence of multiple tryptophan in a protein. Moreover, the limitation of labeling with large size of extrinsic fluorescent probe has led a strong demand for generating the smaller protein tag or site-specific incorporation of unnatural fluorescent amino acids into a protein.[15] Many of the problems for generating extrinsic fluorescently labeled proteins can be solved if a microenvironment sensitive intrinsic fluorescent amino acid can be synthesized and incorporated into a protein site-specifically.[15]

Fluorescent amino acids can be used for in vitro and cellular imaging of protein localization, biomolecular interactions, and conformational changes with the ability to place these small probes at virtually any site in the proteome. The fluorescent proteins are valuable tools in cell biology for monitoring molecular localization and activities of proteins and gene expression in live cells. As for an example, green fluorescent protein (GFP) despite of having few shortcomings is a powerful probe of protein expression, localization, and studying biomolecular interactions.[16] The most important and novel method for the generation of fluorescent proteins is to genetically encoded incorporation of fluorescent amino acids site-specifically.[16c] Thus, Schultz *et al*., have exploited a polarity sensitive fluorescent amino acid, L-(7-hydroxycoumarin-4-yl) ethylglycine, as a probe of the urea dependent denaturation of holomyoglobin. An environmentally sensitive dansyl amino acid (**DansA**) was also genetically encoded and site-specifically incorporated into proteins by the same group and used as an environmentally sensitive reporter of protein unfolding.[17] A fluorescent unnatural amino acid, 6-propionyl-2-(*N*,*N*-dimethyl)aminonaphthalene (**Anap**), has been incorporated into proteins to study ligand-induced local conformational changes in proteins and biomolecular interactions in vitro and to localize proteins in living mammalian cells.[13] Christiane Garbay *et al*., have reported the incorporation of fluorescent coumaryl amino acid into short peptide to generate fluorescent peptide and studied the cell internalization behavior.[17c] There are also reports wherein "click reaction" has been utilized for fluorescent labeling of proteins.[18] Multiple chromophore labeled peptides/proteins have also been developed for investigating folding mechanism, detection of a target protein, enzyme activity detection and studying protein-protein/protein-drug interactions utilising various fluorescence phenomena such as FRET, excimer and exciplex emission.[19, 20] Till the date only a very limited number of such amino acids as discussed have been synthesized or encoded genetically. Therefore, there is a high demand to develop fluorescent unnatural amino acids (FUAA) or fluorescently labelled UAA with high microenvironment sensitivity for genetic encoding or to generate labelled proteins/peptide for studying conformational or diverse functional realm.

Despite the availability of a few of such fluorescent amino acids, no special attentions were taken to develop amino acids with tunable photophysical property and specific conformational adoptability. Therefore, the synthesis of unnatural amino acids with novel photophysical property is currently an emerging area of research which would address the following aspects: (a) labeling a protein via site specific incorporation or a short peptide with such fluorescent "designer amino acid" would enable to study the specific conformational adaptability, functions and dynamics of a protein; (b) these fluorescent unnatural peptide/proteins can be utilized as sensitive probes for visualizing intracellular events and understanding molecular interactions inside a cell such as receptor-ligand binding, monitoring enzyme activity, elucidating protein's structures, functions and dynamics, high-throughput screening, diagnostics and proteomics.[15, 16]

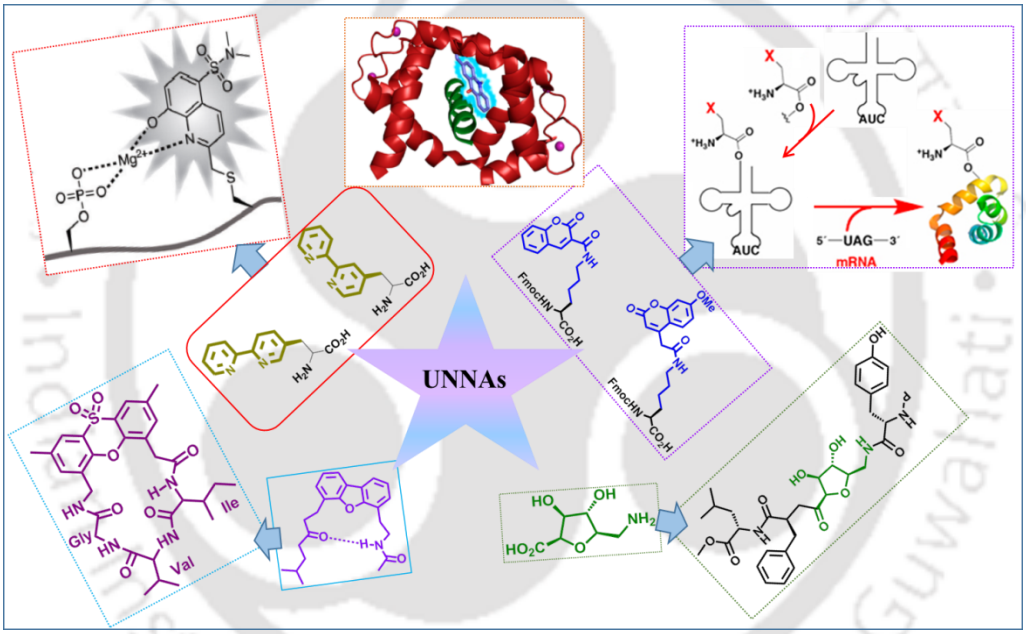

Figure 1.2. Graphical presentation of some reported unnatural amino acids and their applications.

During the past decade, peptides have gained a wide range of applications in medicine and biotechnology. Thus, therapeutic peptide research is currently experiencing a renaissance for commercial reasons as peptides are selective and efficient signaling molecules and trigger intracellular effects through binding to specific cell surface receptors, such as G protein-coupled receptors (GPCRs) or ion channels.[21] Given their attractive pharmacological profile and intrinsic properties, peptides represent an excellent starting point for the design of novel therapeutics. Moreover, high specificity would make peptides as excellently safe, tolerable and effective in humans. Thus, in various aspects of drug market, peptides are in the sweet spot between small molecules and biopharmaceuticals. However, natural peptides seldom can be used therapeutically as drugs, because of the problems associated with

low absorption, rapid metabolism and low oral bioavailability, many efforts aimed to modify the natural sequence of the amino acids of bioactive peptides achieved a desired and a focused effect.[22a] Therefore, harnessing for peptide based therapeutics a great number of researchers all over the world are engaged in the design and synthesis of peptidomimetics or peptide like molecules of clinical importance. Conformationally constrained small, molecular scaffold/ non-peptide isostere are attracting much research interest in this regard because it could induce a particular conformation of a peptide which is the key for showing biological activity by the peptide with high oral viability.[22] Considerable efforts have thus been invested in studying the impact of appended molecular scaffolds in one hand and nucleating β-sheet/β-turn mimics on the other hand, on the conformational preferences of proteins and peptides in solution. Though, an exponential growth on the development of constrained non-peptidic molecular scaffolds as peptidomimetics is observed, very few peptide-based drugs have been developed. Therefore, there is a need to renovate the existing design principles with newer concepts, chemistry and protocols to introduce conformationally constrained nonpeptide isosteres or small molecule scaffold into peptide backbones in order to achieve desirable secondary structures along with pharmacologically viable peptide-based drug candidates of enhanced metabolic stability.[23]

The following sections of this chapter would represent a critical survey of applications of unnatural amino acids and conformationally constrained small, molecular scaffold/ non-peptide isostere in the context of peptidomimetics and generation of functional peptides with novel photophysical properties.

1.2. Need for Unnatural Amino Acids (UNAAs)

The ability to generate proteins with new building blocks (UNAAs), beyond those specified by the genetic code might allow us to generate proteins or even entire organisms with novel functions. The ability to introduce amino acids with precisely tailored steric and electronic properties into proteins would also allow us to carry out "physical organic" studies of proteins much the same way as has been historically done with small molecules.

There are many applications of unnatural amino acids which include the following:

1. The generation of therapeutic proteins with enhanced pharmacology is possible in contrast to the historical, relatively nonspecific methods for the chemical modification of therapeutic proteins with electrophilic moieties or the selective modification of cysteine residues.[24a]
2. Increase the immunogenicity of self-proteins or weakly immunogenic pathogen proteins (e.g., p-nitrophenyl alanine mutants). This method can be applied to the development of cancer and antiviral vaccines.[24b]

3. Photocaged amino acids can activate enzymatic activity or protein phosphorylation in living cells, photochemically, in a temporally and spatially defined fashion. [24c, d]
4. The generation immunotoxins, antibody-based imaging agents, antibody−DNA conjugates, and bispecific antibodies as well as carrier−peptide conjugates with enhanced pharmacokinetics or targeted activities.
5. Fluorescent amino acids can be used for in vitro and cellular imaging of protein localization, biomolecular interactions, and conformational changes with the ability to place these small probes at virtually any site in the proteome.[24e]
6. Multidentate metal ion binding amino acids can enhance the protein's redox and hydrolytic activities.[24f]
7. Redox amino acids can be used as mechanistic probes of electron transfer in enzymes, isotopically labeled amino acids as IR probes of protein dynamics, and sterically modified amino acids as probes of ion channel activation. [24g, h]
8. The mapping biomolecular interactions in cells and identifying orphan ligands and receptors can be achieved by the use of photo-cross-linking amino acids.[24i]
9. Unnatural amino acids (uNAAs) can also used as a probe for the structural and functional study of proteins by biophysical techniques such as nuclear magnetic resonance (NMR), electron paramagnetic resonance (EPR), and infrared (IR) spectroscopy.[24j]

Therefore, looking at the vast applications and importance, research on the development of newer unnatural amino acids is growing at a fast space. There are major three focuses on the development of unnatural amino acids which are: (a) Unnatural Amino Acids for Genetic Incorporation; (b) Fluorescent unnatural amino acids for monitoring protein and (c) Unnatural amino acid based scaffold for peptidomimetics. All these three major research efforts toward the development of unnatural amino acids are presented below in brief.

1.3. Unnatural Amino Acids for Genetic Incorporation

Protein engineering with UNAAs to develope an assemble of new protein building blocks finds several applications, like monitoring protein function, in *vivo* via probe labelling, capturing transient protein-protein interaction via crosslinking and many more. However, incorporation of amino acids into proteins through genetic engineering had been restricted to the 20 natural amino acids until the pioneering discovery of the synthesis or semisynthetic methods for introduction of unnatural amino acids into peptide and proteins by Offord and Kaiser and then the development

of methods for site specific incorporation of more unnatural amino acids into proteins by Schultz *et al*. towards expanding the genetic code.

Three Base (Stop Codon) Codon Method: The genetic code consists of 61 codons for designating 20 naturally occurring amino acids and three codons as stop signals. To incorporate non-natural amino acids into the existing genetic code system, it is necessary to generate new codons that are specific to them. In 1989, introduction of non-natural amino acids into specific position of proteins through amber suppression method developed by P.G. Schultz was found to be an important alternative route to expanding protein function.[25, 26] In this method, amber suppressor tRNAs are aminoacylated with desired non-natural amino acids through chemical aminoacylation (i.e. an enzymatic ligation of an aminoacyl-dinucleotide with a tRNA lacking the terminal dinucleotide unit).[27] The resulting aminoacyl-tRNAs (aa-tRNAs) are added to an *in vitro* translation system or *Xenopus* oocytes together with an mRNA or DNA of interest containing an amber stop codon (UAG) at a desired position. The amber codon is suppressed by the added aa-tRNA, resulting in the incorporation of the non-natural amino acid into the directed position of the target protein (**Figure 1.3**).

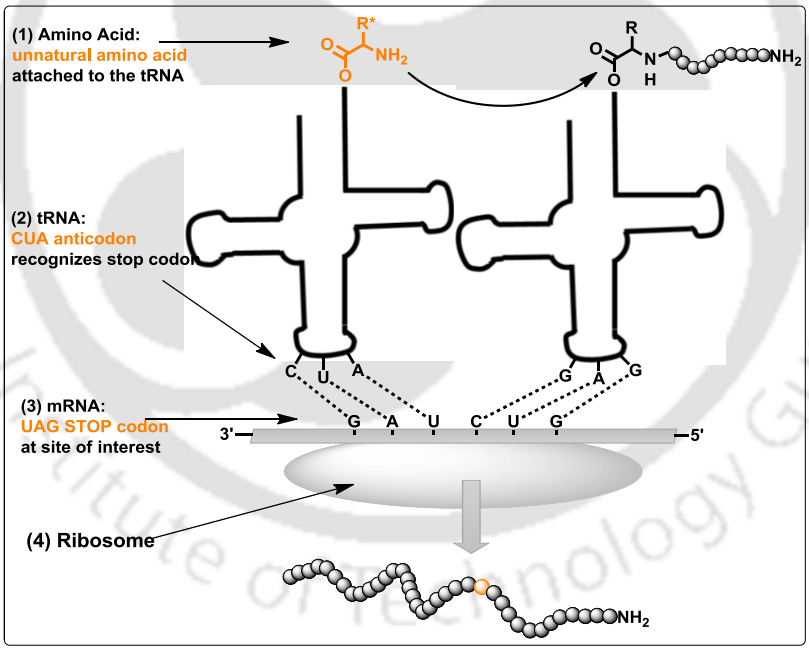

Figure 1.3. Summary of key reagent required for incorporating unnatural amino acids into proteins using nonsense codon suppression.

More than thirty UNAA amino acids have been incorporated selectively and efficiently into proteins in response to nonsense codons up till the 2007 as reported by Peter G. Schultz *at el*., These include metal-binding, photo-reactive, chemically reactive and fluorescent amino acids (**Figure 1.4-1.5**).[1a-b, 24b, 28a-f]

The development of new orthogonal aminoacyl-tRNA synthetase/tRNA pairs by Peter G Schultz *et. al*. has led to the addition of approximately 70 unnatural amino

acids (UAAs) to the genetic codes of *Escherichia coli*, yeast, and mammalian cells until the year of 2010. These UAAs represent a wide range of structures and functions not found in the canonical 20 amino acids and thus provide new opportunities to generate proteins with enhanced or novel properties and probes of protein structure and function.

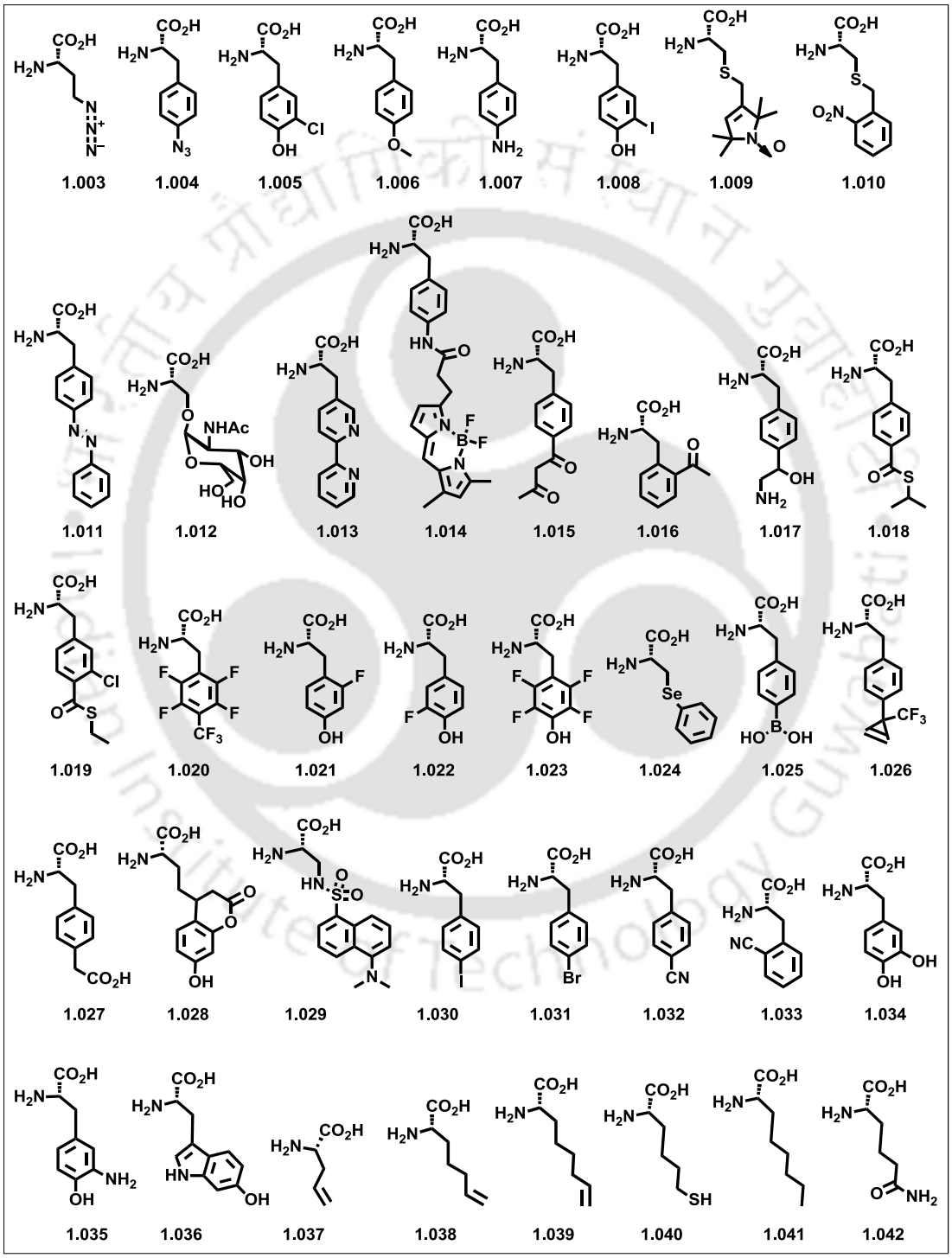

Figure 1.4. Chemical structure of incorporated unnatural amino acids into proteins.

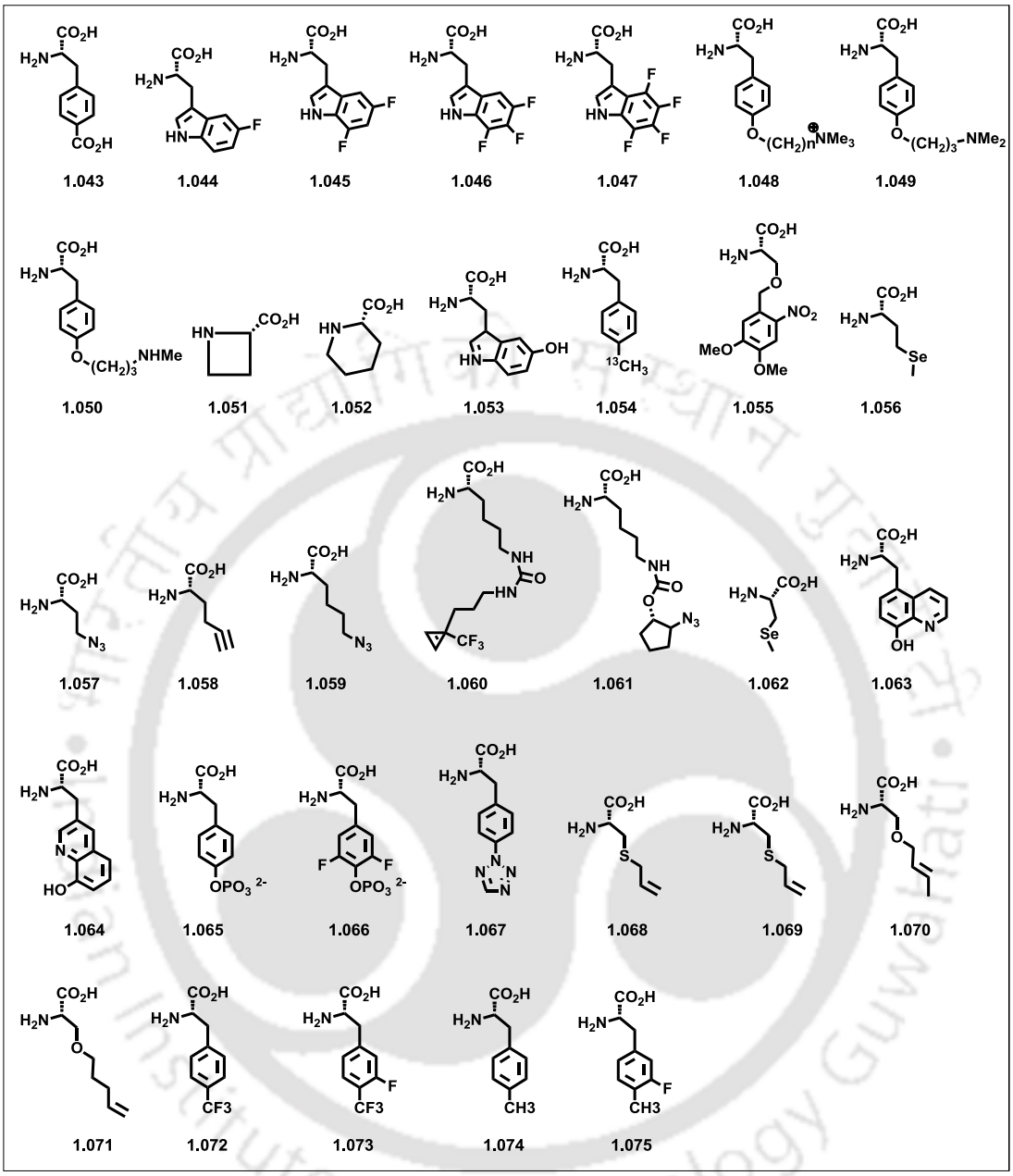

Figure 1.5. Chemical structure of incorporated unnatural amino acids into proteins.

Later on Schultz group published the incorporation of multiple UAAs in the same polypeptide chain, as well as two different UAAs into a single protein utilizing a reassigned nonsense or frameshift codon to encode the UAA, and an orthogonal aminoacyl-tRNA synthetase/tRNA (aaRS/tRNA) pair specific for the UAA which delivers the latter cotranslationally into the target protein. This methodology has been applied to genetically encode a variety of amino acids, such as chemically and photochemically reactive amino acids, biophysical probes, metal-ion chelators and redox-active amino acids.[28] Furthermore, mutually orthogonal aaRS/tRNA pairs capable of suppressing different nonsense/frameshift codons was also developed for

the incorporation of multiple distinct UAAs into one protein in mammalian cells.[13] It has also been shown that the orthogonal PylRS/$tRNA_{UUA}^{Pyl}$ pair was able to efficiently suppress the ochre (TAA) nonsense codon in mammalian cells, and in conjunction with the amber (TAG) suppressing *Ec*TyrRS/$tRNA_{CUA}^{Tyr}$ pair was used to incorporate two different UAAs into distinct sites of the same protein. The utility of this technology was demonstrated by generating full-length anti-HER2 antibody conjugated to auristatin and the fluorophore Alexa Fluor 488 to obtain a defined antibody–drug–fluorophore conjugate.

Four-Base Blank Codon Method: **The** amber codon suppression codon method to incorporate UAAs only allows the replacement with one type of amino acid which is the major drawback. In order to overcome this limitation and to encode multiple distinct UAAs into proteins the use of new "blank" codons has been explored. These blank codons require aaRS and iso-tRNA pairs that can decode these blank codons. One example of an expansion of the genetic code that recognize four- base codons utilize the orthogonal aaRS and iso-tRNA pairs (**Figure 1.6**). This would in theory provide 256 blank quadruplet codons, and with larger codons even more blank codons are theoretically possible.[29] The use of four-base codons is elegantly applied to Ribo-X, which is an evolved orthogonal ribosome developed by J. Chin and coworkers.[29c]

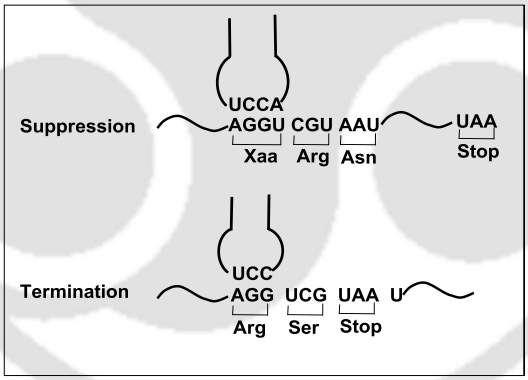

Figure 1.6. Incorporation of UAAs using four base codon method.

In 2010 J. Chin and coworkers were able to incorporate two UAAs into the protein Calmodulin by utilising their evolved ribosomes. Calmodulin fusion protein contained an AGGA codon at position1 and anamber codon at position 40 of calmodulin (**Figure 1.7)**. The full length protein was produced with yields upto 0.5 mg per liter culture.[30]

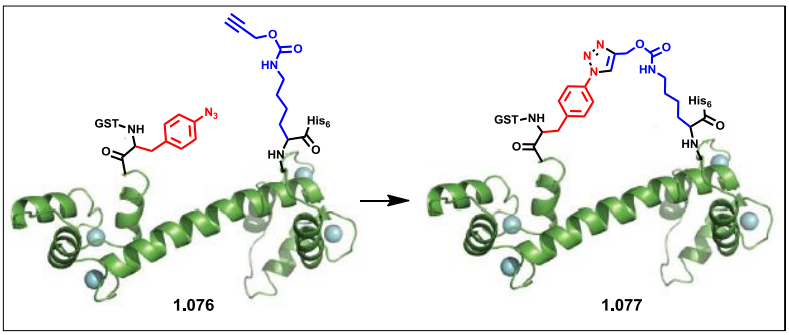

Figure 1.7. Incorporation of two UAAs into the protein Calmodulin.

Five-Base Codon Method: Sisido *et al.* have reported the use of five-base codon–anticodon pairs for the introduction of non-natural amino acids into proteins. Thus, a streptavidin mRNA containing a CGGUA codon at the Tyr54 position and a $tRNA_{UACCG}$ chemically aminoacylated with a non-natural amino acid were added to an *Escherichia coli in vitro* translation system. From the Western blot analysis they reported that the CGGUA codon was decoded by the aminoacyl-tRNA containing the UACCG anticodon. From a HPLC analysis of the tryptic fragment of the translation product they observed the incorporation of nonnatural amino acid corresponding to the CGGUA codon without affecting the reading frame adjacent to the CGGUA codon (**Figure 1.8**).[31]

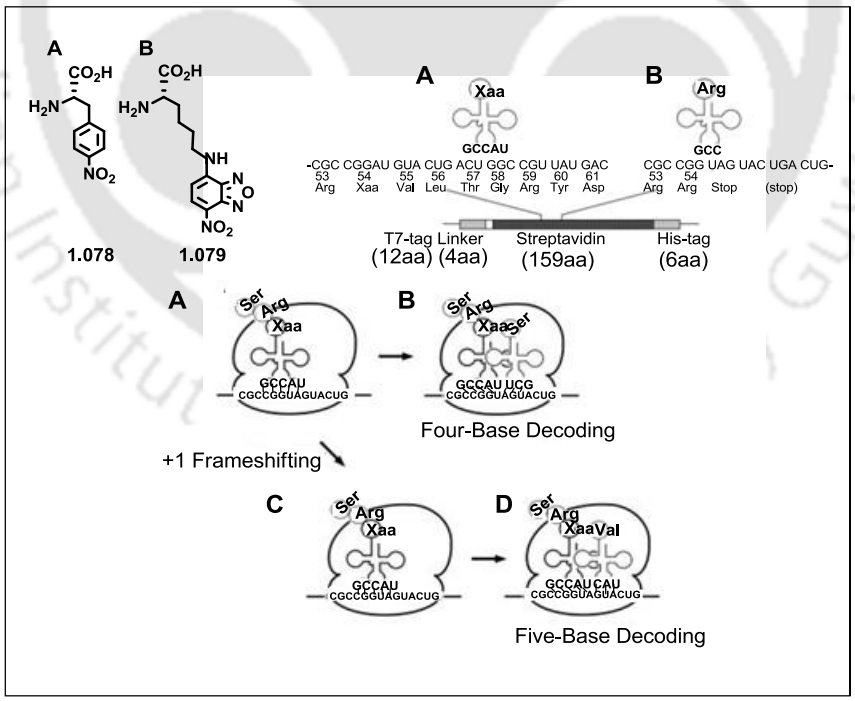

Figure 1.8. Five-base codon–anticodon pairs for the introduction of non-natural amino acids into proteins.

1.4. Fluorescent Unnatural Amino Acids for Protein Monitoring

For visualizing intracellular events and understanding molecular interactions inside a cell such as elucidating protein's structures, functions and dynamics,[4h-i] receptor-ligand binding,[4c-d] monitoring enzyme activity,[4b,h-i] and proteomics,[4m] needs sensing of proteins' microenvironment with the help of highly sensitive fluorescence probe.[4] Though, many of the aspects have been studied either by exploiting intrinsic fluorescence of tryptophan[32] or extrinsic fluorescent probe[33] but these are not free from limitations and thereby not sufficient to fulfill the all research need. Overcoming the shortcomings has led a strong demand for site-specific incorporation of microenvironment sensitive fluorescent unnatural amino acids into a protein.[32-33] Towards this journey, a very few fluorescent amino acids have been synthesized or encoded genetically and site-specifically incorporated into proteins.[34a] Therefore, there is a great demand to develop fluorescent unnatural amino acids (FUAA) or fluorescently labelled UAA for genetic encoding or to generate labelled proteins/peptide for studying conformational or diverse functional realm.[34b] A brief and few literature reported FUAAs are presented in this section.

1.4.1. Fluorescent Unnatural Amino Acids: Tryptophan/Tyrosine Mimics

Toward the development of fluorescent unnatural amino acids, mimicking the size and polarity of tryptophan is a logical approach to minimize perturbation upon incorporation of a modified fluorescent amino acids into protein. Therefore, several such amino acids have been developed and incorporated into protein. Some recent examples of such structures are shown in **Figure 1.9** and include the blue-emitting azulene (azuAla, **1.080**) reported by Moroder, Luis *et al.;*[35] Their study on bioactivity of a heptagastrin analog containing the enantiomerically pure β-(1-azulenyl)-L-alanine suggested that the planar aromatic azulene moiety may indeed mimic the tryptophan side chain to some extent, and the spectral properties of the azulene moiety makes L-Ala of potential value as a UV and fluorescence probe in synthetic peptides. The 5-hydroxytryptophan (5OHTrp, **1.081**)[36] and 7-azatryptophan (7azaTrp, **1.082**)[36, 37] have been synthesised and their spectroscopic properties have been conveniently compared with tryptophan and other tryptophan mimics.[38] It was observed that Both 5OHTrp (**1.081**) and 7azaTrp (**1.082**) displayed a 20 nm bathochromic shift of their absorption maximum relative to tryptophan, facilitating selective excitation even in presence of other tryptophane in a protein.[39] Two other examples of tryptophane mimic includes, benzofuranylalanine (BfAla, **1.083**)[40] and benzothiophenyl (BtAla, **1.084**).[41] These amino acids only differ from tryptophan in their ring heteroatom.[42] Tirrell and co-workers have incorporated BtAla (**1.084**) and other tryptophan mimics to modify the spectral properties of fluorescent proteins.[43, 44, 45].

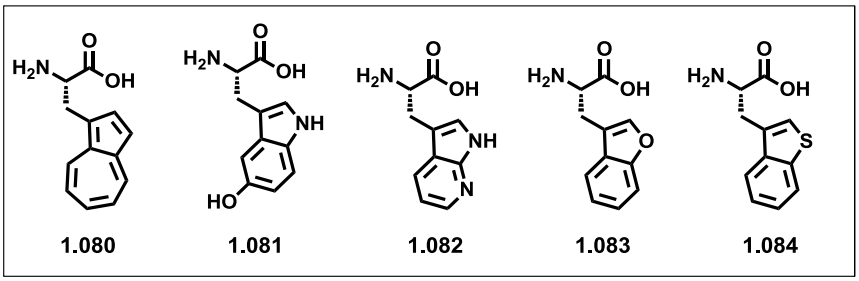

Figure 1.9. Tryptophan mimetic fluorescent unnatural amino acids.

Recently, Sidney M. Hecht reported the synthesis of azaindole tryptophan analogue to overcome the limitations of 4-azatryptophan (**Figure 1.10**). The tricyclic azaindole tryptophan's are more hydrophobic which have larger Stokes shifts (~150−160 nm) and exhibit significantly higher molar absorptivities than that of tryptophan. They incorporated the 1H-pyrrolo[3,2-c]isoquinoline molecule that consists of a benzene ring fused to a bicyclic 4-azaindole ring into dihydrofolate reductase (DHFR) protein with minimal disruption of function. Their study reflected that this tryptophan analogue could be selectively monitored in the presence of five Trp residues in that DHFR.[46]

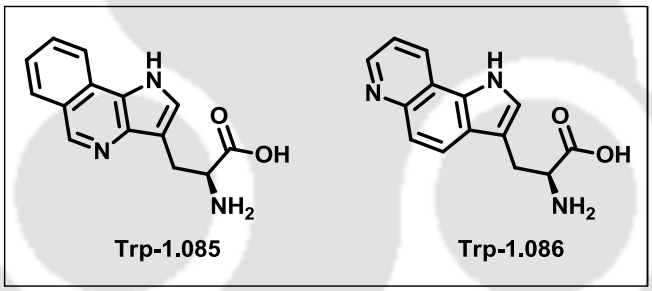

Figure 1.10. Structures of azaindole tryptophan derivative of unnatural amino acid**.**

They also have synthesised cyanotryptophans and incorporated into dihydrofolate reductase (DHFR) protein into two different positions of DHFR. The 6-CNTrp (**1.087**) was found to form an efficient Forster resonance energy transfer (FRET) pair with L-(7-hydroxycoumarin-4-yl)ethylglycine (HCO) at position 17. Analogue **1.087** was also introduced into a single position of the Klenow fragment of polymerase I and was found to transfer energy to DNA substrates containing an acceptor fluorophore, a modified nucleobase. Thus, they demonstrated that a non-natural amino acid could be used as a FRET partner for studying protein−nucleic acid interactions. They also demonstrated that 6-CNTrp (**1.087**) could be utilized as a fluorescence donor for the study of protein conformational events.[47]

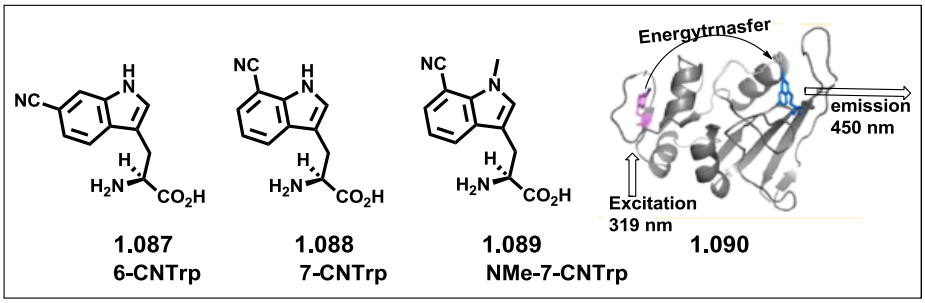

Figure 1.11. Incorporation of cyanotryptophane analogue into dihydrofolate reductase (DHFR) protein

Another approach to generate fluorescent unnatural amino acid is to augment the π-conjugation in tyrosine/phenylalanine to generate structurally novel fluorescent UAAs. These UAAs showed improved photophysical properties than the corresponding tyrosine/phenylalanine amino acids. Thus, Meng-Lin Tsao *et al*. have incorporated the 2-naphthol analogue of tyrosine, 2-amino-3-(6-hydroxy-2-naphthyl)propanoic acid (NpOH) (**1.091**) genetically into proteins in *Escherichia coli*. They also demonstrated that the 2-naphthol side chain in NpOH can serve as the target for site specific protein modifications through the selective azo coupling reaction under neutral pH using diazonium reagents with an electron donating substituent (**Figure 1.12**). This findings provide an alternative way for biocompatible chemical transformation of protein.[48]

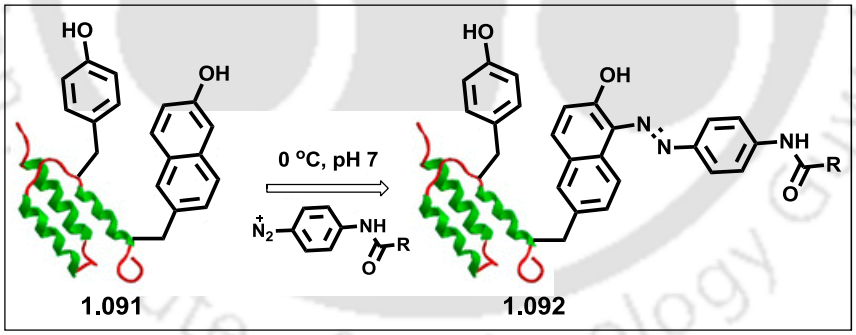

Figure 1.12. Incorporation of 2-naphthol analogue of tyrosine into *Escherichia coli* proteins.

Recently, Sidney M. Hecht described the synthesis and photophysical characterization of four positional isomers of biphenyl-phenylalanine (**Figure 1.13**), all of which were found to exhibit potentially useful fluorescent properties. All four phenylalanine derivatives were incorporated into multiple positions of *ec*DHFR. The protein *ec*DHFR modified with those amino acids at position 16 was found to consume NADPH at rates up to about twice the rate measured for wild type. Their results indicated that biphenyl-phenylalanines can be incorporated into sterically

unencumbered positions in DHFR with minimal impact on the structure or function of the enzyme.[49]

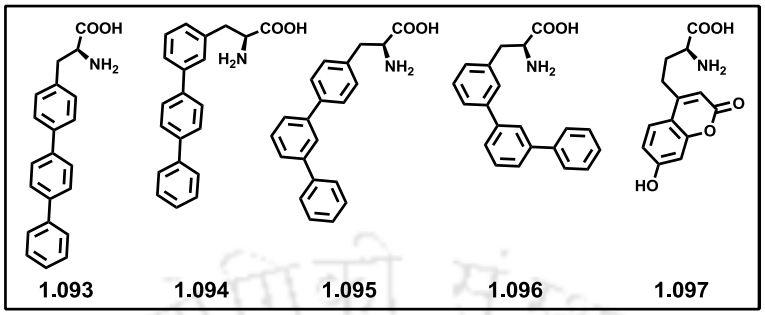

Figure 1.13. Structure of biphenyl-phenylalanines and coumaryl derivative of UAAs.

Two fluorescent amino acids, including the novel fluorescent species 4-biphenyl-l-phenylalanine (**1.093**), and l-(7-hydroxycoumarin-4-yl)ethylglycine (**1.097**) have been incorporated at positions 17 and 115, respectively, of dihydrofolate reductase (DHFR) to enable a study of conformational changes associated with inhibitor binding via Förster resonance energy transfer (FRET). Irradiation of the modified DHFRs at 280 nm (excitation of **1.093)** led to an energy transfer to **1.097** and a FRET emission by **1.097** at 450 nm. These findings demonstrate that amino acids containing small fluorophores can be introduced into DHFR with minimal disruption of function and in a fashion that enables sensitive monitoring of changes in DHFR conformation.[49b]

Recently, Wang *et al.*; have synthesised styryl conjugated tyrosine analogues as a new class of fluorescent UAAs with excellent optical and tunability in emission properties (**Figure 1.14**). These novel fluorescent UAAs consist of stilbene and meta-phenylene vinylene units as fluorophores and cover the emission color from blue to near IR. They were able to show stimuli responsive optical properties with these tyrosine derivatives which showed distinct red, green and blue (RGB) emission spectra simply by controlling the solution pH. They also have utilised these UAAs in solid-phase peptide synthesis (SPPS) to synthesize a cell-penetrating peptide and demonstrated the use of these fluorescent peptides for cell imaging.[50]

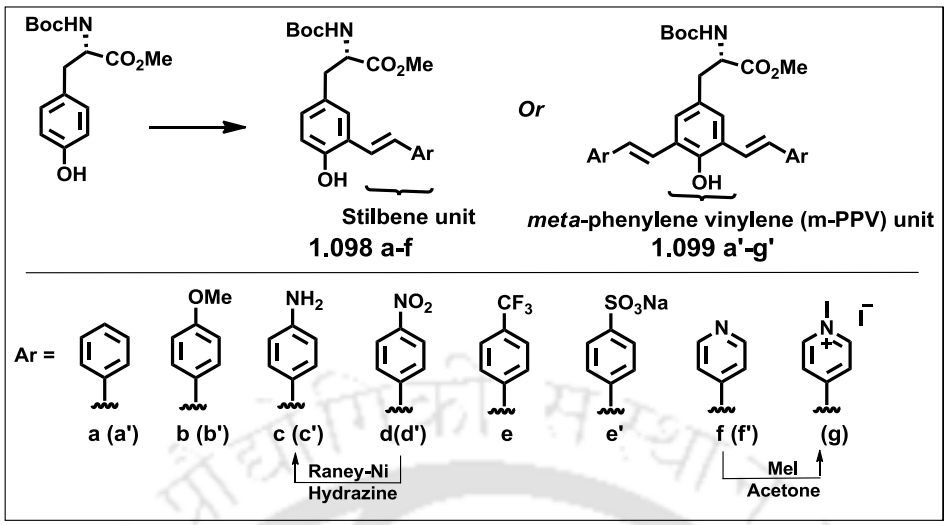

Figure 1.14. Fluorescent UAAs derived from tyrosine/phenylalanine by extending the π-conjugation of aromatic side chain.

Very recently, Sidney M. Hecht et al. have shown the ribosome-mediated incorporation of dipeptides and dipeptide analogues (**1.100**-**1.103**) into proteins in vitro.[51a] They also have synthesised oxazole (**1.103**) and acridon-2-ylalanine (**1.104**) and demonstrated ribosome-mediated incorporation into positions 39 and 66 of GFP, respectively. These two fluorescent amino acids (**1.103**-**1.104**) were found to form an efficient Förster resonance energy transfer (FRET) pair and demonstrated the potential utility of the fluorophores as reporter groups (FRET probe) to monitor protein conformational changes and molecular interactions. [51b]

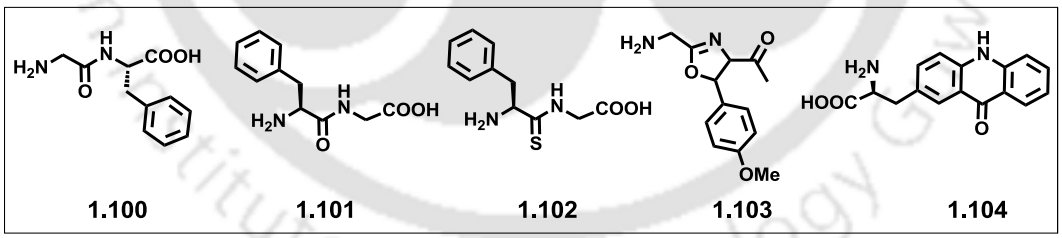

Figure 1.15. Structure of some dipeptide, oxazole (**1.103**) and Acridon-2-ylalanine (**1.104**) derivative which have incorporated into proteins.

1.4.2. Fluorescent Unnatural Amino Acids Carrying Polyaromatic Side Chain

Unnatural amino acids with polyaromatic side chain are useful fluorescent probe in sensing protein's microenvironment that can be widely used for protein engineering. Site specific incorporation of such type of amino acids into proteins is thus important for monitoring the structures, dynamics, and inter-biomolecular interactions. Because of polyaromatic side chain the amino acids are highly electron rich species and thus can act as electron donor for electron transfer in protein.

Toward this end few of such amino acids have been incorporated genetically into proteins which reflected that the efficiency of incorporation was dependent on side chain group. As for an example, *p*-benzoyl phenylalanine has been successfully incorporated into T4 lysozyme and cytochrome*b*2 while amino acid with oxyltetramethylpyrroline was unsuccessful. In 1999, M. Sisido *et al*., have efficiently incorporated various non-natural amino acids with aromatic side chain (**Figure 1.16**). The targeted amino acids were incorporated at the Tyr83 site of streptavidin by using a four-base CGGG-CCCG codon-anticodon pair. From their study of incorporation efficiency via Western Blot techniques revealed that the amino acids with large side groups such as pyrene, dinitrobenzene, and anthraquinone could be incorporated in the rabbit system more efficiently than in the *E. coli* system. This study sugests that the molecular recognition of the rabbit ribosomal A-site is less tight than that of *E. coli* and the former system is more appropriate for preparing proteins incorporated with non-natural amino acids carrying relatively large side groups.[53]

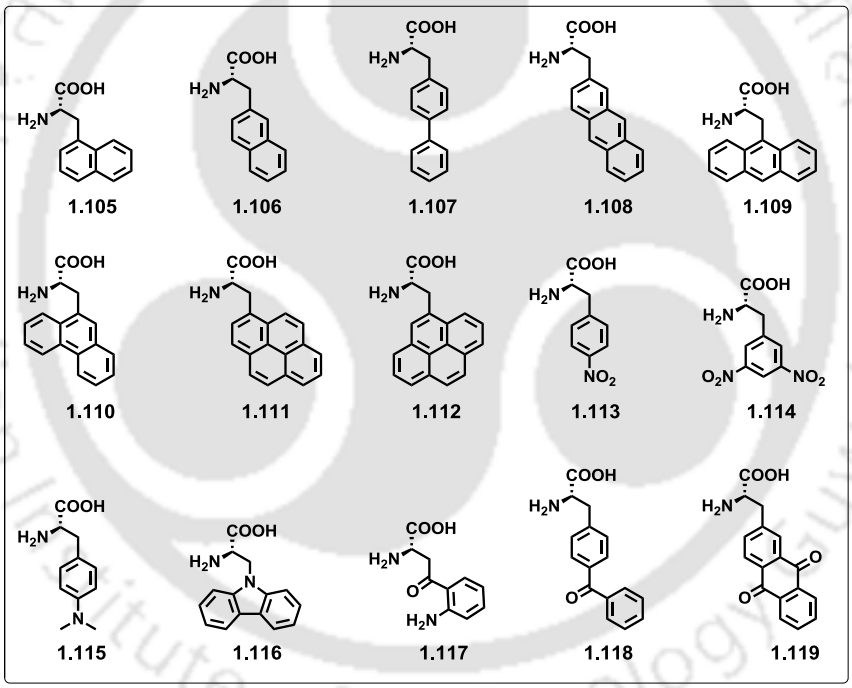

Figure 1.16. Structure of various non-natural amino acids with aromatic side chain.

1.4.3. Coumaryl Fluorescent Nnnatural Amino Acids

The coumarine derivatives are known for their fascinating fluorescence property such as relatively high quantum yields, low bleaching and moderate stability.[54] Furthermore the coumarine labelled amino acids can easily be synthesized from protected aspertic (Asp) and glutamic (Glu) acids as a chiral starting material. These two chiral amino acids can easily be converted into side chain β-ketoester which would undergo condensation with phenols. Coumarines also can easily be synthesised with other procedures such as Pechmann, Perkin, Knoevenagel, Reformatsky and

Wittig reaction. Among these procedures von Pechmann reaction is one of the easiest and direct methods for the synthesis of coumarin derivative.[55]

Coumarin labelled unnatural amino acid is compact in size leading to less or no perturbation if incorporated in a protein and is exhibited highly microenvironment sensitive fluorescence emission property. Moreover, coumarins consists of the largest class of laser dyes for the "blue-green" region[55] and are highly sensitive. These are the most commercially acceptable categories of fluorescent derivatives with the advantages of an extended spectral range, high emission quantum yield, photostability, and good solubility in many solvents. Furthermore, coumaryl amino acid can easily be incorporated into peptide by solid phase peptide synthesis (SPPS) or protein genetically. Thus these amino acids could widely be utilised for biological study in protein system.

In 2004, C. Garbay *et al*., have developed direct synthetic method to prepared optically pure coumarine labelled amino acids from inexpensive chiral materials (**Figure 1.17**).[56] They also have investigated the cellular localization of coumaryl amino acid labeled peptides through confocal fluorescence microscopy.

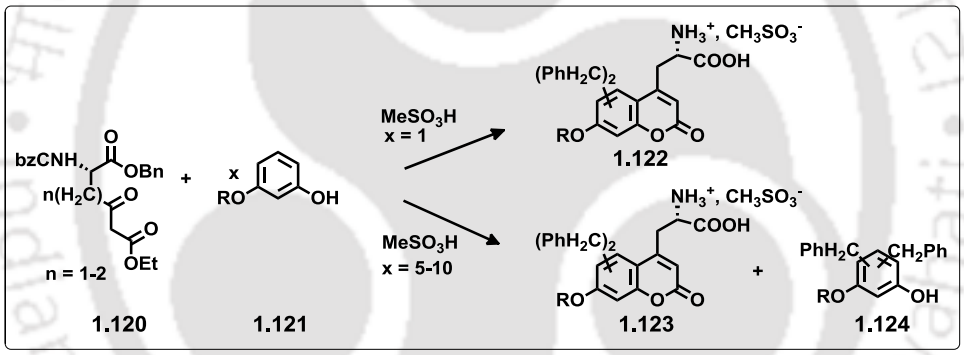

Figure 1.17. General synthesis of coumaryl amino acids.

An optimized protocol for the preparation of the fluorescent amino acid l-(7-hydroxycoumarin-4-yl) ethylglycine on the multi-gram scale has been reported by Martin *et al*., Using standard Fmoc SPPS approaches, the coumaryl amino acid has been incorporated by them into a series of model peptides based upon the Leu-enkephalin (5-mer) and the HIV-Tat (13-mer) peptides and studied the cell internalization behavior.[57a]

Coumarin-labeled lysines are of considerable general interest for the design and synthesis of fluorogenic triple-helical substrates for the analysis of matrix metalloproteinase family members.[57b, 58] Thus, N^{ε}-coumarin-labeled-N^{α}-Fmoc lysines allow successful labeling of peptide substrates by solid phase peptide synthesis for an extracellular matrix metalloprotease and present a powerful tool for proteolysis monitoring.[58]

Katritzky *et al*., have reported[59a, b] straightforward syntheses of coumarin-labeled amino acids and dipeptides which afford enantiomerically pure fluorescent building blocks suitable for solid phase peptide synthesis (SPPS). Thus a two-step synthetic

route provides N^{α}- and N^{ε}-coumarin labeled Cbz- and Fmoc-L-lysines **1.125–1.128** and number of other amino acids **1.129** (**Figure 1.18**) in excellent yields utilizing benzotriazole activated fluorogenic agents as coupling reagents.

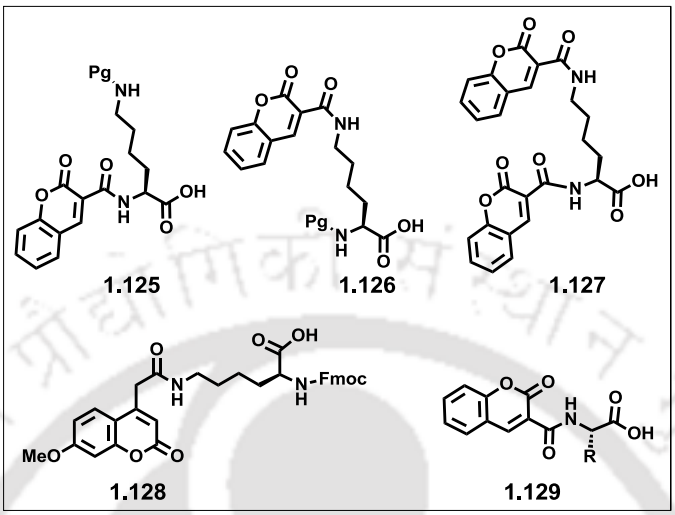

Figure 1.18. Some example of coumarin-labeled amino acids.

They also designed and synthesized a protected monosaccharide containing Fmoc-L-lysine scaffold based on fluorescent amino acid building blocks **1.130–1.133** (**Figure 1.19**).[59c-d] After deprotection, **1.130–1.133** provide water soluble organic fluorophores **1.134** which could be useful for peptide labeling at the C-terminus in inverse solid phase peptide synthesis (SPPS).

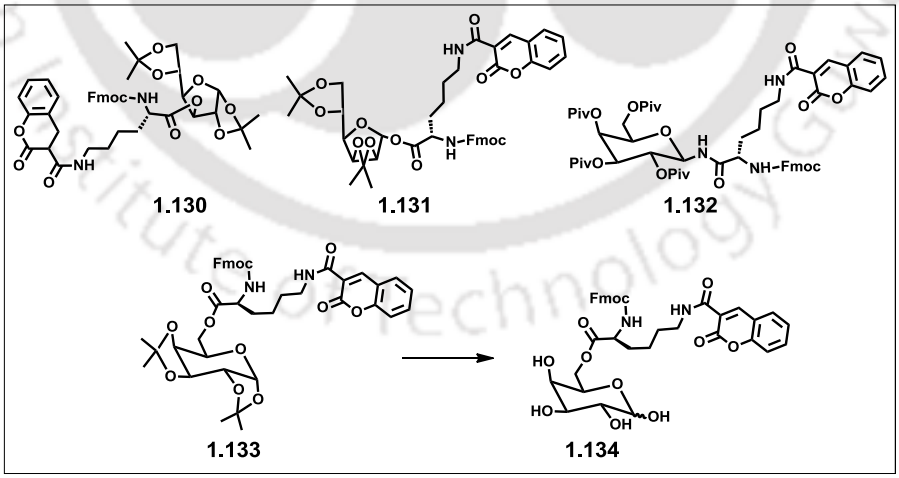

Figure 1.19. Monosaccharide containing Fmoc-L-lysine scaffold based on fluorescent amino acid building blocks.

Very recently, Petersson *et al*., have utilized coumaryl amino acid as a fluorescent signaling unit to study the kinetics of protease enzymes. Thus, in their design of "turn-on" fluorescent protease substrates, a protein was labeled with a thioamide quencher

which can paired with compact coumaryl amino acid. In the native form a weak or no fluorescence from the comaryl amino acid would be observed due to quenching by thioamide, however upon exposer to proteases the thioamide would be free from cumaryl moiety leading to turn-on" fluorescence signal from cumaryl amino acid (**Figure 1.20**). Utilising this strategy, they have tested a variety of serine-, cysteine-, carboxyl-, and metallo-proteases, including trypsin, chymotrypsin, pepsin, thermolysin, papain, and calpain. This technique can be used for real time monitoring of protease activity in crude preparations of virtually any protease.[60]

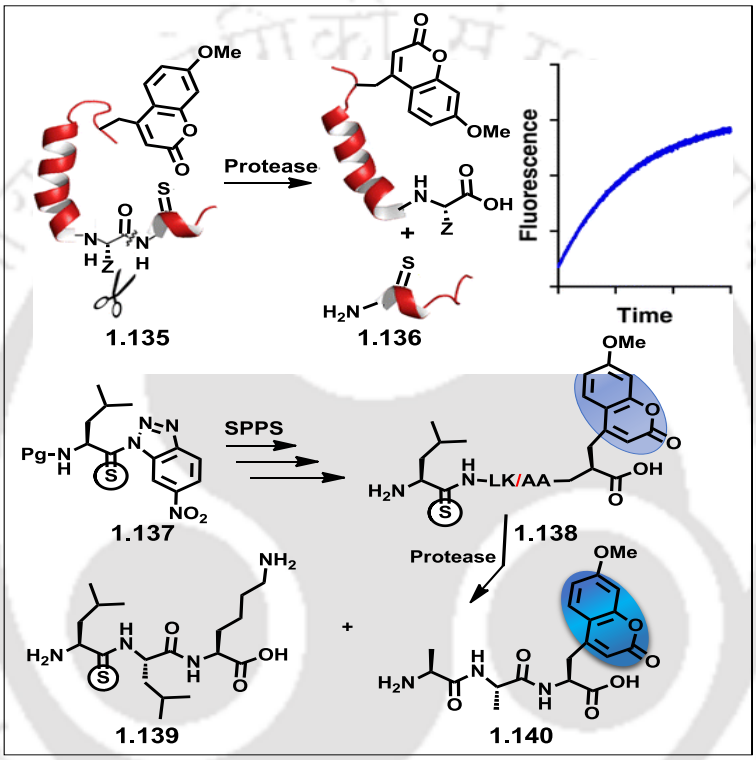

Figure 1.20. Fluorescence turn-on strategy to monitor protease activity.

1.4.4. Fluorescent Unnatural Amino Acids: Microenvironment Sensitivity

The effect of polarity of the solvent on the emission properties of fluorophore is called solvatochroism and the fluorophores are called solvatochromic fluorophore. This is nicely explained in the Jabolonski diagram (**Figure 1.21**). The main reason is that the polarities of ground (S^0) and excited singlet state (S^1) of a fluorophore become different while changing solvent polarities leading to a stabilization of ground and exited state differently. The solvent relaxation causes lowering of energy of the exited singlet state while concomitantly destabilizing the ground state leading to a decreased energy gap between the two states.[61]

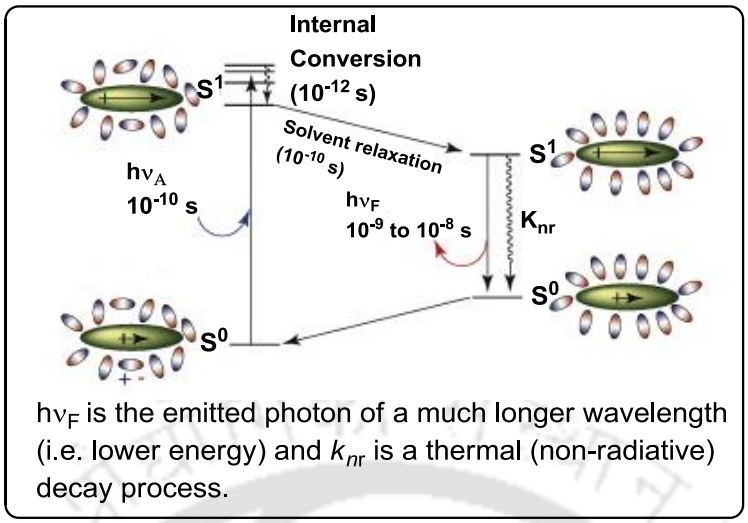

Figure 1.21. Schematic presentation of solvatochroism explained by Jabolonski diagram.

Thus, solvatochromic probes have been recognised as ideal probes to study the polarity of microenvironments within a biomacromolecule and molecular gathering. Therefore, solvatochromic fluorophores are important for investigation of protein folding and dynamics.

An α-amino acid, 6-(2-dimethylaminonaphthoyl) alanine (DANA) containing highly environment-sensitive (solvatochromic) fluorophore 6-propionyl-2-(dimethylamino)naphthalene (PRODAN, **Figure 1.22**) was synthesized in 2002.[62] This amino acid has been utilised in peptides for monitoring peptide–protein and protein–protein interactions, where binding events often bring substrates into contact with more hydrophobic surfaces. An early study with DANA illustrated its potential by reporting the binding of a phosphoserine-containing 14-3-3-binding peptide to the target 14-3-3ζ protein.[63]

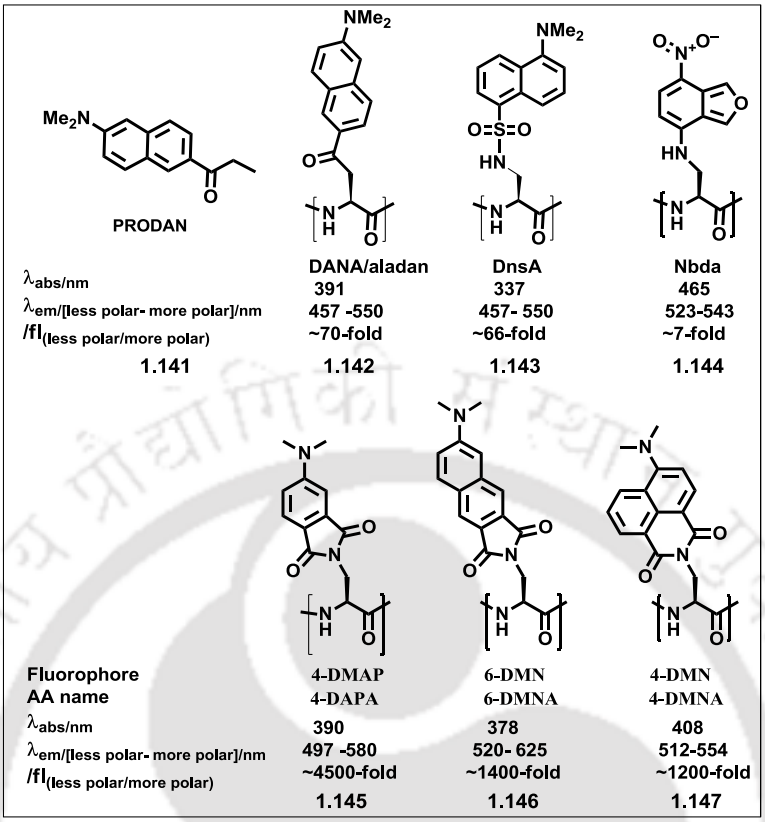

Figure 1.22. Some environment-sensitive fluorophores and their solvachromatic properties.

Aladan (**1.142)** is exceptionally sensitive to the polarity of its surroundings and can be incorporated site-selectively at buried and exposed sites, in both soluble and membrane proteins. Steady-state and time-resolved fluorescence measurements of Aladan residues at different buried and exposed sites in the B1 domain of protein G suggest that its interior is polar and heterogeneous (**Figure 1.22**). Cohen *et al*. employed the amber suppression technique with a chemically charged tRNA bearing the DANA amino acid ("Aladan"), to probe electrostatic character of a protein at multiple sites.[64] Incorporating Aladan into selected sites of Kir2.1 and Shaker potassium channels, it was concluded that Aladan was compatible with the cellular biomachinery. Moreover, substitutions in buried, aqueous, or lipid environments also allowed proper folding and functioning of the protein. As a proof of utility of Aladan to probe protein electrostatics, they incorporated an Fmoc variant of Aladan into the thermally stable IgG binding domain GB1 (~6 kDa) by SPPS. By observing steady-state and time-resolved fluorescence data of GB1 mutants with exposed or buried Aladan, it was concluded that the interior of GB1 is polar and electrostatically heterogeneous. The ability to selectively position Aladan within specified regions of a protein makes it a valuable amino acid for gaining insight into protein electrostatics.

Latter on to improve on the concept of environment-sensitive fluorescent amino acid building blocks, fluorophores based on the dimethylaminophthalimide and dimethylaminonaphthalimide systems were developed, with the goal of increasing the fluorescence changes upon binding in target systems.[65, 66] Thus, the fuluorescent amino acid, 4-(*N*,*N*-dimethylamino)-phthalimide propionic acid (4-DAPA) containing 4-(*N*,*N*-dimethylamino)-phthalimide (4-DMAP, **1.145, Figure 1.22)** was synthesised by Impariali et al. and was found to have the advantage of being a closer size-mimic of tyrosine. Professor Imperiali have investigated that in comparison with DANA (aladan), 4-DAPA gave an approximately six fold enhancement in fluorescence emission upon binding with 14-3-3ζ protein when placed at the phosphoSer(−2) Tyr position in the 14-3-3-binding peptide, with a blue shift of 39 nm in the emission maximum of 570 nm.[67]

Peptide loading onto class II MHC proteins is regulated in antigen-presenting cells. To visualize these processes, Imperiali et al. have developed a series of novel fluorogenic probes containing the environment-sensitive amino acids 6-*N*,*N*-dimethylamino-2-3-naphthalimidoalanine (6-DMNA, **1.146, Figure 1.22**) and 4-*N*,*N*-dimethylaminophthalimidoalanine (4-DAPA, **Figure 1.22**). Upon binding to class II MHC proteins these fluorophores show large changes in emission spectra, quantum yield and fluorescence lifetime. Peptides containing these fluorescent amino acids were found to bind specifically to class II MHC proteins on antigen-presenting cells and can be used to follow peptide binding *in vivo*. Using these probes they have tracked a developmentally regulated cell-surface peptide-binding activity in primary human monocyte-derived dendritic cells.[68] These phthalimide- and naphthalimide-based fluorescence amino acids have also been incorporated into peptides recognizing PDZ and SH2 domains illustrating their versatility in diverse applications.[69a-d]

Impariali *et al*. have also prepared the same series of peptide with the amino acids 4-DMAP, 6-DMN, BADAN,[70] dansyl and NBD (**Figure 1.23**). The environment-sensitive amino acid building blocks based on the dansyl fluorophore has also been exploited for probing protein interactions and protein unfolding.[71] The microenvironment sensitivity of these fluorophores makes them ideal tools for studying structural dynamics in proteins. The Schultz et al. have incorporated dansylalanine into the human superoxide dismutase (hSOD) protein in yeast by using an evolved tRNA/leucyl-tRNA-synthetase pair for monitor protein unfolding phenomena in presence of guanidinium hydrochloride.[72] More they have also genetically incorporated a PRODAN amino acid into the same protein to study conformational changes.[73] The dansylalanine was also incorporated into the voltage sensitive domain (VSD) of the *Ciona intestinalis* voltage-sensitive phosphatase in HCN-A94 cells by Wang *et al*. They found that the dansylalanine was able to report, the conformational change of this domain in response to membrane polarization through environment-sensitive fluorescence emission.[74]

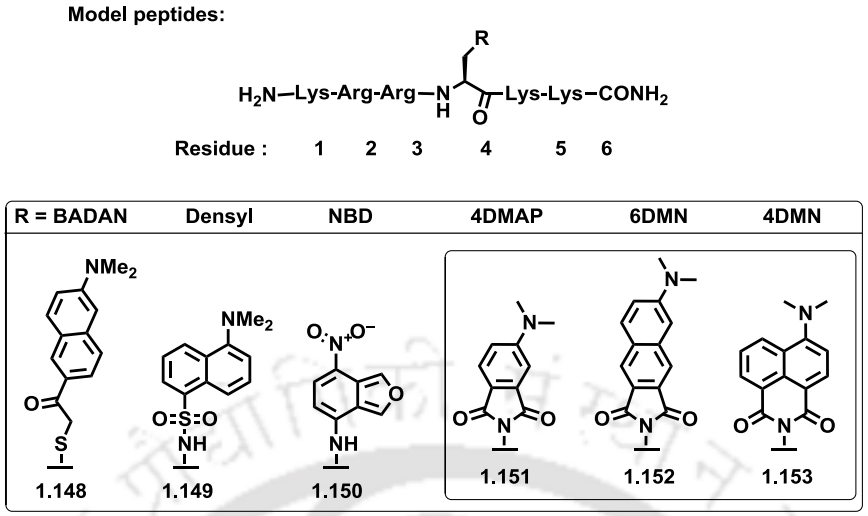

Figure 1.23. Solvatochromic amino acids incorporated model peptide series.

Another polarity-sensitive fluorescent unnatural amino acids L-Anap has been reported and genetically encoded by Wang *et. al*., to image protein modifications and activities in mammalian cells (**Figure 1.24**).[75]

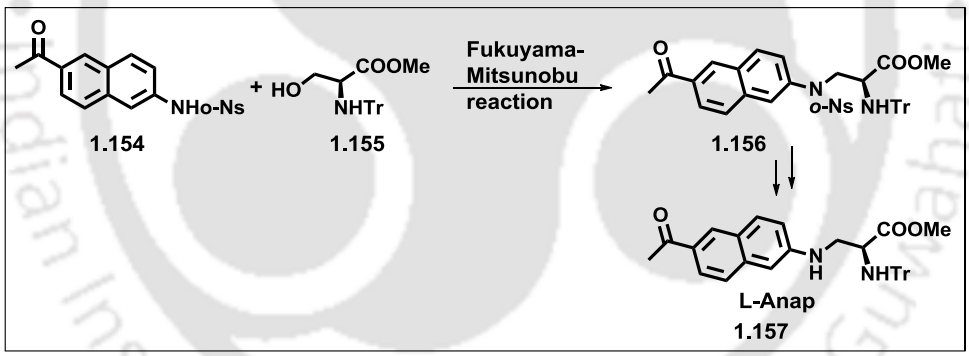

Figure 1.24. Polarity-sensitive fluorescent unnatural amino acids L-Anap.

M. Sisido *et al*., have developed a modern technology for for screening fluorescent peptides containing multiply labeled fluorescent amino acids based on their protein binding specificity. Thus, they synthesized 8-mer peptides modified with a fluorescent several fluorescent unnatural amino acid (**Figure 1.25**). The peptides were mixed with an anti-FLAG antibody and an EGFR before incubation. Then the protein-binding peptides were recovered by gel filtration chromatography. Utilizing a combination of fluorescence analysis with gel filtration method they were able to quantify the binding peptides simultaneously.[53]

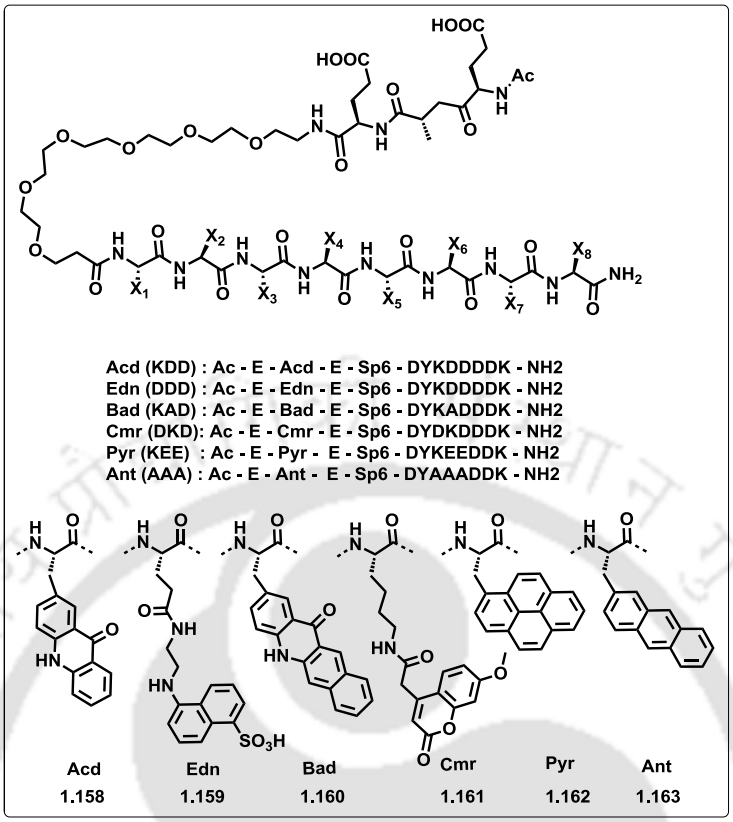

Figure 1.25. Structure of peptides modified with fluorescent amino acids.

1.4.5. Fluorescent Unnatural Amino Acid: Sensing Metal Ion

In 1996, B. Imperiali *et al*., synthesized and characterized three new amino acids **1.164, 1.165 and 1.166** which showed good fluorescence property, metal-coordination property and fluorescence quenching properties respectively (**Figure 1.26**). Mainly they had focused to the development of chemosensor for metal ion in aqueous and non-aqueous medium. They had synthesized three amino acid based peptide building blocks via solid phase synthesis (SPPS) that showed metal-dependent photoinduced electron transfer (PET). Fluorescence quenching was observed upon titration with Zn^{+2} and Co^{+2}.[76]

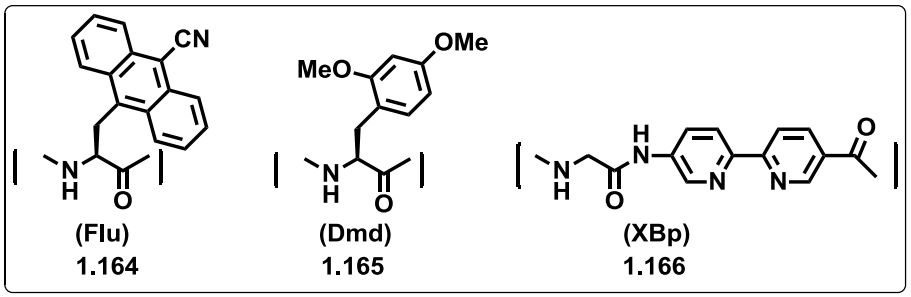

Figure 1.26: Structure of donor/acceptor fluorescent unnatural amino acids.

In presence of complexing metal ion the peptide motif undergoes conformational change which was monitored by exploiting PET leading to a change in fluorescence properties of peptides (**Figure 1.27**).[77a-d] The sensor design is schematically shown in **Table 1**.

Table 1. Sequence of peptide building block modified with chelating ligand

Peptide	Sequences
01	AcFluXBpGlyGlyGlyXBpDmdGlyNH2
02	AcFluXBpGlyGlyGlyXBpDmdThrArgNH2
03	AcArgFluXBpGlySerSerXBpDmdThrArgNH2

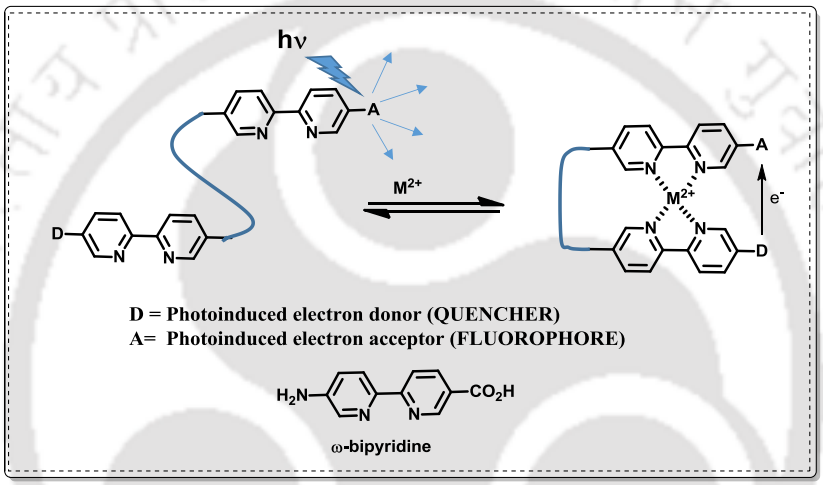

Figure 1.27 Schematic presentation of photon electron transfer**.**

Imperiali *et al*. have reported the syntheses of (*S*)-2-amino-*N*R-9-fluorenylmethoxycarbonyl-3-(oxine-2-yl)propionic acid (Fmoc-2Oxn-OH, **1.167**) and (*S*)-2-amino-*N*R-9-fluorenylmethoxycarbonyl-3-(oxine-5-yl)propionic acid (Fmoc-5Oxn-OH, **1.168**). They have also incorporated these amino acids in short peptides which were found to capable of reporting sub-micromolar levels of Zn(II).[78]

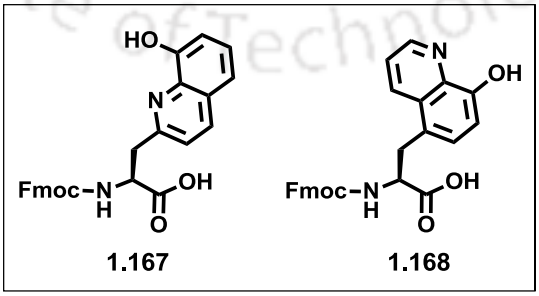

Figure 1.28. Example Zn(II) metal ion sensor FUAAs

Several dansyl alanine amino acids have been designed by Lee *et al*. for detecting concentrations of Hg^{2+} that approach toxic levels (**Figure 1.29**).[79]

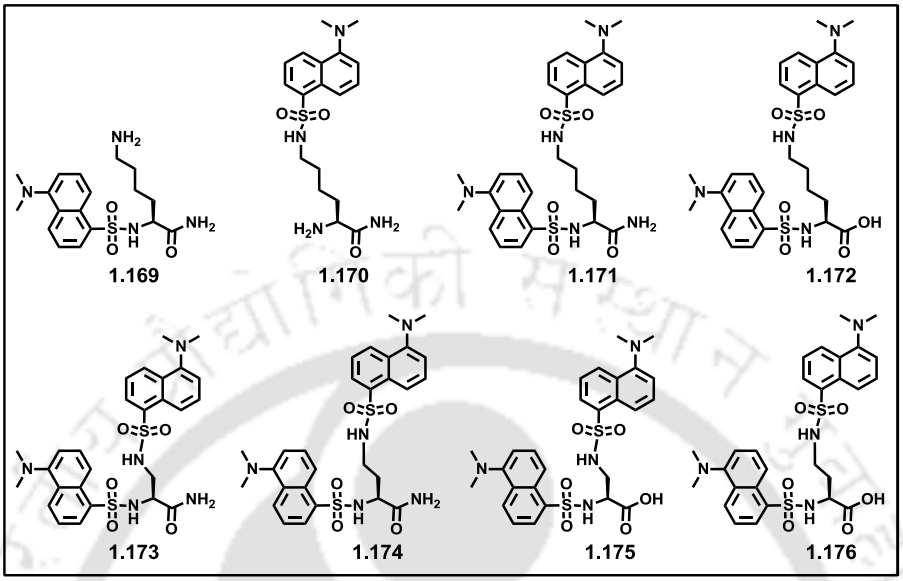

Figure 1.29. Dansyl alanine amino acids derivatives utilized for Hg^{2+} detection.

1.5. Unnatural Amino Acids as Small Molecule Scaffold for Peptidomimetics

From the above discussion on unnatural amino acids it is clear that a lots of efforts have been devoted toward expansion of genetic code, engineering protein, sensing biological events or metal ions and monitoring protein structures, functions, dynamics and interbiomolecular interactions. Now, we will discuss few selected examples in brief toward the design and synthesis of unnatural amino acids for peptidomimetics. Thus, introduction of conformationally constrained non-peptide isosteres or small molecule scaffold into peptide backbones in order to achieve desirable secondary structures along with pharmacologically viable peptide-based drug candidates of enhanced metabolic stability is of great interest in recent time.[22] A great deal of effort has therefore focused on the design and synthesis of small constrained mimetics of protein's secondary structures to provide a better understanding of the molecular basis of peptide and protein interactions in addition to afford potent and selective therapeutic agents. Now a day, a myriad of potential unnatural amino acids with rigid geometry provides a plethora of opportunities for mimicking the protein's secondary structures. Among the various secondary structures, β-turns and β-sheet are important targets for mimicry. Considerable efforts have thus been invested in delineating the impact of appended molecular scaffolds in one hand and nucleating turn and sheet mimics on the other hand, on the conformational preferences of proteins and peptides in solution.[23a-c] Despite an

exponential growth on the development of constrained non-peptidic molecular scaffolds as peptidomimetics, very few peptide-based drugs have been developed, necessitating an overhaul in the existing design principles. Newer concepts, chemistry and protocols are emerging to create unnatural structural entities with properties of inducing desirable structure and pharmacokinetics. The following sub sections will describe few selected examples of constrained molecular scaffold designed mainly for inducing peptide β -sheet or β -turn structures.[23d-f]

1.5.1. Proline Analogue as β-Turns Inducer

Among the all-natural amino acids only proline itself can be induced turn like structure. In 2003, Chakraborty *et al*., have synthesized *E*-vinylogous prolines **1.177** (VPro1) and **1.178** (VPro2) that could act as a nucleators of the *cis*-amide bond and induce the peptide structures to be adopted a type VI β-turns (**Figure 1.30**).[55] They have shown in their designed peptide that placing the nonpolar residue in both side of the proline the peptide adopted well-defined β-turn structure by forming 12 membered intramolecular hydrogen bond.[80]

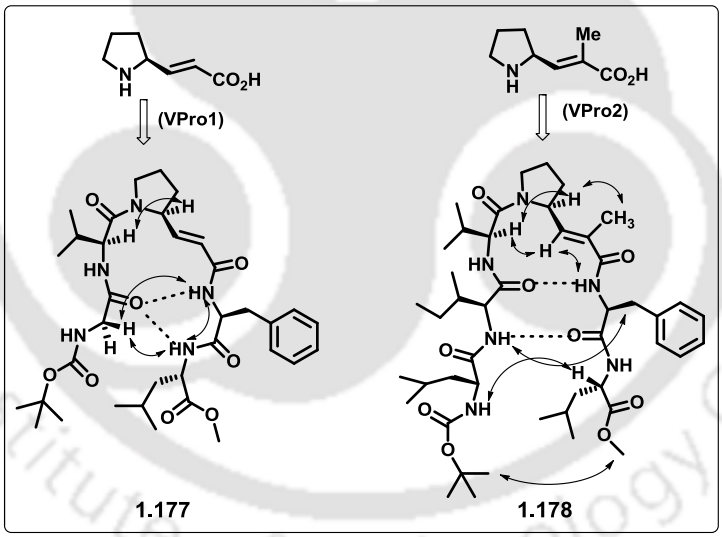

Figure 1.30. Schematic representation of the proposed structures of the *E*-vinylogous proline containing peptides.

1.5.2. Sugar Amino Acids (SAAs) as a Turn Inducer: Leu-Enkephalin Analogue

The five membered sugar ring carrying one carboxyl and one amino functional group was shown to act as a stereo chemically defined and conformational influencing scaffolds to induce turn conformation while present in a backbone of a peptide. The origin of carbohydrate special structure was first described by Hirschmann and his coworkers.[81,82] The deoxy glucose nucleus with amino acid side chain i.e Sugar amino acids (SAAs) were used for generating conformationally constrained turn structure in

peptide building block. Worldwide many research group studied about the conformation when pyranoid and furanoid sugar amino aicds introduced into the peptide backbone.[83]

In 1955, Heyns and Paulsen, first gave a suitable approach for synthesis of sugar amino acids through the oxidation of sugar for example glucosamine. They have first synthesized SAAs by catalytic oxidation of primary hydroxyl group of glucosamine to glucosaminuronic acids. The different size of sugar ring recognized the modification of conformation of the peptidomimmetics.[84]

In 1996, Kessler *et.al*. synthesized rigid pyranose sugar ring having different substituents that have ability to produce linear conformation or distinct turn structures. They have prepared Leu-enkephalin analogues by using such type of pyranose SAAs (**1.179, 1.180**) that replace the natural Gly –Gly dipeptide moiety of Leu-enkephalin (**Figure 1.31**). They analysed the conformation of modified Lue-enkephalin by NMR studies.[85, 86]

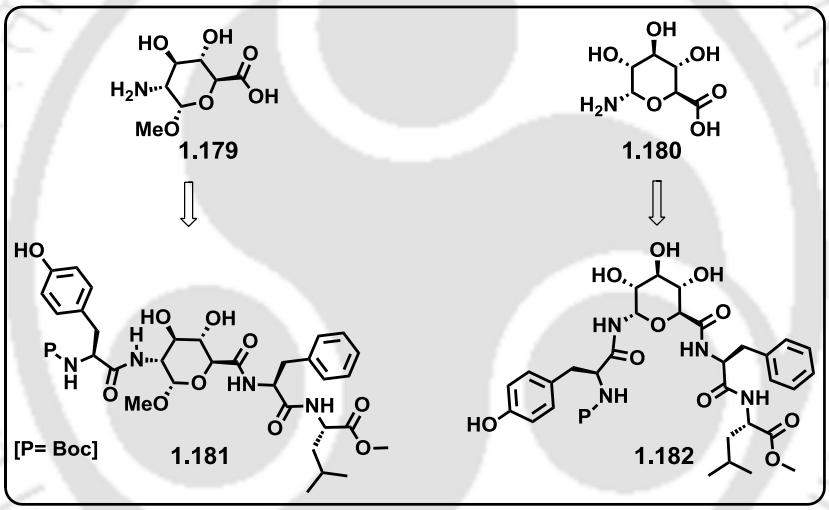

Figure 1.31. Gly-Gly moiety of Leu-enkephalin analogues is replaced by pyranoid SAAs.

In 1999, T. K. Chakraborty, *et al*. reported furanoid sugar amino acids, 6-amino-2,5-anhydro-3,4-di-O-benzyl-6-deoxy-D-gluconic acid (**1.183**), and its mannonic analogue (**1.184**) as rigid scaffold in the design and synthesis of carbopeptoids. Thus, they have synthesized furanoid SAAs as Gly-Gly dipeptide isostere from their cyclic precursor and incorporated into Leu-enkephaline analouges (**Figure 1.32**). Their synthesized analogues showed interesting turn structure which was confirmed from CD and 2D NMR analysis.[87, 88]

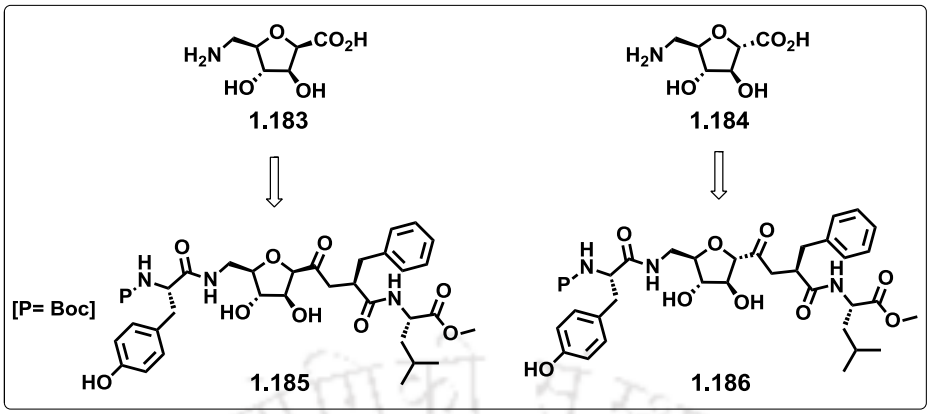

Figure 1.32. Gly-Gly moiety of Leu-enkephalin analogues is replaced by furanoid SAAs**.**

1.5.3. Cyclopentane-Based γ- Amino Acid as a Molecular Backbone

In 2003, Gellman *et al.* synthesized cyclohexyl and cyclopentyl based γ-amino acids building block (**1.187, 1.188, 1.189**) and investigated their power of inducing a particular secondary structure in peptides. They have also studied the effect of substituent at the α, β and γ carbons.[89, 90, 91] Hanessian *et al.* and Seebach *et al.* showed the folding behaviour of γ-amino acids[60a,d] and confirmed that the α, β and γ – trisubstitution pattern influenced the conformation of the peptides (**Figure 1.33**). When cyclic γ-amino acids remained in a backbone, the secondary structure of the peptide mainly depends on the ring size, configuration of the stereogenic centre and location of the ring within the γ-residue.[92]

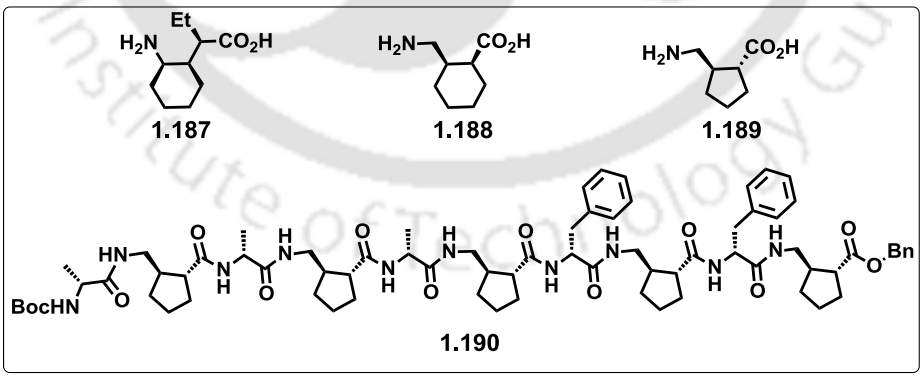

Figure 1.33. γ-Amino acids building block based α/γ-Peptidomimetics

.

1.5.4. Pyrrole and Furan Based Peptidomimetics

In 2009, Chakraborty *et al*., and Jagadeesh *et al*., developed pyrrole and furan based amino acids. They have synthesized two hybrid peptides **1.193** and **1.194** containing these two amino acids **1.191** and **1.192**. (**Figure 1.34**). Peptide **1.193**

adopted type-II' β turn structure stabilized by the formation of H-bond between Pyrrole-NH and furan –CO that led to the formation of H-bonded ten membered stable hairpin structure. The peptide **1.194** also adopted same hairpin like structure through hydrogen bonding interaction as was revealed from their various means of conformational analysis.[93]

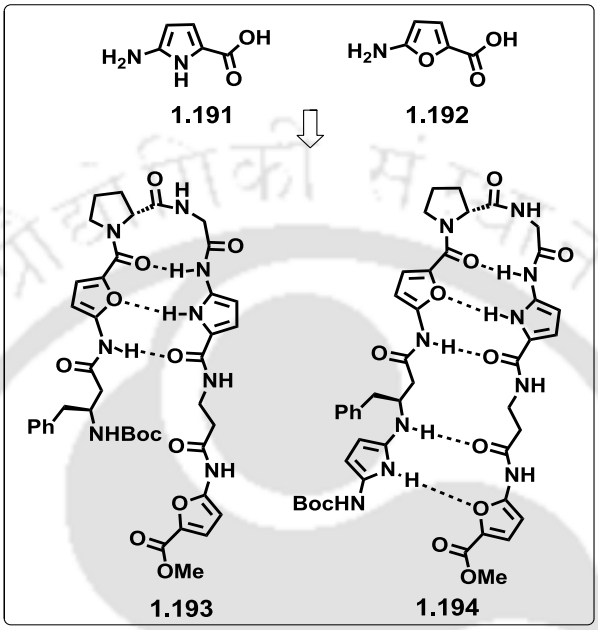

Figure 1.34. Pyrrole and furan based γ-amino acids and hybrid peptides.

1.5.5. Enediynyl Amino Acid as β- Turn Nucleator

Enediynes molecule have great interest because of their cytotoxic activity and possible use as anticancer drug. Z-enediynes was used as possible scaffold for peptide secondary structure mimetic where two arms are attached with peptide motifs. Thus, Bag and Basak *et al*. have incorporated ω- enediynyl amino acid into a peptide chain and study their conformation (**Figure 1.35**).[94] The designed pentapeptide was found β-turn like structure.

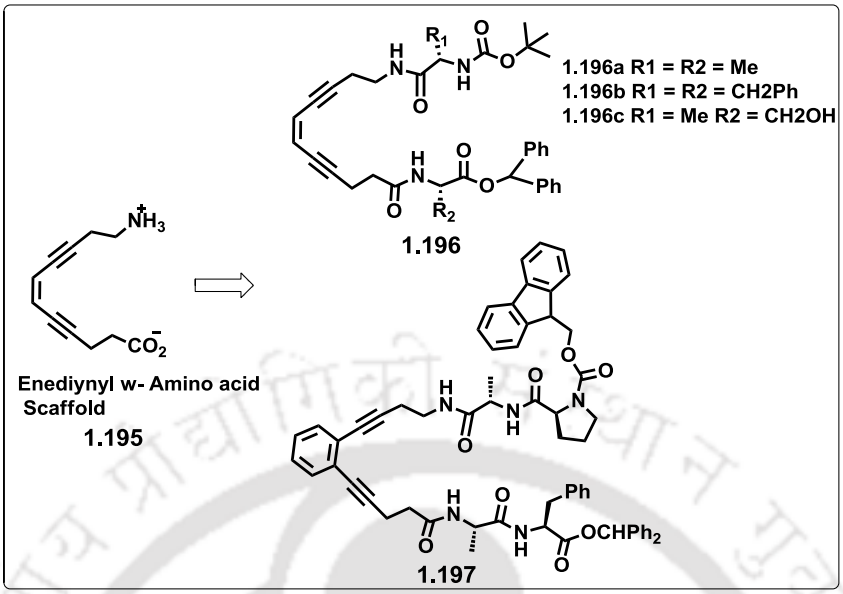

Figure1.35. Example of enediyne based peptidomimetics.

1.5.6. Norbornene Containing Peptide: β-Sheet Nucleator

The endo-(2S,3R)-2-amino-3-carboxynorbornene acts as a conformationally constrained β -amino acid scaffold which act as a turn inducer similar to proline (**Figure 1.36**).[95] The pseudopeptide **1.198** adopted parallel β-sheet conformation in $CDCl_3$ which was confirmed by NOEs, and stabilized by two intramolecular hydrogen bonding involving the NHs of Ala and Val units. The peptide **1.199** adopted antiparallel β-sheet conformation in $CDCl_3$. The peptide **1.200** also exhibited parallel β-sheet structure in DMSO-d_6.[96] The adopted conformations of the peptide where norbornene placed into the peptide backbone clearly suggested that this scaffold act as good β-sheet nucleator. The advantages of norbornene derivative as constrained molecular scaffold are their built-in U-architecture, smaller size and low molecular weight which was exploited in peptidomimetic study.

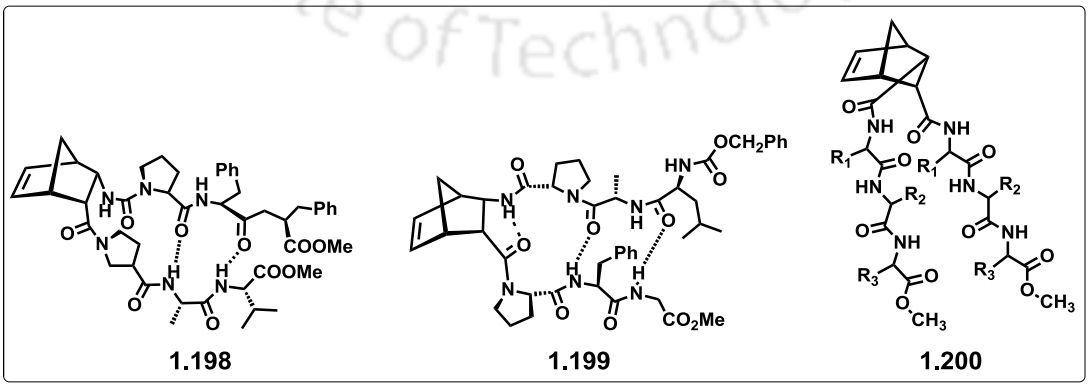

Figure 1.36. Norbornene containing peptidomimetics.

1.5.7. Dibenzofuran-Based Molecular Scaffold

Cyclic structures were first used as turn mimics and nucleators in the mid-1980s and continue to be used for these purposes. In 1992, Kelly and co-workers have used dibenzofuran turn unit **1.201** (**Figure 1.37**) to nucleate anti-parallel β-sheets in water. These compounds adopt conformations in which the dibenzofuran moiety folds against the sheet, forming a hydrophobic cluster with the side chains of the first residues of the sheet, thus stabilizing the turn. Recently, Kelly and co-workers reported a dibenzofuran turn unit that aligns two peptide strands to form a parallel β-sheet-like structure.[97]

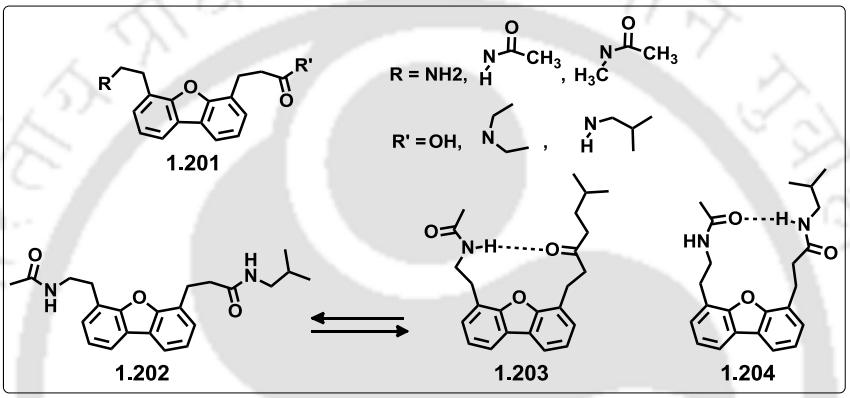

Figure 1.37. Dibenzofuran-based molecular scaffold.

In 2002, Kelly group have reported again 4-(2-aminoethyl)-6-dibenzofuran propionic acid residue as a *β*-turn mimetic which induces a peptide to adopt *β*-hairpin conformation (**Figure 1.38**). Furthermore, they observed that introduction of functional groups at positions 2 and 8 of dibenzofuran ring system, the solubility and stability of the peptides and the scaffold increased. Substitution at this position also helpful for controlling amyloid-like assemblies of peptidomimetics.[98]

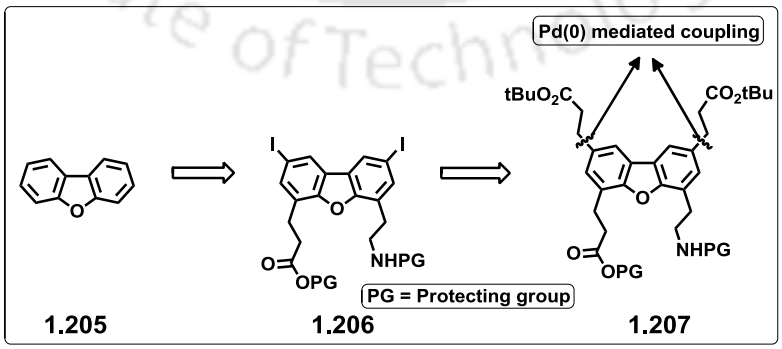

Figure 1.38. Synthetic scheme of dibenzofuran-based side-chain protected, charged molecular scaffold.

1.5.8. Biphenyl Scaffold as a Peptide Backbone

The incorporation of semirigid biphenyl scaffold into the backbone of cyclic peptides is a useful strategy for tuning conformational properties. With this background, The cyclic peptide **1.209** was synthesized by incorporation of biphenyl-containing pseudo-amino acid scaffold **1.208** that pursuing antiparallel β sheet structure (**Figure 1.39**). Due to atropisomerism of biphenyl units the synthesized peptides are interconvertible (R,R)-, (S,S)-, and (R,S)-diastereomers. The NMR (^{1}H NMR, COSY, and ROESY) studies and molecular dynamics calculation support the major diastereomers of cyclic peptide **1.209** adopt the antiparallel β sheet conformation of (R,R)-isomer in DMSO-d_6.[99] The chirality of biphenyl moiety also influenced on the hydrogen bonding pattern.[100]

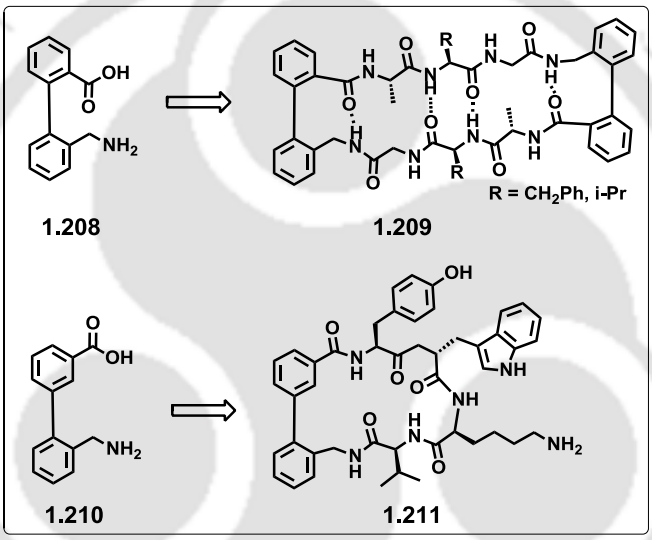

Figure 1.39. Semirigid biphenyl scaffold as a backbone of cyclic peptide.

1.5.9. Pyridine-Based Molecular Scaffolds

In biological system metal ions have great role and exhibit diversity of function in proteins. The metal ions stabilizes the secondary structures through co-ordination chemistry which is very essential for biological function. In that sense, pyridine-based molecular scaffolds **1.212** and **1.213** are placed as peptide backbone which induced β-sheet folding in presence of Cu(II) metal ion.[101] Cu(II) ion have a tendency to bring the attached peptide strand to cissoids square planar conformation through coordination (**Figure 1.40**).

In 1995, Kelly group reported the peptide Lys-Val-Thr-Val-Lys-**1.212**-Lys-Val-Lys-NH_2 (**1.214**) which adopted antiparallel β-sheet structure involving coordination at pH 9.5 in 10 mM borate buffer where as in absence of Cu(II) metal ion the peptide (**1.214)** showed random coil conformation. But in case of peptide Lys-Val-Thr-Val-Lys-Val-**1.213**-Val-Lys-Val-Lys-NH_2 (**1.215)**, here **1.212** is replaced by Val-**1.213** -

Val that is able to forming β-sheet structure even in the absence of Cu(II) through hydrophobic cluster formation at pH 9.1 in 10 mM borate buffer. In this peptide, by addition of Cu(II) increases strengthens of β-sheet structure. Such type of molecular scaffold play a vital role for β-sheet nucleation through Cu(II) binding cisoid conformation or hydrophobic cluster formation in absence metal ion.

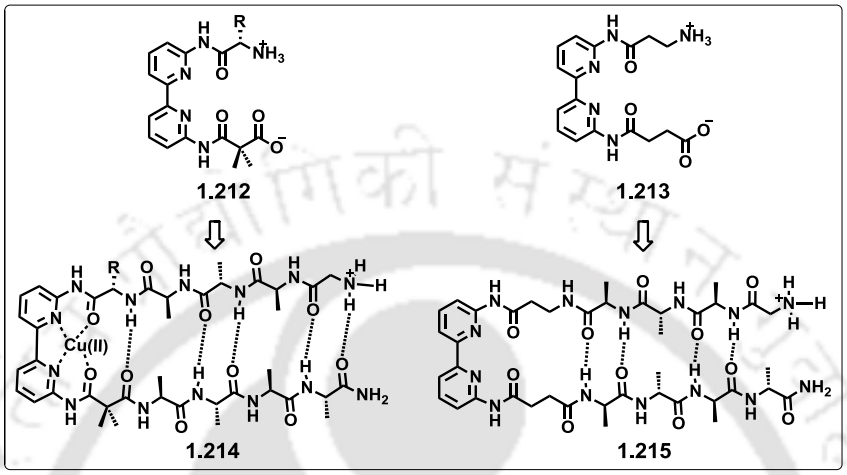

Figure 1.40. Pyridine based β-sheet nucleated molecular scaffold and peptides.

1.5.10. Epindolidione as a β-Sheet Nucleator

Another type of molecular scaffold epindolidione **1.216** having itself hydrogen bonding site that preferred to antiparallel β-sheet structure when attached by L-Pro-D-Ala peptide chain.[102, 103] Is compared to other scaffold the epindolidione scaffold **1.216** is rigid and planner, so when it is incorporated in peptide chain there is no possibility to interaction between two side chain of peptide motif. The antiparallel β-sheet conformation of synthesizes peptide **1.217** was supported by NMR in DMSO-d_6 and temperature dependence of the amide NH chemical shift and NOE effect. So the combination of rigid epindolidione scaffold as a molecular backbone with dipeptide L-Pro-D-Val is a key factor for β-sheet nucleation (**Figure 1.41**).

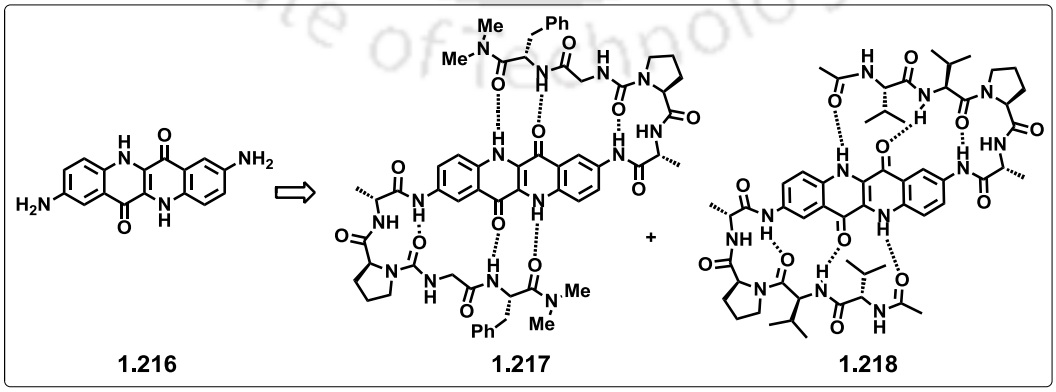

Figure 1.41. Epindolidione act as antiparallel β-sheet nucleator.

So such type of aromatic phenyl group based constrained molecular scaffolds was very useful for generating the β-turn or β-sheet like conformation in short peptidomimetics. We thought, if any fluorescence tag are attached into the two arms of such type of proteins or peptides, we can expected that they have interacted photophysically like FRET, excimer or exciplex emission which would help us to study the protien dynamics and folding nature.

1.5.11. Triazole Scaffold as peptidomimetics

Sze group *et al*., have reported a new class of 1,4 triazole based peptidomimetics which has been self dimerizes in a head to tail fashion and formed organogel in both nonpolar and protic organic solvent. The dimerization constant was strongly affected by the size of the C-terminal end group. The formation of such head-to-tail dimeric structures is very unique and similar of the β-strand structure found in many peptides **(Figure 1.42**). These click peptidomimetics are potentially useful for structural motifs in biomimetic chemistry.[104]

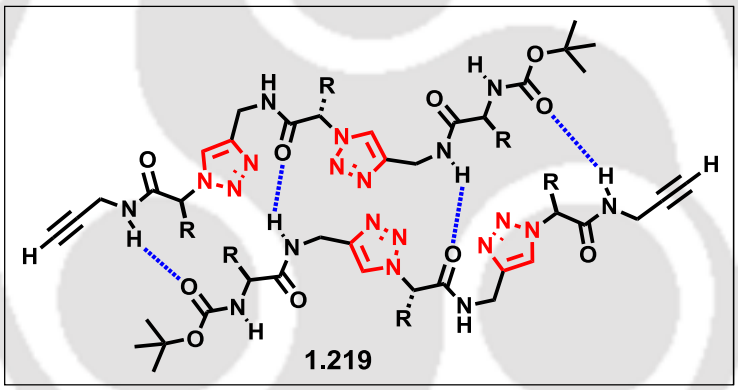

Figure 1.42. Head to tail dimerization of click peptidomimetics.

1.6. Summary and Future Prospect

Design and synthesis of unnatural amino acids towards expansion of genetic code is going at a fast space. At the same various developments of chemistry, platform and protocols are going on for the genetic incorporation of such designer amino acids into a protein system of Eukaryotic cells. As for an example, current efforts by several laboratories are focused on the evolution of new orthogonal aaRS/tRNA pairs for the encoding of additional unnatural amino acids. Efforts toward the transition of these systems are not restricted to E. Coli but expanded to other unicellular and multicellular organisms. With the advent of sophisticated synthetic chemistry more complex amino acids are being designed the encoding of which need the evolution of new aaRS/tRNA pairs that may also allow the *in vivo* synthesis of biopolymers with unnatural backbones. The incorporation of unnatural amino acid into protein

expectedly would generate protein-based therapeutics that would certainly have an impact on medicine.

Furthermore, biomedical researchers are constantly engaged in the development of new peptides/proteins based therapeutics with high metabolic stability, much more selectivity, high efficiency and suitable pharmacokinetics by maintaining the features responsible for biological activity and introducing both structural and functional specific modifications. The challenges in this endeavor have opened a new field of mimicked research, called peptidomimetics. During recent decades the basic concepts and approaches to peptidomimetic constructs have evolved to cover diverse compounds and synthetic strategies such as 'click chemistry' to generate a diverse array of drug candidates. As for an example, β-turn peptidomimetics with a constrained small molecule scaffold ~~have~~ attracted great interest during the last two decades and is finding a rebirth, as the need to target key protein–protein interactions in major diseases such as cancer and CNS diseases requires complex molecular scaffolds capable of mimicking the protein subdomains that play a central role in molecular recognition, which are generally characterized by the presence of α-helix and β-turn motifs. On the other hand, the generation of foldameric structures bearing amino acid side-chain isosteres and displaying a secondary framework such as a β-hairpin/ β-sheet or α-helix conformation is promising for next-generation therapeutics in medicine. Several peptidomimetic inhibitors have been developed and found to be potent against the HIV-1 protease, thus paving the way towards next-generation therapeutics with different modes of action and hopefully with improved therapeutic profile against drug-resistant viral strains. The peptidomimetic approach has thus been powerful in addressing the key recognition elements by scaffold-based peptidomimetic architectures that expectedly would afford a wide array of medicinally important molecules displaying different binding affinity and pharmacokinetic profile.

On the other hand progress towards the design of fluorescent unnatural amino acids (FUAA) are not only restricted to monitor protein's microenvironment, study structure, conformation, function and dynamics of proteins, monitor protein-protein/protein-drug/ protein-DNA interactions but also extended to the cellular imaging with the help of integration of imaging techniques to observe dynamic yet delicate cellular functions in more complex systems through the ongoing advancement of protocols for multiple-FUAA incorporation into protein systems. For example, Chapman *et al.* have incorporated fluorescent 7-hydroxycoumarin amino acid into the bacterial tubulin homologue cytoskeleton protein FtsZ to visualize subcellular localization implying the power of fluorescent amino acids in real-time imaging and the importance of imparting fluorescence to a protein without perturbing its native function.[105] Therefore, with the advancement of knowledge and strategies of chemistry and biology, FUAAs expectedly would continue to be at the forefront in aiding researchers to gain insights into fundamental questions concerning life's essential biological functions involving protein interactions, recognition, and

synthesis.

1.7. References

1. (a) Lang, K.; Chin, J. W. *Chem. Rev*. **2014**, *114*, 4764. (b) Young, T. S.; Schultz, P. G. J. *Biol. Chem.* ***2010***, *285, 11039.* (c) Lajoie, M. J.; Rovner, A. J.; Goodman, D. B.; Aerni, H. R.; Haimovich, A. D.; Kuznetsov, G. Mercer, J. A.; Wang, H. H.; Carr, P. A.; Mosberg, J. A.; Rohland, N.; Schultz, P. G.; Jacobson, J. M.; Rinehart, J.; Church, G. M.; Isaacs, F. J. *Science* ***2013***. *342, 357.* (d) Woese, C. R.; Olsen, G. J.; Ibba, M.; Söll, D. *Microbiol. Mol. Biol. Rev.* ***2000***, *64, 202.* (e) Sakamoto, K. *Nucleic Acids Res*. ***2002***, *30, 4692.* (f) Wang, A.; Nairn, N.; Marelli, M.; Grabstein, K. H. *In Protein engineering with non-natural amino acids* (Kaumaya, P., Ed.) **2012**. 253. InTech.

2. (a) Yuan, J.; O'Donoghue, P.; Ambrogelly, A.; Gundllapalli, S.; Sherrer, R. L.; Palioura, S.; Simonović, M.; Söll, D. *FEBS Lett.* **2010**, *584*, 342. (b) Zhang, Y.; Baranov, P. V.; Atkins, J. F.; Gladyshev, V. N.; *J. Biol. Chem.* **2005,** *280*, 20740. (c) *Liu, C. C.; Schultz, P. G. Annu. Rev. Biochem.* ***2010***, *79, 413.* (d) Wang, Q.; Parrish, A. R.; Wang, L *Chem. Biol.* ***2009***, *16, 323. (*d) Park, H. -S.; Hohn, M. J.; Umehara, T.; Guo, L. –T.; Osborne, E. M.; Benner, J.; Noren, C. J.; Rinehart, J.; Söll, D. *Science* ***2011***, *333, 1151.*

3. (a) Jäckel, C.; Kast. P.; Hilvert, D. *Annu. Rev. Biophys*. **2008**, *37*, 153. (b) Currin, A.; Swainston, N.; Day, P. J.; Kell, D. B. *Chem Soc Rev*. **2015**, *44*, 1172. (c) Michael, S.; Liu, P. D. R. *Nat. Rev. Genet.* **2015**, *16*, 379. (d) *Cobb*, R. E.; Sun, N.; Zhao, H. *Methods* **2013**, *60*, 81. (e) Cardillo, G.; Gentilucci, L.; Tolomelli, A. *Mini. Rev. Med. Chem.* ***2006***, *6, 293.*

4. (a) Liu, Q.; Wang, J.; Boyd, B. J. *Talanta* **2015,** *136*, 114. (b) Pazos, E.; Vázquez, O.; Mascareñas, J. L.; Vázquez, M. E. *Chem. Soc. Rev.* **2009,** *38*, 3348. (c) Tung, C. -H. *Peptide Sci.* **2004**, *76*, 391. (d) Kenworthy, A. K. *Methods* **2001**, *24*, 289. (e) Hoppe, A.; Christensen, K.; Swanson, J. A. *Biophys. J.* **2002**, *83*, 3652. (f) Ozawa, T.; Umezawa, Y. *Supramol. Chem.* **2002**, *14*, 271. (g) Packard, B. Z.; Toptygin, D. D.; Komoriya, A.; Brand, L. *Natl. Acad. Sci. USA* **1996**, *93*, 11640. (h) Bains, G.; Patel, A. B.; Narayanaswami, V. *Biochemistry* **2011**, *16*, 7909. (i) Matsumoto, C.; Hamasaki, K.; Mihara, H.; Ueno, A. *Bioorg. Med. Chem. Lett.* **2000**, *10*, 1857. (k) Chafekar, S. M. *BBA Mol. Bas. Dis*. **2008**, *1782*, 523.

5. (a) Michael, P.; Brunt, V.; Shanebeck, K.; Caldwell, Z.; Johnson, J.; Thompson, P.; Martin, T.; Dong, H.; Li, G.; Xu, H.; D'Hooge, F.; Masterson, L.; Bariola, P.; Tiberghien, A.; Ezeadi, E.; Williams, D. G.; Hartley, J. A.; Howard, P. W.; Grabstein, K. H.; Bowen, M. A.; Marelli, M.; *Bioconjugate Chem.* **2015**, 26, 2249. (b) Sun, M. M. C.; Beam, K. S.; Cerveny, C. G.;

Hamblett, K. J.; Blackmore, R. S.; Torgov, M. Y.; Handley, F. G. M.; Ihle, N. C.; Senter, P. D.; Alley, S. C. *Bioconjugate Chem*. **2005**, *16*, 1282. (c) Axup, J. Y.; Bajjuri, K. M.; Ritland, M.; Hutchins, B. M.; Kim, C. H.; Kazane, S. A.; Halder, R.; Forsyth, J.; Tian, F.; Lu, Y.; Manibusan, A.; Sellers, A.; Tran, H.; Sun, Y.; Phuong, T.; Barnett, R.; Hehli, B.; Song, F. *Natl. Acad. Sci. U. S. A.* **2014**, *111*, 1766.

6. (a) Agrawal, D.; Hackenberger, C. P. R. *Indian J. Chem.* **2013**, *52A*, 973. (b) Pless, S. A.; Christopher, A. A. Annu. Rev. Pharmacol. Toxicol. **2013**, *53*, 211. (c) Wang, L.; Brock, A.; Herberich, B.; Schultz, P. G *Science **2001,** 292, 498.* (d) Wang, A.; Nairn, N.; Marelli, M.; Grabstein, K. H. **2012,** 253. (e) Zimmerman, E. S.; Heibeck, T. H.; Gill, A.; Li, X.; Murray, C. J.; Madlansacay, M. R.; Tran, C.; Uter, N. T.; Yin, G.; Rivers, P. J. *Bioconjugate Chem*. **2014**, *25*, 351.

7. (a) Albericio, F.; Kruger, H. G. Future *Med. Chem.* **2012**, *4*, 1527. (b) Chin, J.; Mahmud, K. A. F.; Kim, S. E.; Park, K.; Byun, Y. *Drug Discov Today Technol*. **2012**, *9*, 105. (c) Park, K.; Kwan, I. C.; Park, K. *React. Funct. Polym*. **2011,** *71*, 280. (d) Vlieghe, P.; Lisowski, V. *Drug Discovery Today* **2010**, *15***,** 40**.**

8. (a) Walensky, L. D.; Kung, A. L.; Escher, I. *Science* **2004**, *305*, 1466. (b) Kharb, R.; Rana, M.; Sharma, P. C.; Yar, M. S. *J. Chem. Pharm. Res*. **2011**, *3*, 173.

9. (a) Hicks, R. P.; Abercrombie, J. J.; Wong, R. K.; Leung, K. P. *Bioorg Med Chem*. **2013**, *21*, 205. (b) Bhonsle, J. B.; Clark, T.; Bartolotti, L.; Hicks, R. P. *Curr. Top. Med. Chem.* **2013**, *13*, 3205. (c) Russell, A. L.; Kennedy, A. M.; Spuches, A. M.; Gibson, W. S.; Venugopal, D.; Klapper, D.; Srouji, A. H.; Bhonsle, J. B.; Hicks, R. P. *Chem. Phys. Lipids*. **2011,** *164*, 740. (d) Hicks, R. P.; Abercrombie, J. J.; Wong, R. K.; Leung, K. P. *Bioorg. Med. Chem.* **2013**, *21*, 205.

10. (a) Xie, J.; Schultz, P. G. *Curr. Opin. Chem. Biol. **2005**, 9, 548.* (b) Santidrian, A. F.; Stafin, K.; Felding-Habermann, B.; Smider, V. V.; Schultz, P. G. *Proc. Natl. Acad. Sci. U. S. A.* **2012**, *109*, 16101. (c) Young, T. S.; Ahmad, I.; Yin, J. A.; Schultz, P. G *J. Mol. Biol. **2010**, 395,* 361

11. (a) Link, A. J.; Mock, M. L.; Tirrell, D. A. *Curr. Opin. Biotechnol*. **2003**, *14*, 603. (b) Pap, E. H. W.; Dansen, T. B.; Summeren, R. V.; Wirtz, K. W. A. *Exp. Cell Res.* **2001,** *265*, 288. (c) Hickman, S. E. *Neurobiol. Dis.* **2008,** *28*, 8354. (t) Liu, J.; Liu, Y.; Gao, M.; Zhang, X.; Proteomics. **2012** *12*, 2258. (d) Ben-Efraim, I.; Strahilevitz, J.; Bach, D.; Shai, Y. *Biochemistry* **1994**, *33*, 6966.

12. (a) Peled, H.; Shai, Y. *Biochemistry* **1994**, *33*, 7211. (b) Hoesl, M. G.; Budisa, N. *Curr. Opin. Biotechnol.* ***2012****. 23. 751*. (c) Bains, G. K.; Kim, S. H.; Sorin, E. J.; Narayanaswami, V. Biochemistry **2012**, *51*, 6207. (d) Fujii, A.; Hirota, S.; Matsuo, T *Bioconjugate Chem*. **2013**, *24*, 1218.

13. (a) Liu, W.; Brock, A.; Chen, S.; Chen, S.; Schultz, P. G. *Nat. Methods* **2007**, *4, 239.* (b) Young, T. S.; Schultz, P. G. *J. Biol. Chem.* **2010**, *285*, 11039. (c) Liu, W.; Brock, A.; Chen, S.; Chen, S.; Schultz, P. G *Nat. Methods* **2000, *7****4***, 239.

14. (a) Chowdhury, S. R.; Chauhan, P. S.; Dedkova, L. M.; Bai, X.; Chen, S.; Talukder, P.; Hecht, S. M. *Biochemistry* **2016**, *55*, 2427. (b) Lampkowski, J. S.; Uthappa, D. M.; Young D. D. *Bioorg. Med. Chem. Lett*. **2015,** *25*, 5277. (c) Chen, S.; Fahmi, N. E.; Wang, L.; Bhattacharya, C.; Benkovic, S. J.; Hecht, S. M. *J. Am. Chem. Soc.* **2013**, *135*, 12924.

15. (a) Merkel, L.; Hoesl, M. G.; Albrecht, M.; Schmidt, A.; Budisa, N. *ChemBioChem* **2010**, *11*, 305. (b) R. F. Wissner, S. Batjargal, C. M. Fadzen, J. E. Petersson, *J. Am. Chem. Soc.* **2013**, *135*, 6529. (c) H. S. Lee, J. Guo, E. A. Lemke, R. D. Dimla, P. G. Schultz, *J. Am. Chem. Soc.* **2009**, *131*, 12921.

16. (a) Shimomura, O.; Johnson, F. H.; Saiga, Y. J. *J. Cell. Comp. Physiol*. **1962**, *59*, 223. (b) Lang, K.; Davis, L.; Torres-Kolbus, J.; Chou, C.; Deiters, A.; Chin, J. W. *Nat. Chem.* **2012**, *4*, 298. (c) Chatterjee, A.; Sun, S. B.; Furman, J. L.; Xiao, H.; Schultz, P. G. *Biochemistry* **2013**, *52*, 1828.

17. (a) Summerer,,D.; Chen, S.; Wu, N.; Deiters, A.; Chin, J. W.; Schultz, P. G. *Proc. Natl. Acad. Sci. USA* **2006**, *103*, 9785. (b) Wang, J.; Xie, J.; Schultz, P. G. *J. Am. Chem. Soc*. **2006**, *128*, 8738. (c) Brun, M. P.; Bischoff, L.; Garbay, C. *Angew. Chem. Int. Ed.* **2004**, *43*, 3432.

18. (a) Thirumurugan, P.; Matosiuk, D.; Jozwiak, K. *Chem. Rev.* **2013**, *113*, 4905. (b) Ievins, A. D.; Wang, X. F.; Moughton, A. O.; Skey, J.; O'Reilly, R. K. Macromolecules **2008**, *41*, 2998. (c) Dirks, A. J.; Cornelissen, J. J. L. M.; Nolte, R. J. M. *Bioconjugate Chem*. **2009**, *20*, 1129.

19. (a) Neuweiler, H.; Schultz, A.; Vaiana, A. C.; Smith, J. C.; Kaul, S.; Wolfrum, J.; Sauer, M. *Angew. Chem., Int. Ed*., **2002**, *41*, 4769. (b) Kohn, J. E.; Plaxco, K. W. *Proc. Natl. Acad. Sci. U.S.A.* **2005**, *102*, 10841.

20. (a) Chen, S. X.; Wang, L.; Fahmi, N. E.; Benkovic, S. J.; Hecht, S. M. *J. Am. Chem. Soc*. **2012**, *134*, 18883. (b) Fujii, A.; Sekiguchi, Y.; Matsumura, H.; Inoue, T.; Chung, W. S.; Hirota, S.; Matsuo, T. *Bioconjugate Chem.* **2015**, *26*, 537.

21. (a) Fosgerau, K.; Hoffmann, T. *Drug Discovery Today* **2015**, 20, 122. (b) Eisenstein, M. *Nat. Methods* **2009**, *6*, 929.

22. (a) Wales, S. M.; Hammer, K. A.; King, A. M.; Tague, A. J.; Lyras, D.; Riley, T. V.; Keller, P. A.; Pyne, S. G. *Org. Biomol. Chem*. **2015**, *13*, 5743. (b) Kemp, D. S. *Trends Biotechnol*. **1990**, *8*, 249. (c) Hirschmann, R. *Angew. Chem. Int. Ed. Engl*., **1991**, *30*, 1278. (d) Schneider, J. P.; Kelly, J. W. *Chem. Rev*. **1995**, *95*, 2169. (e) A. F. Spatola in Chemistry and Biochemutry of Amino Acids,

Peptides, and Proteins, Vol. VII (Eds.: B. Weinstein, M. Dekker), New York, **1983**, p 267. (f) Whitby, L. R.; Boger, D. L. *Acc. Chem. Res*. **2012**, *45*, 1698.

23. (a) Johnson, L. M.; Gellman, S. H. *Methods Enzymol*. **2013**, *523*, 407. (b) Angell, Y. L.; Burgess, K. *Chem. Soc. Rev.* **2007**, *36*, 1674. (c) Basak, A.; Bag, S. S.; Basak, A. *Bioorg. Med. Chem.*, **2005**, *13*, 4096. (d) Tsang, K.Y.; Diaz, H.; Graciani, N.; Kelly, J. W. *J. Am. Chem. Soc.*, **1994**, *116*, 3988. (e) Gardner, R. R.; Liang, G. B.; Gellman, S. H. *J. Am. Chem. Soc.* **1999**, *121*, 1806. (f) Xie, J.; Bogliotti, N. *Chem. Rev.* **2014**, *114*, 7678.

24. (a) Lang, K.; Chin, J. W. *Chem. Rev.* **2014**, *114*, 4764. (b) Chatterjeea, A.; Xiaoa, H.; Bollonga, M.; Aib, H. W.; Schultz, P. G. *PNAS* **2013**, *110***,** 11803. (c) Hohsaka, T.; Kawashima, K.; Sisido, M. *J. Am. Chem. Soc.* **1994**, *116*, 413. (d) Wu, N.; Deiters, A.; Cropp, T. A.; King, D.; Schultz, P. G. *J. Am. Chem. Soc***. 2004**, *126*, 14306. (e) Sinkeldam, R. W.; Greco, N. J.; Tor, Y. *Chem. Rev.* **2010,** *110*, 2579. (f) Jotterand, N.; Pearce, D. A.; Imperiali, B. *J. Org. Chem.* **2001,** *66*, 3224. (g) Yu, Y.; Zhou, Q.; Wang, Li.; Liu, X.; Zhang, W.; Hu, M.; Dong, J.; Li, J.; Lv, X.; Ouyang, H.; Li, H.; Gao, F.; Gong, W.; Lu, Y.; Wang, J. *Chem. Sci*. **2015**, *6*, 3881. (h) Yoder, N. C.; Kumar, K. *Chem. Soc. Rev*. **2002**, *31*, 335**.** (i) Goodman, M.; Kossoy, A. *J. Am. Chem. Soc*. 1966, *88*, 5010. (j) Wang,Y.; Paletta, J. T.; Berg, K.; Reinhart, E.; Rajca, S.; Rajca, A. *Org. Lett*. **2014**, *16*, 5298.

25. (a) Noren, C. J.; Anthony-Cahill, S. J.; Griffith, M. C.; Schultz, P. G. *Science* **1989**, *244*, 182. (b) Hohsaka, T.; Kajihara, D. Ashizuka, Y.; Murakami, H.; Sisido, M. *J. Am. Chem. Soc.* **1999**, *121*, 35. (37)

26. Bain, J. D.; Glabe, C. G.; Dix, T, A.; Chamberlin, A. R.; Diala, E. S *J. Am. Chem. Soc.* **1989**, *111*, 8013. (38)

27. Heckler, T. G.; Chang, L. H.; Zama, Y.; Naka, T.; Chorghade, M. S.; Hecht, S. M *Biochemistry* **1984**, *23*, 1468. (39)

28. (a) Liu, W.; Brock, A.; Chen, S.; Chen, S.; Schultz, P. G.; *Nat. Methods* **2007**, *4*, 239. (b) Xie, J.; Schultz, P. G.; *Nat. Rev. Mol. Cell Biol.* **2006**, 7, 775. (c) Wang, L.; Schultz, P. G.; *Angew. Chem. Int. Edit.* **2005**, *44*, 34. (d) Young, T. S.; Schultz, P. G. *J. Bio. Chem.* **2010**, *285*, 15. (e) Xie, J.; Liu, W.; Schultz, P. G. *Angew. Chem. Int. Ed.* **2007**, *46*, 9239. (f) Hohsaka, T.; Sisido, M. *Current Opinion in Chemical Biology* **2002**, *6*, 809.

29. (a) Anderson, J. C.; Magliery, T.J.; Schultz, P. G. *Chem. Biol.* **2002**, *9*, 237. (b) Wang, K.; Schmied, W.H.; Chin, J. W. *Angew. Chem. Int. Ed. Engl.* **2012**, *51*, 2288. (c) Rackham, O.; Chin, J. W. *Nat. Chem. Biol.* **2005**, *1*, 159.

30. Neumann, H.; Wang, K.; Davis, L.; Garcia-Alai, M.; Chin, J. W. *Nature* **2010**. *464*, 441.

31. Hohsaka, T.; Ashizuka, Y.; Murakami, H.; Sisido, M.; *Nucleic Acids Res*. **2001**, 9, 3646.

32. (a) Martin, L. J.; Imperiali, B. *Methods Mol. Biol.* **2015**, *1248*, 201. (b) Talukder, P.; Chen, S. C.; Liu, T.; Baldwin, E. A.; Benkovic, S. J.; Hecht, S. M. *Bioorg. Med. Chem. Lett.* **2014**, *22*, 5924.

33. (a) Lu, C. H.; Li, J.; Zhang, X. L.; Zheng, A. X.; Yang, H. H.; Chen, Xi.; Chen, G. N. *Anal. Chem*. **2011**, *83*, 7276. (b) Oh, K. J.; Cash, K. J.; Plaxco, K. W. *J. Am. Chem. Soc*. **2006**, *128*, 14018. (c) Marmé, N.; Knemeyer, J. P.; Wolfrun, J.; Sauer, M. *Angew.Chem., Int. Ed. Engl*. **2004**, *43*, 3798.

34. (a) Wang, J.; Xie, J.; Schultz, P. G. *J. Am. Chem. Soc.* 2006, *128*, 8738. (b) Hohsaka, T.; Kajihara, D.; Ashizuka, Y.; Murakami, H.; Sisido, M. *J. Am. Chem. Soc*. **1999**, *121*, 34

35. Loidl, G.; Musiol, H. J.; Budisa, N.; Huber, R.; Poirot, S.; Fourmy, D.; Moroder, L. *J. Pept. Sci.* **2000**, *6*, 139.

36. Steward, L. E.; Collins, C. S.; Gilmore, M. A.; Carlson, J. E.; Ross, J. B. A.; Chamberlin, A. R. *J. Am. Chem. Soc.* **1997**, *119*, 6.

37. De Filippis, V.; De Boni, S.; De Dea, E.; Dalzoppo, D.; Grandi, C.; Fontana, A. *Protein Sci.* **2004**, *13*, 1489.

38. Lotte, K.; Plessow, R.; Brockhinke, A. *Photochem. Photobiol. Sci.* **2004**, *3*, 348.

39. Broos, J.; Gabellieri, E.; Biemans-Oldehinkel, E.; Strambini, G. B. *Protein Sci.* **2003**, *12*, 1991.

40. Erlenmeyer, H.; Grubenmann, W. *Hel*V. *Chim. Acta* **1947**, *30*, 297.

41. Chapman, N. B.; Scrowsto., Rm; Westwood, R. *J. Chem. Soc.* **1969**, 1855.

42. (a) Rajh, H. M.; Uitzetter, J. H.; Westerhuis, L. W.; Vandendries, C. L.; Tesser, G. I. *Int. J. Pept. Protein Res.* **1979**, *14*, 68. (b) Cady, S. G.; Sono, M. *Arch. Biochem. Biophys.* **1991**, *291*, 326. (c) Podea, P. V.; Tosa, M. L.; Palzs, C.; Irimie, F. D. *Tetrahedron: Asymmetry* **2008**, *19*, 500.

43. Kwon, I.; Tirrell, D. A. *J. Am. Chem. Soc.* **2007**, *129*, 10431.

44. (a) Twine, S. M.; Szabo, A. G. *Biophotonics* **2003**, *A360*, 104. (b) Katritzky, A. R.; Narindoshvili, T. *Org. Biomol. Chem.* **2009**, *7*, 627. (c) Budisa, N.; Pal, P. P. *Biol. Chem.* **2004**, *385*, 893. (d) Ross, J. B. A.; Szabo, A. G.; Hogue, C. W. V. *Methods Enzymol.* **1997**, *278*, 151.

45. Sinkeldam, R. W.; Greco, N. J.; Tor, Y *Chem. Rev.* **2010**, *110*, 2579.

46. Talukder, P.; Chen, S.; Arce, P. M.; Hecht, S. M. *Org. Lett*. **2014**, *16*, 556.

47. Talukder, P.; Chen, S.; Roy, B.; Yakovchuk, P.; Spiering, M. M.; Alam, M. P.; Madathil, M. M.; Bhattacharya, C.; Benkovic, S. J. Hecht, S. M. *Biochemistry* **2015**, *54*, 7457.

48. Chen, S.; Tsao, M. –L. *Bioconjugate Chem.* **2013**, *24*, 1645.

49. (a) Chen, S.; Fahmi, N. E.; Bhattacharya, C.; Wang, L.; Jin, Y.; Benkovic, S. J.; Hecht, S. M. *Biochemistry* **2013**, *52*, 8580. (b) Chen, S.; Fahmi, N. E.; Wang, L.; Bhattacharya, C.; Benkovic, S. J.; Hecht, S. M. *J. Am. Chem. Soc.* **2013**, *135*, 12924.

50. Cheruku, P.; Huang, J. –H.; Yen, H. –J.; Iyer, R. S.; Rector, K. D.; Martinez, J. S.; Wang H. –L. *Chem. Sci.* **2015**, ***6***, 1150.

51. (a) Maini, R.; Dedkova, L. M.; Paul, R.; Madathil, M. M.; Chowdhury, S. R.; Chen. S.; Hecht, S. M. *J. Am. Chem. Soc.* **2015**, *137*, 11206. (b) Chowdhury, S. R.; Chauhan, P. S.; Dedkova, L. M.; Bai, X.; Chen, S.; Talukder, P.; Hecht, S. M. *Biochemistry* **2016**, *55* 2427.

52. Cornish, V. W.; Benson, D. R.; Altenbach, C. A.; Hideg, K.; Hubbell, W. L.; Schultz, P. G. *Proc. Natl. Acad. Sci. U.S.A.* **1994**, *91*, 2910.

53. (a) Sisido, M. *Prog. Polym. Sci.* **1992**, *17*, 699. (b) Sisido, M. *Ad*V. *Photochem.* **1997**, *22*, 197. (c) Hohsaka, T.; Ashizuka, Y.; Murakami, H.; Sisido, M. *J. Am. Chem. Soc.* **1996**, *118*, 9778. (d) Hohsaka, T.; Kajihara, D.; Ashizuka, Y.; Murakami, H.; Sisido, M. *J. Am. Chem. Soc*. **1999**, *121*, 34.

54. (a) Wendt, H.; Berger, C.; Baici, A.; Thomas, R. M.; Bosshard, H. R. *Biochemistry* **1995**, *34*, 4097. (b) Wolf, J. H.; Korf, J. *J. Pharm. Biomed. Anal*. **1992**, *11*, 99 (c) Christie, R.M. *Rev. Prog. Color. Relat. Top.* **1993**, *23*, 1.

55. (a) Brufola, G.; Fringuelli, F.; Piermatti, O.; Pizzo, F. *Heterocycles* **1996**, *43*, 127. (b) Yavari, I.; Hekmat-Shoar, R.; Zonouzi, A. *Tetrahedron Lett.* **1998**, *39*, 2391.

56. Brun, M. P.; Bischoff, L.; Garbay, C. *Angew. Chem. Int. Ed.* **2004**, *43*, 3432.

57. (a) Koopmans, T.; Haren, M. V.; Ufford, L. Q. V.; Beekman, J. M.; Martin, N. I. *Bioorg. Med. Chem*. **2013**, *21*, 553. (b) Malkar, N. B.; Fields, G. B. *Lett. Pept. Sci*. **2001**, *7*, 263.

58. (a) Lauer-Fields, J. L.; Kele, P.; Sui, G.; Nagase, H.; Leblanc, R. M.; Fields, G. B. *Anal. Biochem*. **2003**, *321*, 105. (b) Lauer-Fields, J. L.; Broder, T.; Sritharan, T.; Chung, L.; Nagase, H.; Fields, G. B. *Biochem*. **2001**, *40*, 5795. (c) Berthelot, T.; Laïn, G.; Latxague, L.; Deleris, G. *J. Fluoresc*. **2004**, *14*, 671.

59. (a) Katritzky, A. R.; Narindoshvili, T.; Angrish, P.; *Synthesis* **2008**, *13*, 2013. (b) Katritzky, A. R.; Yoshioka, M.; Narindoshvili, T.; Chung, A.; Khashab, N. M.; Johnson, J. V. Submitted to Org. Biomol. Chem. (c) Katritzky, A. R.; Cusido, J.; Narindoshvili, T.; *Bioconj. Chem*. **2008**, *19*, 1471. (d) Johansson, A.; Akerblom, E.; Ersmark, K.; Lindeberg, G.; Hallberg, A. *J. Comb. Chem*. **2000**, *2*, 496.

60. Goldberg, J. M.; Chen, X.; Meinhardt, N.; Greenbaum, D. C.; Petersson, E. J. *J. Am. Chem. Soc.* **2014**, *136*, 2086.

61. (a) Loving, G. S.; Sainlos, M.; Imperiali. B. *Trends Biotechnol.* **2010**, 73. (b) Fakhari M, A.; Rokita, S. E. *Chem. Commun.*, **2011**, *47*, 4222.

62. Nitz, M.; Mezo, A. R.; Ali, M. H.; Imperiali, B. *Chem. Commun*. **2002**, 1912.

63. Vázquez, M. E.; Nitz, M.; Stehn, J.; Yaffe, M. B.; Imperiali, B. *J. Am. Chem. Soc*. **2003**, *125*, 10150.

64. Cohen, B. E.; McAnaney, T. B.; Park, E. S.; Jan, Y. N.; Boxer, S. G.; Jan, L. Y.; *Science* **2002**, *296*, 1700.

65. Grabchev, I.; Chovelon, J. -M.; Qian, X.; *J. Photochem. Photobiol. A* **2003**, *158*, *37*.
66. Martin, E.; Weigand, R.; Pardo, A. *J. Lumin.* **1996**, *68*, 157.
67. Vàzquez, M. E.; Rothman, D. M.; Imperiali, B. *Org. Biomol. Chem*. **2004**, *2*, 1965.
68. Venkatraman, P.; Nguyen, T. T.; Sainlos, M.; Bilsel, O.; Chitta, S.; Imperiali, B.; Stern, L. J. *Nat. Chem. Biol*. **2007**, *3*, 222.
69. (a) Vázquez, M. E.; Blanco, J. B.; Imperiali, B. *J. Am. Chem. Soc.* **2005**, *127*, 1300. *(b)* Sainlos, M.; Iskenderian, W. S.; Imperiali, B. *J. Am. Chem. Soc.* **2009**, *131*, 6680. (c) Sainlos, M.; Tigaret, C.; Poujol, C.; Olivier, N. B.; Bard, L.; Breillat, C.; Thiolon, K.; Choquet, D.; Imperiali, B. *Nat. Chem. Biol*. **2011**, *7*, 81. *(d)* Loving, G. S.; Sainlos, M.; Imperiali, B. *Trends Biotechnol*. **2010**, *28*, 73.
70. (a) Loving, G.; Imperiali, B. *J. Am. Chem. Soc*. **2008**, *130*, 13630. (b) Zhang, J.; Wallar, B. J.; Popescu, C. V.; Renner, D. B.; Thomas, D. D.; Lipscomb, J. D. *Biochemistry* **2006**, *45*, 2913. (c) Zuhlke, R. D.; Pitt, G. S.; Deisseroth, K.; Tsien, R. W.; Reuter, H. *Nature* **1999**, *399*, 159. (d) Torok, K.; Cowley, D. J.; Brandmeier, B. D.; Howell, S.; Aitken, A.; Trentham, D. R. *Biochemistry* **1998**, *37*, 6188. (e) Wang, Q. Z.; Lawrence, D. S. *J. Am. Chem. Soc.* **2005**, *127*, 7684.
71. (a) Turcatti, G.*;* Zoffmann, S.; Lowe III, J. A.*;* Drozda, S. E.; Chassaing, G.; Schwartz, T. W.; A. Chollet, *J. Biol. Chem*. **1997**, *272*, 21167.*(b)* Goguen, B. N.; Loving, G. S.; Imperiali, B. *Bioorg. Med. Chem. Lett*. **2011**, *21*, 5058.
72. Summerer, D.; Chen, S.; Wu, N.; Deiters, A.; Chin, J. W.; Schultz, P. G. *Proc. Natl. Acad. Sci. USA* **2006**, *103*, 9785.
73. Lee, H. S.; Guo, J.; Lemke, E. A.; Dimla, R. D.; Schultz, P. G. *J. Am. Chem. Soc.* **2009**, *131*, 12921.
74. Shen, B.; Xiang, Z.; Miller, B.; Louie, G.; Wang, W.; Noel, J. P.; Gage, F. H.; Wang, L. *Stem Cells* **2011**, *29*, 1231.
75. Xiang, Z.; Wang, L.; *J. Org. Chem.* **2011**, *76*, 6367.
76. Torrado, A.; Imperiali, B. *J. Org. Chem.* **1996,** *61*, 8940.
77. (a) Imperiali, B.; Fisher, S. L. *J. Org. Chem.* **1993**, *58*, 1613. (b) Imperiali, B.; Kapoor, T. M. *Tetrahedron* **1993**, *49*, 3501. (c) Walkup, G. K.; Imperiali, B. *J. Am. Chem. Soc.* **1996**, *118*, 3053. (d) Godwin, H. A.; Berg, J. M. *J. Am. Chem. Soc.* **1996**, *118*, 6514.
78. Walkup, G. K.; Imperiali, B. *J. Org. Chem.* **1998,** *63*, 6727.
79. (a) Lohani, C. R.; Kim, J. M.; Lee, K.-H. *Tetrahedron* **2011**, *67*, 4130. (b) Lohani, C.; Neupane, R. L. N.; Kim, J. –M.; Lee, K. -H. *Sens. Actuators, B* **2012**, *161*, 1088.
80. (a) Grison, C.; Genève, S.; Halbin, E.; Coutrot, P. *Tetrahedron* **2001**, *57*, 4903. (b) Chakraborty, T. K.; Ghosh, A.; Kiran, K. S.; Kunwar, A. C. *J. Org. Chem.* **2003**, *68*, 6459.

81. (a) Guruprasad, K.; Shukla, S. *J. Peptide Res.* **2003**, *61*, 159. (b) Venkatraman, J.; Gowda, G. A. N.; Balaram, P. *J. Am. Chem. Soc.* **2002**, *124*, 4987. (c) Gibbs, A. C.; Bjorndahl, T. C.; Hodges, R. S.; Wishart, D. S. *J. Am. Chem. Soc.* **2002**, *124*, 1203. (d) Haque, T. S.; Little, J. C.; Gellman, S. H. *J. Am. Chem. Soc.* **1996**, *118*, 6975.

82. Hirschmann, R.; Nicolaou, K. C.; Pietranico, S.; Leahy, E. M.; Salvino, J.; Arison, B.; Cichy, M. A.; Spoors, P. G.; Shakespeare, W. C. *J. Am. Chem. Soc*. **1993**, *115*, 12550.

83. (a) Wunberg, T.; Kallus, C.; Opatz, T.; Henke, S.; Schmidt, W.; Kunz, H. *Angew. Chem., Int. Ed. Engl*. **1998**, *37*, 2503. (b) Schweizer, F.; Hindsgaul, O. *Curr. Opin. Chem. Biol*. **1999**, *3*, 291.

84. (a) Lohof, E.; Burkhart, F.; Born, M. A.; Planker, E.; Kessler, H.; Abell, A.; Ed.; JAI Press Inc.: *Stanford, Connecticut* **1999**, *2*, 263. (b) Lohof, E.; Born, M. A.; Kessler, H.; Goodman, M.; Felix, A.; Moroder, L.; Toniolo, C.; *Eds.; Georg Thieme Verlag: Stuttgart*, **2001**; Vol. E *22* (in press).

85. Heyns, K.; Paulsen, H. *Chem. Ber*. **1955**, *88*, 188.

86. (a) Graf von Roedern, E.; Kessler, H. *Angew. Chem., Int. Ed. Engl*. **1994**, *33*, 670. (b) Kessler, H.; Diefenbach, B.; Finsinger, D.; Geyer, A.; Gurrath, M.; Goodman, S. L.; Hölzemann, G.; Haubner, R.; Jonczyk, A.; Müller, G.; Graf von Roedern, E.; Wermuth, *J. Lett. Pept. Sci*. **1995**, *2*, 155.

87. (a) Chakraborty, T. K.; Jayaprakash, S.; Diwan, P. V.; Nagaraj, R.; Jampani, S. R. B.; Kunwar, A. C. *J. Am. Chem. Soc*. **1998**, *120*, 12962. (b) Smith, G. D.; Griffin, J. F. *Science 1978*, **199**, 1214.

88. (a) Chakraborty, T. K.; Ghosh, S.; Jayaprakash, S.; Sharma, J. A. R. P.; Ravikanth, V.; Diwan, P. V.; Nagaraj, R.; Kunwar, A. C. *J. Org. Chem*. **2000**, *65*, 6441. (b) zGraf von Roedern, E.; Lohof, E.; Hessler, G.; Hoffmann, M.; Kessler, H. *J. Am. Chem. Soc*. **1996**, *118*, 10156.

89. (a) Guo, L.; Chi, Y. G.; Almeida, A. M.; Guzei, I. A.; Parker, B. K. Gellman, S. H. *J. Am. Chem. Soc*. **2009**, *131*, 16018. (b) Guo, L.; Almeida, A. M.; Zhang, W.; Reidenbach, A. G.; Choi, S. H.; Guzei, I. A.; Gellman, S. H. *J. Am. Chem. Soc*. **2010**, *132*, 7868. (c) Guo, L.; Zhang, W. C.; Reidenbach, A. G.; Giuliano, M. W.; Guzei, I. A.; Spencer, L. C.; Gellman, S. H. *Angew. Chem., Int. Ed*. **2011**, *50*, 5843. (d) Guo, L.; Zhang, W. C.; Guzei, I. A.; Spencer, L. C.; Gellman, S. H. *Org. Lett*. **2012**, *14*, 2582. (e) Sawada, T.; Gellman, S. H. *J. Am. Chem. Soc*. **2011**, *133*, 7336. (f) Shin, Y.-H.; Mortenson, D. E.; Satyshur, K. A.; Forest, K. T.; Gellman, S. H. *J. Am. Chem. Soc*. **2013**, *135*, 8149.

90. (a) Woll, M. G.; Lai, J. R.; Guzei, I. A.; Taylor, S. J. C.; Smith, M. E. B.; Gellman, S. H. *J. Am. Chem. Soc*. **2001**, *123*, 11077. (b) Seebach, D.; Hook, D. F.; Glattli, A. Biopolymers **2006**, *84*, 23. (c) Jones, C. R.; Qureshi, Truscott, F. R.; Hsu, S. T. D.; Morrison, A. J.; Smith, M. D. *Angew. Chem., Int. Ed*. **2008**, *47*, 7099.

91. (a) Gellman, S. H. *Acc. Chem. Res*. **1998**, *31*, 173. (b) Hill, D. J.; Mio, M. J.; Prince, R. B.; Hughes, T. S.; Moore, J. S. *Chem. Rev*. **2001**, *101*, 3893. (c) Horne, W. S.; Gellman, S. H. *Acc. Chem. Res*. **2008**, *41*, 1399. (d) Martinek, T. A.; Fülöp, F. *Chem. Soc. Rev*. **2012**, *41*, 687.

92. (a) Hanessian, S.; Luo, X. H.; Schaum, R. *Tetrahedron Lett*. **1999**, *40*, 4925. (b) Seebach, D.; Brenner, M.; Rueping, M.; Schweizer, B.; Jaun, B. *Chem. Commun*. **2001**, 207. (c) Seebach, D.; Brenner, M.; Rueping, M.; Jaun, B. *Chem.-Eur. J.* **2002**, *8*, 573. (d) Hanessian, S.; Luo, X. H.; Schaum, R.; Michnick, S. *J. Am. Chem. Soc*. **1998**, *120*, 8569. (e) Seebach, D.; Brenner, M.; Rueping, M.; Schweizer, B.; Jaun, B. *Chem. Commun*. **2001**, 207.

93. (a) Chakraborty, T. K.; Srinivasa, R. K.; Kiran, M. U.; Jagadeesh, B. *Tetrahedron Lett.* **2009**, *50*, 4350. (b) Krishna, Y.; Sharma, S.; Ampapathi, R. S.; Koley, D. *Org. Lett.* **2014**, *16*, 2084. (b) Sun, Q.; Xu, B.; Niu, Y.; Xu, F.; Liang, L.; Wang, C.; Yan, J. G. Y.; Wang, W.; Jin, H.;. Xu, P. *Chem. Med. Chem.* **2015**, *10*, 498.

94. (a) Basak, A.; Bag, S. S.; Basak, A. *Bioorg. Med. Chem. Lett.* **2005**, 13, 4096. (b) Basak A.; Bag, S. S.; Bdour, H. M. M. *Chem. Comm.* **2003**, *20*, 2614. (b) Basak, A.; Rudra.; Rani, K.; Bag, S. S.; Basak, A. *J. Chem. Soc., Perkin Trans. 1*. **2002**, *15*, 1805.

95. (a) Sinkeldam, R.W.; Greco, J. N.; Tor. Y. *Chem. Rev*. **2010**, *110*, 2579. (b) Moriuchi, T.; Hirao, T. *Chem. Soc. Rev*. **2004**, *33*, 294.

96. (a) Ranganathan, D.; Haridas, V.; Kurur, S.; Thomas, A.; Madhusudanan, K. P.; Nagaraj, R.; Kunwar, A. C.; Sarma, A. V. S.; Karle, I. L. *J. Am. Chem. Soc*. **1998**, *120*, 8448. (b) Hackenberger, C. P. R.; Schiffers, I.; Runsink, J.; Bolm, C. *J. Org. Chem*. **2004**, *69*, 739.

97. (a) Lashuel, H. A.; LaBrenz, S. R.; Woo, L.; Serpell, L. C.; Kelly, J. W. *J. Am. Chem. Soc*. **2000**, *122*, 5262. (b) Choo, D. W.; Schneider, J. P.; Graciani, N. R.; Kelly, J. W. *Macromolecules* **1996**, *29*, 355.

98. Kaul, R.; Deechongkit, S.; Kelly, J. W. *J. Am. Chem. Soc*. **2002**, *124*, 11900.

99. (a) Brandmeier, V.; Sauer, W. H. B.; Feigel, M. *Helv. Chim. Acta* **1994**, *77*, 70. (b) Feigel, M. *J. Am. Chem. Soc*. **1986**, *108*, 181.

100. Cheng, R. P.; Suich, D. J.; Cheng, H.; Roder H.; DeGrado, W. F. *J. Am. Chem. Soc*. **2001**, *123*, 12710.

101. Schneider, J. P.; Kelly, J. W. *J. Am. Chem. Soc*. **1995**, *117*, 2533.

102. Kem, D. S.; Bowen, B. R. *Tetrahedron Lett*. **1988**, *29*, 5081.

103. Moriuchi, T.; Hirao, T. *Chem. Soc. Rev*. **2004**, *33*, 294.

104. Ke, Z.; Chow, H. –F.; Chan, M.-C.; Liu, Z.; Sze, K.-H. *Org. Lett*. **2012**, *14*, 1.

105. Krueger, A. T.; Imperiali, B. *ChemBioChem* **2013**, *14*, 788.

Chapter 2

STUDIES ON THE SYNTHESIS AND PHOTOPHYSICAL PROPERTIES OF FLUORESCENT UNNATURAL TRIAZOLYL AMINO ACIDS

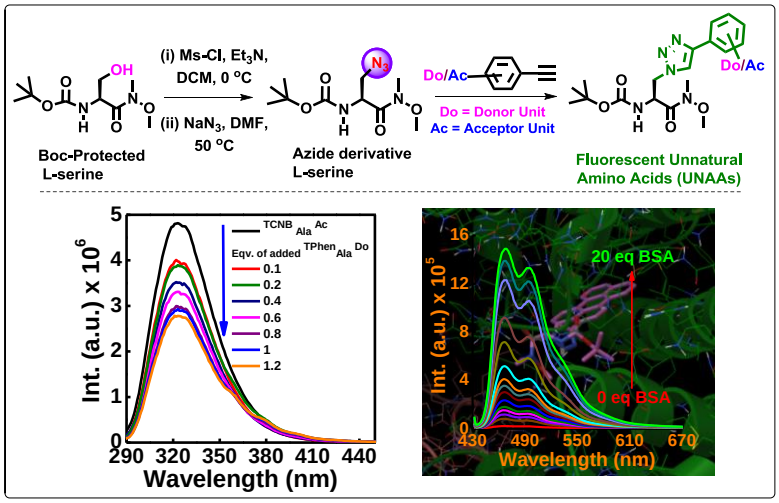

2.1. Introduction

The synthetic or semisynthetic methods for introduction of unnatural amino acids into peptide and proteins by Offord and Kaiser has paved the way to develop protocol for site specific incorporation of more unnatural amino acids into proteins by Schultz *et al.* towards expanding the genetic code and reaching the goal of semisynthetic organism.[1] Towards this end, an increasing amount of research interest has resulted in the acceleration of progress of design of unnatural amino acids for application in protein engineering. Several non-natural amino acids were reported looking after the steric and electronic properties and incorporated into proteins site specifically.[1c-d] However, many of the reported unnatural amino acids are not suitable for giving novel biological properties of the proteins or not containing functionality/signaling elements for labeling the proteins that can offer information about protein's structure, function and dynamics with a fast and easily detectable signal generation. Extremely sensitive fluorescence based detection techniques find widespread applications for probing of structure, function and dynamics of biomolecules, for visualizing intracellular events, understanding molecular interactions inside a cell and for enabling experiments to be measured in solution. Many such aspects have been studied either by exploiting intrinsic fluorescence of tryptophan amino acid in a protein or extrinsic fluorescent label. However, intrinsic fluorescence limits the interpretation of the results in presence of multiple tryptophan in a protein.[2] Moreover, the limitation of labeling with large size of extrinsic fluorescent probe has led a strong demand for generating the smaller protein tag or site-specific incorporation of unnatural fluorescent amino acids into a protein.[2]

To construct such type of unnatural amino acids transition metal catalyzed coupling reaction play a crucial role.[3] Among the various transition metals, copper is more significant because of lower price. Other transition metal ion such as palladium, ruthenium and rhodium were also effective but so much expensive than copper. In particular attention was paid towards the formation of carbon-carbon and carbon-heteroatom bonds mainly utilizing copper as catalyst because of its good functional group tolerance, economically attractiveness and good associative property with heteroatom.[4] Tandem or cascade reactions catalysed by copper salts are efficient tool for the preparation of biologically active hetero cyclic molecules.[5] Among the variety of heterocyclic molecule 1,2,3-Triazole heterocyles have got much attraction in recent time because of its wide applicability in various field ranging from chemistry, biology through medicine to material science.[6] Cu(I)-catalyzed version of the Huisgen 1,3-dipolar cycloaddition reaction became popular to generate 1,4-substituted 1,2,3 – triazoles which was referred to "click reaction" defined by K. B. Sharpless in 2001.[7] The advantages of this reaction lies on the fact that it can easily generate a triazole unit with complete specificity. **Figure 2.1** shows the methods for the generation of 1,2,3-triazole including the Cu(I)-catalysed click reaction. The triazoles are

rotationally restricted small molecular scaffold having high metabolic stability, biocompatibility, easy associability via H-bonding with biomolecules.[8] The triazolyl scaffolds moiety are found in many of biologically active molecules and show biological activities such as anti-HIV, antibiotics, antiviral and antibacterial properties.[9] In recent years click chemistry has got tremendous attention among the scientists worldwide for the generation of medically useful drug candidates and pharmaceutical lead structures.[8, 10] Moreover, click chemistry is one of the powerful and popular reactions for making carbon−heteroatom−carbon bonds in aqueous environment with a wide variety of chemical and biological applications in various fields.[10] Furthermore, the click reaction has widely been used in biological application such as chemical ligation,[11] labeling proteins or to modify proteins in vitro and vivo[11, 12] and in labeling of lipids[13] and nucleic acids.[14]

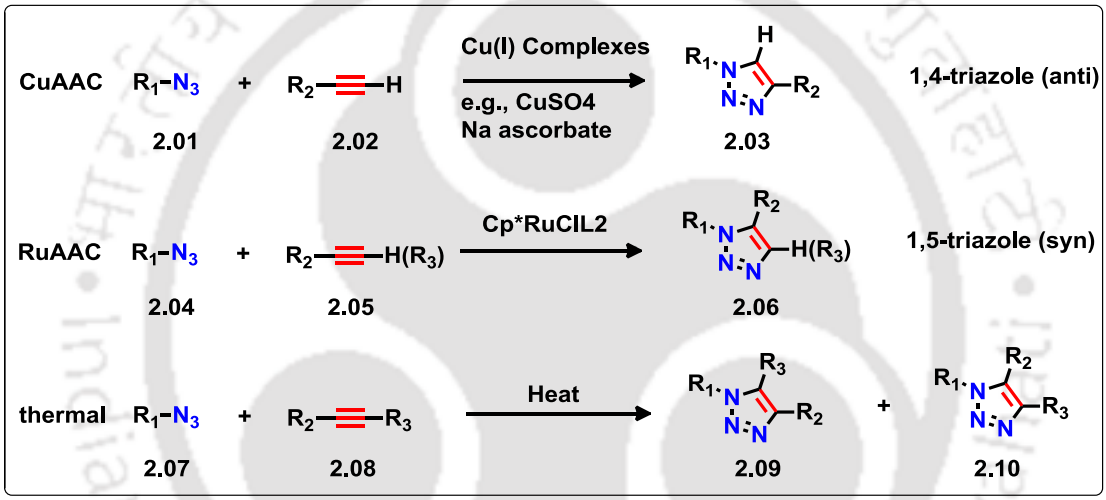

Scheme 2.1. Methods of 1,2,3-triazole synthesis.

Researchers are exploiting the click chemistry to design highly fluorescent biomolecule and molecular scaffold from non-fluorescent starting material containing azides and/or terminal alkynes (**Scheme 2.2**).[15] It has also found a broad application in cell biology and functional proteomics due to high reaction efficiency under mild reaction condition and contrast fluorescence properties of the product than starting material.[16] The main reason behind the using click reaction is that the product "triazole" unit have a resistance to enzymatic degradation, hydrolysis and oxidation, and more labile linker in biologically active compounds.[17]

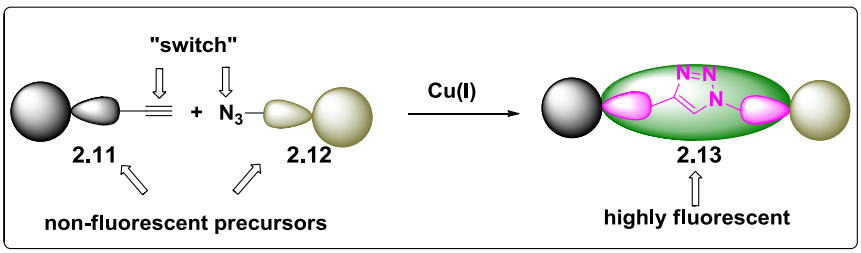

Scheme 2.2. Schematic representation of a fluorogenic Cu(I) catalysed click reaction.

In 2004, two groups are simultaneously reported firstly fluorogenic coumarine derivative using click reaction.[15, 18] Coumarine derivative are easily synthesized from their precursor and studied their photophysical properties by substituting electron donating group at 7-position or electron withdrawing group at the 3- position which strongly enhance the fluorescence emission property. In addition of electron donating group at 4-, 6-, or 7-position or electron withdrawing group at the 3- position can shifted the emission wavelength to longer region.[19] Following this concept Zhou and Fahmi have synthesized the weakly fluorescent azido coumarine **2.15**, and performed the click reaction with a terminal alkyne **2.14** to afford highly fluorescent triazolyl coumarine **2.16** (**Scheme 2.3**).[16, 18]

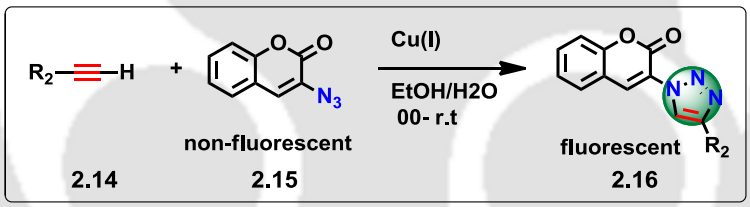

Scheme 2.3. Fluorogenic CuAAC reaction to produce highly fluorescent coumarin derivatives starting from weakly fluorescent coumarine**.**

As protein-polymer conjugates constitute a versatile and interesting class of materials that are beneficial for applications in medicine and biotechnology,[20] click chemistry has got recent interest to generate various protein-polymer conjugate.[21] Cornelissen and coworkers[22] have used click reaction to monitor protein–polymer conjugation. They prepared several 3-azido coumarin terminated poly(ethylene glycol) (**2.18**) and performed the click reaction with alkyne-functionalized bovin serum albumin (BSA), **2.17** to afford a highly fluorescent triazole-linked protein-polymer conjugate **2.19** (**Scheme 2.4**). The generation of the fluorescence can precisely be determined spectroscopically which can provide the information about the efficiency of the click reaction. Thus, it is clear that click chemistry can offer a possibility of monitoring the bioconjugation process by a study of fluorescence assay that is based on the progression of the reaction. This concept might find application in the formation of protein-polymer biohybrid amphiphiles.

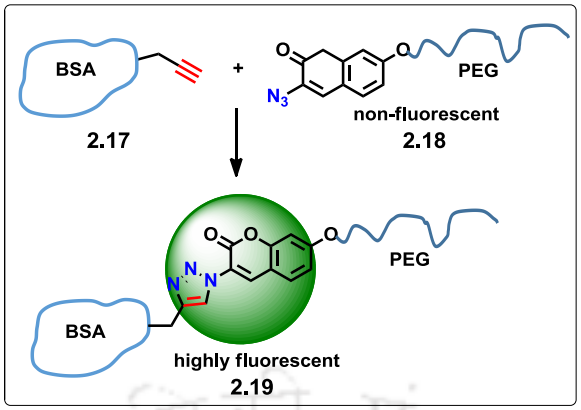

Scheme 2.4. Schematic presentation of copper catalyzed click reaction between alkyne modified protein **2.17** and azide-modified polymer **2.18.**

Our research group also has contributed to this field. Thus, Bag *et al*., have designed the fluorophores in such a way that the donor and the acceptor units are linked *via* the triazole unit thereby the triazolyl donor part can act as full donor to the acceptor unit allowing a charge transfer process leading to installation of emission on to the non fluorescent precursor. In a designed pyrene based fluorophore they have shown that the electron donating properties of triazolyl ring effectively modulate the emission properties of an electronically coupled pyrene when it is coupled with a donor or an acceptor unit. They have designed a series of compounds to show in one hand the installation of fluorescence response on to the non-fluorescent precursor amines or alkynes, on the other hand to show the modulation of the fluorescence response of pyrene (**Figure 2.1**). The concept of design strategy leading to fluorescence installation/modulation is presented in **Figure 2.1**.[23]

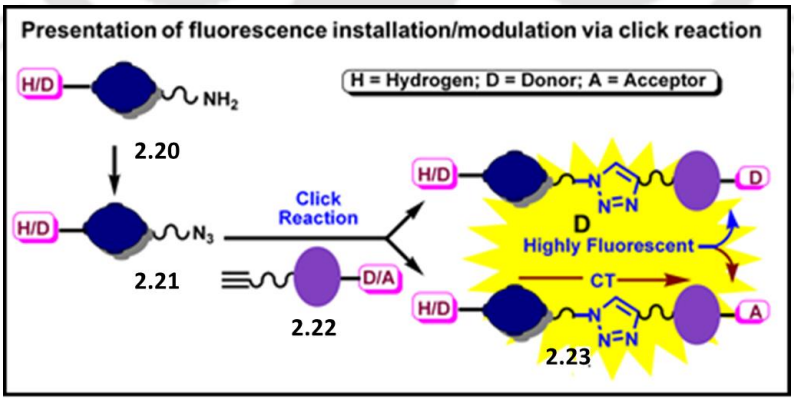

Figure 2.1. Presentation of fluorescence installation/modulation *via* click reaction.

2.2. Click Chemistry and Drug Design

In recent years, high throughput technology has been used to synthesize combinatorial and multi parallel chemical synthesis. Sequencing of human genome as well as the genomes of various pathogens have offered hundreds to thousands of effectively novel biological targets that have poor or no clearly precedented chemical starting point for lead optimization.[24]

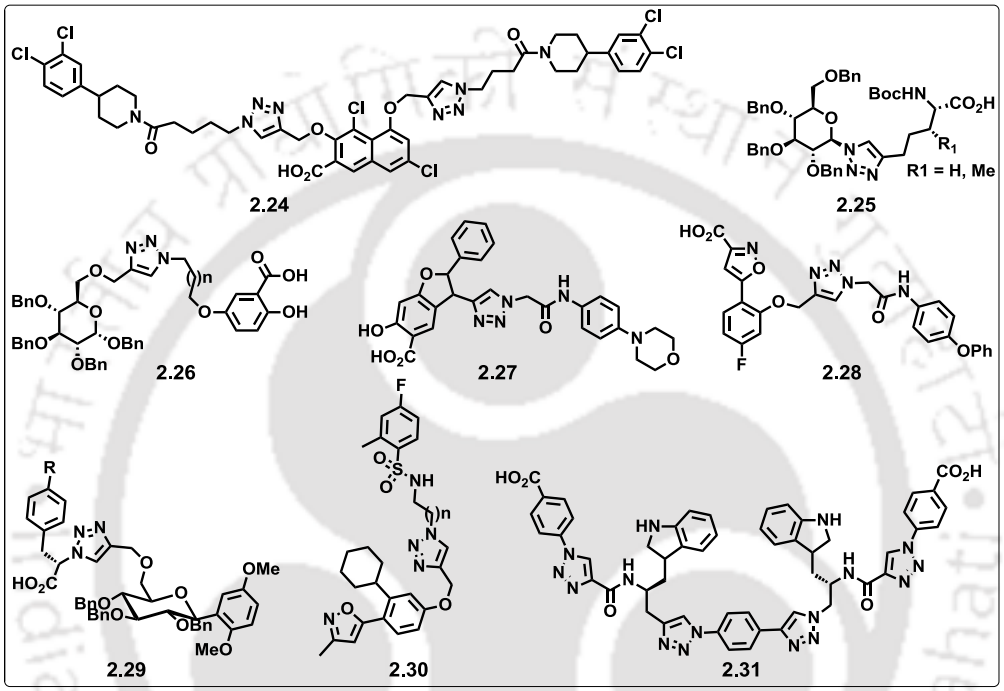

Figure 2.2. Chemical structures of protein tyrosine phosphatase inhibitors synthesized through click chemistry.

Therefore, in this avenue, click chemistry has got attention in synthesizing a combinatorial library of compounds that can be screened after studying the interactions with the unexplored targets. Mainly, click chemistry-based drug discovery falls into three categories (1) high throughput screening, (2) fragment-based drug discovery, and (3) dynamic template-assisted strategies in fragment-based drug discovery. Therefore, click chemistry has been applied for generating an assemble of small molecule libraries that have been broadly applied as distinct inhibitors of enzyme.[10] In such an endeavor, the precursor of click reaction *i.e.* azides and alkynes can be selected looking at the structure of the click products which is a shape mimic of the binding site of enzymes. **Figure 2.2** shows some protein tyrosine phosphatase inhibitors synthesized through click chemistry.

2.3. β-Amino Triazoles Based Unnatuaral Amino Acids

In 2002, Varma *et.al*., reported a new procedure for the synthesis of β-amino triazole based unnatural amino acids using a one pot multi-component reaction of sulfamidates under MW irradiation condition.[25a] This methodology has stereo selectivity as well as regioselectivity and a broad application to produced efficiently side chain modified triazolyl based unnatural amino acids. These amino acids are expected to show wide applicablity to modify biologically active peptide (**Scheme 2.5**).

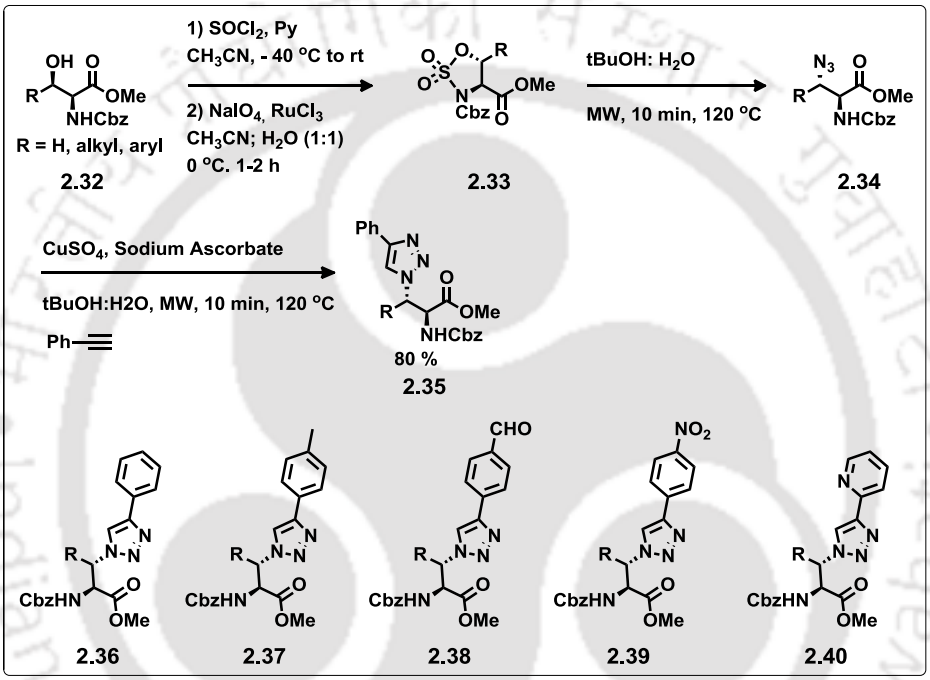

Scheme 2.5. Synthesis and structure of the triazole modified unnatural amino acids.

2.4. Oligo-Triazole Based Peptide Nucleic Acid Analogue (T-PNA)

In 1991, Nielsen was first described about peptide nucleic acids (PNAs) that have been examine to good and favorable DNA/RNA mimics. PNAs are unnatural oligonucleotide sequences in which nucleobases are linked with pseudo-peptide linkage as a neutral and achiral backbone (**Figure 2.3**).[26] They can form very stable hetero duplexes with natural DNA, RNA or other PNA with strong affinity and selectivity.[27] These property of the PNAs can easily explain by their neutral backbone which decreases the electrostatic repulsions present in negatively charged DNA/RNA.[28] PNAs are very useful and important tools in the field of anti-sense therapy or cytogenesis for their high selectivity.[29] They are stable long time within living cell and can escape from hydrolysis of enzyme or protease.[30]

In 2011, Zerrouki and his co-workers[31] described a productive strategy for the synthesis of a series of tri (ethylene glycol)-based oligotriazoles. Copper catalysed click reaction was found to be a high yielding process for the synthesis of a series of novel triazole based oligomers and macrocycles. They have substituted all backbone amide bonds of a PNA oligomer by 1,2,3 triazole moieties (**Figure 2.3**). The excellent conversion rates observed allow to consider the transfer of this strategy to solid support for a further solid phase synthesis of longer polytriazole DNA mimic.

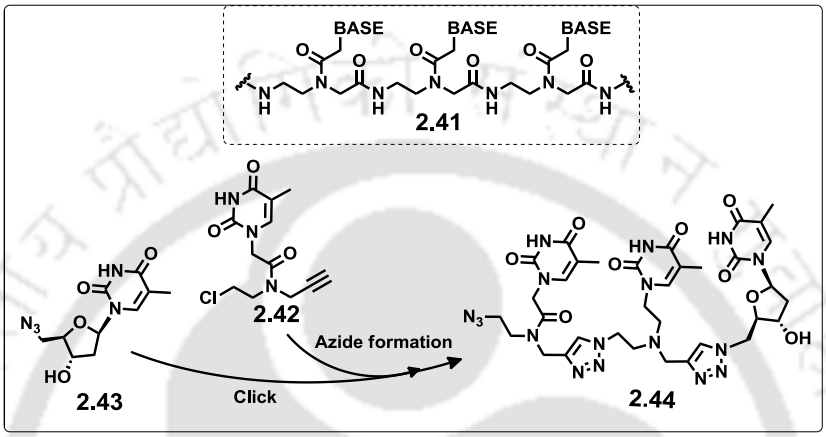

Figure 2.3. Structure of original aminoethylglycine (aeg) PNA (**2.41**) and novel triazole based oligomer (**2.44**).

2.5. Some Examples of Unnatural and Fluorescent Amino Acids

Imperiali and her group in 2001, reported fluorescent peptide based metal ion sensor. They have fluorescent 8-hydroxy quinolinyl alanine amino acids and its analogue wherein a phenyl ring was present in C-5 of 8-hydroxy quinolone (**Figure 2.4**). These two unnatural fluorescent amino acids have been incorporated into short peptidomimetics through solid phase peptide synthesis.[32a] Due to the chelating nature of bidentade ligand 8-hydroxy quinolone, these peptides were found to be effective in sensing Zn(II) ion with a significant red shift of 357 nm to 391 nm in the UV-Visible absorption spectra and exhibited fluorescence emission at 546 nm with modest quantum yield of 0.005 in HEPES buffer at pH 7.0.

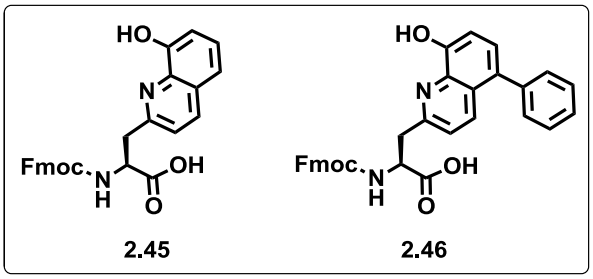

Figure 2.4. 8-Hydroxy quinolone derivative of α-amino acids.

Recently Andrzej Rajca group have reported a series of valuable sterically shielded pyrroline nitroxide functionalized unnatural amino acids. These can act as spin label of protein or peptides and can be utilized for studying the conformation by using ESR spectroscopy. Such types of spin labels are also very important for the study of structure-function of protein in biological environments. Moreover, these spin labels are able to resist the reducing power of ascorbate and ascorbate/glutathione. The structure of modified amino acids with spin labels are shown in **Figure 2.5**.[33]

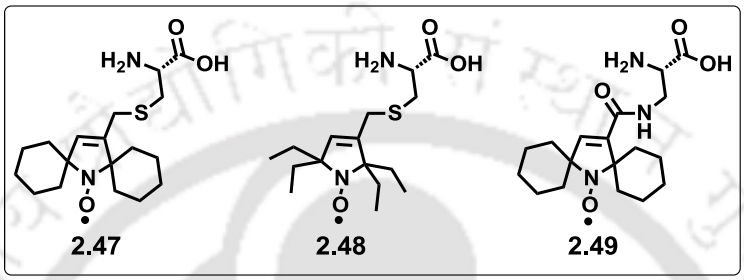

Figure 2.5. Pyrroline nitroxide functionalized unnatural amino acids.

Jin-Quan Yu and his group recently have developed a methodology for the synthesis of anti-β-fluoro-α-amino acids through C-H activation (**Figure 2.6**).[34] The fluorine atom containing unnatural amino acids have been found to show high metabolic stability, lipophilicity and conformational flexibility. Thus, fluorine containing amino acids are expected to be very useful for protein modification, to modulate biological activity of preclinical peptide based drug candidate and also can act as peptide building block.

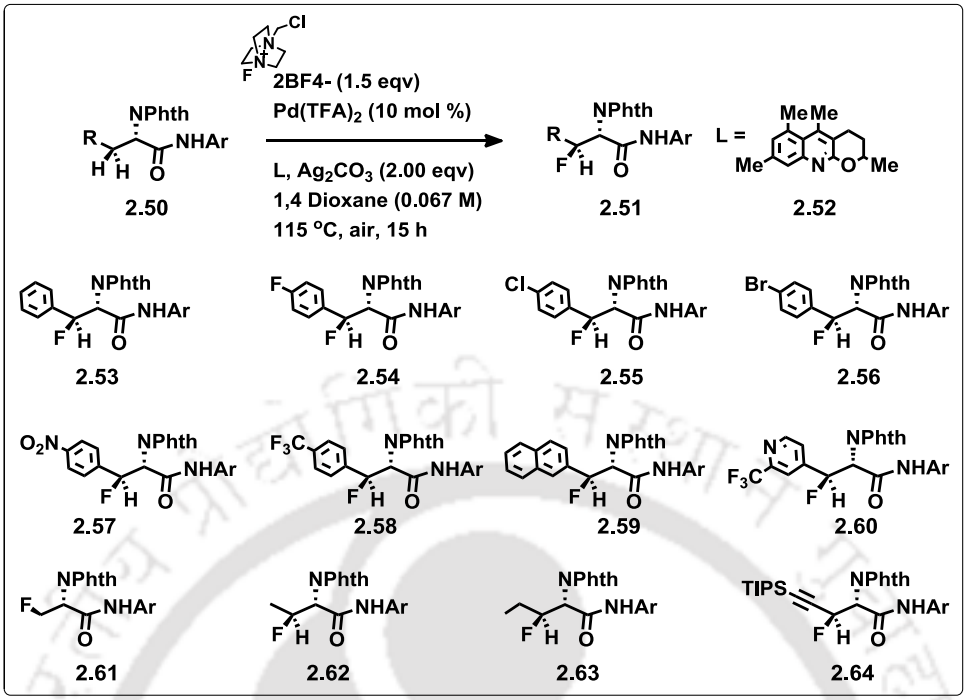

Figure 2.6. Synthetic scheme and the structures of synthesized anti-β-fluoro-α-amino acids.

A new florescent alanine derivative containing (oligo) thiophene and benzoxazole moieties have been reported which possess good photophysical properties (**Figure 2.7**).[35] The benzoxazole moieties exhibited broad spectral windows, high molar absorptivity and fluorescence quantum yield. The thiophene residue and its derivative also exhibited electroluminescent properties. Due to their interesting photophysical properties could find application as fluorescent probe for FRET studies in peptides, sensing of materials, pharmaceutical purpose and optical and electronic devices. These heterocyclic alanine derivatives are very useful building blocks for the cross-linking of peptide chains.

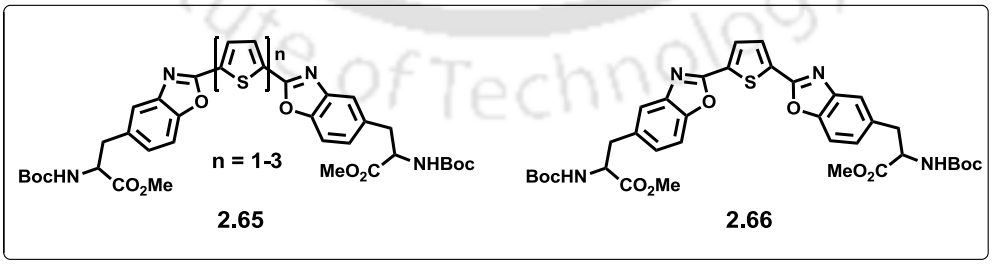

Figure 2.7. Fluorescent bis-amino acids bearing a heterocyclic bridge containing benzoxazole and thiophene.

2.6. Background

From the literature report it is clear that in the fast moving journey of expanding the genetic code, several unnatural amino acids (UNAAs) have been synthesized and incorporated within a protein's framework to afford proteins with novel functionality.[36] The interest in the design and application of novel unnatural amino acids is increasing universally. Moreover, the synthesis of unnatural amino acids with novel functionality is highly demanding and is currently an emerging area of research because of the currently developed technology, "recombinant introduction" of amino acid into proteins.[37] Furthermore, for visualizing intracellular events and understanding molecular interactions inside a cell such as elucidating protein's structures, functions and dynamics,[38] receptor-ligand binding,[39] monitoring enzyme activity,[40] and proteomics,[41] needs sensing of proteins' microenvironment with the help of highly sensitive fluorescence probe.[39, 40] Though, many of the aspects have been studied either by exploiting intrinsic fluorescence of tryptophan[42] or extrinsic fluorescent probe[43] but these are not free from limitations and thereby not sufficient to fulfill the all research need. Overcoming the shortcomings has led a strong demand for site-specific incorporation of microenvironment sensitive fluorescent unnatural amino acids[44] into a protein.[43-44] Towards this journey, a very few fluorescent amino acids have been synthesized or encoded genetically and site-specifically incorporated into proteins a brief introduction of which has already been in described in **chapter 1**.[45] Therefore, there is a great demand to develop fluorescent unnatural amino acids (FUAA) or fluorescently labelled UAA for genetic encoding or to generate labelled proteins/peptide for studying conformational or diverse functional realm.[46] Futhermore, the importance of triazolyl moiety could be utilized for generation of unnatural fluorescent amino acids with tuned photophysical properties of fluorophores.

2.7. Objective

As a part of our current research efforts on synthesis of fluorescent small molecules and biomolecular buildings blocks via azide-alkyne cycloaddition reaction we previously showed that the triazole rings introduces interesting photophysical properties to the generated fluorophores or the building blocks.[23] Previously, we have shown that the triazolyl units are capable of installation of fluorescence property into a non-fluorescent precursor as well as electronically coupling between a triazole and a fluorophore give rise to a modulated emission response to the fluorophore.[23] Therefore, owing to our previous result, we thought that it would be worthwhile to synthesize triazolyl amino acids containing donor and/or acceptor aromatics so as to produce solvatochromic photophysical response into the UNAAs. We, further, envisioned that the fluorescent amino acids could also be useful in the study of

interaction with target biomolecule such as BSA with the help of fluorescence spectroscopy.

The logic behind our choice of triazole linked with donor/acceptor aromatics to be the fluorescent amino acids are: (a) triazoles are metabolically inert[47]; (b) the triazole units are more than just passive linkers [48]; (c) act as *trans*-amide mimetics; (d) they readily associate with biological targets, through hydrogen bonding and dipole interactions [10, 24]; (e) we envisioned that the pseudoaromatic 1,2,3-triazole can modulate the electronic characteristics of the chromophores and endow new properties to the unnatural amino acids[24]; (f) in addition, two of such fluorescent UNAAs if incorporated into two termini of a tripeptide separated by a natural amino acid might adopt a specific peptide secondary structure via backbone H-bonding and could get extra stabilization via hydrophobic, π-π stacking and van der Waals interactions in the side chain; (g) strategically placed triazolyl unnatural amino acids in the specific conformation might involve in photophysical interaction leading to a fluorescent peptide of novel photophysical property. Furthermore, we wanted to explore the pseudoaromatic nature of 1,2,3-triazole to modulate the distribution of electrons and to endow new photophysical properties to the whole unnatural amino acids.

Utilizing the above concept we framed our objectives as follows:

(a) Design and synthesis of few fluorescent unnatural triazolyl amino acids via azide-alkyne cyclo-addition reaction (**Scheme. 2.6**)

(b) Study the photophysical properties.

(c) Investigating the interaction of triazolylperylene amino acid with Bovine serum albumin (BSA) with the help of fluorescence spectroscopy.

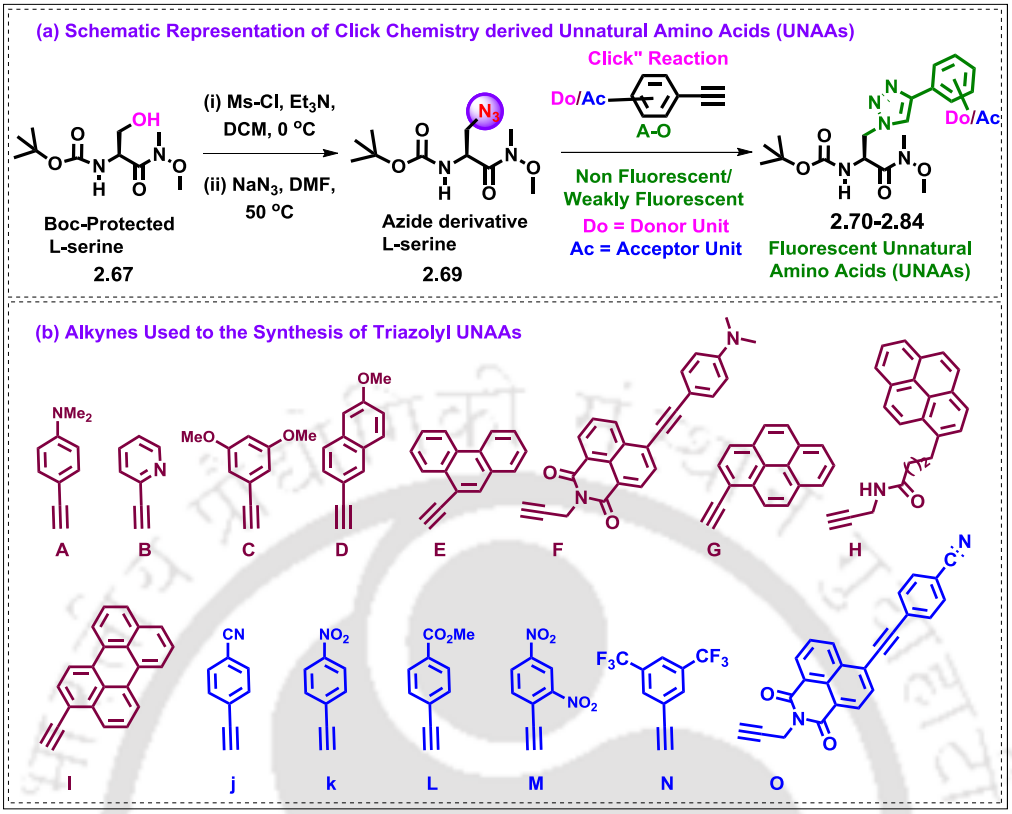

Scheme 2.6. (a) Schematic representation of triazolyl unnatural amino acids (UNAAs) and (b) the alkynes used in this study.

2.8. Result and Discussion

2.8.1 Synthesis of Triazolyl Donor/Acceptor Amino Acids

The synthesis of unnatural triazolyl amino acids was achieved via a 1, 3-dipolar cycloaddition reaction between aromatic alkyne and serine azide which is shown in **Scheme 2.7**. The synthesis started with natural L-serine which was protected first with Boc-anhydried to afford N-Boc-serine. Afterwards, the C-terminus was protected as Weinreb amide (**2.67**) with N-methoxy methyl amine hydrochloride following a peptide coupling protocol. The N, C-protected serine was then allowed to react with mesyl chloride in presence of triethyl amine in dry DCM at room temperature for 30 minutes to afford N, C-protected *O*-mesyl serine (**2.68**). Upon treatment with sodium azide in dry DMF at 40 ^{o}C, mesyl was converted to N, C-protected serine azide (**2.69**).[49] Finally, 1,3-Huisgen azide-alkyne cycloaddition reaction was carried out between the azide derivative of L-serine and various donor-acceptor aromatic alkynes (**A-O, Scheme 2.6**) under click reaction condition at 70 ^{o}C in THF to produce the desired triazolyl donor/acceptor amino acids (**2.70-2.84**) in good yield (70-80%).[25, 47]

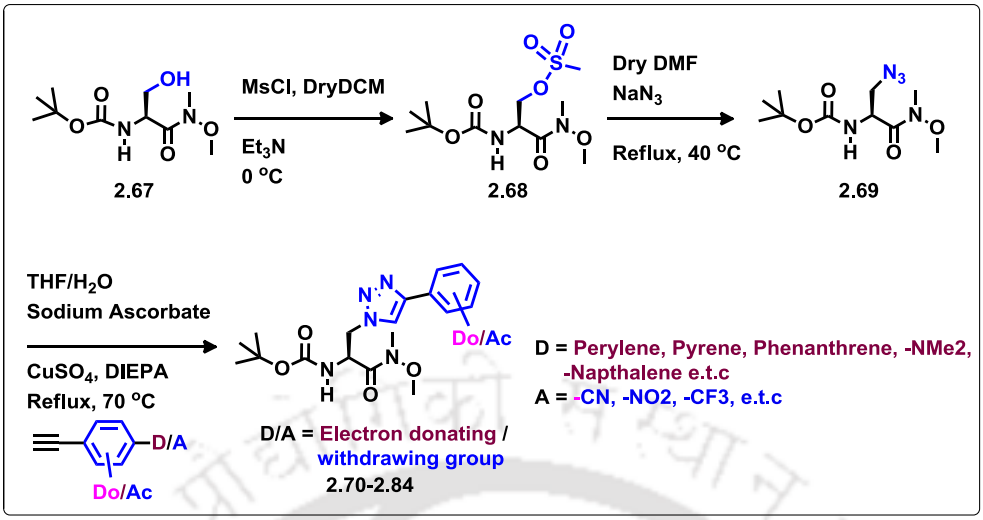

Scheme 2.7. Synthetic scheme for donor-acceptor triazolyl unnatural amino acids.

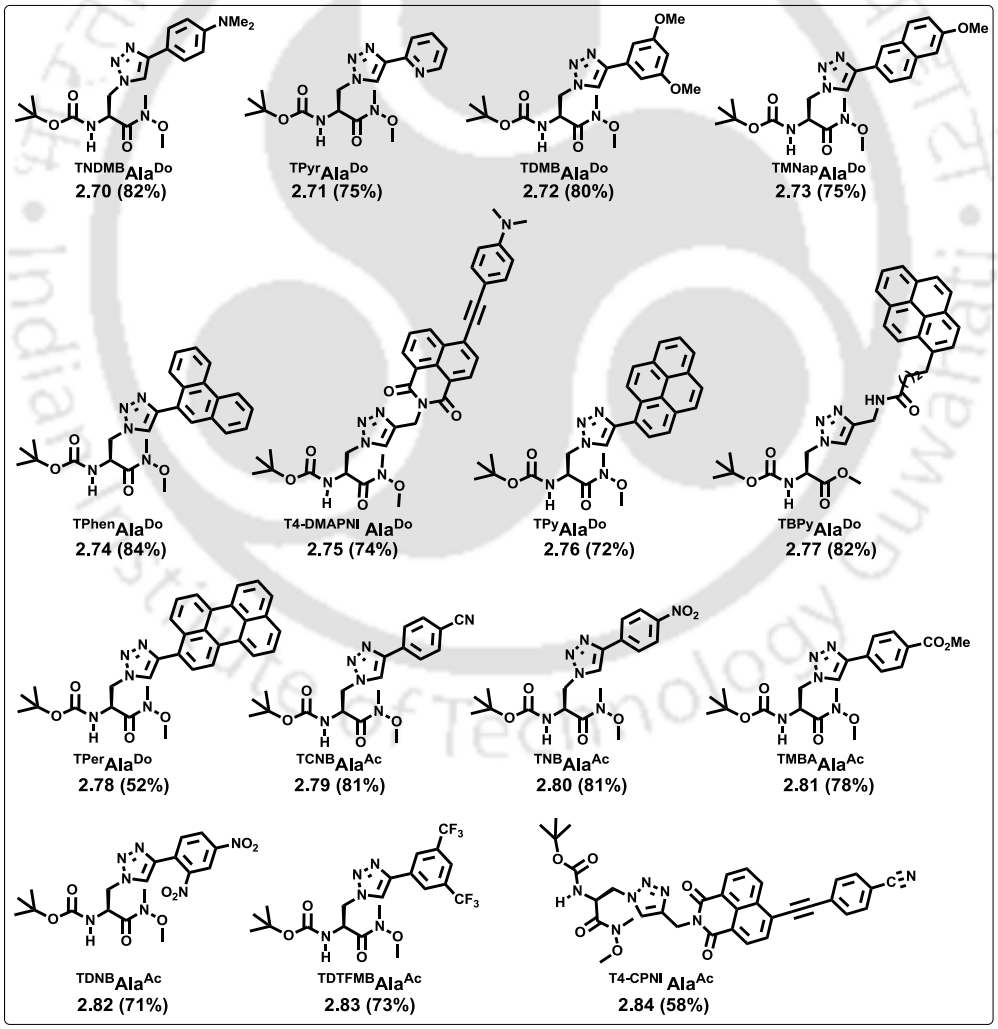

Figure 2.8. Structures of the synthesized N and C- terminal protected triazolyl donor/acceptor unnatural amino acids.

All the synthesized amino acids (^{T}**Ala**$^{Do/Ac}$) were purified by column chromatography and characterised by NMR and HRMS analysis. The structures of the synthesized N, C- protected triazolyl donor/acceptor unnatural amino acids are shown in **Figure 2.8**.

2.8.2 Spectral Characterization of Few Representative Triazolyl Unnatural Fluorescent Amino Acids

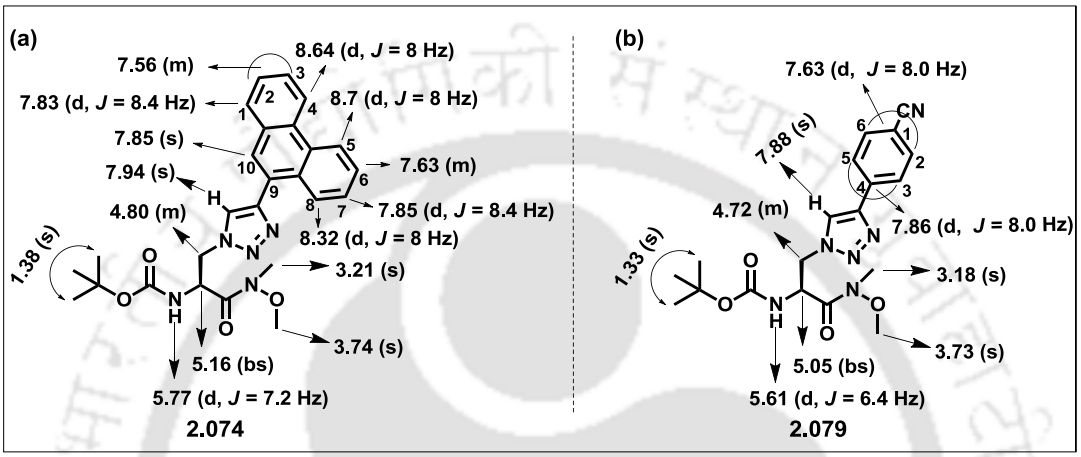

Figure 2.9. ^{1}H NMR of amino acid **2.074 (a)** and **2.079 (b)**

All the amino acids in the fully protected form were characterized mainly by NMR spectroscopy. As representative example the structural assignments of two protected triazolyl amino acids **2.074** and **2.079** are shown in **Figure 2.9**. For amino acid **2.074** (^{TPhen}**Ala**^{Do}), the triazolyl hydrogen appeared as a singlet at the characteristic position of δ 7.94. The C-α hydrogen of alanyl unit resonated as a broad singlet (bs) at δ 5.15. The β-CH_2 hydrogens of alanyl unit appeared as a mutiplet at δ 4.74. The ^{t}Bu hydrogens of Boc- protected group appeared as a singlet at δ 1.38. Methyl hydrogens of NMe and OMe group also resonated as a singlet at δ 3.21 and 3.74 respectively. The C-10 hydrogen of aromatic phenanthrene appeared at 7.85 as a singlet and C-1, C-4, C-5, C-7, C-8 hydrogens resonated as a doublet at δ 7.85, 7.83, 8.64, 8.70, 7.85, 8.32 respectively with coupling constant J = 8.4, 8, 8, 8.4 and 8 Hz. Other three aromatic hydrogens C-2, C-3 and C-6 appeared as a multiplet at δ 7.56 and 7.63 respectively. The N-H appeared as a doublet at δ 5.77 with coupling constant J = 7.2 Hz.

The chemical shift assignment for a representative acceptor aromatic substituted triazolyl unnatural amino acid **2.079** (^{TCNB}**Ala**^{Ac}) is shown in **Figure 2.9**. The detailed assignments are given in the experimental section.

2.8.3. Study of photophysical properties

After getting all the amino acids in hand, we studied their photophysical properites in organic solvents of varying polarities to check the solvatochromic nature. The UV–visible spectra of all the compounds (10 μm) were measured using a UV-visible spectrophotometer with a cell of 1 cm path length at 25 ^{o}C and 1 nm slit width. All the sample solutions were prepared before an hour of the measurement. Fluorescence emission spectra were recorded in a fluorescence spectrophotometer using a cell of 1 cm path length and 3 nm excitation/emission slit width at 25 ^{o}C. The excitation wavelengths for recording the emission spectra was set at maximum wavelength of absorbance (λ_{max}^{abs}) in each case. The fluorescence quantum yield (Φ_f) was determined using quinine sulphate as a reference with the known Φ_f = 0.54 in 0.1 molar solution in sulphuric acid.

From the UV-visible spectra it is clear that the amino acid **2.70** ($^{\mathbf{TNDMB}}\mathbf{Ala}^{\mathbf{Do}}$) containing a *N,N*-dimethylaminobenzene donor exhibited structureless broad absorption maxima at around 280-290 nm in various organic solvents. The absorption spectra experienced about ~7 nm red shift upon increasing the polarity of the solvents. Next, excitation at absorption maxima of each solvent showed fluorescence emission at around 360 nm with a red shift of 26 nm as the solvent polarity was increased. More strikengly, the fluorescence intensity become negligible in polar protic solvents like DMF and MeOH. The fluorescence quenching in polar/protic solvents could be attributed to the radiationless decay assisted by polar solvent–solute interaction or charge transfer or H-bonding interactions (**Figure 2.10a-b**, **Table 2.1**).[50]

Pyridyl triazolyl alanine amino acid **2.71** ($^{\mathbf{TPyr}}\mathbf{Ala}^{\mathbf{Do}}$) showed two absorption bands at around 240 and a long wavelength of absorbance at 285 nm in various organic solvents. Interestingly, the absorbance at 285 nm increases with a slight hypsocromic shift as the solvent porality increased indicating a solvatochromic nature of the amino acid and the band was characterised as charge transfer band. Upon excitation at absorption maxima of each solvent the amino acid showed negligible emission in nonpolar solvents but a strong emission at around 310-330 nm in polar and protic solvents. The intensity of emission gradually increased with slight hypsochromicity as the solvent polarity increases (**Figure 2.10c-d, Table 2.1**). The emission is thus unambiguously characterised as ICT emission. It is expected that in protic solvent like MeOH the pyridyl-N could involve in H-bonding interaction which ultimately would open the channel of charge transfer from donor triazole moiety to the protonated pyridine unit leading to an enhanced fluorescence intensity.[50h-i]

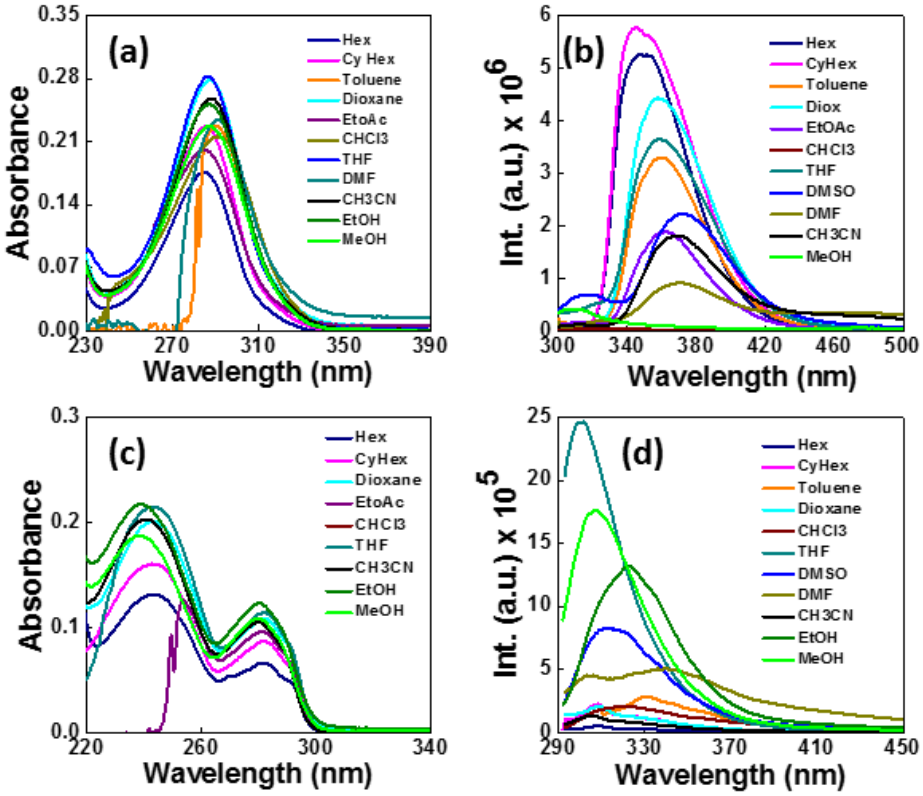

Figure 2.10. UV-visible absorption and fluorescence emission spectra of amino acids in various organic solvents; (a-b) for **2.70** (^{TNDMB}**Ala**^{Do}) and (c-d) for **2.71** (^{TPyr}**Ala**^{Do}). Excitation wavelength was the λ_{max}^{abs} in each solvent and the concentration of amino acids was 10 µM.

Table 2.1. Summary of photophysical properties of amino acids **2.70** (^{TNDMB}**Ala**^{Do}), **2.71** (^{TPyr}**Ala**^{Do}).

Entry →	**2.70 (^{TNDMB}Ala^{Do})**							
Solvents →	**Cyhex**	**Hex**	**Toluene**	**Diox.**	**EtOAc**	**THF**	**ACN**	**MeOH**
Δf	0.000	0.001	0.013	0.021	0.201	0.210	0.307	0.309
λ_{max}^{abs} **(nm)**	285	284	288	286	283	285	286	288
ε_{max} x 10^3	22.7	17.5	22.8	22.8	20.1	28.3	25.82	22.8
λ_{max}^{fl} **(nm)**	345	346	359	358	361	357	368	-----
Φ_f	0.24	0.26	0.15	0.15	0.08	0.13	0.07	-----
2.71 (^{Pyr}Ala^{Do})								
λ_{max}^{abs} **(nm)**	244, 283	244, 283	$CHCl_3$ 244, 281	245, 282	-----	242, 283	241, 281	244, 283
ε_{max} x 10^3	8.6	6.6	10.6	10.8	-----	11.4	10.5	10.8
λ_{max}^{fl} **(nm)**	318	308	309	321	-----	310	307	307
Φ_f	0.014	0.004	0.009	0.012	-----	0.046	0.007	0.045

The UV-visible spectra of amino acid **2.72 (**^{TDMB}**Ala**^{Do}**)** containing a triazolyl dimethoxybenzene aromatic unit displayed three absorption bands at around 260, 290 and 300 nm. The solvent polarity did not affect much on absorption property. Upon excitation at long wavelength absorption maxima (290-300 nm) showed strong emission at around 325 nm in low polar solvent and a red shifted (5-7 nm) emission with enhanced intensity in polar solvents like acetonitrile or methanol (**Figure 2.11a-b, Table 2.2**).

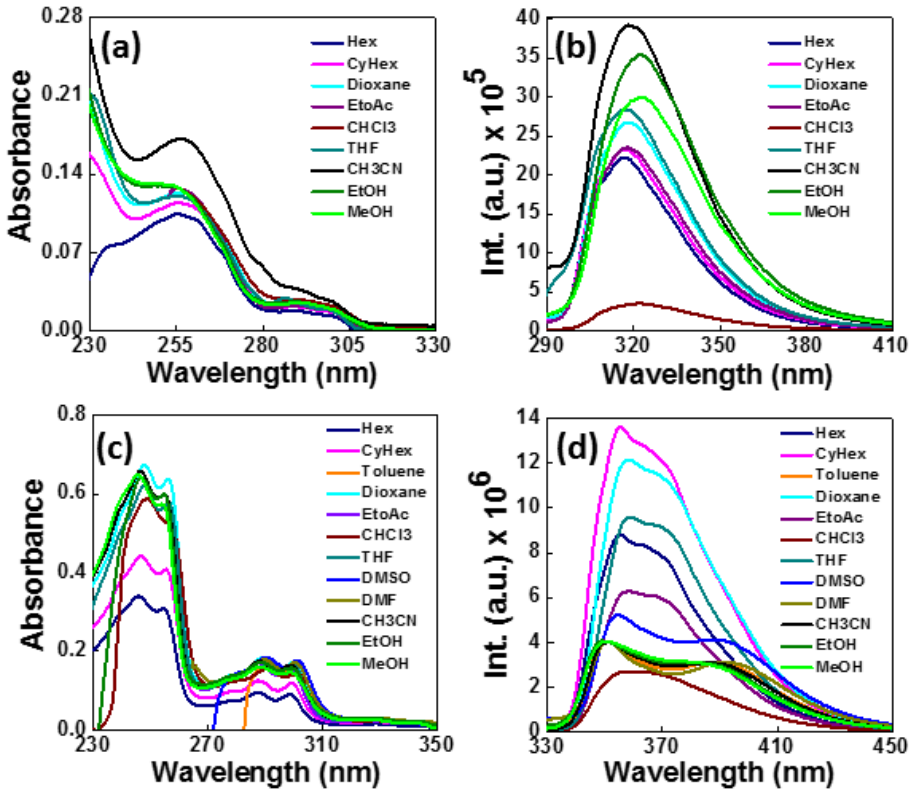

Figure 2.11. UV-visible absorption and fluorescence emission spectra of amino acids in various organic solvents; (a-b) for **2.72** (^{TDMB}**Ala**^{Do}) and (c-d) for **2.73** (^{TMNap}**Ala**^{Do}).

On the other hand, the triazolyl 6-methoxynaphthyl alanine amino acid **2.73** (^{TMNap}**Ala**^{Do}) exhibited solvatochromic and structured absorption bands at 290 and 305 nm. In low polar solvent like cyclohexane, dioxane, it exhibited broad structured emission band at around 350-380 nm; however, increasing solvent polarity the intensity decreases with a red shift of 15 nm indicating its ICT character when excited at 305 nm. The decrease in fluorescence intensity might be attributed to the radiadtionless decay caused due to solvent solute interaction, and H-bonding in protic polar solvents (**Figure 2.11c-d, Table 2.2**).[50] The quantum yield and time resolved fluorescence decay in various solvents followed the same trend as the steady state fluorescence for all the amino acids.

Table 2.2. Summary of photophysical properties of amino acids **2.72 (^{TDMB}Ala^{Do})**, **2.73 (^{TMNap}Ala^{Do})**

Entry →	**2.72 (^{TDMB}Ala^{Do})**							
Solvents →	**Cyhex**	**Hex**	**Diox**	**EtOAc**	**THF**	**EtOH**	**ACN**	**MeOH**
Δf	0.000	0.001	0.021	0.201	0.210	0.290	0.307	0.309
λ_{max}^{abs} **(nm)**	258, 301	257, 300	257, 301	256, 301	257, 300	255, 300	257, 299	254, 300
$\varepsilon_{max} \times 10^3$	21.9	18.1	24.7	22.6	29.6	26.2	37.5	25.3
λ_{max}^{fl} **(nm)**	318	318	318	319	317	323	320	323
Φ_f	0.034	0.035	0.037	0.032	0.42	0.055	0.042	0.047
2.73 (^{TMNap}Ala^{Do})								
λ_{max}^{abs} **(nm)**	288, 300	287, 300	289, 302	288, 300	289, 300	290, 300	288, 300	289, 300
$\varepsilon_{max} \times 10^3$	11.9	9.0	17.4	16.2	16.8	15.8	16.6	14.7
λ_{max}^{fl} **(nm)**	356, 365	355, 363	358, 368	358, 367	359, 368	350, 388	351, 391	350, 388
Φ_f	0.287	0.232	0.269	0.156	0.246	0.121	0.119	0.129
$<\tau>$**[ns]**	----	-----	8.81	-----	-----		7.11	7.23

The amino acid ^{TPhen}Ala^{Do} (**2.74**) exhibited broad and solvatochromic absorption band at around 299-305. The charge transfer absorption band exhibited 10 nm blue shift as the solvent polarity increases. Upon excitation at 300 nm, ^{TPhen}Ala^{Do} showed structured emission at around 400 nm. However, increasing solvent polarity the quantum yields increases (**Figure 2.12a-b, Table 2.3**). On the other hand, donor-acceptor triazolyl 4-(4-N,N-dimethylaminophenylethynyl)-N-(2-propynyl)-1,8 naphthalimide amino acid $^{T4\text{-}DMAPNI}$Ala^{Do} **(2.75)** revealed structureless absorption bands at 300 nm and 443 nm. Changing the solvent polarity from dioxane to ethanol the absorption band at 443 nm experienced a red shift of 9 nm with an increase in intensity (**Figure 2.12c-d, Table 2.3**). The long wavelength and fairly broad solvatochromic band suggested that the ground state of the molecule was significantly polar and thus was unambiguously assigned as intramolecular charge transfer (ICT) band. When excited at absorption maxima, it showed a structureless broad emission band. As the solvent polarity increases from dioxane to chloroform, a strong red shift of about 31 nm ($\lambda_{max,\ Dioxane}$ 580 nm, and $\lambda_{max,\ chloroform}$ 611 nm) was observed which showed a decrease in both the fluorescence intensity and the quantum yield (**Figure 2.12c-d, Table 2.3**).

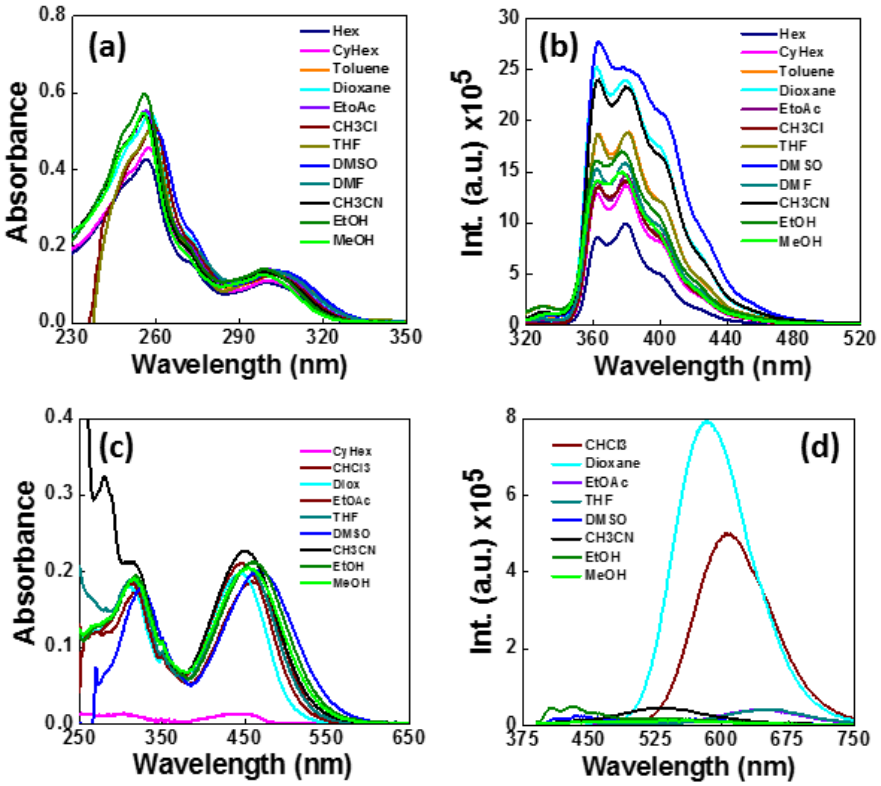

Figure 2.12. UV-visible absorption and fluorescence emission spectra of amino acids in various organic solvents; (a-b) for **2.74** (**^{TPhen}Ala^{Do}**) and (c-d) for **2.75** (**$^{T4\text{-}DMAPNI}$Ala^{Do}**).

Table 2.3. Summary of photophysical properties of amino acids **2.74** (**^{TPhen}Ala^{Do}**), **2.75** (**$^{T4\text{-}DMAPNI}$Ala^{Do}**).

Entry →	**2.74 (^{TPhen}Ala^{Do})**							
Solvents →	**Diox**	**$CHCl_3$**	**EtOAc**	**THF**	**DMF**	**EtOH**	**ACN**	**MeOH**
Δf	0.021	0.148	0.201	0.210	0.275	0.290	0.307	0.309
λ_{max}^{abs} **(nm)**	258, 302	257, 303	259, 303	258, 301	273, 304	256, 300	255, 301	255, 299
$\varepsilon_{max\ X}\ 10^3$	13.9	12.6	14.07	13.7	13.6	14.1	13.2	12.7
λ_{max}^{fl} **(nm)**	363, 380	365, 381	363, 380	364, 382	364, 382	364, 379	363, 380	364, 379
Φ_f	0.32	0.18	0.17	0.24	0.32	0.22	0.20	0.21
$<\tau>$**[ns]**	22.6						13.2	14.2
2.75 ($^{T4\text{-}DMAPNI}$Ala^{Do}).								
λ_{max}^{abs} **(nm)**	444	462	446	453	**DMSO** 469	461	450	453
$\varepsilon_{max\ X}\ 10^3$	19.6	18.5	20.9	20.4	19.9	21.1	22.6	20.4
λ_{max}^{fl} **(nm)**	583	606	645	652	435, 555	431, 549	633	552
Φ_f	0.328	0.225	-----	-----	0.023	0.025	0.025	-----

Therefore, the amino acid **2.75** is highly solvatochromic. The conjugation between the *N*,*N*-dimethyl aminophenyl acetylenic moiety as an electron donor and the naphthalimide core as an electron acceptor played an important role in the large dipole change during excitation and made it highly solvatochromic. However, in aprotic and protic polar solvents negligible emission was observed which might be again due to solvent-solute dipolar interaction and H-bonding mediated radiationless decay.[50]

While triazolyl-pyrenyl-alanine **2.76** (^{TPy}**Ala**^{Do}) showed unstructured broad absorption band at around 348 nm (**Figure 2.13a-b, Table 2.4**), amino acid **2.77** (^{TBAPy}**Ala**^{Do}), pyrenebutaramido triazolyl alanine, displayed characteristic structured absorption bands of pyrene at 313, 327 and 343 nm, in various organic solvents (**Figure 2.13c-d, Table 2.4**). As the solvent polarity increases the absorption experienced a slight blue shift (3 nm) in case of amino acid **2.76**. The disappearance of pyrene structural band in **7** could easily be explained if we consider a strong electronic coupling between the π-cloud of pseudoaromatic triazole and directly linked pyrene (**Figure 2.13a-b**).

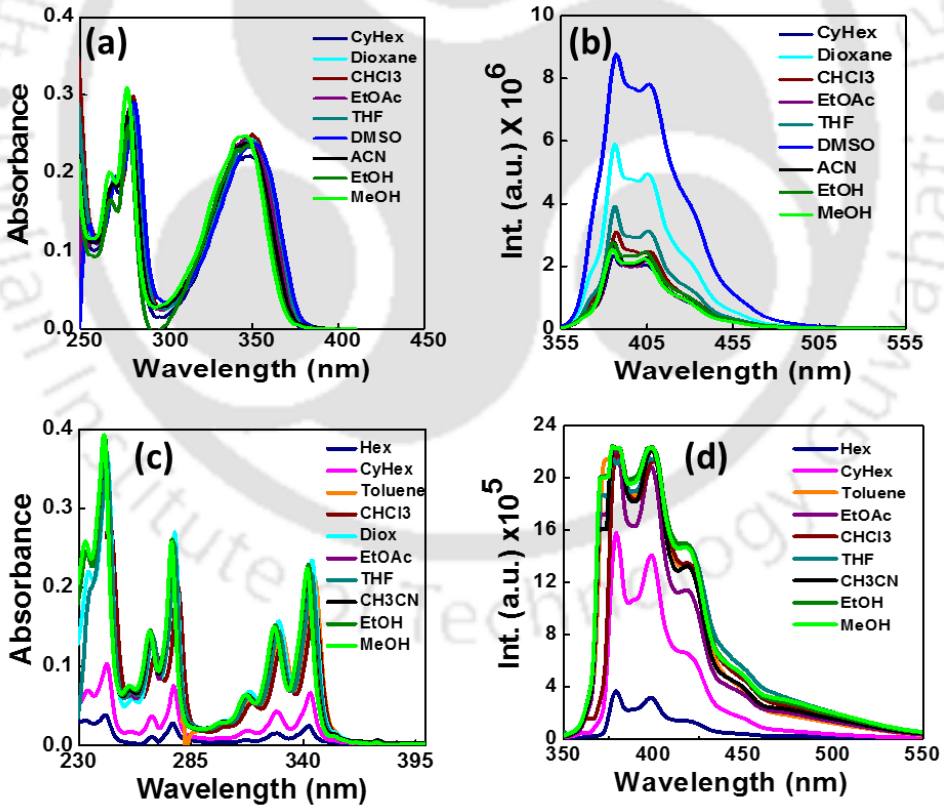

Figure 2.13. UV-visible absorption and fluorescence emission spectra of amino acids in various organic solvents; (a-b) for **2.76** (^{TPy}**Ala**^{Do}) and (c-d) for **2.77** (^{TBAPy}**Ala**^{Do}).

Due to this reason amino acid **2.76** showed a hypsochromic shift of 6-8 nm when solvent polarity increased. However, when excited on their absorption maxima while amino acids **2.77** showed structured emissions at 379, 399 and 418 nm, amino acid **2.76** showed emissions at 389, 407 and 425 nm with a red shift (8-10 nm) of all vibronic bands. The intensity of amino acid **2.77** did not alter much with increasing solvent polarity. The quantum yield and time resolved fluorescence decay in various solvents followed the same trend as the steady state fluorescence for both the cases. On the other hand, amino acid **2.76** experienced a gradual decrease in emission intensity as the solvent polarity increases indicating a solvent-solute or hydrogen bonding interaction mediated fluorescence quenching.[50]

Table 2.4. Summary of photophysical properties of amino acids **2.76 (^{TPy}Ala^{Do}), 2.77 (^{TBAPy}Ala^{Do}).**

Entry →	**2.76 (^{TPy}Ala^{Do})**							
Solvents →	**Cyhex**	**Diox**	**$CHCl_3$**	**EtOAc**	**THF**	**EtOH**	**ACN**	**MeOH**
Δf	0.000	0.021	0.148	0.201	0.210	0.290	0.307	0.309
λ_{max}^{abs} **(nm)**	279, 347	280, 349	280, 349	279, 348	281, 349	279, 347	278, 346	277, 344
$\varepsilon_{max\ X}\ 10^3$	22.1	25.0	25.0	24.3	24.1	23.5	23.9	24.8
λ_{max}^{fl} **(nm)**	385, 405	387, 406	386, 405	385, 406	386, 406	385, 405	385, 405	385, 404
Φ_f	0.126	0.146	0.292	0.123	0.183	0.147	0.130	0.120
$\langle\tau\rangle$ **[ns]**	----	34.1	----	----	----	----	15.16	17.42
2.77 (^{TBAPy}Ala^{Do}).								
λ_{max}^{abs} **(nm)**	327, 343	**Tol.** 345	329, 345	326, 342	327, 344	326, 342	327, 3444	325, 341
$\varepsilon_{max\ X}\ 10^3$	6.64	21.1	18.1	21.9	21.8	22.8	21.7	22.3
λ_{max}^{fl} **(nm)**	379, 398	376, 399	379, 400	379, 398	379, 398	379, 398	379, 397	379, 399
Φ_f	0.255	0.13	0.148	0.163	0.153	0.212	0.188	0.260
$\langle\tau\rangle$ **[ns]**	----	25.8	----	----	----		13.9	14.5

The triazolylperylene amino acid **2.78** (^{TPer}Ala^{Do}) exhibited tuned absorption and fluorescence property compared to perylene indicating a donor-acceptor character. The electron charge density of triazole moiety probably redistributed with the electron deficient aromatic ring of perylene. Because of this charge transfer it showed structured absorption at longer wavelength (399, 422 and 449 nm) than the

characteristic absorption of perylene (387, 409, 435 nm in cyclohexane). As solvent polarity increases from chloroform to methanol, amino acid **2.78** showed hypsochromic shift of 9 nm. Upon excitation at 425 nm, it exhibited less-structured emission at longer wavelength (470 and 502 nm) than perylene (437, 462 and 497 nm). Moreover, the emission of **2.78** experienced a hypsochromic shift of 9-10 nm as the polarity of the solvent increases (**Figure 2.14a-b, Table 2.5**). The quantum yield and time resolved fluorescence decay in various solvents followed the same trend as the steady state fluorescence.

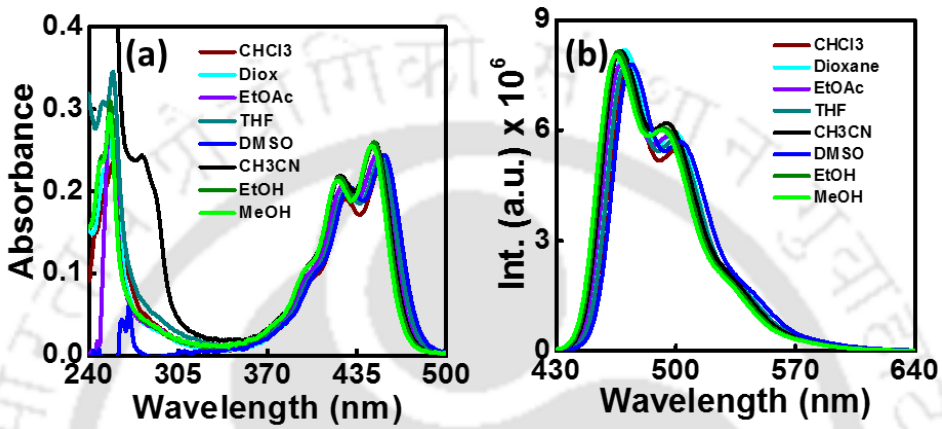

Figure 2.14. UV-visible and fluorescence spectra of amino acid **2.78 (^{TPer}Ala^{Do})** (a-b) in various organic solvents (concentration of amino acids was 10 μM).

Table 2.5. Summary of photophysical properties of amino acids **2.78 (^{TPer}Ala^{Do}).**

Entry →	**2.78 (^{TPer}Ala^{Do})**							
Solvents →	**Diox.**	**$CHCl_3$**	**EtOAc**	**THF**	**DMF**	**EtOH**	**ACN**	**MeOH**
λ_{max}^{abs} **(nm)**	425, 451	427, 452	424, 450	427, 452	429, 455	422, 448	423, 448	420, 446
ε_{max} x 10^3	24.4	22.9	24.4	24.1	24.5	26.0	26.0	25.5
λ_{max}^{fl} **(nm)**	470, 499	471, 500	468, 496	470, 499	474, 502	466, 493	467, 494	465, 492
Φ_f	0.82	0.81	0.78	0.79	0.82	0.77	0.78	0.81
$\langle\tau\rangle$ **[ns]**	----	----	----	----	----	----	4.1	4.2

The amino acid **2.79** (^{TCNB}Ala^{Ac}) containing a triazolyl cyanobenzene aromatic unit as an acceptor possessed strong structure-less absorption at 287 nm in low polar solvent toluene. The absorbance was characterized by a hypsochromic shift of about 10-15 nm as the polarity of the solvent increases. Excitation at 280 nm it showed emission at around 315 nm in toluene which became broad as the solvent polarity

increases. An appearance of an extra band at 335 nm was observed in dioxane which shifted to 358 nm in MeOH. The high intense solvatochromic band was most probably the ICT emission indicating a charge transfer from donor triazolyl moiety to acceptor cyanobenzene moiety (**Figure 2.15a-b, Table 2.6**). On the other hand triazolyl nitrobenzene alanine amino acid ^{TNB}**Ala**^{Ac} (**2.80**) exhibited a strong solvatochromic (hypsochromic) absorbance at 315 nm. However, excitation upon absorbance maxima, it emitted very weak emission band at 355 nm which showed a red shift (of 15 nm) and decreasing intensity of emission as the solvent polarity increases which might be because of polar solvent-solute interaction leading to quenching of fluorescence via dipolar/ H-bonding interaction (**Figure 2.15c-d, Table 2.6**).[50] The quantum yield and time resolved fluorescence decay in various solvents followed the same trend as the steady state fluorescence for both the amino acids.

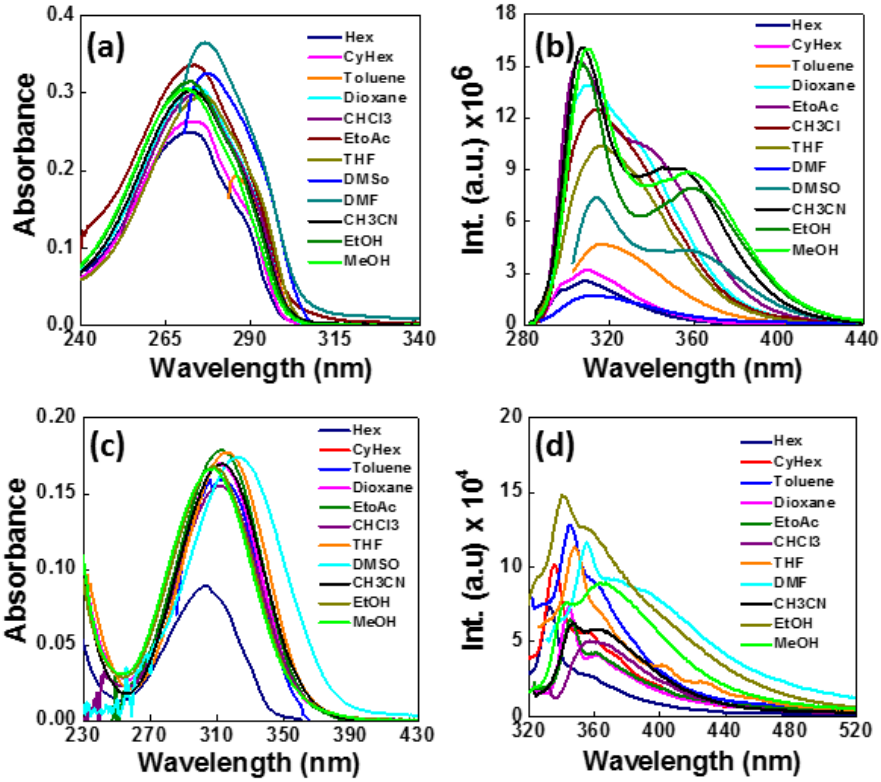

Figure 2.15. UV-visible absorption and fluorescence emission spectra of amino acids in various organic solvents; (a-b) for **2.79** (^{TCNB}**Ala**^{Ac}) and (c-d) for **2.80** (^{TNB}**Ala**^{Ac}).

Table 2.6. Summary of photophysical properties of amino acids **2.79** (**^{TCNB}Ala^{Ac}**), **2.80** (**^{TNB}Ala^{Ac}**)

Entry →	**2.79 (^{TCNB}Ala^{Ac})**							
Solvents →	**Cyhex**	**Diox.**	**$CHCl_3$**	**EtOAc**	**DMF**	**EtOH**	**ACN**	**MeOH**
λ_{max}^{abs} **(nm)**	272	272	273	273	276	271	271	270
$\varepsilon_{max\ X}\ 10^3$	26.3	35.1	33.6	29.8	32.5	31.5	30.4	30.5
λ_{max}^{fl} **(nm)**	310	310, 336	314	306, 338	320	308, 360	307, 352	310, 358
Φ_f	0.09	0.30	0.32	0.34	0.04	0.33	0.36	0.37
<τ> [ns]	----	1.4	----	----	----	----	1.9	3.2
2.80 (^{TNB}Ala^{Ac})								
λ_{max}^{abs} **(nm)**	313	309	314	312	316	304	308	304
$\varepsilon_{max\ X}\ 10^3$	15.5	16.9	15.4	17.9	16.2	16.8	16.9	16.5
λ_{max}^{fl} **(nm)**	356	359	358	357	376	352	357	360
Φ_f	0.003	0.002	0.002	0.002	0.007	0.007	0.002	0.004

The 3,5-trifluoromethylphenyl triazolyl alanine amino acid **^{TDTFMB}Ala^{Ac}** (**2.83**) showed strong broad absorbance at 260 nm which experienced a negligible solvatocromicity. Upon excitation at its absorbance maxima it emitted at 315 nm in cyclohexane which shifted to 329 nm in acetonitrile/methanol. The emission was characterised by a bathochromic shift of 14 nm and a hyperchromic effect as the solvent polarity increases (**Figure 2.16a-b, Table 2.7**). This might be because of internal charge transfer process from donor triazolyl unit to acceptor 3,5-trifluoromethyl benzene in polar solvent. On the other hand, amino acid **2.84**, (**$^{T4\text{-}CPNI}$Ala^{Ac}**) which is an analogue of amino acid **2.75** but with an acceptor cyanophenyl acetyleneic moiety exhibited strong absorption at 351, 369 and 389 nm. The absorption spectra of **2.84** showed a little hypsochromic shift as the polarity of solvent increases. It exhibited structured emission at 404 and 424 nm in low polar solvent like dioxane, ethyl acetate, THF and structureless emission at 435 nm in polar solvents such as acetonitrile, methanol, and ethanol (λ_{ex} = 370 nm). The emission experienced bathochromic shift of about 10 nm with increased intensity and quantum yield (**Figure 2.16c-d, Table 2.7**).

While amino acid **2.75** experienced a large dipole change due to its donor-acceptor character, the amino **2.84** having acceptor-acceptor character did not show such dipole change in increasing the solvent dielectric constant. Therefore, these two amino acids behave oppositely-which was also reflected in the emission intensity as well as in quantum yield.

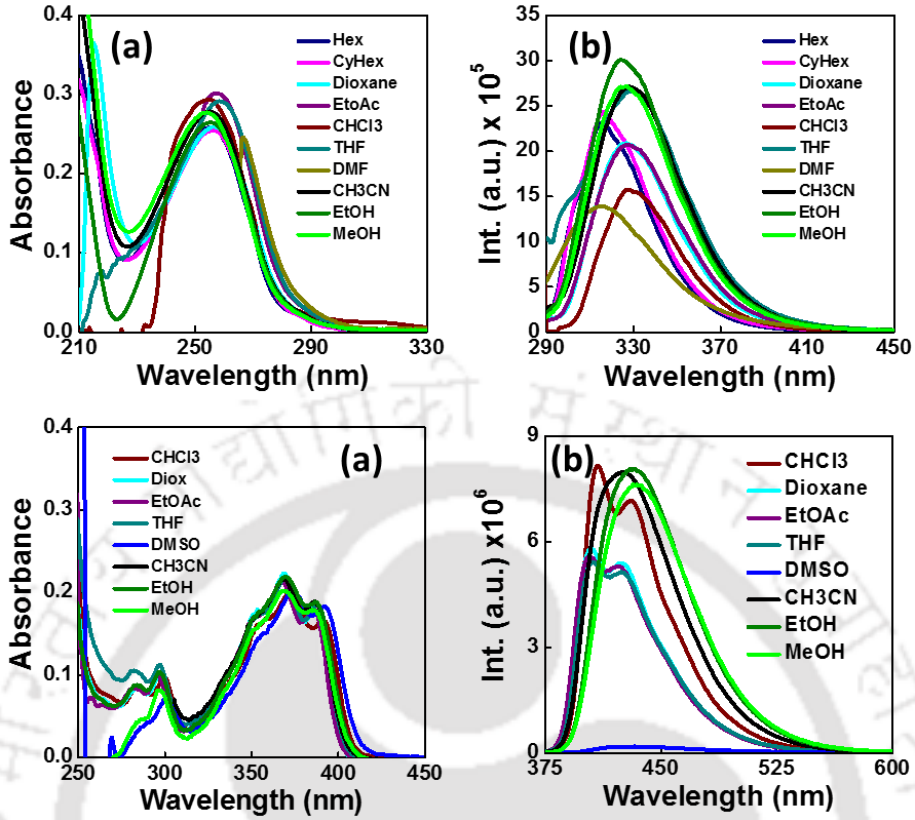

Figure 2.16. UV-visible absorption and fluorescence emission spectra of amino acids in various organic solvents; (a-b) for **2.83** (**$^{TDTFMB}Ala^{Ac}$**) and (c-d) for **2.84** (**$^{T4\text{-}CPENI}Ala^{Ac}$**).

Table 2.7. Summary of photophysical properties of amino acids **2.83** (**$^{TDTFMB}Ala^{Ac}$**), **2.84** (**$^{T4\text{-}CPENI}Ala^{Ac}$**).

Entry →	**2.83 ($^{TDTFMB}Ala^{Ac}$)**							
Solvents →	**Diox**	**$CHCl_3$**	**EtOAc**	**THF**	**DMF**	**EtOH**	**ACN**	**MeOH**
Δf	0.021	0.148	0.201	0.210	0.265	0.290	0.307	0.309
λ_{max}^{abs} **(nm)**	260	257	258	258	266	253	253	252
ε_{max} $x\ 10^3$	25.9	29.2	30.1	29.1	24.6	26.4	27.8	27.7
λ_{max}^{fl} **(nm)**	328	330	329	330	317	325	330	328
Φ_f	0.060	0.040	0.054	0.084	0.046	0.093	0.083	0.085
	2.84 ($^{T4\text{-}CPENI}Ala^{Ac}$)							
λ_{max}^{abs} **(nm)**	369, 388	373, 391	369, 388	369, 386	**DMSO** 392	369, 387	369, 386	368, 385
ε_{max} $x\ 10^3$	18.6	16.5	18.02	18.4	18.3	18.8	18.9	17.9
λ_{max}^{fl} **(nm)**	405, 426	408, 430	403, 422	405, 425	432	431	425	435
Φ_f	0.42	0.64	0.44	0.41	0.02	0.63	0.62	0.68

Therefore, all the triazolyl aromatic amino acids showed a significantly more solvatochromic absorption and emission properties compared to their parent donor/acceptor aromatics. This is attributed to the electronic coupling of triazolyl moiety with π-cloud of aromatic chromophoric unit. The quantum yield and time resolved fluorescence decay in various solvents followed the same trend as the steady state fluorescence for all the amino acids.

Next, the solvatochromic behaviors, particularly ICT originated solvofluorochromicity, of amino acids **2.70**, **2.73**, **2.78** and **2.79** was studied via the correlations of their absorption ($\tilde{\nu}_{max}^{abs}$) and fluorescence maxima ($\tilde{\nu}_{max}^{fl}$) with the solvent polarity function Δf. A linear correlation between the $\tilde{\nu}_{abs}$ and Δf was reflected from the plots in **figure 2.17a, d** that indicated that the ground states of these fluorescent amino acids are moderately polar in nature. However, much more linear correlation was observed between $\tilde{\nu}_{fl}$ and Δf for all these aforementioned amino acids suggesting that the nature of the fluorescent states remained essentially unchanged in all the solvents though solvent induced modulation was reflected in the spectral features.[51a] That the fluorescent states of these amino acids are highly polar in nature and of ICT character was also reflected in the reasonably high slopes of the $\tilde{\nu}_{fl}$ vs Δf plots (**Figure. 2.17a-b**, **d-e**).[52] Moreover, a plot of Stokes' shift ($\Delta\tilde{\nu}$) in different solvents against solvent polarity parameter Δf also showed a good linear correlation with large slopes indicating the highly polar nature of fluorescence states of all the amino acids said above (**Figure. 2.17c, f**).

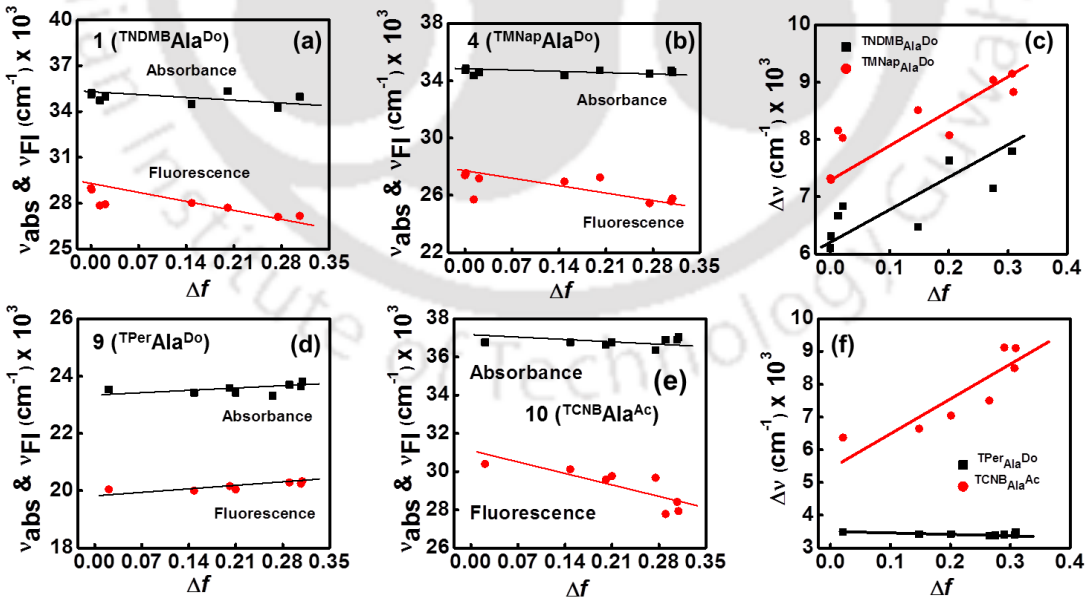

Figure 2.17. Plots of $\tilde{\nu}_{fl}/\tilde{\nu}_{abs}$ and $\Delta\tilde{\nu}$ (Stock shift) against Δf for amino acids **2.70** (a), **2.73** (b), **2.70-2.73** (c), **2.78** (c), **2.79** (d) and **2.78-2.79** (f) in different solvents.

2.9. Study of Possible Photophysical Interaction Among a Donor/Acceptor Pair of Triazolyl Unnatural Fluorescent Amino Acids

Next, we were interested to know whether a mixture of donor-acceptor triazolyl amino acids involved in photophysical interaction. Thus, we titrated a solution of a representative acceptor triazolyl amino acid ^{TCNB}**Ala**^{Ac} (**2.79**) with increasing concentration of a donor triazolyl amino acid, ^{TPhen}**Ala**^{Do} (**2.74**) and measured absorption and emission properties in acetonitrile solvent. A solution of 1: 1 mixture of donor-acceptor amino acids and various other concentration ratios showed characteristic absorptions of both the donor and acceptor amino acids indicating that there was no possibility of ground state charge transfer complexation (**Figure. 2.18**). Next a fluorescence titration experiment was carried out. Thus, upon excitation at absorption maxima of ^{TCNB}**Ala**^{Ac} (λ_{ex} = 270 nm) the emission at 330 nm gradually decreased as the concentration of donor amino acid ^{TPhen}**Ala**^{Do} increases (**Figure. 2.18b**).

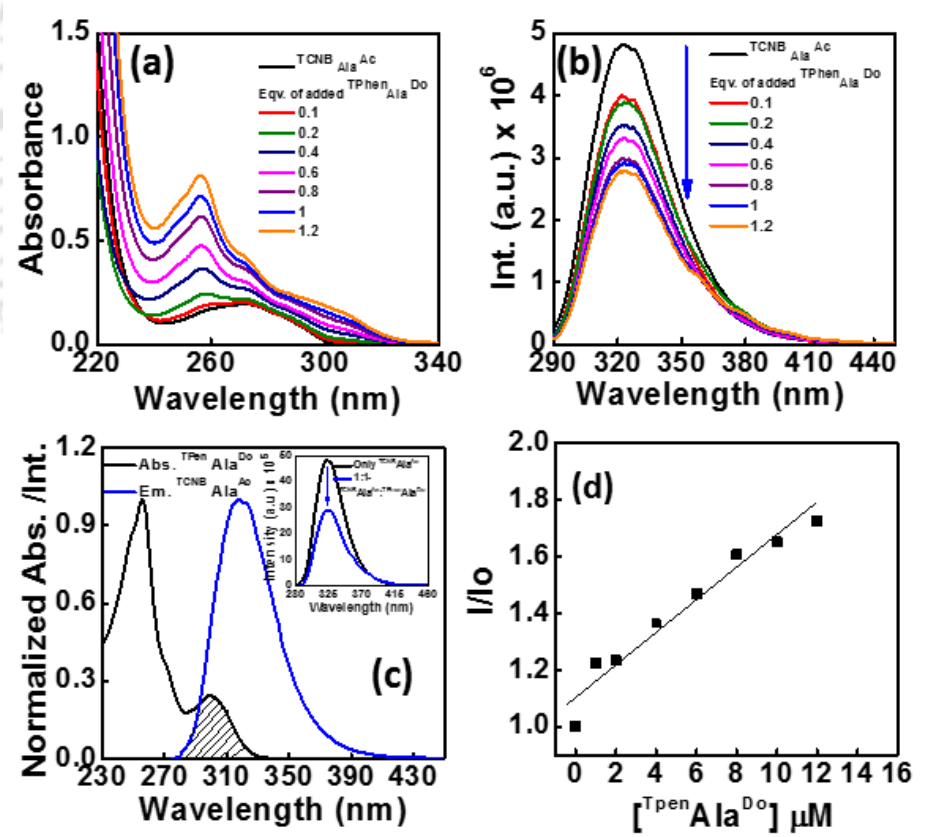

Figure 2.18: UV-visible (a), fluorescence (b) titration spectra of acceptor amino acid **2.79** (^{TCNB}**Ala**^{Ac}) with donor amino acid **2.74** (^{TPhen}**Ala**^{Do}). (c) Overlapped of absorption and fluorescence spectra of **2.74** and **2.79**, respectively. (d) Stern-Volmer plot.

This observation clearly indicated a fluorescence quenching of ^{TCNB}**Ala**^{Ac} in presence ^{TPhen}**Ala**^{Do} via a dynamic quenching process as the static mode of quenching was ruled out from the UV-visible spectroscopic study. The above result of fluorescence knocked us to relook and we observed that emission spectra of ^{TCNB}**Ala**^{Ac} overlapped significantly with the absorption spectra of ^{TPhen}**Ala**^{Do} indicating a possibility of quenching of emission of ^{TCNB}**Ala**^{Ac} via a dynamic quenching mode, the FRET.[53] Therefore, in the mixture, the acceptor triazolyl amino acid ^{TCNB}**Ala**^{Ac} acts as FRET donor and the donor amino acid ^{TPhen}**Ala**^{Do} acts as a FRET acceptor. Therefore as the concentration of FRET acceptor (^{TPhen}**Ala**^{Do}) increases the fluorescence of the FRET donor (^{TCNB}**Ala**^{Ac}) decreases (**Figure. 2.18c**). Stern-Volmer quenching constant was found to be 6 x 10^{-2} (**Figure. 2.18d**). Therefore, a favorable photophysical interaction via FRET was observed between these amino acids pair which might be of great importance in designing FRET-peptide probe usable for studying peptide-protein/protein-protein interaction.[54]

2.10. Theoretical Calculations

Next, to examine the effect of solvent polarity on the absorption and emission property of donor/acceptor aromatic triazolyl amino acids, we studied the TDDFT calculation using Gaussian 09 program package.[55] From the HOMO-LUMO overlap and transition oscillator strength (f) of the donor/acceptor aromatic triazolyl amino acids it was clear that the electronic transition from S_o to S_1 or other possible electronic transitions are feasible. So the reverse transition *i.e.*, $S_0 \leftarrow S_1$, was also fully allowed that revealed the fluorophoric nature of triazolyl unnatural amino acids. Solvatochromicity and intramolecular charge transfer emissions were also explained by redistribution of electronic charge density between HOMO-LUMO (**Figure 2.19-2.20**).[51, 52]

As for example, from the TDDFT calculations the dominant orbital transitions in the low-lying singlet excited states of the studied amino acids is the $S_0 \rightarrow S_1$ transition having highest configuration interaction (CI) values. Thus, the calculated excitation energy for the transition from $S_0 \rightarrow S_1$ of donor triazolyl amino acids ^{TNDMB}**Ala**^{Do} (**2.70**), ^{TMNap}**Ala**^{Do} (**2.73**), ^{TPhen}**Ala**^{Do} (**2.74**), ^{TPy}**Ala**^{Do} (**2.76**) and ^{TPer}**Ala**^{Do} (**2.78**) were found to be 327 (3.8 ev, f = 0.05, CI = 0.7); 324 nm (3.8 ev, f = 0.15, CI = 0.67); 308 nm (4.03 ev, f = 0.19; CI = 0.63); 356 nm (3.48 ev, f = 0.55; CI = 0.69) and 449 nm (2.76 ev, f = 0.56; CI = 0.71) (in vacuum), respectively. These values were in close agreement with the experimental result of 285 nm (cyclohexane), 290 nm (in hexane), 300 nm (in hexane), 310 nm (in hexane), 348 nm (in hexane) and 449 nm (in chloroform) respectively. For amino acid **2.70**, the $S_0 \rightarrow S_1$ transition in lowest excited state appeared at much longer wavelength of 324 nm (f = 0.146) which was far from the experimental value. However, both the transitions at 270 nm (4.54 ev; f = 0.76) in vacuum in the second excited state [$S_0 \rightarrow S_3$ (HOMO→LUMO+2); CI = 0.69]; and

[$S_0 \rightarrow S_2$ (HOMO→LUMO+1; CI = 0.49] correlated well with the observed absorbance at 290 nm (in hexane).[51, 52]

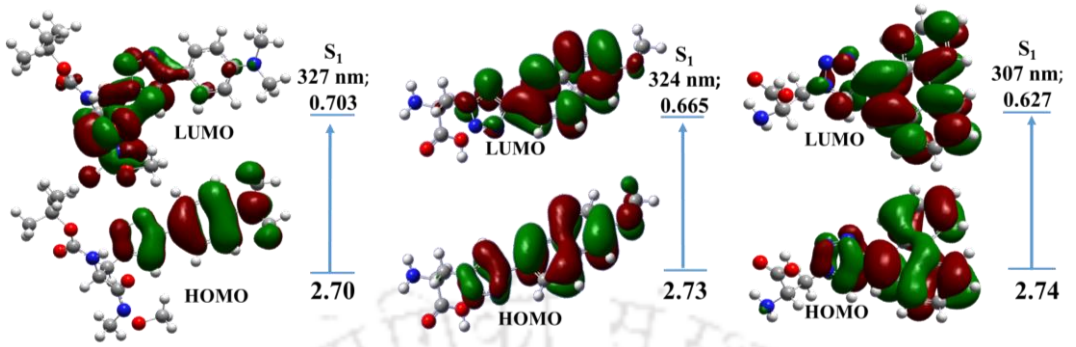

Figure 2.19. Diagram of HOMO-LUMO of amino acids **2.70**, **2.73** and **2.74** calculated at B3LYP//6-31G* level of theory using Gaussian 09 program package.

The emission spectra for all the donor triazolyl amino acids also showed solvatochromic effect and bathochromic shift due to electronic charge redistribution between triazole moiety and fluorophoric unit which was also reflected from their individual HOMO-LUMO diagrams. The emissive states of all the donor triazolyl amino acids were found to be locally excited (LE) states except for the case of amino acid **2.70** (^{TNDMB}**Ala**^{Do}) as was suggested by the HOMO−LUMO distributions. In case of amino acid **2.70** the emissive state was characterized with more significant electron redistribution, *i.e.*, ICT feature. Calculated results of HOMO−LUMO distribution supported our conclusion. [28a,30]

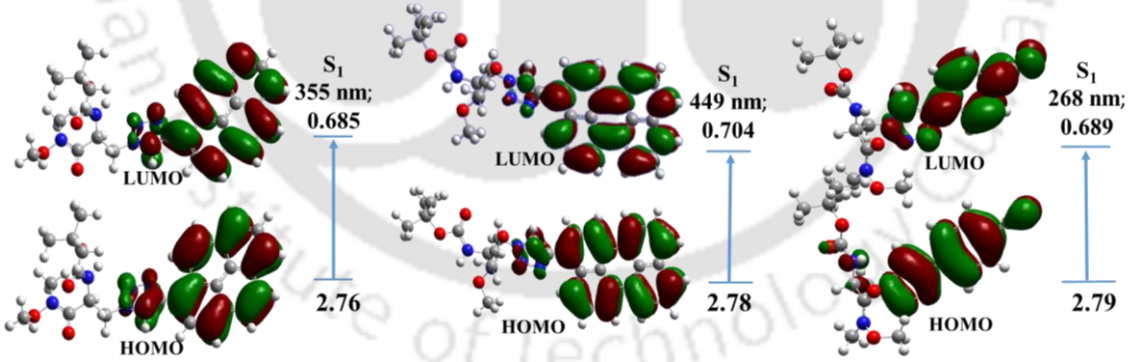

Figure 2.20. Diagram of HOMO-LUMO of amino acids **2.76**, **2.78** and **2.79** calculated at B3LYP//6-31G* level of theory using Gaussian 09 program package.

On the other hand, the dominant orbital transitions in the low-lying singlet excited states of acceptor triazolyl amino acids were found to be $S_0 \rightarrow S_1$ (HOMO→LUMO) for both ^{TCNB}**Ala**^{Ac} (**2.79**) and ^{TNB}**Ala**^{Ac} (**2.80**) with transition wavelength of 268 nm (4.62 ev, f = 0.77; CI = 0.69) and 334 nm (3.71 ev, f = 0.47; CI = 0.70), respectively, in vacuum. These values were in close agreement with the experimental results of 271

and 300 nm in hexane for acceptor triazolyl amino acids **2.79** and **2.80**, respectively. Thus, as revealed from the overlapping of HOMO-LUMO as well as the transition oscillator strength (*f*), the electronic transitions of $S_0 \rightarrow S_1$ are fully allowed for all the acceptor amino acids. This means that reverse transition, *i.e.*, $S_0 \leftarrow S_1$, was also fully allowed indicating their potential fluorophoric nature. The emissive state of $^{TCNB}\mathbf{Ala}^{Ac}$ (**2.79**) showed dual emission at 320 and 360 nm which were well characterized with more significant electron redistribution, *i.e.*, ICT feature which were again supported by the HOMO−LUMO distributions. However, the emissive state of acceptor amino acid $^{TNB}\mathbf{Ala}^{Ac}$ (**2.80**) was basically a locally excited (LE) state as was suggested by the HOMO−LUMO distributions. [51, 52]

The emission spectra for all the donor triazolyl amino acids also showed solvatochromic effect and bathochromic shift due to electronic charge redistribution between triazole moiety and fluorophoric unit which was also reflected from their individual HOMO-LUMO diagrams.

2.11. Study of Interaction of Amino Acid 2.78 ($^{TPer}\mathbf{Ala}^{Do}$) with BSA Protien

Finally, we explored the novel triazolyl perylene amino acid **2.78** ($^{TPer}\mathbf{Ala}^{Do}$) as a possible probe for sensing BSA protein.[56] We envisaged that the triazolylperylene would sense the interaction with BSA via the generation of an enhanced fluorescence signal.[57]

***Study of UV-visible and Fluorescence Photophysical Properties of Triazolyl Perylene Amino Acid (2.78) in Presence of BSA*:** The UV-visible absorption of amino acid **2.78** in phosphate buffer showed a structureless absorption at around 375 nm and weak bands at 440 nm. Addition of an increasing concentration of BSA to the probe solution resulted in a structured absorption at 425 and 450 nm characteristic of perylene which experienced strong hyperchromicity in absorbance. The BSA absorption at 280 nm also shifted to 295 nm. These observations indicated a strong binding interaction between BSA and amino acid **2.78** in the hydrophobic region (**Figure. 2.21a**).

To get more insight into the binding event we next carried out fluorescence titration experiment. In phosphate buffer the amino acid **2.78** showed extremely weak emission at 470 and 495 nm. Upon gradual addition of an increasing amount of BSA, the emission intensity of the probe **2.78** gradually increased when excited at the absorption maximum of **TPer** (420 nm) indicating a strong interaction between the probe and hydrophobic pocket of BSA (**Figure. 2.21b**). The drastic enhancement of fluorescence of **TPer** could be explained if we consider that the **TPer** moiety got accommodated in the hydrophobic pocket of BSA. This was also supported from a solvatochromic emission of **TPer** in various organic solvents. That the **TPer** moiety

of probe **2.78** bound strongly inside the hydrophobic pocket of BSA and experienced a highly restricted rotational motion was supported by a large enhancement of fluorescence anisotropy from 0.02 to 0.3 (**Figure 2.21c**).[58] The enhancement of fluorescence intensity and the quantum yield of probe **2.78** upon binding with BSA were also evident from a time resolve fluorescence study. Thus, we observed a gradual increase in **TPer** life time (λ_{ex} = 405 nm) from 5.3 to 5.5 ns while monitoring the decay at **TPer**-emission (λ_{em} = 495 nm) (**Figure 2.21d**, **Table 2.8**).

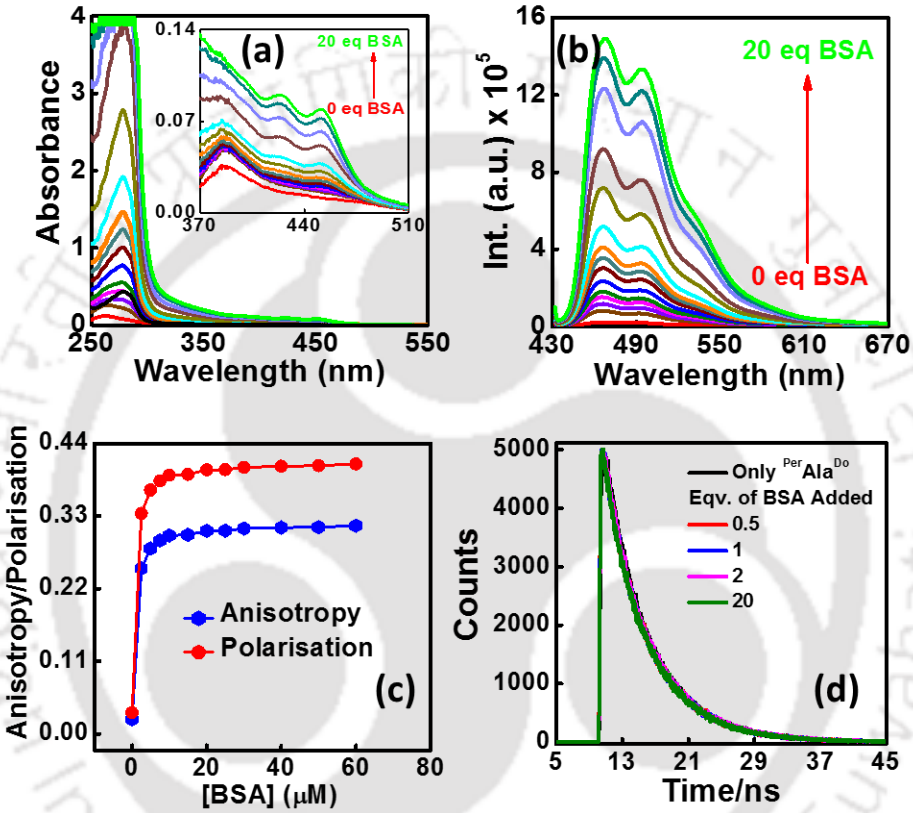

Figure 2.21. (a) UV-visible and (b) fluorescence titration of of amino acid probe **2.78** (**^{TPer}Ala^{Do}**) in absence or in presence of BSA (λ_{ex} = 420 nm). (c) Steady-state anisotropy and polarisation plot (λ_{em} = 490 nm) of triazolyl perylene amino acid fluorophore in presence of increasing BSA concentration. (d) Time resolved fluorescence spectra [**^{TPer}Ala^{Do}**] = 10 μM and [BSA] = 5, 10, 20, 200 μM.

Table 2.8: Summary table of photophysical properties of the triazolyl amino acid **(2.78)** in BSA

Entry	UV-Vis & Fluorescence					
	λ_{max}^{abs} (nm)	ε_{max}	λ_{max}^{fl} (nm)	Φ_f	Anisotropy (λ_{em} = 490 nm)	<τ> [ns]
Compound **2.78**	370, 429	1640	464, 492	0.05	0.0219	5.34
Eqv. of add. BSA						
0.50 eqv.BSA	370, 426	2290	464, 492	0.14	0.28091	5.52
1.00 eqv.BSA	370, 455	2540	465, 492	0.19	0.30054	5.55
1.50 eqv.BSA	370, 454	2620	466, 495	0.24	0.30151	----
2.0 eqv.BSA	370, 453	2780	466, 494	0.29	0.30767	5.46
6.0 eqv.BSA	370, 453	4060	466, 494	0.41	0.3155	----
10.0 eqv.BSA	370, 453	5810	466, 494	0.39	0.31526	----
14.0 eqv.BSA	370, 453	7230	466, 494	0.43	0.31805	----
20.0 eqv.BSA	370, 453	8930	467, 494	0.44	0.31593	5.48

***Benesi-Hildebrand Plot to Evaluation Binding Constant*:** The association constant (K) of the fluorophore with BSA was determined by a Benesi-Hildebrand plot using the following equation 1

$$\frac{1}{(I-I_0)} = \frac{1}{(I_\infty - I_0)} + \frac{1}{(I_\infty - I_0)K[BSA]} \quad \ldots\ldots\ldots\ldots\ldots (1)$$

where I_0, I and I_α are the emission intensities of pentapeptide in the absence of BSA, in the presence of an inetermediate and at infinite concentration of BSA respectively. From the slop of the $1/(I - I_0)$ *vs.*$1/[BSA]$ plot of equation 1, binding constant K was determined and its value is 1.6×10^4 M^{-1}. ΔG = -5.8 Kcal (**Figure. 2.22**)

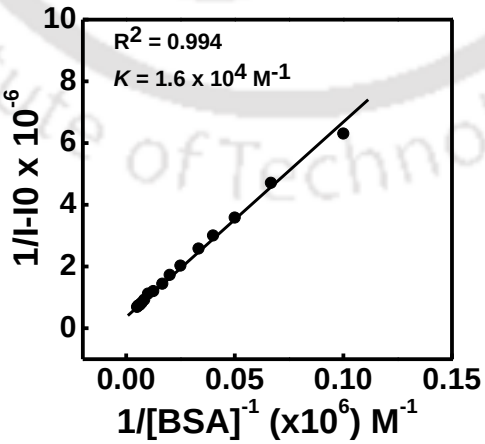

Figure 2.22. The Benesi-Hildebrand plot. [triazolyl perylene amino acid] = 10 μM and [BSA] = 0, 2.5, 5, 7.5, 10, 15, 20, 30, 40, 50, 60, 100, 140, 180, 200 μM.

***Molecular Docking Calculation*:** Docking calculations were carried out using Autodock4 (Bikadi, Hazai, 2009). The amino acid sequence of BSA protein was observed from the NCBI website, http://www.ncbi.nlm.nih.gov/protein/CAA76847.1 The 3D model of the BSA protein was built using the 3D structure 1AO6 chain 'A' as template using the ESyPred3D11 web server. This template shares 72.4% identities with the BSA sequence. Following is the BSA sequence which was used to generate the 3D model. >gi|3336842|emb|CAA76847.1| bovine serum albumin [Bos taurus]
MKWVTFISLLLLFSSAYSRGVFRRDTHKSEIAHRFKDLGEEHFKGLVLIAFSQ
YLQQCPFDEHVKLVNELTEFAKTCVADESHAGCEKSLHTLFGDELCKVASLR
ETYGDMADCCEKQEPERNECFLSHKDDSPDLPKLKPDPNTLCDEFKADEKKF
WGKYLYEIARRHPYFYAPELLYYANKYNGVFQECCQAEDKGACLLPKIETM
REKVLTSSARQRLRCASIQKFGERALKAWSVARLSQKFPKAEFVEVTKLVTD
LTKVHKECCHGDLLECADDRADLAKYICDNQDTISSKLKECCDKPLLEKSHCI
AEVEKDAIPENLPPLTADFAEDKDVCKNYQEAKDAFLGSFLYEYSRRHPEYA
VSVLLRLAKEYEATLEECCAKDDPHACYSTVFDKLKHLVDEPQNLIKQNCDQ
FEKLGEYGFQNALIVRYTRKVPQVSTPTLVEVSRSLGKVGTRCCTKPESERMP
CTEDYLSLILNRLCVLHEKTPVSEKVTKCCTESLVNRRPCFSALTPDETYVPK
AFDEKLFTFHADICTLPDTEKQIKKQTALVELLKHKPKATEEQLKTVMENFVA
FVDKCCAADDKEACFAVEGPKLVVSTQTALA

The association constant of probe with BSA determined by Benesi-Hildebrand plot (**Figure. 2.22**) was found to be 1.6 x 10^4 M^{-1} with an experimental free energy of binding, ΔG = -5.8 kcal/mol. All the results suggested that both the hydrophobic as well as electrostatic interaction played an important role in the present BSA-peptide interaction process. The binding of the **TPer**-moety in the hydrophobic pocket of BSA was also supported by a molecular docking calculation with Autodoc programme[59] which clearly showed that **TPer** moiety of the probe **2.78** was remained surrounded by hydrophobic amino acids of the hydrophobic pocket of subdomain IB of site I of BSA (**Figure 2.23**).

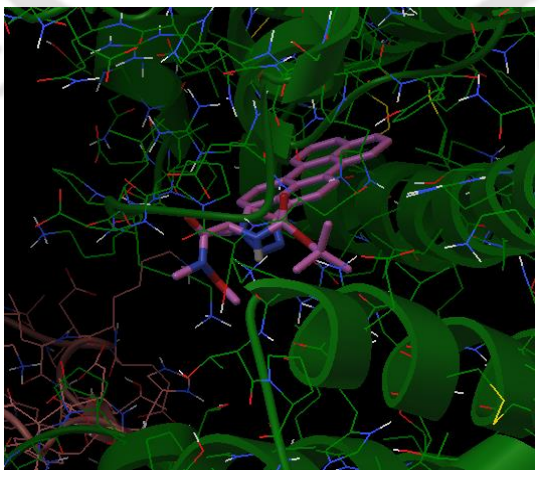

Figure 2.23: Docking pose of **2.78** in hydrophobic pocket of BSA.

Table 2.9: Energy of ^{Per}**Ala**^{Do} **- BSA** complex obtained from Autodock4.

Interaction Energy	kcal/mol
Estimated Free Energy of Binding	-8.53
Final Intermolecular Energy	-10.91
vdW + Hbond + desolv Energy	-10.80
Electrostatic Energy	-0.11
Final Total Internal Energy	-1.85
Torsional Free Energy	+2.39
Unbound System's Energy	-1.85

2.12. Conclusion

In conclusion, we have successfully synthesized few conceptually new triazolyl donor and/or acceptor chromophore decorated fluorescent unnatural amino acids via click reaction which show modulated photophysical properties in various organic solvents. The synthesis is very simple and started with easily available commercial stating materials. The synthesis of azido serine is simple and high yielding. The energy transfer phenomenon was observed in a pair of amino acids ^{TPhen}**Ala**^{Do} and ^{TCNB}**Ala**^{Ac} in acetonitrile solvent wherein ^{TCNB}**Ala**^{Ac} acts as FRET donor and ^{TPhen}**Ala**^{Do} acts as FRET acceptor. This pair might further be exploited in desing FRET-peptide probe for application in studying interaction events between peptide-protein/peptide-DNA. Moreover, we exploited the triazolyl perylene amino acid for studying interaction with BSA protein with the help of fluorescence spectroscopic technique and observed that the hydrophobic triazolyl perylene amino acid is able to sense BSA with a switch on fluorescence response. The other donor/acceptor aromatic triazolyl amino acids might be useful for sensing the biomolecular microenvironment. Furthermore, the present investigation on the photophysical properties of click chemistry derived triazolyl fluorescent amino acids is of great importance for the development of new pair of donor-acceptor amino acids useable for the design of fluorescent peptide/peptidomimetics which could be utilized as probe for studying interbiomolecular interaction.

2.13. Experimental Section

2.13.1. General Experimental

All reactions except N-Boc protection of primary amine were carried out under nitrogen atmosphere in flame-dried glassware, using a nitrogen filled balloon. Organic extracts were dried over anhydrous sodium sulfate. Solvents were removed in a rotary evaporator under reduced pressure. Silica gel (60- 120 mesh size) was used for the

column chromatography. Reactions were monitored by TLC on silica gel 60 F254 (0.25 mm). ^{1}H NMR spectra were recorded at 400MHz and ^{13}C NMR spectra were recorded at 100Mz. Coupling constants (J value) were reported in hertz. The chemical shift were shown in ppm downfield form tetramethylsilane, using residual chloroform (δ =7.24 in ^{1}H NMR, δ = 77.23 in ^{13}C NMR), as an internal standard. Mass spectra were recorded with a HR mass spectrometer and data analyzed by using built-in software. IR spectra were recorded in KBr on a FT-IR spectrometer. BSA, Na_2HPO_4 and $NaH_2PO_4.H_2O$ (for preparation of phosophate buffer) were purchased from Merck, India and used without further purification. Water was taken from a Milli-Q purification system. All solutions were prepared before 1 hour of experiments done. The probe molecules [amino acid **^{TPer}Ala^{Do}** (**2.78**)] was synthesized and purified according to the procedure described.

2.13.2. Synthesis and Characterization

Synthesis of N-t-butyloxycarbonyl-L-Serine: A solution of L-serine (10 mmol) in 1:1 mixture of 1,4 dioxane and water (10 ml each) was treated with NaOH (20 mmol) followed by di-t-butyl dicarbonate (15 mmol) maintaining the pH between 7.5-8.5.

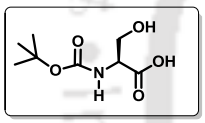

The mixture was stirred room temperature for 20 h. The reation mixture was washed with ethyl acetate (2 x 20 ml) and the aqueous phase was treated with 2(N) HCl to bring pH 2 in cool condition. Immediately the solution was extracted with ethyl acetate and the organic layer was washed with water, brine, dried and evaporated under vaccum to furnish the Boc-protected L-serine viscous liquidin pure form. Yield:95%;^{1}H NMR ($CDCl_3$; 400 MHz) δ 1.42 (9H, s); 3.82 (1H, d, J = 10.4 Hz); 4.02 (1H, d, J = 10 Hz); 4.32 (1H, m); 5.55 (1H, m); 5.82 (1H, d, J = 8.4 Hz).

***Synthesis of weinreb amide Ester of N-protected L-serine (2.67)*:** To a solution N-protected L-serine (2.5 mmol) in 3:1 mixture of dry CH_2Cl_2 and DMF, 1-[3-dimethyl amino propyl]-3-ehtylcarbo- diimide hydrochloride (EDC.HCl) (3mmol) and HOBT

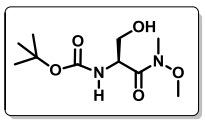

(3mmol) were added and the reaction mixture was stirred for 1h at 0 ^{o}C. Then N,O-dimethyl hydroxylamine hydrochloride (3mmol) added followed by diisopropylethylamine (DIPEA) (6 mmol). The reaction mixture was stirred for another 16-18 h at 0 ^{o}C to room temperature. Then solvent dried by rotary vacuum, after which it was partitioned between EtOAc and aqueous $NaHCO_3$ solution (50 ml each), the organic layer was washed with brine solution. Pure product **2.67** was separated by column chromatography (Si-gel, PE:EtoAc = 1:1); white solid (yield, 55%).^{1}H NMR ($CDCl_3$; 400 MHz) δ 1.33 (9H, s); 3.11 (3H, s); 3.67 (3H, s); 3.70 (2H, d, J = 3.6 Hz); 4.67 (1H, m); 5.72 (1H, d, J = 8.4 Hz); ^{13}C NMR ($CDCl_3$; 100 MHz); δ 27.5, 35.7, 52.1, 60.7, 61.7, 78.7, 155.0, 162.1.

Synthesis of mesylate derivative of N,O protected L-serine (2.68): The N,O protected L-serine (224 mg, 0.903 mmol) was taken in a dry CH_2Cl_2, Mesyl chloride (84.1µl, 1.08mmol) and triethyl amine(150 µl, 1.08 mmol) were added to the reaction mixture maintaining 0 ^oC. The reaction mixture was stirred upto total starting material was consumed, monitored by TLC, after which it was poured into water and CH_2Cl_2 (20 ml each).The organic layer was washed with water two times, dried under Na_2SO_4 and then evaporated. The pure compound was then isolated by column chromatography (si-gel, PE:EA = 2:1) as brown oil (yield, 91%).^{1}H NMR ($CDCl_3$; 400 MHz) δ 1.41 (9H, s); 2.99 (3H, s); 3.20 (3H, s); 3.74 (3H, s); 4.41 (2H, m); 4.90 (1H, m); 5.33 (1H, d, J = 8 Hz); ^{13}C NMR ($CDCl_3$; 100 MHz); δ 27.76, 31.5, 52.1, 60.9, 62.1, 66.4, 79.0, 155.2, 170.7.

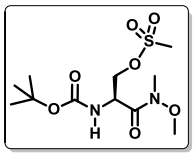

Synthesis of azido derivative of N,O protected L-serine (2.69): To a solution of the Mesylate (269 mg, 0.825mmol) in dry DMF (8 ml), NaN_3 (80 mg, 1.23mmol) was added and stirrer for 18 h at 50 ^oC .The reaction mixture was partitioned between EtOAc and water (20 ml each). The organic layer was washed with brine solution, dried, filtered and then evaporated. The title compound was isolated by column chromatography (si-gel, PE:EA = 2:1), as light brown oil (yield, 76 %). IR (KBr) 3430, 2978, 2104, 1714, 1661, 1505, 1392, 1367, 1251, 1166, 989 cm^{-1}. ^{1}H NMR ($CDCl_3$; 400 MHz) δ 1.31 (9H, s); 3.1 (3H, s); 3.42 (2H, m); 3.64 (3H, s); 4.71 (1H, m); 5.56 (1H, d, J = 8.4 Hz); ^{13}C NMR ($CDCl_3$; 100 MHz); δ 28.2, 32.1, 50.6, 52.1, 61.6, 79.9, 155.0, 169.5;

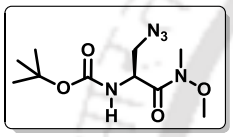

2.13.2.1. General procedure for the synthesis of triazolyl donor/acceptor amino acids by [3+2] cycloaddition reaction

The azido derivative of N,-C terminal protected L-serine **2.69** (1.0 equiv) was taken in a 5:1 dry THF and water mixture solvent and degassed it for 5 min with nitrogen gas. Then, teminal alkyne (1.1 equiv) was added with continuing stirring and degassing for the next 5 min. Then 6 mol % sodium ascorbate and 1 mol% powderd $CuSO_4$ were added. The reaction mixture was degassed and allowed to proceed 18-20 h about 65 to 70 ^oC. After total consumption of the starting azide, the reaction mixture evaporated completely and work up done by EtOAc and NH_4Cl solution. The organic layer was washed with brine, dried over Na_2SO_4. The synthesized trizolyl amino acids were separated by column chromatography (si-gel, PE:EA = 1:1) and characterized. The average yields were 50% to 85%.

Synthesis of (S)-tert-butyl 1-(N-methoxy-N-methylcarbamoyl)-2-(4-(4-(dimethylamino)phenyl)-1H-1,2,3-triazol-1-yl) ethylcarbamate ($^{TNDMB}Ala^{Do}$) : Using general procedure, starting from 0.055 g (0.2 mmol) of chiral serine azide **2.69** and 0.039 g (0.22 mmol) of 4-ethynyl-N,N- dimehtylbenzenamine **A**, 0.068 g (0.162

mmol) of the tilte compound **2.70** was isolated as a redish white gummy material,

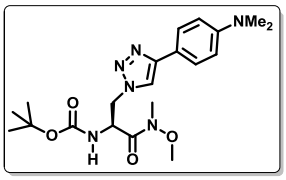

Yield 82%; IR (KBr) 3350, 2920, 1697, 1660, 1520, 1166, 1059, 800, 629 cm^{-1}. ^1H NMR ($CDCl_3$; 400 MHz) δ 1.36 (9H, s); 2.91 (6H, s); 3.16 (3H, s); 3.69 (3H, s); 4.62-4.69 (2H, m); 5.02-5.07 (1H, m); 5.65 (1H, d, *J* = 7.6 Hz), 6.69 (2H, d, *J* = 8.8 Hz); 7.62 (2H, d, *J* = 8.8 Hz); 7.63 (1H, s); ^{13}C NMR ($CDCl_3$; 100 MHz); δ 29.4, 32.4, 40.5, 50.9, 51.2, 61.8, 80.4, 112.5, 118.8, 119.2, 126.7, 148.2, 150.4, 155.1, 169.1, HRMS calcd for $C_{20}H_{31}N_6O_4$ ($[M + H]^+$) 419.2401, found 419.2409.

Synthesis of (S)-tert-butyl 1-(N-methoxy-N-methylcarbamoyl)-2-(4-(pyridin-2-yl)-1H-1,2,3-triazol-1-yl)ethylcarbamate ($^{TPy}Ala^{Do}$) : Using general procedure,

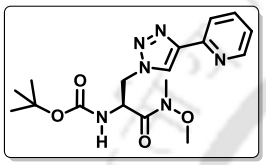

starting from 0.046 g (0.169 mmol) of chiral serine azide **2.69** and 19 µl (0.185mmol) of 2-Ethynylpyridine **B**, 0.048 g (0.127 mmol) of the title compound **2.71** was isolated as a white solid material, Yield 75%; IR (KBr) 3261,3135, 2973, 1717, 1659, 1525, 1166, 1048, 789 cm^{-1}. ^1H NMR ($CDCl_3$; 400 MHz) δ 1.34 (9H, s); 3.21 (3H, s); 3.74 (3H, s); 4.67 - 4.76 (2H, m); 5.02-5.06 (1H, m); 5.64 (1H, d, *J* = 7.6 Hz); 7.15 (1H, t, *J* = 12.4 Hz); 7.7 (1H, t, *J* = 7.6 Hz), 8.09 (1H, d, *J* = 8.0 Hz); 8.13 (1H, s); 8.50 (1H, d, *J* = 4.4 Hz); ^{13}C NMR ($CDCl_3$; 100 MHz) δ 28.3, 32.6, 51.3, 51.5, 61.9, 80.5, 120.4, 122.9, 123.2, 137.0, 148.3, 149.4, 150.2, 155.2, 168.8; HRMS calcd for$C_{17}H_{25}N_6O_4$ ($[M + H]^+$) 377.1932, found 377.1932.

Synthesis of (S)-tert-butyl 1-(N-methoxy-N-methylcarbamoyl)-2-(4-(3,5-dimethoxyphenyl)-1H-1,2,3-triazol-1-yl) ethylcarbamate ($^{TDMB}Ala^{Do}$) : Using general procedure, starting from 0.051 g (0.188 mmol) of chiral serine azide **2.69** and 0.033 g (0.206 mmol) of 1-Ethynyl-3,5-dimethoxybenzene **C**, 0.065 g (0.149 mmol) of the title compound **2.72** was isolated as a grey gummy material, Yield 80 %; IR (KBr)

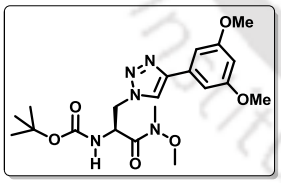

3448, 3342, 2937, 1685, 1594, 1153, 1066, 823 cm^{-1}. ^1H NMR ($CDCl_3$; 400 MHz); δ 1.34 (9H, s); 3.15 (3H, s); 3.68 (3H, s); 3.75 (6H, s); 4.61- 4.65 (2H, m); 5.0 - 5.04 (1H, m); 5.58 (1H, d, *J* = 6.8 Hz); 6.36 (1H, t, *J* = 2.4 Hz); 6.91 (2H, d, *J* = 2.4 Hz); 7.69 (1H, s); ^{13}C NMR ($CDCl_3$; 100 MHz) δ 28.3, 32.5, 51.2, 55.8, 61.9, 80.6, 100.6, 103.8, 121.1, 128.5, 132.4, 147.7, 155.2, 161.2, 168.9; HRMS calcd for $C_{20}H_{30}N_5O_6$ ($[M + H]^+$) 436.2191, found 436.2194.

Synthesis of (S)-tert-butyl 1-(N-methoxy-N-methylcarbamoyl)-2-(4-(2-methoxynaphthalen-6-yl)-1H-1,2,3-triazol-1-yl) ethylcarbamate (^{TMNap}Ala^{Do}) : Using general procedure, starting from 0.047 g (0.173 mmol) of chiral serine azide

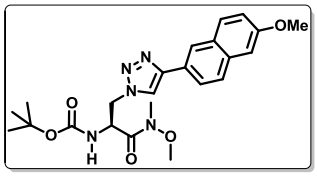

2.69 and 0.034 g (0.19 mmol) of 2-Ethynyl-6-methoxynapthalene **D**, 0.059 g (0.129 mmol) of the title compound **2.73** was isolated as a grey gummy material, Yield 75%; IR (KBr) 3341, 2970, 1660, 1524, 1164, 1029, 855, 653 cm^{-1}. ^1H NMR ($CDCl_3$; 400 MHz) δ 1.38 (9H,

s); 3.21 (3H, s); 3.74 (3H, s); 3.89 (3H, s); 4.7 - 4.77 (2H, m); 5.07-5.13 (1H, m); 5.56 (1H, d, *J* = 6.8 Hz); 7.12 (2H, t, *J* = 4.8 Hz); 7.74 (2H, dd, *J* = 3.6 Hz, 8.4 Hz); 7.82 (1H, s); 7.85 (1H, s); 8.21 (1H, s); ^{13}C NMR ($CDCl_3$; 100 MHz) δ 28.7, 33.0, 51.6, 55.8, 62.3, 81.0, 106.3, 119.7, 120.9, 124.8, 124.9, 126.2, 127.8, 129.0, 129.4, 130.2, 134.8, 148.4, 155.5, 158.4, 169.3; HRMS calcd for $C_{23}H_{29}N_5O_5$ ($[M + H]^+$) 456.2241, found 456.2242.

Synthesis of (S)-tert-butyl 1-(N-methoxy-N-methylcarbamoyl)-2-(4-(phenanthren-9-yl)-1H-1,2,3-triazol-1-yl) ethylcarbamate (^{TPhen}Ala^{Do}): Using

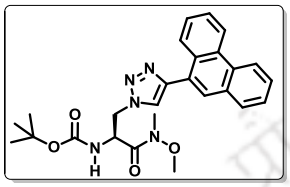

general procedure, starting from 0.048 g (0.176 mmol) of chiral serine azide **2.69** and 0.039 g (0.194mmol) of 9-ethynyl phenanthrene **E**, 0.070 g (0.148 mmol) of the title compound **2.74** was isolated as a light brown gummy material. Yield 84%; IR (KBr) 3347, 2976, 1667, 1552, 1166, 1054, 855, 726 cm^{-1}. ^{1}H NMR ($CDCl_3$; 400 MHz), δ 1.38 (9H, s); 3.21 (3H, s); 3.74 (3H, s); 4.76-4.84 (2H, m); 5.14-5.19 (1H, m); 5.77 (1H, d, *J* = 7.2); 7.53-7.58 (2H, m); 7.6-7.65 (1H, m); 7.85 (1H, s); 7.85 (2H, d, *J* = 8.4 Hz); 7.94 (1H, s); 8.32 (1H, d, *J* = 8 Hz); 8.64 (1H, d, *J* = 8 Hz); 8.7 (1H, d, *J*=8 Hz); ^{13}C NMR ($CDCl_3$; 100 MHz); δ 28.3, 32.5, 51.2, 51.3, 61.9, 80.5, 122.0, 123.0, 124.0, 126.2, 126.9, 128.4, 128.9, 130.0, 130.2, 130.7, 131.3, 146.7, 155.2, 169.0; HRMS calcd for $C_{26}H_{30}N_5O_4$ ($[M + H]^+$) 476.2292, found 476.2294.

Synthesis of (S)-tert-butyl(3-(4-((6-((4-(dimethylamino)phenyl)ethynyl)-1,3-dioxo-1H-benzo[de]isoquinolin-2(3H)-yl)methyl)-1H-1,2,3-triazol-1-yl)-1-(methoxy(methyl)amino)-1-oxopropan-2-yl)carbamate ($^{T4\text{-}DMAPENI}$Ala^{Do}): Using general procedure, starting from 0.058 g (0.212 mmol) of chiral serine azide **2.69** and 0.088 g (0.233 mmol) of *4. 4-(4-N,N-dimethylaminophenylethynyl)-N-(2-propynyl)-1,8-naphthalimide* **F**, 0.102 g (0.156 mmol) of the title

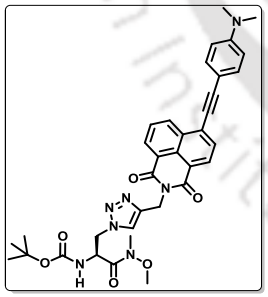

compound **2.75** was isolated as a solid red material. Yield 74 %; IR (KBr) 3343, 2974, 2932, 2188, 1699, 1658, 1583, 1524, 1364, 1236, 1168, 1049, 815, 785 cm^{-1}. ^{1}H NMR ($CDCl_3$; 400 MHz), δ 1.30 (9H, s); 2.97 (6H, s); 3.12 (3H, s); 3.63 (3H, s); 4.58 (2H, d, *J* = 2.4 Hz); 4.96 (1H, d, *J* = 5.6 Hz); 5.39 (2H, q, *J* = 4.8 Hz, *J* = 14.4 Hz); 5.55 (1H, d, *J* = 7.6 Hz); 6.61 (2H, d, *J* = 8.8 Hz); 7.43 (2H, d, *J* = 8.8 Hz); 7.66 (1H, d, *J* = 8.4 Hz); 7.71 (1H, t, *J* = 8 Hz); 7.95 (1H, s); 8.38 (1H, d, *J* = 7.6 Hz); 8.49 (1H, d, *J* = 7.2 Hz); 8.59 (1H, d, *J* = 8.4 Hz) ^{13}C NMR ($CDCl_3$; 100 MHz); δ 28.1, 32.2, 34.9, 36.3, 39.8, 50.6, 51.1, 61.5, 79.9, 85.1, 102.1, 108.1, 111.5, 120.2, 122.2, 124.5, 126.7, 127.7, 128.3, 128.8, 129.3, 130.3, 130.9, 131.3, 132.5, 133.1, 143.4, 150.6, 154.9, 162.5, 163.4, 168.9. HRMS calcd for $C_{35}H_{38}N_7O_6$ ($[M + H]^+$) 652.2878, found 652.2849.

Synthesis of (S) tert-butyl 1-(N-methoxy-N-methylcarbamoyl)-2-(4-(pyrene -9-yl)-1H-1,2,3-triazol-1-yl) ethylcarbamate (^{TPy}Ala^{Do}): Using general procedure, starting from 48 mg (0.18 mmol) of chiral serine azide **2.69** and 44mg (0.19 mmol) of

2-ethynyl pyrene **G**, 65 mg (0.13mmol) of the title compound **2.76** was isolated as a

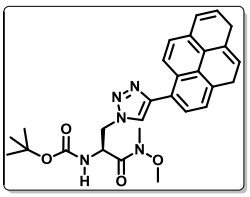

light brown gummy material. Yield 72.4%; IR (KBr) 3421, 2976, 2930 , 2103, 1712, 1663, 1164, 849, 757 cm-1. ^{1}H NMR (CDCl3; 400 MHz), δ 1.395 (9H, s); 3.244 (3H, s); 3.769 (3H, s); 4.835-4.847 (2H, d, J = 4.8 Hz); 5.185-5.203 (1H, m); 5.728-5.747 (1H, d, J = 7.6 Hz); 7.947-8.003 (2H, m); 8.025-8.056 (2H, m); 8.070 (1H, s); 8.124-8.124 (3H, m);8.609-8.632 (1H, d, J=9.2 Hz) ^{13}C NMR (CDCl3; 100 MHz); δ 22.9, 28.5, 29.9, 32.6, 51.4, 62.0, 77.1, 77.4, 77.7, 124.3, 124.8, 125.0, 125.2, 125.3, 125.5, 126.2, 127.4, 127.5, 127.9, 128.2, 128.7, 131.0, 131.4, 131.5, 147.5, 155.4, 169.2 ; HRMS calcd. for C26H30N5O4 ([M + H]+) 500.2376, found 500.2323.

Synthesis of (S)-tert-butyl(1-(methoxy(methyl)amino)-1-oxo-3-(4-((4-(pyren-1-yl)butanamido) methyl)-1H-1,2,3-triazol-1-yl)propan-2-yl)carbamate (^{TBAPy}Ala^{Do}) : Using general procedure, starting from 0.040 g (0.146 mmol) of chiral serine azide **2.69** and 0.054 g (0.176 mmol) of N-(prop-2-yn-1-yl)-4-(pyren-1-yl) butanamide **H**,

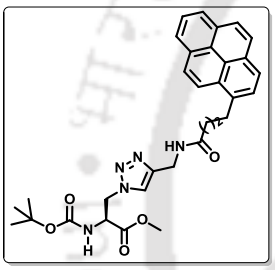

0.069 g (0.121 mmol) of the title compound **2.77** was isolated as a grey solid material. Yield 82 %; IR (KBr) 3326, 2924, 2854, 1745, 1691, 1649, 1531, 1462, 1247, 1061, 843 cm^{-1}. ^{1}H NMR ($CDCl_3$; 400 MHz), δ 1.4 (9H, s); 2.24-2.18 (2H, m); 2.30 (2H, t, J = 7.2 Hz); 3.36 (2H, t, J = 7.2 Hz); 3.74 (3H, s); 4.47 (2H, d, J = 4.8 Hz); 4.69-4.65 (2H, m); 4.73 (1H, s); 5.32 (1H, bs); 6.17 (1H, bs); 7.47 (1H, s); 7.82 (1H, d, J = 8.4 Hz); 8.01-7.96 (3H, m); 8.09 (2H, d, J = 8.8 Hz); 8.15 (2H, d, J = 8 Hz); 8.26 (1H, d, J = 9.6 Hz); ^{13}C NMR ($CDCl_3$; 100 MHz); δ 27.4, 28.4, 32.9, 34.9, 35.9, 51.2, 53.2, 53.8, 80.9, 123.5, 125.0, 125.1, 126.1, 126.9, 127.5, 127.7, 128.9, 130.1, 131.1, 131.6, 135.9, 155.3, 169.6, 173.1. HRMS calcd for $C_{32}H_{36}N_5O_5$ ([M + H]$^+$) 570.2711, found 570.2714.

Synthesis of (S)-tert-butyl (1-(methoxy(methyl)amino)-1-oxo-3-(4-(perylen-3-yl)-1H-1,2,3-triazol-1-yl)propan-2-yl)carbamate (^{TPer}Ala^{Do}): Using general procedure, starting from 0.060 g (0.219 mmol) of chiral serine azide **2.69** and 0.072 g (0.263 mmol) of 1- ethynyl perylene **I**, 0.062 g (0.112 mmol) of the title compound

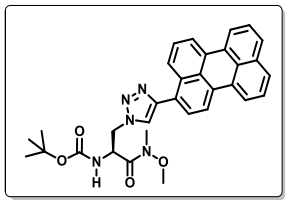

2.78 was isolated as a yellowish red solid material. Yield 52 %; IR (KBr) 3296, 2925, 2103, 1718, 1662, 1498, 1367, 1164, 1023, 809, 765 cm^{-1}. ^{1}H NMR ($CDCl_3$; 400 MHz), δ 1.40 (9H, s); 3.25 (3H, s); 3.78 (3H, s); 4.86-4.77 (2H, m); 5.14 (1H, bs); 5.62 (1H, d, J = 5.6 Hz); 7.43 (2H, d, J = 7.6 Hz); 7.51-7.47 (1H, m); 7.65 (2H, m); 7.82 (1H, s); 7.88 (1H, d, J = 8 Hz); 8.01 (1H, d, J = 8.4 Hz); 8.17-8.05 (4H, m); ^{13}C NMR ($CDCl_3$; 100 MHz); δ 28.4, 32.7, 51.4, 51.5, 62.1, 80.7, 120.1, 120.6, 120.7, 125.6, 126.7, 126.8, 127.2, 128.0, 128.1, 128.2, 128.7, 129.3, 131.1, 131.4, 131.6, 131.8, 134.8, 147.0, 155.3, 169.1; HRMS calcd. for $C_{32}H_{32}N_5O_4$ ([M + H]$^+$) 550.2449, found 550.2450.

Synthesis of (S)- tert-butyl 1-(N-methoxy-N-methylcarbamoyl)-2-(4-(4-cyanophenyl)-1H-1,2,3-triazol-1-yl) ethylcarbamate ($^{TCNB}Ala^{Ac}$) : Using general procedure, starting from 0.11 g (0.402 mmol) of chrial serine azide **2.69** and 0.056 g (0.442 mmol) of 4-ethynyl benzonitrile **J**, 0.13 g (0.324 mmol) of the title compound **2.79** was isolated as a white gummy material. Yield 81%; IR (KBr) 3372, 2978, 2928, 2222, 1697, 1655, 1367, 1173, 1027, 838, 627, 557 cm^{-1}. ^1H NMR ($CDCl_3$; 400 MHz) δ 1.33 (9H, s); 3.18 (3H, s); 3.73 (3H, s); 4.71-4.77 (2H, m); 5.02-5.06 (1H, m); 5.6 (1H, d, J = 6.4 Hz); 7.63 (2H, d, J = 8 Hz); 7.86 (2H, d, J = 8 Hz); 7.88(1H, s); ^{13}C NMR ($CDCl_3$; 100 MHz); δ 28.3, 32.5, 51.2, 51.3, 61.9, 80.6, 111.4, 118.8, 122.0, 126.1, 132.7, 135.0, 145.9, 155.1, 168.7; HRMS calcd for $C_{19}H_{25}N_6O_4$ ($[M + H]^+$) 401.1932, found 401.1935.

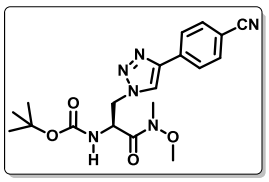

Synthesis of (S)-tert-butyl 1-(N-methoxy-N-methylcarbamoyl)-2-(4-(4-nitrophenyl)-1H-1,2,3-triazol-1-yl) ethylcarbamate ($^{TNB}Ala^{Ac}$) : Using general procedure, starting from 0.051 g (0.187 mmol) of chiral serine azide **2.69** and 0.03 g (0.205 mmol) of 1-Ethynyl-4-nitrobenzene **K**, 0.063 g (0.151mmol) of the tite compound **2.80** was isolated as a white gummy material, Yield 81%; IR (KBr) 3350, 2982, 1693, 1515, 1351, 1165, 853, 625 cm^{-1}. ^1H NMR ($CDCl_3$; 400 MHz) δ 1.39 (9H, s); 3.17 (3H, s); 3.73 (3H, s); 4.67-4.72 (2H, m); 5.02-5.07 (1H, m); 5.61 (1H, d, J = 8.8 Hz); 7.90 (1H, s); 7.93 (2H, d, J = 7.6 Hz); 8.19 (2H, d, J = 8.8 Hz); ^{13}C NMR ($CDCl_3$; 100 MHz) δ 28.3, 32.5, 51.2, 51.4, 62.0, 80.6, 122.4, 124.3, 126.2, 136.9, 145.5, 147.3, 155.1, 168.6; HRMS calcd for $C_{18}H_{25}N_6O_6$ ($[M + H]^+$) 421.1836, found 421.1839.

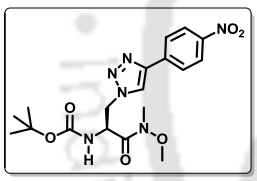

Synthesis of (S)- tert-butyl 1-(N-methoxy-N-methylcarbamoyl)-2-(4-(4-methyl benzoate)-1H-1,2,3-triazol-1-yl) ethylcarbamate ($^{TMBA}Ala^{Ac}$) : Using general procedure, starting from 0.053 g (0.194 mmol) of chiral serine azide **2.69** and 0.034 g (0.213 mmol) of 1-Ethynyl-4-methylbenzoate **L**, 0.067 g (0.154 mmol) of the title compound **2.81** was isolated as a white gummy material, Yield 78 % ; IR (KBr) 3380, 2985, 2949, 1674, 1518, 1286, 1167, 1114, 774, 624 cm^{-1}. ^1H NMR ($CDCl_3$; 400 MHz); δ 1.35 (9H, s); 3.19 (3H, s); 3.73 (3H, s); 3.87 (3H, s); 4.68-4.73 (2H, m); 5.03-5.07 (1H, m); 5.59 (1H, d, J = 7.2 H); 7.83 (1H, s); 7.85 (2H, d, J = 3.2); 8.03 (2H, d, J = 10.4 Hz); ^{13}C NMR ($CDCl_3$; 100 MHz) δ 28.3, 32.5, 51.3, 52.2, 62.0, 80.6, 121.7, 125.6, 129.6, 130.2, 132.14, 134.9, 146.7, 155.1, 166.9, 168.8; HRMS calcd for $C_{20}H_{28}N_5O_6$ ($[M + H]^+$) 434.2034, found 434.2038.

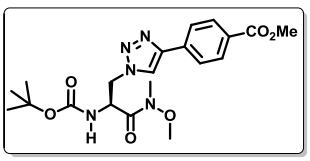

Synthesis of (S)-tert-butyl (3-(4-(2,4-dinitrophenyl)-1H-1,2,3-triazol-1-yl)-1-(methoxy(methyl)amino)-1-oxopropan-2-yl)carbamate ($^{TDNB}Ala^{Ac}$): Using general procedure, starting from 0.07 g (0.256 mmol) of chiral serine azide **2.69** and 0.054 g (0.282 mmol) of 1-Ethynyl-2,4-dinitrobenzene **M**, 0.084 g (0.18 mmol) of the tite compound **2.82** was isolated as a light yellow material, Yield 71%; IR (KBr) 3345, 2980, 1694, 1666, 1531, 1348, 1167, 907, 747 cm^{-1}. ^{1}H NMR ($CDCl_3$; 400 MHz) δ 1.38 (9H,s); 3.22 (3H, s); 3.75 (3H, s); 4.76 (2H, d, J = 4.4 Hz); 5.05-5.01 (1H, m); 5.58 (1H, d, J = 7.2 Hz); 7.89 (1H, s); 8.38 (1H, d, J = 8.8 Hz); 8.44 (2H, dd, J = 1.6 Hz, 8.8 Hz); 8.6 (1H, s); ^{13}C NMR ($CDCl_3$; 100 MHz) δ 28.2, 32.4, 51.2, 51.4, 62.0, 80.6, 119.8, 125.4, 126.7, 130.2, 131.9, 139.8, 146.8, 147.4, 155.1, 168.4. HRMS calcd for $C_{18}H_{24}N_7O_8$ ($[M + H]^+$) 466.1681, found 466.1684.

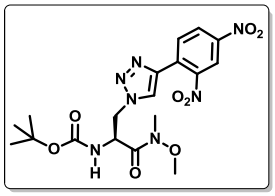

Synthesis of (S) tert-butyl 1-(N-methoxy-N-methylcarbamoyl)-2-(4-(3,5-bis(trifluoromethyl)phenyl)-1H-1,2,3-triazol-1-yl) ethylcarbamate ($^{TFMB}Ala^{Ac}$) : Using general procedure, starting from 0.046 g (0.17 mmol) of chiral serine azide **2.69** and 33 µl (0.187mol) of 1-Ethynyl-3,5-bis (trifluoromethyl)benzene **N**, 0.063 g (0.123mmol) of the title compound **2.83** was isolated as a grey material, yield 73%; IR (KBr) 3354, 2984, 1673, 1523, 1280,1128, 898, 808 cm^{-1}. ^{1}H NMR ($CDCl_3$; 400 MHz) δ 1.35 (9H, s); 3.2 (3H, s); 3.75 (3H, s); 4.67-4.76 (2H, m); 5.05-5.1 (1H, m); 5.65 (1H, d, J = 10.4 Hz); 7.75 (1H, s); 7.97 (1H, s); 8.22 (2H,s); ^{13}C NMR ($CDCl_3$; 100 MHz) δ 28.3, 32.6, 51.3, 51.5, 62.0, 80.8, 121.6, 122.0, 125.8, 132.2, 132.5, 132.9, 145.1, 155.5, 168.8; HRMS calcd for $C_{20}H_{24}N_5O_4F_6$ ($[M + H]^+$) 512.1727, found 512.1728.

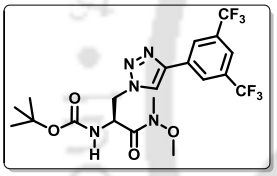

Synthesis of (S)-tert-butyl (3-(4-((6-((4-cyanophenyl)ethynyl)-1,3-dioxo-1H-benzo[de]isoquinolin-2(3H)-yl)methyl)-1H-1,2,3-triazol-1-yl)-1-(methoxy(methyl)amino)-1-oxopropan-2-yl)carbamate ($^{T4\text{-}CPE\ NI}Ala^{Ac}$): Using general procedure, starting from 0.060 g (0.219 mmol) of chiral serine azide **2.69** and 0.086 g (0.240 mmol) of 4-(2-(4-(cyano)phenyl)ethynyl)-1,8-naphthalimide **O**, 0.08 g (0.126 mmol) of the title compound **2.84** was isolated as a light yellow solid material. Yield 58 %; IR (KBr) 3330, 2929, 2225, 1704, 1664, 1585, 1364, 1235, 1163, 1016, 788 cm^{-1}. ^{1}H NMR ($CDCl_3$; 400 MHz), δ 1.29 (9H, s); 2.57 (6H, s); 3.12 (3H, s); 3.65 (3H, s); 4.59 (2H, d, J = 4.4 Hz); 4.96 (1H, bs); 5.39 (2H, q, J = 4.0 Hz, J = 13.6 Hz); 5.57 (1H, d, J = 8.0 Hz); 7.37 (1H, s); 7.73-7.62 (5H, m); 7.83 (1H, d, J = 7.6 Hz); 8.42 (1H, d, J = 7.6 Hz); 8.53-8.49 (2H, m); ^{13}C NMR ($CDCl_3$; 100 MHz); δ 28.2, 32.4, 33.8, 35.2, 40.9, 50.9, 51.1, 61.8, 80.3, 89.9, 96.8, 112.7, 118.2, 122.6, 122.8, 124.6, 126.4, 126.9, 127.8, 127.9, 130.4, 131.2,

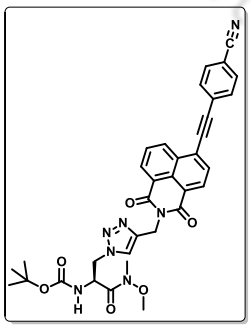

131.4, 131.9, 132.1, 132.3, 132.5, 143.3, 155.1, 163.1, 163.4, 168.8. HRMS calcd for $C_{34}H_{32}N_7O_6$ ([M + H]$^+$) 634.2409, found 634.2390.

2.13.3. Photophysical Studies of the Amino Acids

UV-visible measurements: All the *UV* –visible spectra of the amino acids (10 μM) were measured in different solvents using a UV-Visible spectrophotometer with a cell of 1 cm path length. The measurements were carried out in absorbance mode. The absorbance values of the sample solutions were measured in the wavelength regime of 200–550 nm. All the sample solutions were prepared just before doing the experiment.

Fluorescence experiments: All the sample solutions were prepared as described in UV measurement experiments. Fluorescence spectra were obtained using a fluorescence spectrophotometer at 25 °C using 1 cm path length cell. The excitation wavelengths for all the cases were set at the excitation maxima of each sample in each solvents and emission spectra were measured in the wavelength regime of 300–700 nm with an integration time of 0.2 sec. All the sample solutions were prepared just before doing the experiment. Total volume of 1.0 ml from a stock solution of 2 ml of 10 μM concentration for each case was used for fluorescence experiment in 1 ml cell. Fluorescence emissions were collected exciting the samples at the wave length corresponding to their absorption maxima. Steady-state fluorescence emission spectra were recorded at room temperature as an average of five scans using an excitation slit of 3.0 nm, emission slit 3.0 nm, and scan speed of 120 nm/min. The fluorescence quantum yields (Φ_f) were determined using quinine sulphate as a reference with the known Φ_f (0.55) in 0.1 molar solution in sulphuric acid. The following equation was used to calculate the quantum yield,

$$\Phi_S = \Phi_R \frac{Fl_S^{Area}}{Fl_R^{Area}} \frac{Abs_R}{Abs_S} \frac{n_S^2}{n_R^2}$$

where, Φ_R is the quantum yield of standard reference, Fl_S^{Area} (sample) and Fl_R^{Area} (reference) are the integrated emission peak areas, Abs_S (sample) and Abs_R (reference) are the absorbances at the excitation wavelength, and n_S (sample) and n_R (reference) are the refractive indices of the solutions.

The fluorescence lifetime experiment was carried out using a time resolved fluorescence spectrophotometer at 25 °C using 1 cm path length cell. 290, 405 LED and 375 nm laser was used as excitation light source. The lifetime data were calculated by software with fixed fitting range. The time correlated single photon counting (TCSPC) method was used to calculate the lifetime data. The life time data (Global Analysis) were calculated by the software package with fitting range 205 – 4000 channels.

2.13.4. Studies On the Interaction of Amino Acid $^{TPer}Ala^{Do}$ (2.78) with BSA

***Preparation of BSA solution*:** Phosphate buffer of pH 7.02 was used to prepare the solution of BSA (Merck). A 1200 μM of stock BSA solution was prepared by dissolving 0.08 gm of BSA in 1 mL phosphate buffer (20 mM) of pH 7.0. From that stock solution sub stock of 1000 μM BSA was prepared. The compound stock solution was prepared in DMF because of the poor solubility in water. 1.0 mg of amino acid $^{TPer}Ala^{Do}$ (**2.78**) was dissolved in 1.5 mL DMF to make a stock probe solution of concentration 910.3 μM.

***General experimental on interaction study of BSA by photophysical study*:** All the spectral measurements were carried out at room temperature. To study the interaction of compound with BSA, an aqueous solution of amino acid $^{TPer}\mathbf{Ala}^{Do}$ (**2.78**) (10 μM for amino acid) was titrated with different concentrations of BSA (ranging from 0, 0.25, 0.5, 7.5, 1.0, 1.5, 2, 2.5, 3.0, 4, 5, 6, 10, 14, 18, 20 equivalent). The total volume of the final solution for each sample was 3 mL. The % of DMF content was 2%. The presence of 2% DMF does not induce structural changes to biomolecules. Each sample solution was mixed well before spectral measurements.

***UV-Visible study with BSA*:** The UV–Visible absorbance measurements were performed using UV-visible spectrophotometer with a cell of 1 cm path length at 298 K. All the UV-Visible studies were carried out in 20 mM phosphate buffer of pH 7.02 containing solution at 298 K. 2 % DMF was used to solubilize the probe. The measurements were taken in absorbance mode and the absorbance values of the sample solutions were measured in the wavelength regime of 200– 700 nm. All the experiments were carried out with freshly prepared sample solutions.

Fluorescence study with BSA: All fluorescence and steady state anisotropy experiments were performed using a steady state fluorescence spectrophotometer with a cell of 1 cm path length at 298 K. The excitation wavelength for probe (amino acid $^{TPer}\mathbf{Ala}^{Do}$ (**2.78**) was set at 280 nm, 420 nm and emission spectra were measured in the wavelength regime of 290–650 nm. Steady state anisotropy of the solutions was measured using steady state fluorescence spectrophotometer. The fluorescence lifetime experiment was carried out as described above.

2.14. ^{1}H and ^{13}C NMR Spectra of Few Selected Amino Acids

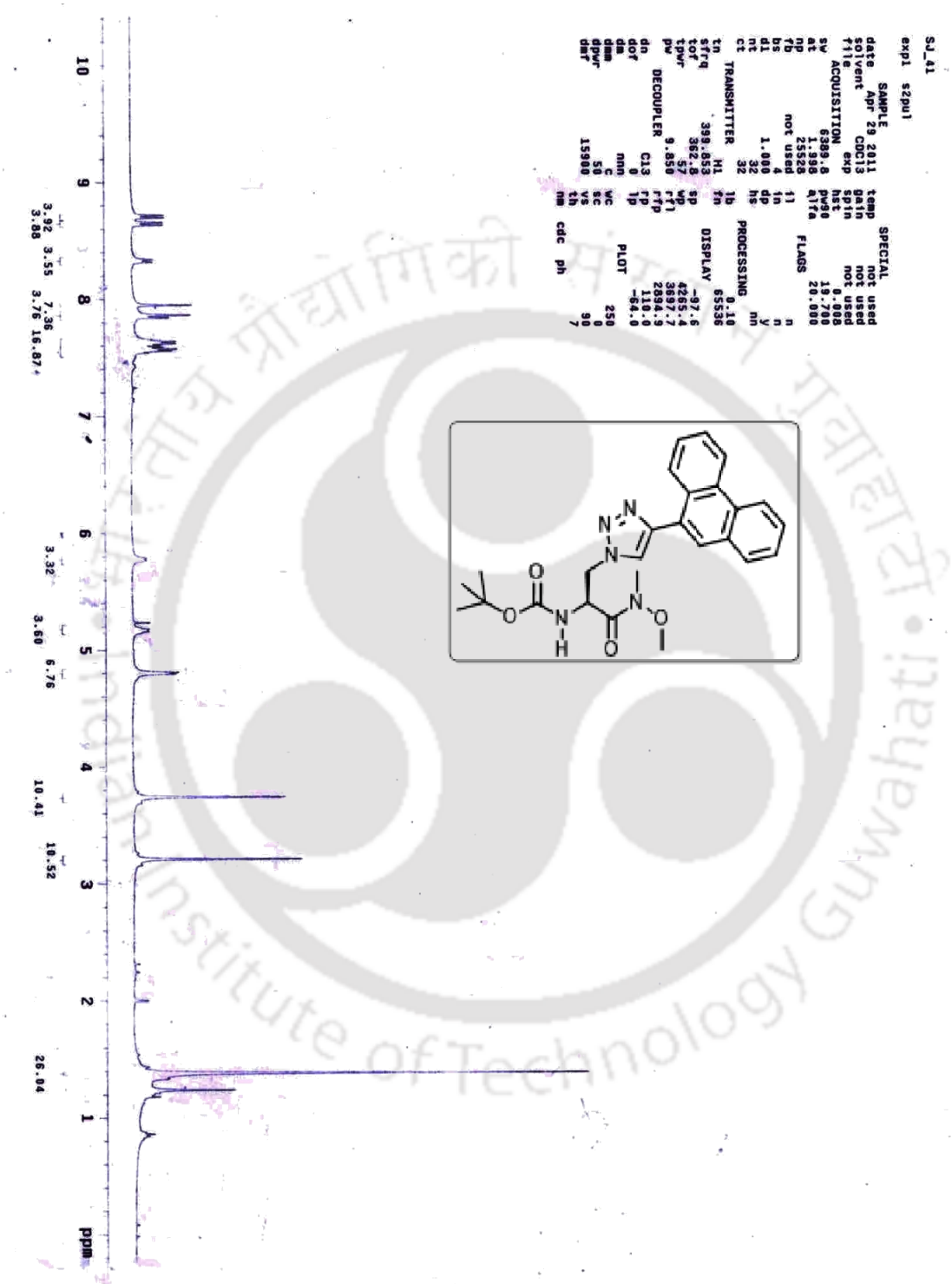

Figure 2.24: ^{1}H NMR spectra of synthesized compound **2.74**

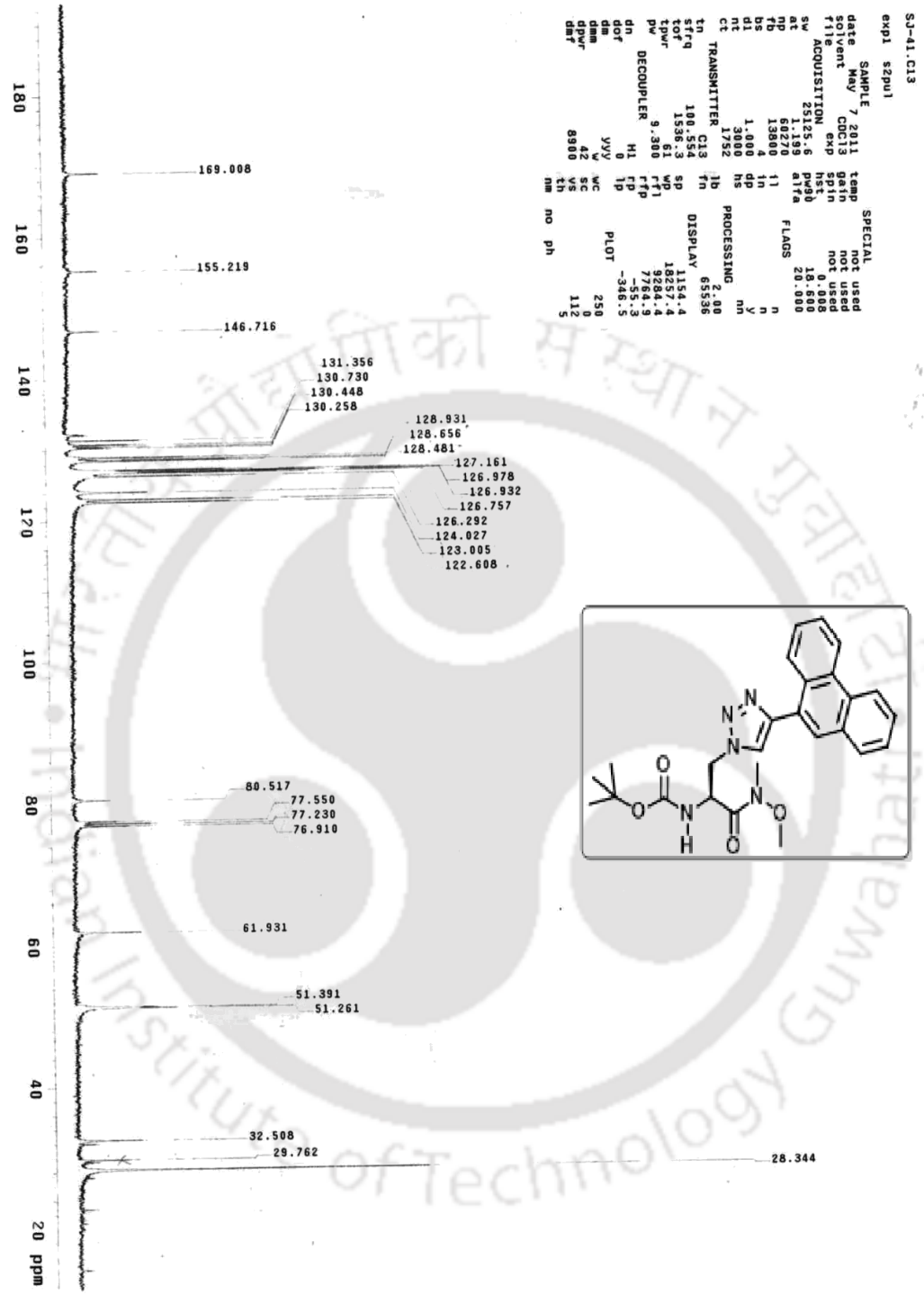

Figure 2.25: ^{13}C NMR spectra of synthesized compound **2.74.**

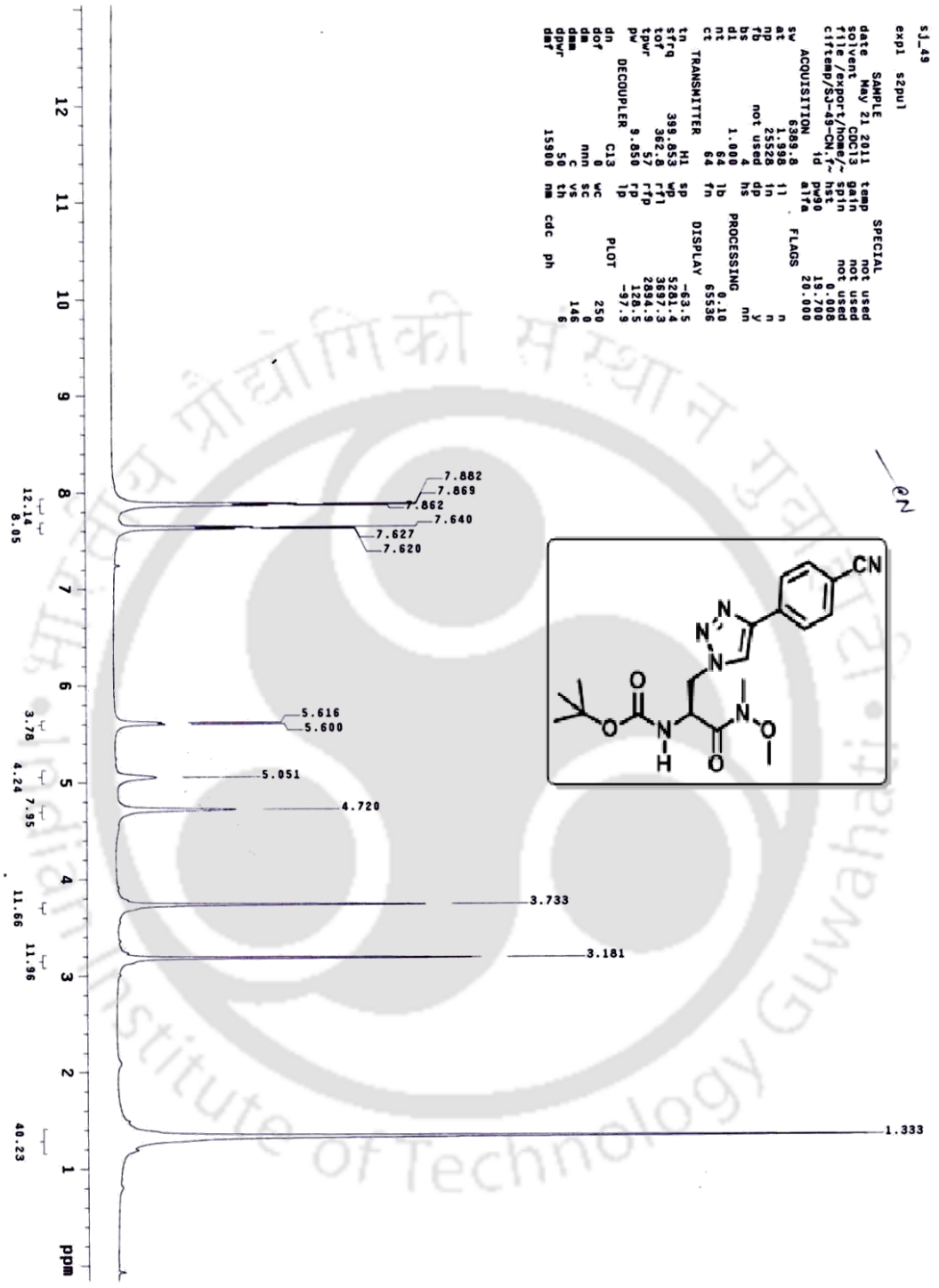

Figure 2.26: ^{1}H NMR spectra of synthesized compound **2.79.**

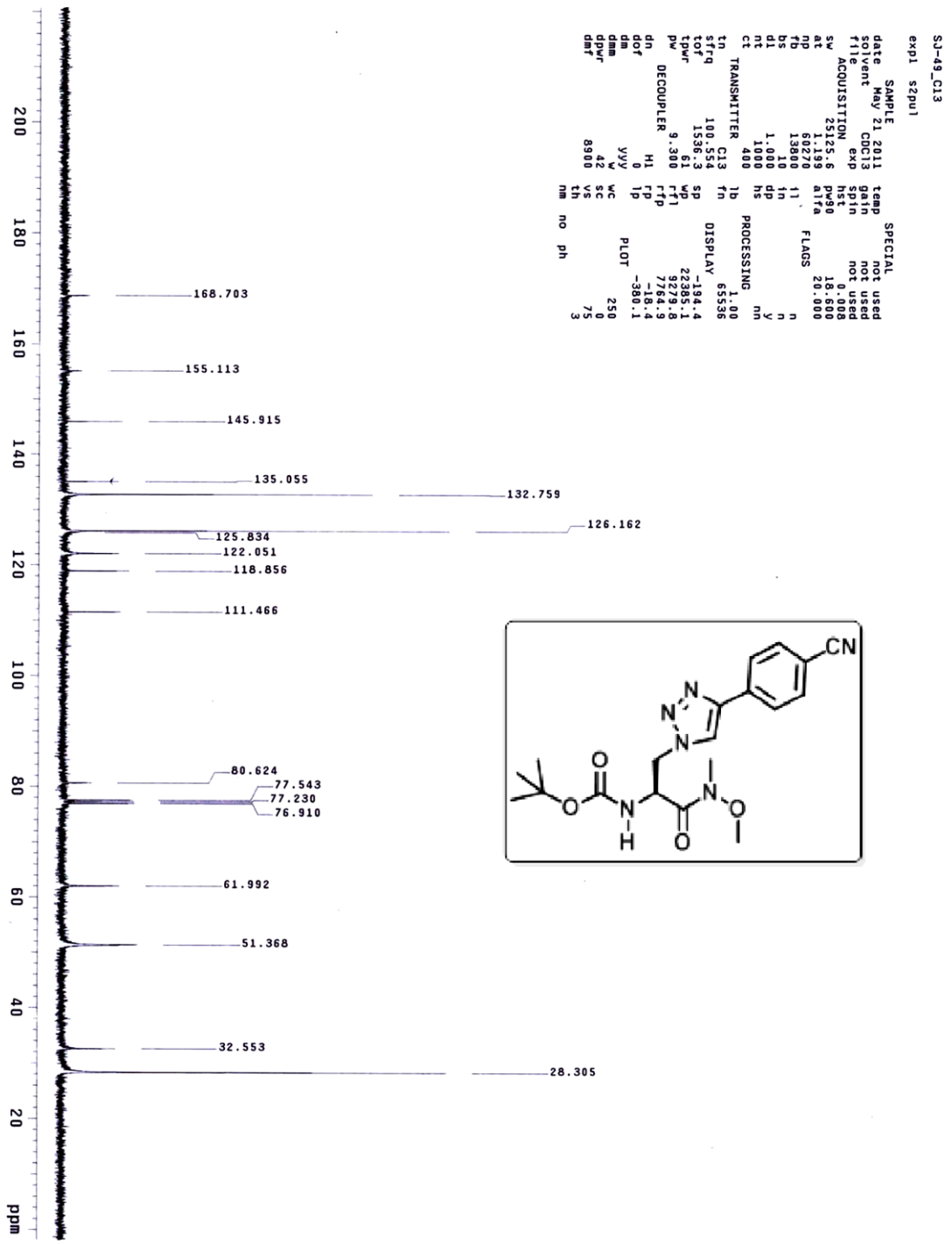

Figure 2.27: ^{13}C NMR spectra of synthesized compound **2.79.**

2.15. References

1. (a) Xie, J.; Schultz, P. G. *Curr. Opin. Chem. Biol.* ***2005***, *9*, *548.* (b) Young, T. S.; Ahmad, I.; Yin, J. A.; Schultz, P. G *J. Mol. Biol.* ***2010***, *395*, 361. (c) Link, A. J.; Mock, M. L.; Tirrell, D. A. *Curr. Opin. Biotechnol*. **2003**, *14*, 603. (d) Liu, J.; Liu, Y.; Gao, M.; Zhang, X.; Proteomics. **2012** *12*, 2258.

2. (a) Merkel, L.; Hoesl, M. G.; Albrecht, M.; Schmidt, A.; Budisa, N. *ChemBioChem* **2010**, *11*, 305. (b) R. F. Wissner, S. Batjargal, C. M. Fadzen, J. E. Petersson, *J. Am. Chem. Soc.* **2013**, *135,* 6529. (c) H. S. Lee, J. Guo, E. A. Lemke, R. D. Dimla, P. G. Schultz, *J. Am. Chem. Soc.* **2009**, *131*, 12921.

3. (a) Diederich, F.; Stang, P. J.; Eds.; Wiley-VCH: New York, **1998**. (b) Nakamura, I.; Yamamoto, Y. *Chem. Rev*. **2004**, *104*, 2127. (c) Cho, S. H.; Kim, J. Y.; Kwak, J.; Chang, S. *Chem. Soc. Rev*. **2011**, *40*, 5068. (d) Shi, W.; Liu, C.; Lei, A. *Chem. Soc. Rev*. **2011**, *40*, 2761. (e) Liu, C.; Zhang, H.; Shi, W.; Lei, A. *Chem. Rev*. **2011**, *111*, 1780.

4. (a) Beletskaya, I. P.; Cheprakov, A. V. Coord. *Chem. Rev*. **2004**, *248*, 2337. (b) Do, H.-Q.; Khan, R. M. K.; Daugulis, O. *J. Am. Chem. Soc*. **2008**, *130*, 15185.

5. Liu, Y.; Wan, J.-P. *Org. Biomol. Chem*. **2011**, *9*, 6873.

6. (a) Agalave, S. G.; Maujan, S. R.; Pore, V. S. *Chem. Asian. J*. **2011**, *6*, 2696. (b) Meldal, M.; Tornøe, C. W. *Chem. Rev*. **2008**, *108*, 2952.

7. (a) Kolb, H. C.; Finn, M. G.; Sharpless, K. B. *Angew. Chem., Int. Ed*. **2001**, *40*, 2004. (b) Wu, P.; Feldman, A. K.; Nugent, A. K.; Hawker, C. J.; Scheel, A.; Voit, B.; Pyun, J.; Frechet, J. M. J.; Sharpless, K. B.; Fokin, V. V. *Angew. Chem., Int. Ed*. **2004**, *43*, 3928.

8. (a) Kolb, H. C.; Finn, M. G.; Sharpless, K. B. *Angew. Chem., Int. Ed*. **2001**, *40*, 2004. (b) Wu, P.; Feldman, A. K.; Nugent, A. K.; Hawker, C. J.; Scheel, A.; Voit, B.; Pyun, J.; Fréchet, J. M. J.; Sharpless, K. B.; Fokin, V. V. *Angew. Chem., Int. Ed*. **2004**, *43*, 3928. (c) Finn, M. G.; Fokin, V. V. *Chem. Rev*. **2010**, *39*, 1231.

9. Tron, G. C.; Pirali, T.; Billington, R. A.; Canonico, P. L.; Sorba, G.; Genazzani, A. A. *Med. Res. Rev*. **2008**, *28*, 278.

10. Kolb, H. C.; Sharpless, K. B. *Drug Discovery Today* **2003**, *8*, 1128. (b) Moses, J. E.; Moorhouse, A. D. *Chem. Rev*. **2007**, *36*, 1249.

11. (a) Bock, V. D.; Hiemstra, H.; van Maarseveen, J. H. *Eur. J. Org. Chem*. **2005**, 51. (b) Briehn, C. A.; Schiedel, M.-S.; Bonsen, E. M.; Schuhmann, W.; Bauerle, P. *Angew. Chem., Int. Ed*. **2001**, *40*, 4680. (c) Sawa, M.; Hsu, T.-L.; Itoh, T.; Sugiyama, M.; Hanson, S. R.; Vogt, P. K.; Wong, C.-H. *Proc. Natl. Acad. Sci. U. S. A.* **2006**, *103*, 12371.

12. Evans, C. E.; Lovell, P. A. *Chem. Commun*. **2009**, 2305.

13. Dirks, A. J.; Cornelissen, J. J. L. M.; Nolte, R. J. M. *Bioconjugate Chem*. **2009**, *20*, 1129.

14. Guo, H. M.; Minakawa, M.; Tanaka, F. *J. Org. Chem*. **2008**, *73*, 3964.
15. Sivakumar, K.; Xie, F.; Cash, B. M.; Long, S.; Barnhill, H. N.; Wang, Q. *Org. Lett*. **2004**, *6*, 4603.
16. Droumaguet, C. L.; Wang, C.; Wang, Q. *Chem. Soc. Rev*. **2010**, *39*, 1233.
17. Holub, J. M.; Kirshenbaum, K. *Chem. Soc. Rev*. **2010**, *39*, 1325
18. Zhou, Z.; Fahrni, C. J. *J. Am. Chem. Soc*. **2004**, *126*, 8862.
19. (a) Wheelock, C. E. *J. Am. Chem. Soc*. **1959**, *81*, 1348. (b) Briehn, C. A.; Schiedel, M.-S.; Bonsen, E. M.; Schuhmann, W.; Bauerle, P. *Angew. Chem., Int. Ed*. **2001**, *40*, 4680.
20. (a) O'Reilly, R. K.; Joralemon, M. J.; Hawker, C. J.; Wooley, K. L. *Chem.–Eur. J*. **2006**, *12*, 6776. (b) Breed, D. R.; Thibault, R.; Xie, F.; Wang, Q.; Hawker, C. J.; Pine, D. J. *Langmuir* **2009**, *25*, 4370. (c) Tornøe, C. W.; Sanderson, S. J.; Mottram, J. C.; Coombs, G. H.; Meldal, M. *J. Comb. Chem.* **2004**, *6*, 312.
21. (a) Ievins, A. D.; Wang, X. F.; Moughton, A. O.; Skey, J.; O'Reilly, R. K. *Macromolecules* **2008**, *41*, 2998. (b) Evans, C. E.; Lovell, P. A. *Chem. Commun*. **2009**, 2305.
22. (a) Dirks, A. J.; Cornelissen, J. J. L. M.; Nolte, R. J. M. *Bioconjugate Chem*. **2009**, *20*, 1129.
23. (a) Bag, S. S.; Kundu, R. *J. Org. Chem*. **2011**, *76*, 3348. (b) Bag, S. S.; Talukdar, S.; Matsumoto, K.; Kundu, R. *J. Org. Chem*. **2013**, *78*, 278.
24. (a) Röper, S.; Kolb, H. C. *Fragment-based Approaches in Drug Discovery*, Wiley-VCH Verlag GmbH & Co. KGaA: Weinheim, Germany, **2006**. (b) Colombo, M.; Peretto, I. *Drug Discovery Today* **2008**, *13*, 677. (c) Borshell, N.; Papp, T.; Congreve, M. *Nat. Rev. Drug Discovery* **2011**, *10*, 166. (d) Welsch, M. E.; Snyder, S. A.; Stockwell, B. R. *Curr. Opin. Chem. Biol*. **2010**, *14*, 347.
25. (a) Baig, R. B. N.; Varma, R. S. *Chem. Commun*. **2012**, *48*, 5853. (b) Dalvie, D. K.; Kalgutkar, A. S.; Khojasteh-Bakht, S. C.; Obach, R. S. J.; Donnell, P. O. *Chem. Res. Toxicol*. **2002**, *15*, 269. (b) Horne, W. S.; Yadav, M. K.; Stout, C. D.; Ghadiri, M. R. *J. Am. Chem. Soc*. **2004**, *126*, 15366.
26. Nielsen, P. E.; Egholm, M.; Berg, R. H.; Buchardt, O. *Science* **1991**, *254*, 1497.
27. Egholm, M.; Buchardt, O.; Christensen, L.; Behrens, C.; Freier, S. M.; Driver, D. A.; Berg, R. H.; Kim, S. K.; Norden, B.; Nielsen, P. E. *Nature* **1993**, *365*, 566.
28. (a) Nielsen, P. E. *Acc. Chem. Res*. **1999**, *32*, 624. (b) Nielsen, P. E. *Mol. Biotechnol*. **2004**, *26*, 233.
29. Pellestor, F.; Paulasova, P.; Macek, M.; Hamamah, S. *Med. Sci*. (Paris), **2005**, *21*, 753.
30. Hanvey, J. C.; Peffer, N. J.; Bisi, J. E. *Science* **1992**, *258*, 1481.
31. (a) Vergnaud, J.; Faugeras, P. -A.; Chaleix, V.; Champavier, Y.; Zerrouki, R.; *Tetrahedron Lett*. **2011**, *52*, 6185. (b) Nuzzi, A.; Massi, A.; Dondoni, A. *QSAR Comb. Sci*. **2007**, *26*, 1191. (c) Isobe, H.; Fujino, T.; Yamazaki, N.; Guillot-

Nieckowski, M.; Nakamura, E. *Org. Lett*. **2008**, *10*, 3729. (d) Binauld, S.; Hawker, C. J.; Fleury, E.; Drockenmuller, E. *Angew. Chem*. **2009**, *48*, 6654. (e) Peng, X.; Li, H.; Seidman, M. *Eur. J. Org. Chem*. **2010**, 4194. (f) Binauld, S.; Damiron, D.; Hawker, C. J.; Drockenmuller, E. *Macromol. Rapid Commun*. **2011**, *32*, 147.

32. (a) Jotterand, N.; Pearce, D. A.; Imperiali, B. *J. Org. Chem.* **2001,** *66*, 3224. (b) Walkup, G. K.; Imperiali, B. *J. Org. Chem.* **1998**, *63*, 6727.

33. Wang,Y.; Paletta, J. T.; Berg, K.; Reinhart, E.; Rajca, S.; Rajca, A. *Org. Lett.* **2014**, *16*, 5298.

34. Zhu, R.-Y.; Tanaka, K.; Li, G.-C.; He, J.; Fu, H.-Y.; Li, S. H.; Yu, J. Q. *J. Am. Chem. Soc*. **2015**, *137*, 7067.

35. (a) Costa, S. P.G.; Batista, R. M. F.; Raposo, M. M. M. *Tetrahedron* **2008**, *64*, 9733. (b) Roncali, J. *Chem. Rev*. **1997**, 97, 173.

36. (a) Xiao, H.; Chatterjee, A.; Choi, S. –H.; Bajjuri, K. M.; Sinha, S. C.; Schultz, P. G. *Angew. Chem. Int. Ed*. **2013**, *52*, 14080. (b) Kiick, K. L.; Saxon, E.; Tirrell, D. A.; Bertozzi, C. R. *PNAS* **2002**, *99*, 119.

37. (a) Liu, C.; Schultz, P. *Annu. Rev. Biochem.* **2010**, *79*, 413. (b) Neumann, H. *FEBS Lett*. **2012**, *586*, 2057. (c) Lang, K.; Chin, J. *Chem Rev.* **2014**, *114*, 4764. (d) Mitra, N. *Mater Methods* **2013**, *3*, 204. (e) Kiick, K. L.; Saxon, E.; Tirrell, D. A.; Bertozzi, C. R. *Proc. Natl. Acad. Sci. U. S. A.* **2002**, *99*, 19.

38. (a) Ben-Efraim, I.; Strahilevitz, J.; Bach, D.; Shai, Y. *Biochemistry* **1994**, *33*, 6966. (b) Marmé, N.; Knemeyer, J. P.; Sauer, M.; Wolfrun, J. *Bioconjugate Chem.* **2003**, *14*, 1133. (c) Bains, G.; Patel, A. B.; Narayanaswami, V. *Molecules* **2011**, *16*, 7909.

39. (a) Pap, E. H. W.; Dansen, T. B.; van Summeren, R.; Wirtz, K.W.A. *Exp. Cell Res*. **2001**, *265*, 288. (b) Tung, C -H. *Peptide Sci.* **2004**, *76*, 391. (e) Kenworthy, A. K. *Methods* **2001**, *24*, 289. (c) Hoppe, A.; Christensen, K.; Swanson, J. A. *Biophys. J.* **2002**, *83*, 3652.

40. (a) Pazos, E.; Vázquez, O.; Mascareñas, J.; Vázquez, M. E. *Chem. Soc. Rev.* **2009**, *38*, 3348. (b) Hoppe, A.; Christensen, K.; Swanson, J. A. *Biophys. J.* **2002**, *83*, 3652. (c) Ozawa, T.; Umezawa, Y. *Supramol. Chem.* **2002**, *14*, 271. (d) Packard, B. Z.; Toptygin, D. D.; Komoriya, A.; Brand, L. *Proc. Natl. Acad. Sci. U. S. A* **1996**, *93*, 11640. (e) Peled, H.; Shai, Y. *Biochemistry* **1994**, *33*, 7211.

41. (a) Vestergaard, M. *Biochem. Biophys. Res. Comm*. **2008**, *725*, 377.

42. (a) Martin, L. J.; Imperiali, B. *Methods Mol. Biol.* **2015**, *1248*, 201. (b) Talukder, P.; Chen, S. C.; Liu, T.; Baldwin, E. A.; Benkovic, S. J.; Hecht, S. M. *Bioorg. Med. Chem. Lett.* **2014**, *22*, 5924.

43. (a) Lu, C. H.; Li, J.; Zhang, X. L.; Zheng, A. X.; Yang, H. H.; Chen, Xi.; Chen, G. N. *Anal. Chem*. **2011**, *83*, 7276. (b) Oh, K. J.; Cash, K. J.; Plaxco, K. W. *J. Am. Chem. Soc***. 2006**, *128*, 14018. (c) Marmé, N.; Knemeyer, J. P.; Wolfrun, J.;

Sauer, M. *Angew.Chem., Int. Ed. Engl*. **2004**, *43*, 3798. (d) Samanta, M.; Petersson, E. J. *Aust. J. Chem.* **2013**, *67*, 686.

44. (a) Bag, S. S.; Jana, S.; Yashmeen, A.; De, S. *Chem. Comm.* **2015**, *51*, 5242**.** (b) Bag, S. S.; Jana, S.; Yashmeen, A.; Senthilkumar, K.; Bag, R. *Chem. Comm.* **2014**, *50*, 433. (c) Loving, G. Imperiali, B. *J. Am. Chem. Soc.* **2008**, *130*, 13630. (d) Krueger, A. T.; Imperiali, B. *ChemBioChem.* **2013**, *14*, 788. (e) Socher, E.; Imperiali, B. *ChemBioChem* **2013**, *14*, 53.

45. (a) Chatterjee, A.; Guo, J.; Lee, H. S.; Schultz, P. G. *J. Am. Chem. Soc.* **2013**, *135*, 12540. (b) Charbon, G.; Brustad, E.; Scott, K. A.; Wang, J.; Løbner-Olesen, A.; Schultz, P. G.; Jacobs-Wagner, C.; Chapman, E. *ChemBioChem*. **2011**, *12*, 1818. (c) Summerer, D.; Chen, S.; Wu, N.; Deiters, A.; Chin, J. W.; Schultz, P. G. Proc. Natl. Acad. Sci. USA. **2006**, *103*, 9785. (d) Pantoja, R.; Rodriguez, E. A.; Dibas, M. I.; Dougherty, D. A.; Lester, H. A. *Biophys. J.* **2009**, *96*, 226.

46. (a) Hohsaka, T.; Kajihara, D.; Ashizuka, Y.; Murakami, H.; Sisido, M. *J. Am. Chem. Soc*. **1999**, *121*, 34. (b) Wendt, H.; Berger, C.; Baici, A.; Thomas, R. M.; Bosshard, H. R. *Biochemistry* **1995**, *34*, 4097. (c) Wolf, J. H.; Korf, J. *J. Pharm. Biomed. Anal*. **1992**, *11*, 99 (d) Christie, R.M. *Rev. Prog. Color. Relat. Top.* **1993**, 23. (e) Yavari, I.; Hekmat-Shoar, R.; Zonouzi, A. *Tetrahedron Lett.* **1998**, *39*, 2391.

47. (a) Li, H.; Aneja, R.; Chaiken, I. *Molecules* **2013**, *18*, 9797. (b) Kolb, H. C.; Finn, M. G.; Sharpless, K. B. *Angew. Chem., Int. Ed*. **2001**, *40*, 2004. (c) Wu, P.; Feldman, A. K.; Nugent, A. K.; Hawker, C. J.; Scheel, A.; Voit, B.; Pyun, J.; Fréchet, J. M. J.; Sharpless, K. B.; Fokin, V. V. *Angew. Chem., Int. Ed*. **2004**, *43*, 3928. (d)Rostovtsev, V. V.; Green, L. G.; Fokin, V. V.; Sharpless, K. B. *Angew. Chem., Int. Ed.* **2002**, *41*, 2596. (e) Meldal, M.; Tornøe, C. W. *Chem. Rev*. **2008**, *108*, 2952.

48. (a) Vlieghe, P.; Lisowski, V.; Martinez, J.; Khrestchatisky, M. *Drug. Discov. Today* **2010**, *15*, 40. (b) Tron, G. C.; Pirali, T.; Billington, R. A.; Canonico, P. L.; Sorba, G.; Genazzani, A. A. *Med. Res. Rev.* **2008**, *28*, 278. (c) Hou, J.; Liu, X.; Shen, J.; Zhao, G.; Wang, P.G. *Expert Opin. Drug Discov.* **2012**, *7*, 489.

49. Panda, G.; Rao, N. V. *Synlett* **2004**, 714.

50. (a) Grabowksi, Z. R.; Rotkiewicz, K.; Rettig, W. *Chem. Rev*. **2003**, *103*, 3899. (b) Badger, G. M.; Walker, I. S. *J. Chem. Soc*. **1956**, 122. (c) Joshi, R.; Meitei, O. R.; Kumar, H.; Jadhao, M.; Ghosh, S. K. *J. Phys. Chem. A* **2016,** *120*, 1000. (d) Chang, D. -H.; Ou, C. –L.; Hsu, H. –Y.; Huang, G. -J.; Kao, C. –Y.; Liu, Y –H.; Peng, S. –M.; Diau, E. W. –G.; Yang, J –S. *J. Org. Chem.* **2015,** *80*, 12431.(e) Barman, N.; Singha, D.; Sahu, K. *J. Phys. Chem. A* **2013**, *117*, 3945. (f) Huang, G. –J.; Ho, J -H.; Prabhakar, C.; Liu, Y. –H.; Peng, S. –M.; Yang, J. –S. *Org. Lett.* **2012**, *14*, 5034. (g) Zhang, Y.; Jiang, M.; Han, G. –C.; Zhao, K.; Tang, B. Z.; Wong, K. S. *J. Phys. Chem. C* **2015,** *119*, 27630. (h) Dobkowski, J.; Kijak, M.; Sazanovich, I. V.; Waluk, J. *J. Phys. Chem. B* **2015,** *119*, 7294. (i)

Kobayashi, A.; Takehira, K.; Yoshihara, T.; Uchiyama, S.; Tobita, S. *Photochem. Photobiol. Sci.* **2012**, *11*, 1368-1376.

51. (a) Ji, L.; Lorbach, A.; Edkins, R. M.; Marder, T. B. *J. Org. Chem*. **2015**, *80*, 5658. (b) Bucevicius, J.; Skardziute, L.; Dodonova, J.; Kazlauskas, K.; Bagdziunas, G.; Jursenas, S.; Tumkevicius, S. *RSC Adv.* **2015**, *5*, 38610. (c) Nagarajan, N.; Velmurugan, G.; Venuvanalingam, P.; R. Renganathan *J. Photochem. Photobiol. A: Chemistry* **2014**, *284*, 36. (d) Denneval, C.; Moldovan, O.; Baudequin, C.; Achelle, S.; Baldeck, P.; Plé, N.; Darabantu, M.; Ramondenc, Y. *Eur. J. Org. Chem.* **2013**, *2013*, 5591. (e) Valeur, B. Molecular Fluorescence: Principles and Applications; Wiley-VCH Verlag: GmbH: Weinheim, Germany, **2001**

52. (a) Fromherz, P. *J. Phys. Chem.* **1995**, *99*, 7188. (b) Albinsson, B. *J. Am. Chem. Soc*. **1997**, *119*, 6369. (c) Shim, T.; Lee, M. H.; Kim, D.; Ouchi, Y. *J. Phys. Chem. B* **2008**, *112*, 1906. (d) Panigrahi, M.; Dash, S.; Patel, S.; Behera, P. K.; Mishra, B. K. *Spectrochim. Acta, Part A* **2007**, *68*, 757. (e) Kim, H. J.; Hong, J.; Hong, A.; Ham, S.; Lee, J. H.; Kim, J. S. *Org. Lett.* **2008**, *10*, 1963. (f) Benniston, A. C.; Harriman, A.; Llarena, I.; Sams, C. A. *Chem. Mater*. **2007**, *19*, 1931. (g) Maeda, H.; Maeda, T.; Mizuno, K.; Fujimoto, K.; Shimizu, H.; Inouye, M. *Chem.—Eur. J.* **2006**, *12*, 824. (h) Perez -Inestrosa, E.; Montenegro, J. -M.; Collado, D.; Suau, R. *Chem. Commun*. **2008**, 1085. (i) Yang, S. -W.; Elangovan, A.; Hwang, K. -C.; Ho, T. -I. *J. Phys. Chem. B* **2005**, *109*, 16628. (m) Senthilkumar, S.; Nath, S.; Pal, H. *Photochem. Photobiol.* **2004**, *80*, 104.

53. (a) Lakowicz, J. R. *Principles of Fluorescence Spectroscopy*; 3rd ed.; Springer: New York, **2006**. (b) Gutow, J. H. *J. Chem. Educ*. **2005**, *82*, 302. (c) Peng, X.; Draney, D. R.; Volcheck, W. M. *Proc. SPIE* **2006**, 6097. (d) Peng, X.; Chen, H.; Draney, D. R.; Schutz-Geschwender, A.; Olive, D. M. *Anal. Biochem*. **2009**, *388*, 220. (e) Arai, S.; Yoon, S. –I.; Murata, A.; Takabayashi, M.; Wu, X.; Lu, Y.; Takeoka, S.; Ozaki, M. *Biochem. Biophys. Res. Commun.* **2011**, *404*, 211. (f) Kuznetsova, S.; Zauner, G.; Schmauder, R.; Mayboroda, O. A.; Deelder, M.; Aartsma, T. J. Canters, G. W. *Anal. Biochem.* **2006**, *350*, 52.

54. (a) Young, R. M.; Arnette, J. K.; Roess, D. A.; Barisas, B. G. *Biophys. J.* **1994**, *67*, 881. (b) Wei, A. P.; Blumenthal, D. K.; Herron, J. N. *Anal. Chem*. **1994**, *66*, 1500. (c) Geoghegan, K. F.; Rosner, P. J.; Hoth, L. R. *Bioconjugate Chem*. **2000**, *11*, 71. (d) Neuweiler, H.; Schultz, A.; Vaiana, A. C.; Smith, J. C.; Kaul, S.; Wolfrum, J.; Sauer, M. *Angew. Chem., Int. Ed*. **2002**, *41*, 4769. (e) Kohn, J. E.; Plaxco, K. W. *Proc. Natl. Acad. Sci. U.S.A.* **2005**, *102*, 10841. (f) Voss, S.; Fischer, R.; Jung, G.; Wiesmuller, K. H.; Brock, R. *J. Am. Chem. Soc*. **2007**, *129*, 554. (g) Wruss, J.; Pollheimer, P. D.; Meindl, I.; Reichel, A.; Schulze, K.; Schofberger, W.; Piehler, J.; Tampe, R.; Blaas, D.; Gruber, H. J. *J. Am. Chem. Soc*. **2009**, *131*, 5478. (h) Chen, S.; Fahmi, N. E.; Wang, L.; Bhattacharya, C.;

Benkovic, S. J.; Hecht, S. M. *J. Am. Chem. Soc*. **2013**, *135*, 12924. (i) Kajihara, D.; Abe, R.; Iijima, I.; Komiyama, C.; Sisido, M.; Hohsaka, T. *Nat. Methods* **2006**, *3*, 923.

55. Frisch, M. J.; Trucks, G. W.; Schlegel, H. B.; Scuseria, G. E.; Robb, M. A.; Cheeseman, J. R.; Scalmani, G.; Barone, V.; Mennucci, B.; Petersson, G. A.; Nakatsuji, H.; Caricato, M.; Li, X.; Hratchian, H. P.; Izmaylov, A. F.; Bloino, J.; Zheng, G.; Sonnenberg, J. L.; Hada, M.; Ehara, M.; Toyota, K.; Fukuda, R.; Hasegawa, J.; Ishida, M.; Nakajima, T.; Honda, Y.; Kitao, O.; Nakai, H.; Vreven, T.; Montgomery, J. A. Jr.; Peralta, J. E.; Ogliaro, F.; Bearpark, M.; Heyd, J. J.; Brothers, E;. Kudin, K. N.; Staroverov, V. N.; Kobayashi, R.; Normand, J.; Raghavachari, K.; Rendell, A.; Burant, J. C.; Iyengar, S. S.; Tomasi, J.; Cossi, M.; Rega, N.; Millam, J. M.; Klene, M.; Knox, J. E.; Cross, J. B.; Bakken, V.; Adamo, C.; Jaramillo, J.; Gomperts, R.; Stratmann, R. E.; Yazyev, O.; Austin, A. J.; Cammi, R.; Pomelli, C.; Ochterski, J. W.; Martin, R. L.; Morokuma, K.; Zakrzewski, V. G.; Voth, G. A.; Salvador, P.; Dannenberg, J. J.; Dapprich, S.; Daniels, A. D.; Farkas, O.; Foresman, J. B.; Ortiz, J. V.; Cioslowski, J.; Fox, D. J. Gaussian, Inc. Wallingford CT, **2009**.

56. (a) Nag, M. Bera, K.; Chakraborty, S.; Basak S. *J Photochem Photobiol B.* **2013**,*127*, 202. (b) Shi, J. H.; Zhu, Y. Y.; Wang, J.; Chen, J.; Shen, Y. J. *Spectrochim Acta A Mol Biomol Spectrosc*. **2013**, *103*, 287. (c) Zhang, X.; Li, L.; Xu, Z.; Liang, Z.; Su, J.; Huang, J.; Li, B. *PLoS One* **2013**, *8*, e59106. (d) Pal, S.; Saha, C. *J Biomol Struct Dyn.* **2014**, *32*, 1132. (e) Hu, Y.; Zhang, G.; Yan, J. *Mol Biol Rep.* **2014**, *41*, 1693.

57. (a) Tao, X. -T.; Wang, L.; Yang, J. -X.; Jiang, M. -H. *J. Phys. Chem. C* **2009**, *113*, 6809. (b) Suzuki, Y.; Yokoyama, K. *J. Am. Chem. Soc*. **2005**, *127*, 17799. (c) Bag, S. S.; Kundu, R.; Jana, S. *Tetrahedron Lett*. **2013**, *54*, 2627. (d) Ni, Y.; Zhu, R.; Kokot, S. *Analyst* **2011**, *136*, 4794. (e) Alvim, H. G. O.; Fagg, E. L.; de Oliveira, A. L.; de Oliveira, H. C. B.; Freitas, S. M.; Xavier, M. –A. E.; Soares, T. A.; Gomes, A. F.; Gozzo, F. C.; Silva, W. A. Neto, B. A. D. *Org. Biomol. Chem.* **2013**, ***11***, 4764. (f) Banerjee, M.; Pal, U.; Subudhhi, A.; Chakrabarti, A.; Basu, S. *J. Photochem. Photobiol. B: Biol.* **2012**, *108*, 23.

58. Bag. S. S.; Kundu, R.; Jana, S. *Tetrahedron Lett*. **2013**, *54*, 2627. (b) Roy, D.; Dutta, S.; Maity, S. S.; Ghosh, S.; Roy, A. S.; Ghosh, K. S.; Dasgupta, S. *J. Lumin.* **2012**, *132*, 1364. (c) Hazra, P.; Chakrabarty, D.; Chakraborty, A.; Sarkar, N. *Biochem. Biophys. Res. Commun.* **2004**, *314*, 543. (d) Paul, B. K.; Guchhait, N. J. *Phys. Chem. B* **2011**, *115*, 10322.

59. (a) Morris, G. M.; Huey, R.; Lindstrom, W.; Sanner, M. F.; Belew, R. K.; Goodsell, D. S.; Olson, A. J. *J. Comput. Chem*. **2009**, *16*, 2785.

Chapter 3

SYNTHESIS, CONFORMATION AND STUDY OF PHOTOPHYSICS OF TRIAZOLYL DONOR–ACCEPTOR UNNATURAL AMINO ACIDS DECORATED TRIPEPTIDES: A FRET EVENT IN β-TURN CONFORMATION

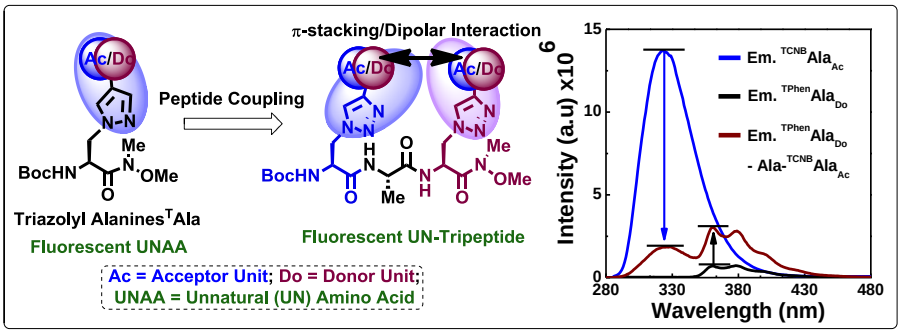

3.1. Introduction: Peptidomimetics and Their Importance

During the past decade, peptides have gained a wide range of applications in medicine and biotechnology. Thus, therapeutic peptide research is currently experiencing a renaissance for commercial reasons as peptides are selective and efficient signaling molecules and trigger intracellular effects through binding to specific cell surface receptors, such as G protein-coupled receptors (GPCRs) or ion channels. Given their attractive pharmacological profile and intrinsic properties, peptides represent an excellent starting point for the design of novel therapeutics. Moreover, high specificity would make peptides as excellently safe, tolerable and effective in humans. Thus, in various aspects of drug market, peptides are in the sweet spot between small molecules and biopharmaceuticals. However, natural peptides seldom can be used therapeutically as drugs, because of the problems associated with low absorption, rapid metabolism and low oral bioavailability, many efforts aimed to modify the natural sequence of the amino acids of bioactive peptides achieved a desired and a focused effect.[1a] Therefore, the discovery of the physiological role of a great number of peptides stimulated researchers all over the world towards design and synthesis of peptidomimetics[1] or peptide like molecules.[2]

The Since natural peptides seldom can be used therapeutically as drugs, because of the problems associated with low absorption, rapid metabolism and low oral bioavailability, many efforts aimed to modify the natural sequence of the amino acids of bioactive peptides achieved a desired, very focused effect. Peptidomimetics, which maintain the key elements required for activity but replace the labile peptide bonds[1g, 3] with more stable features have the advantage of providing new functionalities that can circumvent natural processes in the body. For example, they become able to perform functions that are not available with the natural materials, such as binding to and penetrating cell membranes and resisting degradation by enzymes. Furthermore, to overcome the problems associated with the activity/stability of peptide based drugs,[3] unnatural amino acids could be incorporated into peptides to tune the conformation and stability of the peptide. Those remodeled peptide might be more efficient and biologically active than the natural counterpart.[4]

Peptidomimetics that fold to mimic protein secondary structures[4] have emerged as important targets of bioorganic chemistry. Recently, a variety of compounds that mimic helices,[5] turns,[6] and sheets[7] have been developed, with notable advances in the design of β–peptides that mimic each of these structures. These compounds hold promise as a step toward synthetic molecules with protein like properties and as drugs that block protein-protein[8] interactions. Current speed for the development of unnatural amino acids based peptides/ rigid side chain modified peptides enhances the generation of peptidomimetics with greater stability and conformational rigidity. Therefore, researchers are now involved in synthesizing small peptides and proteins based on unnatural amino acids in the backbone to introduce cumulative properties.[1, 2]

Although initial efforts in peptidomimetic chemistry focused upon the development of enzyme inhibitors[9] and peptide hormone analogues, this field now encompasses both the creation of pharmacologically useful analogues of biologically active peptides and the development of compounds that mimic protein structures. Current objectives include developing new drugs, gaining an enhanced understanding of protein folding, and creating catalysts and new materials with useful properties. Incorporation of non-encoded amino acids into protein ensembles serves to expand the opportunities well beyond the constraints set by nature. Thus, present days protein engineering broadly uses the tools of many fields, allowing us to generate protein/peptide of therapeutic importance in one hand and to investigate protein's structure, function, dynamics and interbiomolecular interactions using a range of biophysical techniques. Therefore, recently, protein engineering has been extensively used for functional studies, biophysical analysis and improving medicinal values of proteins of clinical importance.

However, for studying protein's structure, function, dynamics and interbiomolecular interaction property or monitoring other biological process needs the help of highly sophisticated, sensitive and fast technique such as fluorescence. Moreover, sensing of proteins' microenvironment needs the help of highly sensitive fluorescence probe; though a few reports exist but are not sufficient to fulfill the all research needs.[10] Many of the problems for generating extrinsic fluorescently labeled proteins can be solved if a microenvironment sensitive intrinsic fluorescent amino acid can be synthesized and incorporated into a protein site-specifically. Therefore, extremely sensitive fluorescence based detection techniques find widespread applications for probing of structure, function, dynamics of biomolecules, for visualizing intracellular events, understanding molecular interactions inside a cell and for enabling experiments to be measured in solution.[11] Out of several fluorescence based techniques, the fluorescence resonance energy transfer (FRET) is widely being utilized for such purposes. FRET is a distance dependent phenomenon and unique in generating fluorescence signal associated with molecular conformation, association, separation in the range of 1-10 nm. In this process energy transfer occurs nonradiatively via long rang dipole-dipole interaction in an exited electronic state from donor to an acceptor chromophore. The energy transfer rate depends on the 6^{th} power of donor-acceptor separation (r^6) and other parameters such as, (i) Overlap integral area of donor emission and acceptor absorbance spectra, (ii) relative orientation of donor and acceptor molecule and (iii) refractive index of the enviornment.[12] The FRET process is widely utilized in the elucidation of structures, investigating protein dynamics, studying biomolecular interactions and the conformational distribution of unstructured peptides, along with many other sensory applications.[13,14]

Therefore design of peptide with a particular secondary structure with high proteolytic resistance which would be of medicinal importance in one hand and on the

other hand could be useful as probe would be an attractive research target. In this avenue, fluorescent amino acids based peptides can play a vital role because without much perturbation of the protein conformation, they can serve as probes for in vitro and cellular imaging of protein localization, biomolecular interactions, and conformational changes with the ability to place these small probes at virtually any site in the proteome.

3.2. The Approaches to β-Turn Peptidomimetic

Among the different type of secondary structure β-turn is one of the most important structure of protein.[4] The β-turn[6] (**Figure 3.1** and **3.2**), which has also been referred to as the beta-bend, beta-loop or reverse turn, is one of the three major secondary structural elements of peptides and proteins. The surface localization of turns in proteins, and the predominance of residues containing potentially critita1 pharmacophoric information, has led to the hypothesis that turns play critical roles in a myriad of recognition events in biological systems. These events include but are not limited to the interactions between peptide hormones and their receptors, antibodies and antigens, and regulatory enzymes and their corresponding substrates. Reverse turn mimetics are thus powerful tool for the study of molecular recognition and are providing a unique opportunity to dissect and investigate structure-function relationships in complex proteins. The β-turn can tune the peptide structure that is necessary for compact conformation and is stabilized by intramolecular hydrogen bond.[6] A great deal of effort has therefore focused on the design and synthesis of small constrained mimetics of turn structure to provide a better understanding of the molecular basis of peptide and protein interactions in addition to providing potent and selective therapeutic agents.

β-Turns constitute a tetra peptide unit, which cause a reversal of direction of the peptide chain. Formally, turns can be described by the distance from the Cα of the first residue to the Cα of the fourth residue. When this distance is less than 7 Å and the tetra peptide sequence is not in a α–helical region, it is considered a *β*-turn.[1h] Additionally, a three residue reverse turn, popularly known as *β*-turn, exists but is significantly less widely distributed.

β-Turns are classified[1h, 10] according to the ϕ– and ψ–angles of the i+1 and i+2 residues. In addition to the existence of a number of turn types (I, I', II, II', III, III', IV, V, Va, VIa, VIb, VII, and VIII) the C_α^{i} to C_α^{i+3} distance varies from 4-7 Å.[15]

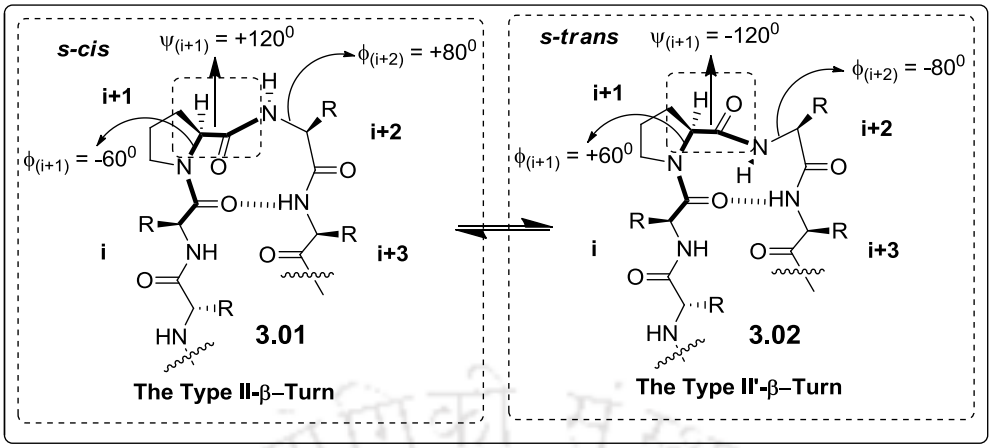

Figure 3.1. The type II- and II'- β-turn motif

While the retention or improvement of biological activity is the ultimate indicator of successful design, the success of many efforts has been measured by the ability of a scaffold to adopt a turn motif using spectroscopic methods such as circular dichroism (CD)[16] or solution phase NMR.[17]

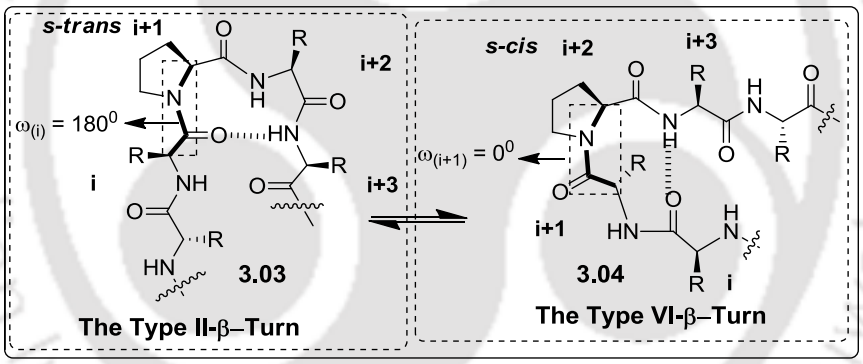

Figure 3.2. The type II- and VI- β--turn motif

In summary, the different type of *β*-turn structures are dependent on the torsional angel of peptide backbone of the residue i+1 and i+2. The ideal value of torsion angles has been estimated by Vankatachalam and is given in the **Table 3.1**. The classification of β-turn structure has been done based on the value of torsion angle phi (ϕ) and psi (ψ) (*) must be a cis-proline.[18]

Table 3.1. Torsional angels for *β*-turn conformation

Torsion angles for classical *β*-turns				
Type	φ_{i+1}	ψ_{i+1}	φ_{i+2}	ψ_{i+2}
I	-60	-30	-90	0
II	-60	120	80	0
VIII	-60	-30	-120	120
I'	60	30	90	0
II'	60	-120	-80	0
VIa1	-60	120	-90	0*
VIa2	-120	120	-60	0*
VIb	-135	135	-75	160*
IV	turns excluded from all the above categories			

The current state of the art of turn mimetic peptides synthesis and scaffold design is now briefly discussed below. The examples are confined to unnatural amino based β-turn peptidomimetics that have been designed with diversity and parallel execution in mind.

3.3. β-Turn Peptidomimetics

Turns are important targets for mimicry, both because they serve as recognition sites in peptides and proteins and because they allow a protein chain to fold back upon itself to form a compact structure. One area of research has focused upon the creation of structures that mimic the conformations and functionality displayed by β-turns and related structures, whereas a second has focused upon the creation of 'nucleating turn mimics' that induce structure in attached groups (typically peptide strands).[19]

Pramanik *et.al.*,[20] have synthesized a series of biologically important small β-turn peptides. They have shown the influenced of solvent polarity and steric interaction on the peptide conformation related to structural interconversion between β-turn and *β*-sheet. They have synthesized model tripeptides I-III, [Boc-Ile-Aib-**Xx**-OMe (**Xx** = Val for peptide I; Leu for II and Phe for peptide III)] with a centrally placed non-coded amino acid Aib (Aib = α-amino isobutyric acid). To investigate the conformational interconversion only steric residue part **Xx** of the tripeptide was changed. From their study it was revealed that the synthesized peptides where Aib was placed in middle of the peptide adopted β-turn structure which was confirmed by X-ray diffraction analysis. From crystal structure of peptide Boc-Ile-Aib-Val-OMe shows Ile(1) and Aib(2) occupying the i+1 and i+2 positions adopting type-II β-turn structure stabilized by intramolecular hydrogen bonding. Another important factor is an intramolecular hydrogen bonding for stabilizing the turn structure between CO of i th residue and NH of i+3 residue creating pseudo ten membered ring (**Figure 3.3**). Most of the β-turn structures are formed by creating intramolecular hydrogen bonding

(about 60%). But some of them do not show an intramolecular hydrogen bond are termed as "open turns".

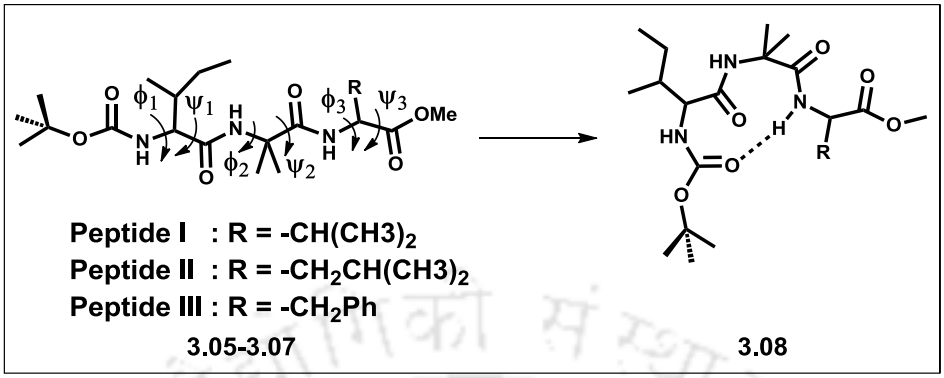

Figure 3.3. Schematic representation of type-II β-turn peptides with unnatural amino acid, **Aib (**α-amino isobutyric acid) in the middle of the peptide strand.

A tetrapeptide mimic focused on biological active neuropeptide substance was designed by Katzenellenbogen *et al*.[21] The peptide **3.11** showed type-1 β -turn conformation as was confirmed by analyzing NMR experiment, X-ray crystallography and molecular modelling study (**Figure 3.4.**). NMR study indicated that the conformations are stable in both the hydrogen bonding and non-hydrogen bonding solvent at various temperature.

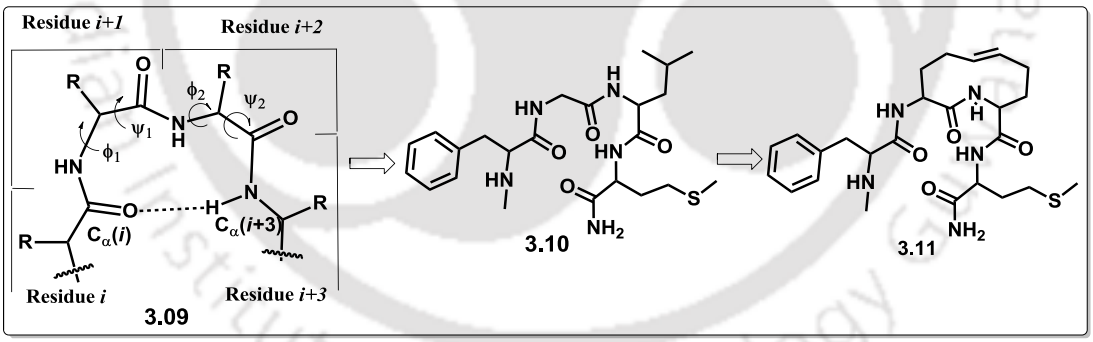

Figure 3.4. Type-I β -turn peptidomimetic.

Gmeiner group[22] developed a novel revers turn peptidomimetic by synthesizing **Asx**-Pro- mimietic **3.12** from the N-allylglycine derivative (**Figure 3.5**). **Asx**-Pro-turn is stabilized by hydrogen bonding between i and i+3 residue and ring-closing olefin metathesis which was established as classical *β*–turn structure. This is also supported by the NMR based conformational studies. The low $\Delta\delta/\Delta T$ value of -4.7 ppb/k suggested a stable intramolecular hydrogen bonding in peptidomimetic **3.12.**

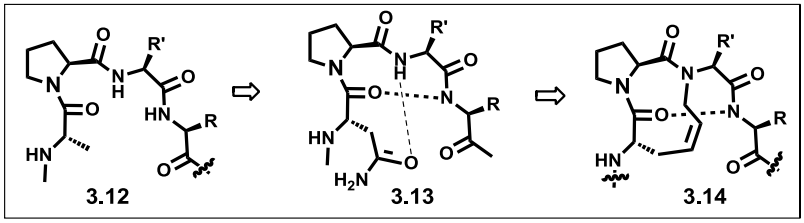

Figure 3.5. Ring-closing olefin metathesis based classical *β* –turn structure.

A bridge depsipeptide (Por/PL/Q, **Figure 3.6**) with donor–acceptor chromophores was reported by Bowler group which adopted a β-turn structure. The donor porphyrin and acceptor quinone are used in Por/PL/Q and PAQ. The main aim of their synthesis was to study hydrogen bond mediated electron transfer through amide CO....NH hydrogen bond.[23] Por/PL/Q and Por/P/Qaa-PMA both were adopted *β*-turn structures. PAQ was connected to the donor and acceptor directly through an amide bond. They have also studied the electron transfer efficiency by replacing the amide linkage with an ester that effect on the *β*-turn folding nature of the peptide. The electron-transfer through-bond between the terminal of the tritolyl-p-carboxyphenylporphyrin donor and the edge of the quinone acceptor are indicated on each structure.

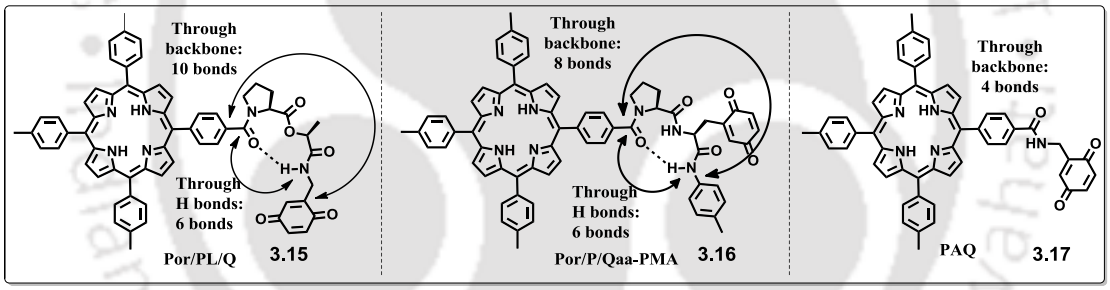

Figure 3.6. Structures of porphyrin-quinone donor-acceptor labeled peptide designed for studying electron transfer through amide linkage.

The great significance of turn structure usually preferred a particular site for many protein-protein interaction or peptidase. Ronald T. Raines and his group have shown that the residues Gly113-Asn113-Pro114-Tye115 form a hairpin like type-VI revers turn in native RNase (**Figure 3.7**). They replaced the turn creating unit, Asn113-Pro114, by two *β* amino acids residues, R-nipecotic acid-S-nipecotic acid (R-Nip-S-Nip, **3.19**) and found that the incorporated unit showed N-H…O=C hydrogen bonded 12- membered ring which was found to be resistant to degradation by protease.[24]

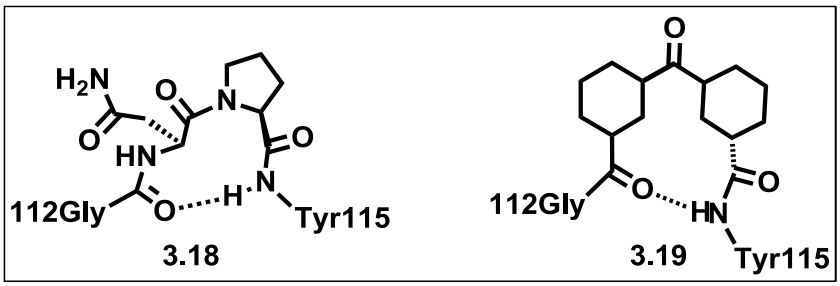

Figure 3.7. Type VI β-turn in ribonuclease A Variants.

Russell group have synthesized a libraries of piperazine acid based turn mimetic peptides.[25] They have defined a common terapeptide sequences with 10 membered hydrogen bonding ring where the distance of i and i + 3 residue varies from 4 to 7 Å. They have studied the effect of diaminopropanoic acid as a source of the key for the synthesis of turn peptidomimetics where the R^3 substituents were missing (**Figure 3.8**).

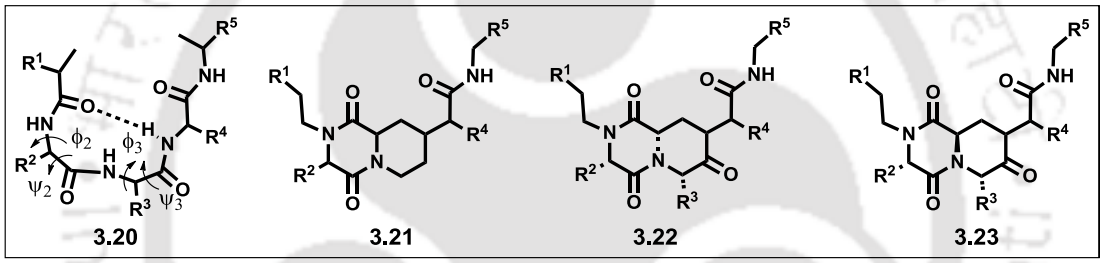

Figure 3.8. Piperazine acid based turn mimetic peptide.

Triazolyl linked peptidomimetics: The most important and challenging work to develop the approaches to control the conformation and shape of the peptide, which are usually flexible. Toward this end in 2011, Liskamp *at al*., have synthesized vancomycine mimetic tripeptide containing 1,4- and 1,5–disubstituted triazole via CuAAC and RuAAC, respectively, catalysed 1,3-dipolar cycloaddition reaction. The product peptides with highly constrained ring structure showed to possess turn like structure (**Figure 3.9**). These peptide derivatives might find application as antibacterial agents similar to antibiotic peptide, gramicidin.[26]

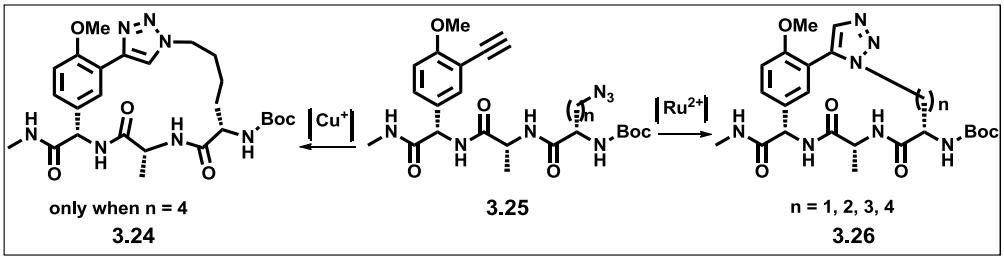

Figure 3.9. 1, 4 and 1, 5–disubstituted triazole based cyclic peptidomimetics.

3.4. Fluorescently Labelled Peptides/Proteins and Application of FRET Process

Over the various available strategies, fluorescence spectroscopic technique is a powerful tool for studying biological events associated with the investigation of biomolecular structures, dynamics and interbiolecular interaction because of its high sensitivity, excellent temporal resolution and good reproducibility.[27] Fluorescent/fluorescently labelled peptides/proteins serve as sensitive probes for visualizing intracellular events and understanding molecular interactions inside a cell.[28] Furthermore, among the various fluorescence photophysical phenomena, Förster resonance energy transfer (FRET) emission find widespread applications in elucidating such events of proteins/peptides in a cell. [29, 30a-b] FRET being a distance dependent phenomenon occurs in donor-acceptor systems is widely being utilized in elucidating structures, dynamics of proteins, in studying biomolecular interactions and conformational distribution of an unstructured peptide and in many other sensory applications.[30c-d] The FRET assay was originally reported by Meldal and co-worker applied for fluorescent donor-acceptor pair, placed between two termini of peptide. When peptidase cleaved the peptide, removes the N-terminal quencher then other part of the peptide becomes fluorescent. So FRET method has many advantages and easily accepted for natural or unnatural fluorescence probe.[31]

Recently, Zuchner *et al.*, have demonstrated a FRET based fluorescence assay system for the determination of protease activities, which in author's hope could in principle be adapted for the detection of all proteases.[32] The assay is based on the cleavage of a FRET peptide substrate, which results in a dramatic increase of the donor fluorescence after the cleavage (**Figure 3.10**). The assay was tested in complex biological mixtures using two proteases such as trypsin and enteropeptidase and was found to work efficiently with highly sensitivity. Therefore such a sensitive and simple assay system without having any background signal even in the presence of high concentration of other proteases can be utilized in complex biological mixtures for the detection of proteases.

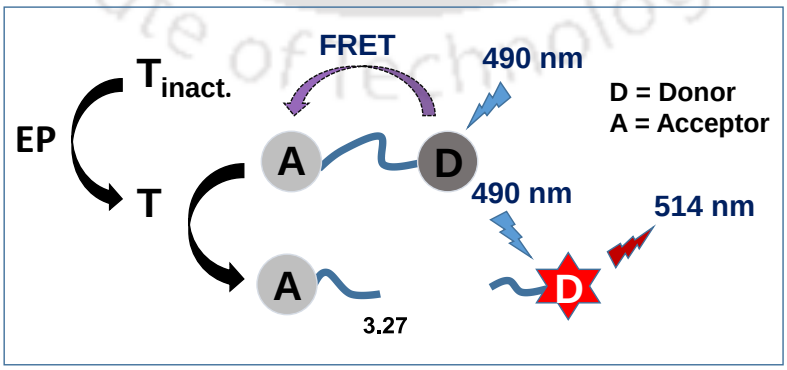

Figure 3.10. FRET peptide for the fluorimetric determination of protease activities.

Pei group[33] have reported earlier a similar fluorescent donor/acceptor labeled solid supported peptide probe system for monitoring the cleavage by proteases. Their strategy was based on a fluorophore-quencher pair which before cleavage showed no or little fluorescence. However, the cleavage of the peptide by protease separate the donor acceptor and a strong enhanced fluorescent could be observed from the Donor fluorophore. This strategy was utilized for systematic profiling the substrate specificity of endopeptidases (**Figure 3.11)**.

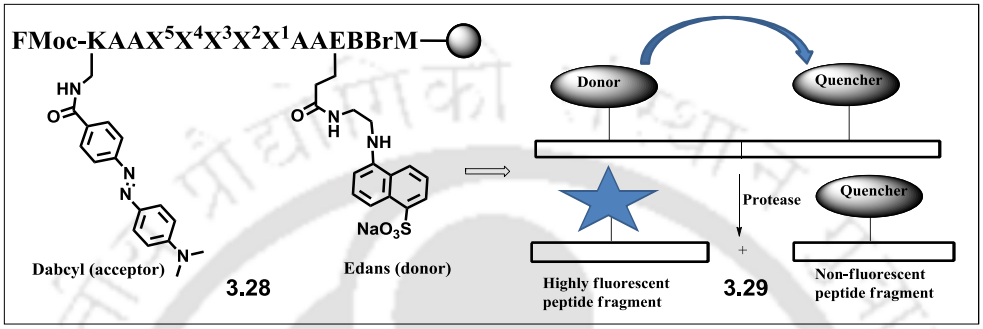

Figure 3.11. Schematic presentation of FRET based peptide designed for systematic profiling the substrate specificity of endopeptidases.

Peptide–membrane interactions play a crucial role in many biological processes[34] such as membrane lysis, fertilization, and viral infection. Toward this end Gai *et al.* have studied the kinetics of the helix formation accompanied by the peptide–membrane association utilising FRET phenomenon among a FRET pair, *p*-cyano-l-phenylalanine and tryptophan.

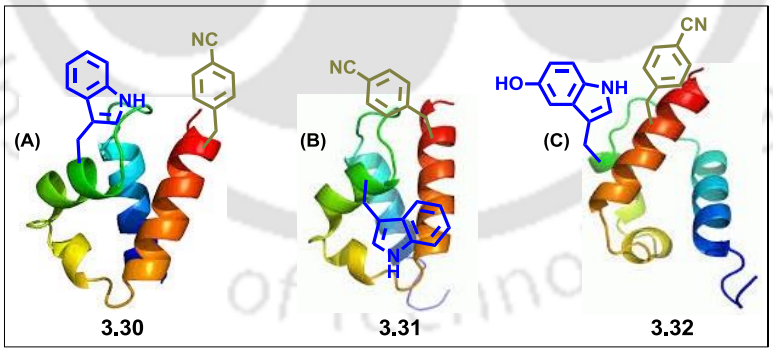

Figure 3.12. (A) FRET based protein for study the kinetics of the helix formation accompanied by the peptide–membrane association utilising FRET phenomenon among a FRET pair, *p*-cyano-l-phenylalanine and tryptophan. (B) FRET phenomena for studying the urea-induced unfolding transitions of two small proteins. (C) The 7-azatryptophane (7AW) and 5-hydroxytryptophane (5HW) as FRET acceptor to Phe-CN in proteins utilized to demonstrate the urea-induced unfolding transitions of protein.

They have studied the membrane-mediated helix folding dynamics of a mutant of magainin 2, which is an antibiotic peptide found in the skin of the African clawed frog, *Xenopus laevis*. Their results indicated that the coil-to-helix transition occurs during the binding of the peptide to the lipid vesicle but prior to the full insertion of the peptide into the hydrophobic region of the lipid bilayers (**Figure 3.12A**).[35a]

The same group has applied the same FRET phenomena for studying the urea-induced unfolding transitions of two small proteins, the villin headpiece subdomain (HP35) and the lysin motif (LysM) domain. Depending on whether Phe_{CN} is exposed to solvent, they were able to extract either qualitative information about the folding pathway or quantitative thermodynamic and structural information.

Their results showed that Phe_{CN}–Trp FRET pair is capable of monitoring unfolding transitions with site-specific resolution (**Figure 3.12B**).[35b] They also have demonstrated recently that 7-azatryptophane (7AW) and 5-hydroxytryptophane (5HW) can also act as FRET acceptor to Phe-CN. Thus, these FRET pairs were utilized to demonstrate the urea-induced unfolding transitions of the villin headpiece subdomain (HP35), a designed ββα motif (BBA5), and the human Pin1 WW domain (**Figure 3.12C**). They also have shown that Phe_{CN}, Trp, and 7AW can be used together to form a multi-FRET system, allowing more structural information to be extracted from a single FRET experiment. Therefore, such multi-FRET systems might find applications in studies concerning relative motions of peptide chains such as those taking place in protein folding process. [35c]

Janda and his group reported a FRET based assay for monitoring of HIV gp41 core disruption.[36] For this purpose they have chosen a well-known FRET pair 7-methoxycoumerin-4-acetic acid (MCA) and 2,4 dinitrophenyl (Dnp) groups as fluorophore and quencher. This FRET pair is attractive and has the advantage of being small size and avoiding large polycyclic entities could interact with peptide or nonpeptide inhibitor through π-stacking interaction. Thus, both the MCA and Dnp modified amino acids were hooked in a peptide synthesized through automated solid-phase peptide synthesis. Thus, they have reported the design, synthesis, and development of a N- and C- terminal peptide FRET pair for screening of gp41 six-helix bundle disruption (**Figure 3.13**). It was concluded that that by strategically placing two FRET probes on two peptides, they were able to monitor the intermolecular co-association by fluorescence quenching between the fluorescence donor and acceptor.

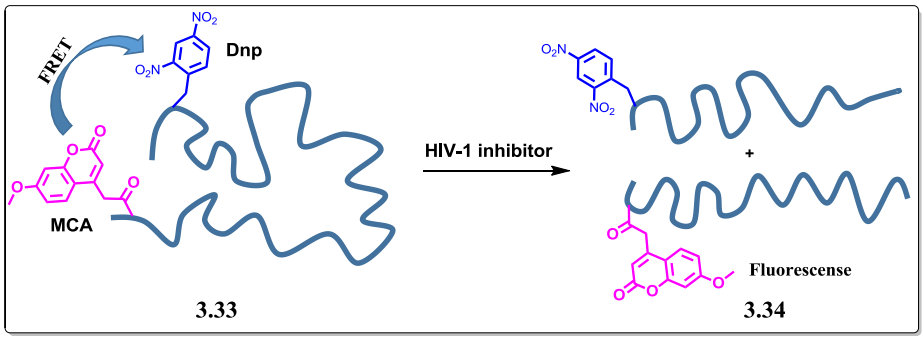

Figure 3.13. Schematic presentation of HIV-1 fusion protein gp41 and the effect of viral entry.

A 23 residue FRET-peptide (sequence: dansyl-Gly-Gly-Thr-Leu-Ala-Val-Pro-Gly-Met-Thr-Cys-Ala-Ala-Cys-Pro-Ile-Thr-Val-Lys-Lys-Gly-Gly-Trp-CONH2) was synthesized by Holcombe *et.al.*,[38] for studying the mechanism of detecting metal ion using the enhancement of fluorescence emission through fluorescence resonance energy transfer from tryptophan as donor and dansyl as acceptor. The turn on "FRET" enhancement was recognized for Hg^{2+} as well as for Zn^{2+}, Cd^{2+} and Ag^{+} in pure aqueous solution at pH 7.0. But it does not response to other transition, alkali and alkaline earth metal. The fluorescent enhancement observed is unique for Hg^{2+} since this metal generally quenches fluorescence.

Recently, Erqun Song *et al.* have developed a graphene oxide (GO) based peptide FRET sensor for the sensitive, rapid, and accurate detection of matrix metallopeptidase 2 (MMP-2) in complex serum samples. In this study, fluorescein isothiocyanate-labeled peptide (Pep-FITC) was covalently conjugated onto the GO surface to construct a GO-Pep-FITC FRET sensor which is found to be superior compared to sensor fabricated through physical adsorption in their detection of MMP-2 with high sensitivity (**Figure 3.14**). Moreover, it allows for rapid MMP-2 detection even in complex biological samples with satisfactory accuracy. Our studies further suggest that such a platform developed here for sensitive, rapid, and accurate detection of biomarkers holds great promise for clinical diagnosis of protease-related diseases. This is the first report demonstrating the application of a GO-Pep-FITC FRET sensor for MMP-2 detection in real human serum samples, showing the potentials of GO-Pep-FITC FRET sensors for both basic research and clinical applications, especially rapid disease diagnosis. Based on the simple preparation and facile manipulation and sensitivity it can be concluded that the GO-Pep-FITC sensor can be easily applied for the detection of other biomolecules by changing the peptide substrate sequence, which should greatly enlarge the areas of application for such GO-based sensors.[38]

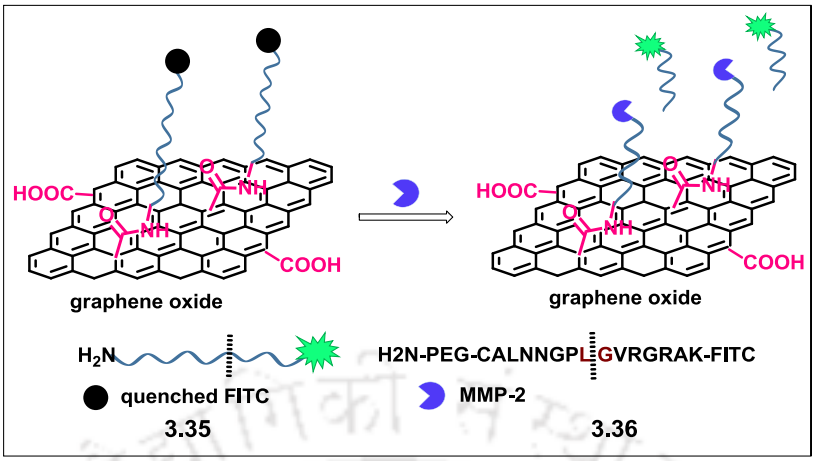

Figure 3.14. Schematic illustration of MMP-2 detection by a GO-Pep-FITC FRET sensor.

3.5. Background

From the literature study it is revealed that there exist a very limited no of fluorescent amino acids that have been synthesized or encoded genetically or incorporated into short peptide to generate fluorescent peptides which might adopt/mimic a particular secondary structure of protein and can show very interesting photophysical properties. Moreover, a limited number of fluorescent amino acid have been incorporated into short peptides to study the protein–protien interaction. Multiple chromophore labelled peptides/proteins have also been developed as sensitive probes for visualizing intracellular events and understanding inter-biomolecular interactions inside a cell via FRET or excimer emission. Therefore, designing fluorescent peptides is currently an attractive research area to study photophysics for various biophysical applications.

3.6. Objective

As discussed above, there exist only few reports of fluorescent amino acid containing peptides. The main aim of synthesis of triazolyl unnatural amino acids which is discussed in **Chapter 2** was to use them to design peptide of defined conformation and to study their modulated photophysical interaction property in that conformation. Thus, we envisaged that upon incorporation of two of such fluorescent UNAAs into two termini of a tripeptide separated by a natural alanine might adopt β-turn conformation via backbone H-bonding interaction.[39] We also expected that the hydrophobic, π-π stacking and van der Waals interactions in the side chain would stabilize the conformation and allow the two terminal triazolyl aromatics to involve in dipolar photophysical interaction, most likely Förster resonance energy transfer

(FRET) process.[30c] FRET being a distance dependent phenomenon is widely being utilized in elucidating structures, dynamics of proteins, in studying biomolecular interactions and conformational distribution of an unstructured peptide and in many other sensory applications.[40] Thus, we were interested in β-turn peptidomimetic capable of showing FRET interaction between two terminally placed fluorescent unnatural amino acids.

With this background and concept we framed our objectives as below:

(a) Synthesis of tripeptides containing two donor/acceptor fluorescent triazolyl amino acids (^{TPhen}**Ala**^{Do} and ^{TCNB}**Ala**^{Ac}) separated by a natural alanine -(i) ^{TPhen}**Ala**^{Do} – Ala – ^{TCNB}**Ala**^{Ac} **(3.37)**, (ii) ^{TPhen}**Ala**^{Do}–Ala – ^{TPhen}**Ala**^{Do} (**3.38**), and (iii) ^{TCNB}**Ala**^{Ac} –Ala –^{TCNB}**Ala**^{Ac} (**3.39**).

(b) Tripeptide **3.37** is designed to examine the possibility of H-bonding, hydrophobic and/or π-stacking interactions guided formation and stabilization of β-turn conformation as well as photophysical dipolar interaction between Do/Ac pair.

(c) Peptide **3.38** (Do/Do) and **3.39** (Ac/Ac) are designed to compare the results.

(d) Study of peptide secondary structure.

(e) Study of photophysical interaction among the fluorescent amino acids at the two termini.

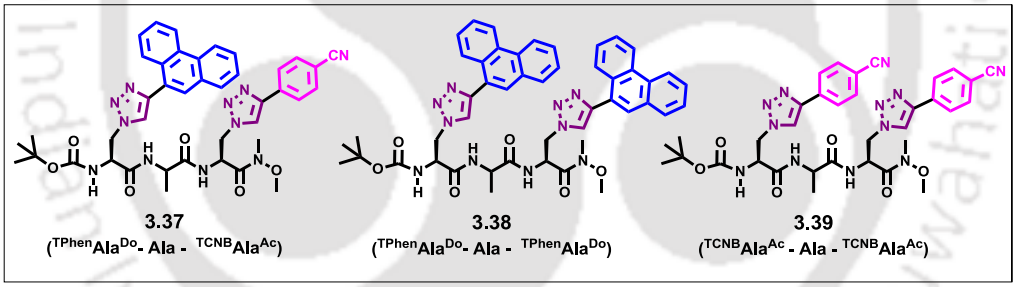

Figure 3.15. The chemical structures of target triazolyl Do/Ac chromophore decorated fluorescent tripeptides.

Logic behind Choosing ^{TPhen}Ala^{Do} and ^{TCNB}Ala^{Ac} Pair for Incorporation into Short Peptide: Study of Dipolar / Charge Transfer Interaction Property:

Study of possible photophysical interaction behavior among a pair of donor/acceptor triazolyl unnatural amino fluorescent acids, as was described already in **Chapter 2**, **Section 2.8**, revealed that an UV-visible titration of a solution of an acceptor triazolyl amino acid ^{TCNB}**Ala**^{Ac} (**2.79**) with increasing concentration of a donor triazolyl amino acid, ^{TPhen}**Ala**^{Do} (**2.74**) showed characteristic absorptions of both the donor and acceptor amino acids indicating that there was no possibility of ground state charge transfer complexation (**Figure. 2.18**). However, upon excitation at absorption maxima of ^{TCNB}**Ala**^{Ac} (λ_{ex} = 270 nm) the emission at 330 nm was found

to decrease gradually as the concentration of donor amino acid ^{TPhen}**Ala**^{Do} was increased (**Figure. 2.18b**). This observation clearly indicated a fluorescence quenching of ^{TCNB}**Ala**^{Ac} in presence ^{TPhen}**Ala**^{Do} via a dynamic quenching process as the static mode of quenching was ruled out from the UV-visible spectroscopic study. Furthermore, it was observed that emission spectra of ^{TCNB}**Ala**^{Ac} overlapped significantly with the absorption spectra of ^{TPhen}**Ala**^{Do} indicating a possibility of quenching of emission of ^{TCNB}**Ala**^{Ac} via a dynamic quenching mode, the FRET. Therefore, this donor/acceptor pair amino acid could potentially act as a FRET pair if they can be incorporated into a peptide construct wherein the, the acceptor triazolyl amino acid ^{TCNB}**Ala**^{Ac} would act as FRET donor and the donor amino acid ^{TPhen}**Ala**^{Do} act as a FRET acceptor. Therefore, a favorable photophysical interaction via FRET was observed between these amino acids pair which we exploited herein in this **Chapter 3** for the design of FRET-peptide with β-turn conformation.

Therefore, we have chosen phenanthrene/cyanobenzene pair for incorporation in short peptidomimetics and expected that they could able to do the possible photophysics when come to close. Exploration of the photophysics of other possible fluorescent donor/acceptor amino acids pair is the future scope of this thesis.

3.7. Results and Discussion

3.7.1. Synthesis of Triazolyl Donor/Acceptor Amino Acid Decorated Tripeptides

To synthesize our designed tripeptides decorated with our synthesized donor/acceptor unnatural amino acids (described in **Chapter 2**), at first we have prepared Ser-Ala dipeptide (**3.42**) by EDC.HCl and HOBT mediated solution phase peptide coupling protocol. Then the serine–OH of Ser-Ala dipeptide (**3.42**) was transformed to corresponding dipeptidyl azide derivative (**3.44**) via the mesylate (**3.43**).[41] Finally the dipeptidyl azide **3.44** was made to undergo click reaction with 9-phenanthrene acetylene/p-cyanophenyl acetylene to afford corresponding triazolyl derivative donor/acceptor dipeptide (**3.47-3.48**) in very good yield (**Scheme 3.1**). Next, the LiOH mediated hydrolysis of Wienreb amide moiety of dipeptide **3.47** and **3.48** afforded the correspond acid (**3.49-3.50**) which was undergone a EDC.HCl and HOBT mediated solution phase peptide coupling with Boc-deprotected monomeric triazolyl amino acids (**3.51-3.52**) to afford our targeted tripeptides [(Do/Do (**3.38**), Do/Ac (**3.37**), Ac/Ac (**3.39)]** in very good yields (**Scheme 3.1**). All the synthesized peptides were characterised by NMR, HRMS and IR analysis.

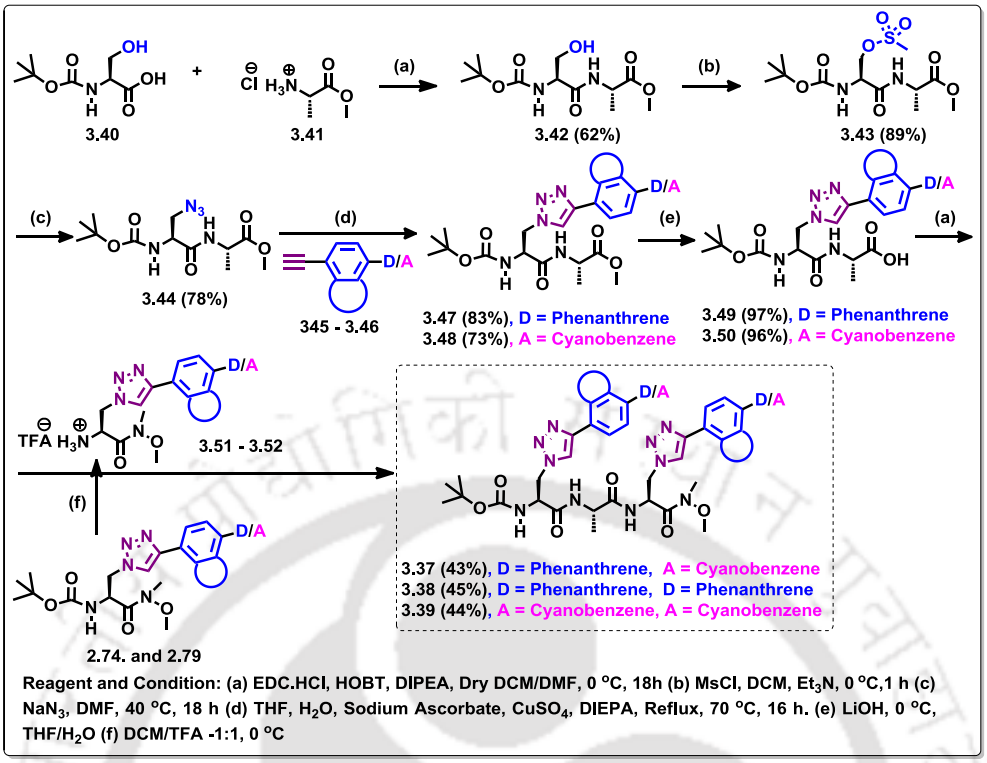

Scheme 3.1. Synthetic procedure of triazolyl decorated donor/acceptor tripeptides.

3.7.2. Spectral Characterisation of the Synthesized Tripeptides

The synthesized three tripeptides in the fully protected form were characterized mainly by NMR spectroscopy. As representative example the structural assignments of peptides **3.37** and **3.38** are shown in **Figure 3.16a** and **3.16b**, respectively. For peptide **3.37 (**^{TPhen}**Ala**^{Do}**- Ala-**^{TCNB}**Ala**^{Ac}**)**, the triazolyl hydrogen of ^{TPhen}**Ala**^{Do} and ^{TCNB}**Ala**^{Ac} appeared as a singlet at the characteristic position of δ 8.50 and 8.56 respectively. The C-α hydrogen of N-terminal Serine, alanine and C-terminal serine resonated as a broad singlet (bs) at δ 4.81, 4.35 and 5.33, respectively. The β-CH_2 hydrogens of ^{TPhen}**Ala**^{Do} and ^{TCNB}**Ala**^{Ac} unit appeared as a doublet at δ 4.46 and 4.70 with coupling constants J = 13.2 and 13.5 Hz respectively. The ^{t}Bu-hydrogens of Boc-protected group appeared as a singlet at δ 1.17. The methyl hydrogens of NMe and OMe groups resonated as singlets at δ 3.16 and 3.75, respectively. The methyl hydrogens of alanyl unit appeared as a doublet at δ 1.10 with coupling constant J = 6.8 Hz. The C-10 hydrogen of aromatic phenanthrene appeared at δ 7.95 as a singlet and C-1, C-2 and C-7 hydrogens resonated as a multiplet at δ 8.58 and 7.87 respectively. The C-3 and C-6 hydrogens resonated as a triplet at δ 8.06 and 7.79 with coupling constants J = 3.9 and 4.5 Hz respectively. Other three aromatic hydrogens at C-4, C-5 and C-8 of phenanthrene appeared as a doublet at δ 8.93, 8.84

and 8.44 with coupling constants J = 7.8, 8.1 and 9.0 Hz respectively. Whereas, C-12, C-16 hydrogens in cyanobenzene unit resonated as doublet at δ 7.65 with coupling constant J = 6.4 Hz, the C-13, C-15 hydrogens appeared as a doublet at δ 7.72 with coupling constant J = 6.0 Hz. The hydrogens of N-1, N-2 and N-3 appeared as a doublet at δ 6.90, 8.25, 8.36 with coupling constants J = 7.5, 6.6 and 5.7 Hz respectively.

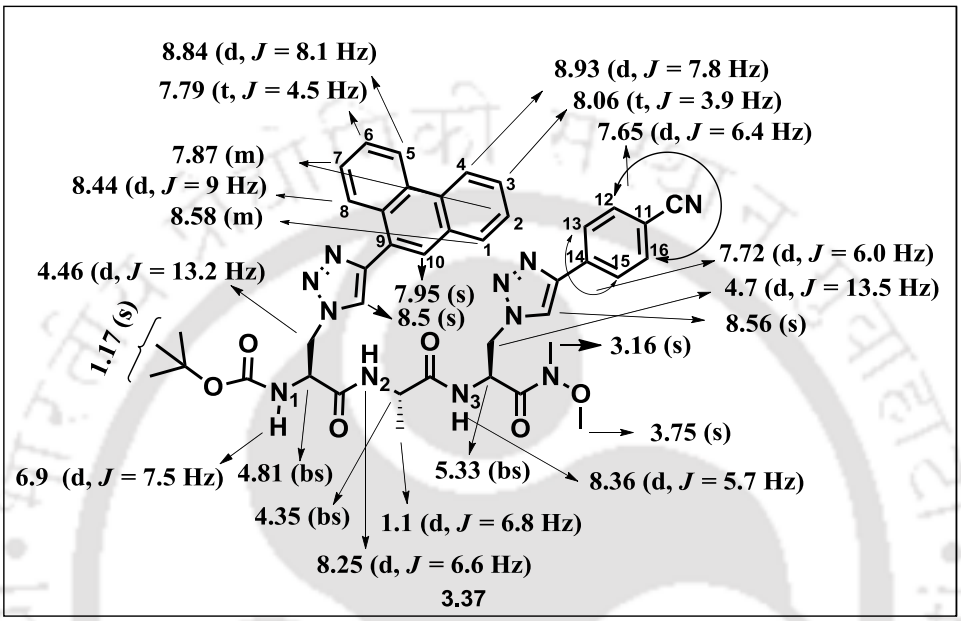

Figure 3.16a. ^{1}H NMR assignment of tripeptide **3.37.**

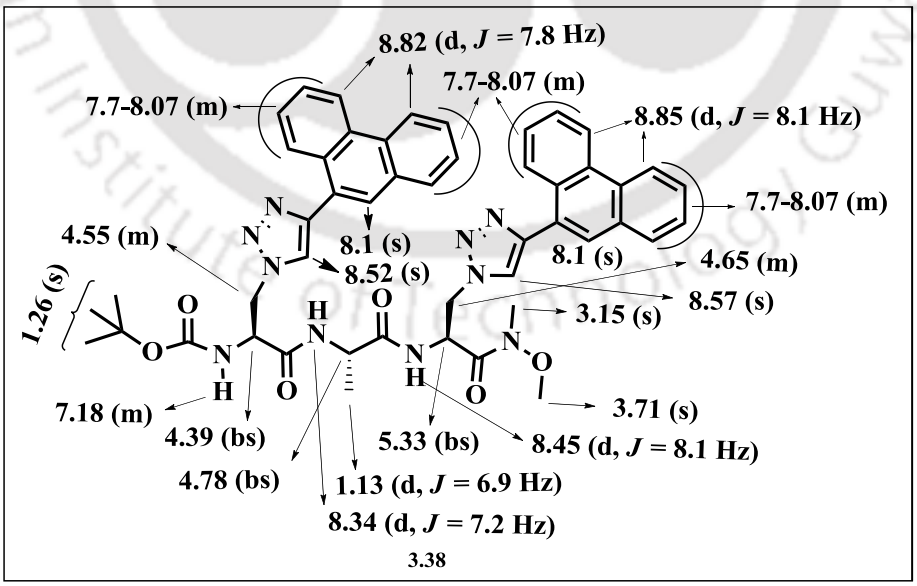

Figure 3.16b. ^{1}H NMR assignment of tripeptide **3.38.**

The chemical shift assignment for a representative tripeptide **3.38 (**^{TPhen}**Ala**^{Do}**-Ala-**^{TPhen}**Ala**^{Do}**)** is shown in **Figure 3.16b**. The detailed assignments for all the cases are given in the experimental section.

3.7.3. Study of Conformation of Peptides 3.37, 3.38 and 3.39 Using CD, IR, NMR, Spectroscopic Techniques and Macromodel Calculation

***Study of Circular Dichroism Spectroscopy*:** The secondary structure of peptide **3.37** was estimated by recording its CD spectrum in acetonitrile and methanol, which showed a maximum at ~ 205–212 nm and a sudden switch from a positive to a negative band at 240–266 nm indicating a β-turn conformation (**Figure 3.17**). Aromatic absorption or a π-π stacking interaction between two aromatic moieties of terminal amino acids (^{TPhen}**Ala**^{Do} and ^{TCNB}**Ala**^{Ac}) was also evident from the appearance of a signature negative band at 297–301 nm in all solvents studied. The hypsochromic shift in wavelength and hypochromism of the bands at 266 and 301 nm in the variable temperature CD spectrum suggest a weakening of the π-π stacking interaction between the triazolylphenanthrene (**TPhen**) unit of ^{TPhen}**Ala**^{Do} and the triazolyl cyanobenzene (**TCNB**) moiety of ^{TCNB}**Ala**^{Ac} (**Figure 3.17a**). Other two peptides, **3.38** and **3.39** also showed more or less similar characteristics.[42] The β-turn structure in the peptides indicated the presence of intramolecular back bone H-bonds the presence of which was also confirmed from IR and VT-NMR spectroscopic study as described below.

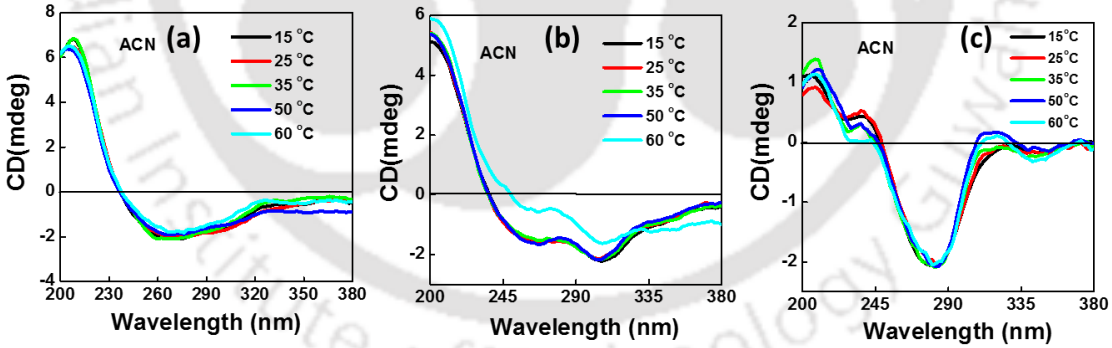

Figure 3.17: Circular dichroism Spectra of (a) **3.37**, ^{TPhen}**Ala**^{Do}**-Ala -** ^{TCNB}**Ala**^{Ac} (b) **3.38**, ^{TPhen}**Ala**^{Do} **-Ala -** ^{TPhen}**Ala**^{Do} (c) **3.39**, ^{TCNB}**Ala**^{Ac} **-Ala -** ^{TCNB}**Ala**^{Ac} in CH_3CN (30 μM, various temperature of each solvent).

Probing the Intramolecular H-Bonding: Study of FT-IR Spectroscopy: IR spectra were recorded using dry KBr with solid and dry compound. The IR spectrum of peptide ^{TPhen}**Ala**^{Do}**-Ala-**^{TCNB}**Ala**^{Ac} showed absorption due to intramolecular H-bonding and free amide –NH stretching at 3320 and 3450 cm^{-1} respectively. The ratio of absorption was significantly larger in peptide **3.37** than in other two peptides,

indicating that the hydrogen-bonded form of amide –NH was more favorable in the case of peptide **3.37**. Thus, the IR spectrum also supported the formation of a β-turn type structure.[43]

Probing the Intramolecular H-Bonding: Study of Variable Temperature ^{1}H NMR (VT-NMR): We next study the variable temperature NMR (VT-NMR) to know the status of intramolecular H-bonding in a representative peptide **3.37**. The presence of intramolecular H-bonds was assessed by determining the variation of chemical shifts of the various NHs with temperature (**Table 3.2A**), in d_6-DMSO in which all the 3 NHs exhibited different chemical shifts. The triazole C-H of C-terminal amino acid also exhibited temperature effect. All the amide NH's, and triazole C-H exhibited Δδ/ΔT values that are close to Kessler limit of –3 ppb/K indicating strong intramolecular H-bonding and supported the predominant turn like structure of the peptide (**Table 3.2B**). The presence of strong intramolecular H-bonding involving the carbamate carbonyl at i and the amide –NH (of ^{TCNB}**Ala**^{Ac}) at i + 3 was observed from the variable temperature NMR experiment.[44]

Table 3.2. (A) Plot of Δδ vs. T. (B) Values of Δδ/ΔT in ppb/K.

(A) Plot of Δδ vs. T.	**(B)** Values of Δδ/ΔT in ppb/K			
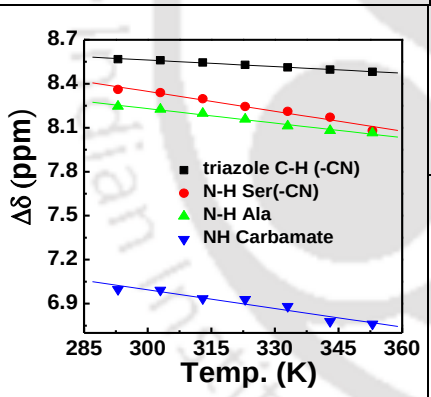	Carbamate N-H (^{TPhen}**Ala**^{Do})	N-H (**Ala**)	N-H (^{TCNB}**Ala**^{Ac})	Triazole-C-H (^{TCNB}**Ala**^{Ac})
	- 4.25	- 3.30	- 4.52	- 1.49

Solution Conformational Analysis Using 2D NMR Study Experiment: The NOESY spectrum of peptide **3.37** (**^{TPhen}Ala^{Do}-Ala-^{TCNB}Ala^{Ac}**) in d_6-DMSO revealed interactions among the aromatic hydrogens of the TPhen and TCNB units of the two terminal amino acids. It was also evident that the triazolyl C–H of the N-terminal amino acid (^{TPhen}**Ala**^{Do}) interacted with the methylene (–CH2–) proton of the C-terminal amino acid (^{TCNB}**Ala**^{Ac}). Moreover, the triazolyl C–H of the C terminal amino acid (^{TCNB}**Ala**^{Ac}) interacted with the aromatic hydrogens (of the **TPhen** unit) of the N-terminal amino acid (^{TPhen}**Ala**^{Do}). Furthermore, ^{t}Boc–H and NMe–H of the two terminal amino acids showed NOESY interactions (**Figure 3.18**). All these

interactions in the side chain of peptide **3.37** possibly played a role in stabilizing the β-turn structure and in bringing the two terminal aromatics closer for a dipole–dipole interaction. However, these side chain interactions were weak in case of other two peptides, probably because of the steric repulsion between two bulky phenanthrenes in peptide **3.38** and the dipolar repulsion between two TCNB units in peptide **3.39**. Therefore, they also adopted similar but deformed structures, which could be seen in the corresponding CD spectra.

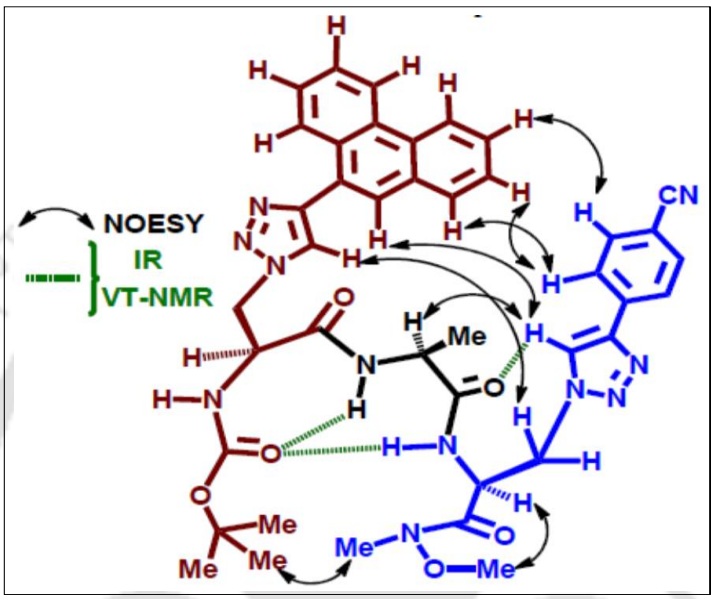

Figure 3.18. Possible various interactions are shown in pictorial form for peptide **3.37**.

***Conformational Analysis Using Macromodel Study*: *Geometry Optimisation*:** Molecular modeling study of the peptides is carried out using Schrodinger Macro Model (Maestro vs. 9.0) software with MMFFs force field in water. After optimization we carried out conformational search using MMFFs force field at constant dielectric in water with "large scale low-frequency-mode conformational search" (Mixed torsional/Largescale low-mode sampling = MCMM/LMCS) method using Schrodinger Macromodel (Maestro vs. 9.0) software package.[45]

A total of 500 structures were processed with 500 maximum no. of steps iteration. A global search analysis eliminates redundant conformers using RMS deviation for all compared atoms exceed the threshold Cutoff of 0.5 Å. An optimal minimization method was chosen for minimizing the generating conformers.

The geometry minimization, molecular dynamics calculation using MMFFs force field supported β-turn conformation with H-bonding between CO(*i*)–NH(*i+3*) (**Figure 3.19**).[39b-c, 45] Therefore, the spectroscopic evidences and the modelling study supported the β-turn conformation of peptide **3.37** which was mostly originated from backbone H-bonding interaction and stabilized by other side chain interactions like

hydrophobic, π-π stacking interactions between the terminal **TPhen** and **TCNB** moieties.

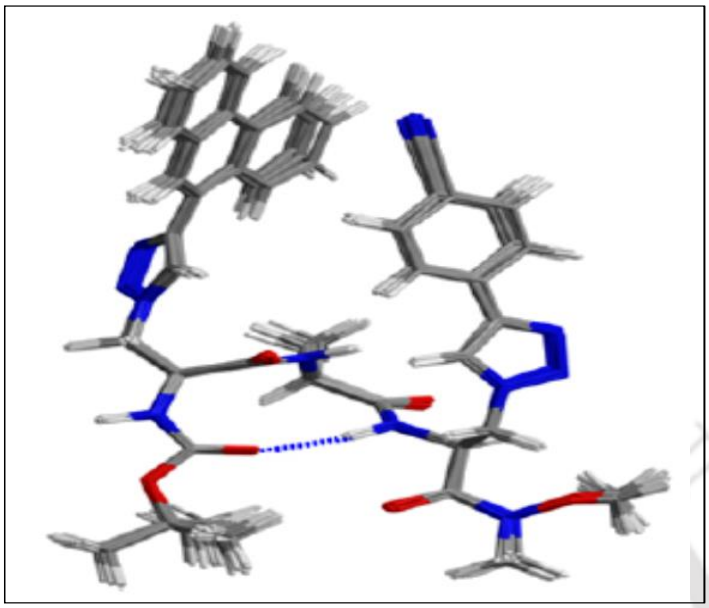

Figure 3.19: Superimposed structures of various conformations of peptide ^{TPhen}**Ala**^{Do}-**Ala**-^{TCNB}**Ala**^{Ac} derived from a conformational search using MMFFs force field.

3.7.4. Study of Photophysical Properties of Synthesized Tripeptides

After getting three pure tripeptides in hand, we next studied their UV-visible and fluorescence photophysical properties in various organic solvents to test their microenvironment sensitive property. The donor/acceptor pair decorated tripeptide **3.37** (^{TPhen}**Ala**^{Do}-**Ala**-^{TCNB}**Ala**^{Ac}) containing a triazolyl phenanthrene and a triazolyl cyanobenzene amino acid separated by natural alanine exhibited four absorption maxima at around 260-310 nm in various organic solvents with small blue shift (~5 nm) as solvent polarity increases. Excitation at absorption maxima in each solvent resulted in characteristic emission bands of two triazolyl amino acid units at around 330, 364 nm and 381 nm. The intensity of ^{TCNB}**Ala**^{Ac} moiety is less than ^{TPhen}**Ala**^{Do} in all organic solvent that indicated that the dipolar interaction existed between two triazolyl fluorophoric moieties (**Figure 2.20a-b, Table 3.3**).[46]

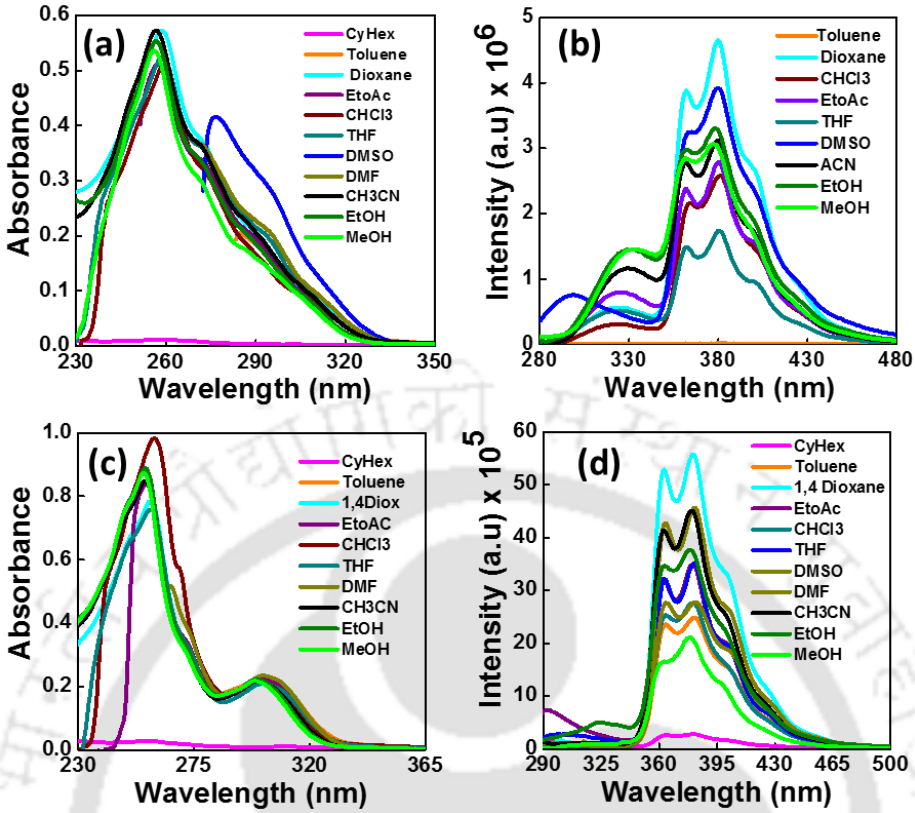

Figure 3.20. UV-visible and fluorescence spectra (**a-b**) of tripeptide **3.37** (**^{TPhen}Ala^{Do}-Ala-^{TCNB}Ala^{Ac}**) and (**c-d**) of tripeptide **3.38** (**^{TPhen}Ala^{Do}-Ala-^{TPhen}Ala^{Do}**) in various organic solvents (concentration of tripeptide was 10 μM).

The tripeptide **3.38** (**^{TPhen}Ala^{Do}-Ala-^{TPhen}Ala^{Do}**) containing a two triazolyl phenanthrene amino acids separated by a natural alanine exhibited broad and solvatochromic absorption band at around 300-305 nm in various organic solvents. The absorption band exhibited ~ 8-10 nm blue shift as the solvent polarity increases. Excitation at absorption maxima of each solvent shows characteristic emission at around 364 nm and 381 nm with hypochromicity with increasing solvent polarity which might be due to the polar solvent–solute interaction via dipolar or H-bonding interactions (**Figure 2.20c-d, Table 3.3**).[46]

Table 3.3. Summary table of photophysical properties of the tripeptide **3.37 and 3.38**.

Solvents	Δf	UV-Vis & Fluorescence			
		λ_{max}^{abs} (nm)	λ_{max}^{fl} (nm)	Φ_f	$<\tau>$[ns]
^{TPhen}Ala^{Do}-Ala-^{TCNB}Ala^{Ac} (3.37)					
Toluene	0.013	285, 294, 312	327, 365, 382, 403	0.11	-----
Dioxane	0.021	258, 274, 292, 310	319, 363, 381, 399	0.20	23.9
$CHCl_3$	0.148	260, 274, 292, 310	319, 365, 382, 401	0.13	-----
EtOAc	0.201	257, 272, 291, 310	320, 363, 381, 399	0.18	-----
THF	0.210	259, 273, 294, 312	321, 364, 383, 401	0.09	-----
DMSO	0.265	277, 295, 312	330, 364, 383, 403	0.12	-----
DMF	0.275	268, 296, 311	332, 364, 383, 401	0.16	-----
EtOH	0.290	257, 272, 290, 309	328, 364, 379, 400	0.23	-----
ACN	0.307	257, 273, 290, 310	326, 363, 380, 397	0.23	13.5
MeOH	0.309	256, 272, 290, 310	309, 361, 378, 401	0.29	14.8
Buffer (pH 7.0)	0.318	260, 309	330, 364, 379, 404	0.03	17.8
^{TPhen}Ala^{Do} -Ala - ^{TPhen}Ala^{Do} (3.38)					
Toluene	0.013	302	366, 382, 402	0.07	-----
Dioxane	0.021	259, 303	364, 381, 401, 422	0.21	23.1
$CHCl_3$	0.148	260, 302	365, 381, 403	0.09	-----
EtOAc	0.201	258, 304	365, 383, 402, 426	0.14	-----
THF	0.210	258, 303	364, 382, 402, 423	0.13	-----
DMF	0.275	267, 304	365, 382, 399, 422	0.15	-----
EtOH	0.290	257, 301	324,365, 380, 397, 424	0.16	-----
ACN	0.307	257, 302	364, 381, 400, 422	0.17	13.5
MeOH	0.309	256, 301	364, 380, 401	0.19	14.3
Buffer (pH 7.0)	0.318	266, 312	368, 386	0.02	9.1

The acceptor triazolyl cyanobenzene containing tripeptide **3.39** (**^{TCNB}Ala^{Ac}-Ala-^{TCNB}Ala^{Ac})** showed structure-less absorption band at 275-285 nm same as monomeric amino acid (**^{TCNB}Ala^{Ac})** with high absorbance value. Excitation at 280 nm it showed comparatively broad emission band (310 nm-360 nm) than monomeric unit. However, increasing solvent polarity the quantum yields increases (**Figure 3.21, Table 3.4**).[46]

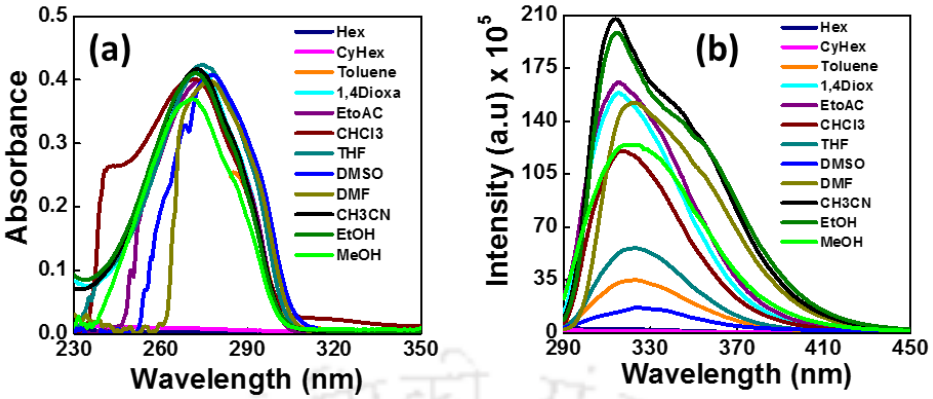

Figure 3.21. UV-visible and fluorescence spectra of (a-b) tripeptide **31** (**^{TCNB}Ala^{Ac}-Ala-^{TCNB}Ala^{Ac}**) in various organic solvents (concentration of tripeptide was 10 μM).

Table 3.4: Summary table of photophysical properties of the tripeptide **3.39.**

Solvents	Δf	UV-Vis & Fluorescence			
		λ_{max}^{abs} (nm)	λ_{max}^{fl} (nm)	Φ_f	$<\tau>$[ns]
^{TCNB}Ala^{Ac} -Ala - ^{TCNB}Ala^{Ac} (3.39)					
Toluene	0.013	286	324	0.07	-----
Dioxane	0.021	273	317	0.12	1.8
$CHCl_3$	0.148	272	318	0.09	-----
EtOAc	0.201	274	316	0.14	-----
THF	0.210	276	324	0.05	-----
DMSO	0.265	278	330	0.02	-----
DMF	0.275	277	322, 342	0.18	-----
EtOH	0.290	273	316, 342	0.24	-----
ACN	0.307	274	315, 336	0.27	1.7
MeOH	0.309	271	326	0.19	2.0
Buffer (pH 7.0)	0.318	272	330	0.10	8.3

3.7.5. Study of Förster Resonance Energy Transfer (FRET) in Peptide 3.37 ^{TPhen}Ala^{Do}-Ala-^{TCNB}Ala^{Ac}

After establishing the β-turn conformation in all the peptides and in detail in case of Donor/Acceptor peptide **3.37**, we next studied the possibility of photophysical interactions between the terminal Do–Ac amino acid pair in peptide **^{TPhen}Ala^{Do}-Ala-^{TCNB}Ala^{Ac}**. The UV-visible and fluorescence spectra of the individual donor and acceptor amino acids revealed that the fluorescence spectrum of **^{TCNB}Ala^{Ac}** overlapped significantly with the absorption spectrum of **^{TPhen}Ala^{Do}** (**Figure 3.22a**).

Moreover, the peptide **3.37** containing these two amino acids can be selectively excited at 272 nm (the maximum absorbance of ^{TCNB}**Ala**^{Ac}) where there is very low absorbance of ^{TPhen}**Ala**^{Do}. Therefore, these two amino acids should form a FRET pair in our designed tripeptide where the conceptual donor amino acid **2.74** (^{TPhen}**Ala**^{Do}) and the acceptor amino acid **2.79** (^{TCNB}**Ala**^{Ac}) acted as a FRET acceptor and donor, respectively. With this observation we turned our attention to study the FRET process. It was observed that the fluorescence intensity of ^{TPhen}**Ala**^{Do} increased almost four-fold from that of the monomer emission in the presence of ^{TCNB}**Ala**^{Ac} in peptide **3.37** when it was excited at the maximum absorbance of ^{TCNB}**Ala**^{Ac} (λ_{max} = 272 nm). On the other hand, the fluorescence intensity of ^{TCNB}**Ala**^{Ac} in the peptide decreased almost seven to eight times that of the monomer fluorescence. This ratiometric change in fluorescence intensity provided visual evidence of the FRET process from ^{TCNB}**Ala**^{Ac} to ^{TPhen}**Ala**^{Do} (**Figure 3.22b**).[30a-b]

FRET process also supported by the time-resolved fluorescence study that revealed a decrease in donor lifetime (^{TCNB}**Ala**^{Ac}; λ_{ex} = 308 nm, λ_{em} = 340 nm) from 1.9 ns to 1.2 ns in peptide **3.37**, indicating the occurrence of the FRET process. More interestingly, the acceptor (^{TPhen}**Ala**^{Do}) exhibited a biexponential profile (λ_{ex} = 308 nm, λ_{em} = 380 nm) having a distinct rise component of 3.2 ns and a decay component of 14.1 ns. Thus, the lifetime of the acceptor in the presence of the donor in peptide **3.37** increases from 13.2 ns (in the absence of the donor) to 14.1 ns (in the presence of the donor) which is also clearly an indication of FRET (**Table 3.5**).[47]

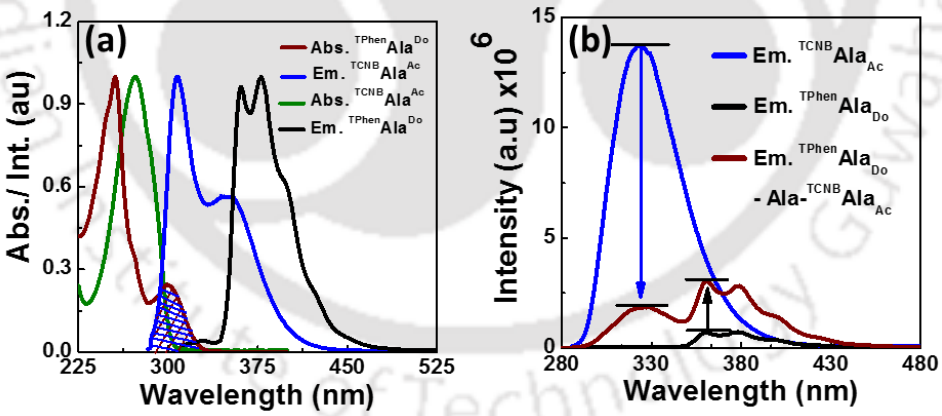

Figure 3.22: (a) Overlaping spectra of ^{TCNB}**Ala**^{Ac} (act as a FRET donor) emission and ^{TPhen}**Ala**^{Do} (act as a FRET acceptor) absorption, (b) Fluorescence spectra of individual donor amino acid ^{TCNB}**Ala**^{Ac} and acceptor amino acid ^{TPhen}**Ala**^{Do} and the tripeptide ^{TPhen}**Ala**^{Do}**-Ala-**^{TCNB}**Ala**^{Ac} which contain this two amino acids (10 μM each, r.t.; λ_{ex} = 272 nm in CH_3CN).

Table 3.5. Time resolved fluorescence spectra of amino acid ^{TPhen}**Ala**^{Do} (**2.74**) (λex = 308 nm, λem = 380 nm); ^{TCNB}**Ala**^{Ac} (**2.79**) (λex = 308 nm, λem = 330 nm); and the tripeptide ^{TPhen}**Ala**^{Do}**-Ala -**^{TCNB}**Ala**^{Ac} **(3.37)** (λex = 308 nm, λem = 330, 380 nm) in acetonitrile solvent. Concentration = 10 μM in each case.

(A) Time resolved fluorescence spectra.

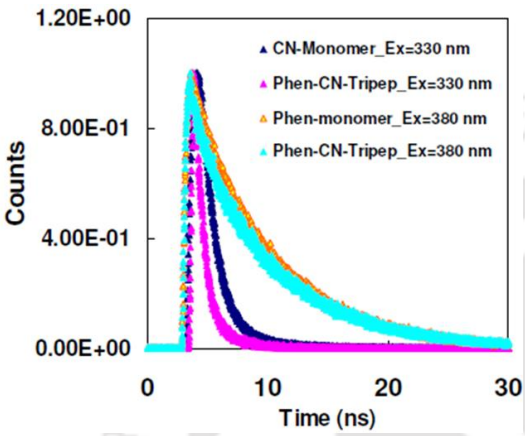

(B) Lifetime values

Amino acids/ peptides	λ_{em} **(nm)**	τ_1 **(ns)**	τ_2 **(ns)**	$\langle\tau\rangle$ **(ns)**
^{TCNB}**Ala**^{Ac} **2.79**	330	1.2 (93%)	4.5 (7%)	1.9
^{TPhen}**Ala**^{Do} **2.74**	380	13.2 (100%)	----	13.2
^{TPhen}**Ala**^{Do} **-Ala –**	330	1.2 (100%)	----	1.2
^{TCNB}**Ala**^{Ac} **3.37**	380	2.9 (8%)	14.1 (92%)	13.5

***Calculation of the Förster distance and FRET efficiency*:** The fluorescence resonance energy transfer (FRET) and the Förster distance for the FRET were calculated using the following three equations. The efficiency of energy transfer, *E*, was calculated using the equation (1)

$$E=\frac{R_0^6}{R_0^6+r^6}=1-\frac{F}{F_0} \quad \text{.....(1)}$$

where *F* and F_0 are the fluorescence intensity of donor in the presence and absence of acceptor, *r* is the distance between donor and the acceptor and R_0 is the critical distance when the energy transfer efficiency is 50% . The Förster distance R_0 (Å) was calculated by the following equation (2)[48]

$$R_0=[8.79\times10^{-5}\kappa^2 n^{-4}\Phi_D J(\lambda)]^{1/6} \quad \text{.....(2)}$$

where κ^2 is the orientation, *n* is the refractive index of the medium, Φ_D is the quantum yield of the donor in the absence of acceptor $J(\lambda)$ is the overlap integral of the fluorescence emission spectrum of the donor and the absorption spectrum of the acceptor given by the following equation (3)

$$J=\frac{\int_0^\infty F_D(\lambda)\varepsilon_A(\lambda)\lambda^4 d\lambda}{\int_0^\infty F_D(\lambda)d\lambda} \quad \text{.....(3)}$$

where $F_D(\lambda)$ is the fluorescence intensity of the donor in the wavelength range λ to $\lambda + \Delta\lambda$ with the total intensity normalized to unity. $\varepsilon_A(\lambda)$ is the molar extinction coefficient of the acceptor as a function of wavelength (λ).

Using the values of $\kappa^2 = 2/3$, $n = 1.346$, $\Phi_D = 0.36$, and the obtained overlap integral, $J(\lambda) = 5.8643 \times 10^{13}$, the R_0 and r values were calculated which were found to be $R_0 = 20$ Å and $r = 15$ Å. R_0 is the critical distance when the energy transfer efficiency is 50 % and r is the distance between the donor and acceptor.

Energy Transfer efficiency (E) = 1- F/F_0 = 85 %. F and F_0 are the fluorescence intensity of donor in the presence and absence of acceptor.

3.7.6. Solvent Assisted Modulation of FRET Emission

While examining the polarity sensitive emission of peptide ^{TPhen}**Ala**^{Do}**-Ala-**^{TCNB}**Ala**^{Ac}, we observed that FRET-induced fluorescence could be modulated. Thus, as the polarity of the solvents increased, FRET emission from ^{TPhen}**Ala**^{Do} (at 390 nm) decreased slightly (**Figure 3.23a**). This could be due to the influence of the solvent polarity on the FRET parameters and association within the TPhen–TCNB pair that led to a slight decrease in FRET emission intensity, which was also supported by a fluorescence lifetime measurement study. A very weak FRET emission was observed in phosphate buffer which could be due to non-radiative deactivation. However, the FRET signal could be optimized upon addition of DMSO to give a 296% enhancement (**Figure 3.23b**) with increasing quantum yield 0.029 to 0.115. This addition of DMSO possibly fine-tuned the donor–acceptor interaction to minimize the non-radiative deactivation process, thereby leading to an increase in intensity. The solvent assisted modulation/fine tuning the emission property would be useable in amplifying the detection signals FRET-based bioassays.[30]

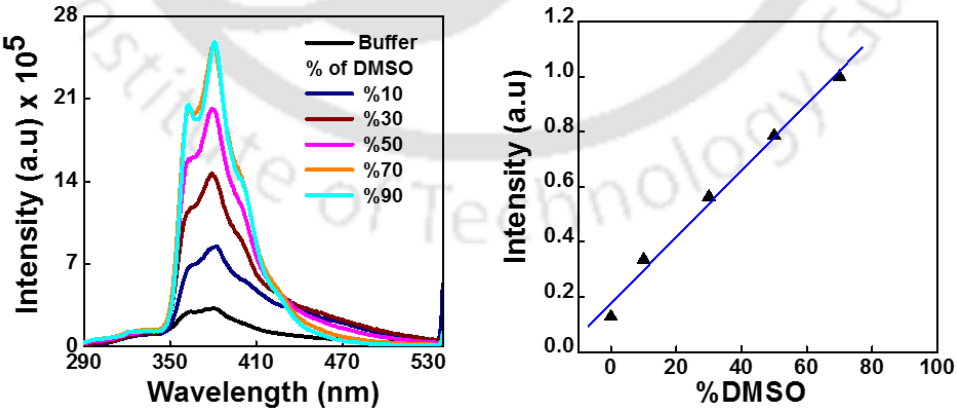

Figure 3.23. (a) Emission spectra of ^{TPhen}**Ala**^{Do}**-Ala-**^{TCNB}**Ala**^{Ac} in Buffer tritated with increasing percentage of DMSO (% of DMSO = 0, 10, 30, 50, 70, 90)**. (b)** Plot of Intensity Vs % of DMSO added (Buffer tritated with DMSO).

3.8. Conclusion

In summary, we have successfully synthesized conceptually placed donor/acceptor triazolyl unnatural amino acids decorated tripeptide. After all spectroscopic study we have concluded that our designing tripeptide adopted β-turn conformation which stabilized by intra molecular hydrogen bonding. Studied their photophysical properties and established Förster resonance energy transfer (FRET) in the conceptually designed novel unnatural β-turn peptide containing a new class of fluorescent unnatural donor/acceptor amino acids. The FRET process occurred from **TCNB** moiety of $^{TCNB}\mathbf{Ala}^{Ac}$ (FRET donor) to **TPhen** unit of $^{TPhen}\mathbf{Ala}^{Do}$ (FRET acceptor). Our developed FRET pair, $^{TCNB}\mathbf{Ala}^{Ac}$ - $^{TPhen}\mathbf{Ala}^{Do}$, wherein both the partners are unnatural amino acid, is new to the best of our knowledge. As FRET can provide information about peptide/protein conformation, our unnatural amino acid pair (FRET pair) and the FRET peptide might find application in studying solution conformational distribution of an unstructured peptide and FRET based bioassay. The modulation of FRET emission would find application in FRET-based bioassay to improve the detection sensitivity.

3.9. Experimental Section

3.9.1. General Experimental

All reactions were carried out under nitrogen atmosphere in flame-dried glassware, using a nitrogen filled balloon. Organic extracts were dried over anhydrous sodium sulfate. Solvents were removed in a rotary evaporator under reduced pressure. Silica gel (60- 120 mesh size) was used for the column chromatography. Reactions were monitored by TLC on silica gel 60 F254 (0.25 mm). ^{1}H NMR spectra were recorded at 400MHz and ^{13}C NMR spectra were recorded at 100Mz. Coupling constants (J value) were reported in hertz. The chemical shift were shown in ppm downfield form tetramethylsilane, using residual chloroform (δ =7.24 in ^{1}H NMR, δ = 77.23 in ^{13}C NMR), as an internal standard. Mass spectra were recorded with a HR mass spectrometer and data analyzed by using built-in software. IR spectra were recorded in KBr on a FT-IR spectrometer.

3.9.2. Synthesis and Characterization

***Synthesis of L-Alanine methyl ester (3.41)*:** To a degassed and cold solution of L-Alanine in dry methanol, thionyl chloride (1.5 equivalent) was added at 0 ^{o}C. After 15 minutes the reaction mixture was refluxed at 75-80 ^{o}C overnight. The solvent was evaporated in vacuum. Material was washed

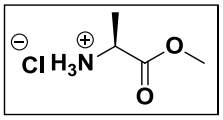

with toluene three times to remove excess thionyl chloride and the amine salt of methyl ester -L-alanine was isolated, washed with ether twice, dried and used for the next step.

***Synthesis of methyl 2-(2-(tert-butoxycarbonyl)-3 hydroxypropanamido) propanoate (3.42)*:** To a solution N-protected L-serine **3.40**, (378 mg, 1.84 mmol) in 3:1 mixture of dry CH_2Cl_2 and DMF , 1-[3-dimethyl amino propyl]-3-ehtylcarbo-diimide hydrochloride (EDC.HCl) (422 mg, 2.21 mmol) and HOBT (373 mg, 2.21mmol) were added and the reaction mixture was stirred for 1h at 0 ^oC. Then the

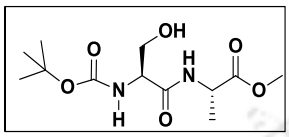

amine salt of methyl ester -L-alanine (257 mg, 1.84 mmol) was added followed by diisopropyl-ethylamine (DIPEA) (0.8 ml, 4.41 mmol). The reaction mixture was stirred for another 18-20 h at 0 ^oC to room temperature. Then solvent was dried by rotary evaporator, after which it was partitioned between EtOAc and aqueous $NaHCO_3$ solution (50 ml each). The organic layer was washed with brine solution. Pure product **3.42 (**300 mg, 1.03 mmol) was isolated in pure form by column chromatography (Si-gel, PE : EtOAc = 1:1) as colourless oil. Yield 62%; ^1H NMR ($CDCl_3$; 400 MHz) δ 1.38 (3H, d, J = 7.2 Hz); 1.42 (9H, s); 2.303 (1H, m); 3.62 (1H, q, J = 5.6, 10.8 Hz); 3.72 (3H, s); 4.02 (1H, dd, J = 3.6, 12.4 Hz); 4.16 (1H, m); 4.52 (1H, m); 5.5 (1H, d, J = 8.0 Hz); 7.02 (1H, d, J = 4.8 Hz); ^{13}C NMR (CDCl3; 100 MHz); δ 17.1, 28.1, 48.3, 52.6, 55.7, 62.7, 80.34, 156.0, 171.4, 173.6.

***Synthesis of methyl 2-(2-(tert-butoxycarbonyl)-3(methylsulfonyloxy) propanamido) propanoate (3.43)*:** Dipeptide **3.42** (190 mg, 0.61 mmol) was taken in dry DCM and was cooled to 0 ^oC. Methane sulphonyl chloride (61 µl, 0.72 mmol) and triethyl amine (109 µl, 0 .72 mmol) were added to the reaction mixture and stirred for

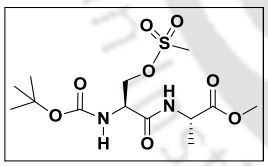

an hour till the total reactant was consumed. After that reaction mixture was poured into water and CH_2Cl_2 (20 ml each).The organic layer was washed with water two times, dried over Na_2SO_4 and then evaporated. The pure compound **3.43**, was then isolated by column chromatography (si-gel, PE:EA = 2:1) as brown oil (yield, 89%). ^1H NMR ($CDCl_3$; 400 MHz) δ 1.40 (3H, d, J = 8 Hz); 1.44 (9H, s); 3.30 (3H, s); 3.73 (3H, s); 4.31 (1H, dd, J = 4.8 Hz, 10.4 Hz); 4.53 (2H, m); 4.61 (1H, dd, J = 4 Hz, 10.4 Hz); 5.37 (1H, d, J = 8 Hz); 6.94 (1H, d, 5.6 Hz).

***Synthesis of methyl 2-(3-azido-2-(tert-butoxycarbonyl) propanamido) propanoate (3.44)* :** To a solution of the mesylate **3.43** (180 mg, 0.49 mmol) in dry DMF (6 ml), NaN_3 (48.75 mg, 0.75 mmol) was added and stirrer for 18 h at 40 ^oC. The reaction

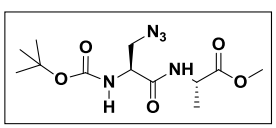

mixture was partitioned between EtOAc and water (20 ml each). The organic layer was washed with brine solution, dried, filtered and then evaporated. The title compound **3.44** was isolated by column chromatography (Si-gel, PE:EA = 2:1), as light brown oil (yield, 78 %). IR (KBr) 3425, 2981, 2107, 1661, 1515, 1368, 1251, 1163, 1062, 859. ^1H NMR ($CDCl_3$; 400 MHz) δ 1.35 (3H, d, J = 7.2); 1.39 (1H,

s); 3.49 (2H, dd, *J* = 2.8, 11.6 Hz); 3.69 (3H, s); 4.31(1H, m); 4.52 (1H, m); 5.52(1H, d, *J* = 5.2 Hz); 7.09 (1H, s); ^{13}C NMR ($CDCl_3$; 100 MHz); δ 18.2, 28.3, 48.4, 52.4, 52.6, 53.8, 80.8, 155.3, 169.2, 173.

***General procedure for the synthesis triazolyl unnatural dipeptide*:** Using the azido derivative of dipeptide (Boc-NH-Ser.Ala-OMe) **3.44**, we have prepared three different unnatural tri-peptide using Donor/Acceptor terminal alkynes.

General procedure for the synthesis triazolyl unnatural dipeptide (Boc-NH-Ser.Ala-OMe) by [3+2] cycloaddition reaction: The azido derivative of dipeptide (Boc-NH-Ser.Ala-OMe) **3.44** (1.0 equiv) was taken in 5:1 dry THF and water and degassed for 5 min with N_2. Then, alkyne (1.1 equiv) was added and both the stirring and degassing were continued for the next 5 min. After that a 6 mol % sodium ascorbate and 1 mol% powderd $CuSO_4$ were added. Then the reaction mixture was degassed and allowed to proceed for 18-20 h about 65 to 70 ^oC. After total consumption of the starting azide, the reaction mixture was evaporated completely and work up was done by EtOAc and NH_4Cl solution. The organic layer was washed with brine, dried over Na_2SO_4.The title trizolyl derivative of dipeptides **3.47** and **3.48** were separated by column chromatography and characterized.

Synthesis of methyl 2-(2-(tert-butoxycarbonyl)-3-(4-(phenanthren-9-yl)-1H-1,2,3-triazol-1-yl) propanamido) propanoate (3.47): Using general procedure, starting from 155 mg (0.49 mmol) of azido derivative of dipeptide **3.44** and 109 g (0.54 mmol) of 9- ethynylphenanthrene (**3.45**), 210 mg (0.41 mmol) of the title compound **3.47** was isolated as a light brown gummy material. Yield 83%. ^{1}H NMR ($CDCl_3$; 400 MHz) δ =1.27 (3H, d, *J* = 6.8 Hz); 1.46 (9H, s); 3.69 (3H, s); 4.48 (1H, t, *J* = 7.6 Hz); 4.82 (2H, m); 5.03 (1H, m); 5.79 (1H, d, *J* = 7.60 Hz); 7.11 (1H, d, *J* = 6 Hz); 7.62 (4H, dd, *J* = 8.4, 24 Hz); 7.95 (1H, d, *J* = 5.2 Hz); 8.26 (2H, d, *J* = 6.8 Hz); 8.32 (1H, d, *J* = 7.6 Hz); 8.71 (2H, dd, *J* = 8 Hz, 25.6 Hz); ^{13}C NMR ($CDCl_3$; 100 MHz); δ 17.7, 28.2, 48.4, 51.4, 52.4, 54.3, 80.7, 122.5, 122.9, 124.9, 126.1, 126.8, 128.4, 128.8, 129.9, 130.3, 130.6, 131.2, 146.5, 155.53, 169.0, 172.7.

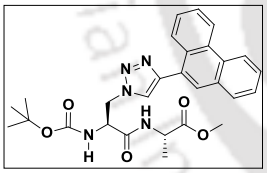

Synthesis of methyl 2-(2-(tert-butoxycarbonyl)-3-(4-(4-cyanophenyl)-1H-1,2,3-triazol-1yl)propanamido) propanoate (3.48): Using general procedure, starting from 162 mg (0.51 mmol) of azido derivative of dipeptide **3.44** and 71 mg (0.56 mmol) of 4-ethynyl benzonitrile (**3.46**), 165 mg (0.37 mmol) of the title compound **3.48** was isolated as a colourless gummy material. Yield 73%. ^{1}H NMR ($CDCl_3$; 400 MHz) δ 1.24 (3H, d, *J*=7.2 Hz); 3.69 (3H, s); 4.43 (1H, m); 4.73 (2H, d, *J* = 10.4 Hz); 4.93 (1H, m); 5.66 (1H, d, *J* = 5.2 Hz); 7.02 (1H, d, *J* = 6.4 Hz); 7.68 (2H, d, *J* = 7.6 Hz); 7.89 (2H, d, *J* = 7.2 Hz); 7.98 (1H, s);

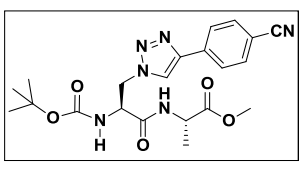

^{13}C NMR ($CDCl_3$; 100 MHz); δ 18.0, 28.3, 48.5, 51.4, 52.7, 54.3, 81.3, 111.7, 118.8, 123.1, 126.1, 132.9, 134.8, 146.0, 155.5, 168.6, 172.8.

General procedure for the deprotection of the methyl ester. To a solution of the respective methyl ester protected peptide in Water : THF = 1 : 10, lithium hydroxide (1.5 equivalent) was added at 0 ^{o}C. Then the reaction mixture was stirred about 2-3 hour until starting material was consumed. Reaction was monitored by TLC. After completion of the reaction, solvent dried by rotary evaporator. Then water (4-5 ml) was added to the reaction mixture and cooled to 0 ^{o}C. The dilute acetic acid was added to the reaction mixture to adjust pH ~ 3 to 4. The reaction mixture was extracted with CH_2Cl_2. The combined organic layers were dried over anhydrous Na_2SO_4. The hydrolysed compound was isolated by column chromatography (Si-gel, $CHCl_3$:MeOH = 10:1). Yield was 96-97%.

***Synthesis of 2-(2-(tert-butoxycarbonyl)-3-(4-(phenanthren-9-yl)-1H-1,2,3-triazol-1-yl)propanamido) propanamido) propanoic acid (3.49)*:** Using general procedure of deprotection of the methyl ester, starting from 205 mg (0.40 mmol) of **3.47**, 193 mg (0.38 mmol) of the title compound **3.49** was isolated as a white solid material and used for the next step without characterization. Yield 97%.

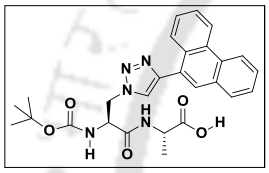

***Synthesis of 2-(2-(tert-butoxycarbonyl)-3-(4-(4-cyanophenyl)-1H-1,2,3-triazol-1-yl) propanamido) propanoic acid (3.50)*:** Using general procedure of deprotection of the methyl ester, starting from 159 mg (0.36 mmol) of **3.44**, 148 mg (0.35 mmol) of the title compound **3.50** was isolated as a white solid material and used for the next step without characterization. Yield 96%.

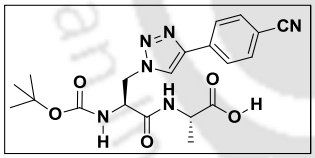

General procedure for the deprotection of the Boc-group. The respective protected amino acid or peptide was dissolved in CH_2Cl_2 and cooled to 0 ^{o}C. TFA (equal amount as the solvent) was added and the solution was allowed to warm to room temperature. After stirring at room temperature until starting material was consumed (TLC monitoring), the reaction mixture was evaporated *in vacuo*. The residual TFA was evaporated by titurating the mixture with dry toluene thrice, evaporated thrice and dried to afford the product in quantitative yield.

Synthesis of 3.51 and 3.52 : Using the general procedure of Boc-deprotection, compound **2.74** (170 mg, 0.42 mmol) and **2.79** (200 mg, 0.42 mmol) were reacted. The products **3.51** and **3.52** were obtained in quantitative yield and were used without further purification and characterization.

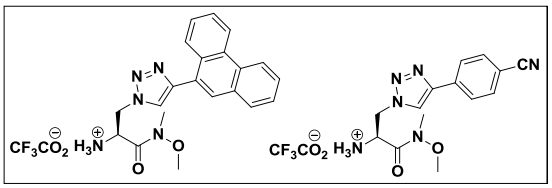

Synthesis of triazolyl donor/acceptor tripeptides*:* The target tripeptides **3.37-3.39** were synthesized following the general procedure of peptide coupling protocol as was discussed for the synthesis of dipeptides. The pure product was isolated by column chromatography (Si-gel, $CHCl_3$:MeOH = 30:1).

Synthesis of tert-butyl 3-(4-(4-cyanophenyl)-1H-1,2,3-triazol-1-yl)-1-(1-(1-(methoxy(methyl)amino)-1-oxo-3-(4-(phenanthren-9-yl)-1H-1,2,3-triazol-1-yl)propan-2-ylamino)-1-oxopropan-2-ylamino)-1-oxopropan-2-ylcarbamate (3.37): Using general procedure, starting from 144 mg (0.28 mmol) of **3.49** and 126 mg (0.31 mmol) of **3.52**, 95 mg (0.12 mmol) of the title compound **3.37** was isolated as a gummy material, after washing with ether it converted to white solid. Yield 43%. IR (KBr) 3320, 2973, 2931, 2226, 1660, 1516, 1452, 1367, 1248, 1164, 1053, 849, 729, 556 cm^{-1}. ^1H NMR (d_6-DMSO; 400 MHz) δ 1.1 (3H, d, J = 6.9 Hz); 1.17 (9H, s); 3.16 (3H, s); 3.75 (3H, s); 4.35 (1H, bs);4.46 (2H, d, J = 13.2 Hz); 4.7 (2H, d, J = 13.5 Hz); 4.81 (1H, bs); 5.33 (1H, bs); 6.99 (1H, d, J = 7.5 Hz); 7.65 (2H, d, J = 6.4 Hz); 7.72 (2H, d, J = 6.0 Hz); 7.87 (2H, m); 7.79 (1H, t, J = 4.5 Hz); 7.95 (1H, s); 8.06 (1H, t, J = 3.9 Hz); 8.25 (1H, d, J = 9.0 Hz); 8.44 (1H, d, J = 9.0 Hz); 8.36 (1H, d, J = 5.7 Hz); 8.44(1H, d, J = 9.0 Hz); 8.50 (1H, s); 8.56 (1H, s); 8.58 (1H, m); 8.84 (1H, d, J = 8.1 Hz); 8.93 (1H, d, J = 7.8 Hz); ^{13}C NMR ($CDCl_3$; 100MHz); δ 17.7, 28.1, 32.4, 36.3, 49.2, 50.3, 60.3, 61.8, 66.9, 80.4, 110.8, 118.7, 122.4, 122.9, 124.8, 125.5, 126.0, 126.4, 126.8, 128.2, 128.7, 129.8, 130.1, 130.5, 131.0, 132.3, 134.4, 145.2, 146.3, 156.1, 168.2, 169.0, 172.2. HRMS calcd for $C_{41}H_{44}N_{11}O_6$ ([M + H]$^+$) 786.3471, found 786.3476. $C_{41}H_{43}N_{11}O_6Na$ ([M + Na]$^+$) 809.3376, found 809.3374.

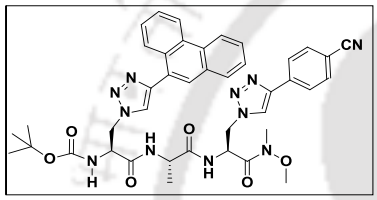

Synthesis of tert-butyl 1-(1-(1-(methoxy(methyl)amino)-1-oxo-3-(4-(phenanthren-9-yl)-1H-1,2,3-triazol-1-yl)propan-2-ylamino)-1-oxopropan-2-ylamino)-1-oxo-3-(4-(phenanthren-9-yl)-1H-1,2,3-triazol-1-yl)propan-2-ylcarbamate (3.38) : Using general procedure, starting from 193 mg (0.37 mmol) of **3.49** and 182 mg (0.37 mmol) of **3.51,** 147 mg (0.17 mmol) of the title compound **3.38** was isolated as a brown solid compound after washing with ether.

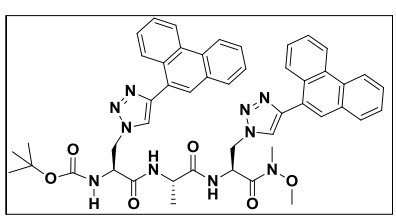

Yield 45%. IR (KBr) 3327, 2979, 1655, 1519, 1451, 1367, 1248, 1165, 1054, 728 cm^{-1}. ^1H NMR 1H NMR (d6-DMSO; 300 MHz) δ 1.13 (3H, d, J = 6.9 Hz); 1.26 (9H, s); 3.15 (3H, s); 3.71 (3H, s); 4.39 (1H, bs);4.69- 4.53 (4H, m); 4.78 (1H, bs); 5.33 (1H, bs); 7.24-7.13 (1H, m); 7.72-7.66 (8H, m); 8.07-8.01 (4H, m); 8.34 (1H, d, J = 7.2 Hz); 8.45 (3H, d, J = 8.1 Hz); 8.52 (1H, s); 8.57 (1H, s); 8.82 (2H, d, J = 7.8 Hz); 8.85 (2H, d, J = 8.1 Hz); ^{13}C NMR ($CDCl_3$; 100 MHz); δ 17.3, 28.3, 32.5, 49.5, 50.4, 51.0, 51.3, 54.9, 61.9, 80.8, 122.5, 122.9, 124.8, 126.8, 126.9, 128.4, 128.9, 130.0, 130.4, 130.7, 131.3, 146.7, 155.9, 168.2, 169.6, 172.1. HRMS calcd for $C_{48}H_{49}N_{10}O_6$ ([M + H]$^+$) 861.3831, found 861.3837. $C_{48}H_{48}N_{10}O_6Na$ ([M + Na]$^+$) 884.3734, found 884.3731.

Synthesis of tert-butyl 3-(4-(4-cyanophenyl)-1H-1,2,3-triazol-1-yl)-1-(1-(3-(4-(4-cyanophenyl)-1H-1,2,3-triazol-1-yl)-1-(methoxy(methyl)amino)-1-oxopropan-2-ylamino)-1-oxopropan-2-ylamino)-1-oxopropan-2-ylcarbamate (3.39): Using general procedure, starting from 148 mg (0.35 mmol) of **3.50** and 159 mg (0.39 mmol) of **3.52**, 100 mg (0.14 mmol) of the title compound **3.39** was isolated as a transparent gummy material which became solid particle after ether wash. Yield 44%. IR (KBr) 3325, 2979, 2931, 2227, 1664, 1517, 1368, 1237, 1164, 1049, 848, 556 cm^{-1}. ^1H NMR ($CDCl_3$; 400 MHz) δ = 1.18 (3H, d, J = 7.2 Hz); 1.34 (9H, s); 3.2 (3H, s); 3. 77 (3H, s); 4.41 (1H, m); 4.78 (2H, m); 4.89 (2H, m); 5.27 (1H, m); 5.80 (1H, m); 6.43 (1H, d, J = 8 Hz); 6.65 (1H, d, J = 6.8 Hz); 6.83 (1H, d, J = 7.6 Hz); 7.65 (4H, d, J = 7.2 Hz); 7.89 (6H, m); ^{13}C NMR ($CDCl_3$; 100 MHz); δ 17.9, 28.1, 32.4, 49.4, 50.0, 51.7, 53.4, 54.2, 61.9, 80.8, 111.1, 111.2, 118.7, 122.8, 126.0, 132.6, 134.7, 135.0, 145.5, 145.7, 155.3, 167.8, 169.2, 172.2. HRMS calcd for $C_{34}H_{39}N_{12}O_6$ ([M + H]$^+$) 711.3116, found 711.3110. $C_{34}H_{38}N_{12}O_6Na$ ([M + Na]$^+$) 734.3013, found 734.301.

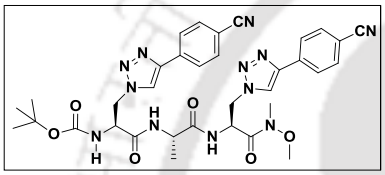

3.9.3. Photophysical Studies of the Peptides

UV-visible measurements: All the *UV* –visible spectra of the amino acids (10 µM) were measured in different solvents using a UV-Visible spectrophotometer with a cell of 1 cm path length. The measurements were carried out in absorbance mode. The absorbance values of the sample solutions were measured in the wavelength regime of 200–550 nm. All the sample solutions were prepared just before doing the experiment.

Study of circular dichroism spectroscopy: Circular dichroism spectra were recorded using a CD spectropolarimeter with a cell path length of 10 nm at 25 ^oC. All the samples were prepared in spectroscopic grade acetonitrile/methanol solvent with 30 µM concentration.

Fluorescence experiments: All the sample solutions were prepared as described in UV measurement experiments. Fluorescence spectra were obtained using a fluorescence spectrophotometer at 25 °C using 1 cm path length cell. The excitation

wavelengths for all the cases were set at the excitation maxima of each sample in each solvents and emission spectra were measured in the wavelength regime of 300–700 nm with an integration time of 0.2 sec. All the sample solutions were prepared just before doing the experiment. Total volume of 1.0 ml from a stock solution of 2 ml of 10 μM concentration for each case was used for fluorescence experiment in 1 ml cell. Fluorescence emissions were collected exciting the samples at the wave length corresponding to their absorption maxima. Steady-state fluorescence emission spectra were recorded at room temperature as an average of five scans using an excitation slit of 3.0 nm, emission slit 3.0 nm, and scan speed of 120 nm/min. The fluorescence quantum yields (Φ_f) were determined using quinine sulphate as a reference with the known Φ_f (0.55) in 0.1 molar solution in sulphuric acid. The following equation was used to calculate the quantum yield,

$$\Phi_S = \Phi_R \frac{Fl_S^{Area}}{Fl_R^{Area}} \frac{Abs_R}{Abs_S} \frac{n_S^2}{n_R^2}$$

where, Φ_R is the quantum yield of standard reference, Fl_S^{Area} (sample) and Fl_R^{Area} (reference) are the integrated emission peak areas, Abs_S (sample) and Abs_R (reference) are the absorbances at the excitation wavelength, and n_S (sample) and n_R (reference) are the refractive indices of the solutions.

The fluorescence lifetime experiment was carried out using a time resolved fluorescence spectrophotometer at 25 °C using 1 cm path length cell. 290, 405 LED and 375 nm laser was used as excitation light source. The lifetime data were calculated by software with fixed fitting range. The time correlated single photon counting (TCSPC) method was used to calculate the lifetime data. The life time data (Global Analysis) were calculated by the software package with fitting range 205 – 4000 channels.

3.10. ^{1}H and ^{13}C NMR Spectra Few Selected Peptides

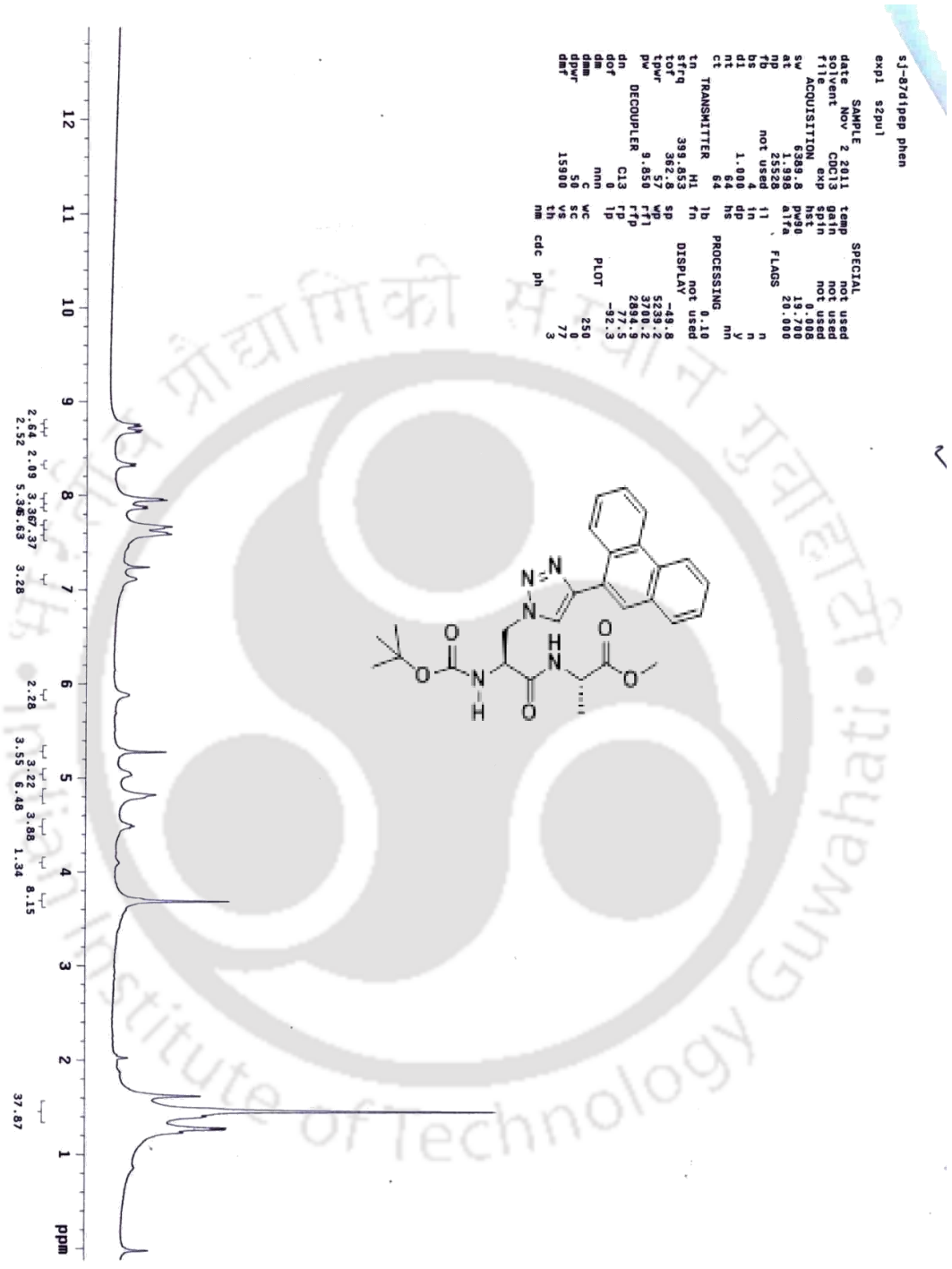

Figure 3.24: ^{1}H NMR spectra of compound **3.47**.

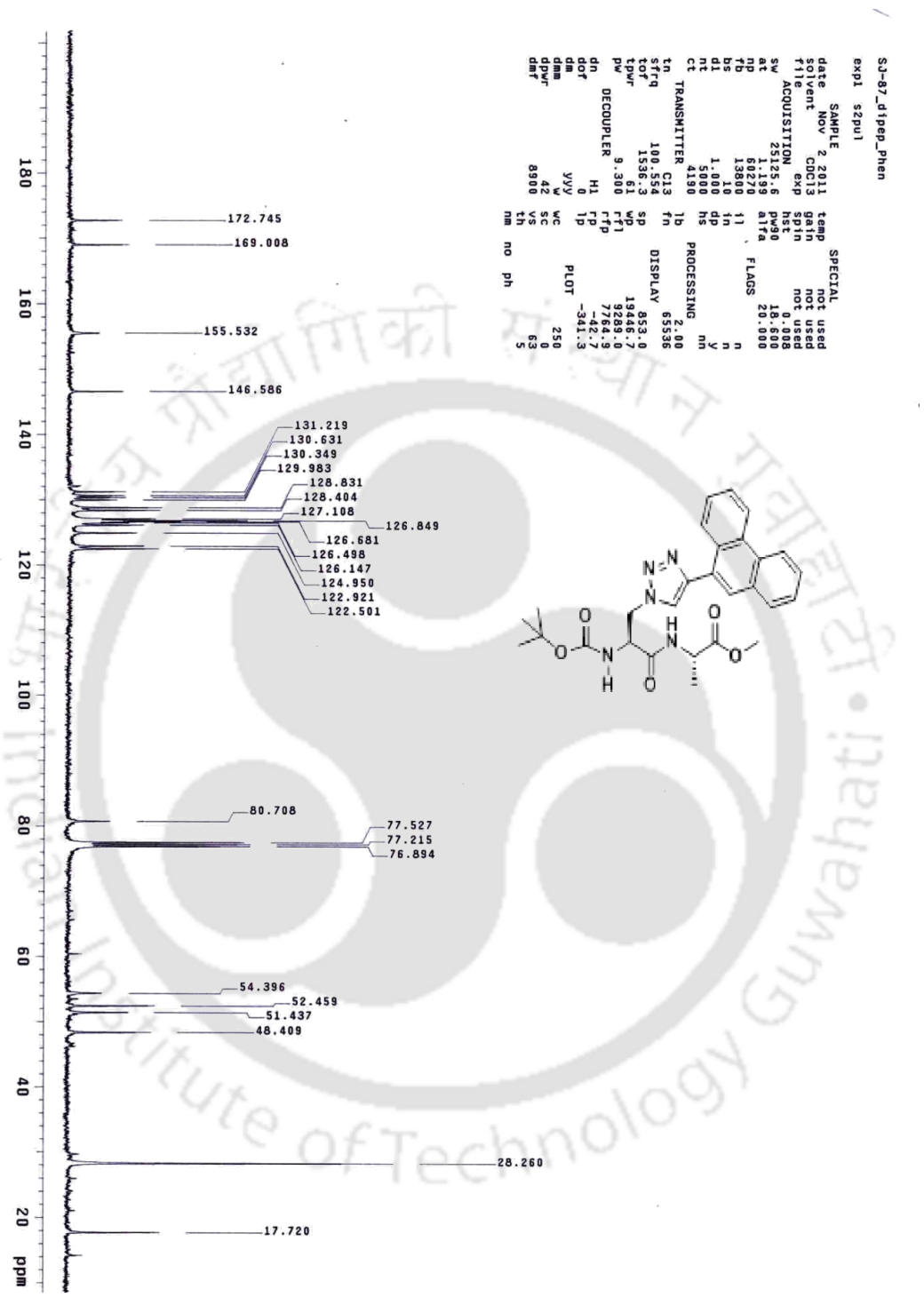

Figure 3.25: ^{13}C NMR spectra of compound **3.47**.

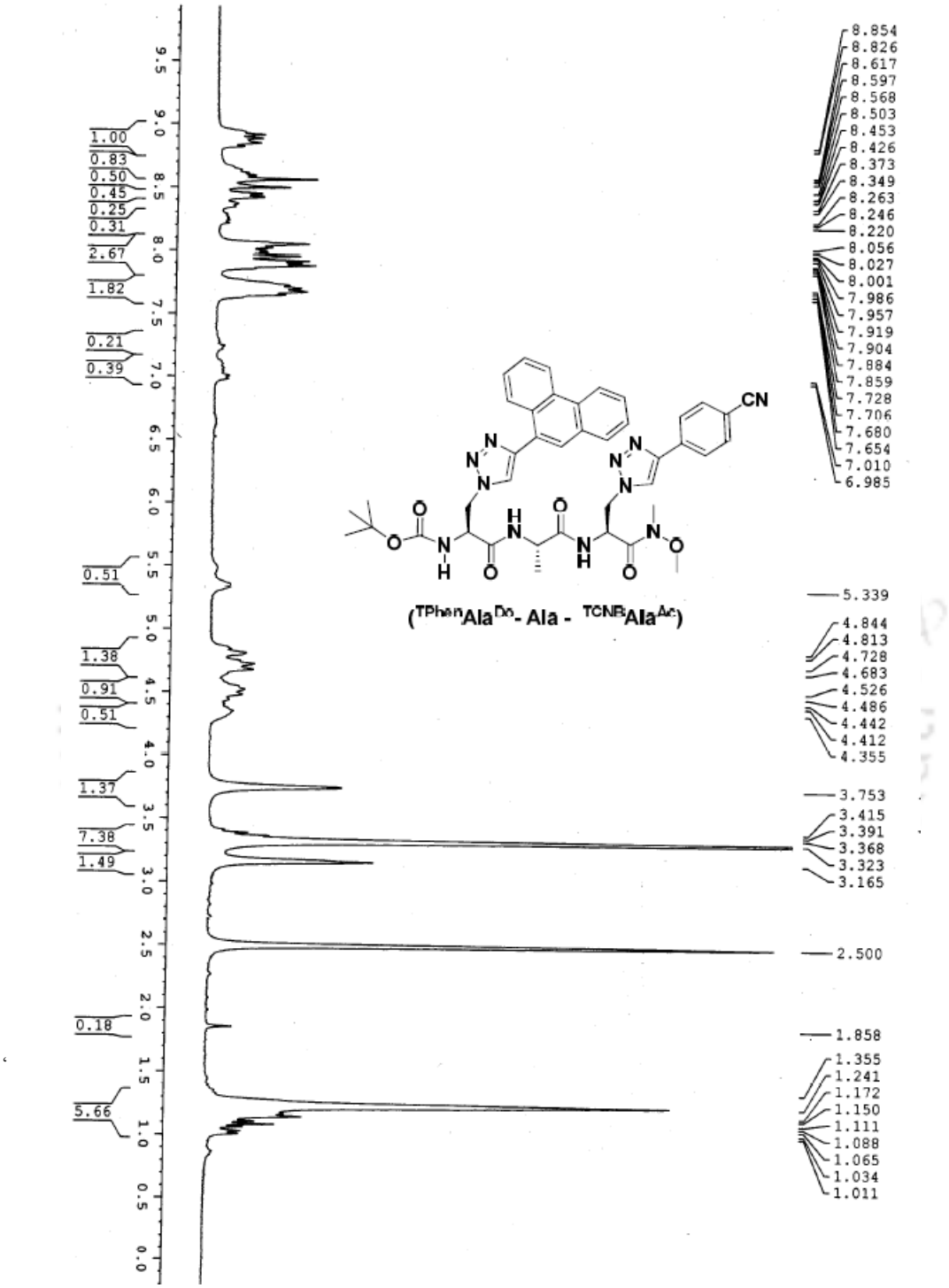

Figure 3.26: ^{1}H NMR spectra of tripeptide **3.37.**

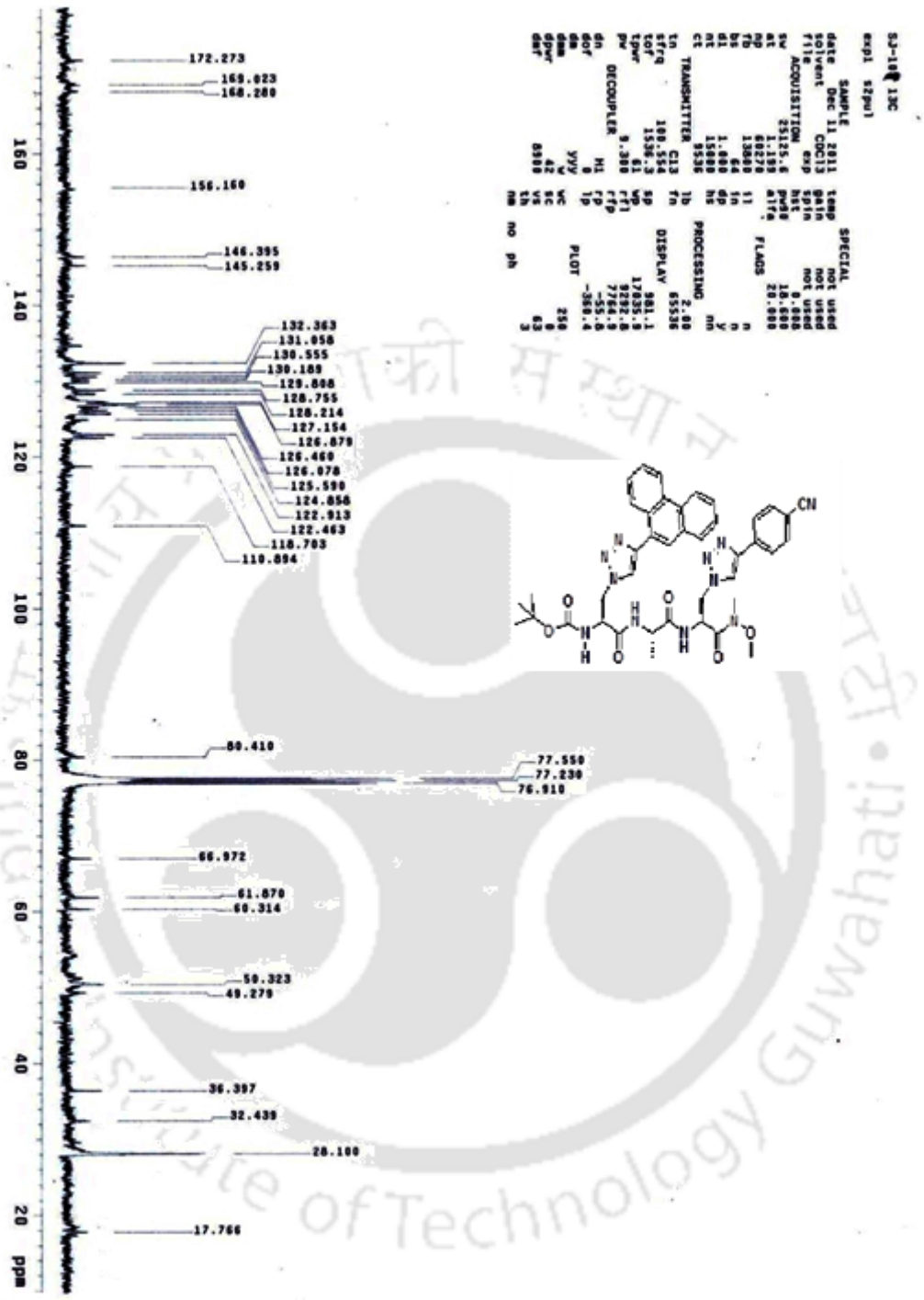

Figure 3.27: ^{13}C NMR spectra of tripeptide **3.37.**

3.11. References:

1. (a) Wales, S. M.; Hammer, K. A.; King, A. M.; Tague, A. J.; Lyras, D.; Riley, T. V.; Keller, P. A.; Pyne, S. G. *Org. Biomol. Chem*. **2015**, *13*, 5743. (b) Kemp, D. S. *Trends Biotechnol.* **1990**, *8*, 249. (c) Giannis, A.; Kolter, T. *Angew.Chem. Int. Ed. Engl.* **1993**, *32*, 1244. (d) Schneider, J. P.; Kelly, J. W. *Chem. Rev.* **1995**, *95*, 2169 (e) Ramurthy, S.; Lee, M. S.; Nakanishi, H.; Shen, R.; Kahn, M. *Bioorg. Med. Chem. Lett.* **1994**, *4*, 1007. (f) Olson, G. L.; Bolin, D. R.; Bonner, M. P.; Bos, M.; Cook,C. M.; Fry, D. C.; Graves, B. J.; Hatada, M.; Hill, D. E.; Kahn, M.; Madison, V. S.; Rusiecki,V. K.; Sarabu, R.; Sepinwall, J.; Vincent, G. P.; Voss, M. E. *J. Med. Chem.* **1993**, *36*, 3039. (g) Kahn, M. *Synlett.* **1993**, 821.
2. (a) Ottaviani, E.; Cossarizza, A. *FEBS Lett.* **1990**, *267*, 250. (b) Gray, R. A.; Vander V. D. G.; Burke, C. J.; Manning, M. C.; Middaugh, C. R.; Borchardt, R. T. *Biochemistry* **1994**, *33*, 1323. (c) Rich, D. H.; Bursavich M. G.; Estiarte, M. A. *Biopolymers* **2002**, *66*, 115. (d) Kleinert, H. D.; Baker, W. R.; Stein, H. H. *Biopharm* **1993**, *6*, 36,
3. (a) Spatola, A. F. In *Chemistry and Biochemutry of Amino Acids*, *Peptides*, and *Proteins*; Weinstein, B., Ed.; Marcel Dekker: New York, **1983**, VII, 267. (b) Rich, D. H. Peptidase Inhibitors. In *Comprehensive Medicinal Chemistry*; Hanach, C.; Sammes, P. G.; Taylor, J. B. Eds.; Pergamon Press: Oxford, **1989**, *2*, 391.
4. (a) Schulz, G. E.; R. Schirmer, H. In *Principles of Protein Structure*; Springer, New York, **1979**. (b) Branden, C.; Tooze, J. In *Introduction to Protein Structure*; Garland, New York, **1991**.
5. (a) Appella, D. H.; Christianson, L. A.; Karle, I. L.; Powell, D.R.; Gellman, S. H. *J. Am. Chem. Soc.* **1996**, *118*, 13071. (b) Appella, D. H.; Barchi, J. J.; Durell, S. R.; Gellman, S. H. *J. Am. Chem. Soc.* **1999**, *121*, 2309. (c) Hanessian, S.; Luo, X.; Schaum, R.; Michnick, S. *J. Am. Chem. Soc.* **1998**, *120*, 8569. (d) Kemp, D. S.; Curran, T. P.; Davis, W. M.; Boyd, J. G.; Muendel, C. *J. Org. Chem.* **1991**, *56*, 6672.
6. (a) Souers, A. J.; Rosenquist, A.; jarvie, E. M.; Ladlow, M.; Fenuik, W.; Ellman, J. A. *Biorg. Med. Chem. Lett*. **2000**, *10*, 2731. (b) Souers, A. J.; Virgilio, A. A.; Rosenquist, A.; Fenuik, W.; Ellman, J. A. *J. Am. Chem. Soc.* **1999**, *121*, 1817. (c) Gardner, B.; Nakanishi, H.; Kahn, M. *Tetrahedron* **1993**, *49*, 3433. (d) Giannis, A.; Kolter, T. *Angew. Chem. Int. Ed. Engl.* **1993**, *32*, 1244.
7. (a) Nowick, J. S. *Acc. Chem. Res.* **1999**, *32*, 287. (b) Nowick, J. S.; Smith, E. M.; Pairish, M. *Chem. Soc. Rev.* **1996**, 401. (c) Junquera, E.; Nowick, J. S. *J. Org. Chem.* **1999**, *64*, 2527. (d) Schneider, J. P.; Kelly, J. W. *J. Am. Chem. Soc.* **1995**, *117*, 2533.

8. (a) Cochran, A. G. *Chem. Biol.* **2000**, *7*, R85. (b) Stites, W. E. *Chem. Rev.***1997**, *97*, 1233. (c) Bogan, A. A.; Thorn, K. S. *J. Mol. Biol*. **1998**, *280*, 1. (d) Jones, S.; Thornton, J. M. *Proc. Natl. Acad. Sci.* USA. **1996**, *93*, 13. (e) Peczuh, M. W.; Hamilton, A. D. *Chem. Rev.* **2000**, *100*, 2479. (f) Burgess, K. *Acc. Chem. Res.* **2001,** *34*, 826.

9. (a) G. MacBeath, S. L. Schreiber, *Science* **2000**, *289*, 1760. (b) J. Zhang, R. E. Campbell, A. Y. Ting, R. Y. Tsien, *Nat. Rev. Mol. Cell Biol.* **2002**, *3*, 906. (c) B. N. G. Giepmans, S. R. Adams, M. H. Ellisman, R. Y. Tsien, *Science* **2006**, *312*, 217.

10. (a) R. F. Wissner, S. Batjargal, C. M. Fadzen, J. E. Petersson, *J. Am. Chem. Soc.* **2013**, *135*, 6529. (b) H. S. Lee, J. Guo, E. A. Lemke, R. D. Dimla, P. G. Schultz, *J. Am. Chem. Soc.* **2009**, *131*, 12921.

11. G. Loving, B. Imperiali, *J. Am. Chem. Soc.* **2008**, *130*, 13630.

12. (a) Clegg, R. M. *Methods Enzymol*. **1992**, *211*, 353. (b) Clegg, R. M. (John Wiley & Sons), New York, **1996**. (c) Weib Van Der Meer, B.; Coker, G.; Simon Chen, S. –Y. Theory and Data, VCH, New York, **1994**.

13. (a) Förster, T. *Discuss. Faraday Soc*. **1959**, *27*, 7. (b) Royer, C. A.; *Chem. Rev*. **2006**, *106*, 1769. (c) Lakowicz, J. R. Principles of Fluorescence Spectroscopy, Springer, New York, 3rd edn, **2006**. (d) Rogers, J. M. G.; Lippert, L. G.; Gai, F. *Anal. Biochem*. **2010**, *399*, 182.

14. (a) Nedumpara, R. J.; Manu, P. J.; C. Vallabhan, P. G.; Nampoori, V. P. N.; Radhakrishnan, P. *Opt. Laser Technol*. **2008**, *40*, 953. (b) Kang, M.; Nag, O. K.; Hwang, S.; Kim, I.; Yang, H.; Kyhm, K.; Woo, H. Y. *Phys. Chem. Chem. Phys*. **2010**, *12*, 15482 (c) Tamiaki, H.; Maruyama, K. *Chem. Lett*. **1993**, 1499.

15. Wilmot, C. M.; Thornton, J. M. *J. Mol. Biol.* **1988**, *203*, 221.

16. (a) Toniolo, C.; Polese, A.; Formaggio, F.; Crisma, M.; Kamphuis, J. *J. Am. Chem. Soc.* **1996**, *118*, 2744. (b) Engel, M.; Williams, R. W.; Erickson, B. W. *Biochemistry* **1991**, *30*, 3161. (c) Kemp, D. S.; Allen, T. J.; Oslick, S. L. *J. Am. Chem. Soc.* **1995**, *117*, 6641.

17. (a) Plateau, P.; Gueron, M. *J. Am. Chem. Soc.* **1982**, *104*, 7310. (b) Wishart, D. S.; Sykes, B. D.; Richards, F. M. *J. Mol. Biol.* **1991**, *222*, 311. (c) Plateau, P.; Gueron, M. *J. Am. Chem. Soc.* **1982**, *104*, 7310. (d) Wishart, D. S.; Sykes, B. D.; Richards, F. M. *J. Mol. Biol.* **1991**, *222*, 311. (e) Dyson, H. J.; Wright, P. E. *Ann. Rev. Biophys. Biophys. Chem.* **1991**, *20*, 519.

18. Venkatachalam, C. M. *Biopolymers* **1968**, *6*, 1425.

19. Schneider, J. P.; Kelly, J.W. *Chem. Rev.* **1995**, ***95***, 2169.

20. (a) Dutt, A.; Frohlich, R.; Pramanik, A. *Org. Biomol. Chem*. **2005**, *3*, 661. (b) Dutt, A.; Drew, M. G. B.; Pramanik, A. *Tetrahedron* **2005**, *61*, 11163. (c) Dutt, A.; Dutta, A.; Mondal, R.; Spencer, E. C.; Howardb, J. A. K.; Pramanik, A. *Tetrahedron* **2007**, *63*, 10282.

21. Fink, B. E.; Kym, P. R. Katzenellenbogen, J. A. *J. Am. Chem. Soc*. **1998**, *120*, 4334.

22. (a) Pinsker, A.; Einsiedel, J.; Härterich, S.; Waibel, R.; Gmeiner, P. *Org. Lett*. **2011**, *13*, 13. (b) Bittermann, H.; Gmeiner, P. *J. Org. Chem*. **2006**, *71*, 97.

23. Williamson, D. A.; Bowler, B. E. *J. Am. Chem. Soc*. **1998**, *120*, 10902.

24. Arnold, U.; Hinderaker, M. P.; Nilsson, B. L. Huck, B. R.; Gellman, S. H.; Raines, R. T. *J. Am. Chem. Soc*. **2002**, *124*, 8522.

25. Golebiowski, A.; Klopfenstein, S. R.; Shao, X.; Chen, J. J.; Colson, A.-O.; Grieb, A. L. Russell, A. F *Org. Lett*. **2000**, *2*, 17.

26. Zhang, J.; Kemmink, J.; Rijkers, D. T. S.; Liskamp, R. M. J. *Org. Lett*. **2011**. *13*, 13.

27. (a) Talukder, P.; Chen, S. C.; Liu, T.; Baldwin, E. A.; Benkovic, S. J.; Hecht, S. M. *Bioorg. Med. Chem. Lett.* **2014**, *22*, 5924. (b) Marmé, N.; Knemeyer, J. P.; Wolfruna, J.; Sauer, M. *Angew. Chem. Int. Ed. Engl*. **2004**, *43*, 3798.

28. (a) Tung, C-H. *Peptide Sci.* **2004**, *76*, 391. (b) Pazos, E.; Vázquez, O.; Mascareñas, J.; Vázquez, M. E. *Chem. Soc. Rev.* **2009**, *38*, 3348. (e) Bains, G. K.; Kim, S. H.; Sorina, E. J.; Narayanaswami, V. *Biochemistry* **2012**, *51*, 6207.

29. (a) Neuweiler, H.; Schultz, A.; Vaiana, A. C.; Smith, J. C.; Kaul, S.; Wolfrum, J.; Sauer, M. *Angew. Chem., Int. Ed*. **2002**, *41*, 4769. (b) Chen, S.; Fahmi, N. E.; Wang, L.; Bhattacharya, C.; Benkovic, S. J.; Hecht, S. M. *J. Am. Chem. Soc.* **2013**, *135*, 12924.

30. (a) Fujii, A.; Sekiguchi, Y.; Matsumura, H.; Inoue, T.; Chung, W. S.; Hirota, S.; Matsuo, T. *Bioconjugate Chem.* **2015**, *26*, 537. (b) Oh, K. J.; Casha, K. J.; Plaxco, K. W. *J. Am. Chem. Soc.* **2006**, *128*, 14018. (c) Nedumparaa, R. J.; Manua, P. J.; Vallabhanb, C. P. G.; Nampooria, V. P. N.; Radhakrishnana, P. *Opt. Laser Tech.* **2008**, *40*, 953. (d) Kang, M.; Nag, O. K.; Hwang, S.; Kim, I.; Yang, H.; Kyhm, K.; Woo, H. Y. *Phys. Chem. Chem. Phys.* **2010**, *12*, 15482.

31. (a) Meldal, M.; Tornøe, C. W. *Chem. Rev*. **2008**, *108*, 2952. (b) Tornøe, C. W.; Christensen, C.; Meldal, M. *J. Org. Chem*. **2002**, *67*, 3057. (c) Tornøe, C. W.; Sanderson, S. J.; Mottram, J. C.; Coombs, G. H.; Meldal, M. *J. Comb. Chem.* **2004**, *6*, 312.

32. Zauner, T.; Berger-Hoffmann, R.; Müller, K.; Hoffmann, R.; Zuchner, T. *Anal Chem*. **2011**, *83*, 7356.

33. Ekici, O. D.; Zhu, J.; Chung, I. Y. W.; Paetzel, M.; Dalbey, R. E.; Pei, D. *Biochemistry* **2009**, *48*, 5753.

34. (a) Zasloff, M. *Nature* **2002**, *415*, 389. (b) Rinaldi, A. C. *Curr. Opin. Chem. Biol.* **2002**, *6*, 799.

35. (a) Tucker, M. J.; Tang, J.; Gai, F. *J. Phys. Chem. B*. **2006**, *110*, 8105. (b) Glasscock, J. M.; Zhu, Y.; Chowdhury, P.; Tang, J.; Gai, F. *Biochemistry*

2008, *47*, 11070. (c) Rogers, J. M. G.; Lippert, L. G.; Gai, F. *Anal. Biochem*. **2010**, *399*, 182.

36. Xu, Y.; Hixon, M. S.; Dawson, P. E.; Janda, K. D. *J. Org. Chem*. **2007**, *72*, 6700.

37. White, B. R.; Liljestrand, H. M.; Holcombe, J. A. *Analyst* **2008**, *133*, 65.

38. Song, E.; Cheng, D.; Song, Y.; Jiang, M.; Yu, J.; Wang, Y. Biosens. Bioelectron. **2013**, *47*, 445.

39. (a) Angell, Y. L.; Burgess, K. *Chem. Soc. Rev.* **2007**, *36*, 1674. (b) Barbaras, D.; Gademann, K. *ChemBioChem*, **2008**, *9*, 2398. (c) Chouhan, G.; James, K. *Org. Lett*. **2013**, *15*, 1206. (d) Oh, K.; Guan, Z. *Chem. Commun*. **2006**, 3069 (e) Ball, J. B.; Hughes, R. A.; Alewood, P. L.; Andrews, P. R. *Tetrahedron* **1993**, *49*, 3467.

40. (a) Förster, T. *Discuss. Faraday Soc.* **1959**, 7. (b) Royer, C. A. *Chem. Rev.* **2006**, *106*, 1769. (c) Lakowicz, J. R. *Principles of Fluorescence Spectroscopy*, 3rd ed.; Springer: New York, **2006**. (d) Kang, M. O.; Nag, K.; Hwang, S.; Kim, I.; Yang, H.; Kyhm, K.; Woo, H. Y. *Phys. Chem. Chem. Phys.* **2010**, *12*, 15482.

41. Panda, G.; Rao, N. V. *Synlett.* **2004**, *1*, 13.

42. (a) Halab, L.; Lubell, W. D. *J. Am. Chem. Soc.* **2002**, *124*, 2474. (b) Proulx, C.; Lubell, W. D. *J. Org. Chem.* **2010**, 75, 5385. (c) Tiffany, M. L.; Krimm, S. *Biopolymers* **1972**, *11*, 2309.

43. (a) Kim, K.; Germanas, J. P. *J. Org. Chem.* **1997**, *62*, 2847. (b) Oh, K.; Guan, Z. *Chem. Commun*. **2006**, 3069.

44. Kessler, H. *Angew. Chem. Int. Ed. Engl.*, **1982**, *21*, 512.

45. (a) Maestro, version 9.0, Schrödinger, LLC, New York, NY, **2009**. (b) Lee, H.-J.; Park, H. M.; Lee, K. B. *Biophys. Chem*. **2007**, *125*, 117.

46. (a) Grabowksi, Z. R.; Rotkiewicz, K.; Rettig, W. *Chem. Rev*. **2003**, *103*, 3899. (b) Zhang, Y.; Jiang, M.; Han, G. –C.; Zhao, K.; Tang, B. Z.; Wong, K. S. *J. Phys. Chem. C* **2015,** *119*, 27630. (c) Dobkowski, J.; Kijak, M.; Sazanovich, I. V.; Waluk, J. *J. Phys. Chem. B* **2015,** *119*, 7294. (d) Kobayashi, A.; Takehira, K.; Yoshihara, T.; Uchiyama, S.; Tobita, S. *Photochem. Photobiol. Sci*. **2012**, *11*, 1368-1376.

47. (a) Adhikari, A.; Das, D. K.; Sasmal, D. K.; Bhattacharyya, K. *J. Phys. Chem. A* **2009**, *113*, 3737. (b) Banerjee, C.; Kundu, N.; Ghosh, S.; Mandal, S.; Kuchlyan, J.; Sarkar, N. *J. Phys. Chem. B* **2013**, *117*, 9508.

48. Das, D. K.; Das, A. K.; Mandal, T.; Mandal, A. K.; Bhattacharyya, K. *J. phys. Chem. B* **2010**, *114*, 13159

Chapter 4

SYNTHESIS OF TRIAZOLO β - AZA - ε- AMINO ACID AS NOVEL SCAFFOLD FOR β - TURN PEPTIDOMIMETICS

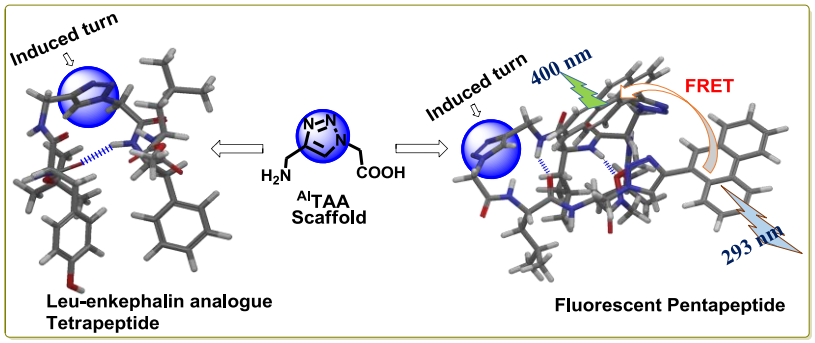

4.1. Introduction

During the last three decades, peptides have gained a wide range of attractions from a diverse range of scientific corners. As a result, an important numbers of biologically active peptides have been discovered and characterized and several of them have been tested as medicinally active. However, natural peptides often are not suitable as therapeutics because of the conformational flexibility leading to shortcomings such as-(a) multiple conformations that are energetically accessible for each residue of medium-sized polypeptides, (b) low metabolic stability, (c) poor absorption after oral ingestion, (d) low diffusion in the central nervous system, (e) rapid excretion and (f) undesired effects, due to flexibility, on interaction with several receptors.[1]

Besides all these drawbacks, biomedical researchers are constantly engaged in the development of new peptides/proteins based therapeutics, by maintaining the features responsible for biological activity and introducing both structural and functional specific modifications so as to get rid of the above shortcomings. The challenges in this endeavor have opened a new field of mimicked research, called peptidomimetics.[2, 3] A peptidomimetic compound is a substance with a desired secondary structure retaining other structural features similar to native peptide to enable the substance therapeutically more useful compared to native peptide. Peptidomimetics are thus found to show greater oral bioavailability, biological activity[4, 5] much more selectivity and efficiency and hence resulting in a fewer side effects than native peptides. Thus, for developing drug candidates, peptidomimetics have shown great promise both in organic and medicinal chemistry.

4.2. Peptidomimetics: Design and Classifications

Peptidomimetics Design Criteria: Peptidomimetics is basically a knowledge based design focusing the electronic and conformational features of the native peptide and its mechanism of biological acidity such as receptor or enzyme's active site binding. Thus, the development of peptidomimetics follows some basic principles which includes.[6]

(a) Replacement of peptide backbone with a non-peptide framework

(b) Preservation of side-chains involved in biological activity: when they constitute the pharmacophore.

(c) Second generation peptidomimetics: Modifications may be introduced to improve biological activity: (i) chain length modification, (ii) introduction of constraints, (iii) cyclopeptide bond replacement and (iv) introduction of isosteric replacements.[7]

(d) Maintenance of flexibility: First-generation peptidomimetics: For a biological active flexible mimetic, the introduction of rigidity to side-chains is welcome to improve the activity observed.

(e) Structure–activity relationship: Kknowledge of the structure–activity relationship or the three-dimensional structure of bioactive conformation/pharmacophore hypothesis can be applied to achieve the best peptidomimetic compound.

Types of Peptidomimetics: It may be divided into three classes depending on their structural and functional characteristics: [8]

(1) Type I mimetics: It is the structural mimetics of a native substrate with all the functionalities in a well-defined spatial orientation.

(2) Type II mimetics: It is a functional mimetics designed based on the mechanism of interaction with the target in a similar fashion as the native peptides do to show the biological activity.

(3) Type III mimetics: It is both structural and functional mimetics which can be adopted via introduction of a scaffold with a structure different from that of the substrate. However all the biologically important and active functional groups are mounted in a well-defined spatial orientation. Examples include an unnatural constrained small molecular framework present/substitute the peptide backbone.

4.3. Approaches to Peptidomimetic Design

The major approaches in peptidomimetic chemistry deals with-

(a) Introduction of Local Modification/Constraints:

- **(i) Introduction of Novel Amino acids:** Replacing one or more amino acids of a peptide sequence with a modified novel amino acid without altering the biological activity of the native peptide is one of the important approaches in peptide mimetic design.
- **(ii) Introduction of isosteres of the peptide bond**
- **(iii) Side-Chain Isosteres**

(b) Introduction of global constraints to define the bioactive conformation.

(c) Molecular Scaffolds Mimicking the Peptidic Backbone

4.3.1. Introduction of Local Modification/Constraints

(i) ***Introduction of Novel Amino acids*:** The most conservative approach to modify a peptide is to replace an amino acid by a modified one which can introduce only a local structural change into the peptide. The modification

can be at the side chain or in the back bone which would introduce conformational restrictions and stabilization towards proteaolytic degradation.

One approach is to replace proteinogenic amino acids locally and systematically with their corresponding Dd-variants, Cα-alkylated, Cβ-alkylated or *N*α-alkylated amino acids. As for an example, substitution of any one of native amino acid in a leu-enkephalin peptide (H-Tyr-Gly-Gly-Phe-Leu-OH) by an α-amino cycloalkane carboxylic acid(s) resulted in a peptidomimetic with greater *in vivo* activity (**Figure 4.1.A**).[9] Proline analogues are important for introducing strong conformational constraints to the peptide which favors the formation of β-turns over α-helix formation by virtue of N-Cα bond constraint (the φ angle). This has been exemplified in a peptidomimetic wherein Pro was replaced by 5,5-dimethylthiazolidine-4-carboxylic acid (Dtc) in angiotensin II, a key peptide in blood pressure regulation, and found to offer 39% greater agonist activity than the natural peptide (**Figure 4.1.B**).[10]

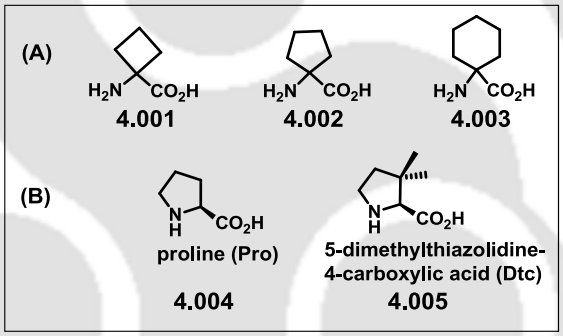

Figure 4.1. (A) α-Aminocycloalkane carboxylic acids and (B) 5,5-Dimethylthiazolidine-4-carboxylic acid (Dtc) as a proline analogue for peptidomimetics.

Other unnatural amino acids such as unsaturated, cyclic, β-amino acids, proline analogues and conformationally locked phenylalanine amino acid isosteres, introduction of dipeptide isosteres, retro-inverso isomeric moieties, double bond fragments and cyclic *cis*-amide bond isosteres also have been investigated to generate constrained peptide conformation (**Figure 4.2**).[11, 12-14]

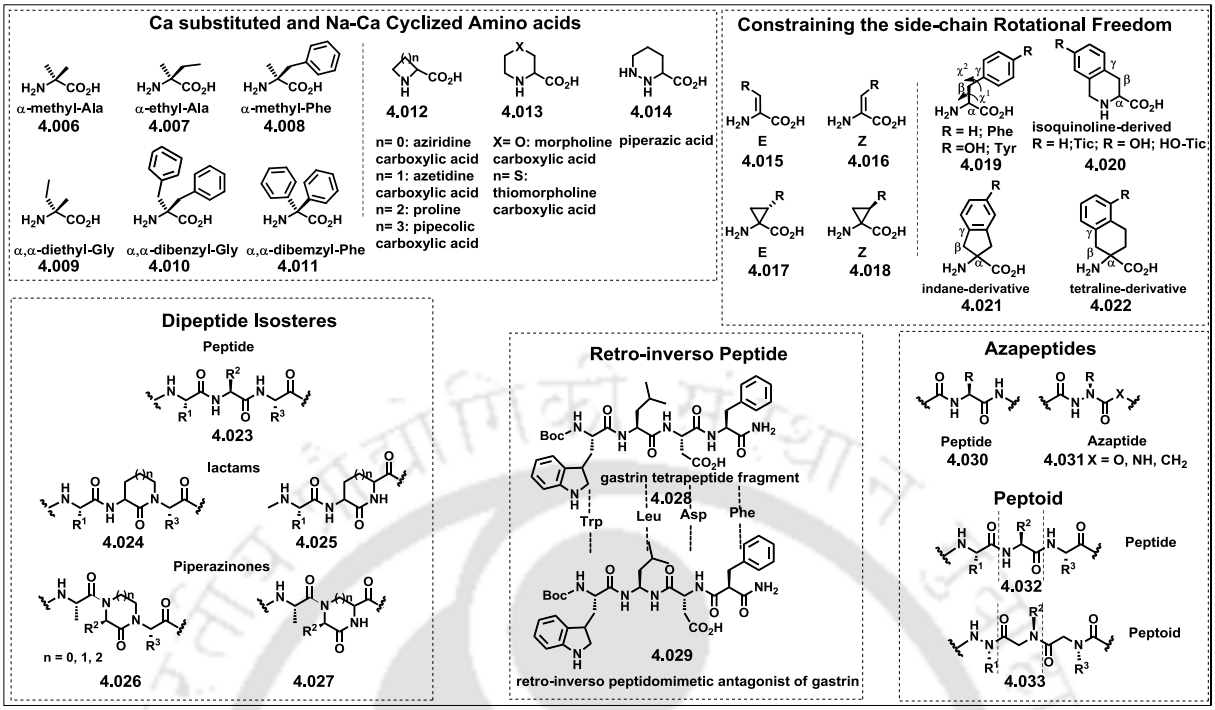

Figure 4.2. Examples of generation of constrained peptide conformation using various local constraints/novel amino acids.

(ii) ***Introduction of Isosteres/Bioisosteres of the Peptide Bond*: M**imicking the structural features of the peptide bond and modify the conformational profile and the hydrogen-bonding capability is another approach for backbone modification by replacing amide bond with isoelectronic chemical entity to improving the stability of the peptide *in vivo.*[15] 1 Such isoelectronic replacement was conceptualized first and the concept of isosterism between relatively simple chemical entities was originally contemplated by James Moir in 1909. He was the Irving Langmuir who in 1919 formulated isosterism and coined the term "isostere" based on experimental observations. In 1925, H.G. Grimm [3] extended the concept of isosterism, introduced by Langmuir, with his hydride displacement law.[16-18] Extending the earlier work conducted by Karl Landsteiner, Erlenmeyer[19] in 1932 redefined the term as atoms, ions or molecules in which the peripheral layers of electrons can be consider identical which is the origin of conceptualization of "bioisoteres", the term ultimately introduced by Harris Friedman in 1950 who defined it as compounds eliciting a similar biological effect if they fit the broadest definition for isosteres.[20].Later on in 1979, Thornber[21] extended the concept and defined the Bioisosters as Groups or molecules which have chemical and physical similarities producing broadly similar biological effects.

The development and application of bioisosteres have been adopted, in the contemporary practice of medicinal chemistry, as a fundamental tactical approach to address a number of aspects associated with the design and development of drug candidates.[16, 17, 22-23] The established utility of bioisosteres is broad in nature- (a) extending to improving potency, (b) enhancing selectivity, (c) altering physical properties, (d) reducing or redirecting metabolism, (e) eliminating or modifying toxicophores, and (f) acquiring novel intellectual property. Bioisosteres are also classified into two categories (a) classical bioisostere and (b) non-classical bioisostere.

The same concept was utilized in search of peptide based drug candidates, in peptidomimetics. Therefore, several amide bond isosteres have been proposed which that augments the conformational flexibility locally without altering the topology, modulates the hydrogen-bonding capabilities and enhances the stability against biodegradation. There exist a diverse range of amide bond isosteres which are given in **Figure 4.3**.

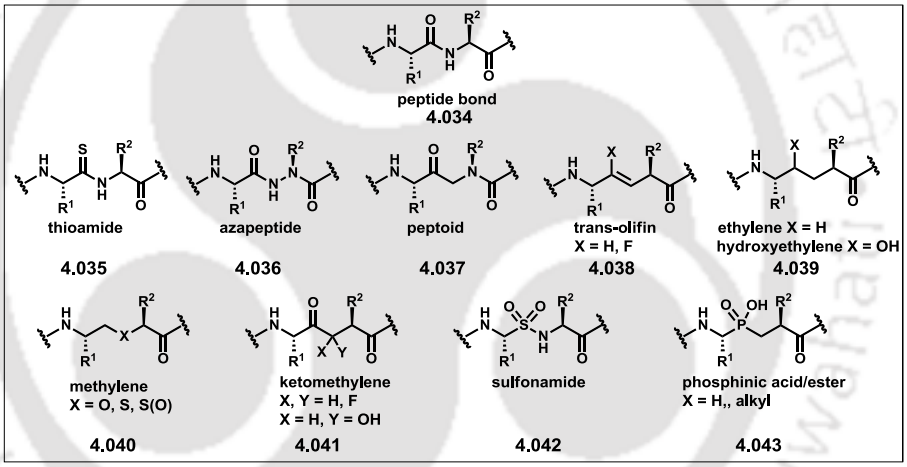

Figure 4.3. Bio isosteres of the peptide bond.

(i) ***Side-Chain Isosteres*:** Moreover, side-chain modifications have also been introduced to explore pharmacophoric steric and electronic interactions. The aim of introduction of local modifications around side-chains is mainly to modulate the conformational profile of the peptide. As for an example, guanidines are strongly basic which leads to poor membrane permeability of the peptides/proteins rich with arginine. Therefore, significant efforts have been devoted towards the development of isosteric replacements of guanidines with aim of reducing their basicity and maintaining key ionic interactions. As for an example arginine mimetics are conceived to reduce the basicity in order to enhance oral bioavailability.[24] Similarly, for acidic amino acids such as glutamate and aspartate, the mimetic design involves the replacements of side chain

carboxylic acid alone with their isosteres.[25] Some examples of both are depicted in **Figure 4.4** below.

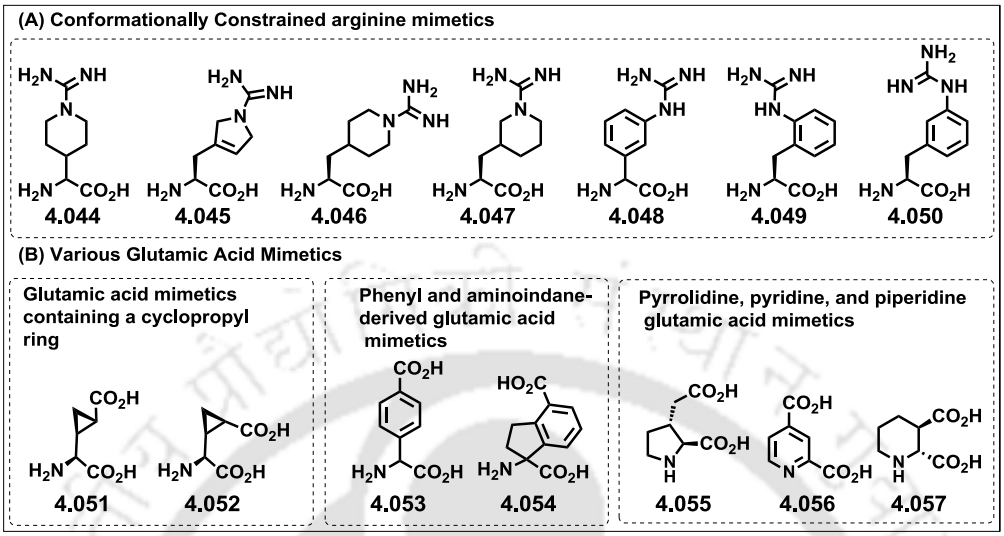

Figure 4.4. (A) Structures of conformationally constrained arginine mimetics and (B) various glutamic acid mimetics.

Peptidomimetic bioisosteres has been mainly applied for addressing local modifications of bioactive peptides by introducing isosteres (a) of the peptide bond, (b) of side chains and (c) chemical moieties resembling dipeptide motifs or tripeptide isosteres. This modification is a first-generation peptidomimetics generated from modifications that can allow important structure–activity relationship to be utilised to develop non-peptide peptidomimetics consisting of a central molecular entity containing suitable chemical appendages mimicking the pharmacophoric unit of original peptide bond responsible for biological activity. Such constraint small structural entity/molecules constitute a "subset of bioisosteres" and called molecular "scaffold" for peptidomimetics, incorpotation of which in the peptide backbone allow the peptide to adopt a particular desired conformation of peptide secondary structure such as β-sheet or β-turn.

4.3.2. Introduction of Global Restrictions

Much higher *in vivo* stability of a linear peptide could be achieved by imposing global restrictions into it by cyclization the advantage of which was also taken by Nature as can be revealed from the many biologically active macrocyclic peptides that are found in nature. As for an example, somatostatin is a macrocyclic peptide hormone, formed in the hypothalamus, which regulates the release of growth hormone.[26] The cyclic motif of the macrocyclic peptidomimetics offers an entropic

advantage over an acyclic peptide leading to enhanced binding selectivity with increased biological activity.

There are several strategies for cyclization according to the chemical moieties used for the introduction of the constraint utilizing either backbone or side chain

(a) **Cyclization between Backbone Elements**: This includes the followings-
   (i) **Backbone to Backbone**: This can be achieved (a) by tethering two amide nitrogen atoms with a linker and side-chains and/or (b) by introducing a chemical junction between a Cα and a nitrogen atom
   (ii) **Head to Backbone**: This can be done by linking a *N*-terminal amino group with an amide nitrogen atom with a spacer
   (iii) **Head-to-Tail**: By cyclizing the two *N*- and *C*-terminal ends of a peptidomimetic structure with an amide could lead to Head-to-Tail macrocyclic peptidomimetics.

(b) **Cyclization between Side Chain Elements**: This can be achieved by performing bond forming reaction among the two side chain functionalities (**Scheme 4.1**).

The most popular approach for the generation of a cyclic peptidomimetics is Cyclization between Side Chain Elements such as by exploiting (i) basic and amino acid residues, (ii) cysteine amino acids through disulfide bridges or (iii) ring closing metathesis.[27]

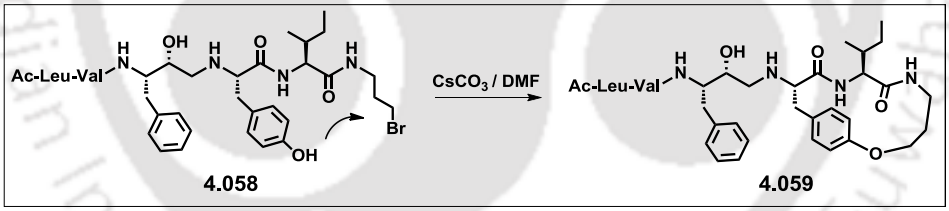

Scheme 4.1. Macrocyclic HIV-protease inhibitor generated through macrocyclisation between side chain and spacer unit at the C-terminal backbone.[28]

4.3.3. Molecular Scaffolds Mimicking the Peptidic Backbone: Peptidomimetic Scaffolds

An important development in peptide/peptide secondary structure mimicry has been the emergence of molecules that are analogues of peptide secondary structures and mainly present in the main-chain polyamide backbone. These small molecules are the non-peptide peptidomimetics consisting of a central molecular entity containing suitable chemical appendages mimicking the pharmacophoric unit of original peptide bond responsible for biological activity. Thus, a peptidomimetic compound/molecule is thought of as a small molecule mimicking the biological activity of a peptide although being no longer a peptide in chemical nature.[29] In generally, these molecules

do not contain any peptide bonds and possess a modular structure deriving from amino acids, carbohydrates or other types of building blocks. The ideal peptidomimetic molecules are those which possess (a) favorable pharmacokinetics properties for oral administration, (b) improved proteolytic stability and specificity with respect to the parent bioactive peptide. Such constraint small structural entity/molecules constitute a "subset of bioisosteres" replacing a peptide bond(s) and called molecular "peptidomimetic scaffold". The incorpotation of such scaffold in the peptide backbone allow the peptide to adopt a particular desired conformation of peptide secondary structure such as α-helix, β-sheet or β-turn.

Peptidomimetic scaffolds are basically developed according in two ways:(a) rational design approach based on structural information about the target or the biological activity of the parent peptide or conformational models of the parent peptide to ascertain the rationale for molecular recognition and (b) random screening method which relies on the random screening of wide arrays of small molecule mimetics of the parent bioactive peptide, followed by structural elaboration of hit compounds according to a rational approach based on available structural data. A combination of both approaches is the most successful route. A remarkable example of such a combined approach has been reported for the development of peptidomimetic ligands of the bradykinin receptor.[30]

In nature there are several secondary structures which are essential in protein function- α-helix, β- and γ-turn and, β-sheets. The goal of creating peptidomimetics of peptide secondary structures is a well-established approach in drug discovery aiming at fixing the bioactive conformations of a native peptide. This resulted in the development of peptidomimetic molecules of α-helix and β-sheet secondary structures, as well as in the design of a wide array of molecular scaffolds capable of replacing β- turns and loops, which are essential conformational components for peptides and proteins. Early examples of peptide secondary structure mimetics with designer scaffolds were reported by Hirschmann and Smith, who designed β-turn analogues based on sugar,[31] steroid,[32]or even catechol[33] backbones. Similarly, Hamilton[34-56] and others[37] used biphenyl,[37a] terphenyl,[38, 39] and related[40] scaffolds to mimic helices. Due to difficulties of protein folding in sheet structures, scaffolds that induce these β-sheet secondary structures are necessary in developing protein mimics. *Kemp* and co-workers displayed in 1988 the first induced β-sheet mimic by utilizing hydrogen bonding and the rigidity of proline to artificially construct a β-sheet structure.

In the previous chapter (**Chapter 3**), a more detailed discussion was provided in respect of *β*-turn secondary structure. Herein, a sort and selective report of constraints molecular scaffolds is presented which demonstrate β-turn mimetics or act as β-turn inducing scaffolds.

4.3.3.1. Molecular Scaffolds Mimicking/Inducing The β-Turns

As discussed, in the previous chapter, β-Turns are the most frequently mimicked protein secondary structures. It is the most prevalent turn motif found in proteins and is the four-residue β-turn, in which the *i* and *i* + 3 residues are hydrogen-bonded [41, 42–43]. The β-Turns are categorized based on the φ and ψ dihedral angles of the *i* + 1 and *i* + 2 amino acid residues, with the most common types being I, I′, II, and II′. An ideal mimic will have a rigid scaffold that can orient the side-chain residues in the same direction as the natural peptide thereby conferring better solubility and/or resistance to enzymatic degradation.

The generation of β-turn mimetics has been approached by two ways-(a) designing scaffolds that mimick the whole peptide motif (**4.061**) or (b) developing dipeptide isosteres capable of inducing a turn in a peptide motif (**4.062**). Furthermore, to stabilize *β*-turn structures, chemical tethers can be introduced as constraining elements within a (**4.063**) (**Figure 4.5**).

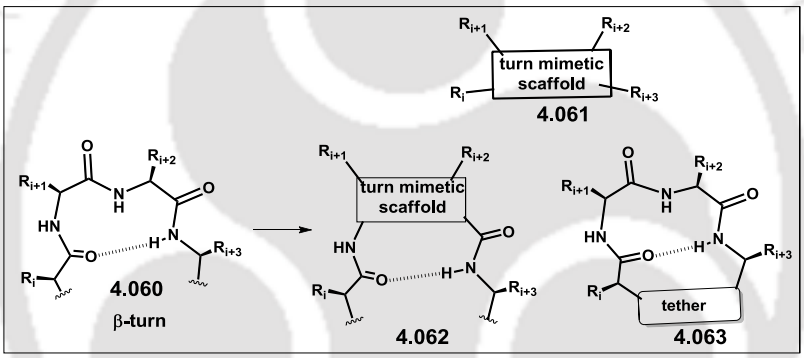

Figure 4.5. Approaches to β-turn mimetics.

The most popular approaches to reverse-turn peptidomimetics are based on the use of proline mimetics either at the *i*+1 or *i*+2 position to constrain a peptide conformation in a turn structure and to introduce δ-amino acids as dipeptide isosteres to replace the *i*+1−*i*+2 peptide moiety with a constrained scaffold.

4.3.3.1.1. ***Proline Analogues in β-Turn Peptidomimetics***: Proline (**4.064-4.065**) and lactam-bridged molecular scaffolds (**4.066**) generated from proline by introducing suitable constraint elements, were reported as a powerful β-turn mimetics.[44] Marshall *et al*. showed that the model peptides containing 2-azaproline (azPro) have a general tendency to prefer the type VI β-turn both in crystals and in organic solvents (**4.067-4.068**) (**Figure 4.6**).[45] A bicyclic α-amino acid scaffold, BGS, as turn inducers was reported which was incorporated at the *i*+1 position. The conformational study showed to adopt type II β-turn by the tetrapeptide containg BGS which was comparable to the conformation adopted by Val-d-Pro-Gly-Leu sequence as the reference peptide.[46] The prevalence of the *trans* isomer at the Val–BGS amide bond in the model tetrapeptide demonstrated that a BGS compound can mimic exactly the

trans-d-proline commonly found at the *i*+1 position of a type II β-turn. However, in a more competitive CD_3CN solution it showed a preference for a more compact structure described by a γ-turn stabilized by 7- and 11-membered ring hydrogen-bonds, and in equilibrium with a β-hairpin-like structure (**Figure 4.6**).

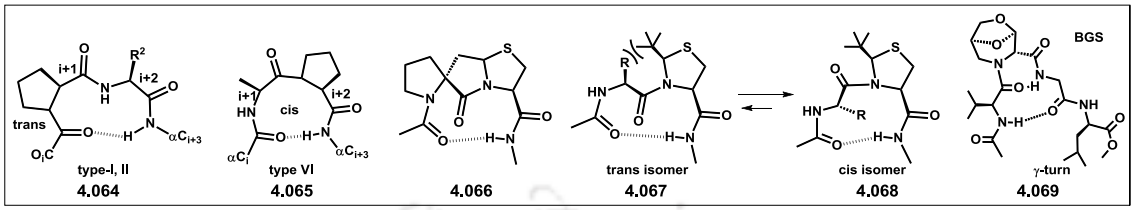

Figure 4.6. β-Turns mimitics with proline/proline derived molecular scaffolds.

Many types of scaffolds have been employed, spanning from bi- and tricyclic molecules to spirolactam structures, which aim to nucleate a reverse-turn, to maintain the ten-membered ring intramolecular hydrogen-bond, and also to introduce additional constraints to the system.[47, 48] Numerous mimics of β-turn substructures have been prepared over the past few decades, including those designed to act as folding nucleators.[49] Examples of other scaffolds include (a) δ-amino acid analogues in β-turn peptidomimetics, (b) biomolecular building blocks as scaffold for β-turn peptidomimetics some examples of all types are given below in **Figure 4.7**.

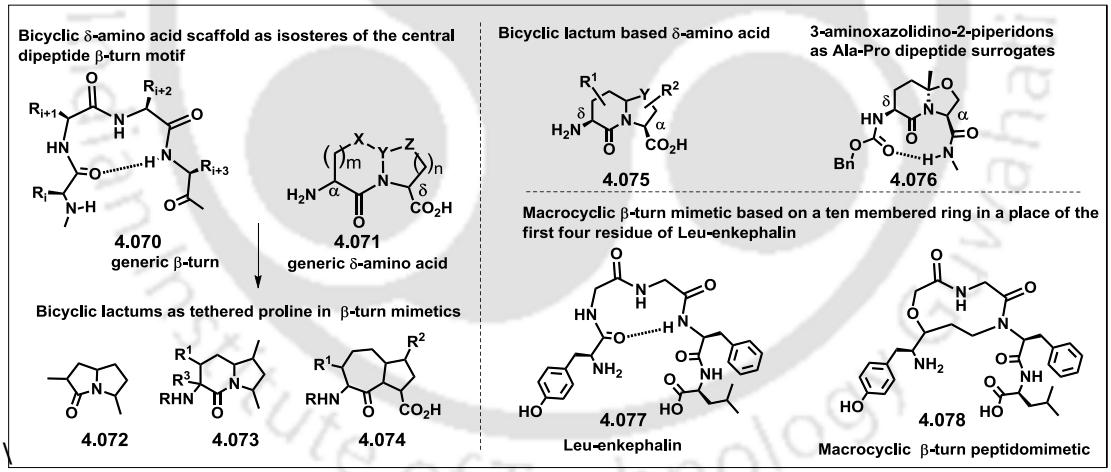

Figure 4.7. Several β-turn mimetics.

4.4. The Triazole Ring as a Peptidomimetic Scaffold

Controlling the Protein-protein interactions- the driving force behind biochemical pathways- is highly important to potential understanding of the mechanism of specific pathways as well as potential drug analogues that specifically can mediate how cell interactions proceed. Over the course of the evolution of life, nature has made the complex systems that we know today through a relatively small number, of small

molecules, which are used to create larger biological molecules.[50] In peptidomimetic chemistry, it is often found that biologically active peptidomimetics have turned out to be good drug candidates. These peptidomimetic molecules are usually have higher affinity for specific receptors, higher metabolically stablity towards endogenous protease, as well as greater oral bio-availability and more rapid excretion in contrast to their natural analogues.[51] Such conformationally restricted small peptidomimetic molecules i.e. scaffolds or dipeptide isosteres when functionalised with molecules of biological interest /short peptides would then show potential biological activity, conformational rigidity and found even more attractive than their natural or unfunctionalised analogues. As for an example the functionalisation of peptidomimetics with lipophilic or hydrophobic appendages may improve peptide-receptor affinity by interacting with hydrophobic or hydrophilic pockets. Moreover it is also possible to conjugate peptidomimetics scaffolds such as amino acids derived from natural or unnatural building blocks with peptide strands or other biologically active molecules to generate full peptide with desired secondary structures and may find more applicational/functional potentiality.[52]

A practical examples of application was demonstrated by C. Scolastico et al., by synthesising several 6,5- and 7,5-fused-2-oxo-1-azabicyclo[X.3.0] alkane amino acids which are regarded as conformationally restricted scaffold amino acid and Ala-Pro/Phe-Pro dipeptide isosteres. These amino acids present in peptide backbone showed efficient β-turn inducing potentiality. These amino acids scaffolds can be used to replace the central (i + 1 and i + 2) residue of β-turns.[53] Therefore, conjugating the peptidomimetic scaffolds or to synthesise them it is desirable to manipulating the reactions found in nature as well as to expand the chemical reaction toolbox. In this endeavor, it is beneficial to find diversified and biologically novel chemical reactions that are similar to those of nature in their simplicity and ability to fit the framework biological systems. "Click" chemistry is one such specific reaction that fulfills these demands. Among different available methodologies found in literature to assist the assembly of compounds/scaffold, peptidomimetic scaffold/bioconjugation, 'click chemistry', pioneered by Sharpless et al.[54] is highly versatile and has become increasingly popular for generating new chemical entities in medicinal chemistry, in bioconjugating strategies and in material chemistry. Of all the reactions meeting the requirements of 'click chemistry', the Huisgen 1,3-dipolar cycloaddition of alkynes and azides, also called Cu-catalysed azide-alkyne cycloaddition (CuAAC), to yield 1,2,3-triazoles is undoubtedly the most important example. The features of CuAAC and the triazoles ring and its applications are already described in **Chapter 3**, a summary of which in the present context is only pointed out herein. Specifically, CuAAC has several advantages in peptidomimetic chemistry:

(a) Triazole rings formed by CuAAC are often used as passive linker with excellent stability which makes it an attractive moiety to replace more labile

linkers in biologically active compounds.

(b) The triazole ring is planar and displays similar electronic con- tent and dipole moment as the amide bond.[55]

(c) It is considered to be a good non-classical bioisostere of the peptidic bond with an improved stability in biological systems (**Figure 4.8**).[56]

(d) It possesses an analogous H-bonding profile as an amide bond does. The C2 atom acts as H-bond donor, and N-4 and N-5 atoms as H-bonding acceptors with their lone pairs in a same way to the nitrogen and oxygen atoms of the amide bond, respectively.

(e) The ring can work as a peptidomimetic scaffold

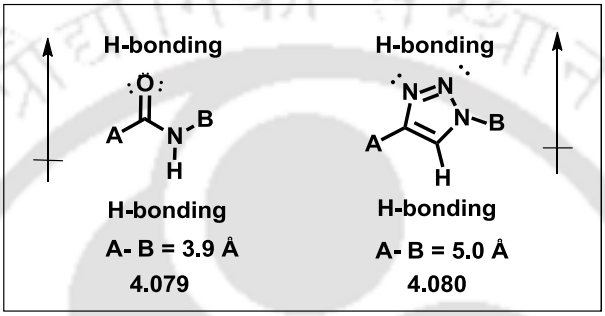

Figure 4.8. Bioisosteric relationship between triazole ring and the amide bond.

(f) The reaction is compatible with the side-chains of all the amino acids, at least in the protected form and is high yielding with few by-products.

Therefore, the CuAAC reaction has widely been utilized as a conjugation strategy in the design and synthesis of complex biomimetic architectures while triazole linkage replaces peptide and phosphodiester bonds. Moreover, several reports demonstrated that 1,2,3-triazoles can be used as surrogates for biologically relevant amide bonds. Few selected examples of triazole-containing peptidomimetics are highlighted below.

4.4.1. Triazole-Containing Peptidomimetics

Triazoles as Amide Bond Isosteres in Macrocyclic Peptidomimetics: Constraining bioactive oligomers via macrocyclisation is an important strategy to reduce conformational flexibility, and render potential interaction in the binding site by preorganizing side-chain pharmacophores into optimal orientations. Cyclic peptides are thus generated via CuAAC reaction which showed high conformational stability, enhanced proteolytic resistance and ability to display protein-like epitopes. Thus, these peptides could be a potentially valuable class of therapeutic agents (**Figure 4.9**).

McAlpine et al. reported a cyclic sansalvamide A peptidomimetics by embedding a triazole heterocycles by replacing the Leu-Val amide bond (**Figure 4.9a**).[57] This constraint triazolo sansalvamide A exhibited similar cytotoxicity which is an example

of modulation of the pharmacological profile of a lead compound via CuAAC.

In connection to the synthesis of cyclic peptide-based tyrosinase inhibitors, cyclisation of peptides consisting of Tyr-Pro-Val-Pro sequences were difficult. However, 'click chemistry' has been adopted by many researchers to circumvent this issue were able to synthesise cyclic Tyr-Pro-Val-Pro tetramers incorporating a triazole ring within the peptide backbone (**Figure 4.9b**).[58] The triazole analogue of tyrosinase inhibitor showed a threefold increase in tyrosinase inhibitory activity relative to the natural peptide product.

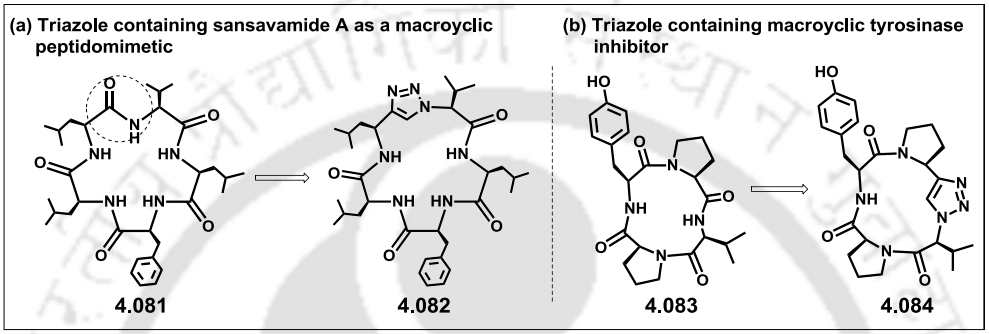

Figure 4.9. Triazoles as amide bond isosteres in macrocyclic peptidomimetics-(a) Triazole-containing sansalvamide A as a macrocyclic peptidomimetic and (b) Triazole-containing macrocyclic tyrosinase inhibitor.

Triazoles as Amide Bond Isosteres in Linear Peptidomimetics-HIV Protease Inhibitors: Wong, et al., reported an important application of CuAAC for the development of triazole-based HIV protease inhibitors.[59] They adopted the strategy of replacing of the amide bond of central peptide substrate with the triazole ring as the isostere. Interestingly, the triazole-based peptidomimetic displayed inhibition towards the HIV protease possessing IC_{50} and K_i values in the nanomolar range. The central nitrogen of the triazole unit showed a hydrogen-bond with the water molecule similar to what is generally observed under the protease flaps. This water molecule also formed a hydrogen-bond with the sulfonamide similar to what is seen in the crystallographic structure of amprenavir when bound to HIV-1 protease. Therefore the triazole inhibitor showed an interesting peptidomimetic inhibition profile as compared to the reference inhibitor (**Figure 4.10**).

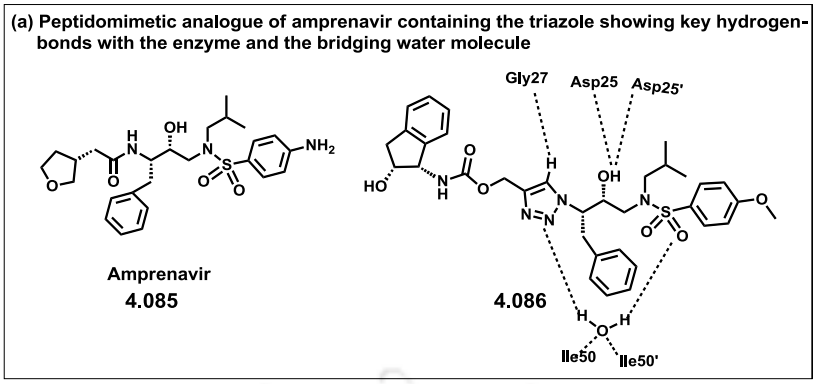

Figure 4.10. (a) Peptidomimetic analogue of amprenavir containing the 1,2,3-triazole as amide bond isostere in the central unit.

***Triazoles as Side chain-Side chain Lock in Macrocyclic Peptidomimetics*:** A conformationally constrained macrocyclic compound as STAT3 (signal transducers and activators of transcription 3) inhibitor was synthesised via intramolecular 'click chemistry' by Wang and coworkers (**Figure 4.11**).[60]

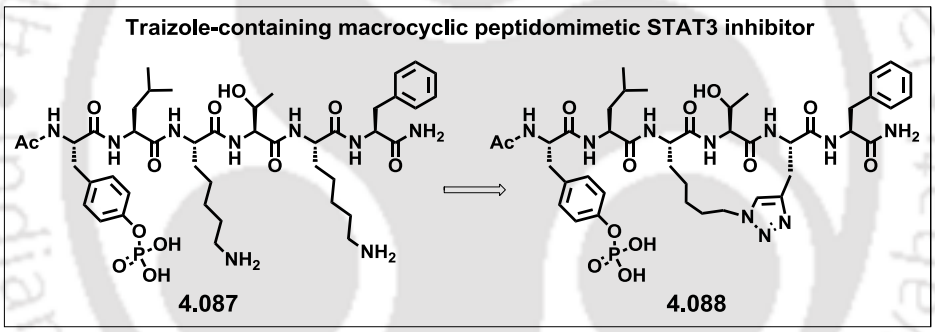

Figure 4.11. Traizole-containing macrocyclic peptidomimetic STAT3 inhibitor.

4.4.2. Triazoles as β-Turn Inducers (a Small Molecule Scaffold/Dipeptide Isosteres/Dipeptide Mimic) in Secondary Structures

In Short Acyclic Peptide: Ghadiri et al. demonstrated that triazole units can be used as dipeptide isosteres with minimal consequence to the overall peptide secondary structure.[61a] To utilize this property triazole scaffold was exploited as an isostere addressing the overall structural features of -Pro-Gly- sequences in some β-turns. Thus, Guan et al. utilized this strategy to conjugate two peptide strands derivatized with terminal alkynes and azides, respectively, so as to generate triazole linked peptides.[61b] Elucidation of the structural properties of peptides containing a single triazole unit revealed a β-turn structure and was concluded that the triazole unit as a reverse turn inducer. However, they indicated that for facilitating proper folding into the β-turn structure three methylene units on either side of the triazole moiety are required (**Figure 4.12**).

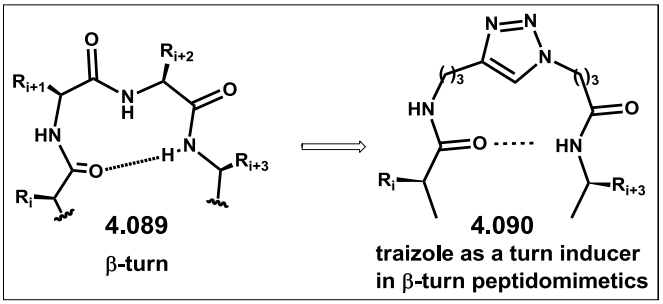

Figure 4.12. Comparison between a β-turn and β-turn peptidomimetics containing the triazole ring connecting the two peptide β-strands.

This short turn motif was successively applied in the generation of higher structures. Specifically, Liu et al. utilized CuAAC-based polymerization[62] using CuAAc as a catalyst to ligate block-peptide sequences. This strategy allowed the triazole unit at either end of the fibrils to induce β-turn mimetics and inducing the peptide sequences to fold into antiparallel β-strands, ultimately resulting in the organization of the overall structure in higher order nanofibrils.

In Macrocyclic Peptides: Burgess *al*.[63] *et* used the CuAAC to form cyclic peptide derivatives from linear peptide substrates. They showed that tethering the triazole unit β-turn structures become highly stabilize as demonstrated by computational, nuclear magnetic resonance (NMR) and circular dichroism (CD) analyses. Their study revealed that the triazole was able to nucleate the cyclic peptide in to adopt type I and type II β-turn conformations (**Figure 4.13**).

A similar approach of using 'click chemistry' to tether a peptide moiety into a macrocyclic structure was applied by Wan et al.[64] A very few reports exist showing the specific application of the triazole ring in the RGD moiety, both (a) as a turn mimetic constraint and (b) as a scaffold in non-peptide RGD peptidomimetics containing Arg and Asp side-chain isosteres. Thus, Pan and his colleagues[64] utilized the triazole ring as an amino acid replacement to achieve a cyclic RGD tripeptide, cyclo[-Arg-Gly-Asp-(triazole)-Gly-Xaa-] via 'click chemistry' (**Figure 4.13b**). Finally, a study of cytotoxic effect on different human endothelial and carcinoma cell lines by these cyclopeptides differing by the Xaa amino acid was evaluated indicating cytotoxic activity in the sub-micromolar range for several peptides of this class, and similarly to the very well known ligand *c*[RGDfK].

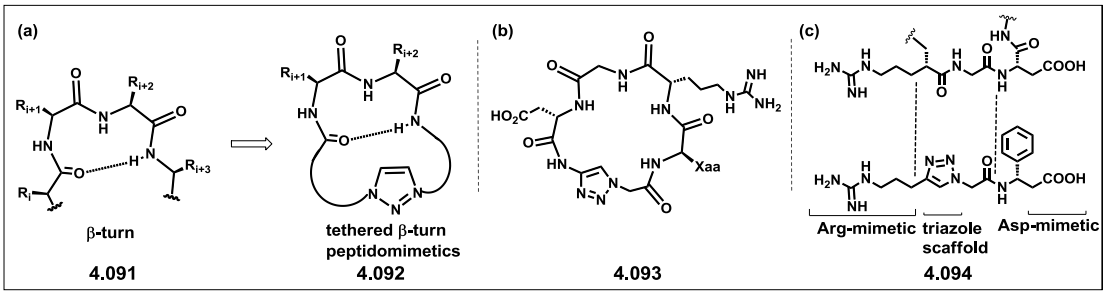

Figure 4.13. (a) The triazole ring as the inducer/scaffold for macrocyclic β-turn peptidomimetics (b) Cyclic RGD peptidomimetic with the triazole ring as a turn-inducing element.[65] (b) Triazole-scaffolded RGD peptidomimetic with the isosteric replacements for the amino acids.

Recently, Guarna et al., utilized the CuAAC click chemistry reaction to generate linear RGD peptidomimetics containing the triazole ring as the scaffold to attach the arginine and aspartic acid side-chain isosteres.[66] In the design, the position of the triazole in the linear peptidomimetic was found to be crucial to attain a judicious presentation of both Arg and Asp isosteres and also to address additional hydrophobic contacts within the active site of the receptor. Biological assays showed this RGD peptidomimetic capable of binding αvβ3 integrin with nanomolar affinity according to a two-site model (**Figure 4.13c**).

In 2013, James group reported copper-tris(triazole) ligand catalyzed click mediated cyclic tetrapeptide. They have synthesized a series of β-turn cyclic tetrapeptide with high yield and got the crystal structure of several synthesized peptide (**Figure 4.14**). The crystallographic study clearly showed the existing of intramolecular hydrogen bonding between carbonyl of phenyl alanine at *i* and NH of glycine at *i*+3 that formed *β*- turn secondary structure. The two hydrogen bonds were existed in compound **4.096**, one of them involved with triazole N-atom. This structural conformation also supported by 1D, 2D (ROSEY spectrum) and variable temperature (VT)- ^{1}H NMR spectroscopy.[67]

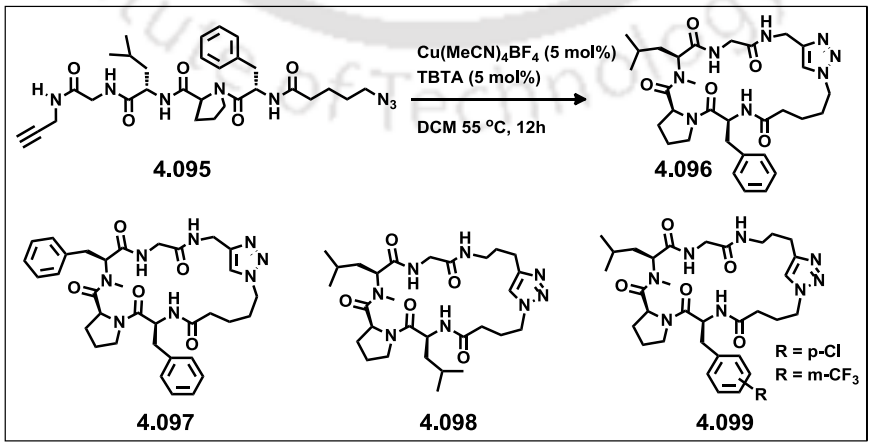

Figure 4.14. Copper catalyzed synthesis of β-turn cyclic tetrapeptide.

4.5. Background

Introduction of conformationally constrained nonpeptide isosteres into peptide backbones in order to achieve desirable secondary structures along with pharmacologically viable peptide-based drug candidates of enhanced metabolic stability is of great interest in recent time. Among the various secondary structures, *β*-turns are important targets for mimicry, both because they serve as recognition sites in peptides and proteins as well as they allow a protein chain to fold back upon itself to form compact structures. Now a days scientist are able to increase the stability and constraint of peptide or protein structure by incorporating molecular scaffold through replacing amide bond. Different types of approaches have been applied for backbone modification like as replacing non-natural amino acid, cyclisation, terminal protection etc. From literature it is clear that, the click reaction product 1, 2, 3 triazole and amide bond of peptide both have more or less same size, polarity and hydrogen bonding capability and unlike stability. The CuAAC has gained high popularity due to the ease of synthesis and high regioselectivity and compatibility with aqueous conditions. The attractive structural feature of triazolyl unit permitted several applications as a peptidomimetic building block as turn inducer and amide bond isosteres to create better structural property and functional potentiality.

4.6. Objective

Our continuous research effort on the design of unnatural biomolecular building blocks via click chemistry and β-turn peptidomimetics and the recent advancement on the design of conformationally constrained small molecular scaffold for peptidomimetics prompted us to relook into the rigid framework of pseudo-aromatic triazole unit. A comparison of the backbone bonds and the dihedral angles of the dipeptide isostere **4.100** (**^{Al}TAA**) with those of a natural dipeptide showed that the triazole unit of **4.100** fixes the ω_i (*trans*-amide bond) and ϕ_{i+1} angles at about 180^o and it had "free rotation" about the ϕ_i, ψ_i, and ψ_{i+1} and θ angles. Accordingly, peptidomimetic **4.100** could be used to replace two adjacent amino acids (Gly-β^3Ala) having conformational restriction at ω_i and ϕ_{i+1} angle (**Figure 4.15**). We observed that a designed triazolo amino acid with constrained backbone angles ω(i) and ϕ(i+1), would expected to induce folded conformations in linear peptides. Moreover, the triazole unit is metabolically inert, can easily associate with biological targets, act as *trans*-amide mimetics and tolerate various reactions conditions used in peptide synthesis.[68] Though the click chemistry has been utilised in mimicking protein's secondary structures, to the best of our knowledge, the triazolo amino acid as a scaffold has not been explored. We envisioned that upon incorporation into a backbone a linear peptide might adopt β-turn conformation. This is again obvious if we could incorporate **^{Al}TAA** into Leu-enkephalin by replacing its Gly-Gly dipeptide

segment that is known to be flexible and amenable to different conformations depending on the binding environment.

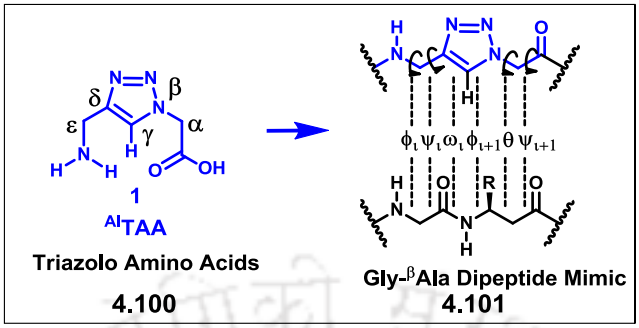

Figure 4.15. Dihedral angle relationship between scaffold amino acid **^{Al}TAA** and Gly-βAla dipeptide representing scaffold as a dipeptide mimetic.

With this background and concept we focused on the following objectives as follows:

(a) Synthesis of triazolo-β-aza-ε-amino acid, **^{Al}TAA** (**4.100**)

(b) Study of its effect on the structural properties of linear peptide, a Leu-enkephalin analogue, (**4.102**) wherein the scaffold present in the peptide backbone.

(c) Synthesis of a model fluorescent pentapeptide **4.103**, (Boc-**^{TPy}Ala^{Do}**-Leu-**^{Al}TAA**-Leu-**^{TPhen}Ala^{Do}**-CO_2Me), wherein two fluorescent unnatural triazolo amino acids, (**^{TPy}Ala^{Do}** and **^{TPhen}Ala^{Do}**), are at the two arms of the scaffold via an intervening leucine in each arm.

(d) Study of fluorescent photophysics of the pentapeptide and photophysical interaction, if at all, among the terminal fluorescent amino acids.

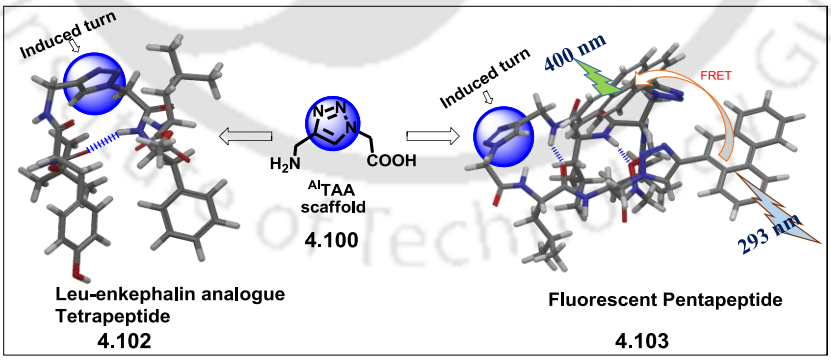

Figure 4.16. Structure of scaffold Amino acid **4.100** and the peptides (**4.102** and **4.103**) and conceptual FRET process in the pentapeptide **4.103.**

4.7. Result and Discussion

4.7.1. Synthesis of Aliphatic Triazolyl Amino Acid Scaffold (4.100, ^{Al}TAA) and Corresponding Peptides

Synthesis of aliphatic triazolyl amino acid scaffold is based on Cu(I) catalyzed click chemistry. For the synthesis of aliphatic triazolyl amino acid, we first synthesized ethyl azidoacetate (**4.105**) from ethyl bromoacetate (**4.104**) using NaN_3 in water/aceton (1:3) solvent mixture under 60 ^oC. The synthesized ethyl azidoacetate, **4.105** undergoes cycloaddition reaction with propargyl alcohol under click reaction condition and produced corresponding triazolyl alcohol (**4.106**) which was converted to mesylate derivative (**4.107**) in presence of triethyl amine and mesyl chloride under 0 ^oC in dry DCM solvent. Then it was treated with NaN_3 under dry DMF solvent at 50 ^oC to afford azido derivative of triazolyl scaffold (**4.108**). Lithium hydroxide mediated hydrolysis of ethyl ester followed by the reduction of azide under Pd/C and hydrogen atmosphere in dry methanol solvent afforded the unnatural triazolyl amino acid, **4.100, ^{Al}TAA**. Boc-protection of synthesized scaffold using Boc-anhydried in dioxane–water system finally yielded the BocNH-triazoly amino acid scaffold **(4.110, ^{Al}TAA)** (**Scheme 4.2**).

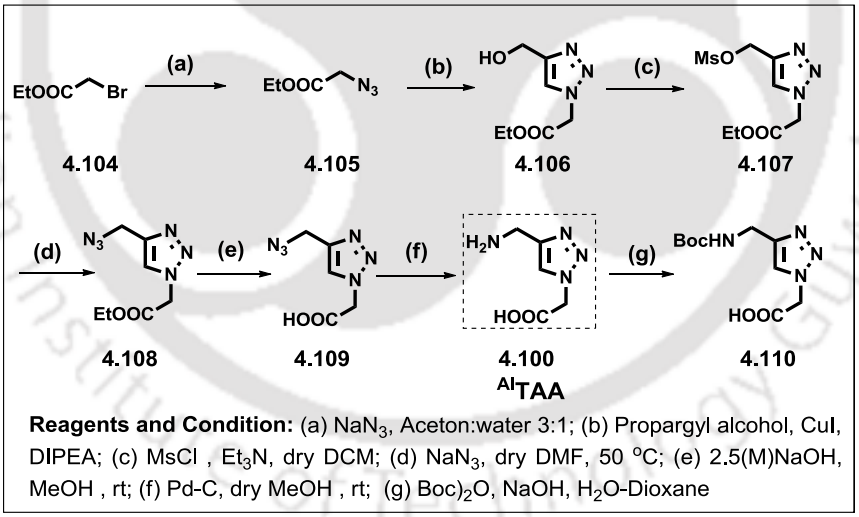

Scheme 4.2. Synthesis of aliphatic triazoly amino acid scaffold **(4.100, ^{Al}TAA)**.

To explore the constrained properties of the scaffold **4.100**, we, next, incorporated it into a linear Leu-enkephalin analogue peptide **4.102** and a designed pentapeptide, containing two of our triazolyl fluorescent UAAs into two termini (**4.103**) (**Figure 4.16**). All the peptides were synthesized by a solution phase peptide coupling protocol. The synthetic protocol is shown in **Scheme 4.3-4.4**. Thus, to synthesize Leu-enkephaline analogue peptidomimetics **4.102**, at first we synthesized dipeptide (**4.113**) of phenyl alanine and leucine using EDC.HCl and HOBt mediated coupling

method. Next, dipeptide **4.113** was treated with TFA:DCM (1:1) at 0 ^{o}C- r.t for about 1 hour to obtain Boc-deprotected dipeptide **4.114** which was then coupled with N-Boc protected aliphatic triazolyl amino acid scaffold **4.110** following EDC.HCl/DMAP mediated peptide coupling protocol to afford tripeptide **4.115**. A second round of peptide coupling between the Boc-deprotected tripeptide (**4.116**) and N-Boc-tyrosine yielded our target Leu-enkephaline analogue tetrapeptide **4.102** (**Scheme 4.3**).

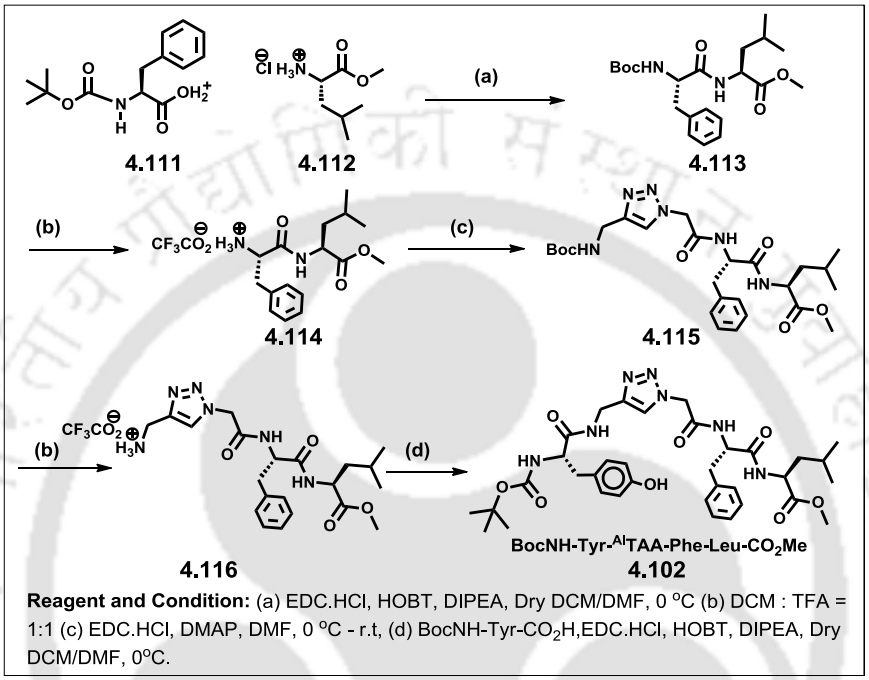

Scheme 4.3. Synthetic procedure of triazolyl aliphatic amino acid scaffold based Leu-enkephalin mimetic tetrapeptide **4.102 (**BocNH-Tyr-^{Al}**TAA**-Phe-Leu-CO_2Me**).**

Next, the fluorescent pentapeptide **4.103** was synthesized in a similar via the coupling of Boc-deprotected tripeptide (TFA.NH_3-^{Al}**TAA**-Lue-^{TPhen}**Ala**^{Do}-CO(NMe)OMe, **4.123**), and N-Boc-protected dipeptide (BocNH-^{TPy}**Ala**^{Do}-Leu-CO_2H, **4.125**), containing unnatural fluorescent triazolyl amino acids [^{TPhen}**Ala**^{Do} and ^{TPy}**Ala**^{Do}, respectively] wherein the scaffold ^{Al}**TAA** (**4.100**) was placed in the middle of the peptide backbone (**Scheme 4.4**). Synthetic procedure of fluorescent triazolyl dipeptide derivatives was discussed in **Chapter 3** (**Section 3.7.1**).

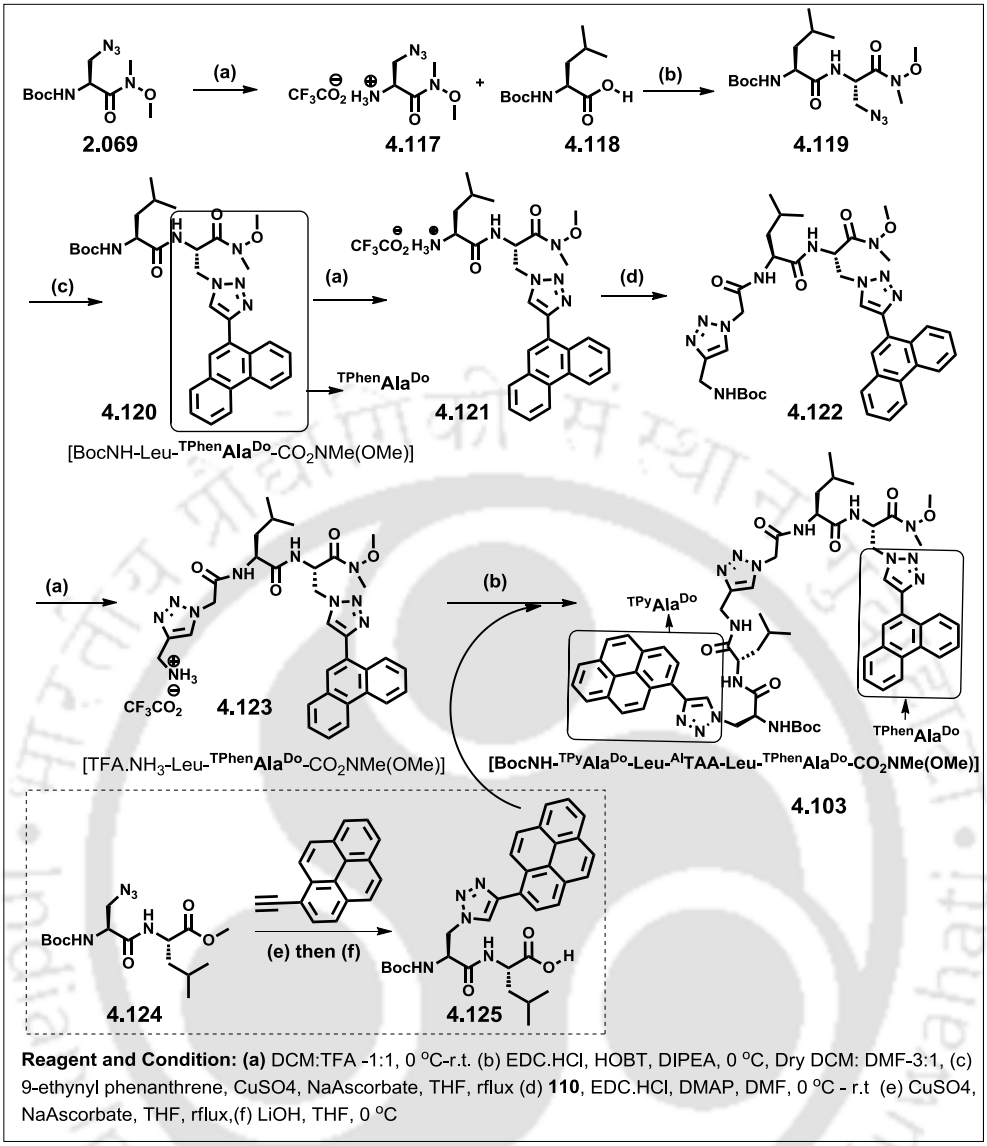

Scheme 4.4. Synthetic scheme of aliphatic triazolyl amino acid scaffold based unnatural pentapeptide **4.103 [**BocNH-^{TPy}**Ala**^{Do}-Leu-^{Al}**TAA**-Leu-^{TPhen}**Ala**^{Do}-CO_2NMe(OMe**)].**

All the intermediate peptides and final peptides were purified by silica-gel (60-120 mesh) column chromatography and characterized by both 1D and 2D NMR, IR, and HR-mass spectrometry. After getting our target peptides in pure form in hand, we, next, studied their secondary structure using various spectroscopic techniques.

4.7.2. Spectral Characterization of the Synthesized Peptides

The synthesized peptides **4.102** and **4.103** in the fully protected form were characterized mainly by NMR spectroscopy. For peptide **4.102** (Boc-NH-Tyr-^{Al}**TAA**-Phe-Lue-CO_2Me), the triazolyl hydrogen appeared as a singlet at δ 7.33. The C-α hydrogens of tyrosine, phenyl alanine resonated as a broad singlet (bs) at δ 4.59, 4.38, respectively, and leucine as multiplate at δ 4.01. The β-CH_2 hydrogens of tyrosine, phenyl alanine and leucine units appeared as a broad singlet (bs) at δ 2.81 and multiplate at δ 3.03, 1.58, respectively. The γ and δ hydrogens of leucine unit appeared as a multiplate at δ 1.50 and doublet at δ 0.85 with coupling constant of δ hydrogen J = 7.2 Hz. The ^{t}Bu-hydrogens of Boc-protected group appeared as a singlet at δ 1.36. The methyl hydrogens of OMe group also resonated as a singlet at δ 3.61. The N-and C-terminal CH_2 hydrogens of scaffold ^{Al}**TAA** appeared as a quartet at δ 5.03 with coupling constant 15.0 Hz and as a broad singlet at δ 4.30, respectively. The C-2, C-3, C-4 and C-5 aromatic hydrogens of tyrosine appeared as a doublet at δ 7.09, 6.61, 7.01 and 6.69 with coupling constants J = 5.4, 6.6, 6.6 and 4.8 Hz respectively. The aromatic hydrogens of phenyl alanine unit resonated as a singlet at δ 7.25. The hydrogens of N-1, N-2, N-3 and N-4 appeared as a doublet at δ 6.92, 5.03, 8.52 and 8.6 with coupling constant J = 7.2, 7.8, 4.8 and 7.2 Hz, respectively. The structural assignment of tetra peptides **4.102** is shown in **Figure 4.17a**.

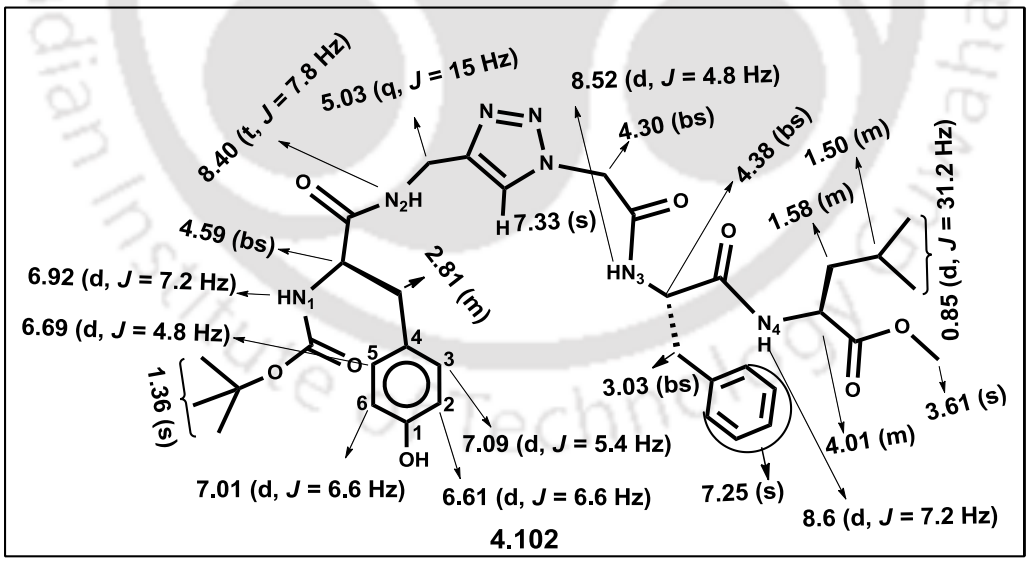

Figure 4.17a. ^{1}H NMR assignment of tetrapeptide **4.102.**

The chemical shift assignment for the fluorescent pentapeptide **4.103** is shown in **Figure 4.17b**. The detailed assignments are given in the experimental section.

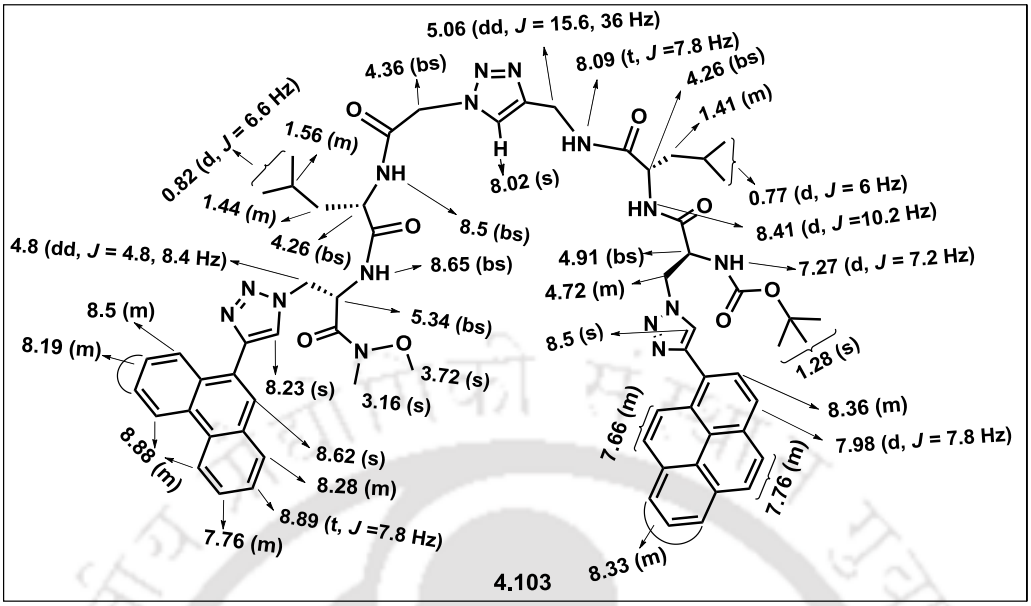

Figure 4.17b. ^{1}H NMR assignment of pentapeptide **4.103.**

4.7.3. Study of Conformation of Peptides 4.102 and 4.103 Using CD, IR, NMR, Spectroscopic Techniques and Macromodel Calculation

Study of Circular Dichroism Spectroscopy: The secondary structure of tetrapeptide **4.102**, a Leu-enkephalin analogue, was estimated by recording its CD spectrum in methanol **(**60 µM concentration), which showed a strong positive band at 206 nm and a negative band at 191 nm indicating a type II β-turn conformation.[69] Moreover, the signature of aromatic π-π stacking interaction between Phe and Tyr in peptide **4.102** was also evident from the appearance of a positive band at 217 nm. The estimation of the secondary structure of the peptide using CD estima program showed 100% β-turn structure in peptide **4.102**, the existence of which implied the possible presence of intramolecular H-bonds between the peptide strands. The fluorescent pentapeptide **4.103** also exhibited a strong positive band at 207 nm and a negative band at 193 nm indicating a predominantly type II β-turn conformation (**Figure 4.18**).[69] The positive bands at 308 and 350 nm indicated the absorption due to the fluorescent triazolyl phenanthrene and pyrene respectively, amino acids. The β-turn structure in the peptides indicated the presence of intramolecular back bone H-bonds between CO_i and NH_{i+3} residues.

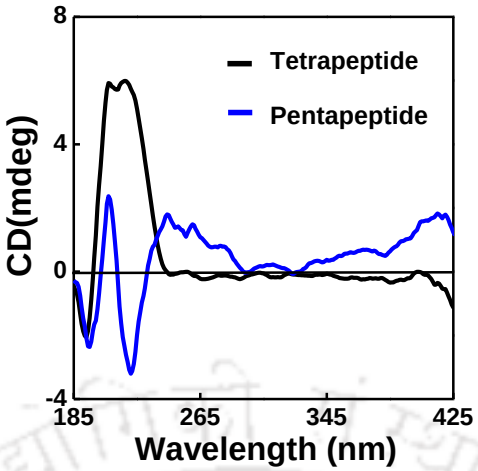

Figure 4.18. CD spectra of peptides **4.102** and **4.103** in methanol solvent **(**60 µM concentration).

Probing the Intramolecular H-Bonding: Study of FT-IR Spectroscopy: To probe the intramolecular H-bonding, IR spectroscopic technique was utilized. Thus, IR spectra were recorded using dry KBr with solid and dry compound. The IR spectrum showed the presence of intramolecular H-bonded and free amide -NH stretching absorptions at 3281-3314 and 3409-3440 cm^{-1}, respectively, for all the peptides supporting β-turn structure.[70] The IR spectrum of peptide **4.102** displayed a sharp N-H stretching absorption at $\tilde{\nu}$ =3314 cm^{-1}, C=O stretching at $\tilde{\nu}$=1658 cm^{-1}, and N-H bending and C-N stretching at $\tilde{\nu}$ = 1517 cm^{-1}, which were independent of the sample concentration. Similar concentration independent IR absorptions were observed for peptide **4.103**. These results confirmed the presence of intramolecular H-bonds in both the peptides **4.102** and **4.103**.[70b]

Probing the Intramolecular H-Bonding: Study of Variable Temperature ^{1}H NMR (VT-NMR): The presence of intramolecular H-bonds was next assessed by determining the variation of chemical shifts of the various NHs with temperature (**Figure 4.19**), in d_6-DMSO in which all NHs exhibited different chemical shifts. From the VT-NMR experiment, strong intramolecular H-bonding involving the amide NH (of Phe) at i+3 was observed in peptide **4.102**, wherein the temperature coefficient of the chemical shift ($\Delta\delta/\Delta T$) was found to be medium to close to Kessler limit supporting the type II β-turn structure (**Figure 4.19a, Table 4.1**).[71]

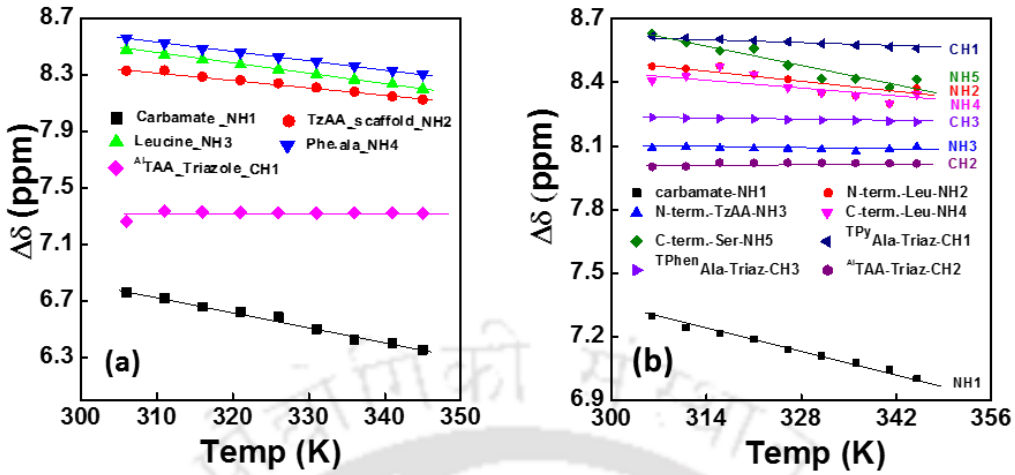

Figure 4.19. Temperature dependence of NH chemical shift of (**a**) tetrapeptide **4.102** and (**b**) pentapeptide **4.103.**

Table 4.1. Values of NH/CH chemical shifts with temperature for tetrapeptide **4.102** and **4.103**

Kessler limit (Δ*δ*/ΔT) ppb/k			
Tetrapeptide **4.102**		Pentapeptide **4.103**	
Carbamate N-H1	- 9.1	Carbamate N-H1	-7.23
^{Al}**TAA**-scaffold-N-H2	- 5.5	N-terminal-Leu-N-H2	- 4.33
C-terminal Phe-N-H3	- 6.43	^{Al}**TAA**- scaffold -N-H3	- 0.363
C-terminal-Leu-N-H4	-7.03	C-terminal -Leu-N-H4	-3.43
^{Al}**TAA**- Triazole-C-H	0.0005	C-terminal-Ser-N-H5	-6.45
----	----	^{TPy}**Ala**-Triaz-C-H2	-1.47
----	----	^{TPhen}**Al** -Triaz-C-H3	-0.506

In pentapeptide **4.103**, The Triazole C-H (^{TPy}**Ala**) of N-terminal amino acid also exhibited temperature effect. All the amide NH's, and triazole C-H exhibited (Δ*δ*/ΔT) values that are moderate to close to Kessler limit of -3 to -6 ppb/K indicating presence of strong to moderate intramolecular H-bonding and supported the predominant turn like structure of the peptide (**Figure 4.19b, Table 4.1**).

Solution Conformational Analysis using 2D NMR Experiment: Next, the solution conformations of β-turn peptides **4.102-4.103**, were determined by studying, in detail, their 2D ^{1}H NMR spectra in DMSO-d_6. ^{1}H-^{1}H TOCSY (Total Correlated Spectroscopy) is useful for dividing the proton signals into groups or coupling. So, TOCSY experiment was carried out in d_6-DMSO for both the tetrapeptide (**4.102**) and pentapeptide (**4.103**) to identify various NH's protons and triazole CH's. From the coupling of side chain protons of tetrapeptide **4.102** in ^{1}H NMR spectra it was observed that the Leu-side chain was very rigid and adopted predominantly one single

conformation about χ_1 and χ_2 with an anti-relationship between βH(pro-S) and γH. Strong ROESY interaction between Leuβ-H/CH2(C-terminal) of the scaffold also supported this observation. The cross peak in the ROESY spectrum between LeuCαH and LeuδCH3(pro-S) provided additional evidence of the rigidity of the Leu side-chain. The Phe and Tyr-side chains also showed their rigidity as well as the presence of one single conformation about χ_1. The NOESY and ROESY spectra of peptide **4.102** revealed the interactions among the aromatic hydrogens of Tyr and Phe. Long-range ROESY cross-peaks among Tyrβ-H/Phe-ArH; Triazole-CH/Tyrβ-H, Pheβ-H, Tyr-ArH; and Pheβ-H/Tyr-ArH suggested the close proximity of Tyr and Phe as well as their rigidity in one single conformation in tetrapeptide **4.102**. The presence of NOESY cross peak between $H_\alpha(i^{th})$/NH (i+1) also revealed a type-II β-turn conformation (**Figure 4.20a**). The NOESY and ROESY spectra of pentapeptide **4.103** showed the interaction between H_α (of ^{TPy}**Ala**^{Do})/OMe-H (of ^{TPhen}**Ala**$_{Do}$); ^{TPy}**Ar**-H (of ^{TPy}**Ala**$_{Do}$)/$CH_{2(N\text{-terminal})}$ of the scaffold, triazole-CH, $LeuNH_{(C\text{-terminal})}$; and $CH2_{(N\text{-terminal})}$ of the scaffold/$LeuNH_{(C\text{-terminal})}$, which supported the turn structure with the pyrene moiety inside the loop closer to the triazole unit of the scaffold (**Figure 4.20b**).

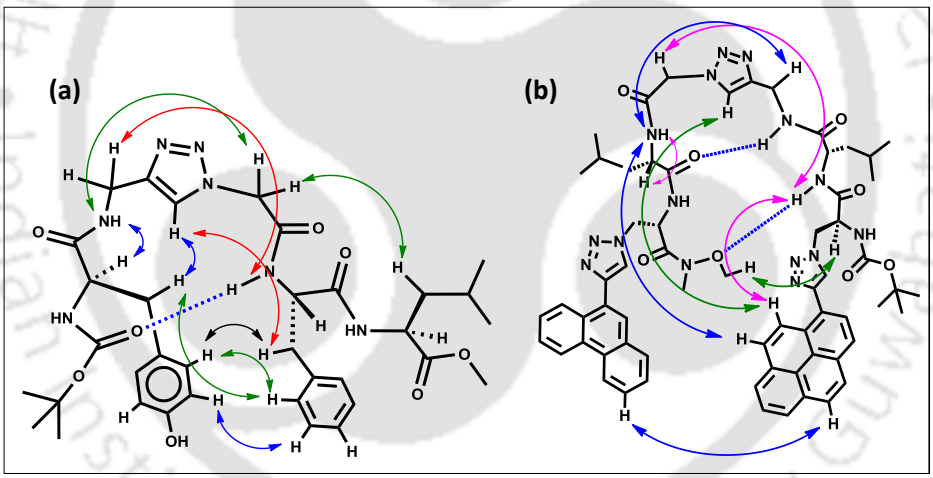

Figure 4.20. Pictorially presentation of long range proton-proton interaction of tetrapeptide **4.102** (a) and pentapeptide **4.103** (b) as evident from 2D NMR.

Conformational Analysis Using Macromodel Study: Geometry Optimisation: Molecular modeling study of the peptides is carried out using Schrodinger Macro Model (Maestro vs. 9.0) software with OPLS 2005 force field in water. A conjugate gradient minimization scheme [PRCG (Polak-Ribiere Conjugate Gradient)] that uses the Polak-Ribiere first derivative method with restarts every 3N iterations were employed for the minimization of the peptides

Conformational Search of Optimized Structure For the Peptides and MD Simulations: Conformational Search of Optimized structure for the peptides we carried out conformational search using OPLS 2005 force field at constant dielectric

in water with "large scale low frequency-mode conformational search" (Mixed torsional/Largescale low-mode sampling = MCMM/LMCS) method using Schrodinger Macromodel (Maestro vs. 9.0) software package. It is a hybrid functional method wherein Low-Mode Conformational Search Methods is hybridized with Monte Carlo Multiple Minimum (MCMM) global searching. This method uses a combination of the random changes in torsion angles and/or molecular position from the MCMM method, together with the low-mode steps from the LLMOD method used in Large scale low-mode.[72]

A total of 500 structures were processed with 500 maximum no. of steps iteration. A global search analysis eliminates redundant conformers using RMS deviation for all compared atoms exceed the threshold Cutoff of 0.5 Å. An optimal minimization method was chosen for minimizing the generating conformers.

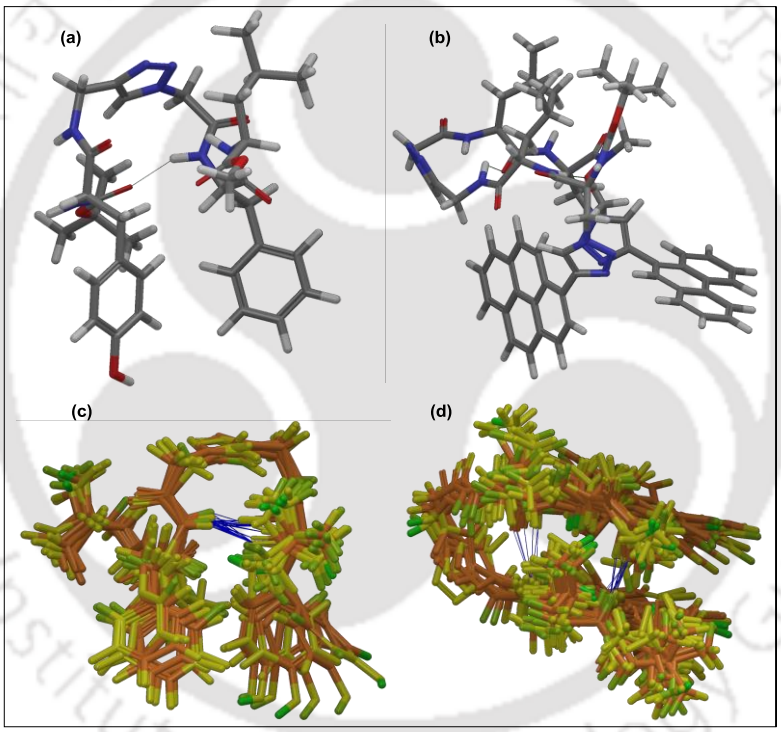

Figure 4.21. OPLS 2005 force field energy minimized conformations and well converged structures obtained from molecular dynamics simulation of tetrapeptide **4.102** (a, c) and pentapeptide **4.103** (b, d).

A total of 84 (for Pentapeptide **4.103**) and 91 (for tetrapeptide **4.102**) minimized and well converged conformers were generate out of which the one conformer appeared 4 times (for Pentapeptide **4.103**), and 6 times (for tetrapeptide **4.102**) which remained within 1.00 k.cal/mole (4.18 kJ/mole) global minimum with a convergence threshold of 0.031 to 0.007 RMSD (threshold cutoff = 0.05). The relative potential energy is 0 and force field energy which correspond to global minimum is -603.34 k J/mole and -492.7 k J/mole for the conformer of tetrapeptide **4.102** (BocNH-Tyr-

^{Al}**TAA**-Phe-Leu-OMe) and pentapeptide **4.103** (BocNH-^{TPy}**Ala**^{Do}-Leu-^{Al}**TAA**-Leu-^{TPhen}**Ala**^{Do}-CO_2NMe(OMe)). These conformers were taken as the starting structures for MD simulation studies.

Molecular Dynamics Simulation of Optimized Structure of the Peptides: We carried out MD simulations for the peptides using an OPLS 2005 force field. The starting structures for the peptides were the global minimum conformers obtained in a conformational search as stated above. The MD simulations were performed using Schrodinger Macromodel (Maestro vs. 9.0) software package with OPLS 2005 force field in which the systems were subjected to 100 ps simulations time (with time step of 1.5 fs and equilibrium time 1.0 ps) at constant temperature (300 K) and pressure (1 atm) with shaking bonds to hydrogens.[72] An optimal minimization method was chosen for minimizing the generating structure (with maximum iteration of 1000) with gradiant convergence threshold of 0.05.

The optimized geometry, conformational search and the MD simulation of the tetrapeptide **4.102** and pentapeptide **4.103** containing aliphatic triazolo amino acid scaffold (^{Al}**TAA**) in the backbone fully supported the type II β-turn conformation with H-bond involving >CO at i and NH at i+3.

4.7.4. Study of Photophysical Properties

After established the β-turn conformation of our synthesized fluorescent peptide **4.103**, we next studied their photophysical property in various organic solvents. The UV-visible spectra of the ^{TPhen}**Ala**^{Do}–Leu dipeptide **4.120** (**Scheme 4.4**) containing a triazolyl phenanthrene exhibited broad and solvatochromic absorption band at around 300-305 nm in various organic solvents. Excitation at absorption maxima of each solvent showed characteristic emission band at 360 nm, 380 nm and 400 nm same as ^{TPhen}**Ala**^{Do}. (**Figure 4.22a-b**, **Table 4.2**).[73] ^{TPy}**Ala**^{Do}**–Leu** dipeptide in methyl ester protected form of **4.125** (**Scheme 4.4**) showed structureless absorption at 346 nm in dioxane which shifted to 343 nm as the solvent polarity increases from dioxane to methanol. However, when excited on their absorption maxima 345 nm it showed a structured emission at 384, 404 and 422 nm. The emission intensity of dipeptide **4.125** decreases with increasing solvent polarity (**Figure 4.22c-d, Table 4.2**). The quantum yield also follows the same trend as the intensity in various organic solvents.[73]

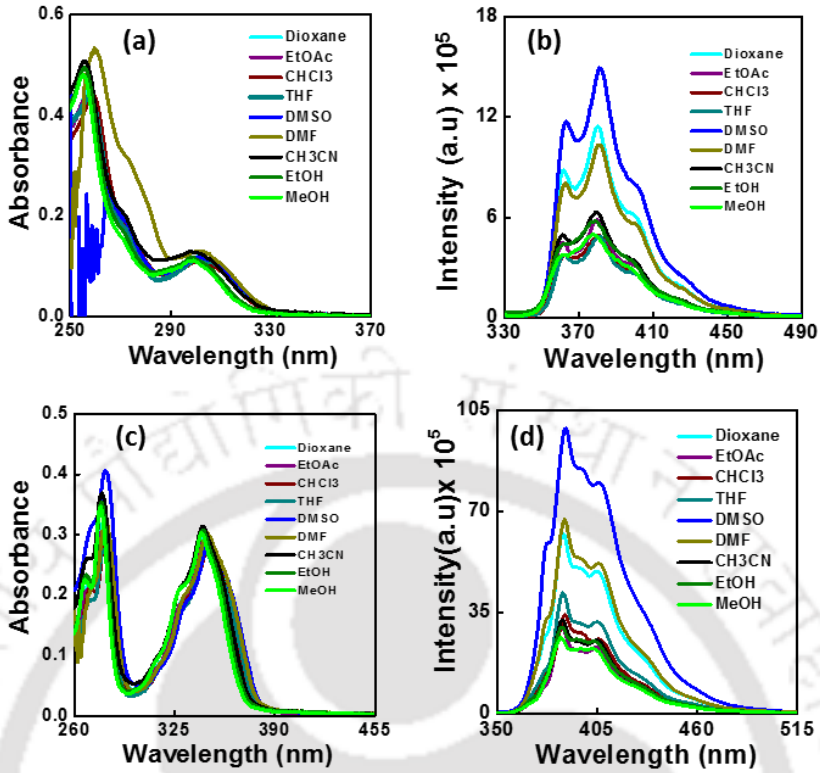

Figure 4.22. UV-Visible and Fluorescence spectra of dipeptide **4.120** (a, b) and dipeptide **4.125** (c, d) in different solvents (10 μM, r.t.; $\lambda_{ex} = \lambda_{max}$ 300, 345 nm respectively of each solvent).

Table 4.2. Summary table of photophysical properties of the peptides **4.120 and 4.125.**

Entry	Solvents	Δf	UV-Vis & Fluorescence		
			λ_{max}^{abs} (nm)	λ_{max}^{fl} (nm)	Φ_f
^{TPhen}Dipeptide 4.120	Dioxane	0.021	258, 269, 301	362, 380, 399	0.12
	$CHCl_3$	0.148	259, 270, 301	361, 380, 395	0.05
	EtOAc	0.201	257, 269, 300	361, 381, 398	0.06
	THF	0.210	258, 271, 302	361, 380, 397	0.05
	DMSO	0.265	265, 271, 301	362, 381, 399	0.14
	DMF	0.275	259, 270, 302	362, 380, 397	0.10
	EtOH	0.290	254, 269, 298	361, 378, 396	0.07
	ACN	0.307	255, 269, 299	360, 379, 395	0.06
	MeOH	0.309	255, 270, 298	361, 377, 395	0.06
	Buffer (pH=7.0)	0.318	256, 300	362, 376, 395	0.09

^{TPy}Dipeptide 4.125	Dioxane	0.021	279, 331, 345	386, 405, 423	0.22
	$CHCl_3$	0.148	280, 334, 346	386, 406, 426	0.13
	EtOAc	0.201	278, 330, 343	387, 406, 426	0.10
	THF	0.210	279, 332, 344	386, 405, 425	0.15
	DMSO	0.265	280, 334, 344	387, 406, 428	0.40
	DMF	0.275	280, 333, 346	387, 406, 426	0.23
	EtOH	0.290	277, 330, 343	385, 403, 422	0.11
	ACN	0.307	278, 331, 343	386, 404, 424	0.10
	MeOH	0.309	276, 329, 342	385, 403, 422	0.10
	Buffer (pH=7.0)	0.318	283,330,344,355	383, 396, 466	0.05

The pentapeptide **4.103** containing a two functionality exhibited absorption band at around 305 nm due to **TPhen** moiety and very strong absorption band at 350 nm for **TPy** unit in all the solvents tested. The absorption spectra showed 5 nm blue shift of as the solvent polarity increases. When excited at two absorption maxima (λ_{ex} = 300 and 350 nm) showed characteristic high intense emission band at 386, 405 and 425 nm **(Figure 4.23, Table 4.3)**.[73]

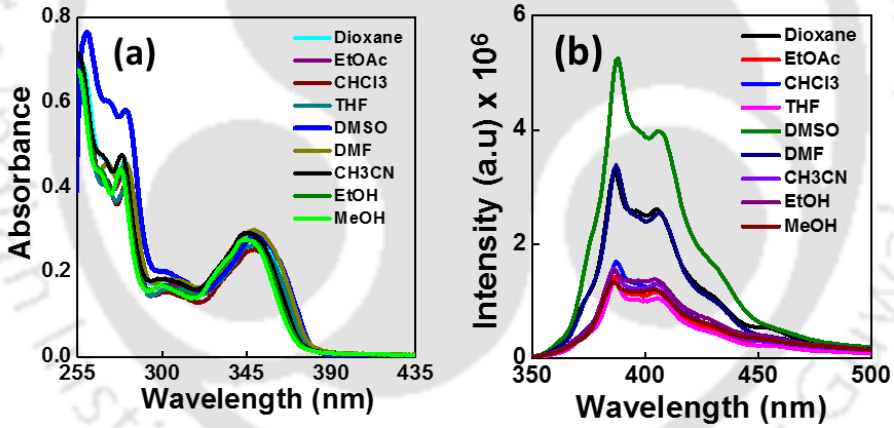

Figure 4.23. UV-Visible (a) and fluorescence spectra (b) of Pentapeptide **4.103** in different solvents (10 µM, r.t.; $\lambda_{ex} = \lambda_{max}$ of each solvent).

Table 4.3. Summary table of photophysical properties of the peptide **4.103**

Entry	Solvents	Δf	UV-Vis & Fluorescence		
			λ_{max}^{abs} (nm)	λ_{max}^{fl} (nm)	Φ_f
TPhen-TPy Pentapeptide 4.103	Dioxane	0.021	280, 305, 348	386, 405, 424	0.33
	$CHCl_3$	0.148	280, 301, 349	386, 405, 425	0.19
	EtOAc	0.201	279, 304, 346	386, 404, 426	0.16
	THF	0.210	280, 305, 348	386, 405, 424	0.15
	DMSO	0.265	280, 301, 350	387, 406, 427	0.46
	DMF	0.275	281, 305, 349	387, 406, 426	0.32
	EtOH	0.290	278, 299, 345	386, 404, 423	0.19
	ACN	0.307	278, 299, 346	385, 404, 423	0.16
	MeOH	0.309	277, 299, 344	385, 403, 423	0.18
	Buffer (pH=7.0)	0.318	284, 308, 357	385, 398, 466	0.02

4.7.5. Study of Förster Resonance Energy Transfer (FRET) in Pentapeptide 4.103

As per our design concept, we next studied the possibility of photophysical interaction between the terminal fluorophoric amino acid pair in the pentapeptide **4.103**. The UV-visible and fluorescence spectra of the individual **^{TPhen}Ala^{Do}–Leu** dipeptide **4.120** and **^{TPy}Ala^{Do}–Leu** dipeptide **4.125** showed that the fluorescence spectrum of **^{TPhen}Ala^{Do}–Leu** dipeptide **4.120** overlapped significantly with the absorption spectrum of **^{TPy}Ala^{Do}–Leu** dipeptide **4.125** (**Figure 4.24a**). The emissions from these two dipeptides were considered as monomer emissions. Therefore, these two amino acids (**^{TPhen}Ala^{Do}**/**^{TPy}Ala^{Do}**) should form a FRET pair in our designed pentapeptide where the amino acid **2.74** (**^{TPhen}Ala^{Do}**, donor chromophore) and the amino acid **2.76** (**^{TPy}Ala^{Do}**, acceptor chromophore) acted as a FRET donor and acceptor, respectively. Furthermore, the peptide **2.103** containing these two amino acids can be selectively excited at 300 nm (the maximum absorbance of **^{TPhen}Ala^{Do}**), wherein there is small absorbance of **^{TPy}Ala^{Do}**. These observations motivated us to study FRET process in detail.[74] It was observed that the fluorescence intensity of **^{TPy}Ala^{Do}** increased almost five times from that of the monomer emission whereas the fluorescence intensity of **^{TPhen}Ala^{Do}** in the peptide decreased almost 3 times that of the monomer fluorescence when the pentapeptide **4.103** was excited at 300 nm. This ratiometric change in fluorescence intensity provided visual evidence of the FRET process from **^{TPhen}Ala^{Do}** to **^{TPy}Ala^{Do}** in pentapeptide **4.103** (**Figure 4.24b**).[74c]

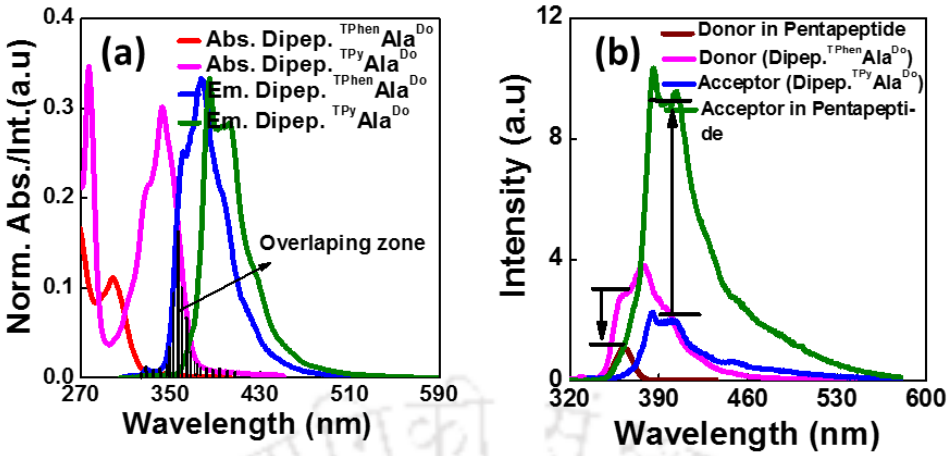

Figure 4.24. (a) Overlapped emission spectra of **^{TPhen}Ala^{Do}-Leu dipeptide 4.120** (act as a FRET donor) and absorption spectra of **^{TPy}Ala^{Do}-Leu dipeptide 4.125** (act as a FRET acceptor) (b) Fluorescence spectra of individual donor dipeptide **4.120** and acceptor dipeptide **4.125** and the pentapeptide **4.103** which contain this two dipeptide (10 µM each, r.t.; λ_{ex} = 300 nm in MeOH).

The occurrence of the FRET process was also evident from time resolved fluorescence study wherein we observed a decrease in the donor lifetime (**^{TPhen}Ala^{Do}-Leu**; λ_{ex} = 293 nm, λ_{em} = 370 nm) from 13.7 ns to 2.0 ns. More interestingly, the lifetime of an acceptor (**^{TPy}Ala^{Do}-Leu**; λ_{ex} = 293 nm, λ_{em} = 400 nm) in the presence of a donor was found to increase from 18.2 ns (in the absence of a donor) to 19.0 ns (in the presence of a donor) evidencing the FRET process (**Table 4.4**, **Figure 4.25**).[74d]

Table 4.4. Summary table of fluorescence lifetimes of the peptides **4.120, 4.125, & 4.103** in MeOH at 25 °C

Compound	λ_{ex}	λ_{em} [nm]	τ_1 [ns]	τ_2 [ns]	$<\tau>$ [ns]	k_f [$10^8 s^{-1}$]	k_{nr} [$10^8 s^{-1}$]	χ^2
Dipeptide **4.120**	293	370	1.99 (49%)	13.78 (51%)	12.2	0.04	0.77	1.1
Dipeptide **4.125**	293	400	5.55 (41%)	18.2 (59%)	15.9	0.06	0.56	1.08
	340	400	3.93 (42%)	17.64 (58%)	15.7	0.06	0.57	1.1
Pentapeptide **4.103**	293	370	1.95 (73%)	16.5 (26%)	12.8	0.14	0.64	1.1
Pentapeptide **4.103**	293	400	2.95 (42%)	19.01 (58%)	17.4	0.10	0.47	1.1
	340	400	3.3 (35%)	18.4 (65%)	17.1	0.10	0.48	1.1
For lifetimes of the fluorescent peptides λex = 293 and 343 nm; Concentration of each fluorescent amino acid = 10 µM; $<\tau>$, k_f, and k_{nr} are weighted means from the biexponential fits: $<\tau> = 1/(\alpha_1/\tau_1 + \alpha_2/\tau_2)$, $k_f = \Phi_f/<\tau>$, and $k_{nr} = (1-\Phi_f)/<\tau>$.								

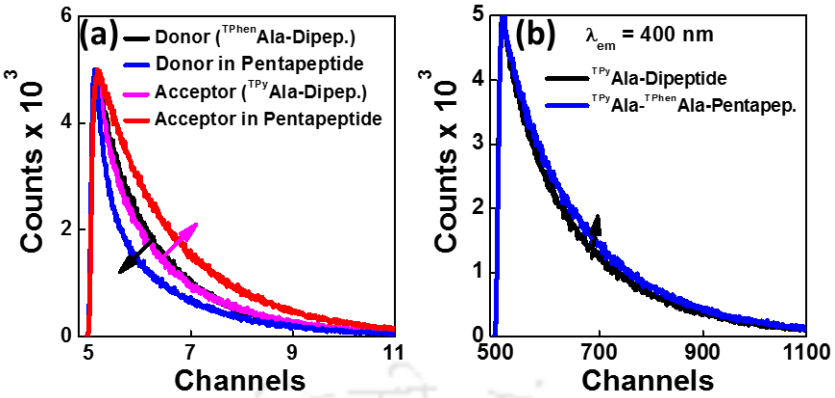

Figure 4.25. Time resolved fluorescence spectra of ^{TPhen}Ala-Leu dipeptide **4.120** and ^{TPy}Ala-Leu dipeptide **4.125** and pentapeptide **4.103** using (a) 293 LED in methanol and (c) 343 LED in methanol solvent. (1ns = 10 chan.).

Following the calculation as described in **Chapter 3, Section 3.7.5** and using the values of κ^2= 2/3, n = 1.329, Φ_D = 0.06, and the obtained overlap integral, $J(\lambda)$ = 1.1085 x 10^{15}, the R_0 and r values were calculated which were found to be $\boldsymbol{R_0}$ **= 31 Å and** $\boldsymbol{r}$ **= 23 Å**. R_0 is the critical distance when the energy transfer efficiency is 50 % and r is the distance between the donor and acceptor .

Energy Transfer efficiency (E) = 1- τ/τ_0 = 85 %. τ and τ_0 are the fluorescence life time of donor in the presence and absence of acceptor.

4.8. Conclusion

In conclusion, the easily accessible aliphatic triazolo amino acid scaffold **4.100** was introduced for the first time as a β-turn-mimetic constrained molecular scaffold. The structural and conformational analysis of Leu-enkephalin analogue peptide **4.102** and fluorescent peptide **4.103** by various spectroscopic techniques and molecular dynamics (MD) simulation studies established well-defined type II β-turn structure induced by the novel β-turn-mimetic constrained molecular scaffold, the triazolo amino acid scaffold **4.100**. Moreover, we established the FRET process in peptide **4.103** containing a new class of fluorescent unnatural triazolyl amino acids at the two termini. Exploration of turn mimetics and the sequence specific DNA binding event of tetra-amides of this molecular scaffold might lead to the generation of a new family of distamycin analogue.

4.9. Experimental Section

4.9.1. General Experimental

Except N-Boc protection of primary amine all reaction were carried out under nitrogen atmosphere in flame-dried glassware, using a nitrogen filled balloon. Organic extracts were dreid over anhydrous sodium sulfate. Solvents were removed in a rotary evaporator under reduced pressure. Silica gel (60- 120 mesh size) was used for the column chromatography. Reactions were monitored by TLC on silica gel 60 F254 (0.25). 1H NMR spectra were recorded either at 400MHz or at 600MHz and 13C NMR spectra were recorded either at 100 MHz or at 150 MHz (mentioned accordingly). Coupling constants (J value) were reported in hertz (Hz). The chemical shift were shown in ppm downfield form tetramethylsilane, using residual chloroform (δ = 7.26 in ^{1}H NMR, δ = 77.23 in ^{13}C NMR), DMSO (δ = 2.5 in ^{1}H NMR, δ = 39.5 in ^{13}C NMR), as an internal standard. Mass spectra were recorded with a HR mass spectrometer and data analysed by using built-in software. IR spectra were recorded in KBr on a FT-IR spectrometer.

All 2D NMR Experiments were carried out on 600 MHz (Bruker Ascend^{TM} Aeon) spectrometer at room temperature using 7 - 10 mM concentration in d_6-DMSO solvent. Spectra were acquired with 2048 x 256 in both dimension (F2 and F1) and other parameter are given below. Parametre of

TOCSY : Free induction decay (FID) with NS = 16 and DS =32, relaxation delay (D1) 2s, mixing time (D9) 0.08s, acquisition time (AQ) 0.085s, spectral width 12019 Hz.

ROESY : Free induction decay (FID) with NS = 16 and DS =16, relaxation delay (D1) 2s, mixing time (P15) 0.02s, acquisition time (AQ) 0.085s, spectral width (SWH) 12019 Hz.

NOESY : Free induction decay (FID) with NS = 8 and DS =16, relaxation delay (D1) 2s, mixing time (D8) 0.6s, acquisition time (AQ) 0.085s, spectral width (SWH) 12019 Hz.

4.9.2. Synthesis and Characterization

***General Procedure for the Peptide Coupling*:** To a solution N-protected amino acids in 3:1 mixture of dry DCM and DMF, 1-[3-dimethyl amino propyl]-3-ehtylcarbo-diimide hydrochloride (EDC.HCl) (1.2 equiv) and HOBT (1.2 equiv) were added and the reaction mixture was stirred for 1h at 0 ^{o}C. Then the amine salt of wienreb amide or methyl ester protected corresponding amino acids or dipeptide (1.1 equiv) were added followed by diisopropylethylamine (DIPEA) (2.4 equiv). The reaction mixture was stirred for another 18-20 h at 0 ^{o}C to room temperature. Then solvent was dried by rotary evaporator, after which it was partitioned between EtOAc

and aqueous $NaHCO_3$ solution (50 ml each). The organic layer was washed with brine solution. Pure product was isolated in pure form by column chromatography (Si-gel, PE : EtOAc = 1:1).

***General procedure of [3+2] cyclo-addition reaction* :** The azido derivative of dipeptide was taken in 5:1 dry THF and water and degassed for 5 min with nitrogen gas. After adding alkyne (1.1 equiv) degassing were continued for the next 5 min. Then, 6 mol % sodium ascorbate and 1 mol% powderd CuSO4 were added. Then 1.2 eqv Et_3N was added and reaction mixture was degassed and allowed to proceed for 18-20 h about 65 to 70 ^{O}C. After total consumption of the starting azide, the reaction mixture was evaporated completely and work up was done by EtOAc and NH_4Cl solution. The organic layer was washed with brine, dried over Na_2SO_4.The title trizolyl unnatural dipeptides were separated by column chromatography and characterized.

***General procedure for the deprotection of the methyl ester* :** To a solution of the respective methyl ester protected peptide in THF : H_2O = 5 : 1, lithium hydroxide (1.5 equivalent) was added at 0 ^{o}C. The reaction mixture was stirred about 3-4 hour until starting material was consumed. Reaction was monitored by TLC. After completion of the reaction, solvent dried by rotary evaporator. Then water (4-5 ml) was added to the reaction mixture and cooled to 0 ^{o}C. The dilute acetic acid was added to the reaction mixture to adjust pH- 3 ~ 4. The reaction mixture was extracted with EtOAc. The combined organic layers were dried over Na_2SO4. The hydrolysed compound was isolated by column chromatography (Si-gel, $CHCl_3$:MeOH = 10:1). Yield was 90-96%.

General procedure for the deprotection of the Boc-group : The respective both side protected amino acids or peptides was dissolved in CH_2Cl_2 and cooled to 0 °C. TFA (equal amount as the solvent) was added and the solution was allowed to warm to room temperature. After stirring at room temperature until starting material was consumed (TLC monitoring). The reaction mixture was evaporated *in vacuo.* The residual TFA was evaporated by triturating the mixture with dry toluene thrice, evaporated thrice and dried to afford the product in quantitative yield. But in some cases to get free amine, water (4-5 ml) was added to the reaction mixture after evaporation and cooled to 0 ^{o}C. Then diluted aq.Et_3N was added to the reaction mixture to adjust pH- 8. The reaction mixture was extracted with EtOAc. The combined organic layers were dried over Na_2SO_4 and evaporated *in vacuo* to yield the crude product in quantitative yield to use for next step.

***Synthesis of ethyl azido acetate* (4.105)**: To a solution of ethyl bromoacetate **4.104** (1510 mg, 9.04 mmol) in water/acetone (1:3, 0.25 M) was added NaN_3 (881.6 mg, 13.56 mmol) and the mixture was heated at 60 ^{o}C for 4 hours. Then the reaction mixture was diluted with DCM and washed with water. The organic layer was dried over anhydrous Na_2SO_4 and evaporated in *vacuo*. The crude material in quantitative yield to use

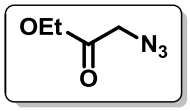

for next step without purification. The product **4.105** is oily liquid, 1132 mg. Yield 97%. IR (KBr) 2955, 2103, 1741, 1441, 1372, 1175, 1064 cm^{-1}.

***Synthesis of ethyl 2-(4-(hydroxymethyl)-1H-1,2,3-triazol-1-yl) acetate* (4.106):** The prepared ethyl azido acetate **4.105** (500 mg, 3.876 mmol) was taken in dry THF and water (3:1) and degassed for 5 min with N_2. Then propargyl alcohol (0.246 ml, 5.8 mmol) was added and both the stirring and degassing were continued for the next 5 min. Consequently 0.06 eqv. sodium ascorbate and 0.01 eqv. powder $CuSO_4$ were added to the reaction mixture. Then the reaction mixture was degassed and allowed to proceed for 12 hours at room temperature. After total consumption of the starting azide, the reaction mixture was evaporated completely and work up was done by EtOAc and NH_4Cl solution. The organic layer was washed with brine, dried over Na_2SO_4. The title compound **4.106** was isolated by column chromatography (si-gel, PE:EA = 1:1) in pure form as white solid (560 mg, Yield 79 %). %). ^{1}H NMR ($CDCl_3$; 600 MHz) δ 1.266-1.204 (3H, m); 4.238-4.190 (2H, m); 4.744-4.731 (2H, d , J = 7.8 Hz); 5.104 (2H, s); 7.630 (1H, s). ^{13}C NMR ($CDCl_3$; 125 MHz) δ 13.9, 50.7, 55.7, 62.3, 123.8, 148.2, 166.6. HRMS calcd for $C_7H_{12}N_3O_3$ ($[M + H]^+$) 186.0808, found 186.0887

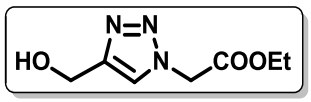

Synthesis of ethyl 2-(4-(((methylsulfonyl)oxy)methyl)-1H-1,2,3-triazol-1-yl) acetate(4.107): Compound **4.106** (100 mg, 0.54 mmol) was taken in a dry CH_2Cl_2, mesyl chloride (0.06 ml, 0.81 mmol) and triethyl amine (0.113 ml, 0.81 mmol) were added to the reaction mixture at 0 ^{o}C. The reaction mixture was stirred at 0 ^{o}C till the starting material was consumed. After that the reaction mixture was diluted with DCM and washed with water and dried over Na_2SO_4 and then evaporated in *vacuo*. The pure compound **4.107** was then isolated by column chromatography (si-gel, PE:EA = 2:1) as a colourless oil (129 mg, Yield 83%) and utilised immediately for the next step.

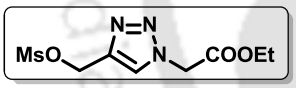

***Synthesis of ethyl 2-(4-(azidomethyl)-1H-1,2,3-triazol-1-yl)acetate* (4.108):** To a solution of the mesyl derivative of **4.107** (129 mg, 0.523mmol) in dry DMF (5 ml), NaN_3 (40.7 mg, 0.627 mmol) was added and stirrer for 18 h at 50 ^{o}C. The reaction mixture was partitioned between EtOAc and water (20 ml each). The organic layer was washed with brine solution, dried with Na_2SO_4, filtered and then evaporated. The title compound **4.108** was isolated by column chromatography (si-gel, PE:EA = 5:1) in pure form as white solid (98 mg, Yield 89%). IR (KBr) 3447, 3138, 3006, 2108, 1739, 1634, 1464, 1407, 1259, 1021, 771 cm^{-1}. ^{1}H NMR ($CDCl_3$; 600 MHz) δ 1.29 (3H, t, J = 6.6 Hz); 4.27 (2H, q, J = 7.2 Hz); 4.51 (2H, s); 5.17 (2H, s); 7.17 (1H, s). ^{13}C NMR ($CDCl_3$; 125 MHz) δ 14.0, 45.5, 50.9, 62.5, 124.0, 142.9, 166.2. HRMS calcd for $C_7H_{10}N_6O_2$ ($[M + H]^+$) 211.0899, found 211.0950.

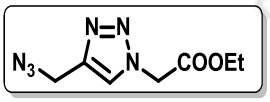

Synthesis of 2-(4-(azidomethyl)-1H-1,2,3-triazol-1-yl)acetic acid **(4.109)**: To a solution of compound **4.108** in methanol, 1.5 eqv. lithium hydroxide was added and

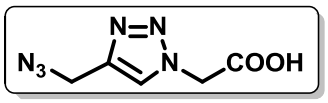

stirred about 2-3 hours at room tempr until starting material is vanished. After that in the reaction mixture, dilute HCl is added until it becomes pH = 3 then it was partitioned between EtOAc and water (20 ml each). The organic layer was washed with brine solution, dried with Na_2SO_4, filtered and then evaporated. The prepared title compound **4.109** can be used for next step without further purification. IR (KBr) 3153, 2101, 1725, 1557, 1447, 1414, 1362, 1333,1231, 1068, 822 cm^{-1}. ^1H NMR (CD_3OD; 400 MHz) δ 4.49 (2H, s); 5.30 (2H, s); 8.06 (1H, s). ^{13}C NMR (CD_3OD; 100 MHz) δ 46.1, 51.8, 126.6, 144.0, 169.9.

Synthesis of 2-(4-(aminomethyl)-1H-1,2,3-triazol-1-yl)acetic acid **(4.100)**: To solution of the compound **4.109** in methanol solvent (200 mg, 1.1 mmol) Pd/C is

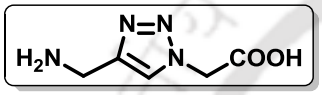

added in hydrogen atmosphere and stir the reaction mixture for 3-4 hours. The reaction mixture solvent methanol is evaporated and the crude is dissolved in water and then filtered, filtrate is evaporated to afford the title compound **4.100** with quantitative yield. IR (KBr) 3418, 3153, 1614, 1393, 1308, 1233 cm^{-1}. ^1H NMR (D_2O; 600 MHz) δ 4.34 (2H, s); 5.06 (2H, s); 8.07 (1H, s). ^{13}C NMR (D_2O; 125 MHz) δ 34.0, 53.2, 126.3, 139.6, 173.1.

Synthesis of N-t-butyloxycarbonyl-2-(4-(azidomethyl)-1H-1,2,3-triazol-1-yl)acetic acid **(4.110):** In a solution of 2-(4-(azidomethyl)-1H-1,2,3-triazol-1-yl)acetic acid **4.100** (200 mg, 1.28 mmol) in 1:1 mixture of 1,4 dioxane and water (3 ml each) was added NaOH (102.6 mg, 2.56 mmol) followed by di-t-butyl dicarbonate

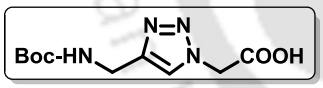

(0.44 ml, 1.92 mmol) maintaining the pH between 7.5-8.5. The reaction mixture was stirred at room temperature for 20 h. The reaction mixture was washed with ethyl acetate (2 x 10 ml) and the aqueous phase was treated with dil. HCl to bring pH ~ 4 in cold condition. Immediately the solution was extracted with ethyl acetate and the organic layer was washed with water, brine, dried and evaporated under *vacuo* to furnish the Boc-protected 2-(4-(azidomethyl)-1H-1,2,3-triazol-1-yl) acetic acid **4.110** as white solid in pure form (265.4 mg, Yield 81%). ^1H NMR (CD_3OD; 400 MHz) δ 1.43 (9H, s); 4.31 (2H, s); 5.25 (2H, s); 7.87 (1H, s). ^{13}C NMR (CD_3OD; 100 MHz) δ 28.9, 36.8, 51.8, 80.6, 125.6, 147.4, 158.4, 170.0. HRMS calcd for $C_{10}H_{15}N_4O_4$ ([M - H]$^-$) 255.2540, found 255.2255.

Synthesis of ((S)-methyl 2-((S)-2-((tert-butoxycarbonyl)amino)-3phenylpropanamido) methylpentanoate **(4.113):** Using general procedure of peptide coupling starting N-protected L-phenylalanine **4.111** (1500 mg, 5.66 mmol),

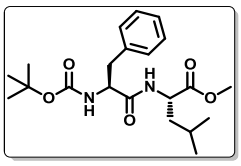

and the amine salt of methyl ester -L-leucine **4.112** (991 mg, 6.79 mmol)**,** the title compound **4.113 (**1464.3 mg, 3.73 mmol) was isolated as white solid. Yield 66%; IR (KBr) 3391, 3067, 2966, 2937, 1751, 1683, 1648, 1545, 1390, 1200, 703 cm^{-1}. ^1H

NMR ($CDCl_3$; 400 MHz) δ 0.90 (6H, t, J = 6 Hz); 1.26 (1H, s); 1.432 (9H, s); 1.66-1.58 (2H, m); 3.10 (2H, ddd, J = 6 Hz, 9.2 Hz); 3.694 (3H, s); 4.12 (1H, m); 4.84 (1H, d, J = 6.8 Hz); 4.98 (1H, d, J = 7.6); 6.66 (1H, d, J = 7.2 Hz); 7.10 (2H, d, J = 7.6 Hz); 7.29-7.20 (3H, m); ^{13}C NMR ($CDCl_3$; 100 MHz); δ 22.1, 22.7, 24.7, 28.4, 31.7, 38.1, 41.3, 52.4, 53.2, 80.1, 127.2, 128.6, 129.4, 135.9, 155.6, 171.8, 172.4. HRMS calcd for $C_{21}H_{32}N_2O_5Na$ ($[M + Na]^+$) 415.2201, found 415.2222.

***Synthesis of Boc deprotected ((S)-methyl 2-((S)-2-((tert-butoxycarbonyl)amino)-3- phenylpropanamido)-4-methylpentanoate* (4.114):** Using the general procedure of Boc deprotection, compound **4.113** (212 mg, 0.54 mmol) was reacted. The product

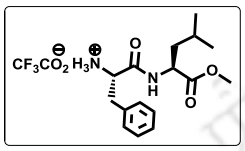

4.114 was obtained in quantitative yield and were used without further purification and characterization.

***Synthesis of (S)-methyl 2-((S)-2-(2-(4-(((tert-butoxycarbonyl)amino)methyl)-1H-1,2,3-triazol-1-yl)acetamido)-3-phenylpropanamido)-4-methylpentanoate* (4.115) :**To a solution N-protected **^{Al}TAA 4.110**, (140 mg, 0.54 mmol) in dry DMF was cooled to 0 ^{o}C by ice bath. Consequently 1-[3-dimethyl amino propyl]-3-ehtylcarbo-diimide hydrochloride (EDC.HCl) (156 mg, 0.817 mmol), DMAP (200 mg, 1.64

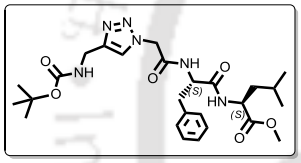

mmol) and amine salt of methyl ester protected dipeptide **4.114** were added and the reaction mixture was stirred for 18h at 0 ^{o}C to room tempareture. Then solvent was dried by rotary evaporator, after which it was partitioned between EtOAc and water (50 ml each). The organic layer was washed with brine solution. Pure product **4.115 (**262 mg, 0.494 mmol) was isolated in pure form by column chromatography (Si-gel, PE : EtOAc = 1:1) as solid compound. Yield 81%. IR (KBr) 3438, 3314, 3066, 2957, 2100, 1746, 1690, 1657, 1533, 1454, 1367, 1252, 1169, 1052, 746, 702 cm^{-1}. ^{1}HNMR ($CDCl_3$; 400 MHz) δ 0.84 (6H, d, J = 5.2 Hz); 1.43 (9H, s); 1.58-1.48 (3H, m); 3.09-2.93 (2H, ddd, J = 6.4 Hz, 20 Hz), 3.69 (3H, s); 4.36 (2H, d, J = 5.2 Hz); 4.49 (1H, q, J = 7.6 Hz, 6 Hz); 4.76 (1H, q, J = 6.8 Hz, 7.6 Hz); 4.96 (2H, bs); 5.48 (1H, bs); 6.77 (1H, d, J = 6.8 Hz); 7.19 (2H, d, J = 6.4 Hz); 7.23 (3H, d, J = 6.8 Hz); 7.58 (1H, s); 7.61 (1H, d, J = 7.6 Hz); ^{13}C NMR ($CDCl_3$; 100 MHz) δ 21.8, 22.5,24.6, 28.3, 35.9, 38.5, 40.5, 51.1, 51.9, 52.2, 54.6, 79.3, 123.6, 126.8, 128.4, 129.3, 136.2, 145.5, 155.9, 165.6, 171.3, 172.8. HRMS calcd for $C_{26}H_{39}N_6O_6$ ($[M + H]^+$) 531.2930, found 531.2856.

***Synthesis of Boc deprotected (S)-methyl 2-((S)-2-(2-(4-(((tert-butoxy carbonyl) amino)methyl)-1H-1,2,3-triazol-1-yl)acetamido)-3-phenylpropanamido)-4-methylpentanoate* (4.116):** Using the general procedure of Boc deprotection, compound **4.115** (262.8 mg, 0.496 mmol) was reacted. The product **4.116** was obtained in quantitative yield and were used without further purification and characterization.

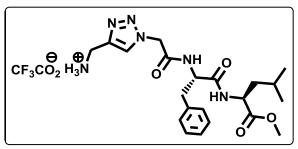

Methyl2-((S)-2-(2-(4-(((S)-2-((tert-butoxycarbonyl)amino)-3-(4-hydroxyphenyl) propanamido) methyl)-1H-1,2,3-triazol-1-yl)acetamido)-3-phenylpropanamido)-4-methylpentanoate **(4.102) :** Using general procedure of peptide coupling, starting from 140 mg (0.496 mmol) of Boc protected L-tyrosine and 214 mg (0.496 mmol) of

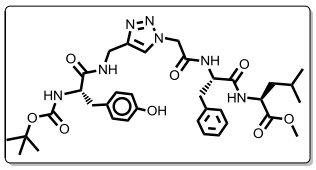

4.116, 165 mg (0.238 mmol) of the title compound **4.102** was isolated as a white solid (Si-gel, EtOAc). Yield 48%. IR (KBr) 3439, 3371, 2958, 2931, 2871, 1751, 1690, 1658, 1516, 1367, 1252, 1166, 1052, 749 cm^{-1}. ^1H NMR (d_6-DMSO; 600 MHz) δ 0.85 (6H, d, J = 31.2 Hz); 1.36 (9H, s); 1.58-1.50 (3H, m); 2.81-2.72 (2H, m); 3.03 (2H, bs); 3.61 (3H, s); 4.06-4.01 (1H, m); 4.3 (2H, bs); 4.38 (1H, bs); 4.59 (1H, bs); 5.03 (2H, q, J = 15 Hz); 6.61 (1H, d, J = 6.6 Hz); 6.69 (1H, d, J = 4.8); 6.92 (1H, d, J = 7.2 Hz); 7.01 (1H, d, J = 6.6 Hz); 7.09 (1H, s); 7.25 (5H, s); 7.33 (1H, s); 8.40 (1H, t, J = 7.8 Hz); 8.52 (1H, d, J = 4.8 Hz); 8.6 (1H, d, J = 7.2 Hz); ^{13}C NMR (d_6-DMSO; 125 MHz) δ 21.3, 22.7, 24.2, 28.1, 34.3, 35.6, 36.8, 50.4, 51.4, 51.9, 53.7, 59.8, 78.6, 114.8, 115.1, 120.9, 121.3, 124.1, 126.4, 129.2, 130.1, 130.2, 130.3, 137.3, 144.6, 155.6, 165.1, 170.4, 171.0, 171.8, 172.6. HRMS calcd for $C_{35}H_{48}N_7O_8$ ($[M + H]^+$) 694.3550, found 694.3540.

Synthesis of (S)-tert-butyl (3-azido-1-(methoxy(methyl)amino)-1-oxopropan-2 yl)carbamate **(2.069):** Using our previous method from 1000 mg (5 mmol) of NBoc-protected L-serine, 540 mg (1.97 mmol) of the title compound **2.069** was preapred. Overall Yield 75 %.

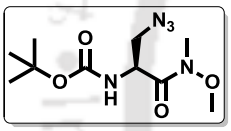

Synthesis of Boc deprotected (S)-tert-butyl (3-azido-1-(methoxy(methyl)amino)-1-oxopropan-2-yl)carbamate **(4.117):** Using the general procedure of Boc deprotection, compound **2.069** (500 mg, 1.832 mmol) was reacted. The product **4.117** was obtained in quantitative yield and were used without further purification and characterization.

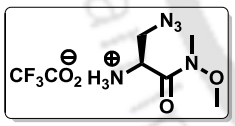

Synthesis of *tert-butyl ((S)-1-(((S)-3-azido-1-(methoxy(methyl)amino)-1-oxopropan-2- yl)amino)-4-methyl-1-oxopentan-2-yl)carbamate* **(4.119) :** Using general procedure of peptide coupling, starting from 1000 mg (4.32 mmol) of NBoc-protected leucine **4.118** and 752 mg (4.32 mmol) of N-deprodected serine azide **4.117**,

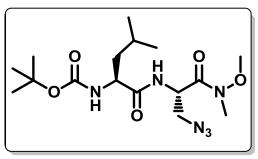

900 mg (2.33 mmol) of the title compound **4.119** was isolated. Pure product was isolated in pure form by column chromatography (Si-gel, PE : EtOAc = 2:1) as colourless oil. Yield 54%. IR (KBr) 3335, 3244, 2966, 2105, 1685, 1643, 1523, 1272, 1170, 928 cm^{-1}. ^1H NMR ($CDCl_3$; 400 MHz) δ 0.89 (6H, d, J = 3.2 Hz); 1.4 (9H, s); 1.47-1.43 (1H, m); 1.63 (2H, m); 3.19 (3H, s); 3.55-3.51 (1H, m); 3.63-3.60 (1H, m); 3.72 (3H, s); 4.15 (1H, bs); 5.03 (1H, bs); ^{13}C NMR ($CDCl_3$; 100 MHz) δ 21.8, 23.1, 24.8, 28.3, 32.3, 41.4, 49.6, 51.9, 53.6, 61.8, 80.1, 155.6, 169.1, 172.8. HRMS calcd for $C_{16}H_{31}N_6O_5$ ($[M + H]^+$) 387.2277, found 387.2165.

***Synthesis of tert-butyl ((S)-1-(((S)-1-(methoxy(methyl)amino)-1-oxo-3-(4-(phenanthren-9-yl)-1H-1,2,3-triazol-1-yl)propan-2-yl)amino)-4-methyl-1-oxopentan-2-yl)carbamate* (4.120):** Using general procedure of [3+2] cyclo-addition reaction, starting from 250 mg (0.647 mmol) of azide derivative of dipeptide **4.119**

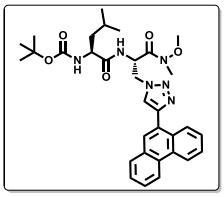

and 157 mg (0.78 mmol) of 9-ethynyl phenanthrene, 320 mg (0.54 mmol) of the title compound **4.120** was isolated as a light brown gummy material (Si-gel, PE : EtOAc = 1:1). Yield 84%; IR (KBr) 3331, 2958, 2929, 2136, 1657, 1518, 1366, 1165, 1048, 729 cm^{-1}. ^{1}H NMR ($CDCl_3$; 400 MHz); δ 0.86 (6H, d, J = 5.2 Hz); 1.32 (9H, s); 1.47-1.41 (1H, m); 1.63-1.54 (2H, m); 3.25 (3H, s); 3.8 (3H, s); 4.06 (1H, bs); 4.82 (2H, dd, J = 4.4 Hz, 9.6 Hz); 4.99 (1H, d, J = 13.6 Hz); 5.29 (1H, bs); 7.11 (1H, d, J = 6.4 Hz); 7.66-7.54 (4H, m); 7.87 (1H, d, J = 7.6 Hz); 8.01 (1H, s); 8.17 (1H, s); 8.14 (1H, d, J = 8 Hz); 8.69 (2H, dd, J = 8 Hz, 15.6 Hz); ^{13}C NMR ($CDCl_3$; 100 MHz); δ 21.5, 22.8, 24.5, 28.1, 32.3, 41.1, 50.1, 50.2, 53.4, 61.7, 79.6, 122.3, 122.7, 124.4, 126.2, 126.5, 126.6, 126.7,126.8, 128.1, 128.7, 129.9, 130.1, 130.5, 131.1, 146.5, 155.6, 162.4, 168.2, 173.1. HRMS calcd for $C_{32}H_{41}N_6O_5$ ($[M + H]^+$) 589.3137, found 589.3039.

***Synthesis of Boc deprotected tert-butyl ((S)-1-(((S)-1-(methoxy(methyl)amino)-1-oxo-3-(4-(phenanthren-9-yl)-1H-1,2,3-triazol-1-yl)propan-2-yl)amino)-4-methyl-1-oxopentan- 2-yl)carbamate* (4.121):** Using the general procedure of Boc deprotection, compound **4.120** (319.5 mg, 0.543 mmol) was reacted. The product **4.121** was obtained in quantitative yield and were used without further purification and characterization.

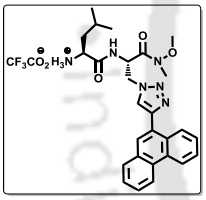

***Synthesis of tert-butyl ((1-((5S,8S)-8-isobutyl-3-methyl-4,7,10-trioxo-5-((4-(phenanthren-9-yl)-1H-1,2,3-triazol-1-yl)methyl)-2-oxa-3,6,9-triazaundecan-11-yl)-1H-1,2,3-triazol-4-yl)methyl)carbamate* (4.122) :** To a solution N-protected **^{Al}TzAA 4.110**, (160 mg, 0.625 mmol) in dry DMF was cooled to 0 ^{o}C by ice bath. Consequently 1-[3-dimethyl amino propyl]-3-ehtylcarbo-diimide hydrochloride

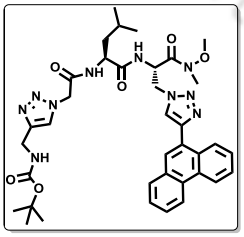

(EDC·HCl) (178 mg, 0.937 mmol), DMAP (288 mg, 1.87 mmol) and amine salt of weinreb amide protected corresponding dipeptide **4.121** were added and the reaction mixture was stirred for 18h at 0 ^{o}C to room temperature. Then solvent was dried by rotary evaporator, after which it was partitioned between EtOAc and water (50 ml each). The organic layer was washed with brine solution. Pure product **4.122** (300 mg, 0.414 mmol) was isolated in pure form by column chromatography (Si-gel, EtOAc) as solid compound. Yield 66%. IR (KBr) 3449, 3422, 3314, 2958, 2869, 2100, 1680, 1660, 1524, 1366, 1250, 1168, 1054, 729 cm^{-1}. ^{1}HNMR ($CDCl_3$; 400 MHz) δ 0.84 (6H, t, J = 6 Hz); 1.39 (9H, s); 1.63-1.46 (3H, m); 3.29 (3H, s); 3.85 (3H, s); 4.24 (2H, d, J = 4.4 Hz); 4.46-4.41 (1H, m); 4.87-4.82 (2H, m); 4.96 (2H, d, J = 7.2 Hz); 5.13 (1H, bs); 5.35 (1H, q, J = 5.2 Hz, 7.2 Hz);

6.69 (1H, bs); 7.55 (1H, s); 7.62 (2H, t, *J* = 7.2 Hz); 7.69 (2H, q, *J* = 6.8 Hz, 4.8 Hz); 7.91 (1H, d, *J* = 7.2 Hz); 7.97 (2H, d, *J* = 6 Hz); 8.33 (1H, d, *J* = 8 Hz); 8.7 (1H, d, *J* = 8 Hz); 8.76 (1H, d, *J* = 8.4 Hz). ^{13}C NMR ($CDCl_3$; 100 MHz) *δ* 21.8, 22.8, 24.7, 28.4, 32.5, 36.1, 40.4, 50.2, 50.4, 52.3, 52.4, 62.0, 79.5, 122.5, 123.1, 123.8, 124.6, 126.3, 126.5, 126.8, 127.1, 127.3, 128.4, 128.9, 130.1, 130.3, 130.6, 131.2, 145.6, 146.6, 155.9, 165.9, 168.2, 172.1. HRMS calcd for $C_{37}H_{47}N_{10}O_6$ ([M + H]$^+$) 727.3679, found 727.3658.

***Synthesis of Boc deprotected tert-butyl ((1-((5S,8S)-8-isobutyl-3-methyl-4,7,10-trioxo-5-((4-(phenanthren-9-yl)-1H-1,2,3-triazol-1-yl)methyl)-2-oxa-3,6,9-triazaundecan-11- yl)-1H-1,2,3-triazol-4-yl)methyl)carbamate* (4.123):** Using the general procedure of Boc deprotection, compound **4.122** (300.0 mg, 0.414 mmol) was reacted. The product **4.123** was obtained in quantitative yield and were used without further purification and characterization.

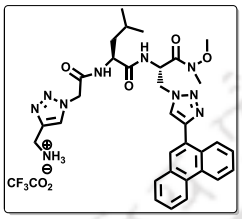

Synthesis of *(S)-methyl 2-((S)-3-azido-2-((tert-butoxycarbonyl)amino)propanamido)-4-methylpentanoate* (4.124): Using general procedure of peptide coupling, starting from 1000 mg (4.34 mmol) of N-protected serine azide **3.040** and 570 mg (4.34 mmol) of N-deprodected amine salt of methyl ester -L-leucine, 870 mg (2.43 mmol) of the title compound **4.124** was isolated. Pure product was isolated in pure form by column chromatography (Si-gel, PE : EtOAc = 2:1) as light yellow oil. Yield 56%. IR (KBr) 3326, 2960, 2873, 2105, 1745, 1666, 1524, 1368, 1250, 1023, 858, 780 cm^{-1}. ^{1}H NMR ($CDCl_3$; 400 MHz) *δ* 0.88 (6H, d, *J* = 5.6 Hz); 1.41 (9H, s); 1.63-1.51 (3H, m); 3.51 (1H, dd, *J* = 4.8 Hz, 6.8 Hz); 3.68 (3H, s); 3.74-3.70 (1H, m); 4.30 (1H, bs); 4.56 (1H, bs); 5.51 (1H, d, *J* = 6.4 Hz); 6.97 (1H, d, *J* = 6.4 Hz); ^{13}C NMR ($CDCl_3$; 100 MHz) *δ* 21.9, 22.8, 24.8, 28.3, 41.3, 51.0, 52.2, 52.4, 53.7, 80.8, 155.5, 169.5, 173.1. HRMS calcd for $C_{15}H_{27}N_5O_5Na$ ([M + Na]$^+$) 380.1908, found 380.1909.

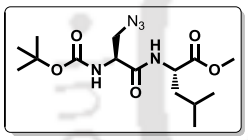

***Synthesis of (S)-methyl 2-((S)-2-((tert-butoxycarbonyl)amino)-3-(4-(pyren-1-yl)-1H-1,2,3-triazol-1-yl)propanamido)-4-methylpentanoate* (protected form of 4.125):** Using general procedure of [3+2] cyclo-addition reaction, starting from 200 mg (0.56 mmol) of azide derivative of dipeptide **4.124** and 152 mg (0.78 mmol) of 1-ethynyl pyrene, 210 mg (0.36 mmol) of the title compound **4.125** was isolated as a light brown gummy material (Si-gel, PE : EtOAc = 1:1). Yield 64%; IR (KBr) 3336, 2961, 1669, 1515, 1258, 1165, 847, 724 cm^{-1}. ^{1}H NMR ($CDCl_3$; 400 MHz); *δ* 0.69 (6H, d, *J* = 6.4 Hz); 0.88-0.086 (2H, m); 1.46 (9H, s); 1.54-1.49 (2H, m); 3.67 (3H, s); 4.57 (1H, m); 4.87 (2H, bs); 5.05 (1H, m); 6.05 (1H, d, *J* = 8.4 Hz); 7.19 (1H, d, *J* = 6.8 Hz); 8.02-7.97 (1H, m); 8.09-8.05 (3H, m); 8.11 (1H, s); 8.16-8.13 (3H, m); 8.22-8.19 (1H, m); 8.66 (1H, d, *J* = 8.8 Hz); ^{13}C NMR ($CDCl_3$; 100 MHz); *δ* 21.7, 22.8, 24.9, 28.4, 41.3, 43.5, 51.1, 52.5, 54.6, 81.3, 124.6, 124.8,

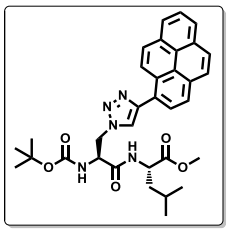

124.9, 125.1, 125.2, 125.3, 125.5, 126.2, 127.2, 127.4, 128.0, 128.3, 128.6, 131.0, 131.3, 131.5, 147.5, 155.7, 169.0, 172.8. HRMS calcd for $C_{33}H_{38}N_5O_5$ ($[M + H]^+$) 584.2867, found 584.2874.

Synthesis of tert-butyl ((S)-1-(((S)-1-(((1-((5S,8S)-8-isobutyl-3-methyl-4,7,10-trioxo-5-((4-(phenanthren-9-yl)-1H-1,2,3-triazol-1-yl)methyl)-2-oxa-3,6,9-triazaundecan-11-yl)-1H-1,2,3-triazol-4-yl)methyl)amino)-4-methyl-1-oxopentan-2-yl)amino)-1-oxo-3-(4-(pyren-1-yl)-1H-1,2,3-triazol-1-yl)propan-2-yl)carbamate

(4.103) : Using general procedure of peptide coupling, starting from 180 mg (0.316 mmol) of **4.125** and 198 mg (0.316 mmol) of **4.123**, 170 mg (0.15 mmol) of the title compound **4.103** was isolated as a gummy material, after washing with ether it converted to light yellow solid (CH_3Cl:MeOH = 20:1). Yield 46%. IR (KBr) 3472, 3421, 3281, 3076, 2955, 2103, 1674, 1649, 1636, 1543, 1367, 1248, 1166, 1050, 847, 729 cm^{-1}. ^1H NMR (d_6-DMSO; 600 MHz) δ 0.77 (3H, d, J = 6 Hz); 0.82 (3H, d, J = 6.6 Hz); 1.28 (9H, s); 1.44-1.41 (4H, m); 1.56-1.53 (2H, m); 3.16 (3H, s); 3.72 (3H, s); 4.26 (2H, bs); 4.36 (2H, bs); 4.72-4.69 (2H, m); 4.8 (2H, dd, J = 4.8 Hz, 8.4 Hz); 4.91 (1H, d, J = 8.4 Hz); 5.06 (2H, dd, J = 15.6, 36 Hz); 5.34 (1H, bs); 7.27 (1H, d, J = 7.2 Hz); 7.66-7.65 (2H, m); 7.76-7.69 (3H, m); 7.98 (1H, d, J = 7.8Hz); 8.02 (1H, s); 8.09 (1H, t, J = 7.8 Hz); 8.22-8.19 (3H, m); 8.23 (1H, s); 8.33-8.28 (3H, m); 8.36-8.35 (1H, m); 8.41 (1H, d, J = 10.2 Hz); 8.5 (3H, bs); 8.62 (1H, s); 8.65 (1H, bs); 8.86-8.81 (2H, m); 8.89 (1H, t, J = 7.2 Hz); ^{13}C NMR (d_6-DMSO; 125 MHz) δ 21.4, 22.9, 23.1, 24.0, 24.1, 28.0, 30.8, 34.3, 35.8,40.9, 49.4, 49.7, 50.6, 51.2, 51.3, 51.4, 54.4, 78.8, 122.8, 123.3, 123.9, 124.1, 124.3, 124.8, 125.1, 125.2, 125.3, 125.5, 126.2, 126.5, 126.7, 126.9, 127.0, 127.1, 127.2, 127.3, 127.5, 127.7, 127.9, 128.7, 129.5, 129.7, 130.2, 130.4, 130.5, 130.8, 130.9, 144.4, 145.2, 145.7, 155.1, 162.4, 165.3, 168.7, 171.8, 171.9. HRMS calcd for $C_{64}H_{72}N_{15}O_8$ ($[M + H]^+$) 1178.5767, found 1178.5771.

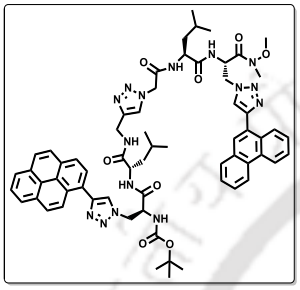

4.9.3. Study of Photophysical Properties of Fluorescence Peptides

The procedures for study of all the photophysical properties such as UV-visible, Steady state fluorescence, Time resolved fluorescence were already described in **Chapter 3** and the same was followed for this chapter also.

4.10. ^{1}H and ^{13}C NMR Spectra of Few Selected Peptides and Intermediates

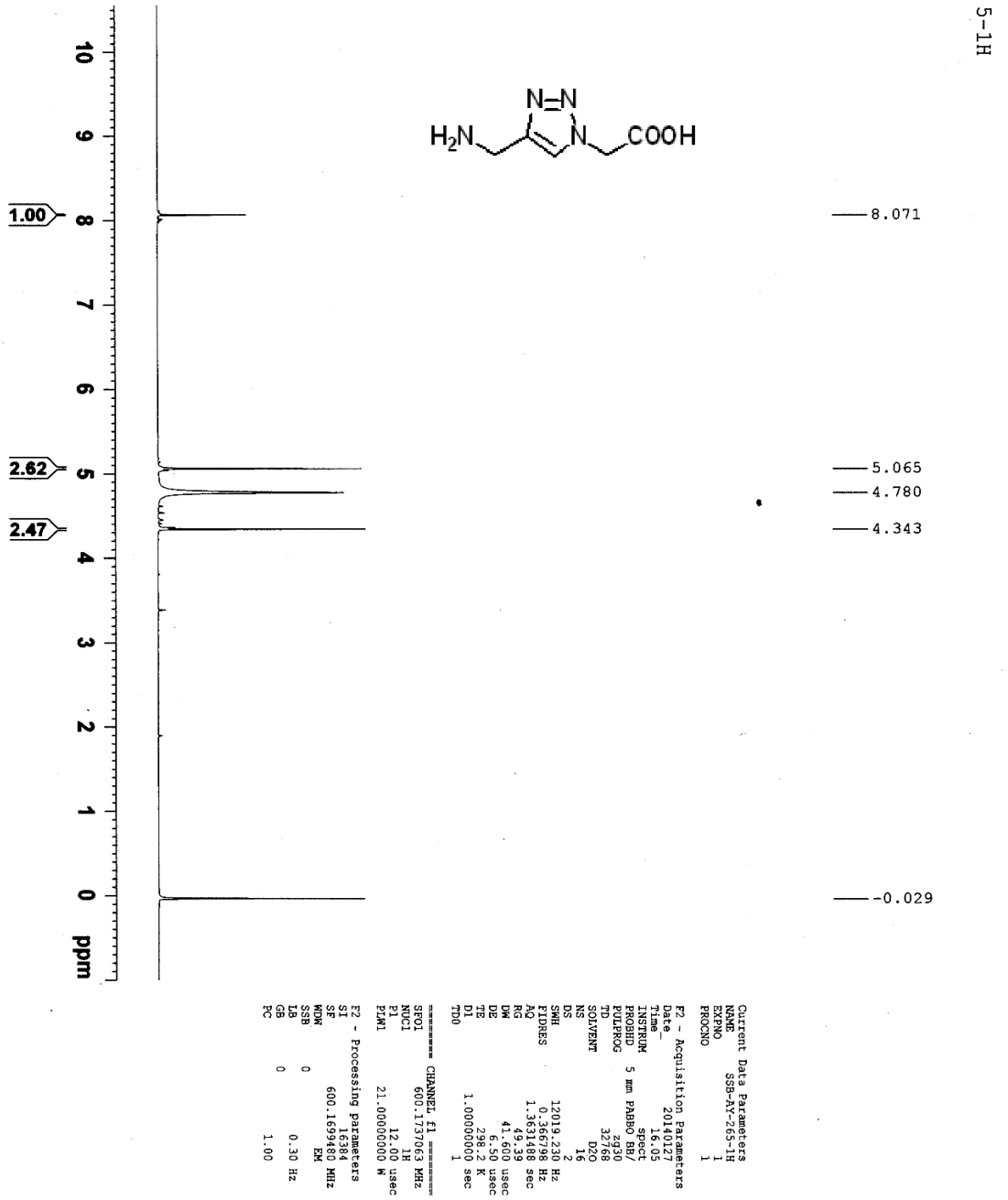

Figure 4.26. ^{1}H NMR spectra of synthesized compound **4.100.**

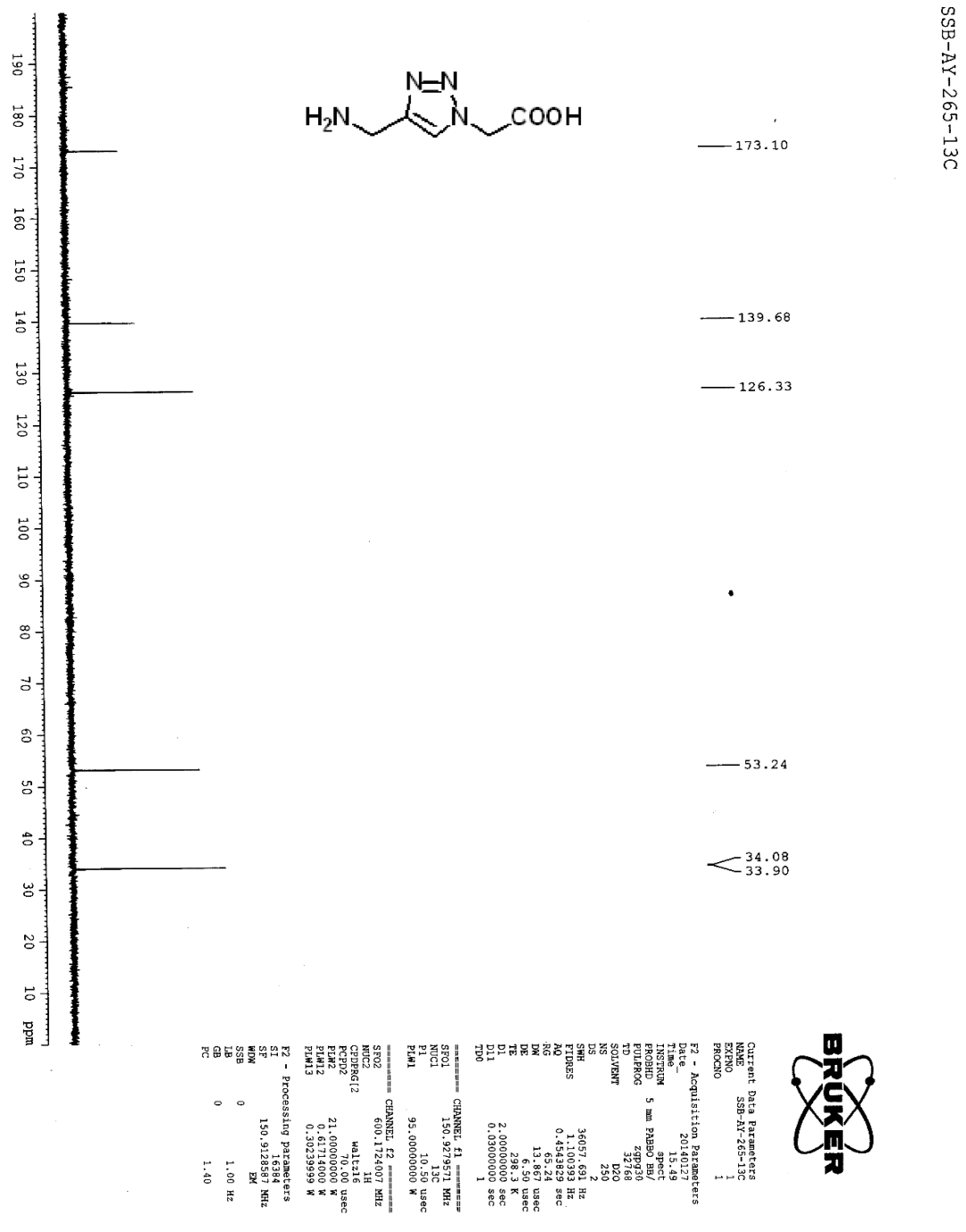

Figure 4.27. ^{13}C NMR spectra of synthesized compound **4.100.**

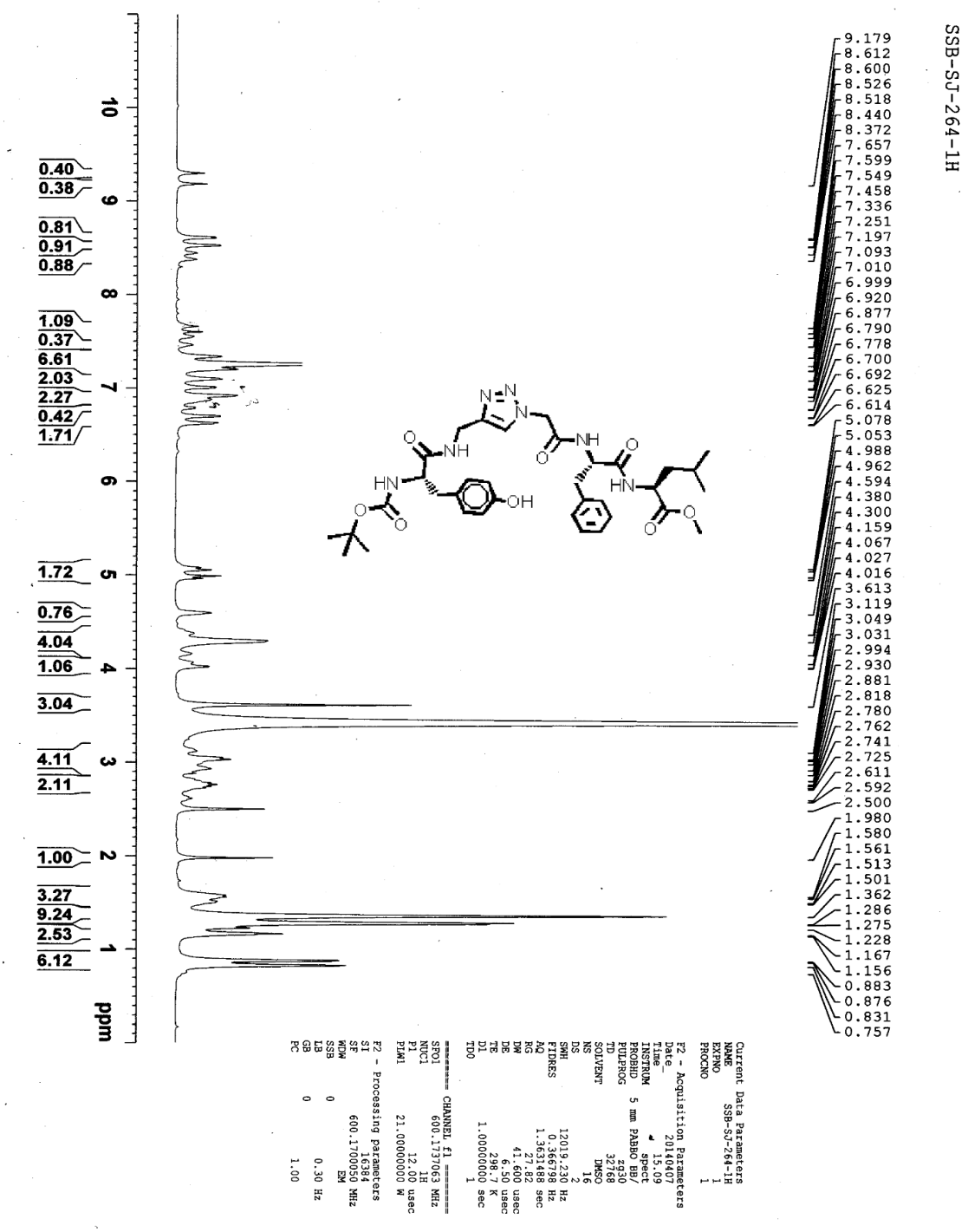

Figure 4.28. ^{1}H NMR spectra of synthesized compound **4.102.**

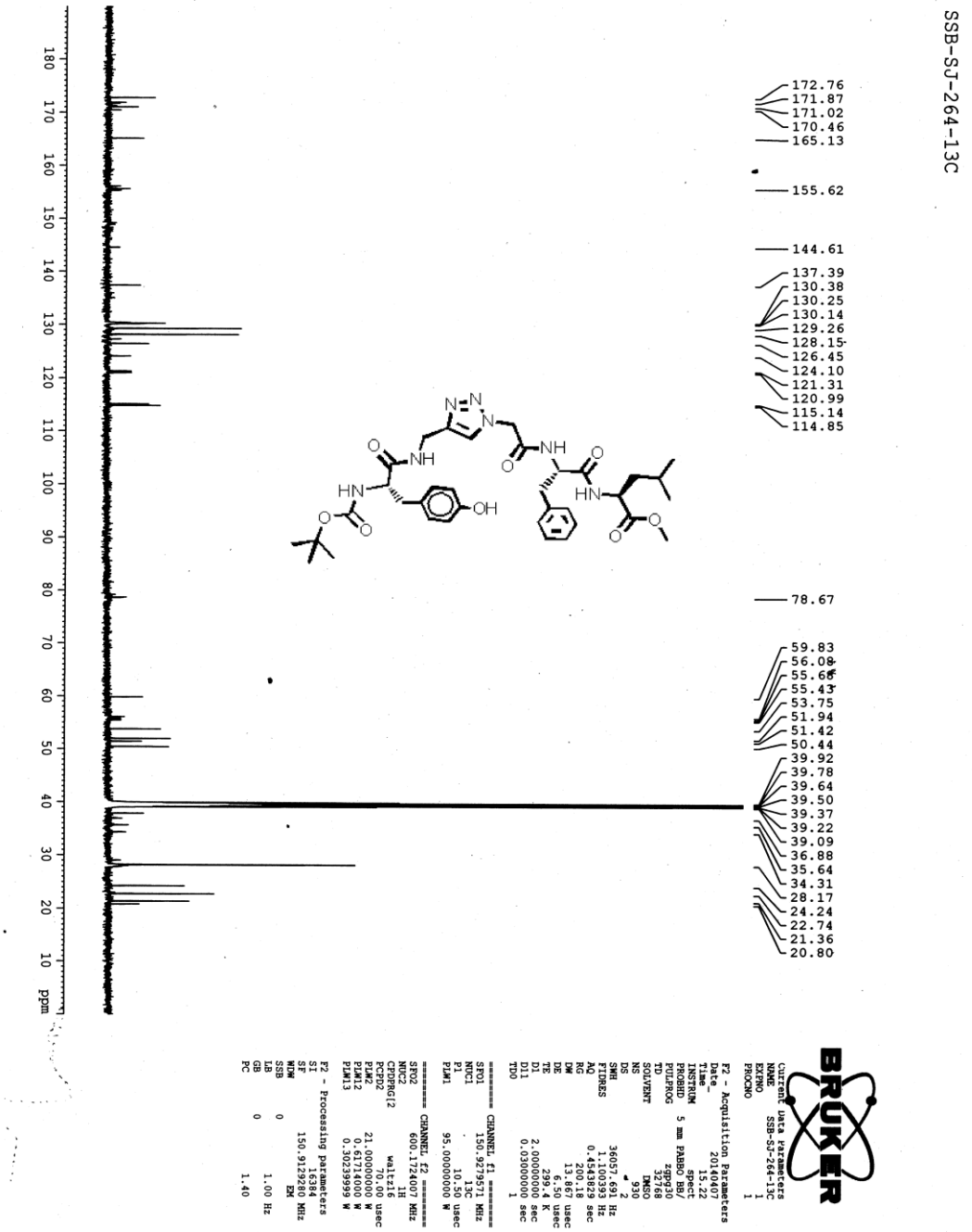

Figure 4.29. ^{13}C NMR spectra of synthesized compound **4.102.**

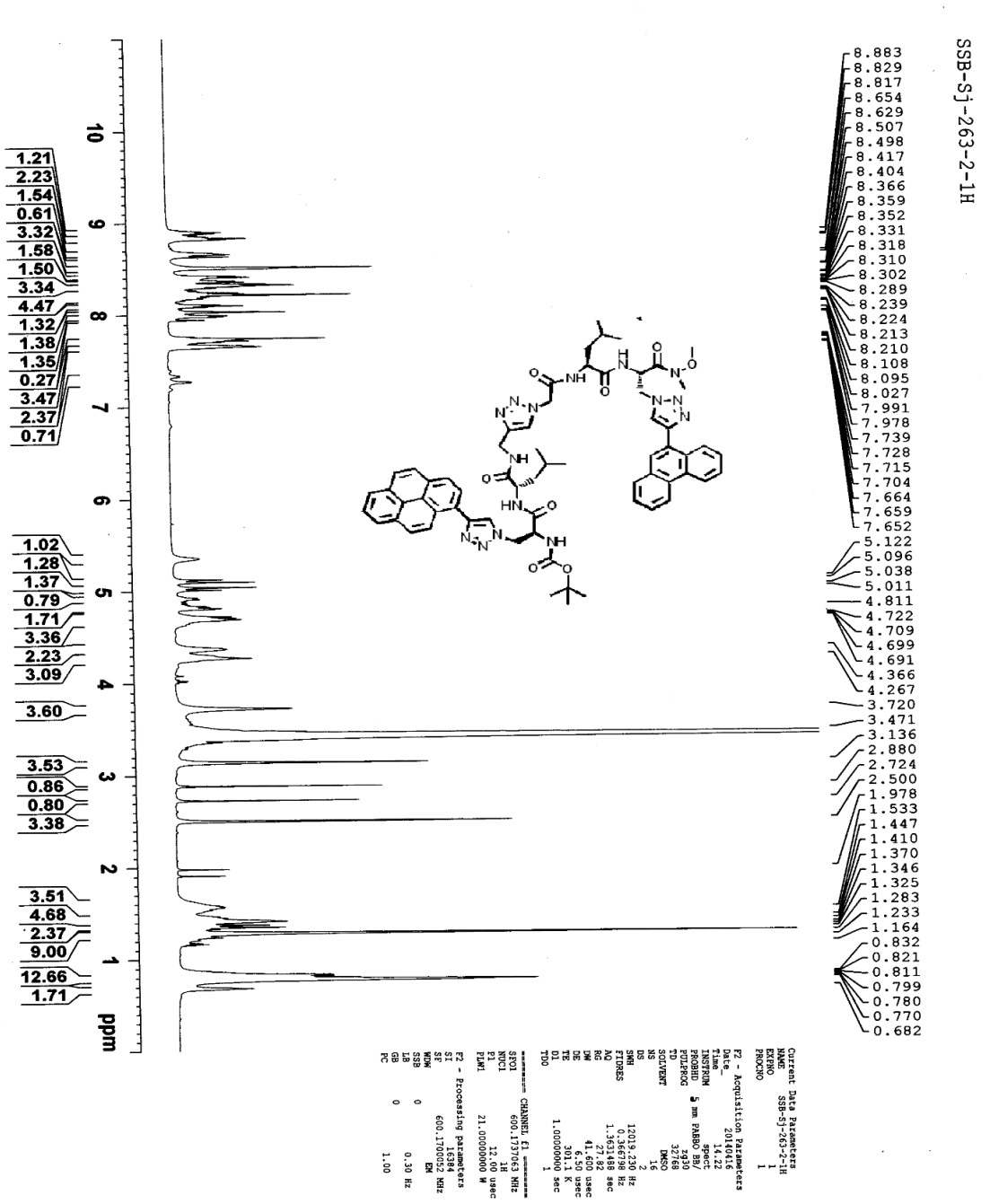

Figure 4.30. ^{1}H NMR spectra of synthesized compound **4.103.**

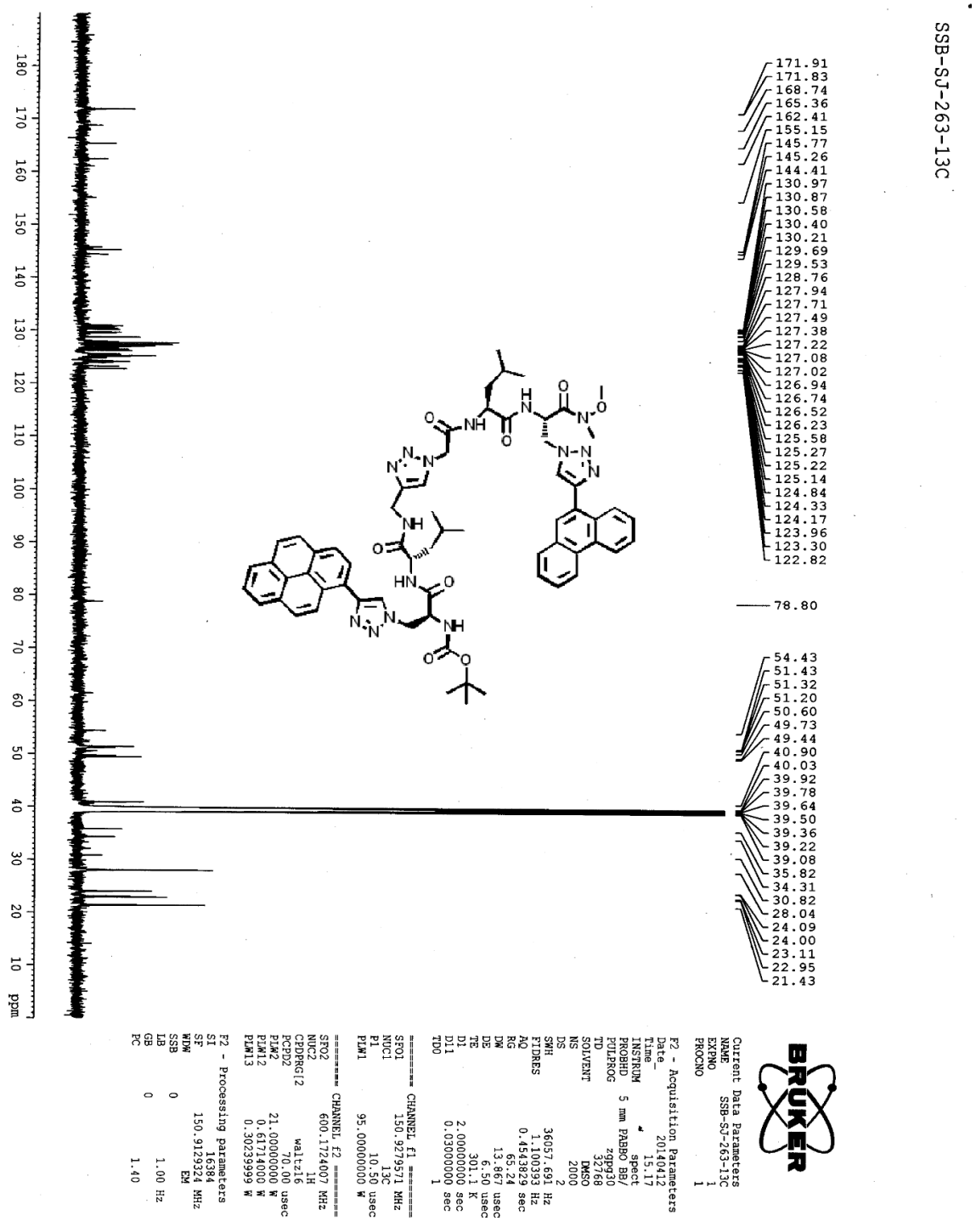

Figure 4.31. ^{13}C NMR spectra of synthesized compound **4.103.**

4.11. References

1. Giannis, A.; Kolter, T. *Angew. Chem., Int. Ed. Engl.*, **1993,** *32*, 1244.
2. Gante, J. *Angew. Chem., Int. Ed. Engl.* **1994**, *33*, 1699.
3. Adessi, C. Soto, C. *Curr. Med. Chem.* **2002**, *9*, 963.
4. Liskamp, R. M. J. *Recl. Trav. Chim. Pays-Bas* **1994**, *113*, 1.
5. Olson, G. L.; Bolin, D. R.; Bonner, M. P. *J. Med. Chem.* **1993**, *36*, 3039.
6. Farmer, P.S. *Drug Design*, (ed E.J. Ariëns), Academic Press, New York, **1980**, 119.
7. Marshall, G. R. *Tetrahedron* **1993**, *49*, 3547.
8. Ripka, A. S.; Rich, D. H. *Curr. Opin. Chem. Biol.*, **1998**, *2*, 441.
9. Toniolo, C.; Crisma, M.; Valle, G. *Peptide Res.* **1989**, *2*, 275
10. Samanen, J.; Cash, T.; Narindray, D. *J. Med. Chem.* **1991,** *34*, 3036.
11. Hart, S. A.; Etzkorn, F. A. *J. Org. Chem.* **1999**, *64*, 2998.
12. Wang, X. J.; Xu, B.; Mulllins, A. B. *J. Am. Chem. Soc.* **2004**, *126*, 15533.
13. (a) Karle, I. L.; Balaram, P. *Biochemistry,* **1990**, *29*, 6747. (b) Thorsett, E. D.; Harris, E. E.; Aster, S. D. *Biochem. Biophys. Res. Commun.*, **1983**, *111*, 166.
14. (a) Rodriguez, M.; Dubreuil, P.; Bali, J. P. Martinez, J. *J. Med. Chem.*, **1987**, *30*, 758. (b) Simon, R. J.; Kania, R. S.; Zuckermann, R. N. *Proc. Natl. Acad. Sci. U.S.A.* **1992**, *89*, 9367.
15. Choudhary, A.; Raines, R. T. *ChemBioChem*. **2011**, *12*, 1801.
16. Burger, A.; *Prog. Drug Res*. **1991**, *37*, 288.
17. Patani, G. A.; LaVoie, E. J. *Chem. Rev*. **1996**, *96*, 3147.
18. Langmuir, I. *J. Am. Chem. Soc*. **1919**, *41*, 1543.
19. (a) Erlenmeyer, H.; Berger, E. *Biochem. Z.* **1932**, *252*, 22. (b) Erlenmeyer, H.; Berger, E.; Leo, M *Helv. Chim. Acta* **1933**, *16*, 733.
20. Friedman, H. *LNAS-NRS*: Washington, DC, **1951**, *206*, 295.
21. Thornber, C. W. *Chem. Soc. Rev*. **1979**, 8, 563.
22. (a) Lipinski, C. A. *Annu. Rep. Med. Chem*. **1986**, *21*, 283. (b) Wermuth, C. G. Ed. Academic Press: San Diego, CA, **1996**; Chapters 12-16, pp 181-310 (2nd ed., **2003**). (c) Olsen, P. H. *Curr. Opin. Drug Discovery Dev*. **2001**, *4*, 471.
23. (a) Sheridan, R. P. *J. Chem. Inf. Comput. Sci*. **2002**, *42*, 103. (b) Wermuth, C. G. *Drug Discov. Today* 2005, 11, 348–354. (c) Lima, L. M.; Barriero, E. J. *Curr. Med. Chem*. **2005**, *12*, 23.
24. (a) Peterlin-Mǎsic, L. Kikelj, D. *Tetrahedron*, **2001**, *57*, 7073. (b) Peterlin-Mǎsic, L. *Curr. Med. Chem.* **2006,** *13*, 3627.
25. Marinozzi, M.; Natalini, B.; Constantino, G. *Farmaco*, **1996,** *51*, 121.
26. Burgus, R.; Ling, N.; Butcher, M.; Guillemin, R. *Proc. Natl. Acad. Sci. U.S.A.* **1973**, *70*, 684.
27. (a) Blackwell, H. E.; Grubbs, R. H. *Angew. Chem., Int. Ed.*, **1998**, *37*, 3281. (b) Blackwell, H. E.; Sadowsky, J. D.; Howard, R. J. *J. Org. Chem.*, **2001**, *66*, 5291.

28. (a) Grauer, A.; König, B. *Eur. J. Org. Chem.*, **2009,** 5099. (b) March, D. R.; Abbenante, G.; Bergman, D. A. *J. Am. Chem. Soc.*, **1996,** 118, 3375.

29. Adessi, C.; Soto, C. *Curr. Med. Chem.*, **2002,** *9*, 963.

30. Chakravarty, S.; Mavunkel, B. J.; Goehring, R. R.; Kyle, D. J. *Immunopharmacology*, **1996,** *33*, 61.

31. (a) Hirschmann, R.; Nicolaou, K. C.; Pietranico, S.; Salvino, J.; Leahy, E. M.; Sprengeler, P. A.; Furst, G.; Smith, A. B. *J. Am. Chem. Soc.* **1992**, *114*, 9217. (b) Hirschmann, R. *J. Am. Chem. Soc.* **1993**, *115*, 12550.

32. Hirschmann, R.; Sprengeler, P. A.; Kawasaki, T.; Leahy, J. W.; Shakespeare, W. C.; Smith, A. B. *J. Am. Chem. Soc.* **1992**, *114*, 9699.

33. Mowery, B. P.; Prasad, V.; Kenesky, C. S.; Angeles, A. R.; Taylor, L. L.; Feng, J. J.; Chen, W. L.; Lin, A.; Cheng, F. C.; Smith, A. B.; Hirschmann, R. *Org. Lett.* **2006**, *8*, 4397.

34. (a) Kim, I. C.; Hamilton, A. D. *Org. Lett.* **2006**, *8*, 1751. (b) Yin, H.; Lee, G.; Sedey, K. A.; Kutzki, O.; Park, H. S.; Orner, B. P.; Ernst, J. T.; Wang, H.-G.; Sebti, S. M.; Hamilton, A. D. *J. Am. Chem. Soc.* **2005**, *12* 10191. (c) Davis, J. M.; Truong, A.; Hamilton, A. D. *Org. Lett.* **2005**, *7*, 5405.

35. Ernst, J. T.; Becerril, J.; Park, H.; Yin, H.; Hamilton, A. D. *Angew. Chem., Int. Ed.* **2003**, *42*, 535.

36. (a) Kutzki, O.; Park, H. S.; Ernst, J. T.; Orner, B. P.; Yin, H.; Hamilton, A. D. *J. Am. Chem. Soc.* **2002**, *124*, 11838. (b) Peczuh, M. W.; Hamilton, A. D. *Chem. Rev.* **2000**, *100*, 2479. (c) Wilson, A. J.; Hong, J.; Fletcher, S.; Hamilton, A. D. *Org. Biomol. Chem.* **2007**, *5*, 276. (d) Davis, J. M.; Tsou, L. K.; Hamilton, A. D. *Chem. Soc. Rev.* **2007**, *36*, 326. (e) Becerril, J.; Hamilton, A. D. *Angew. Chem., Int. Ed.* **2007**, *46*, 4471.

37. (a) Fletcher, S.; Hamilton, A. D. *Curr. Top. Med. Chem.* **2007**, *7*, 922. (b) Yin, H.; Lee, G. I.; Hamilton, A. D. *Drug Discovery Res.* **2007**, 281. (c) Yin, H.; Hamilton, A. D. In *Chemical Biology: From Small Molecules to System Biology and Drug Design*; Schreiber, S. L., Kapoor, T. M., Wess, G., Eds.; Wiley-VCH: Weinheim, **2007**; Vol. 1, pp 250-269. (d) Becerril, J.; Rodriguez, J. M.; Saraogi, I.; Hamilton, A. D. *Foldamers* **2007**, 195. (e) Rodriguez, J. M.; Hamilton, A. D. *Angew. Chem., Int. Ed.* **2007**, *46*, 8614. (f) Fletcher, S.; Hamilton, A. D. *J. R. Soc., Interface* **2006**, *3*, 215..

38. (a) Jacoby, E. *Bioorg. Med. Chem. Lett.* **2002**, *12*, 891. (b) Jiang, H.; Leger, J. M.; Huc, I. *J. Am. Chem. Soc.* **2003**, *125*, 3448. (c) Che, Y.; Brooks, B. R.; Marshall, G. R. *J. Comput.-Aided Mol. Des.* **2006**, *20*, 109. (d) Okuyama, M.; Laman, H.; Kingsbury, S. R.; Visintin, C.; Leo, E.; Eward, K. L.; Stoeber, K.; Boshoff, C.; Williams, G. H.; Selwood, D. L. *Nat. Methods* **2007**, *4*, 153. (e) Ahn, J. M.; Han, S. Y. *Tetrahedron Lett.* **2007**, *48*, 3543. (f) Ahn, J. -M.; Han, S. -Y. *Tetrahedron Lett.* **2007**, *48*, 3543. (g) Volonterio, A.; Moisan, L.; Rebek, J. Jr. *Org. Lett.* **2007**, *9*, 3733. (h) Shaginian, A.; Whitby, L. R.; Hong,

S.; Hwang, I.; Farooqi, B.; Searcey, M.; Chen, J.; Vogt, P. K.; Boger, D. L. *J. Am. Chem. Soc.* **2009**, *131*, 5564.

39. (a) Yin, H.; Lee, G.; Sedey, K. A.; Kutzki, O.; Park, H. S.; Orner, B. P.; Ernst, J. T.; Wang, H. -G.; Sebti, S. M.; Hamilton, A. D. *J. Am. Chem. Soc.* **2005**, *127*, 10191. (b) Davis, J. M.; Truong, A.; Hamilton, A. D. *Org. Lett.* **2005**, *7*, 5405. (c) Kutzki, O.; Park, H. S.; Ernst, J. T.; Orner, B. P.; Yin, H.; Hamilton, A. D. *J. Am. Chem. Soc.* **2002**, *124*, 11838. (d) Yin, H.; Lee, G. -I.; Hamilton, A. D. *Drug Disco*V*ery Res.* **2007**, 281. (e) Becerril, J.; Rodriguez, J. M.; Saraogi, I.; Hamilton, A. D. *Foldamers* **2007**, 195.

40. (a) Orner, B. P.; Ernst, J. T.; Hamilton, A. D. *J. Am. Chem. Soc.* **2001**, *123*, 5382. (b) Ellard, J. M.; Zollitsch, T.; Cummins, W. J.; Hamilton, A. L.; Bradley, M. *Angew. Chem. Int. Ed.* **2002**, *41*, 3233. (c) Yin, H.; Lee, G. -i.; Park, H. S.; Payne, G. A.; Rodriguez, J. M.; Sebti, S. M.; Hamilton, A. D. *Angew. Chem., Int. Ed.* **2005**, *44*, 2704.

41. (a) Ernst, J. T.; Becerril, J.; Park, H.; Yin, H.; Hamilton, A. D. *Angew. Chem., Int. Ed.* **2003**, *42*, 535. (b) Davis, J. M.; Tsou, L. K.; Hamilton, A. D. *Chem. Soc. Rev.* **2007**, *36*, 326. (c) Yin, H.; Lee, G. -I.; Hamilton, A. D. *Drug Discovery Res.* **2007**, 281. (d) Rodriguez, J. M.; Hamilton, A. D. *Tetrahedron Lett.* **2006**, *47*, 7443. (e) Marimganti, S.; Cheemala, M. N.; Ahn, J .-M. *Org. Lett.* **2009**, *11*, 4418.

42. (a) Cheng, R. P.; Gellman, S. H.; DeGrado, W. F. *Chem. Rev.* **2001**, *101*, 3219. (b) Davis, J. M.; Tsou, L. K.; Hamilton, A. D. *Chem. Soc. Rev.* **2007,** *36*, 326. (c) Bautista, A. D.; Craig, C. J.; Harker, E. A.; Schepartz, A. *Curr. Opin. Chem. Biol.* **2007,** *11*, 685. (d) Garner, J.; Harding, M. M. *Org. Biomol. Chem.*, **2007,** *5*, 3577. (e) Goodman, C. M.; Choi, S.; Shandler, S.; DeGrado, W. F. *Nat. Chem. Biol.*, **2007,** *3*, 252. (f) Murray, J. K.; Gellman, S. H. *Biopolymers*, **2007**, *88*, 657.

43. (a) Chou, P. Y.; Fasman, G. D. *J. Mol. Biol*. **1977**, *115*, 135. (b) Rose, G. D.; Gierasch, L. M.; Smith, J. A. *Adv. Protein Chem*. **1985**, *37*, 1. (c) Stanfield, R. L.; Fieser, T. M.; Lerner, R. A.; Wilson, I. A. Science, **1990**, *248*, 712.

44. (a) Belvisi, L.; Gennari, C.; Mielgo, A. *Eur. J. Org. Chem*. **1999**, 389. (b) Creighton, C. J.; Leo, G. C.; Du, Y.; Reitz, A. B. *Bioorg. Med. Chem*. **2004**, *12*, 4375.

45. (a) Nagai, U.; Sato, K. *Tetrahedron Lett*. **1985,** *26*, 647. (b) Feigel, M. *J. Am. Chem. Soc*. **1986**, *108*, 181. (c) Diaz, H.; Espina, J. R.; Kelly, J. W. *J. Am. Chem. Soc*. **1992**, *114*, 8316. (d) Genin, M. J. Johnson, R. L. *J. Am. Chem. Soc*., **1992**, *114*, 8778.

46. Zhang, W. J.; Berglund, A.; Kao, J. L. -F. *J. Am. Chem. Soc*. **2003**, *125*, 1221.

47. Trabocchi, A.; Potenza, D.; Guarna, A. *Eur. J. Org. Chem*. **2004**, 4621.

48. (a) Haque, T. S.; Gellman, S. H. *J. Am. Chem. Soc.* **1997,** *119*, 2303. (b) Kemp, D. S. Sites, W. E. *Tetrahedron Lett.*, **1988**, *29*, 5057. (c) Brandmeier, V.; Feigel, M. *Angew. Chem.* **1989**, *102*, 466. (d) Gardner, B.; Nanashi, H.;

Khan, M. *Tetrahedron*, **1993,** *49*, 3433. (e) Nagai, U.; Sato, K.; Nakamura, R.; Kato, R. *Tetrahedron*, **1993,** *49*, 3577. (f) Gardner, R. R.; Liang, G. -B. Gellman, S. H. *J. Am. Chem. Soc.* **1995**, *117*, 3280.

49. (a) Schneider, J. P.; Kelly, J. W. *J. Am. Chem. Soc*. **1995**, *117*, 2533. (b) Kemp, D. S.; Li, Z. Q. *Tetrahedron Lett*. **1995**, *36*, 4179. (c) Nowick, S.; Smith, E. M.; Noronha, G. *J. Org. Chem*. **1995**, *60*, 7386. (d) Nesloney, C. L.; Kelly, J. W. *J. Am. Chem. Soc*. **1996**, *118*, 5836. (e) Holmes, D. L.; Smith, E. M.; Nowick, J. S. *J. Am. Chem. Soc*. **1997**, *119*, 7655. (f) Smith, E. M.; Holmes, D. L.; Shaka, A. J.; Nowick, J. S. *J. Org. Chem.* **1997,** *62*, 7906. (g) Krauthäuser, S.; Christianson, L. A.; Powell, D. R.; Gellman, S. H. *J. Am. Chem. Soc*. **1997**, *119*, 11719.

50. (a) Haque, T. S.; Little, J. C.; Gellman, S. H. *J. Am. Chem. Soc*. **1996**, *118*, 6975. (b) Welsh, J. H.; Zerbe, O.; von Philipsborn, W.; Robinson, J. A. *FEBS Lett.* **1992**, *297*, 216.

51. (a) Gellman, S. H.; Daughtery, D. L. *J. Am. Chem. Soc.* **1999**, *121*, 4325. (b) Kolb, H. C.; Finn, M. G.; Sharpless, B. K *Angew. Chem., Int. Ed.* **2001**, *40*, 2004.

52. (a) Gante, J. *Angew. Chem., Int. Ed. Engl*. **1994,** *33*, 1699. (b) Giannis, A.; Kolter, T. *Angew. Chem., Int. Ed. Engl*. **1993**, 32, 1244.

53. (a) Tornøe, C. W.; Christensen, C.; Meldal, M. *J. Org. Chem*. **2002**, 67, 3057, (b) Angell, Y.; Burgess, K. *J. Org. Chem*. **2005**, *70*, 9595. (c) Lin, H.; Walsh, C. T. *J. Am. Chem. Soc*. **2004,** *126*, 13998. (d) Arosio, D.; Bertoli, M.; Manzoni, L.; Scolastico, C.; *Tetrahedron Lett*. **2006**, *47*, 3697.

54. Belvisi, L.; Colombo, L.; Manzoni, L.; Potenza, D.; Scolastico, C. *Synlett*, **2004**, *9*, 1449. (b) Belvisi, L.; Bernardi, A.; Manzoni, L.; Potenza, D.; Scolastico, C. *Eur. J. Org. Chem.* **2000**, 2563. (c) Belvisi, L.; Gennari, C.; Mielgo, A.; Potenza, D.; Scolastico, C. *Eur. J. Org. Chem*. **1999**, 389.

55. Kolb, H. C.; Sharpless, K. B. *Drug Discov. Today* **2003**, *8*, 1128.

56. (a) Himo, F.; Lovell, T.; Hilgraf, R. *J. Am. Chem. Soc.* **2005,** *127*, 210. (b) Bock, V. D.; Hiemstra, H.; van Maarseveen, J. H. *Eur. J. Org. Chem.*, **2006,** 68.

57. (a) Tron, G. C.; Pirali, T.; Billington, L. A. *Med. Res. Rev*. **2008**, *28*, 278. (b) Davis, M. R.; Singh, E. K.; Wahyudi, H. *Tetrahedron* **2012**, *68*, 1029.

58. Bock, V. D.; Speijer, D.; Hiemstra, H.; van Maarseveen, J. H. *Org. Biomol. Chem*. **2007**, *5*, 971.

59. (a) Brik, A.; Muldoon, J.; Lin, Y. -C. *ChemBioChem* **2003**, *4*, 1246. (b) Brik, A.; Alexandratos, J.; Lin, Y. -C. *ChemBioChem*, **2005**, *6*, 1167.

60. (a) Darnell, J. E. Jr. *Nat. Rev. Cancer* **2002**, *2*, 740. (b) Yu, H.; Jove, R. *Nat. Rev. Cancer* **2004**, *4*, 97. (c) Chen, J.; Nikolovska-Coleska, Z.; Yang, C.-Y.; *Bioorg. Med. Chem. Lett*. **2007**, *17*, 3939.

61. (a) Horne, W. S.; Yadav, M. K.; Stout, C. D.; Ghadiri, M. R. *J. Am. Chem. Soc*. **2004**, *126*, 15366. (b) Oh, K.; Guan, Z. *Chem. Commun*., **2006**, 3069.

62. Liu, Y.; Diaz, D. D.; Accurso, A. A. *J. Polym. Sci., Part A: Polym. Chem*. **2007**, *45*, 5182.

63. Ko, E.; Liu, J.; Perez, L. M.; Lu, G.; Schaefer, A.; Burgess, K. *J. Am. Chem. Soc.* **2011**, *133*, 462.

64. Liu, Y.; Zhang, L.; Wan, J. *Tetrahedron*, **2008,** *64*, 10728.

65. (a) Garanger, E.; Boturyn, D.; Dumy, P. *Anticancer Agents Med. Chem*. **2007**, *7*, 552. (b) Haubner, R.; Decristoforo, C. *Front Biosci*. **2009**, *14*, 872. (c) Tateishi, U.; Oka, T.; Inoue, T. *Curr. Med. Chem*. **2012,** *19*, 3301.

66. Trabocchi, A.; Menchi, G.; Cini, N. *J. Med. Chem.* **2010,** *53*, 7119.

67. Chouhan, G.; James, K. *Org. Lett*. **2013**, *15*, 1206.

68. (a) Rostovtsev, V. V.; Green, L. G.; Fokin, V. V.; Sharpless, K. B. *Angew. Chem., Int. Ed.* **2002**, *41*, 2596. (b) Meldal, M.; Tornøe, C. W. *Chem. Rev.* **2008**, *108*, 2952.

69. (a) Woody, R. W. In *Circular Dichroism. Principles and Applications;* Nakanishi, K. Berova, N.; Woody, R. W. Eds., **1994**, 473–496, VCH, New York. (b) Proulx, C.; Lubell, W. D. *J. Org. Chem.* **2010**, *75*, 5385. (c) Chen, Y. H.; Yang, J. T. *Biochem. Biophys. Res. Commun.*, **1971**, *44*, 1285. (d) Krysmann, M. J.; Castelletto, V.; Kelarakis, A.; Hamley, I. W.; Hule, R. A.; Pochan, D. J. *Biochemistry* **2008**, *47*, 4597.

70. (a) Oh, K.; Guan, Z. *Chem. Commun*., **2006**, 3069. (b) Feher-Voelger, A.; Borges-Gonzlez, J.; Carrillo, R.; Morales. E. Q.; Gonzlez-Platas, J.; Martn, T. *Chem. Eur. J.* **2014**, *20*, 1.

71. Kessler, H. *Angew. Chem., Int. Ed. Engl.*, **1982**, *21*, 512.

72. (a) MacroModel, Version 9.9 Schrodinger, LLC, New York, NY, **2012**. (b) Kolossvry, I. W.; Guida, C. *J. Am. Chem. Soc.***1996**, *118*, 5011.

73. (a) Zhang, Y.; Jiang, M.; Han, G. –C.; Zhao, K.; Tang, B. Z.; Wong, K. S. *J. Phys. Chem. C* **2015**, *119*, 27630. (b) Dobkowski, J.; Kijak, M.; Sazanovich, I. V.; Waluk, J. *J. Phys. Chem. B* **2015**, *119*, 7294. (d) Kobayashi, A.; Takehira, K.; Yoshihara, T.; Uchiyama, S.; Tobita, S. *Photochem. Photobiol. Sci.* **2012**, *11*, 1368.

74. (a) Förster, T. *Discuss. Faraday Soc.* **1959**, 7. (b) Rogers, J. M. G.; Lippert, L. G.; Gai, F. *Anal. Biochem.* **2010**, *399*, 182. (c) Nedumparaa, R. J.; Manua, P. J.; Vallabhanb, C. P. G.; Nampooria, V. P. N.; Radhakrishnana, P. *Opt. Laser Tech.* **2008**, *40*, 953. (d) Banerjee, C.; Kundu, N.; Ghosh, S.; Mandal, S.; Kuchlyan, J.; Sarkar, N. *J. Phys. Chem. B* **2013**, *117*, 9508.

Chapter 5

DESIGN AND SYNTHESIS OF AROMATIC TRIAZOLO AMINO ACID AS CONFORMATIONALLY CONSTRAINED MOLECULER SCAFFOLD AND ITS APPLICATION IN β –SHEET NEUCLEATING PEPTIDOMIMETICS AND SENSING BSA PROTEIN

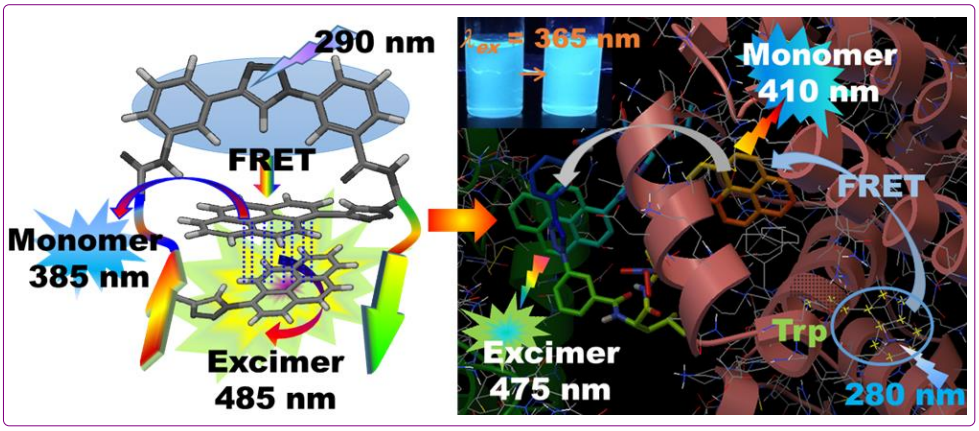

5.1. Introduction: Importance of β-Sheet Peptidomimetic

Defining β-Sheet: The simplest peptide structural element is the β-strand that is a linear or saw-toothed arrangement of amino acids. In β-strand the amide bonds are almost coplanar and side chains alternating above and below the plane of the peptide backbone with no intramolecular hydrogen bonds between the amino acid residues (**Figure 5.1**). The β-strands are the fundamental structural elements recognized by biomolecular receptors though isolated β-strands are not common.[1, 2] A pair of β-strands are usually found hydrogen bonded form which gives them stability and ultimately the network form is known as β-sheet structures in proteins. The β-sheet or β-pleated sheet is the second form of regular secondary structure in proteins. It is only somewhat less common than alpha helix. The β-sheets not only act as important scaffolding elements to stabilize protein structures, but also are the key recognition motifs that bind to other proteins or DNA. The β-sheet secondary structure of peptides/proteins accounts for over 30% of all protein structure.

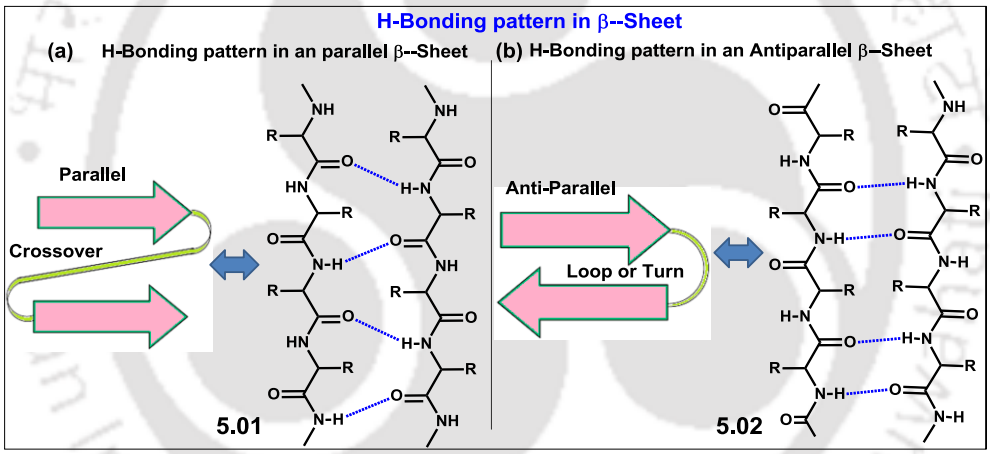

Figure 5.1. The structure of β-sheets- (a) parallel and (b) anti-parallel.

Types of β-Sheet: According to the interstrand H-bonded arrangement of a pair of β-strand β-sheets are of three types-(a) parallel, (b) antiparallel, or (c) mixed. As for an example structures of Lectin and Carbonic anhydrase are anti-parallel β-sheets and parallel β-sheet, respectively. While parallel β-sheets contain strands that run in the same direction and are characterized by a series of 12-membered hydrogen-bonded rings (**Figure 5.1a**), the strands of antiparallel β-sheets run in opposite directions and are characterized by an alternating series of 10- and 14-membered hydrogen-bonded rings (**Figure 5.1.b**). Mixed β-sheets contain mixtures of both patterns. The β-pleated sheets are defined as a state of optimal hydrogen-bonding interactions between strands, forcing contiguous side chains to opposite sides of the peptide chain. The dihedral angles commonly found in various β-sheets are given below in **Table 5.1.**

Table 5.1. Ideal Phi (Φ) and Psi (Ψ) Angles for a β-sheet in comparison to a-helix and one β-turn

	secondary structure	Φ	Ψ
	parallel β-sheet	−119	113
	antiparallel β-sheet	−139	135
	α-helix	−58	−47
	β-turn Type I	−60	−30

Importance of β-sheet: The β-sheet plays mainly a scaffolding role in protein architecture. However, it often acts as a key recognition motif in some protein−protein and protein−DNA interactions that are important in many biological processes and in some diseases. As for an example, the higher-level association of β-sheets has been implicated in formation of the protein aggregates and fibrils responsible for generating many human diseases, notably the amyloidoses such as Alzheimer's disease.[4] Normal gene regulation by the *met* repressor requires its dimerization through β-sheet domains. The resulting β-sheet is known to recognize the major groove of DNA.[5] Two Arc represser protein dimers in the β-sheet form can bind and make complex with 21-base-pair DNA duplex. The antiparallel β-sheet is formed from a single strand from each monomer that binds to the center of the major groove of DNA (**Figure 5.2a**).[6] An extensive β-sheet interactions between the TATA box-binding protein (TBP) and DNA was also reported involving hydrogen bonds, van der Waals interactions, and base stacking interactions with phenyl alanine (**Figure 5.2b**).[7-8] Silk and spider webs are the real examples of naturally occurring β-sheets.[9] HIV virus requires a β-strand mediated interaction of viral gp-120 with CD4 receptors located on the surface of target immune cells causing infection of human.[10]

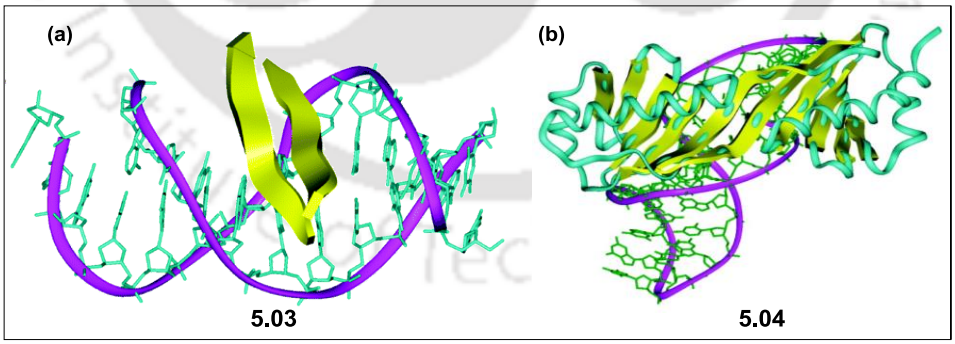

Figure 5.2. DNA recognition of β-sheets. (a) Complex of two arc repressor protein dimers with DNA illustrating the β-sheet interaction (PDB entry: 1par). (b) Positioning of the β-sheet of TATA box-binding protein (TBP) over the DNA strand (PDB entry: 1ytb).

Therefore, design of β-sheet conformation of a peptide or protein is highly important which could find application as competitive ligands for receptors/enzymes that typically bind to β-sheets, or as inhibitors of β-sheet formation when β-sheets themselves are undesirable. However, use of small natural peptides having β-sheet conformation for such purpose is not feasible because of their low oral availability and poor pharmacokinetics as being degraded easily by endogeneous proteases. Therefore, to overcome the shortcomings mimicking the protein's β-sheet conformation is highly desirable. These secondary structure mimics could find applications in pharmacology. Although several reports exist for β-sheet mimetics,[11] there are currently no therapeutics involving β-sheet mimicry. However, β-sheet mimetics can provide useful information for the design of improved β-sheet mimetics.

5.2. Approaches to β-Strand Peptidomimetic to Antagonize β-Sheet

Examination of protein−protein interactions associated with disease, followed by the design of small molecules/peptides that can mimic or bind to one of the interacting proteins is often the basis of design of small molecule drugs or peptide based therapeutics. Drug in a small localized region of particular secondary structure.[12, 13] Again the drug bindings in proteins occurs only in a small localized region of a protein surface created by secondary structural elements (such as α-helices, β- or γ-turns, or β-strands/sheets). Therefore, the small molecules/peptidomimetics based on these structures are expected to act as antagonists. Often the bioactivity of proteins/peptides stems from mimicking β-strands to provoke β-sheet formation or recognition represents a viable therapeutic strategy toward the prevention or treatment of diseases associated with β-sheet structures.

The simplest approach for β-strand/sheet recognition would be to use short peptides corresponding to strand/sheet regions of proteins recognized by other proteins or DNA. However, short peptides suffer from a number of disadvantages which do not permit them to be valuable drug candidates-(a) they are conformationally flexible, (b) susceptible to proteolytic degradation, (c) have low bioavailability, (d) exhibit poor pharmacological profiles, and (e) poor membrane permeability.[14, 15] Thus, while biomolecular interactions with peptides provide very useful clues for drug design, changes need to be made to create more pharmacologically acceptable drug candidates.

The molecules which are conformationally preorganized and/or are fixed into shapes are expected to be recognized by a receptor with higher affinity due to the reduced entropy penalty for adopting the receptor-binding shape. However, unlike the case for turns and helices, there are only few reported conformationally restricted, surrogates for the β-strand. However, several reports exists which consider restricting the conformational freedom which is done via several ways-(a) Peptide macrocyclisation: (i) side chain to side chain, (ii) side chain to main chain, or (iii)

main chain to main chain linkages. (b) Incorporation of Conformational Constraints in Back Bone: One or more amino acid residues could be replaced in a peptide sequence by one or more rigid organic units. Such replacements can produce peptidomimetics with drug-like components.[16] Conformationally and metabolically stable peptidomimetics or nonpeptidic mimetics are the goals of β-strand mimicry. Therefore, design of small constraint molecules that mimic the β-strand for β-sheet formation is important research target.[17] A significant amount of advances have been made in the synthesis of conformationally constrained β-sheet mimetics. There exist several strategies for design of β-sheet conformation out of which β-sheet though nucleation strategy will be discussed below briefly.

5.3. β-Sheet Formation Through the Nucleation Strategy

β-Sheets are not only important for normal biological activities, but also involved in many diseases including HIV, cancer, and neurodegenerative diseases. Therefore creating model systems that fold to form β-sheet-like structures or participate in intermolecular β-sheet interactions would provide valuable tools to study β-sheet folding and interactions.[18] β-sheet formation can be adopted by (a) designing β-strand mimetics and/or (b) nucleation strategy. The nucleation to b-sheet is highly interesting and can be arrived via the use of (i) natural amino acid as b-sheet nucleator or (ii) synthetic scaffold/template as nucleator of β-sheet. In artificial β-sheets, β-turn mimics, β-strand mimics, and other templates help nucleate and stabilize β-sheet structures or enforce intermolecular β-sheet interactions.[19]

β-Turn mimics induce β-sheet/β-Hairpins structure: Reverse turns induce β-sheet structure in proteins by aligning protein chains. β-Turn mimics have been used extensively to nucleate β-sheet folding in β-hairpins. As for example, Achiral α-aminoisobutyric acid (Aib) induces a β-turn conformation when combined with either a D-α-amino acid or an achiral α-amino acid. Thus, the β-turn peptides such as Gellman's *^{D}Pro-Gly*, Balaram's *Aib-^{D}Ala*, and achiral *Aib-Gly* (**Figure 5.3a**) all fold into superimposable β-hairpin structures in water. Collectively, these findings show that achiral turn units, like chiral turn units with appropriate chirality can induce. Balaram *et al*. reported several expanded β-turn mimics that contain ^{D}Pro in the $i + 1$ position and a β-, γ-, or δ-amino acid in the $i + 2$ position of a peptide strand and observed that peptide with a α,δ turn unit adopts a β-hairpin structure in solid state, while peptides with α,β and α,γ turn units adopt β-hairpin structures in methanol (**Figure 5.3b**).[20]

β-Turn mimics that undergo a rapid light-triggered conformational change permit studying β-sheet folding processes. It has been shown that the *cis* isomer of an *m,m′*-substituted azobenzene amino acid induces a β-hairpin conformation in peptides, while the *trans* isomer disfavors this conformation (**Figure 5.3c**).[21]

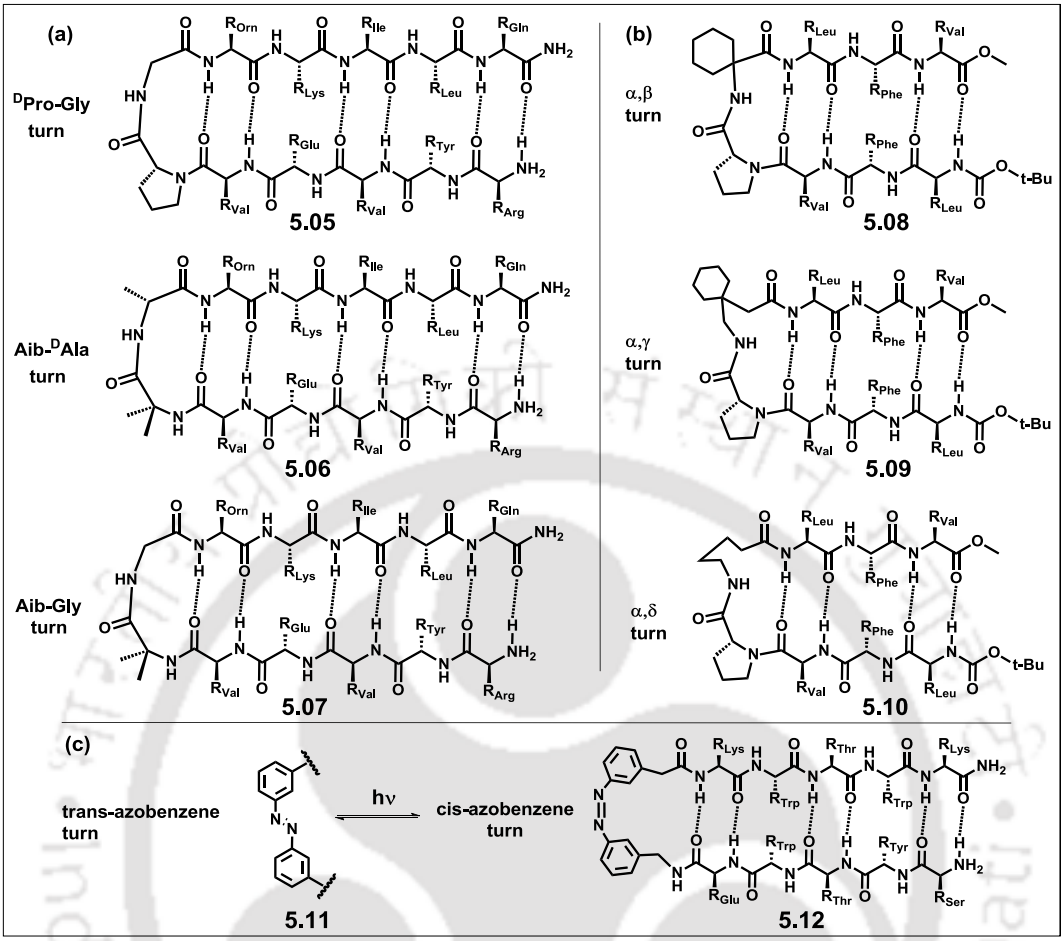

Figure 5.3. β-Turn mimics as nucleator for β-Hairpins. (a) β-Hairpins with Aib-based or *^{D}Pro-Gly* turn units. (b) β-Hairpins with extended α,β, α,γ, and α,δ turn units. (c) Light-controlled azobenzene-based turn unit as nucleator of β-hairpin.

Gogoll *et al*. reported an *m*, *m'*-substituted stilbene derivative in linear and cyclic peptides and observed that both the *cis* and *trans* isomers of the stilbene derivative fail to induce β-hairpin structures in methanol and in DMSO in linear peptides, however, only the *cis* isomer supports β-sheet folding in cyclic peptides containing both the stilbene turn unit and a *^{D}Pro-Gly* turn unit.[22] Several other research groups have reported new β-turn mimics that induce β-hairpin folding in peptides.[23, 24]

However, the most attractive and alternative approach to fold into β-sheet is the nucleation strategy by small molecules scaffolds/template which often is the β-turn mimetic. We will now examplify few selected templates which help nucleating b-sheet.

Constrained Small Molecular Scaffolds/Templates Nucleating β-Sheet: Molecular templates useable for generating folded, synthetic polypeptides may be used in two distinct ways. (a) First, the designed templates may represent or may provide a preorganized folding nucleus with properly oriented hydrogen-bonding

groups that sets up and propagate a regular secondary structure, such as β-sheet. (b) Second, the scaffold/templates may be used to organize proposed modules of secondary structure in order to generate compact tertiary folds. In this section, we consider few selected aromatic scaffold/templates used for nucleating β-sheet secondary structures.

The β-hairpin structures with H-bonded β-sheet arrangements are quite often nucleated by tight two-residue loops, β-turns. In the β-turn conformation of the template, chain reversal is achieved with the nucleus which can be stabilized by a 10-atom 4→1 hydrogen bond (**Figure 5.4**). Several templates for designing β-hairpin/β-sheet peptidomimetics have been synthetically constructed and their utility demonstrated in model sequences. **Figure 5.4** shows some representative templates that nucleate β-sheet In all cases, the templates with two reactive functional handles are utilized to attach N- and C-terminal polypeptide chain segments and the size of the template helps the pendant antiparallel and parallel peptide chains to involve into hydrogen-bonding interaction.[25, 26] Few selected scaffolds that nucleate β-sheet formation via formation of a β-strand hydrogen-bonded network are presented below.

In 1985, Feigel and his co-workers reported the use nonpeptidic molecular spacer **5.13** to organize hydrogen bonding and hence formation of β-sheet structure between two antiparallel peptide strands hooked in two arms of the scaffold (**5.13**) which itself is a *β*-turn mimetic.[27a]

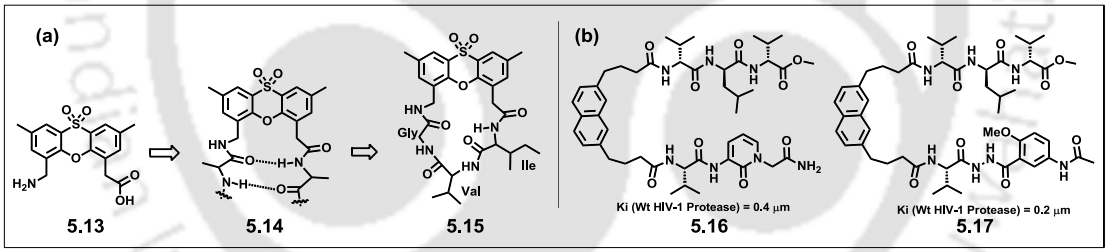

Figure 5.4: (a) Feigel's template as a β-reverse turn mimetic β-sheet nucleator. (b) Naphthalene scaffold based β-hairpin peptide backbone.

Naphthalene based diacid was also reported to act as small molecular scaffold which was exploited to developed the HIV protease inhibitors showed *β*-hairpin structure among the two peptide strands (**Figure 5.4b**).[28]

Most notable example includes Kelly's dibenzofuran-based templates.[29] Kelly and coworkers used dibenzofuran-based amino acid to attach two tripeptide arms to yield a hairpin structure *via* stabilization of the β-sheet conformations (**Figure 5.5a**). Their study demonstrated that hydrophobic cluster formation involving interactions between the aromatic template and the attached nonpolar residue is necessary for β-hairpin formation.

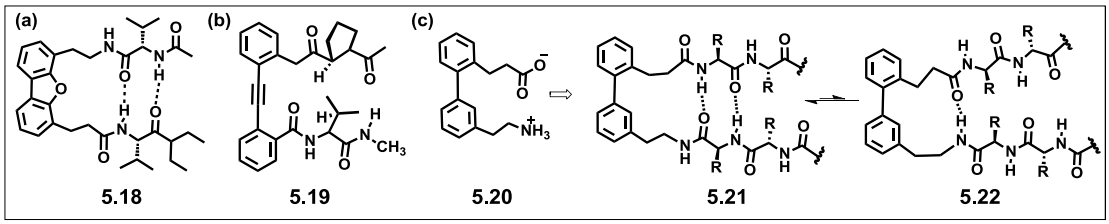

Figure 5.5. The Kellys' dibenzofuran (a), biphenyl scaffold (c) and Kemp's biphenyl acetylene template (b) as β-sheet nucleators.

The same group synthesized the 2,3'-substituted biphenyl-based amino acid, [3'-(2-aminoethyl)-2-biphenyl]propionic acid, which was found as a β-hairpin nucleator (**Figure 5.5c**).[30] The tripeptide segments have been added to the two arms of the template yielding a heptapeptide which was stabilized not only by H-bonded b-sheet structure but also by hydrophobic interaction. Extension of the chains to yield a 13-residue peptide results in the formation of a β-hairpin structure which then aggregates.[30].

5.3.1. Click-Triazoles as Constrained Small Molecular Scaffolds/Templates for Nucleating β-Sheet

A vast majority of research works on peptidomimetic drug design have been reported based on click chemistry. The β-turn peptidomimetic based on click reaction has already been placed in previous **Chapter 4**. Herein, few selected examples relating to β-sheet peptidomimetics are presented.

The triazole as short turn motif was successively applied in the generation of higher structures. Specifically, the CuAAC was used to polymerize short-chain peptide sequences, resulting in the formation of β-sheet nanofibrils[31] using hexamers containing repeating -Ala-Gly- dipeptide units to favour the nucleation of stable sheet-like architectures and installing azides and alkynes at their *N*- and *C*-termini. CuAAC-based polymerization[32] using $Cu(OAc)_2$ as a catalyst was then employed to ligate block-peptide sequences, allowing the triazole unit at either end of the fibrils to induce β-turn mimetics and inducing the peptide sequences to fold into antiparallel β-strands, ultimately resulting in the organization of the overall structure in higher order nanofibrils.

In 2012, Zhan-Ting Li and his co-workers introduced a series of 1,4 –diphenyl -1,2,3-triazole-based β-turn mimic. They studied the conformations of synthesized compounds both in solution and solid phase and also analyzed their ability to nucleate a β-hairpin or β-sheet like structure. They designed compound **5.26** as a model of β-turn mimic, while compound **5.27-5.29** attached with terminal alkyl group and different spacer lengths which influenced the stability of β-turn mimic. On the other side compound **5.30** also was synthesized to examine the ability for the formation of

β-sheet conformation from β-turn structure (**Figure 5.6**). Their study revealed that with the stabilization via hydrogen bonding, compound **5.26** adopted planar U-shaped conformation, mimicking a *β*-turn unit and helps formation of β-sheets conformations among the peptide strands attached in the two arms.[33]

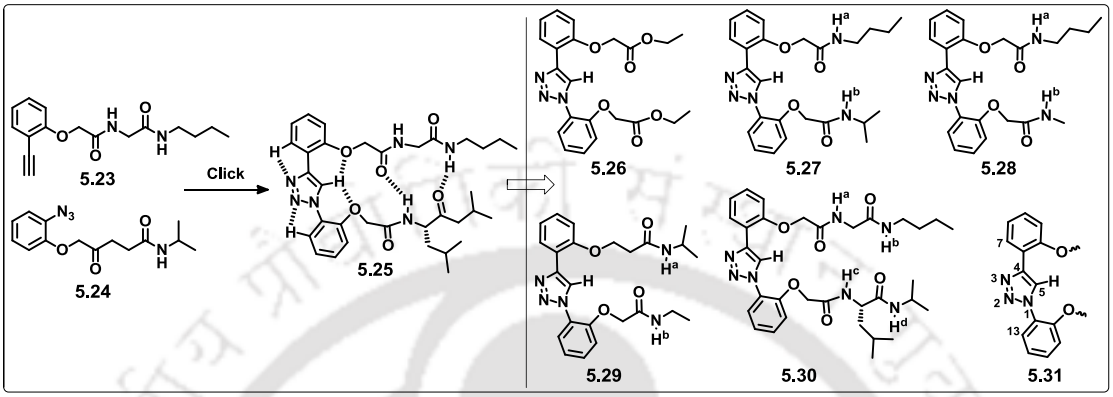

Figure 5.6: 1,4 –diphenyl -1,2,3-triazole-based *β*-turn mimic as *β*-sheet nucleator.

Therefore, design of constrained small molecular scaffold to nucleate *β*-sheet like secondary structure of short peptide motifs is a very useful nucleation strategy to adopt *β*-sheets which are not only important for normal biological activities, but also involved in many diseases including HIV, cancer, and neurodegenerative diseases. Creating templates/scaffolds that fold to form β-sheet-like structures or participate in intermolecular β-sheet interactions would provide valuable tools to study β-sheet folding and protein-protein interactions which is the key to gather information inside the cell.[34, 35] In addition to generate β-sheet recognition unit, if a fluorescent tag is attached the generated β-sheet peptidomimetic would find widespread application in studying protein−protein or peptide-DNA interactions in a living cell. There exists several fluorescent based techniques which can be utilized for such a purpose. Thus, there exists several examples of peptide/protein based fluorescent probes out of which few selected examples of such probes with excimer emission property are given below.

5.4. Application of Excimer Emission

The fluorescent/fluorescently labelled peptides/proteins serve as sensitive probes for visualizing intracellular events and understanding molecular interactions inside a cell.[36] Many of such aspects have been studied either by exploiting intrinsic fluorescence of a protein or with the help of an extrinsic fluorescent label.[37] However, intrinsic fluorescence limits the interpretation of results in presence of multiple tryptophan.[37c] Moreover, shortcomings of labeling with large size of extrinsic probes[38]

have led to a strong demand for generating a small protein tag[38] or site-specific incorporation of unnatural fluorescent amino acids[39] into a protein.[38-39] Such fluorescent proteins or small peptides are currently attracting much research interests to gain a deeper insight into the nature, regulation and functions inside living cells.[40] Over the various available strategies, fluorescence spectroscopic technique is a powerful tool for studying such biological events because of its high sensitivity, excellent temporal resolution and good reproducibility.[37c, 38c] Furthermore, among the various fluorescence photophysical phenomena, Förster resonance energy transfer (FRET)[6] and excimer[7] emission find widespread applications in elucidating such events of proteins/peptides in a cell.[41-42] .In general, because of lower sensitivity to small changes in distances accessible FRET pair, the excimer formation is more sensitive due to very short distance involvement. The excimer formation involves the complexation between excited state and ground state molecule that is characterized by red shifted fluorescence emission compared to monomer emission and long radiative decay time. As for an example, the excimer formation by pyrene molecule need an electronically excited pyrene with a second pyrene in its ground state (**Figure 5.7).** explain the energy diagram for the formation of Py-Py excimer wherein D* and E* denote the ground state and first excited state for a pair of Pyrene.[43]

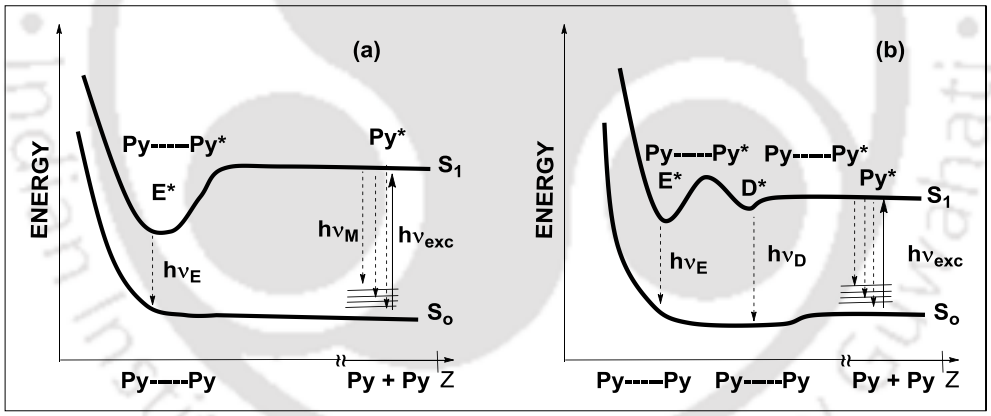

Figure 5.7. Schematic potential energy diagrams for pyrene excimer formation in the absence of ground-state association (a) and with pyrene ground state association (b).

The excimer emission of pyrene is depended on modes of stacking that are again affected by structural flexibilities. This property of pyrene is very useful for investigating biomolecular interaction and protein folding nature. To evaluate the structural effect on pyrene excimer emission, Matsuo group reported a tree type pyrene probe with different linker length that are linked with cysteine residue in the A55C/C77S/V169C mutant of adenylate kinase (Adk), an enzyme that shows a structural transition between OPEN and CLOSED forms.[44] They showed that all the proteins are able to form the CLOSED form with a similar distance between Cys55 and Cys169. However, the mechanism of excimer emission in the CLOSED Adk_{tm}s is

strongly dependent on the linker length of the pyrene probes (**Figure 5.8**). They presented a series of spectroscopic data demonstrating the significance of probe structure design and the utility of the probe for the precise evaluation of the association modes between fluorescent probe-labeled biomolecules.

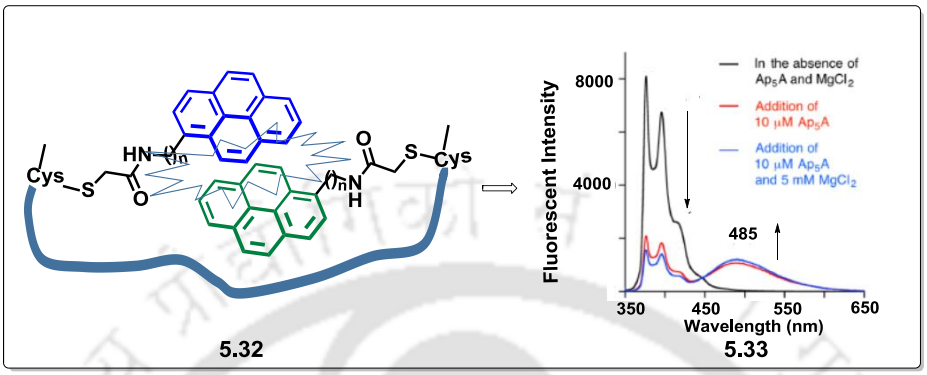

Figure 5.8: Pyrene labelled biomolecules with different linker length (Adopted from Ref. 44)

In 2012, Hecht group elaborated the synthesis of (S)-pyren-1-ylalanine attached at 3'-terminus of a suppressor t-RNA transcript, that introduced to 16 and 49 position of dihydrofolate reductase (DHFR) by suppression of UAG codons, which showed excimer formation (**Figure 5.9)**.[45] The excimer formation has been used to monitor the conformational changes that is directly associated with product release from DHFR. The emission spectra of modified DHFRs containing pyren-1-ylalanine at position 16 (black curve), position 49 (green curve) or positions 16 and 49 (red curve, excimer emission, 481 nm) (**Figure5.9)**.[45]

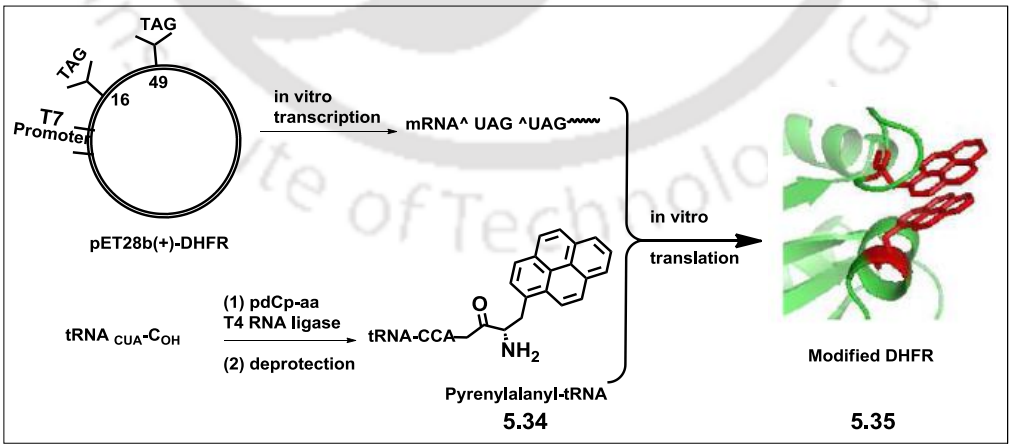

Figure 5.9: Modification and application of DHFR by Pyren-1-ylalanine at Positions 16 and 49.

Protein phosphorylation is a ubiquitous post-translation modification, which serves, among other roles, as a switch to control proteins' activation state. Gunning and co-workers have reported pyrene excimer based turn-on fluorescent sensor for the selective detection of proximally diphosphorylated proteins in aqueous solution.[46] To detect diphosphorylated proteins, they have synthesized pyrene ligated Zn(II)-cyclen macrocycle that preferentially formed 1:1 complex with a peptide/protein containing two proximal phosphorylated amino acids (pX, X = any amino acid). As the complexation occur the pyrenyl units come closer to form excimer. However, for a peptide/protein containing a single phosphorylated amino acid, complexation with Zn would lead to only a monomer emission at pyrene but no excimer emission could be observed (**Figure 5.10b**).

Upon excitation at 350 nm, sensor **5.36** showed the emission at 380 nm which shifted to 480 nm in pY-pY containing peptide (diphosphorylated peptide). This result strongly was observed for the study of α- and β- caseins only both of which contained diphosphorylated motifs and hence 30 times enhancement of fluorescence intensity was observed. These result of pyrene based excimer emission is very use full for detection of proximally diphosphorylation status proteins.

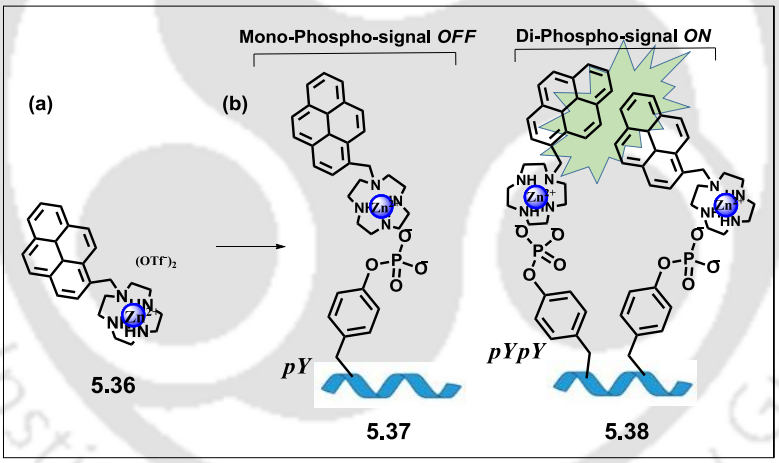

Figure 5.10: (a) Chemical structure of sensor **5.36**, (b) mechanism for the sensor signaling.

5.5. Background

Among the various bioactive conformations, the β-sheet accounts more than 30% of all protein structures i.e. the second most common structural motif of protein. The β-sheet not only plays a scaffolding role, but also serves as a key recognition motif in many important biological processes involving protein-protein and protein-DNA interactions. As a result of tremendous research efforts, the field of β-sheet peptidomimetic encompases from several successful design of constrained molecular scaffolds that nucleate intermolecular β-sheet formation between two peptide chains

for mimicking secondary structures to the mimicry of β-sheet quaternary interactions with simple model systems. Moreover, the mimicry of β-sheet secondary structures in a designed fluorescent peptide to test the fundamental aspects that a particular conformation can have an impact on the photophysics has received little attention. Investigating such impact might find widespread applications in studying peptide-protein or protein-protein or peptide-DNA interactions in a living cell.[47]

5.6. Objective

Currently, a variety of small molecular scaffolds have been designed to resemble β-turns which help inducing artificial β-sheet structures when two peptide strands are attached in the two arms of such scaffolds. The representative examples include (a) 2,2′-substituted tolan adopted by the Kemp group,[48] (b) phenoxathiin derivatives developed by Feigel and Sogah,[49] (c) dibenzofuran-based amino acids reported by Kelly,[11a, 30] (d) tetrasubstituted alkenes reported by the Gellman group [50], as well as (e) amino(oxo)piperidinecarboxylate scaffolds designed by Borggraeve and co-workers. [51] Though the click chemistry has been utilised in mimicking the protein's secondary structures, however there is no report of triazolo amino acids or aromatic triazolo amino acid as scaffold resembling a turn like shape and can induce a specific peptide secondary structure. The rigid frameworks of pseudo-aromatic triazole unit with constrained backbone angles ω(i) and ϕ(i+1), would expected to induce folded conformations in linear peptides (**Figure 5.11**).

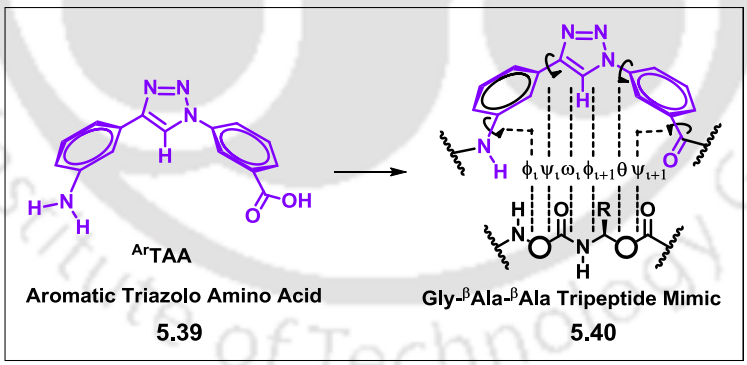

Figure 5.11. Presentation of aromatic triazolo amino acid scaffold as tripeptide isostere.

As a part of our ongoing research effort on the design of unnatural biomolecular building blocks via click chemistry and β-turn peptidomimetics with unnatural fluorescent amino acid (discussed in **Chapter 3**) and aliphatic triazolo amino acid scaffolded β-turn peptidomimetics (designed in **Chapter 4**) we thought that more rigid triazolo amino acid scaffold such as an aromatic analogue in the turn

conformation might act as a "β-turn mimic as β-sheet folding nucleator". Moreover, design of a fluorescent peptide which in a folded β-sheet conformation might have impact on its photophysical outcome would be fundamentally of great importance owing to their possible applications in gaining insight into the living cell *via* studying their inter-biomolecular interaction property.

Therefore, with this background and concept we framed our objective as follows:

(a) Synthesis and study the photophysical properties of aromatic triazolo amino acid.

(b) Incorporation of scaffold aromatic triazolo amino acid into a short linear peptide and study of conformation induced by the scaffold.

(c) Design and synthesis of aromatic triazolo amino acid scaffolded trichromophoric fluorescent pentapeptide and study of conformation and photophysical properties.

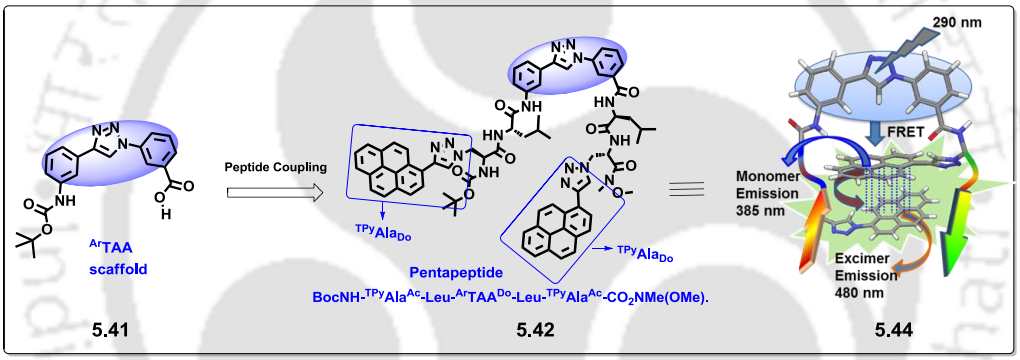

Figure 5.12. Graphical presentation of the constrained molecular scaffold triazolo aromatic amino acids (**5.41**, **^{Ar}TAA)** and the possible photophysics of the designed fluorescent pentapeptide **5.42**.

(d) **Our Concept:** We envisaged that the mechanism of excimer/exciplex formation via FRET would become possible by judicious designing and proper positioning a donor/acceptor pair with respect to a third chromophore in a probe wherein a pair of chromophores involve in π-π stacking interaction. Thus, we designed an aromatic triazolo amino acid scaffolded pentapeptide **5.42** wherein the scaffold (**5.41**, **^{Ar}TAA**, **Figure 5.12**) itself is a chromophore. The fluorescent triazolylpyrene (**TPy**) unnatural amino acids (**^{TPy}Ala^{Do}**) were chosen as other two chromophores attached to the N-and C-terminus, respectively, of the scaffold via an intervening natural amino acid, leucine. We thought that excitation at the absorption maximum of the scaffold would lead to an energy transfer to a second chromophore, **^{TPy}Ala^{Do}**, which then release its excitation energy as emission (monomer) and form π-stacked complex (excimer) with the proximally positioned third chromophore, **^{TPy}Ala^{Do}**. The π-

stacked complex would thus show excimer emission at a longer wavelength. Establishing dual door entry to excimer emission in the designed fluorescent pentapeptide.

(e) Application of dual door entry to excimer emissive peptide as fluorescent light-up probe for studying protein-peptide interaction.

5.7. Result and Discussion

5.7.1 Synthesis of Aromatic Triazolyl Amino Acid Scaffold (5.41,^{Ar}TAA) and Corresponding Peptides

To synthesise aromatic triazolyl amino acid scaffold, we first synthesised, 3-trimethylsilylethynyl-N-Boc protected aniline (**5.50**) from *m*-bromo aniline (**5.48**) via $PdCl_2(PPh_3)_2$ catalyzed sonogashira coupling. Deprotection of the TMS group with KOH at room temperature afforded 3-ethynyl-N-Boc protected aniline **5.51**. On the other side, 3-azido methyl benzoate **5.47** was prepared starting from 3-amino benzoic acid (**5.45**) as shown in the **Scheme 5.1**. Next, 3-azido methyl benzoate **5.47** and alkyne **5.51** were undergone cycloaddition reaction under click reaction condition to yield aromatic triazolyl amino acid scaffold **5.52** in bisprotected form. A LiOH mediated deprotection of methyl ester ultimately afforded the desired scaffold **5.41** (**Scheme 5.1**).[39c-d]

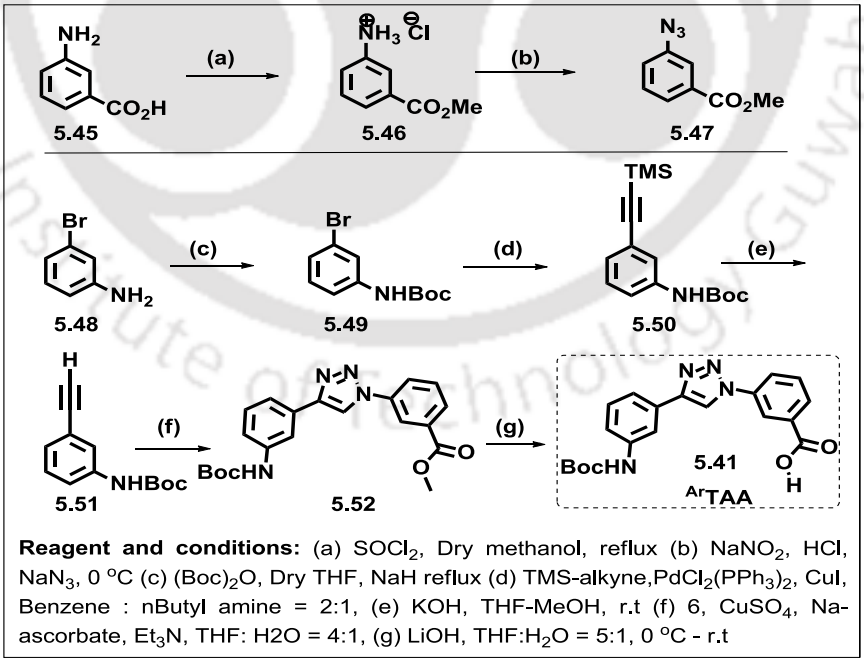

Reagent and conditions: (a) $SOCl_2$, Dry methanol, reflux (b) $NaNO_2$, HCl, NaN_3, 0 °C (c) $(Boc)_2O$, Dry THF, NaH reflux (d) TMS-alkyne,$PdCl_2(PPh_3)_2$, CuI, Benzene : nButyl amine = 2:1, (e) KOH, THF-MeOH, r.t (f) 6, $CuSO_4$, Na-ascorbate, Et_3N, THF: H2O = 4:1, (g) LiOH, THF:H_2O = 5:1, 0 °C - r.t

Scheme 5.1. Synthetic scheme for the triazolyl aromatic amino acid scaffold (**5.41**, ^{Ar}**TAA**).

To investigate the constrained properties of the scaffold **5.41**, we, next, synthesized a designed fluorescent pentapeptide **5.42** and a linear Leu-enkephalen analogue **5.43** wherein our scaffold has been placed in the middle of the peptide chain. All the peptide strands were synthesized by a solution phase peptide coupling protocol. Thus, the triazolyl amino acid scaffold **5.41** was coupled with triazolylpyrenyl dipeptide **5.54** via a peptide coupling protocol to afford N, C-diprotected tripeptide **5.55**. Finally, deprotection of N-Boc from **5.55** and subsequent coupling with N-Boc-protected dipeptide **4.125** (BocNH-^{TPy}Ala^{Do}-Leu-CO_2H) afforded the desired fluorescent pentapeptide **5.42** (**Scheme 5.2**). [39c-d]

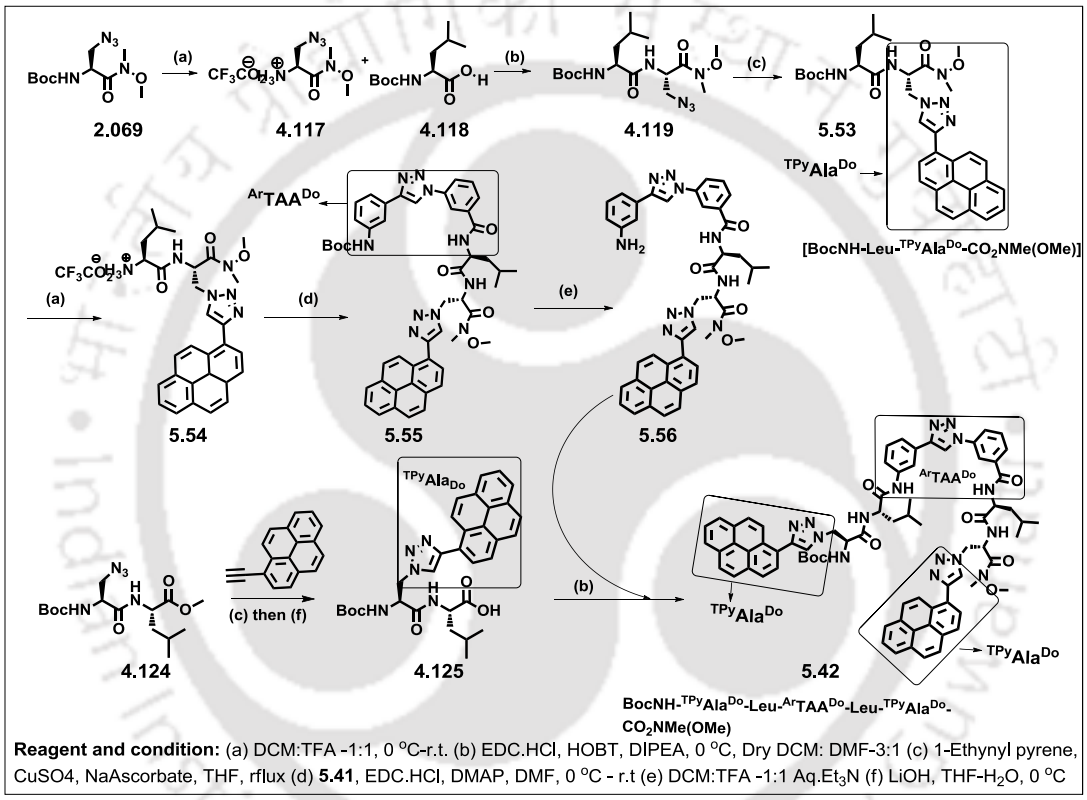

Scheme 5.2: Synthetic scheme of aromatic triazolyl amino acid scaffold based unnatural pentapeptide **5.42 [**BocNH-^{TPy}**Ala$_{Do}$**-Leu-^{Ar}**TAA$_{Do}$**-Leu-^{TPy}**Ala$_{Do}$**-CO_2NMe(OMe**)].**

The peptide **5.43**, a Leu-enkephalen analogue, was also synthesised in a similar way to study the conformation induced by the scaffold **5.41** (**Scheme 5.3**).[10] Thus, N-Boc-deprotected dipeptide **4.114** was coupled with scaffold **5.41** following EDC.HCl/DMAP mediated peptide coupling protocol to afford tripeptide **5.57**. The tyrosine was then attached to the N-terminus of N-Boc-deprotected tripeptide **5.58** (**Scheme 5.3**) and produced our targeted tetrapeptide **5.43** where ^{Ar}**TAA** (**5.41**) remain in the backbone of the peptide. [39c-d]

\

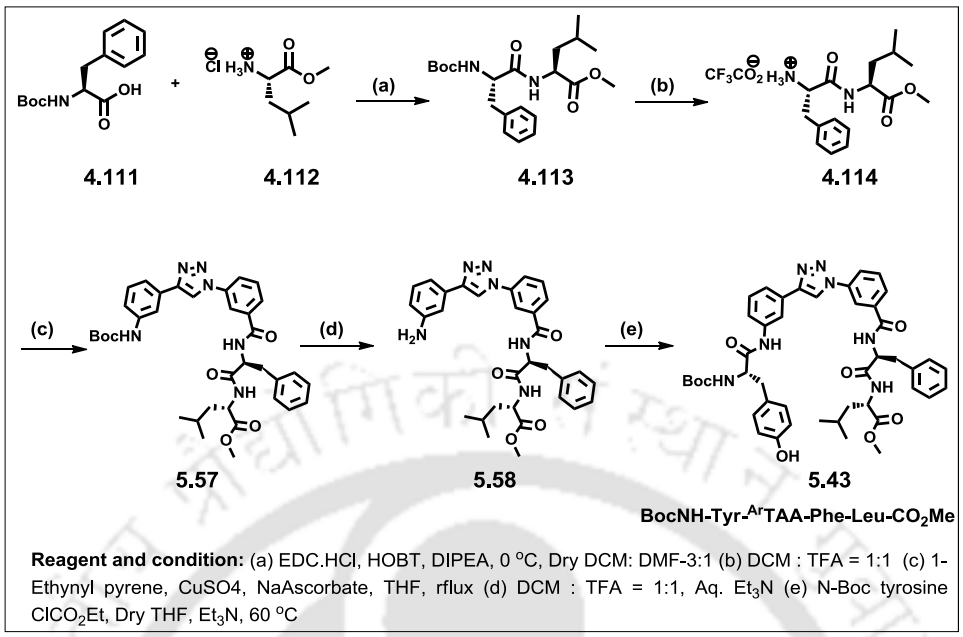

Scheme 5.3: Synthetic scheme of triazolyl aromatic amino acid scaffold based Leu-enkephalin analogue natural tetrapeptide **5.43 (**BocNH-Tyr-^{Ar}**TAA**-Phe-Leu-CO_2Me**).**

All the intermediate peptides and final peptides were purified by silica-gel (60-120 mesh) column chromatography and characterized by both 1D and 2D NMR, IR, and HR-mass spectrometry. After getting our target peptides in pure form in hand, we, next, studied their secondary structure using various spectroscopic techniques.

5.7.2. Spectral Characterisation of the Synthesized Scaffold/Peptides

The scaffold and the peptides were characterized mainly by NMR spectroscopy. The X-ray single crystal analysis was carried out for the scaffold confirming its structure and provided important information which is given below. The synthesized peptides **5.42** and **5.43** in the fully protected form were characterized mainly by NMR spectroscopy. The chemical shift assignment for pentapeptide **5.42** is shown in **Figure 5.13b**. The detailed assignments are given in the experimental section. The structural assignments of peptides **5.43** is shown in **Figure 5.13a** and described below.

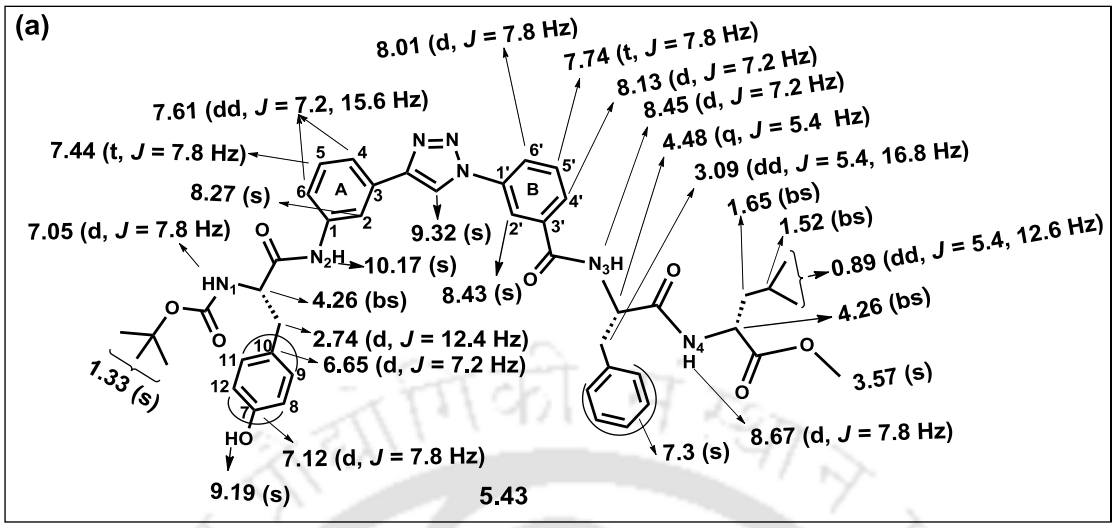

Figure 5.13a. ^{1}H NMR assignment of Leu-enkephalin analogue tetrapeptide **5.43.**

The structural assignment of fluorescent pentapeptide **5.43** is shown in **Figure 5.13b**. Thus, for peptide **5.43** (Boc-NH-Tyr-^{Ar}**TAA**-Phe-Lue-CO_2Me), the triazolyl hydrogen appeared as a singlet at δ 9.32. The C-α hydrogens of tyrosine and leucine resonated as a broad singlet (bs) at δ 4.26 and 4.62, respectively. The C-α hydrogens of phenyl alanine appeared as a quartet at δ 4.48 with coupling constant J = 5.4. The β-CH_2 hydrogens of tyrosine and phenyl alanine appeared as a doublet and as a doublet of doublet at δ 2.74 and 3.09 with coupling constant J = 12.4 Hz and 5.4, 16.8 Hz, respectively. The β-CH_2 hydrogens of leucine unit appeared as a broad singlet at δ 1.65. The γ and δ hydrogens of leucine unit appeared as a broad singlet at δ 1.52 and doublet of doublet at δ 0.89 with coupling constant J = 5.4 and 12.6 Hz. The ^{t}Bu hydrogens of Boc- protected group appeared as a singlet at δ 1.33. The methyl hydrogens of OMe group also resonated as a singlet at δ 3.57. The aromatic hydrogens of ^{Ar}**TAA** scaffold at C-2 (N-terminal Ar, Ring A) and C-2′ (C-terminal Ar, Ring B) appeared as singlet at δ 8.27 and 8.43, respectively. While, C-4 and C-6 hydrogens (N-terminal Ar, Ring A) appeared as a doublet of doublet at δ 7.61 with coupling constants J = 7.2 and 15.6 Hz. The C-6′ and C-4′ (C-terminal Ar, Ring B) hydrogens resonated as a doublet at δ 8.01 and 8.13 with coupling constant J = 7.8 and 7.2 respectively. The hydrogens at C-5 (N-terminal Ar, Ring A) and C-5′ (C-terminal Ar, Ring B) appeared as triplet at δ 7.44 and 7.74 with same coupling constant 7.8 Hz respectively. The C-9, C-11 and C-8, C-12 aromatic hydrogens of tyrosine appeared as a doublet at δ 6.65, 7.12 with coupling constant 7.2 and 7.8 Hz respectively. The aromatic hydrogens of phenyl alanine unit resonated as a singlet at δ 7.30. The hydrogens of N-1, N-2, N-3 and N-4 appeared as a doublet, singlet, doublet and doublet at δ 7.05, 10.15, 8.45 and 8.67 with coupling constant 7.8, 7.2 and 7.8 Hz respectively.

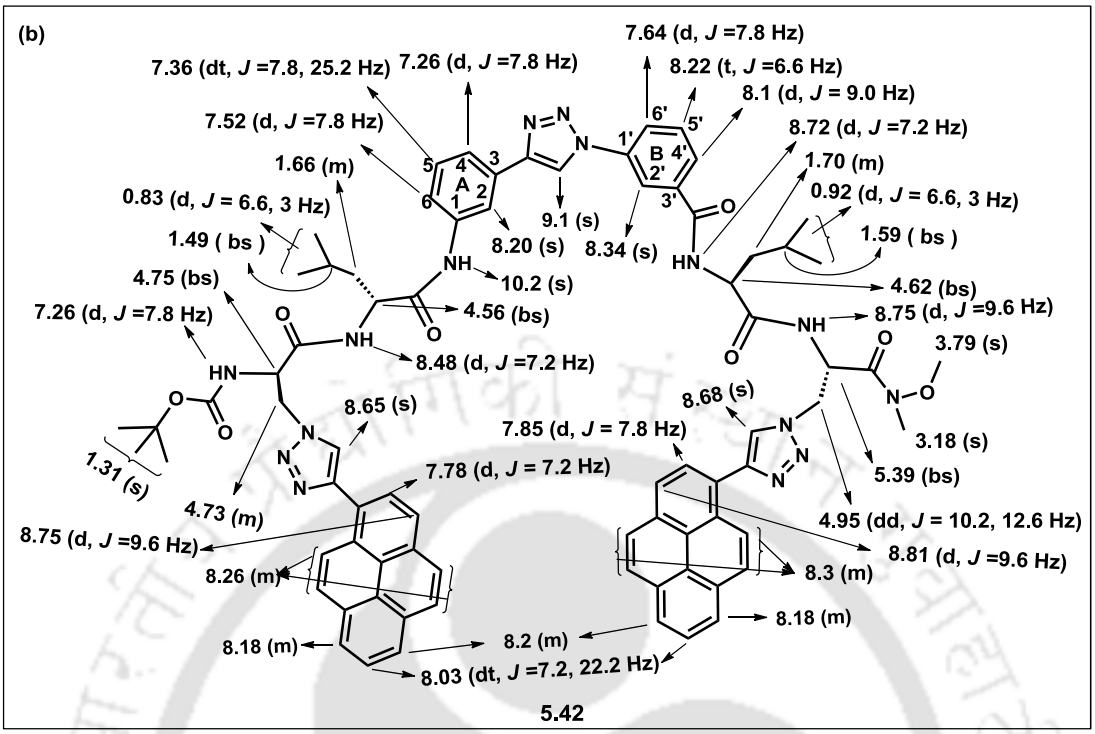

Figure 5.13b. ^{1}H NMR assignment of fluorescent pentapeptide **5.42.**

***The Single Crystal X-Ray Structure*:** The crystal structure analysis of scaffold **5.52** revealed an interesting observation. Recrystallization of **5.52** from acetonitrile yielded beautiful brown needle-shaped crystal (mp 168 ^{o}C). Single crystal X-ray diffraction analysis showed that the crystals were orthorhombic and classified into the chiral space group $P2_12_12_1$. This interesting observation knocked us to examine the possible origin of the solid state chirality as well as to examine whether the same chirality is maintained in solution. The specific rotation ($\alpha_D^{20} + 1.5$) of the scaffold in MeOH showed the maintenance of induced chirality in solution. The packing diagram showed that the scaffold had a 2-fold screw axis of symmetry, unit cell contained four molecules and the aminophenyl unit was 25.1 ^{o} out of plane with respect to triazole unit. The other phenyl unit remained almost in the plane of triazole. Overall the scaffold adopted a hairpin shape wherein the two hairpins packed face-to-face via weak H-bonding interaction leading to "S"-shaped structure (**Figure 5.14**). The molecular arrangement revealed that each "S"-shaped units were linked each other via ArCH….$N_{Triazole}$, ArCH-π bonding (side way) and hydrophobic interaction through ^{t}Butyl-units to link "S"- units linearly leading to a helical like construct (**Figure 5.14c**) [CCDC 997089].

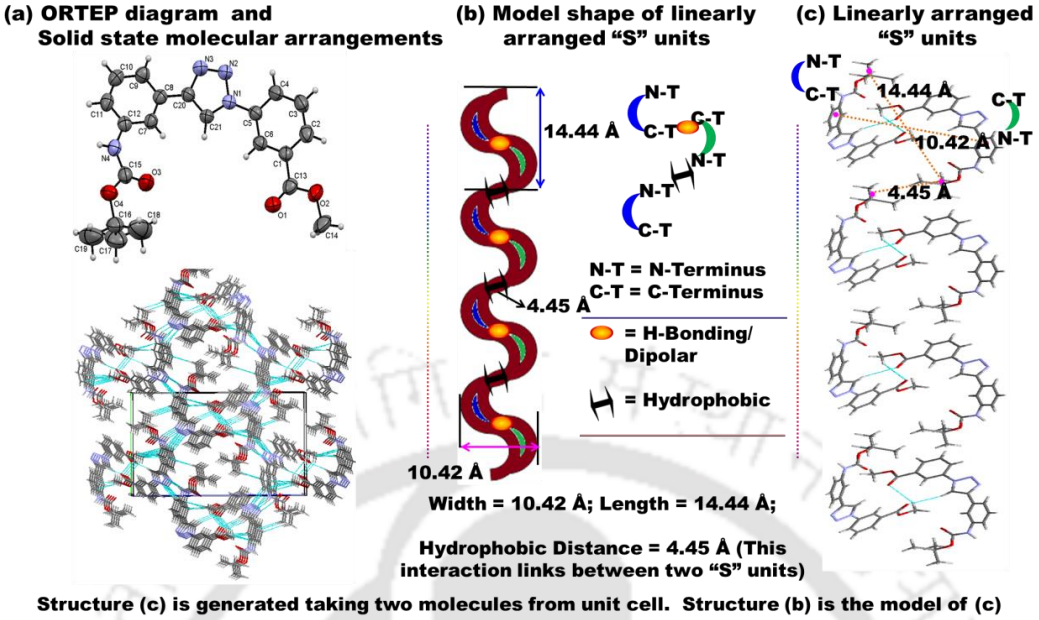

Figure 5.14. (a) ORTEP diagram with 50% thermal ellipsoid and molecular arrangement; (b-c) Model shape and linearly arranged "S" units.

Table 5.2: Summary table of crystal parameter of scaffold **5.52** (^{Ar}**TAA**).

Empirical formula	$C_{21}H_{22}N_4O_4$
CCDC Number	CCDC 981750
Formula weight	394.43
Crystal habit, colour	needle, brown
Crystal size, mm^3	0.40 x 0.24 x 0.22
Temperature, T	296(2) K
Wavelength, λ	0.71073 Å
Crystal system	orthorhombic
Space group	$P2_12_12_1$, No.19
Unit cell dimensions	a = 5.9906(6) Å
	b = 15.7335(18) Å
	c = 21.9353(19) Å
	$\alpha = \beta = \gamma = 90°$
Volume, V	2067.5(4) Å^3
Z	4
Calculated density	1.267 Mg/m^3
Absorption coefficient, μ	0.090 mm^{-1}
F(000)	832
θ range for data collection	1.59° to 24.99°
Limiting indices	$-7 \leq h \leq 7$, $-18 \leq k \leq 12$, $-24 \leq l \leq 25$
Reflection collected / unique	10672 / 3576 [R(int) = 0.0668]
Completeness to θ	99.2 %

Max. and min. transmission	0.974 and 0.980
Refinement method	Full–matrix least–squares on F^2
Data / restraints / parameters	3576 / 0 / 266
Goodness–of–fit on F^2	0.973
Final R indices [I>2sigma(I)]	$R1$ = 0.0501, $wR2$ = 0.1086
R indices (all data)	$R1$ = 0.0877, $wR2$ = 0.1248
Largest diff. peak and hole	0.161d –0.164 e.Å^{-3}

After getting our targeted peptide in hand, we, next, studied their conformation using various spectroscopic techniques.

5.7.3. Study of Conformation of Peptides 5.42 and 5.43 Using CD, IR, NMR, Spectroscopic Techniques and Macromodel Calculation

Study of Circular Dichroism Spectroscopy: Circular dichroism spectra were recorded using a CD spectropolarimeter with a cell path length of 1 mm at in different solvent at room temperature and variable temperature. All the samples were prepared in spectroscopic grade solvent with 100 μM concentration.

The secondary structure elucidation of fluorescent peptide **5.42** via CD spectroscopy at 20 ºC revealed the presence of a strong positive band at around 194 nm and a broad negative band at around 215-239 nm in ethanol indicating sheet conformation (**Figure 5.15b**).[52] Moreover, the signature of negative band at 287 nm due to aromatic scaffold and positive bands at 331 and 360 nm due to the absorption of the fluorescent triazolyl pyrene indicated π-π stacking interaction between two terminal triazolyl pyrene moieties that was also supported from variable temperature CD spectra in EtOH solvent.[52] While the tripeptide **5.55** (**Scheme 5.2**) containing a single **TPy** showed a positive induced CD signal (**Figure 5.15a**), the pentapeptide **5.42** showed a negative Cotton effect in the absorption range of **TPy** indicating π-π-stacking interaction between two terminal **TPy** units.[52d-e]

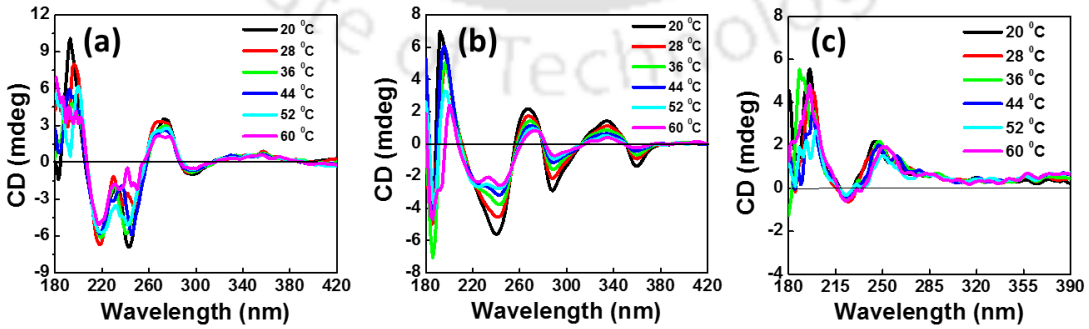

Figure 5.15. Variable temperature CD spectra of synthesized (a) tripeptide **5.55**, (b) pentapeptide **5.42** and (c) tetrapeptide **5.43** in ethanol solvent (100 μM concentration).

The tetrapeptide **5.43** containing the aromatic scaffold in the backbone showed a positive band at 197 nm and a broad negative band at around 209-225 nm indicating sheet conformation.[52] Moreover, the presence of a positive band at 238 and 276 nm signified the absorption of chiral aromatic triazolyl amino acid scaffold as well of the tyrosine in the tetrapeptide **5.43 (Figure 5.15c)**. Overall, the synthesized peptides **5.42** and **5.43** showed β-sheet like structure with some contribution of turn conformation the existence of which implied the possible presence of intramolecular H-bonds between the peptide strands.

All of these observations indicated that the aromatic triazolo amino acid scaffold **5.41** (**^{Ar}TAA**) acts as a turn mimetic β-sheet nucleator.

Probing the Intramolecular H-Bonding: Study of FT-IR Spectroscopy: To probe the intramolecular H-bonding, IR spectroscopic technique was utilized. IR spectra were recorded using dry KBr with solid and dry compound. Thus, the presence of intramolecular H-bonded and free amide -NH stretching absorptions at 3289-3331 and 3419-3441 cm^{-1}, respectively, in the IR spectra of all the peptides supported predominant β-sheet conformations.[53] Fourier self-deconvolution (FSD) trace of IR spectra of peptide **5.42-5.43** showed amide I band absorptions at 1689-1685 cm^{-1} and 1644-1635 cm^{-1} supported the predominant β-sheet conformation along with a contribution from turn reflecting in the FSD trace at 1665-1670 cm^{-1} (**Figure 5.16a-b**).[53]

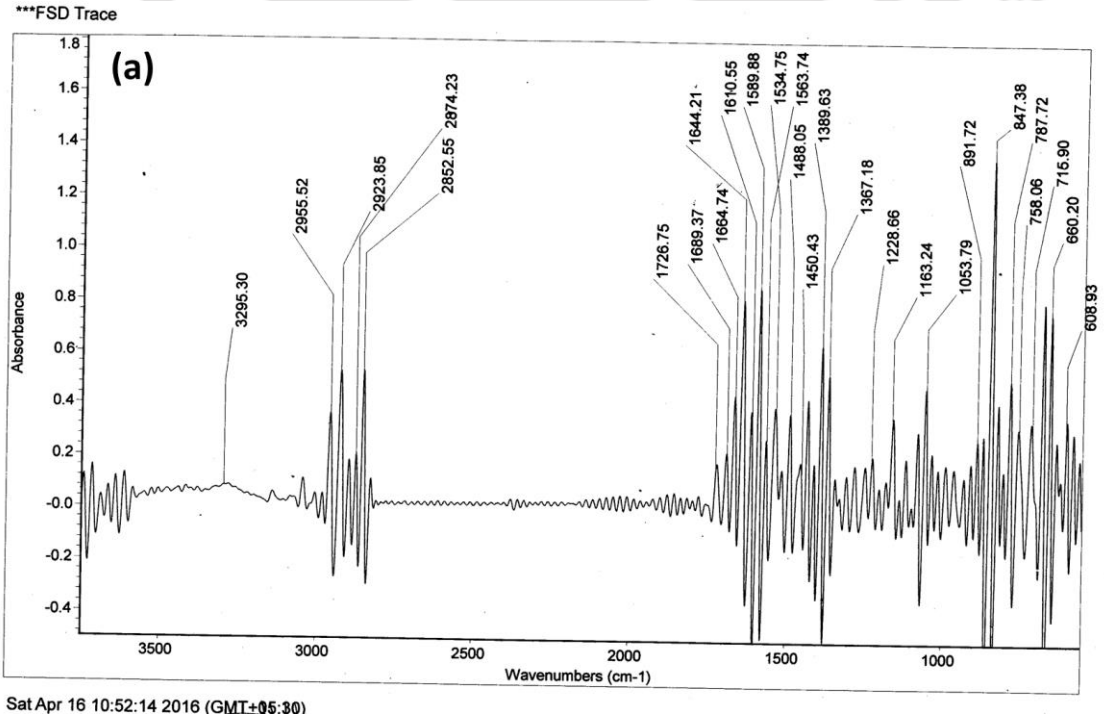

Figure 5.16a. Fourier self-deconvolution (FSD) traces of IR spectra of pentapeptide **5.42**

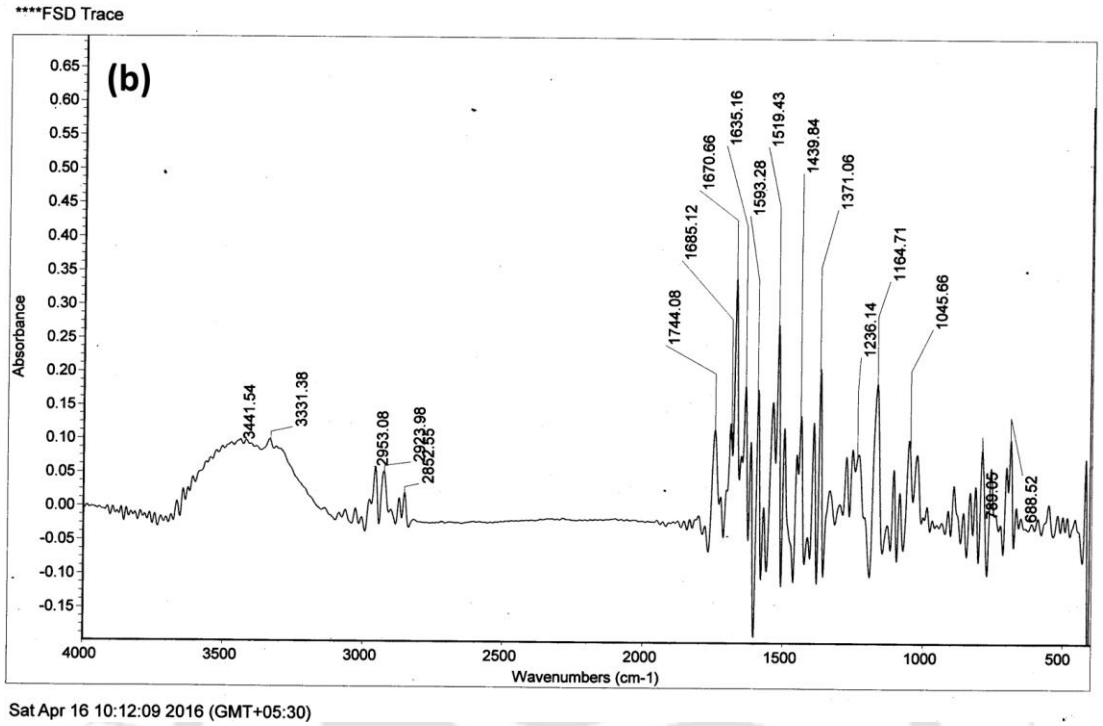

Figure 5.16b. Fourier self-deconvolution (FSD) traces of IR spectra of tetrapeptide **5.43**.

Probing the Intramolecular H-Bonding: Study of Variable Temperature ^{1}H NMR (VT-NMR): In pentapeptide **5.42**, the triazole C-H and all amide NH's shows temperature effect. All the amide NH's, and triazole C-H exhibited ($\Delta\delta/\Delta T$) values are close to Kessler limit of -3 to -6 ppb/K indicating presence of moderately H-bonding and supported β-sheet like structure of the peptide. While all the amide NHs of pentapeptide **5.43** were strongly H-bonded, the peptide **5.42** showed H-bonding involving the amide NH of C-terminal-Leu only (**Figure 5.17, Table 5.3**).[54]

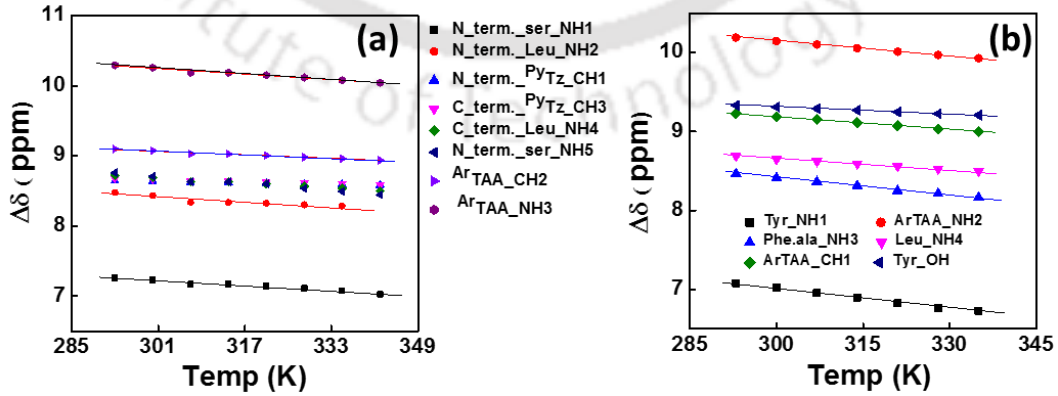

Figure 5.17: Temperature dependence of amide-NH/triazole-CH chemical shift of (a) pentapeptide **5.42** and (b) tetrapeptide **5.43**.

Table 5.3. Values of temperature coefficients of chemical shifts of amide NH's or triazole-CH's in Pentapeptide **5.42** and **5.43**.

Kessler limit (Δδ/ΔT) ppb/k			
Pentapeptide 5.42		**Tetrapeptide 5.43**	
N-terminal-Ser-NH1	- 4.45	N-terminal-Tyr-NH1	- 8.68
N-terminal-Leu-NH2	- 4.37	^{Ar}TAA-NH2	- 6.29
N-terminal-^{Py}Tz_CH1	- 1.27	C-terminal-Phe.ala-NH3	-7.2
C-terminal-^{Py}Tz-CH3	-1.79	C-terminal -Leu-NH4	-4.51
C-terminal-Leu-NH4	-4.31	^{Ar}TAA-triazole-CH1	-3.02
N-terminal-Ser-NH5	-6.1	Tyr-OH	-5.56
^{Ar}TAA-NH3	-4.86	----	----
^{Ar}TAA-CH2	-3.13	----	----

Solution Conformational Analysis Using 2D NMR Study Experiment: The study of solution conformation using NOESY and ROESY spectra of both the peptides **5.42-5.43** revealed that the scaffold itself adopted hairpin shape with overall sheet like conformation. The peptide **5.43** showed no interaction between Phe and Tyr. The spatial proximity between two terminal **TPy** units in peptide **5.42** is evident from both NOESY and ROESY spectra. Thus, the observed interstrand backbone-side chain interactions, such as, NH(i)-CH2(i+4), CH2(i)-NH(i+4), NH(i+1)-CH2(i+4), are indicative of close proximity between the two termini. Moreover, peptide **5.42** showed interactions among the aromatic hydrogens of two terminal triazolylpyrenes (**TPy**) suggesting their close proximity as well as rigidity in a single conformation. Thus, 2D NMR supported the close proximity and hence a possibility of photophysical interaction among the scaffold, ^{Ar}**TAA**, and the C-terminal triazolylpyrene (**TPy**) in pentapeptide **5.42** (**Figure 5.18**).

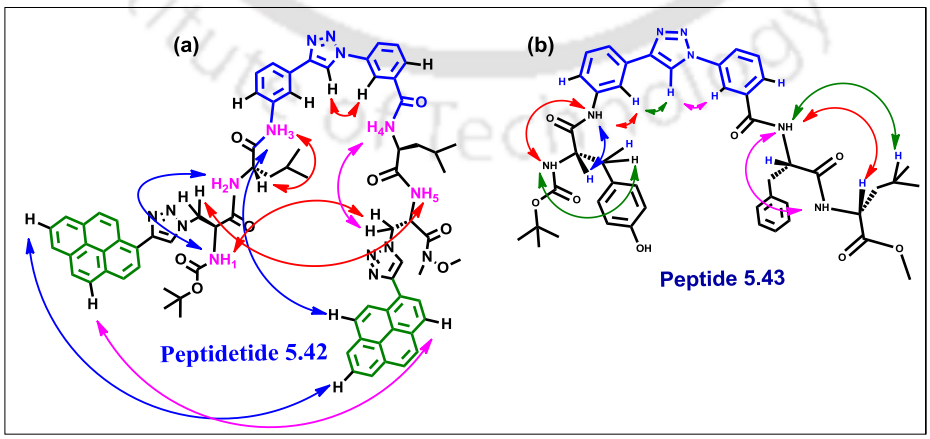

Figure 5.18. Pictorially presentation of long range proton-proton interaction of (a) pentapeptide **5.42** and (b) tetrapeptide **5.43**.

Conformational Analysis Using Macromodel Study: Geometry Optimisation: Using Schrodinger Macromodel (Maestro vs. 9.1) software we optimized the geometry and carry out the conformational search for both the peptides **5.42** and **5.43** with OPLS 2005 force field in water following the same method as was already described in **Chapter 4, section 4.7.3**.[39c-d]

A total of 65 (for Pentapeptide **5.42**) and 116 (for tetrapeptide **5.43**) minimized and well converged conformers were generated out of which the one conformer appeared 3 times (for Pentapeptide **5.42**), and 5 times (for tetrapeptide **5.43**) which remained within 1.00 k.cal/mole (4.18 kJ/mole) global minimum with a convergence threshold of 0.047 to 0.045 RMSD (threshold cutoff = 0.05). These two conformers were taken as the starting structures for MD simulation studies (**Figure 5.19a-b)**.

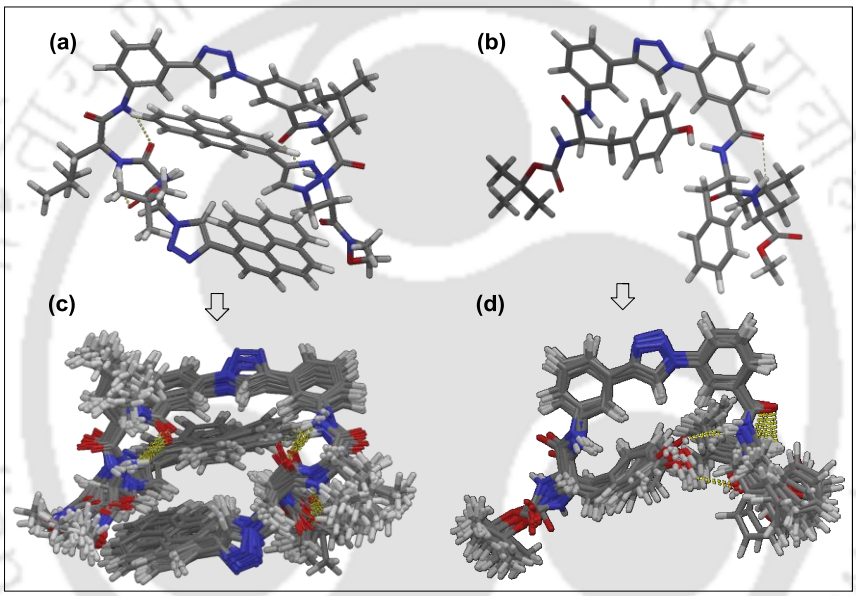

Figure 5.19. OPLS 2005 force field energy minimized conformations and well converged structures obtained from molecular dynamics simulation of pentapeptide **5.42** (a,c) and tetrapeptide **5.43** (b,d).

Molecular Dynamics Simulation of Energy Optimised Conformers of the Peptides 5.42 and 5.43: The MD simulations were done by Schrodinger Macromodel (Maestro vs. 9.1) software package with OPLS 2005 force field in which the systems were subjected to 100 ps simulations time (with time step of 1.5 fs and equilibrium time 1.0 ps) at constant temperature (300 K) and pressure (1 atm) with shaking all bonds. An optimal minimization method was chosen for minimizing the generated structures (with maximum iteration of 1000) with gradiant convergence threshold of 0.05. The MD simulated cluster of conformers within 21 kJ/mole from the global minima of peptide **5.42-5.43** is shown in **Figure 5.19c-d** respectively.[55]

The optimized geometry, conformational search and the MD simulation of the tetrapeptide **5.43** and pentapeptide **5.43** containing aromatic triazolo amino acid

scaffold (**^{Ar}TAA**) in the backbone fully supported the β-sheet conformation (**Figure 5.19**).

In summary, all the above spectroscopic technique and macro model study supported the close proximity of **^{Ar}TAA**, and the C-terminal triazolylpyrene (**TPy**) and two terminal **TPy** units each other in peptide **5.42** and hence a possibility of photophysical interaction among the scaffold **^{Ar}TAA** and two terminal **TPy** unit in pentapeptide **5.42**. To establish the fundamental concept of entry to excimer emission either via FRET and/or via direct excitation of a FRET acceptor **TPy** study their detailed photophysical properties**.**

5.7.4. Study of Photophysical Properties of the Peptides

After establishing the β-sheet like structure for the synthesized fluorescent peptide **5.42**, we first studied its photophysical property in various organic solvent. The UV-visible spectra of the triazolylpyrene dipeptide **5.53** (**Scheme 5.2)** shows structureless absorption at 351 nm in dimethyl sulfoxide (DMSO) which shifted to 346 nm as the solvent polarity increases from DMSO to methanol. However, when excited at the absorption maxima of 350 nm it showed a structured emission at 381, 401 and 424 nm. The intensity of emission of spectra decreases with increasing solvent polarity (**Figure 5.20a-b**). The quantum yield also follows the same trend with emission properties (**Table 5.4**).[56]

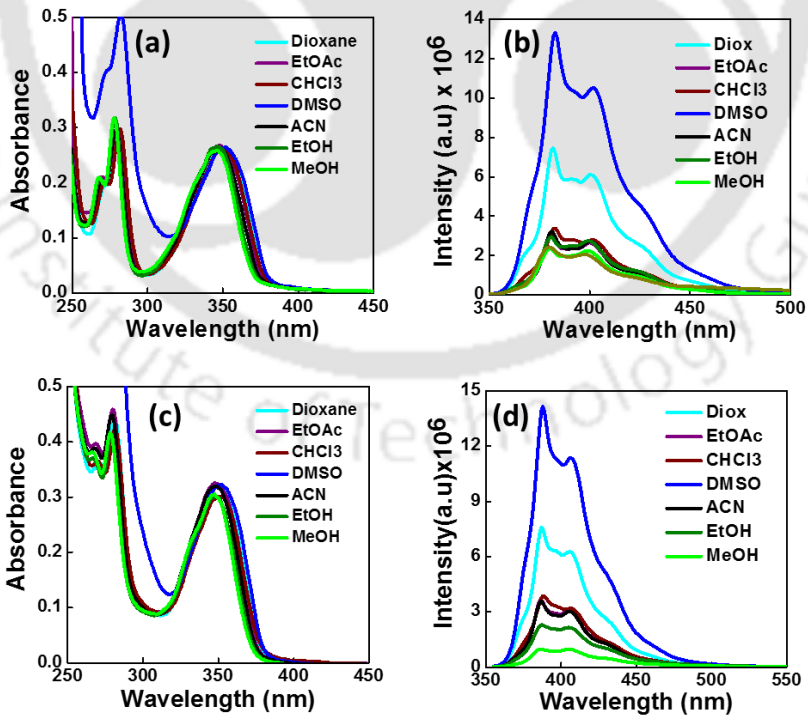

Figure 5.20. UV-Visible and Fluorescence spectra of dipeptide **5.53** (a, b) and tripeptide **5.55** (c, d) in different solvents (10 μM, r.t.; $\lambda_{ex} = \lambda_{max}$ (345 nm) of each solvent).

Tripeptide containing ^{Ar}**TAA 5.42** and dipeptide **5.53** showed very little blue shifted absorbance as the polarity of the solvent increases from dimethyl sulfoxide (λ_{max} = 251 nm) to methanol (λ_{max} = 345 nm). Upon excitation at 350 nm, the tripeptide **5.55** shows slightly red shifted structured emission band at 386, 406 and 426 nm with respect to triazolyl pyrene dipeptide **5.55**. With increasing solvent polarity fluorescence intensity decreased (**Figure 5.20c-d)**.

To test our hypothesis, we, next, examined the possible photophysical interaction behavior among the terminal triazolyl unnatural amino acids and the scaffold in fluorescent pentapeptide **5.42**. The UV-visible spectra of peptide **5.42** exhibited very strong and structureless absorption band at 348 ~ 353 nm. The absorbance is characterized by a hypsochromic shift of ~5 nm and little hypochromism as the polarity of the solvent increases. Upon excitation at absorption maxima (350 nm) of each solvent the emission at around 388, 408, 431 for triazolyl pyrene and 485 nm due to pyrene-pyrene excimer emission were observed the intensity of which was found to decrease as the solvent polarity increases (**Figure 5.21, Table 5.4**).[56] Furthermore, excitation at the absorption of Scaffold (290 nm) also gave rise to excimer emission in the peptide **5.42** which satisfied our designing concept. Thus the mechanism was investigated in details.

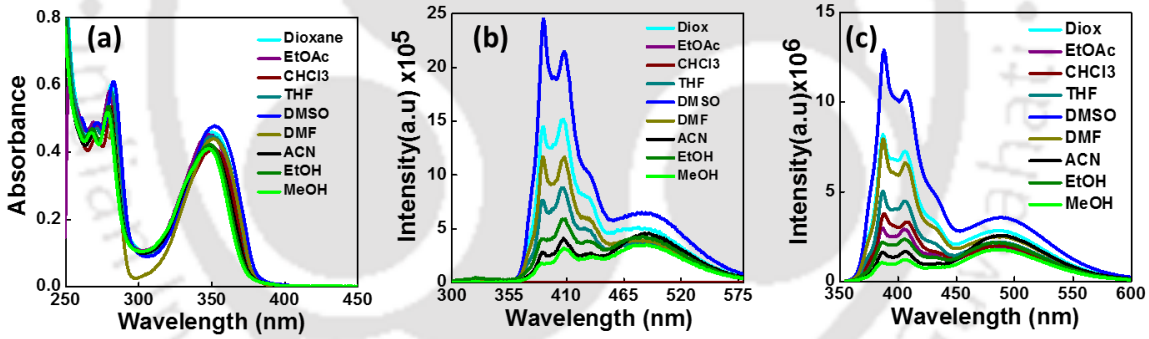

Figure 5.21. (a) UV-Visible and Fluorescence spectra of pentapeptide **5.42** in different solvents (b) λ_{ex} = 290 nm, (c) λ_{ex} = 345 nm (10 μM, r.t.; of each solvent).

Table 5.4: Summary table of photophysical properties of the peptides **5.53**, **5.55** and **5.42**

Entry	Solvents	Δf	UV-Vis & Fluorescence		
			λ_{max}^{abs} (nm)	λ_{max}^{fl} (nm)	Φ_f
Dipep. 5.53	Dioxane	0.021	281, 349	382, 400, 423	0.326
	$CHCl_3$	0.148	281, 350	382, 401, 422	0.158
	EtOAc	0.201	279, 347	381, 499, 421	0.133
	DMSO	0.265	282, 350	383, 402, 425	0.56
	EtOH	0.290	278, 345	380, 400, 421	0.140
	ACN	0.307	279, 345	380, 400, 422	0.137
	MeOH	0.309	278, 344	380, 399, 418	0.110
Tripep. 5.55	Dioxane	0.021	281, 349	387, 406, 429	0.303
	$CHCl_3$	0.148	281, 351	387, 406, 430	0.173
	EtOAc	0.201	280, 348	386, 406, 426	0.139
	DMSO	0.265	280, 350	387, 406, 428	0.57
	EtOH	0.290	279, 348	387, 405, 427	0.114
	ACN	0.307	279, 347	386, 406, 428	0.138
	MeOH	0.309	278, 346	386, 407, 430	0.051
Pentapep. 5.42	Dioxane	0.021	281, 351	387, 406, 426, 488	0.358
	$CHCl_3$	0.148	281, 351	388, 407, 428, 486	0.225
	EtOAc	0.201	280, 349	388, 407, 428, 485	0.183
	THF	0.210	279, 351	388, 407, 431, 488	0.246
	DMSO	0.265	282, 352	387, 406, 428, 488	0.498
	DMF	0.275	280, 351	387, 406, 429, 487	0.338
	EtOH	0.290	279, 349	324, 386, 406, 426, 485	0.192
	ACN	0.307	279, 349	386, 406, 487	0.191
	MeOH	0.309	278, 348	385, 406, 485	0.140

5.7.5. Study of Mechanism of Excimer Emission: Either via FRET and/or via Direct Excitation of the FRET Acceptor in Pentapeptide 5.42

We designed the trichromophoric pepntapetide **5.42** with a concept to uncover a dual door entry to the excimer/exciplex formation. We envisaged that excitation at the absorption maximum of the scaffold (290 nm) would lead to an energy transfer (FRET) to a second chromophore, ^{TPy}**Ala**^{Do}, which then release its excitation energy as emission (monomer) and form π-stacked complex (excimer) with the proximally positioned third chromophore, ^{TPy}**Ala**^{Do} in the trichromophoric pentapeptide **5.42**. The π-stacked complex would thus show excimer emission at a longer wavelength (**Figure 5.22**).

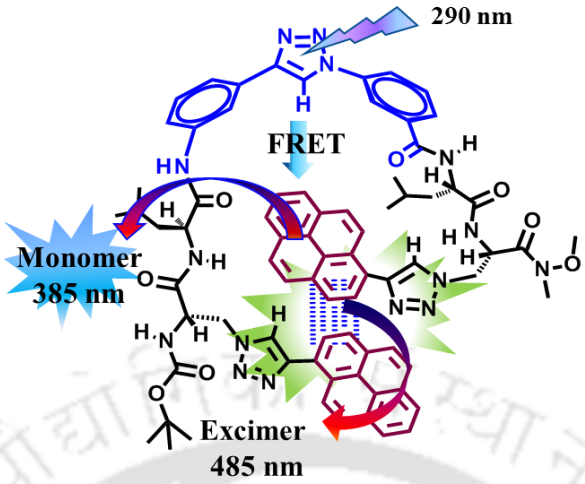

Figure 5.22. Schematic presentation of dual door entry to excimer emission through FRET in pentapeptide **5.42.**

To establishing dual door entry to excimer emission in the designed fluorescent pentapeptide **5.42**, we, next, proceeded to study in detail.

Proof of Excimer Emission via FRET: Based on our designing concept we found that the fluorescence spectrum of the aromatic triazolo amino acid scaffold (**5.41**, **^{Ar}TAA**) overlapped significantly with the absorption spectrum of **^{TPy}Ala^{Do}** containing dipeptide, **5.53** indicating a possibility of FRET process to occur (**Figure 5.23a**). Moreover, the peptide **5.42** could selectively be excited at 290 nm (λ_{max}^{abs} of **^{Ar}TAA**) where there is very low absorbance of **^{TPy}Ala^{Do}**. With this observation we turned our attention to study the FRET process in detail.[41, 57] When excited at absorption maximum of the donor, **^{Ar}TAA** (λ_{ex} = 290 nm), the pentapeptide **5.42** showed three emission bands at 330, 405 and 486 nm corresponding to emission from scaffold, **^{Ar}TAA**, monomer emission from **TPyAla^{Do}** and excimer emission from the π-stacked excited state complex between two terminal **^{TPy}Ala^{Do}**, respectively. Moreover, we observed that the fluorescence intensity of the acceptor, **^{TPy}Ala^{Do}**, increased from that of the free acceptor emission by almost two times in presence of donor. On the other hand, the fluorescence intensity of the donor, **^{Ar}TAA**, in pentapeptide **5.42** decreased almost two times of that of the free donor fluorescence in presence of an acceptor, **^{TPy}Ala^{Do}** (**Figure 5.23b**). These observations revealed the visual evidence of FRET process from **^{Ar}TAA** to **^{TPy}Ala^{Do}** in peptide **5.42**.[57c] The FRET process between the scaffold and the **TPy** was also evident from an emission of a tripeptide **5.55** wherein a single **TPy** was attached with the scaffold via an intervening Leu (**Figure 5.23b**). The phenomena were also reflected in the change and differences in intensities of

fluorescence images under UV-irradiation of various peptides at λ_{ex} = 290 and 350 nm, respectively (**Figure 5.23c-h**).

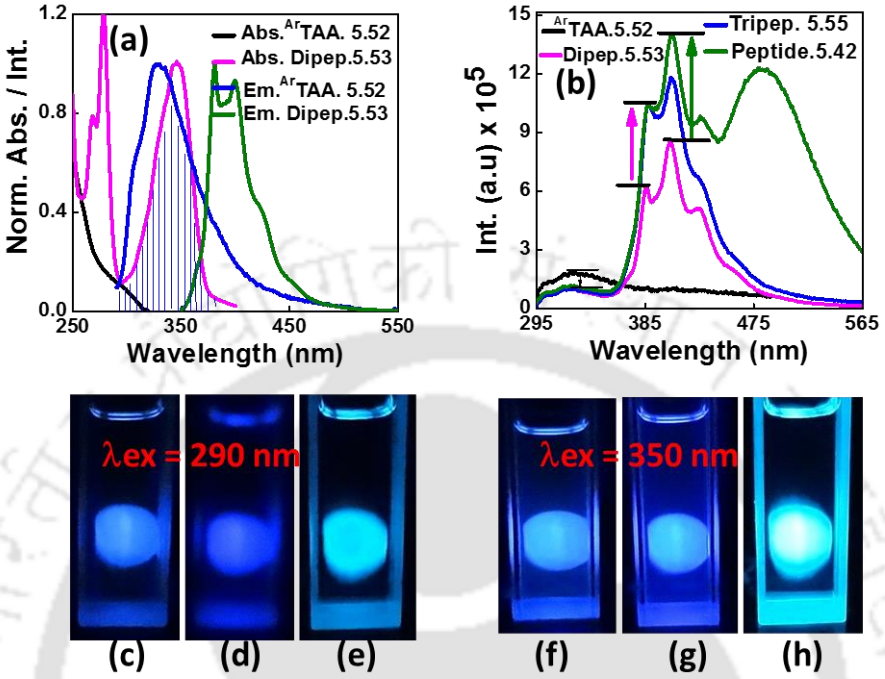

Figure 5.23. (a) Overlapping spectra of scaffold **^{Ar}TAA**, **5.41** (act as a FRET donor) emission and **^{TPy}Ala^{Do}**-Leu dipeptide **5.55** (act as a FRET acceptor) absorption, (b) Fluorescence spectra of individual donor **^{Ar}TAA 5.41**, acceptor dipeptide **5.53** and the tripeptide **5.55** (contain scaffold and **^{TPy}Ala^{Do}**-Leu dipeptide **5.53**) and the pentapeptide **5.42** (contain scaffold and double strand **^{TPy}Ala^{Do}**-Leu dipeptide **5.53, 4.125)** (10 µM each, r.t.; λ_{ex} = 290 nm in EtOH). (c-h) Photographs under fluorescence light of Dipeptide **5.53** (c, f); Tripeptide **5.55** (d, g); and Pentapeptide **5.42** (e, h) in ethanol solvents.

Further evidence of FRET process came from a time resolved fluorescence study wherein we observed a decrease in life time of both the components of donor (**^{Ar}TAA**; λ_{ex} = 293 nm, λ_{em} = 330 nm) from 3.7 to 2.0 ns and 8.9 to 6.4 ns (**Table 5.5**). While monitoring the decay at excimer emission (λ_{em} = 485 nm), the life time of **TPy** excimer was found to increase from 22.4 ns (λ_{ex} = 336 nm) to 25.9 ns (λ_{ex} = 293 nm) (**Table 5.5**).[52d-e, 57d-f] All these observations evident our hypothesis of FRET mediated excimer emission. Based on 2D NMR observation we can propose that the FRET occurred between the scaffold (**^{Ar}TAA)** and the C-terminal **TPy** of **^{TPy}Ala^{Do}**. The FRET mediated excimer emission is a new concept and might find wide applications in chemical biology.

Table 5.5: Summary table of fluorescence lifetimes of the peptides **5.41**, **5.53, 5.55 and 5.42** at λ_{ex} = 290 nm and 336 nm.

Entry	Solvents	Φ_f	λ [nm]	τ_1 [ns]	τ_2 [ns]	$<\tau>$ [ns]	k_f [$10^8 s^{-1}$]	k_{nr} [$10^8 s^{-1}$]	χ^2
λ_{ex} = 290 nm									
^{Ar}TAA. **5.41**	EtOH	0.07	330	3.65 (49%)	8.85 (51%)	6.21	0.112	1.5	1.03
Tripep. **5.55**	EtOH	0.005	330	2.15 (14%)	6.7 (86%)	6.07	0.008	1.64	1.03
Pentapep. **5.42**	EtOH	0.004	330	2.05 (15%)	6.38 (85%)	5.69	0.007	1.75	0.98
λ_{ex} = 290 nm									
Dipep. **5.53**	EtOH	0.152	405	20.83 (100%)	----	20.8	0.072	0.407	0.99
Tripep. **5.55**	EtOH	0.116	405	14.01 (100%)	----	14.1	0.046	0.748	0.92
Pentapep. **5.42**	EtOH	0.059	405	4.69 (18%)	14.34 (82%)	12.6	0.046	0.074	0.91
	EtOH	0.119	485	25.9 (100%)	----	25.9	0.045	0.340	1.05
λ_{ex} = 336 nm									
Dipep. **5.53**	EtOH	0.140	405	21.39 (100%)	----	21.39	0.065	0.402	1.03
Tripep. **5.55**	EtOH	0.114	405	14.39 (100%)	----	14.39	0.079	0.616	0.96
Pentapep. **5.42**	EtOH	0.057	405	5.2 (20%)	14.28 (80%)	12.45	0.045	0.757	0.93
	EtOH	0.136	485	1.54 (4%)	23.19 (96%)	22.42	0.060	0.385	1.01

For lifetimes of the fluorescent amino acids λ_{ex} = 290 nm and 336 nm; Concentration of each fluorescent amino acid = 10 μM; $<\tau>$, k_f, and k_{nr} are weighted means from the biexponential fits: $<\tau> = 1/(\alpha_1/\tau_1 + \alpha_2/\tau_2)$, $k_f = \Phi_f/<\tau>$, and $k_{nr} = (1- \Phi_f)/<\tau>$.

***Calculation of Energy Transfer efficiency*:** In a same way as described in **Chapter 3**; **Section 3.7.5**, using the values of κ^2= 2/3, n = 1.36, Φ_D = 0.068, and the obtained overlap integral, $J(\lambda)$ =5.9255 x 10^{16} the R_0 and r values were calculated which were found to be R_0 = 58 Å and r = 63 Å. R_0 is the critical distance when the energy transfer efficiency is 50 % and r is the distance between the donor and acceptor. **Energy Transfer efficiency** (E) = 1- F/F_0 = 38 %. F and F_0 are the fluorescence intensity of donor in the presence and absence of acceptor.

Proof of Excimer Emission via Direct Excitation of the FRET Acceptor: To establish the second path of excimer emission, i.e. via direct excitation of a FRET acceptor, **^{TPy}Ala^{Do}**, we excited the pentapeptide **2** at the absorption maxima of

^{TPy}**Ala**^{Do} (λ_{max} = 350 nm) and in reality we observed both the emission-the monomer emission at 405 nm as well as the excimer emission at 486 nm which was also supported from a time resolve fluorescence experiment (**Figure 5.21c**, **Table 5.5**). Therefore, we established our concept of dual mechanism of excimer emission-either via FRET or via direct excitation of the FRET acceptor. To the best of our knowledge this fundamental phenomenon is new and will attract scientists for designing such probes for application in chemical biology as well as in material sciences.

5.8. Studies On the Interaction of Pentapeptide 5.42 With BSA Protein

Finally, we explored the novel dual door entry system to excimer emissive pentapeptide **5.42** as a possible probe for sensing BSA protein.

UV-visible, Fluorescence and Circular Dichroism (CD) Study of Probe 5.42 (Pentapeptide) in Presence BSA Protein: We envisaged that the trichromophoric fluorescent pentapeptide would sense the interaction with BSA via the generation of an enhanced fluorescence signal-either via FRET mediated monomer emission from triazolylpyrene or excimer emission.

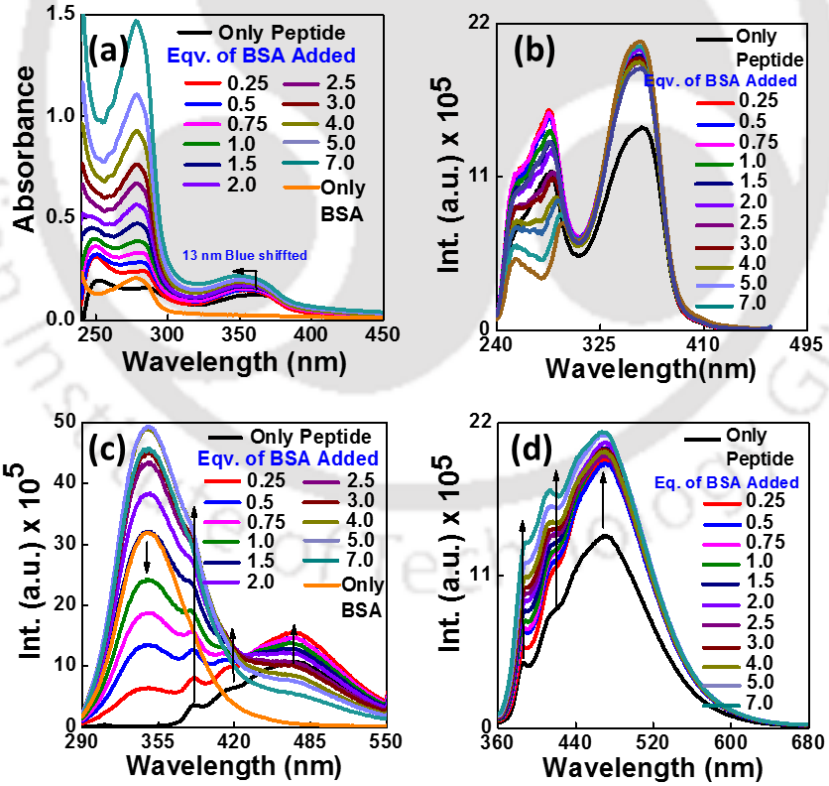

Figure 5.24. (a) UV-visible and (b) excitation spectra (λ_{ex} = 470 nm), (c) emission spectra (λ_{ex} = 280 nm) and (d) emission spectra (λ_{ex} = 350 nm) of Pentapeptide **5.42** in presence of increasing BSA concentration at 298K. [Pentapeptide] = 4 μM and [BSA] = 0, 1, 2, 3, 4, 6, 8, 12, 16, 20, 24, 28 μM.

Analysis of UV-visible absorption of probe peptide **5.42** in phosphate buffer showed a structureless absorption at around 360 nm corresponding to triazolyl pyrene (**TPy**) absorption. Addition of an increasing concentration of BSA to the probe solution resulted in a hyperchromicity in absorbance along with a blue shift of wavelength (13 nm) indicating a strong binding interactions between BSA and probe **5.42** in the hydrophobic region (**Figure 5.24a**).

A fluorescence titration experiment was carried out to investigate protein sensing ability and to get insight into the interaction with BSA. In phosphate buffer the probe exhibited a broad excimer emission at around 470 nm along with an overlapped monomer emission at 410 nm. Upon gradual addition of an increasing amount of BSA, the monomer emission intensities of the probe **5.42** increased when excited at the absorption maximum of **TPy** (350 nm, **Figure 5.24d**) indicating a strong interaction among the probe and hydrophobic pocket of BSA. On the contrary, upon excitation at 280 nm (absorption of the scaffold, **^{Ar}TAA** and BSA), a gradual increase in **TPy** monomer emission intensity at 385 nm was observed (**Figure 5.24c**). However, a minimal change in excimer/monomer intensity indicated a hindrance in the formation of π-π- stacked excited state complex between two **TPy** as the concentration of BSA increased. Moreover, **TPy** moieties got accommodated in the hydrophobic pocket of BSA leaving aside peptide chain on the surface which ultimately resulted in an increased monomer emission. This was supported by a large enhancement of fluorescence anisotropy from 0.02 to 0.15 (monitored at 385) which indicated that the **TPy** moiety of probe **2** bound strongly inside the hydrophobic pocket of BSA and experienced a highly restricted rotational motion (**Figure 25a**, **Table 5.6**).[58a, 59]

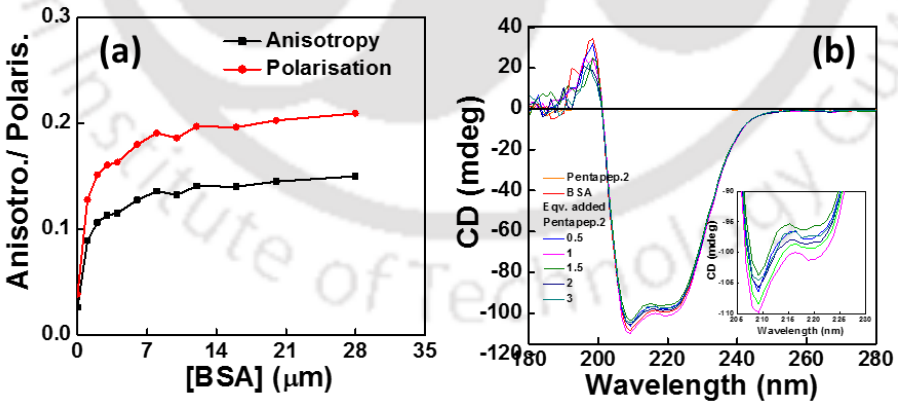

Figure 5.25. Steady-state anisotropy and polarisation plot (a) λ_{em} = 385 nm of pentapeptide **5.42** in presence of increasing BSA concentration. [Pentapeptide] = 4 μM and [BSA] = 0, 1, 2, 3, 4, 6, 8, 12, 16, 20, 24, 28 μM. (b) CD spectra of BSA in presence of increasing concentration of fluorophoric pentapeptide **5.42** in phosphate buffer (3% EtOH). [BSA] = 10 μM and [Pentapeptide] = 2.5, 5, 10, 15, 20, μM.

However, a small change in anisotropy corresponding to the excimer (from 0.01 to 0.04; monitored at 472) indicated a less perturbation of the excimer emission intensity of the probe **5.42** upon gradual addition of BSA. The slight change in the %α-helicity of BSA as was observed in the CD spectra in presence of the probe-peptide **2** indicated a possible conformational adjustment of BSA upon association in the hydrophobic region (**Figure 25b**).[60] Circular dichroism spectra were recorded using a CD spectropolarimeter with a cell path length of 1 mm at 25 ^{o}C, samples concentration 10 µM.

Table 5.6. Summary table of photophysical properties of the peptides **5.42-BSA tritation**.

Entry	**UV-Vis & Fluorescence**				
	λ_{max}^{abs} **(nm)**	λ_{max}^{fl} **(nm)**	Φ_f	**Anisotropy monitored at**	
				385 nm	**470 nm**
Compound **2.78**	284, 364	385, 411, 472	0.073	0.025	0.02278
Only BSA	278	346	0.058	----	----
Eqv. of add.BSA					
0.25 eqv.BSA	283,354	342, 385, 414, 472	0.083	0.08887	0.03089
0.50 eqv.BSA	282, 353	344, 384, 412, 471	0.083	0.10623	0.02869
0.75 eqv.BSA	280, 353	345, 484, 411, 472	0.084	0.11312	0.03049
1.00 eqv.BSA	281, 352	345, 383, 410, 473	0.078	0.11492	0.033
1.50 eqv.BSA	280, 350	346, 382, 410, 472	0.079	0.12768	0.03575
2.0 eqv.BSA	279, 350	346, 381, 409, 471	0.079	0.13569	0.04261

Study of Binding Events: The association constant (K) of the fluorophore with BSA was determined by a Benesi-Hildebrand plot[58] using the following equation 1,

$$\frac{1}{(I-I_0)} = \frac{1}{(I_\infty - I_0)} + \frac{1}{(I_\infty - I_0)K[BSA]} \quad \ldots\ldots\ldots\ldots\ldots (1)$$

Where I_0, I and I_α are the emission intensities of pentapeptide **5.42** in the absence of BSA, in the presence of an intermediate and at infinite concentration of BSA respectively. From the slop of the $1/(I - I_0)$ *vs.*$1/[BSA]$ plot of equation 1, binding constant K was determined and its value is 1.8×10^5 M^{-1}. ΔG = -7.16 Kcal (**Figure 26a)**.

The binding thermodynamics was also supported by an isothermal calorimetry (ITC)[61] measurement. Thus, the ITC tritation of BSA with pentapeptide **5.42** was performed at 298 K in phosphate bufffer pH 7.02. The protien solution (1 µm) was taken in a sample cell and titrant solution of pentapeptide **5.42** (15 µm) was fitted in the syringe. Thus, the plot of the amount of heat liberated per injection as a function of the molar ratio of the peptide **5.42** to BSA was best fitted with a standard nonlinear

least squares regression binding model involving two binding sites (**Figure 26b)**. The ITC titrations indicated mostly an exothermic binding process for site II. Binding events with pentapeptide **5.42** in the flexible site I and small site II pocket of BSA were found to be comparable with binding constants of 1.43-1.78 x 10^4 $mol^{-1}$and free energy change of -5.6 to -5.8 kcal/mol (**Table 5.7**). All the results suggested that both the hydrophobic as well as electrostatic interaction played an important role in the present BSA-peptide interaction process.

Table 5.7. Thermodynamical parameter of **BSA-peptide** system from ITC

Two sites binding				
K_1 (M^{-1})	N_1	ΔH_1 (cal/mol)	ΔS_1 (cal/mol/deg)	ΔG_1 (Kcal)
1.78 x 10^4	0.939	4.106 x 10^6	1.38 x 10^4	-5.8
K_2 (M^{-1})	N_2	ΔH_2 (cal/mol)	ΔS_2 (cal/mol/deg)	ΔG_2 (Kcal)
1.43 x 10^4	0.946	-5.349 x 10^6	-1.79 x 10^4	- 5.6

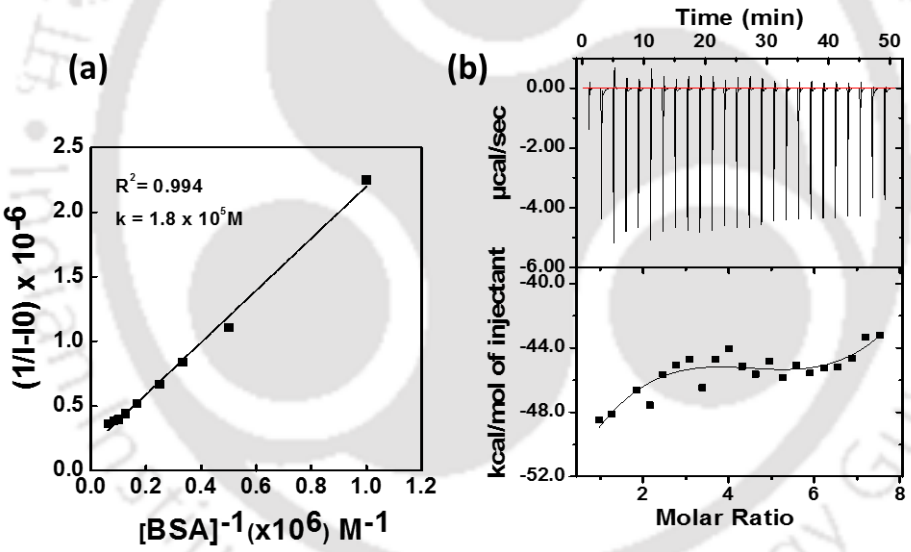

Figure 5.26: Benesi- Hildebrand plot of pentapeptide **5.42** in presence of increasing BSA concentration. . [pentapeptide] = 4 µM and [BSA] = 0, 1, 2, 3, 4, 6, 8, 12, 16, 20, 24, 28 µM. (b) Plot of isothermal titration calorimetry.

Study of FRET Between Pentapeptide 5.42 and BSA Protein: The spectroscopic study indicated that the probe might involve in energy transfer (FRET) with Trp unit of hydrophobic sub-domain that was again suggested from an overlapped emission spectrum of BSA and absorption spectrum of the probe (**Figure 27a**).[62] Interestingly, excitation at the BSA absorption (280 nm) we observed a FRET from Trp to **TPy** with a concomitant decrease in intensity of donor Trp emission at 345 nm and two to

three times enhancement of emission of **TPy** monomer at 385 nm acting as an acceptor (**Figure 27b**). The excimer intensity at 470 nm was also increased slightly. The FRET event in pentapeptide **5.42** upon binding with BSA was also evident from a time resolve fluorescence study. Thus, we observed a decrease in both the components of donor life time (Trp; λ_{ex} = 293 nm, λ_{em} = 350 nm) from 4.0 to 2.8 ns and 7.0 to 6.4 ns.[57d-f] While monitoring the decay at excimer emission (λ_{em} = 470 nm), the life time of **TPy** excimer remained almost unchanged (**Table 5.8**).

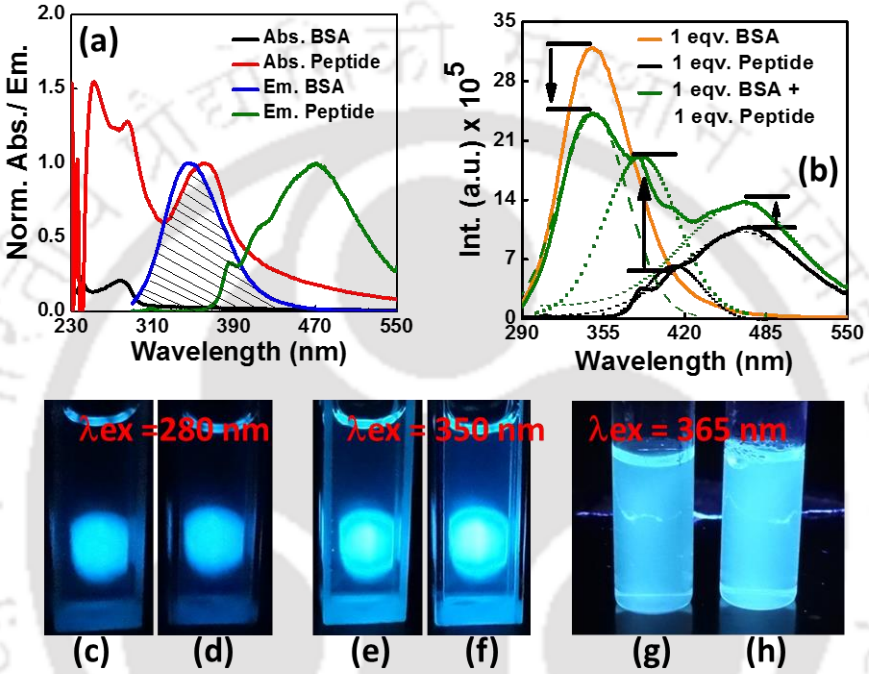

Figure 5.27. (a) Overlapped emission spectra of BSA (act as a FRET donor) and the absorption spectra of pentapeptide **5.42** (act as a FRET acceptor). (b) Steady state emission of BSA in absence or in presence of pentapeptide **5.42** showing a FRET process and FRET mediated excimer emission. Dotted lines represent the resolved spectra. (4 μM each, r.t.; λ_{ex} = 280 nm in buffer). (c-h) Picture under fluorescence light of pentapeptide **5.42** (**c**, **e** and **g**); Pentapeptide **5.42** –**BSA** (**d**, **f** and **h**) in phosphate buffer.

Both the FRET and excimer emissions were also reflected in the differences in intensities of fluorescence images of pentapeptide **5.42** in presence of BSA under UV-irradiation at λ_{ex} = 280, 350 and 365 nm, respectively (**Figure 5.27c-h**).

Table 5.8. Summary table of fluorescence lifetimes of the peptides **5.42** with increasing BSA concentation **at λ_{ex} = 290 nm**

Entry	Φ_f	λ [nm]	τ_1 [ns]	τ_2 [ns]	$<\tau>$ [ns]	k_f [$10^8 s^{-1}$]	k_{nr} [$10^8 s^{-1}$]	χ^2
Only BSA	0.058	350	4.03 (35%)	7.00 (65%)	6.51	0.097	1.57	1.01
1 eqv peptide+ 0. 5 eqv BSA	0.048	350	2.32 (24%)	5.57 (76%)	4.84	0.010	1.96	1.06
1 eqv peptide+ 1.00 eqv BSA	0.049	350	2.82 (17%)	6.42 (83%)	5.79	0.077	1.64	1.01
1 eqv peptide+ 2.00 eqv BSA	0.045	350	2.99 (17%)	6.49 (83%)	5.89	0.066	1.63	0.98
Only Peptide 2	0.041	470	2.92 (33%)	13.79 (66%)	10.1	0.03	0.94	1.04
1 eqv peptide+ 0.5 eqv BSA	0.046	470	3.25 (36%)	14.61 (63%)	10.4	0.046	0.906	1.04
1 eqv peptide+ 1 eqv BSA	0.044	470	3.41 (34%)	14.49 (65%)	10.6	0.042	0.896	1.03
1 eqv peptide+ 2.00 eqv BSA	0.044	470	3.40 (33%)	14.56 (67%)	10.8	0.035	0.886	1.03
For lifetimes of the peptide-BSA, λ_{ex} = 290 nm; Concentration of the peptide = 10 μM; $<\tau>$, k_f, and k_{nr} are weighted means from the biexponential fits: $<\tau> = 1/(\alpha_1/\tau_1 + \alpha_2/\tau_2)$, $k_f = \Phi_f/<\tau>$, and $k_{nr} = (1-\Phi_f)/<\tau>$.								

Calculation Of The Forster Distance and FRET Efficiency: Using the values of $\kappa^2 = 2/3$, n = 1.33, Φ_D = 0.058, and the obtained overlap integral, $J(\lambda)$ = 4.33113 x 10^{17} the R_0 and r values were calculated which were found to be R_0 = 82.59 Å and r = 99 Å. R_0 is the critical distance when the energy transfer efficiency is 50 % and r is the distance between the donor and acceptor. **Energy Transfer efficiency** (E) = 1-F/F_0 = 25 %. F and F_0 are the fluorescence intensity of donor in the presence and absence of acceptor.

Study of Binding Event-Docking Calculation: Among the various conformation of Peptide **5.42** with BSA from docking result, the docking pose (rank-2) was shown in **Figure (5.28)**. The close proximity of TPy of probe 2 and Trp of BSA and hence the possibility of occurrence of FRET process was also supported by a molecular docking calculation with Autodoc programme[63] which clearly showed that C-terminal TPy moiety of the probe-peptide 2 was located in the vicinity of tryptophan (Trp-134) and remained surrounded by other hydrophobic amino acids of the hydrophobic pocket of subdomain IB of site I of BSA (Fig. 5b). The free energy of binding (ΔG) obtained from a docking calculation was found to be in (-7.10 kcal/mol) excellent agreement with our experimental value (**Table 5.9)**.

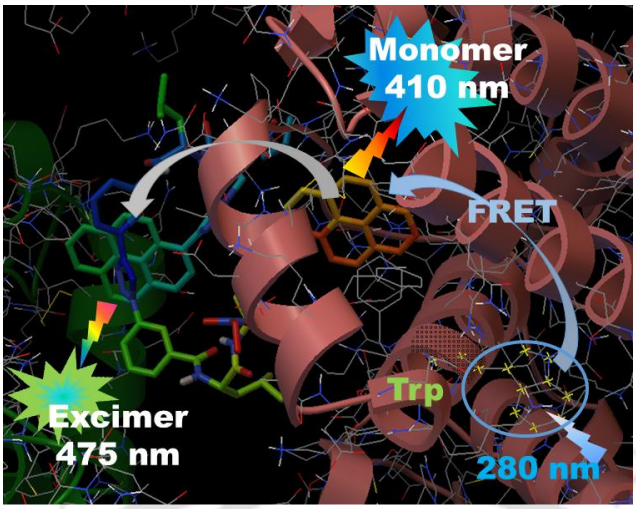

Figure 5.28. Docking pose of pentapeptide **5.42 – BSA.**

Table 5.9. Energy of Pentapeptide **5.42-BSA** complex obtained from Autodock4

Interaction Energy	kcal/mol
Estimated Free Energy of Binding	-7.10
Final Intermolecular Energy	-14.55
vdW + Hbond + desolv Energy	-13.45
Electrostatic Energy	-1.11
Final Total Internal Energy	-8.67
Torsional Free Energy	+7.46
Unbound System's Energy	-8.67

All these observations clearly proved the occurrence of excimer emission in the triazolo aromatic amino acid scaffolded trichromophoric β-sheet fluorescent pentapeptide **5.42** both via FRET as well as through excitation of a FRET acceptor. Furthermore, the probe was found to be efficient in sensing BSA protein via the generation of an enhanced **TPy** fluorescence via FRET and FRET-mediated **TPy-TPy** excimer emission.

5.9. Conclusion

In summary, the newly designed trichromophoric β-sheet pentapeptide represents a scerendipitus discovery of a dual door entry system for excimer emission. Both the processes of excitation of **TPy** of ^{TPy}**Ala**^{Do}-either energy transfer from excited scaffold amino acid, ^{Ar}**TAA** (FRET) to **TPy** or direct excitation of **TPy**-led to the excimer emission in pentapeptide **5.42**. This study would provide fundamental guidelines to design such conceptual fluorescent probe of dual door entry system to excimer emission. To the best of our knowledge this is the start of a new generation of

probes which would find wide applications in the field of chemical biology. Moreover, the novel probe of dual door entry to excimer emission system was found to be an effective fluorescence light-up probe for detecting and studying protein–peptide interactions in solution. Studying other specific protein–peptide interactions of significant clinical interest utilizing conceptual fluorescent peptide-probe is our current research focus.

5.10. Experimental Section

5.10.1. General Experimental: It is the same as was described in Chapter 4.

5.10.2. Synthetic Procedure and Characterization Data of Synthesized Peptides

Some General Procedures: All the general procedures such as, (a) for the Peptide coupling, (b) for [3+2] Cyclo-addition reaction, (c) for the deprotection of the methyl ester, and (d) for the deprotection of the Boc-group which were also adopted in this chapter were already described in the previous **Chapter 4**. Therefore these are excluded here.

***Synthesis of 3-(methoxycarbonyl) benzenaminium chloride* (5.46):** *m*-Amino benzoic acid **5.45** (1500 mg) was taken in a dried RB then it is dissolved by adding dry methanol. Under ice cold condition 1.2 equivalent $SOCl_2$ was added into the reaction mixture. After 15 minute reaction mixture was refluxed for 5-6 hours. After that reaction solvent was dried in rotary evaporator and washed the reaction mixture with toluene 3 times. The title compound **5.46** was isolated in quantitative yield.

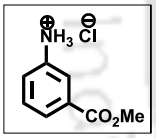

***Synthesis of methyl 3-azidobenzoate* (5.47) :** Starting material **5.46** (1500 mg) was taken in a conical then it dissolved by adding water and it was acidified with dil. HCl under ice cool condition. Then drop by drop 1.5 equivalent $NaNO_2$ solution was added to the reaction mixture. Consequently 1.5 eqv. NaN_3 solution was added slowly to the reaction mixture. After few minute to complete the reaction it was work up by ethyl acetate. The combined organic layer was washed by brine solution dried over Na_2SO_4. The title compound **5.47** was isolated by column chromatography (si-gel, PE) in pure form as colourless oil (1079 mg, Yield 76 %). IR (KBr) 2953, 2844, **2115**, 1727, 1585, 1484, 1443, 1300, 1140, 752 cm^{-1}.

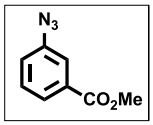

***Synthesis of tert-butyl (3-bromophenyl)carbamate* (5.49) :** In a dry THF, NaH (1.1 eqv) (washed by hexane) and 3-bromo aniline **5.48** (1 ml, 8.7 mmol) were taken. The reaction mixture was heated to reflux for one hour then cooled to room temperature. Boc anhydride (1.5 ml, 10.4 mmol) was added and reaction mixture was stirred for 30 minute. A second portion of sodium hydride (same eqv. amount again) was added to the reaction

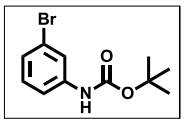

mixture and refluxed overnight. The reaction mixture was cooled to room temperature, carefully quenched by water. The reaction mixture was extracted with EtOAc. The combined organic layers were dried over Na_2SO_4. The Pure product **5.49** was isolated by column chromatography (Si-gel, PE : EtOAc = 10:1). (2070 mg, 7.6 mmol, Yield 88 %).

***Synthesis of tert-butyl (3-((trimethylsilyl)ethynyl)phenyl)carbamate* (5.50) :** In a dry R.B, compound **5.49** (800 mg, 2.95 mmol) was taken with dry solvent benzene : n-butyl amine = 2:1 then catalyst $PdCl_2(PPh_3)_2$ (103.6 mg, 0.147 mmol) was added and degassed by N_2 gas. After fifteen minute of stirring the reaction mixture, TMS acetylene (600 µl, 4.42 mmol) and CuI (11.2 mg, 0.06 mmol) was added and heated to 80 ^{0}C temperature for 12 hour. Then solvent was dried by rotary evaporator, then it was partitioned between EtOAc and aqueous NH_4Cl solution (20 ml each). The organic layer was washed with brine solution. Pure product **5.50** (665 mg, 2.3 mmol) was isolated in pure form by column chromatography (Si-gel, PE : EtOAc = 10:1). Yield 78 %. ^{1}H NMR ($CDCl_3$; 400 MHz) δ 0.15 (9H, s); 1.42 (9H, s); 6.52 (1H, bs); 7.04 (1H, d, J = 6.8 Hz); 7.1 (1H, t, J = 8.2 Hz); 7.17 (1H, d, J = 8.4 Hz); 7.48 (1H, s); ^{13}C NMR ($CDCl_3$; 100 MHz) δ 0.1, 28.4, 80.8, 94.3, 104.9, 118.8, 121.8, 126.7, 128.9, 130.3, 138.4, 152.7.

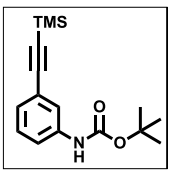

***Synthesis of tert-butyl (3-ethynylphenyl)carbamate* (5.51) :** Compound **5.50,** 650 mg (2.24 mmol) was dissolved in 8 ml THF with 1 ml methanol, 314 mg (5.6 mmol) KOH was added to the solution at room temperature and stirrer overnight. Then solvent was dried by rotary evaporator, then it was partitioned between EtOAc and water. The organic layer was washed with brine solution. Pure product **5.51** (468 mg, 2.15 mmol) was isolated in pure form by column chromatography (Si-gel, PE : EtOAc = 10:1). Yield 96 %. ^{1}H NMR ($CDCl_3$; 400 MHz) δ 1.5 (9H, s); 3.04 (1H, s); 6.63 (1H, s); 7.14 (1H, d, J = 7.6 Hz); 7.19 (1H, t, J = 8 Hz); 7.43 (1H, d, J = 8 Hz); 7.53 (1H, s); ^{13}C NMR ($CDCl_3$; 100 MHz) δ 28.4, 77.3, 80.9, 83.5, 119.2, 122.1, 122.8, 126.8, 129.1, 138.5, 152.7.

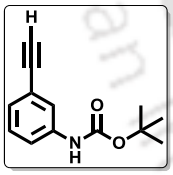

***Synthesis of methyl 3-(4-(3-((tert-butoxycarbonyl)amino)phenyl)-1H-1,2,3-triazol-1-yl)benzoate* (5.52) :** The ethynyl derivative **5.51**, 450 mg (2.06 mmol) was taken in a 5:1 dry THF and water system and degassed for 5 min with nitrogen gas. Methyl 3-azidobenzoate **5.47**, 403 mg (2.3 mmol), 6 mol % sodium ascorbate and 1 mol% powderd CuSO4 were added followed by. Then 1.2 eqv Et_3N was added and reaction mixture was degassed and refluxed for 18-20 hour. After finishing starting material, the reaction mixture was evaporated completely and it was partitioned by EtOAc and NH_4Cl solution. The organic layer was washed with brine, dried over Na_2SO_4. Pure product **5.52** (670 mg, 1.7 mmol) was isolated in pure form by column chromatography (Si-gel, PE : EtOAc = 2:1). Yield 82 %. IR (KBr)

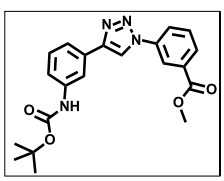

3328, 3137, 2965, 2919, 1718, 1593, 1448, 1289, 1151, 762 cm^{-1}. ^1H NMR (d_6-DMSO; 600 MHz) δ 1.48 (9H, s); 3.91 (3H, s); 7.38-7.34 (2H, m); 7.52 (1H, d, *J* = 6.6 Hz); 7.78 (1H, t, *J* = 7.8 Hz); 8.06 (1H, d, *J* = 7.8 Hz); 8.17 (1H, s), 8.24 (1H, d, *J* = 7.8 Hz); 8.49 (1H, s); 9.33 (1H, s); 9.45 (1H, s); ^{13}C NMR (d_6-DMSO; 150 MHz) δ 28.5, 52.9, 79.7, 115.4, 118.7, 119.9, 120.1, 120.6, 124.8, 129.5, 129.8, 130.7, 131.1, 131.7, 137.1, 140.4, 147.9, 153.3, 165.8. HRMS calcd for $C_{21}H_{23}N_4O_4$ ($[M + H]^+$) 395.1713, found 395.1712.

***Synthesis of 3-(4-(3-((tert-butoxycarbonyl)amino)phenyl)-1H-1,2,3-triazol-1-yl)benzoic acid* (5.41):** Using the general procedure of methyl ester hydrolysis, starting from 500 mg (1.26 mmol) of **5.52**, 463 mg (1.2 mmol) of the title compound **5.41** (445 mg, 1.17 mmol) was isolated as a white solid material in pure form by column chromatography (Si-gel, PE : EtOAc = 1:2). Yield 93%. ^1H NMR (d_6-DMSO; 400 MHz) δ 1.47 (9H, s); 7.36 (2H, s); 7.51 (1H, s); 7.75 (1H, t, *J* = 7.6 Hz); 8.04 (1H, d, *J* = 6.8 Hz), 8.16 (1H, s); 8.08 (1H, d, *J* = 8.0 Hz); 8.46 (1H, s); 9.33 (1H, s); 9.47 (1H, s); ^{13}C NMR (d_6-DMSO; 100 MHz) δ 28.4, 79.6, 115.3, 118.5, 119.9, 120.1, 120.6, 120.7, 124.4, 129.5, 130.8, 132.9, 137.1, 140.4, 147.9, 153.2, 166.7. HRMS calcd for $C_{20}H_{19}N_4O_4$ $[M + H]^+$ 381.1557, found 379.1558.

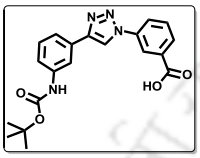

***Synthesis of (S)-tert-butyl (3-azido-1-(methoxy(methyl)amino)-1-oxopropan-2-yl)carbamate* (2.069):** This is already given in **Chapter 2**.

***Synthesis of Boc deprotected (S)-tert-butyl (3-azido-1-(methoxy(methyl)amino)-1-oxopropan-2-yl)carbamate* (4.117):** This is already given in **Chapter 4**.

Synthesis of *tert-butyl ((S)-1-(((S)-3-azido-1-(methoxy(methyl)amino)-1-oxopropan-2- yl)amino)-4-methyl-1-oxopentan-2-yl)carbamate* (4.119) : This is already given in **Chapter 4**.

***Synthesis of tert-butyl ((S)-1-(((S)-1-(methoxy(methyl)amino)-1-oxo-3-(4-(pyren-1-yl)-1H-1,2,3-triazol-1-yl)propan-2-yl)amino)-4-methyl-1-oxopentan-2-yl)carbamate* (5.53) :** Using the general procedure of [3+2] cyclo-addition reaction, starting from 200 mg (0.52 mmol) of azide derivative of dipeptide **4.119** and 140 mg (0.62 mmol) of 1-ethynyl pyrene, 247 mg (0.40 mmol) of the title compound **5.53** was isolated as a light brown solid material (Si-gel, PE : EtOAc = 1:1). Yield 78%; IR (KBr) 3450, 2958, 2928, 2102, 1653, 1509, 1390, 1167, 1049, 848 cm^{-1}. ^1H NMR ($CDCl_3$; 600 MHz); δ 0.89 (6H, d, *J* = 5.4 Hz); 1.38 (9H, s); 1.52-1.48 (1H, m); 1.67-1.59 (2H, m); 3.29 (3H, s); 3.7 (3H, s); 4.11 (1H, bs); 4.89 (1H, dd, *J* = 4.2 Hz, 9.6 Hz); 4.95 (1H, d, *J* = 6.6 Hz); 5.05 (1H, bs); 5.36 (1H, bs); 7.22 (1H, d, *J* = 5.4 Hz); 7.99 (1H, t, *J* = 7.2 Hz); 8.06 (2H, d, *J* = 4.8 Hz); 8.09 (1H, t, *J* = 9.0 Hz); 8.18-8.15 (3H, m); 8.30 (1H, s); 8.31 (1H, s); 8.79 (1H, d, *J* = 9.0 Hz); ^{13}C NMR ($CDCl_3$; 150 MHz); δ 21.9, 23.1, 24.9, 28.4, 32.9, 41.1, 50.4, 50.7, 53.9, 62.1, 80.4, 124.8, 124.9, 125.0, 125.2, 125.3, 125.4, 126.1, 127.4, 127.5,127.8, 128.2, 128.7,

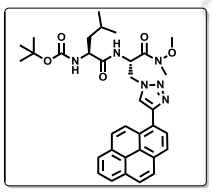

131.1, 131.4, 131.5, 147.8, 155.9, 168.2, 173.2. HRMS calcd for $C_{34}H_{41}N_6O_5$ ([M + H]$^+$) 613.3133, found 613.3132.

***Synthesis of Boc deprotected (S)-1-(((S)-1-(methoxy(methyl)amino)-1-oxo-3-(4-(pyren-1-yl)-1H-1,2,3-triazol-1-yl)propan-2-yl)amino)-4-methyl-1-oxopentan-2-aminium 2,2,2-trifluoroacetate* (5.54):** Using the general procedure of Boc-deprotection, compound **5.53** (240 mg, 0.40 mmol) was deprotected. The product **5.54** was obtained in quantitative yield and were used without further purification and characterization.]

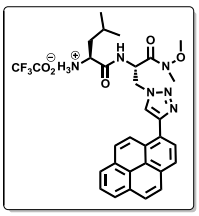

***Synthesis of tert-butyl (3-(1-(3-(((S)-1-(((S)-1-(methoxy(methyl)amino)-1-oxo-3-(4-(pyren-1-yl)-1H-1,2,3-triazol-1-yl)propan-2-yl)amino)-4-methyl-1-oxopentan-2-yl)carbamoyl)phenyl)-1H-1,2,3-triazol-4-yl)phenyl)carbamate* (5.55):** To a solution of N-protected ^{Ar}**TAA, 5.41** (130 mg, 0.342 mmol) in dry DMF was cooled to 0 ^{o}C by ice bath. Consequently 1-[3-dimethyl amino propyl]-3-ehtylcarbo-diimide hydrochloride (EDC.HCl) (98 mg, 0.513 mmol), DMAP (125 mg, 1.02 mmol) and amine salt of weinreb amide protected corresponding dipeptide **5.54** were added and the reaction mixture was stirred for 18 hour at 0 ^{o}C to room temperature. Then solvent was dried by rotary evaporator, after which it was partitioned between EtOAc and water (50 ml each). The organic layer was washed with brine solution. Pure product **5.55** (230 mg, 0.259 mmol) was isolated in pure form by column chromatography (Si-gel, EtOAc) as solid compound. Yield 76%. IR (KBr) 3452, 3325, 2931, 1726, 1654, 1530, 1385, 1524, 1236, 1160, 1051, 842 cm^{-1}. ^{1}HNMR ($CDCl_3$; 400 MHz) δ 0.87 (6H, d, J = 5.2 Hz); 1.53 (9H, s); 1.74-1.63 (3H, m); 3.30 (3H, s); 3.84 (3H, s); 4.78 (1H, q, J = 6.8 Hz); 4.87 (1H, dd, J = 8.0 Hz, 6.0 Hz); 5.01 (1H, bs); 5.48 (1H, bs); 6.91 (1H, t, J = 8.0 Hz); 7.05 (1H, bs); 7.24 (1H, s); 7.33-7.29 (2H, m); 7.41 (1H, d, J = 8 Hz); 7.51 (1H, d, J = 7.6 Hz); 7.66 (1H, d, J = 6.8 Hz); 7.74 (1H, s); 7.81 (1H, s); 7.90-7.87 (4H, m); 7.99-7.94 (4H, m); 8.08 (2H, t, J = 7.6 Hz); 8.20 (1H, s); 8.51 (1H, d, J = 8.4 Hz); ^{13}C NMR ($CDCl_3$; 100 MHz) δ 21.7, 22.9, 24.8, 28.3, 32.5, 36.4, 40.4, 50.5, 52.8, 61.9, 80.4, 115.7, 117.9, 118.3, 118.5, 120.1, 122.4, 124.4, 124.6, 124.7, 124.8, 124.9, 125.2, 125.9, 127.1, 127.2, 127.6, 127.9, 128.2, 129.2, 129.4, 130.3, 130.6, 131.0, 131.1, 134.5, 136.2, 139.3, 147.2, 147.8, 153.2, 162.7, 168.3, 173.1. HRMS calcd for $C_{49}H_{51}N_{10}O_6$ ([M + H]$^+$) 875.3988, found 875.3993.

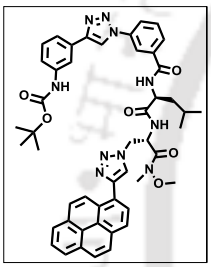

Synthesis of *(S)-methyl 2-((S)-3-azido-2-((tert-butoxycarbonyl)amino)propanamido)-4-methylpentanoate* (4.124): This is already given in **Chapter 4**.

***Synthesis of (S)-methyl 2-((S)-2-((tert-butoxycarbonyl)amino)-3-(4-(pyren-1-yl)-1H-1,2,3-triazol-1-yl)propanamido)-4-methylpentanoate* (4.125) :** This is already given in **Chapter 4**.

Synthesis of tert-butyl ((S)-1-(((S)-1-((3-(1-(3-(((S)-1-(((S)-1-(methoxy(methyl)amino)-1-oxo-3-(4-(pyren-1-yl)-1H-1,2,3-triazol-1-yl)propan-2-yl)amino)-4-methyl-1-oxopentan-2-yl)carbamoyl)phenyl)-1H-1,2,3-triazol-4-yl)phenyl)amino)-4-methyl-1-oxopentan-2-yl)amino)-1-oxo-3-(4-(pyren-1-yl)-1H-1,2,3-triazol-1-yl)propan-2-yl)carbamate **(5.42):** Starting material **4.125,** 160 mg (0.281 mmol) was taken in a dry 50 ml RB. With creating nitrogen atmosphere and maintaining 0 ^{o}C temperature by ice bath we are added dry THF solvent, ethyl chloroformate and tri-ethylamine followed by. Then free amine of tripeptide **5.56**, 218 mg (0.281 mmol) was added to the reaction mixture and allowed to stirrer about half an hour. After removing ice bath the reaction mixture was refluxed approximate 4 to 5 hour and monitored by TLC. The pure product **5.42**, 156 mg (0.12 mmol) was isolated as a solid material (CH_3Cl:MeOH = 10:1). Yield 42%. IR (KBr) 3440, 3323, 2953, 2914, 2849, 1716, 1653, 1586, 1539, 1497, 1388, 1367, 1156, 1052, 849, 757 cm^{-1}. ^{1}H NMR (d_6-DMSO; 600 MHz) δ 0.83 (6H, bs); 0.92 (6H, dd, *J* = 6.6 Hz, 3 Hz); 1.31 (9H, s); 1.49 (1H, bs); 1.59 (1H, bs); 1.65-1.73 (4H, m); 3.18 (3H, s); 3.79 (3H, s); 4.56 (1H, bs); 4.62 (1H, bs); 4.77-4.70 (3H, m); 4.95 (2H, dd, *J* = 10.2 Hz, 12.6 Hz); 5.39 (1H, bs); 7.26 (1H, d, *J* = 7.8 Hz), 7.36 (2H, dt, *J* = 25.2 Hz, 7.8 Hz); 7.52 (1H, d, *J* = 7.8 Hz); 7.64 (1H, d, *J* = 7.8 Hz); 7.78 (1H, d, *J* = 7.2 Hz); 7.85 (1H, d, *J* = 7.8 Hz); 8.03 (2H, dt, *J* = 22.2 Hz, 7.2 Hz); 8.10 (1H, d, *J* = 9.0 Hz); 8.20-8.17 (5H, m); 8.22 (1H, t, *J* = 6.6 Hz); 8.31-8.24 (8H, m); 8.34 (1H, s); 8.48 (1H, d, *J* = 7.2 Hz); 8.65 (1H, s); 8.68 (1H, s); 8.72 (1H, d, *J* = 7.2 Hz); 8.75 (2H, d, *J* = 9.6 Hz); 8.81 (1H, d, *J* = 9.6 Hz); 9.1 (1H, s); 10.2 (1H, s); ^{13}C NMR (d_6-DMSO; 150 MHz) δ 21.4, 21.5, 23.0, 23.1, 24.2, 24.3, 28.1, 31.5, 49.5, 49.9, 50.7, 52.1, 52.3, 54.3, 61.6, 78.8, 116.2, 118.8, 119.3, 119.6, 120.7, 122.4, 123.8, 123.9, 124.2, 124.3, 124.8, 124.9, 125.0, 125.1, 125.2, 125.3, 125.39, 125.4, 125.5, 126.3, 126.4, 126.9, 127.1, 127.2, 127.3, 127.4, 127.6, 127.8, 127.9, 129.4, 129.5, 130.3, 130.4, 130.5, 130.6, 130.8, 130.9, 135.3, 136.3, 139.4, 145.8, 146.1, 147.2, 155.1, 165.1, 168.9, 171.1, 172.4.; HRMS calcd for $C_{76}H_{76}N_{15}O_8$ ($[M + H]^+$) 1326.5998, found 1326.6014.

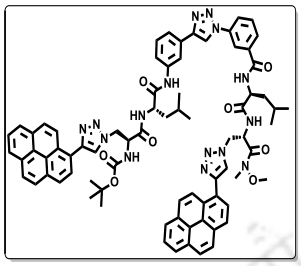

Synthesis of ((S)-methyl 2-((S)-2-((tert-butoxycarbonyl)amino)-3-phenylpropanamido)-4-methylpentanoate **(4.113):** This is already given in **Chapter 4**.

Synthesis of Boc deprotected ((S)-methyl 2-((S)-2-((tert-butoxycarbonyl)amino)-3-phenylpropanamido)-4-methylpentanoate **(4.114):** This is already given in **Chapter 4**.

(S)-Methyl-2-((S)-2-(3-(4-(3-((tert-butoxycarbonyl)amino)phenyl)-1H-1,2,3-triazol-1-yl)benzamido)-3-phenylpropanamido)-4-methylpentanoate (5.57): In a dry DMF, N-protected aromatic triazolyl amino acid **^{Ar}TAA, 5.41** (200 mg, 0.526 mmol) was taken in a dry R.B. Under ice cold condition 1-[3-dimethyl amino propyl]-3-ehtylcarbo-diimide hydrochloride (EDC.HCl) (150.69 mg, 0.789 mmol),

DMAP (192.52 mg, 1.578 mmol) were added and stirred for 15 minutes. After that the amine salt of methyl ester protected dipeptide **4.114** was added and the reaction mixture was stirred for another 18 h at 0 ^{o}C to room temperature. After completion of

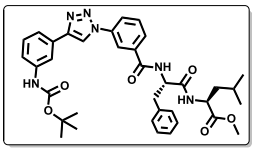

the reaction, the solvent was dried by rotary evaporator, after which it was partitioned between EtOAc and water (30 ml each). The organic layer was washed with brine solution. Pure product **5.57 (**250 mg, 0.389 mmol) was separated in pure form by column chromatography (Si-gel, PE: EtOAc = 1:1) as solid compound. Yield 73%; ^{1}H NMR (d$_6$-DMSO; 400 MHz) δ 0.85 (6H, dd, *J* = 6 Hz, 16.8 Hz); 1.49 (9H, s); 1.56-1.52 (1H, m); 1.69-1.59 (2H, m); 3.00 (1H, t, *J* = 12.4 Hz); 3.14 (1H, dd, *J* = 3.2 Hz, 13.6 Hz); 3.62 (3H, s); 4.32 (1H, m); 4.84 (1H, m); 7.17 (1H, q, *J* = 8.0 Hz); 7.26 (2H, t, *J* = 7.6 Hz); 7.37 (3H, s); 7.39 (1H, s); 7.52-7.50 (1H, m); 7.70 (1H, t, *J* = 8 Hz); 7.94-7.89 (1H, m); 8.10 (1H, dt, *J* = 1.2 Hz, 8.4 Hz); 8.21 (1H, s); 8.36 (1H, s); 8.58 (1H, d, *J* = 7.6 Hz); 8.87 (1H, d, *J* = 8 Hz); 9.25 (1H, s); 9.51 (1H, s); ^{13}C NMR (d$_6$-DMSO; 100 MHz); δ 21.4, 22.8, 24.3, 28.2, 37.1, 40.1, 50.5, 51.9, 54.7, 79.2, 115.1, 118.3, 119.1, 119.5, 119.7, 122.8, 126,3, 127.5, 128.1, 129.2, 129.3, 129.4, 130.0, 130.6, 135.7, 136.6, 138.2, 140.2, 147.6, 152.9, 165.2, 171.7. 172.9. HRMS calcd for $C_{36}H_{43}N_6O_6$ ([M + H]$^+$) 655.3239, found 655.3231.

***(S)-methyl-2-((S)-2-(3-(4-(3-((S)-2-((tert-butoxycarbonyl)amino)-3-(4 hydroxyphenyl)propanamido)phenyl)-1H-1,2,3-triazol-1-yl)benzamido)-3-phenylpropanamido)-4-methylpentanoate* (5.43):** In a dry THF at 0 ^{o}C temperature N-Boc tyrosine (60.93 mg, 0.213 mmol), ethyl chloroformate (24µl , 0.256 mmol) and trimethyl amine (35 µl, 0.256 mmol) were added. After five minutes free amine and C-terminal protected tripeptide **5.58** (106 mg, 0.192 mmol) was added and stirred at half an hour at cold condition. Then reaction mixture was refluxed about 4 to 5 hour and reaction monitor by TLC. After completion of the reaction, the solvent was dried by rotary evaporator, after which it was partitioned between EtOAc and water (50 ml each). The organic layer was washed with brine solution. Pure product **5.43 (**80 mg, 0.098 mmol) was isolated in pure form by column chromatography (Si-gel, PE : EtOAc = 1:1) as solid compound. Yield 46%; %; IR (KBr) 3441, 3331, 2953, 2923, 1744, 1670, 1519, 1439, 1371, 1236, 1164, 1045, 789, 688 cm^{-1}. ^{1}H NMR (d$_6$-DMSO; 600 MHz) δ 0.89 (6H, dd, *J* = 5.4 Hz, 12.6 Hz); 1.33 (9H, s); 1.52 (1H, bs); 1.65 (2H, bs); 2.74 (1H, d, *J* = 12.4 Hz); 2.89 (1H, bs); 3.01 (2H, dd, *J* = 5.4 Hz, 16.8 Hz); 3.57 (3H, s); 4.26 (1H, bs); 4.48 (1H, q, *J* = 5.4 Hz); 4.62 (1H, bs); 6.65 (2H, d, *J* = 7.2 Hz); 7.05 (1H, d, *J* = 7.8 Hz); 7.12 (2H, d, *J* = 7.8 Hz); 7.15 (1H, s); 7.21 (4H, s); 7.44 (1H, t, *J* = 7.8 Hz); 7.61 (2H, dd, *J* = 7.2 Hz, 15.6 Hz); 7.74 (1H, t, *J* = 7.8 Hz); 8.01 (1H, d, *J* = 7.8 Hz); 8.13 (1H, d, *J* = 7.2 Hz); 8.27 (1H, s); 8.43 (1H, s); 8.45 (1H, s); 8.67 (1H, d, *J* = 7.8 Hz); 9.19 (1H, s); 9.32 (1H, s); 10.17 (1H, s); ^{13}C NMR (d$_6$-DMSO; CDCl$_3$; 150 MHz); δ 22.2, 22.8, 24.9, 28.3, 37.7, 40.9, 52.4, 52.5, 53.5,

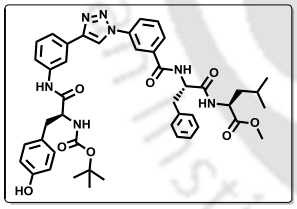

54.0, 57.4, 80.3, 115.6, 116.9, 117.9, 118.0, 119.7, 121.2, 123.4, 127.0, 128.0, 128.1, 128.6, 129.0, 130.0, 130.2, 130.3, 130.7, 134.7, 136.1, 136.7, 147.6, 155.6, 156.5, 166.2, 171.9, 173.5 HRMS calcd for $C_{45}H_{52}N_7O_8$ ([M + H]$^+$) 818.3872, found 818.3871.

5.11. ^{1}H and ^{13}C NMR Spectra of Some Selected Intermediates and Final Peptides

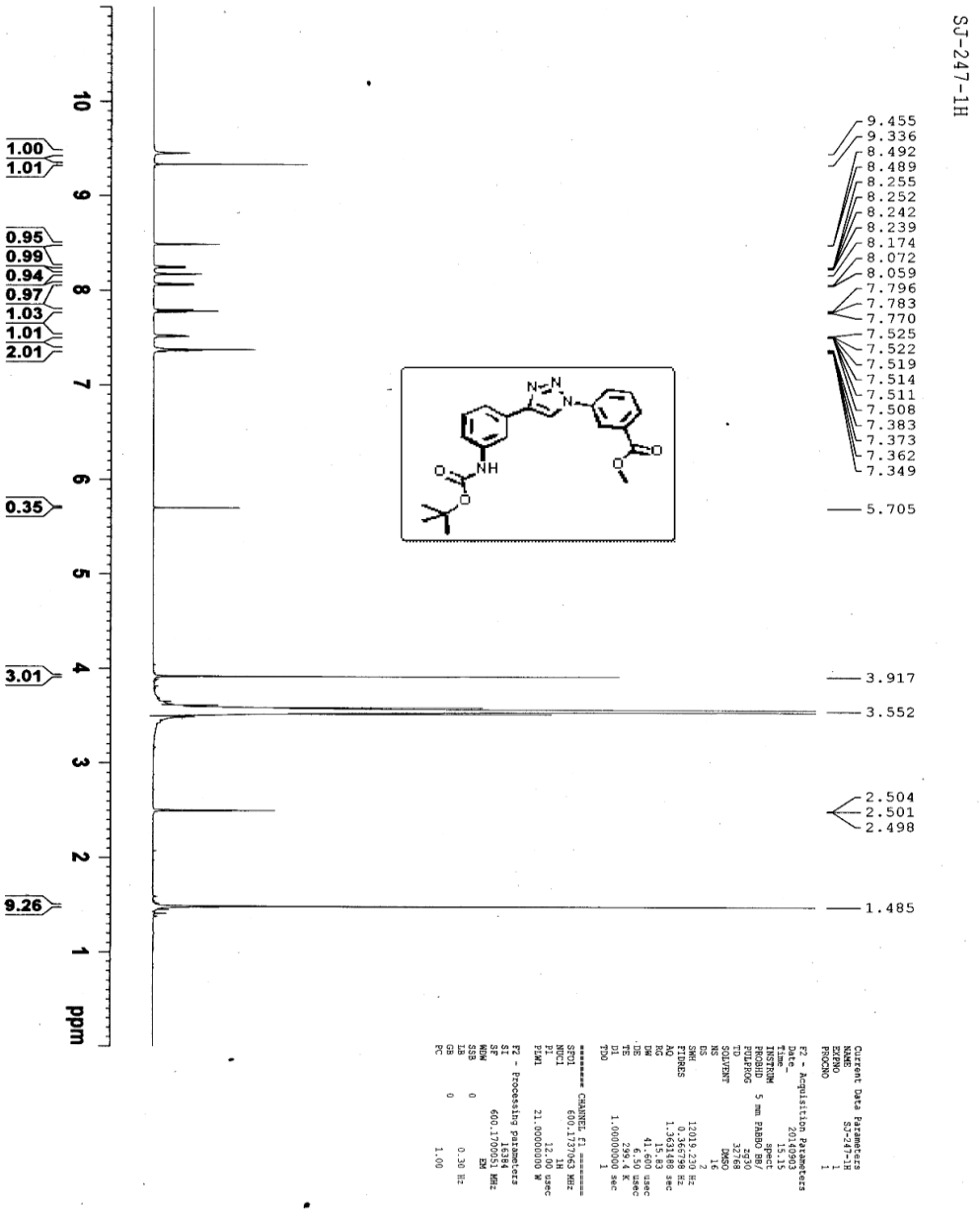

Figure 5.29. ^{1}H NMR spectra of synthesized compound **5.52.**

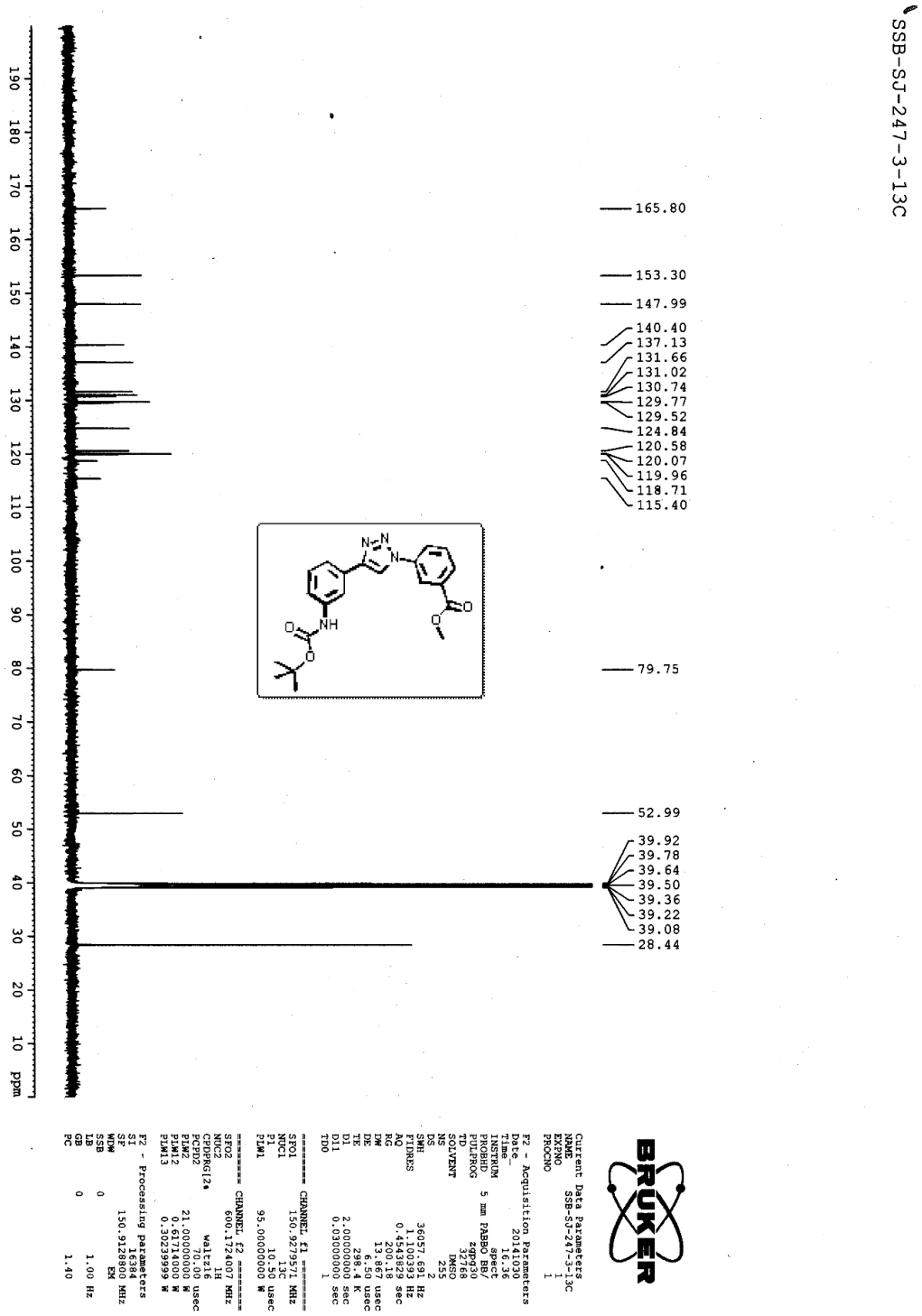

Figure 5.30. ^{13}C NMR spectra of synthesized compound **5.52.**

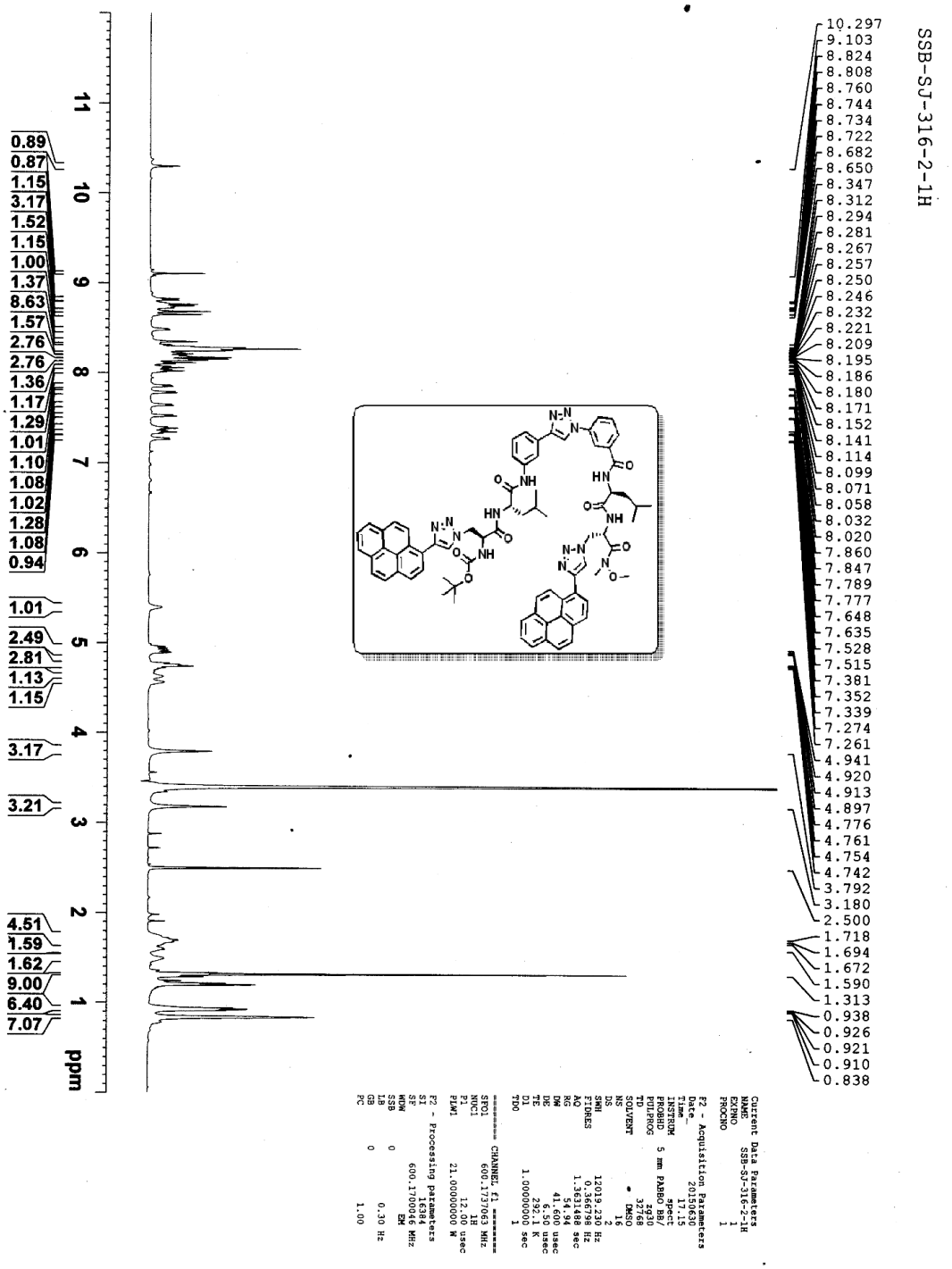

Figure 5.31. ^{1}H NMR spectra of synthesized compound **5.42.**

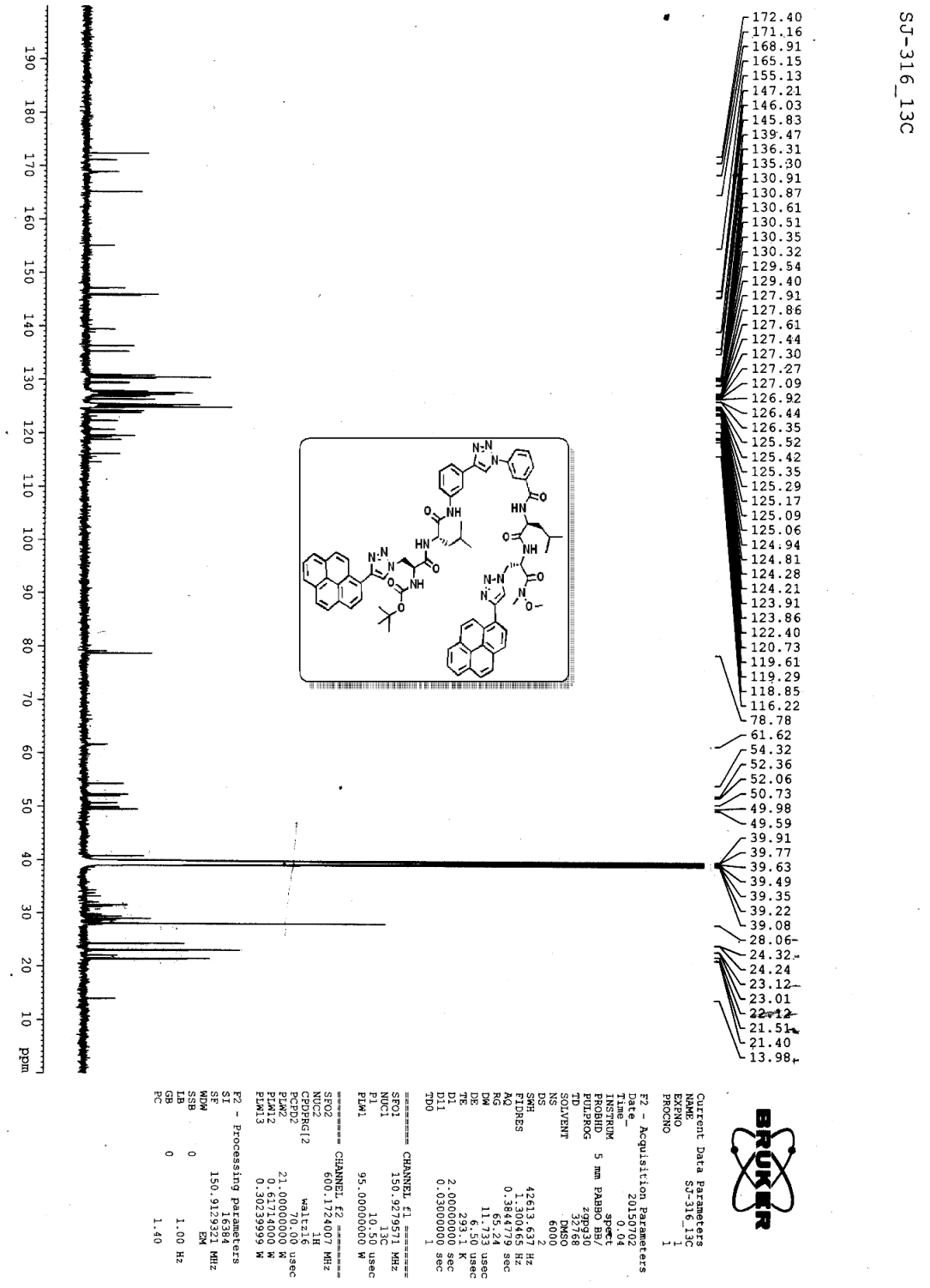

Figure 5.32. ^{13}C NMR spectra of synthesized compound **5.42.**

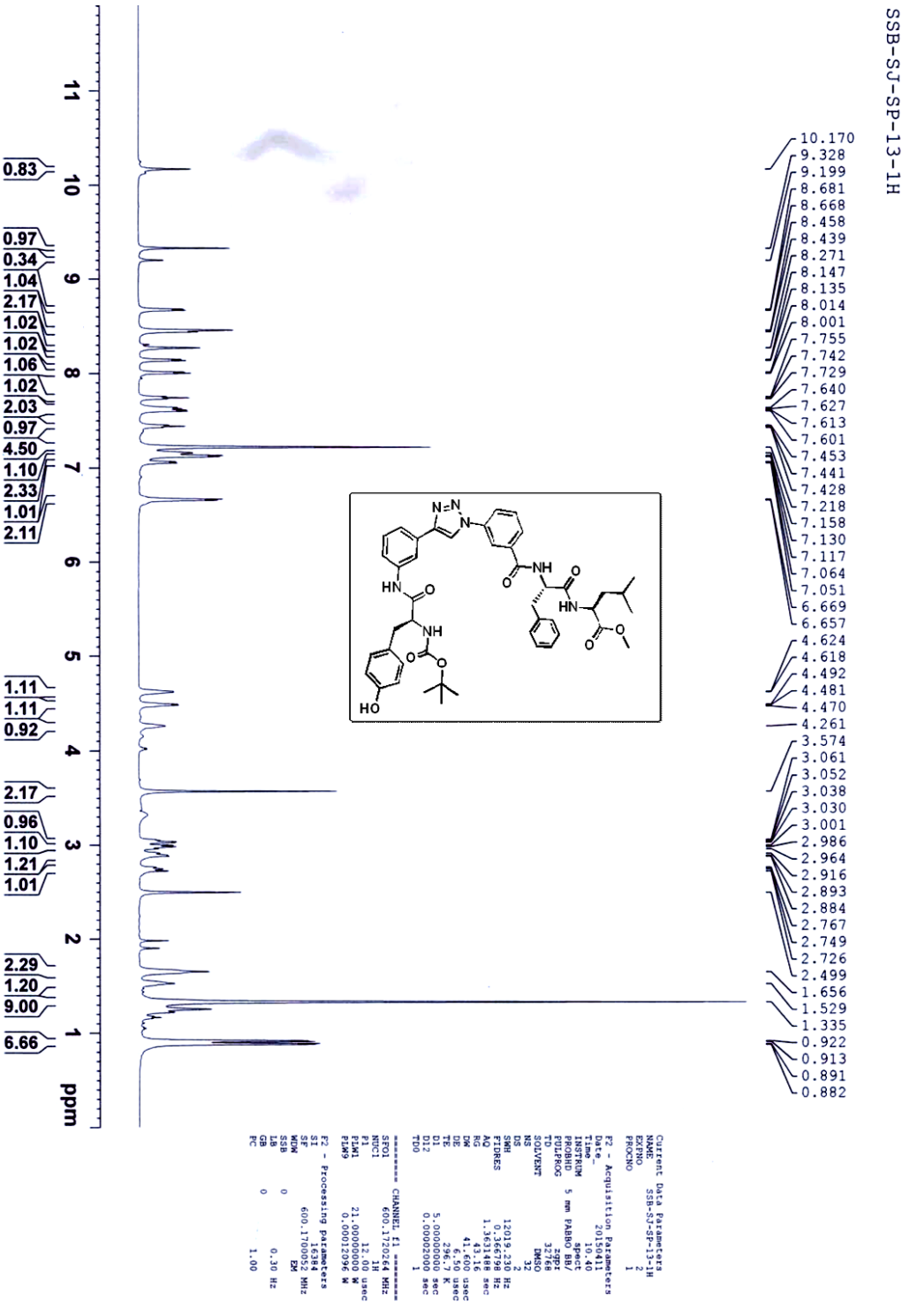

Figure 5.33. ^{1}H NMR spectra of synthesized compound **5.43.**

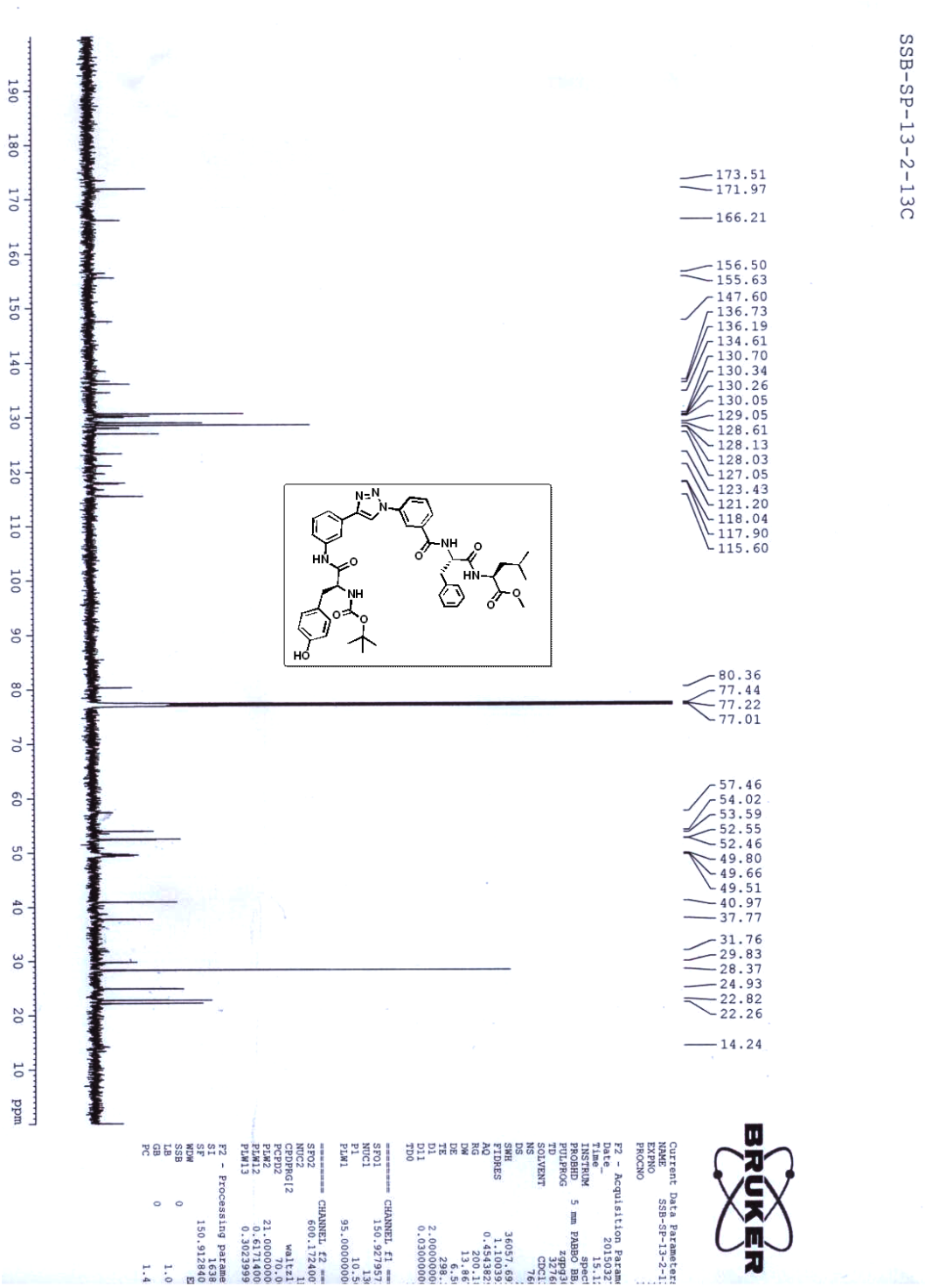

Figure 5.34. ^{13}C NMR spectra of synthesized compound **5.43.**

5.12. References

1. (a) Fairlie, D. P.; Tyndall, J. D. A.; Reid, R. C.; Wong, A. K.; Abbenante, G.; Scanlon, M. J.; March, D. R.; Bergman, D. A.; Chai, C. L. L.; Burkett, B. A. *J. Med. Chem.* **2000**, *43*, 1271. **(b)** Tyndall, J. D. A.; Fairlie, D. P. *J. Mol. Recognit.* **1999**, *12*, 363.
2. (a) Brown, J. H.; Jardetzky, T. S.; Gorga, J. C.; Stern, L. J.; Urban, R. G.; Strominger, J. L.; Wiley, D. C. *Nature* **1993**, *364*, 33 **(**b**)** Qian, Y.; Blaskovich, M. A.; Saleem, M.; Seong, C. M.; Wathen, S. P.; Hamilton, A. D.; Sebti, S. M. *J. Biol. Chem.* **1994**, *269*, 12410.
3. (a) Loughlin, W. A.; Tyndall, J. D. A.; Glenn, M. P.; Fairlie, D. P. *Chem. Rev.* **2004,** *104*, 6085. (a) Gillespie, P.; Cicariello, J.; Olson, G. L. *Biopolymers* **1997**, *43*, 191. (b) Voet, D.; Voet, J. G.; Pratt, C. W. *Fundamentals of Biochemistry*; Wiley: New York, **1999**.
4. (a) Harper, J. D.; Lansbury, P. T. Jr. *Annu. Rev. Biochem.* **1997**, *66*, 385. **(b)** Verbeek, M. M.; Ruiter, D. J.; De Waal, R. M. W. *Biol. Chem.* **1997**, *378*, 937. **(c)** Selkoe, D. J. *J. Neuropath. Exp. Neurol.* **1994**, *53*, 438. **(d)** Lansbury, P. T. Jr. *Acc. Chem. Res.* **1996**, *29*, 317.
5. Somers, W. S.; Phillips, S. E. V. *Nature* **1992**, *359*, 387.
6. (a) Raumann, B. E.; Rould, M. A.; Pabo, C. O.; Sauer, R. T. *Nature* **1994**, *367*, 754. (b) Meador, W. E.; Means, A. R.; Quiocho, F. A. *Science* **1993**, *262*, 1718.
7. (a) Nikolov, D. B.; Chen, H.; Halay, E. D.; Usheva, A. A.; Hisatake, K.; Lee, D. K.; Roeder, R. G.; Burley, S. K. *Nature* **1995**, *377*, 119. (b) Kim, J. L.; Nikolov, D. B.; Burley, S. K. *Nature* **1993**, *365*, 520.
8. Kim, Y.; Geiger, J. H.; Hahn, S.; Sigler, P. B. *Nature* **1993**, *365*, 512.
9. (a) Iconomidou, V. A.; Vriend, G.; Hamodrakas, S. J. *FEBS Lett*. **2000**, *479*, 141. (b) Kenney, J. M.; Knight, D.; Wise, M. J.; Vollrath, F. *Eur. J. Biochem.* **2002**, *269*, 4159.
10. Moebius, U.; Clayton, L. K.; Abraham, S.; Diener, A.; Yunis, J. J.; Harrison, S. C.; Reinherz, E. L. Proc. *Natl. Acad. Sci. U.S.A.* **1992**, *89*, 12008.
11. (a) Schneider, J. P.; Kelly, J. W. *Chem. Rev.* **1995**, *95*, 2169. (b) Nowick, J. S.; Smith, E. M.; Pairish, M. *Chem. Soc. Rev.* **1996**, *25*, 401.
12. (a) Leung, D.; Abbenante, G.; Fairlie, D. P. *J. Med. Chem.* **2000**,*43*, 305. (b) Babine, R. E.; Bender, S. L. *Chem. Rev.* **1997**, *97*, 1359. (c) West, M. L.; Fairlie, D. P. *Trends Pharmacol. Sci.* **1995**, *16*, 67.
13. (a) Walkinshaw, M. D. *Med. Res. Rev.* **1992**, *12*, 317. (b) Fairlie, D. P.; Abbenante, G.; March, D. R. *Curr. Med. Chem.* **1995**, *2*, 654. (c) Wade, R. C. *Structure* **1997**, *5*, 1139. (d) Fairlie, D. P.; West, M. L.; Wong, A. K. *Curr. Med. Chem.* **1998**, *5*, 29.

14. (a) West, M. L.; Fairlie, D. P. *Trends Pharmacol. Sci.* **1995**, *16*, 67. (b) Hirschmann, R. *Angew. Chem., Int. Ed. Engl.* **1991**, *30*, 1278. (c) Smith, A. B.; Hirschmann, R.; Pasternak, A.; Akaishi, R.; Guzman, M. C.; Jones, D. R.; Keenan, T. P.; Sprengeler, P. A.; Darke, P. L.; Emini, E. A.; Holloway, M. K.; Schleif, W. A. *J. Med. Chem.* **1994**, *37*, 215.

15. (a) Scholtz, J. M.; Baldwin, R. L. *Annu. Rev. Biophys. Biomol. Struct.* **1992**, *21*, 95. (b) Milner-White, E. J. *Trends Pharmacol. Sci.* **1989**, *10*, 70. (c) McGeary, R. P.; Fairlie, D. P. *Curr. Opin. Drug Discovery Dev.* **1998**, *1*, 208.

16. Fairlie, D. P.; Abbenante, G.; March, D. R. Curr. Med. Chem. **1995**, *2*, 654.

17. Kahn, M.; Qabar, M. N.; McMillan, M. K.; Ogbu, C. O.; Eguchi, M.; Kim, H. -O.; Boatman, P. D. Jr.; Urban, J.; Meara, J. P.; Babu, S.; Ferguson, M. D.; Lum, C. T. PCT Int. Appl., Molecumetics Ltd., USA, WO 9805333, **1998**; *Chem. Abstr.* **1998**, *128*, 192934.

18. (a) Man, S. H *Curr Opin Chem Biol* **1998**, 2, 717. (b) Searle, M. S. *J. Chem. Soc. Perkin Trans.* **2001**, *2*, 1011. (c) Venkatraman, J.; Shankaramma, S. C.; Balaram, P.; *Chem Rev.* **2001**, *101*, 3131. (d) Searle, M. S.; Ciani, B.; *Curr. Opin. Struct. Biol.* **2004**, *14*, 458. (e) Hughes, R. M.; Waters, M. L.; *Curr Opin Struct Biol* **2006**, *16*, 514.

19. (a) Nowick, J. S.; Smith, E. M.; Pairish, M.; *Chem Soc Rev* **1996**, 401. (b) Nowick, J. S.; *Acc Chem Res* **1999**, *32*, 287. (c) Moriuchi, T.; Hirao, T. *Chem Soc Rev*. **2004**, *33*, 294. (d) Loughlin, W. A.; Tyndall, J. D. A.; Glenn, M. P.; Fairlie, D. P. *Chem Rev.* **2004**, *104*, 6085.

20. Rai. R.; Vasudev. P. G.; Ananda, K.; Raghothama, S.; Shamala, N.; Karle, I. L.; Balaram, P. *Chem. –Eur. J.* **2007**, 13, 5917.

21. (a) Dong, S. L.; Löweneck, M.; Schrader. T. E.; Schreier, W. J.; Zinth, W.; Moroder, L.; Renner, C.; *Chem. –Eur. J.* **2006**, *12*, 1114. (b) Aemissegger, A.; Krautler, V.; Van Gunsteren, W. F.; Hilvert, D. A. *J. Am. Chem. Soc.* **2005**, *127*, 2929.

22. (a) Erde lyi M, Karle´ n A, Gogoll A: A new tool in peptide engineering: a photoswitchable stilbene-type b-hairpin mimetic. *Chem—Eur J* **2006**, *12*, 403.

23. (a) Lesma, G.; Meschini, E.; Recca, T.; Sacchetti, A.; Silvani, A.; *Tetrahedron* **2007**, 63, 5567. (b) Ressurreic¸ M.; Bordessa, A.; Civera, M.; Belvisi, L.; Gennari, C.; Piarulli, U. *J Org Chem* **2008**, *73*, 652. (c) Fisk, J. D.; Gellman, S. H.; *J. Am. Chem. Soc.* **2001**, 343. (d) Fisk, J. D. *J Am Chem Soc* **2006**, *128*, 7148.

24. (a) Freire, F.; Fisk, J. D.; Peoples, A. J.; Ivancic, M.; Guzei, I. A.; Gellman, S. H. *J. Am. Chem. Soc.* **2008**, *130*, 7839. (b) Fooks, H. M.; Martin, A. C. R.; Woolfson, D. N.; Sessions, R. B.; *J. Mol. Biol.* **2006**, *356*, 32.

25. (a) Aurora, R.; Creamer, T. P.; Srinivasan, R.; Rose, G. D. *J. Biol. Chem.* **1997**, *272*, 1413. (b) Nowick, J. S. *Acc. Chem. Res.* **1999**, *32*, 287.

26. (a) Stigers, K. D.; Soth, M. J.; Nowick, J. S. *Curr. Opin. Chem. Biol.* **1999**, *3*, 714 (b) Robinson, J. A. *Synlett.* **1999**, 429.

27. (a) Feigel, M. *J. Am. Chem. Soc*. **1986**, *108*, 181. (b) Brandmeier, V.; Sauer, W. H. B.; Feigel, M. *Helv. Chim. Acta* **1994**, *77*, 70.

28. (a) Bannwarth, L.; Kessler, A.; Pethe, S.; Collinet, B.; Merabet, N.; Boggetto, N.; Sicsic, S.; Reboud-Ravaux, M.; Ongeri, S. *J. Med. Chem*. **2006**, *49*, 4657. (b) Bannwarth, L.; Rose, T.; Dufau, L.; Vanderesse, R.; Dumond, J.; Jamart-Gregoire, B.; Pannecouque, C.; De Clercq, E.; Reboud- Ravaux, M. *Biochemistry* **2009**, *48*, 379.

29. (a) Diaz, H.; Kelly, J. W. *Tetrahedron Lett.* **1991**, *32*, 5725. (b) Diaz, H.; Tsang, K. Y.; Choo, D.; Kelly, J. W. *Tetrahedron* **1993**, *49*, 3533.

30. Nesloney, C. L.; Kelly, J. W. *J. Am. Chem. Soc.* **1996**, *118*, 5836.

31. Yu, T. B.; Bai, J. Z.; Guan, Z. *Angew. Chem. Int. Ed*. **2009**, *48*, 1097.

32. Liu, Y.; Diaz, D. D.; Accurso, A. A. *J. Polym. Sci., Part A: Polym. Chem.*, **2007,** *45*, 5182.

33. Wu, C. -F.; Zhao, X.; Lan, W. –X.; Cao, C.; Liu, J. –T.; Jiang, X. –K.; Li, Z. -T. *J. Org. Chem*. **2012**, *77*, 4261.

34. (a) Gellman, S. H. *Curr. Opin. Chem. Biol.* **1998**, *2*, 717. (b) Searle, M. S. *J. Chem. Soc. Perkin Trans.* **2001**, *2*, 1011. (c) Venkatraman, J.; Shankaramma, S. C. *Chem Rev* **2001**, *101*, 3131.

35. (a) Searle, M. S.; Ciani, B. *Curr. Opin. Struct. Biol*. **2004**, *14*, 458. (b) Hughes, R. M.; Waters, M. L. *Curr Opin Struct Biol* **2006**, *16*, 514.

36. (a) Liu, J.; Liu, Y.; Gao, M.; Zhang, X. *Proteomics*. **2012**, *14*, 2258. (b) Liu, Q.; Wang, J.; Boyd, B. J. *Talanta* **2015**, *136*, 114. (c) Pelay-Gimeno, M.; Glas, A.; Koch, O.; Grossmann, T. N. *Angew. Chem., Int. Ed.* **2015**, *54*, 8896. (d) Houimel, M.; Mach, J- P.; Corthésy-Theulaz, I.; Corthésy, B.; Fisch, I. *Eur. J. Biochem.* **1999**, *262*, 774. (e) Tung, C-H. *Peptide Sci.* **2004**, *76*, 391. (f) Pazos, E.; Vázquez, O.; Mascareñas, J.; Vázquez, M. E. *Chem. Soc. Rev.* **2009**, *38*, 3348. (g) Fujii, A.; Hirota, S.; Matsuo, T. *Bioconjugate Chem*. **2013**, *24*, 1218.

37. (a) Niu, T-f.; Gu, L.; Wang, L.; Yi, W.-b.; Cai, C.; *Eur. J. Org. Chem.* **2012,** *2012*, 6767. (b) Park, S-H.; Raines, R. T. *Protein Sci*. **1997**, *6*, 2344. (c) Lakowicz, J. R. In *Principles of Fluorescence Spectroscopy,* Third Ed., *New York: Springer*, **2006**, *ch 16*, pp 529. (d) Martin, L. J.; Imperiali, B. *Methods Mol. Biol.* **2015**, *1248*, 201. (e) Talukder, P.; Chen, S. C.; Liu, T.; Baldwin, E. A.; Benkovic, S. J.; Hecht, S. M. *Bioorg. Med. Chem. Lett.* **2014**, *22*, 5924.

38. (a) Lu, C. H.; Li, J.; Zhang, X. L.; Zheng, A. X.; Yang, H. H.; Chen, Xi.; Chen, G. N. *Anal. Chem*. **2011**, *83*, 7276. (b) Samanta, M.; Petersson, E. J. *Aust. J. Chem.* **2013**, *67*, 686 (c) Oh, K. J.; Cash, K. J.; Plaxco, K. W. *J. Am. Chem. Soc***. 2006**, *128*, 14018. (d) Marmé, N.; Knemeyer, J. P.; Wolfrun, J.; Sauer, M. *Angew.Chem., Int. Ed. Engl*. **2004**, *43*, 3798.

39. (a) Loving, G. Imperiali, B. *J. Am. Chem. Soc.* **2008**, *130*, 13630. (b) Socher, E.; Imperiali, B. *ChemBioChem.* **2013**, *14*, 53. (c) Bag, S. S.; Jana, S.; Yashmeen, A.; De, S. *Chem. Comm.* **2015**, *51*, 5242. **(**d) Bag, S. S.; Jana, S.; Yashmeen, A.; Senthilkumar, K.; Bag, R. *Chem. Comm.* **2014**, *50*, 433. (e) Krueger, A. T.; Imperiali, B. *ChemBioChem.* **2013**, *14*, 788.

40. (a) Cusick, M. E.; Klitgord, N.; Vidal, M.; Hill, D. E. *Hum. Mol. Genet*. **2005**, *14*, R171. (b) Schütz, V.; Mootz, H. D. *Angew. Chem., Int. Ed*. **2014**, *53*, 4113. (c) Ryan, D. P.; Matthews, J. M. *Curr. Opin. Struct. Biol*. **2005**, *15*, 441.

41. (a) Schreier, W. J.; Aumüller, T.; Haiser, K.; Koller, F. O.; Löweneck, M.; Musiol, H.-J.; Schrader, T. E.; Kiefhaber, T.; Moroder, L.; Zinth, W. *Peptide Sci*. **2013**, *100*, 38. (b) Neuweiler, H.; Schultz, A.; Vaiana, A. C.; Smith, J. C.; Kaul, S.; Wolfrum, J.; Sauer, M. *Angew. Chem., Int. Ed*. **2002**, *41*, 4769. (c) Kohn, J. E.; Plaxco, K. W. *Proc. Natl. Acad. Sci. U.S.A.* **2005**, *102*, 10841. (d) Chen, S.; Fahmi, N. E.; Wang, L.; Bhattacharya, C.; Benkovic, S. J.; Hecht, S. M. *J. Am. Chem. Soc.* **2013**, *135*, 12924. (e) Kajihara, D.; Abe, R.; Iijima, I.; Komiyama, C.; Sisido, M.; Hohsaka, T. *Nat. Methods* **2006**, *3*, 923.

42. (a) Goedeweeck, R.; Ruttens, F.; López-Arbeloa, F.; Schryver, F. C. D. *Biopolymers*, **1987**, *26*, 1833. (b) Häner, R.; Biner, S. M.; Langenegger, S. M.; Meng, T.; Malinovskii, V. L. *Angew. Chem., Int. Ed.* **2010**, *49*, 1227. (c) Chen, S. X.; Wang, L.; Fahmi, N. E.; Benkovic, S. J.; Hecht, S. M. *J. Am. Chem. Soc*. **2012**, *134*, 18883. (d) Fujii, A.; Sekiguchi, Y.; Matsumura, H.; Inoue, T.; Chung, W. –S.; Hirota, S.; Matsuo, T. *Bioconjugate Chem.* **2015**, *26*, 537. (e) Honda, K.; Fujishima, S. -H.; Ojida, A.; Hamachi, I. *ChemBioChem*. **2007**, *8*, 1370.

43. Winnik, F. M. *Chem. Rev.* **1993**, *93*, 587-614

44. Fujii, A.; Sekiguchi, Y.; Matsumura, H.; Inoue, T.; Chung, W.; Hirota, S.; Matsuo, T. *Bioconjugate Chem*. **2015**, *26*, 537.

45. Chen, S.; Wang, Lin.; Fahmi, N. E.; Benkovic, S. J.; Hecht, S. M. *J. Am. Chem. Soc*. **2012**, *134*, 18883.

46. (a) Kraskouskaya, D.; Bancerz, M.; Soor, H. S.; Gardiner, J. E.; Gunning, P. T. *J. Am. Chem. Soc*. **2014**, *136*, 1234. (b) Schmidt, F.; Stadlbauer, S.; Konig, B. *Dalton Trans*. **2010**, *39*, 7250.

47. (a) Freire, F.; Gellman, S. H. *J. Am. Chem. Soc.* **2009**, *131*, 7970. (b) Moriuchi, T.; Hirao, T. *Chem. Soc. Rev.* **2004**, *33*, 294. (c) Ross, N. T.; Katt, W. P.; Hamilton, A. D. *Phil. Trans. R. Soc. A* **2010**, *368*, 989. (d) Ko, E.; Liu, J.; Perez, L. M.; Lu, G.; Schaefer, Burgess, A. K. *J. Am. Chem. Soc.* **2011**, *133*, 462. (e) Lutz, J.-F.; Zarafshani, Z. *Adv. Drug Delivery Rev.* 2008, *60*, 958–970.

48. Kemp, D. S.; Li, Z. Q. *Tetrahedron Lett.* **1995**, *36*, 4179.

49. (a) Feigel, M. *J. Am. Chem. Soc*. **1986**, *108*, 181. (b) Brandmeier, V.; Sauer, W. H. B.; Feigel, M. *Helv. Chim. Acta* **1994**, *77*, 70.

50. Gardner, R.; Liang, R. G.; Gellman, S. H. *J. Am. Chem. Soc.* **1999**, *121*, 1806.
51. Verbist, B. M. P.; Borggraeve, W. M. D.; Toppet, S.; Compernolle, F.; Hoornaert, G. J. *Eur. J. Org. Chem.* **2005,** *2005*, 2941.
52. (a) Rubinov, B.; Wagner, N.; Rapaport, H.; Ashkenasy, G. *Angew. Chem., Int. Ed*. **2009**, *121*, 6811. (b) Tsang, K. Y.; Diaz, H.; Graciani, N.; Kelly, J. W. *J. Am. Chem. Soc.*, **1994**, *116*, 3988. (c) Fuller, A. A.; Du, D.; Liu, F.; Davoren, J. E.; Kroon, G.; Powers, E. T.; Wipf, P.; Gruebele, M.; Kelly, J. W. *Proc. Natl. Acad. Sci.* **2009**, *106*, 11067. (d) Fujii, A.; Hirota, S.; Matsuo, T. *Bioconjugate Chem*. **2013**, *24*, 1218. (e) Fujii, A.; Sekiguchi, Y.; Matsumura, H.; Inoue, T.; Chung, W. –S.; Hirota, S.; Matsuo, T.; *Bioconjugate Chem*. **2015**, *26*, 537. (f) Micsonaia, A.; Wienb, F.; Kernyaa, L.; Leec, Y. –H.; Gotoc, Y.; Réfrégiersb, M.; Kardosa, J. *PNAS* **2015**, E3095.
53. (a**)** Oh, K.; Guan, Z. *Chem. Commun*. **2006**, *29*, 3069. (b) Feher-Voelger, A.; Borges-Gonzlez, J.; Carrillo, R.; Morales, E. Q.; Martn, J. G-P. T. *Chem. Eur. J.* **2014**, *20*, 1. (c) Kong, J.; Yu, S. *Acta. Biochim. Biophys. Sin.* **2007**, *39*, 549.
54. (a) Kessler, H. *Angew. Chem., Int. Ed. Engl*. **1982**, *21*, 512.
55. (a) MacroModel, Version 9.9 Schrodinger, LLC, New York, NY, **2012**. (b) Kolossvry, I. W.; Guida, C. *J. Am. Chem. Soc.* **1996**, *118*, 5011.
56. (a) Zhang, Y.; Jiang, M.; Han, G. –C.; Zhao, K.; Tang, B. Z.; Wong, K. S. *J. Phys. Chem. C* **2015**, *119*, 27630. (b) Dobkowski, J.; Kijak, M.; Sazanovich, I. V.; Waluk, J. *J. Phys. Chem. B* **2015**, *119*, 7294. (d) Kobayashi, A.; Takehira, K.; Yoshihara, T.; Uchiyama, S.; Tobita, S. *Photochem. Photobiol. Sci*. **2012**, *11*, 1368.
57. (a) Förster, T. *Discuss. Faraday Soc.***1959**, 7. (b) Rogers, J. M. G.; Lippert, L. G.; Gai, F. *Anal. Biochem.* **2010**, *399*, 182. (c) Nedumparaa, R. J.; Manua, P. J.; Vallabhanb, C. P. G.; Nampooria, V. P. N.; Radhakrishnana, P. *Opt. Laser Tech.* **2008**, *40*, 953. (d) Forster, T. *Angew. Chem., Int. Ed. in Engl*. **1969**, *8*, 333. (e) Ueno, A.; Suzuki, I.; Osa, T. *J. Am. Chem. Soc*. **1989**, *111*, 6391. (f) Winnik, F. M. *Chem. Rev*. **1993**, *93*, 587.
58. (a) Bag, S. S.; Kundu, R.; Jana, S. *Tetrahedron Lett.* **2013**, *54*, 2627. (b) Sar, D.; Bag, R.; Yashmeen, A.; Bag, S. S.; Punniyamurthy, T. *Org. Lett.*, **2015**, *17*, 5308. (c) Roy, D.; Dutta, S.; Maity, S. S.; Ghosh, S.; Roy, A. S.; Ghosh, K. S.; Dasgupta, S. *J. Luminescence* **2012**, *132*, 1364.
59. (a) Hazra, P.; Chakrabarty, D.; Chakraborty, A.; Sarkar, N. *Biochem. Biophys. Res. Commun.* **2004**, *314*, 543. (b) Paul, B. K.; Guchhait, N. *J. Phys. Chem. B* **2011**, *115*, 10322.
60. (a) Nielsen, B. G.; Jensen, M. Ø.; Bohr, H. G. *Pept. Sci.* **2003**, *71*, 577. (b) Gardner, R. R.; Liang, G. B.; Gellman, S. H. *J. Am. Chem. Soc*. **1999**, *121*, 1806. (c) Aldrich, J. V.; Wolff, M. E. Ed. *Burger's Medicinal Chemistry and Drug Discovery*, John Wiley & Sons: New York, **1996**, *3*, 321. (d) Smith, G. D.; Griffin, J. F. Science **1978**, *199*, 1214.

61. a) Leavitt, S.; Freire, E. *Current Opin. Struct. Biol.* **2001**, *11*, 560. (b) Ojha, H.; Mishra, K.; Hassan, M. I.; Chaudhurya, N. K. Thermochim. Acta **2012**, *548*, 56.

62. (a) Hazra, P.; Chakrabarty, D.; Chakraborty, A.; Sarkar, N. *Biochem. Biophys. Res. Commun.* **2004**, *314*, 543. (b) Paul, B. K.; Guchhait, N. *J. Phys. Chem. B* **2011**, *115*, 10322.

63. Morris, G. M.; Huey, R.; Lindstrom, W.; Sanner, M. F.; Belew, R. K.; Goodsell, D. S.; Olson, A. J. *J. Comput. Chem*. **2009**, *16*, 2785.

Chapter 6

APPLICATION OF AROMATIC TRIAZOLYL AMINO ACID SCAFFOLD AND ITS MONO- AND BIS-PYRENYL AMIDES AS FLUORESCENCE LIGHT-UP SENSORS OF ETHANOL

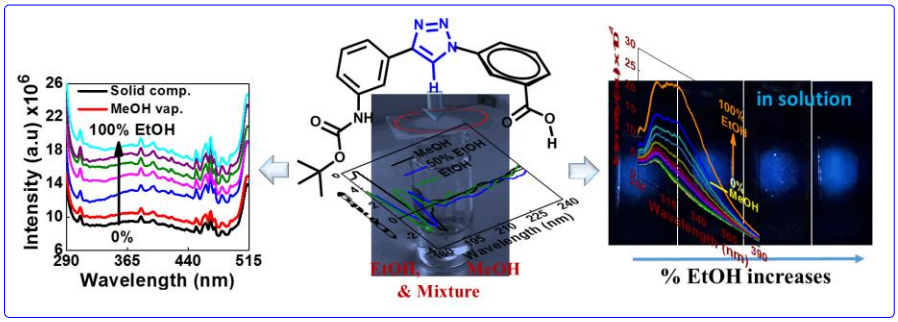

6.1. Introduction

Organic solvents are ubiquitously used both in industrial applications and in academic research. As for example both the methanol and ethanol are of current interest in public due to their use in direct-methanol-fuel-cells and as bio-fuel.[1] Ethanol is an important alcohol which is also widely used in perfumery, paints industries, liquor industries.[2] Therefore, measuring the concentration of ethanol is highly importance in clinical, biochemical and beverage industry. On the other hand methanol is highly toxic substance that causes serious effect on health mainly mental illness, disorders, liver diseases are mostly related to the use of excess alcohol.[3] The methanol though is a common organic solvent but is toxic because of its metabolic acidosis causes blindness and badly effect on nerve system of our body.[3] The enzyme's affinity for ethanol is 10-20 times higher than methanol.[4]

Therefore, development of reliable methods for the discrimination of alcohols is highly important primarily due to their differential health and environmental impacts, use in industrial applications and in academic research.[5] However, both methanol and ethanol are colorless liquids and are structurally similar solvents. While, ethanol is the primary constituent in alcoholic beverages, methanol may be found as a toxic byproduct which results in severe health issues upon ingestion. Over the last 30 years substantial development has been made to reduce the use and exposure to alcohol and tobacco. However, there has been little or no success in preventing the effect caused by alcohol, other psychoactive substances and obesity.

As methanol is poisonous to health, it is important to determine the percentage methanol content to control the quality of alcoholic beverages. Sensing minor quantity of methanol in presence of ethanol is also not easy by simple means such as smell or test.[5] Moreover, as the boiling points are similar these alcohols can't be separated out of another. So discrimination of ethanol−methanol mixtures and quantitative determination is growingly vital primarily due to health concerns involved with these two solvents. Methanol and ethanol both are colorless, chemically very similar and indispensable liquid as a fuels for direct-methanol-fuel-cells (DMFC) and biomass ethanol.[6] So without proper analytical instrumentation or any other costly methodology it is difficult to discriminate the ethanol and methanol.[7] Now a days many polymer or nanomaterial based optical sensor and colorimetric sensor are reported for sensing alcohol.[8, 9] Several fluorescence-based optical alcohol sensors also have been introduced which found promising as alcohol sensor (Mohr and Spichiger-Keller 1997; Mohr et al. 1997; Blum et al. 2001; Chang et al. 1997; Orellana et al. 1995). However, many of these sensors suffer from various shortcomings as the success solvatochromic dyes lies with reasonable polarity differences among various analytes. Thus, discrimination of methanol and ethanol with subtle differences in polarities is a difficult task and remains as a challenge.

6.2. Various Approaches to Ethanol Sensors

Several methodologies, chemistry have been discovered addressing these challenges. However, none of them met all research needs. Therefore continuous research is going on to find out best discriminating methods, chemistry and platform. Over the years, many analytical methods have been developed the measurement of ethanol and other alcohols. They can be classified in three major categories: (a) chromatographic, (b) enzymatic, and (c) optical.

***The Chromatographic Method for the Determination of Ethanol*:** The chromatographic method is the most accurate and sensitive (Buttler et al. 1993; Johansson et al. 1993) method for the determination of ethanol, with a lower limit of ethanol detection on the order of 0.005% v/v (Zinbo 1994). However, it suffers from several shortcomings such as high cost, the necessity for sample pretreatment and time consuming operational process. Many more advancement on this chromatographic techniques either GC-FID, GC-MS or HPLC, are also being developed for detection/discrimination of methanol-ethanol.[10]

Infrared Spectrometry based method for the determination of ethanol was, also an highly sensitive and accurate detection techniques, reported by Battiste et al.[11] Recently, Fourier Transform Infrared (FTIR) spectroscopy in combination with chemometrics were applied for the quality control of 26 fruit brandies by Floria et al. By principal component analysis of FTIR areas (1170 -1000 cm^{-1}), they were able to discriminate between samples of various biological and geographical origin of brandy samples.[12] Their FTIR study was found to correlate well with GC-FID based method indicating that the FTIR technique could offer a good prediction and statistical correlation with GC-FID technique for methanol quantification.

***Enzymatic Method for the Determination of Ethanol*:** In comparison to chromatographic method, somewhat less precise but more rapid measurements can be achieved by the use of enzymes. In general, the determination of ethanol concentration is based on either of two enzymes, alcohol oxidase or alcohol dehydrogenase, by monitoring O_2 consumption or H_2O_2 formation (Azevedo *et al.* **2005**; Boujitita *et al.* **2000**). The specificity of the enzyme binding sites provides highly selective and accurate sensitivity in detecting ethanol. However, the disadvantage of the sensors lies in their instability due to the denaturation of the enzymes when exposed to high temperature, pressure, or extreme pH condition.

To get rid of such shortcomings, attempts have been made to place the enzyme which is used for the sensing purpose in close proximity to a transducer (Guilbalt *et al.* **1983**) or to immobilize them in a matrix (Belghith *et al.* **1987**; Mitsubayashi *et al.* **1994**) which increases the stability of the enzymes and allows for continuous

monitoring. Screen-printing technology has also been used for the mass production of low cost disposable enzymatic sensors (Boujitita *et al.* **2000**).

Optical Method for the Determination of Ethanol: Optical sensing methodologies are the most promising with respect to their several advantages which include: (a) low-cost manufacturability, (b) less time consuming, (c) highly sensitive, (d) miniaturization and can be used in real-time, (c) in situ monitoring. Fluorescence based detection techniques have been used for such purposes. Some examples include-lifetime–based (Chang *et al*. 1997) and fluorescence-based (Mohr and Spichiger-Keller 1997; Mohr *et al*. 1997; Blum *et al*. 2001; Orellana *et al*. 1995) alcohol sensors have been introduced utilizing various alcohol-sensitive dyes. Fluorescence based methods are in general robust and extremely promising though these methods also suffers from shortcomings such as dye leaching, cross-sensitivity to pH, low specificity, dye may lack high temperature/photo stability and are subject to interference due to auto fluorescence. Few selected examples of this category will be discussed below.

6.3. Fluorescence Optical Sensor for Ethanol

The need for low-cost, robust alcohol sensors has increased with the renewed interest in alternative fuels as well as high-throughput screening of biological processes involving the production of ethanol. Towards this end several research laboratory have contributed to develop fluorescent optical sensor for ethanol or discriminating between ethanol and methanol.

***Reversible Liquid Ethanol/Methanol Sensor*:** Kessler *et al.* developed fluorescent optical sensor for on-line determination of solvent mixtures based on solvent polarity sensitive probe.[13] For alcohol sensing Podgorsek *et.al*., in 1998, used a glassy polyamide for the discrimination of ethanol and methanol but it was not suitable for mixture.[14] An optical ratiometric sensor for alcohol measurements was reported by Taylor et al.[15] A ratiometric fluorescence ethanol sensor was developed and reported in 2007 by Kostov et al.[16] The sensor is based on the fluorescent dye Nile Blue Chloride (**Figure 6.1**) which in solution exhibited a single fluorescence peak. However, a dual emission peak was observed upon immobilization of the dye in the hydrogel poly (ethylene glycol) dimethacrylate. The dual emission of the probe dye allowed for ratiometric sensing of ethanol with high sensitivity, selectivity and response time. Using this immobilization technique, the author's found that the sensor was sensitive through a broad range of ethanol concentrations, from 5% to 90% v/v with good reproducibility. This ratiometric approach circumvents many of the problems of the intensity-based methods,[17] including signal variations due to dye bleaching, fluctuations in source intensity or temperature, and coloring of the media.

Moreover, the sensor is most sensitive in acidic and neutral environments reflecting its broad range utility such as for studying yeast- based alcohol fermentations.

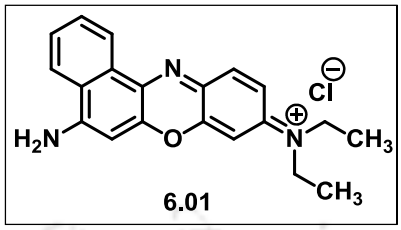

Figure 6.1. (a) Chemical structure of Nile Blue Chloride (NB) used for determination of ethanol.

Chang *et al*. in 2012 developed a novel hydrogen-bridged cholesteric liquid crystal (CLC) polymer networks with a porosity for distinguishing methanol from ethanol (**Figure 6.2**). Their strategy was based on the diversity of molecular affinities in ethanol and methanol with the hydrogen-bridged cholesteric polymer networks. Because of differential affinities, cholesteric polymer networks generates different coloration upon the uptake of the alcohol solutions with different ratios of methanol/ethanol. They also demonstrated that the reduction of cross-link density and increasing amount of alkyloxybenzoic acid in polymer networks enhanced the distinguishing ability between methanol and ethanol. Thus, **t**he colorimetry of the cholesteric liquid crystal is an effective means of identifying the concentration of methanol indicating its potentiality for fabrication into a device to be applicable for sensing alcohol.[18]

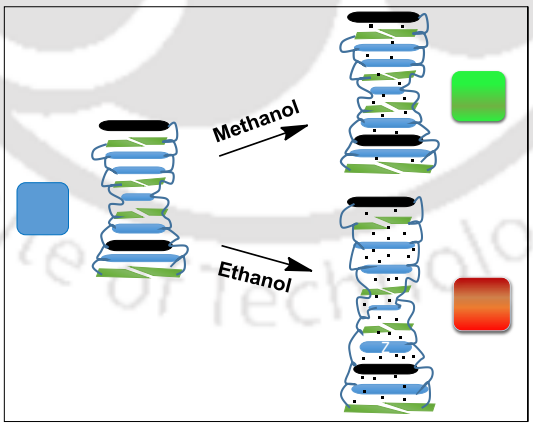

Figure 6.2. Schematic presentation of hydrogen-bridged cholesteric liquid crystal (CLC) polymer networks.

Ishihara *et al.*, in 2013 developed a composite film of oxoporphyrinogen and layered double hydroxide for visual discrimination of methanol from ethanol (**Figure 6.3**). The composite film underwent a long time persistent visible color change (from

magenta to purple) when exposed to methanol while upon exposure to ethanol no colour change was observed. Even after removal of methanol under reduced pressure the film retained its changed coloration. However, the original state of the OxPLDH composite film could be recovered by rinsing it with tetrahydrofuran (THF), enabling repeated usage of the composite film and indicating its reversibility in detecting MeOH and discriminating from ethanol. The mechanism of color variation was proposed to be anion transfer from LDH to OxP triggered by methanol exposure.[19]

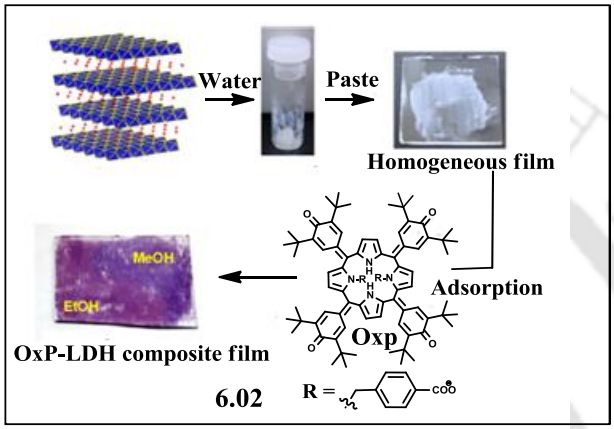

Figure 6.3. Schematic illustration for the OxP-LDH composite film based discrimination of ethanoil from methanol via visible color variation.

Certain phenol derivatives are known to exhibit increases in fluorescence intensity in the solid state when treated with solutions of basic substances. With this idea, very recently in 2015, Katsuhiko Ariga *et al.*[20] developed a solid state fluorescent optical sensor based on terphenyl-ol (TPhOH) derivatives for the ethanol contents of various alcoholic beverages.Their investigation showed that the compound **6.05** weak dark-blue fluorescent at 380 nm in solid state. However, in presence of Na_2CO_3 and ethanol the emission wavelength shifted from 380 nm to 472 nm (bright sky –blue fluorescence) with a detection limit of ~ 5 v/v %. Furthermore, the emission returned to the initial position after evaporation of EtOH over 15 minutes implying the reversibility of the sesor in contrary to other non-reversible optical ethanol sensor such as colorimetric detection involving reduction of chromates or ethanol sensor using semiconductor devices developed by Win *et al.*[21a] The emission properties of TPhOHs have been again tuned through synthesising other phenols (**Figure 6.4**) derivatives. They followed the same strategy and also examined the effect of different solvent such as water, chloroform, tetrahydrofuran, acetone, acetonitrile, ethanol, methanol, dimethyl formamide and dimethyl sulfoxide which showed the fluorescence colour change of compound **6.05** from blue to green depending on the solvent.[21b]

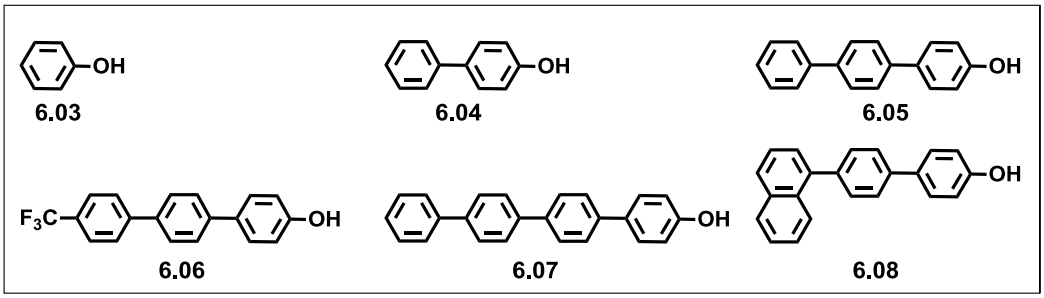

Figure 6.4: A series of phenol derivatives as alcohol sensor.

Recently, a high performance colorimetric sensor was reported by Warner, *et.al.*, in 2015 based on single ionic liquid (IL), ditrihexyl(tetradecyl)phosphonium bromothymol blue ($[P_{66614}]_2$[BTB]), for accurate detection and identification of different alcohol and mixture of alcohols.[22] They studied the total eight alcohols and seven binary mixtures of alcohols. The IL in alcoholic solution showed two different characteristic absorption bands in at 410 nm and 630 nm in the UV-visible spectra. The ratios of two absorption bands were found to be highly sensitive to polarity of the alcohols. Compared to methanol in 2- butanol the band at 410 nm was bathochromically shifted by 15 nm and band at 630 nm was blue shifted by 9 nm. They used for this study a more sensitive and efficient sensor a single IL, i.e., this IL was synthesized by redesign of a commercially available pH indicator dye bromo ethyl blue (BTB), known as 3', 3''-dibromothymolsulfonephthalein. The dissociation of BTB can be described as shown in **Figure 6.5**. H_2R, HR^- (Yellow) and R^{2-} (Blue) are the biprotonated, monoprotonated and deprotonated form of BTB respectively. A group of structurally and chemically similar alcohols and alcohol mixtures were chosen as representative analytes to test the performance of their sensor array. The sensor was found to show a unique ratiometric absorption signal (630/410) in organic solvents in distinct contrast to that of the parent BTB compound. In addition, the authors observed an excellent correlation between the 630/410 absorption ratio and alcohol polarity and found that the 630/410 ratio was increased with decreasing polarity of alcohols and vice versa, inferring a polarity-dependent equilibrium shift between HR− and R2− forms. It was concluded that a single IL concentration itself was able to achieve discrimination among the majority of the analytes tested.

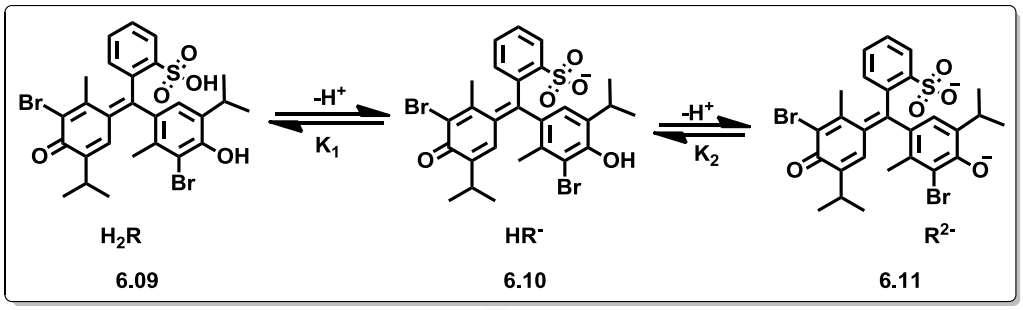

Figure 6.5: Dissociation of bromo ethyl blue (BTB).

***Irreversible Liquid Ethanol/Methanol Sensor*:** Gao group in 2010 have reported a novel comb like Cu_2O nanorod-based material which was found to act as a good ethanol sensor. The material was synthesized through an interface etching route using salicylaldehyde as ligand and reducing agent in a water–toluene system. They prepared Cu_2O nanomaterial modified GC electrode in 0.1 M sodium hydroxide solution with different alcohol concentration. They observed that the redox peak changed with changing ethanol concentration and it became stronger with increasing alcohol concentration from 10 to 500 mM. This observation clearly indicated that the Cu_2O nanostructure showed electrolytic activity which responses for ethanol oxidation.[22] Their electrochemical and gas sensing studies demonstrated that the Cu2O nanorod-based structures have great application potentials as both electrochemical and gas sensor for detection of ethanol.[23]

***Ethanol/Methanol Vapor Sensor*:** There exist several reports of sensing ethanol/methanol vapor. As for an example, Kimmel et developed optochemical sensors for polar solvent vapors based on substituted 3,3-diphenylphthalides.[24] Later on in 2002, Kieser et al. developed a strategy for the discrimination of methanol and ethanol vapors by the use of a single optical sensor with a microporous sensitive layer based on glassy polycarbonate.[25] They used time resolved measurement where sorption occurs into the micropores of the polymer. They analyzed their work with respect to change in the refractive index over the analyte exposure time. Both analytes were adsorbed into the micropores of the polymer showing different diffusion kinetics. The sensor response during analyte exposure is subdivided into different time channels. By this a quantitative multicomponent analysis of ethanol and methanol was possible using the sensor response of only one single sensor. However, a detection of both analytes in mixtures was not performed. They claimed that the polycarbonate Makrolon provided a sensitive, stable, and reversible sensor layer, which is highly selective due to the sorption of the analytes into the micropores of the polymer (**Figure 6.6**).

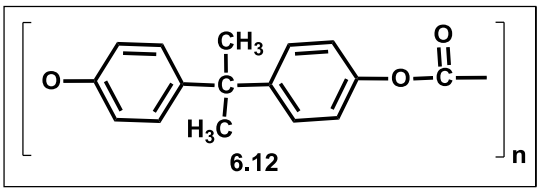

6.12

Figure 6.6: Structure of the polycarbonate Makrolon M2400.[17]

Zhang *et al*., [26] in 2011 have synthesized two types of α-Fe_2O_3 nanostructure one is flower like and another one three dimensional hierarchical through two step process of solvothermal and calcination. Because of large surface area and mesoporosity it was applied to gas sensing purpose. After fabrication it was tested for ethanol sensing. Their study reflected that the hierarchical α-Fe_2O_3 sensor exhibited significantly improved ethanol sensing performances in comparison with the compact α-Fe_2O_3 structures. Furthermore, the sensitivity of the flower like α-Fe_2O_3 enhanced to nine fold compared to compact structure. The amplitude of response of flower like α-Fe_2O_3 nanostructured simultaneously increases with concentration of ethanol. The enhancement of sensing properties is attributed to the unique porous and well-aligned nanostructure.

Hess *et al*., in 2014 have reported highly sensitive and superior indium oxide based ethanol sensor. The metal oxide reacted with ethanol catalytically by two way, one is dehydration to ethane or the dehydrogenation to acetaldehyde. Both routes are oxidation of the ethanol to carbon dioxide but latter one is more efficient and sensitive. From literature, so many SnO_2 and In_2O_3 sensor material reported that interact with ethanol. But in case of In_2O_3 based ethanol sensor, oxidation reaction took place where ethanol converted to actaldehyde. Here, they were measured DC electrical conductivity, Raman spectra of the sensor and Fourier transform infrared (FTIR) material for ethanol sensing by indium oxide materials to study the ethanol sensing mechanism. This work was done in different temperature and gas environment. After that they have correlated the results of the sensor signal in presence of absorbates, the indium oxide oxidation state and intensity of surface hydroxyl group. In conclusion, after analyzed all the data they have proposed the reaction mechanism of ethanol sensing by indium oxide was that the indium oxide surface adsorbed ethanol gas then at 190 ^{O}C temperature adsorbed gas reacted and converted to acetate or decompose to formate partially in presence of oxygen. With increasing temperature at 325 ^{O}C adsorbate decomposes and deposited in the form of carbon which is oxidised to carbon dioxide and water in presence of oxygen.[27]

In 2015, Anglos group developed a new optical gas sensor nanohybrids from ZnO nanoparticles which was dispersed in an inert soft flexible cross-linked polydimethylsiloxane (PDMS) matrix.[28] The synthesized polymer nanohybride showed highly luminescent character. They carried out UV-visible and photoluminescence of ZnO to investigate the sensitivity and sensing capability of

ethanol vapor at room temperature (**Figure 6.7a**). The nanocomposite showed linear Langmuir –type adsorption when exposed to low ethanol vapor pressure to saturated high pressure. The nanocomposites exhibited a clear increase in their photoluminescence (PL) emission, which showed a nearly Langmuir dependence on the alcohol vapor pressure. The limit of ethanol vapor detection was found to be 0.4 Torr. Interestingly, the sensor remained unaffected by the presence of water vapor indicating the potential of the ZnO–PDMS system as an optical gas sensing device.

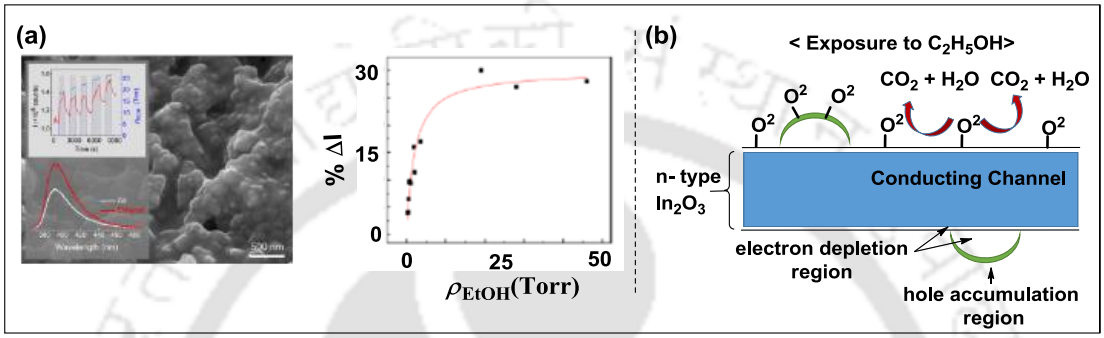

Figure 6.7: (a) ZnO− polydimethylsiloxane (PDMS) nanohybrids as ethanol sensor. (b) Schematic diagrams showing the depletion layer and potential barrier forming at the In_2O_3-Bi_2O_3 junction upon exposure to air and C_2H_5OH gas.

Recently Lee *et al.*,[29] in 2015 reported the synthesis of Bi_2O_3 nanoparticle decorated In_2O_3 nanorods for sensing ethanol because nanorod type sensors are more superior than thin film. Both sample were responded strongly with increasing ethanol concentration. But Bi_2O_3 decorated In_2O_3 nanorods showed vigorous response than pure In_2O_3. The Bi_2O_3-decorated In_2O_3 nanorod sensor showed responses of 171–1774% at ethanol concentrations of 10–200 ppm at 200 °C. The responses of the Bi_2O_3-decorated In_2O_3 nanorod sensor were found to be stronger than those of the simple In_2O_3 nanorod sensors by 1.5–4.9 times. The Bi_2O_3-decorated In_2O_3 nanorod sensor showed high selectivity for ethanol gas over other gases. The mechanism of ethanol sensing by Bi_2O_3 nanoparticle decorated In_2O_3 nanorods was explained considering the modulation of the depletion layer width near the In_2O_3−Bi_2O_3 interface and change in the potential barrier of the same places (**Figure 6.7b**).

6.4. Background

Monitoring organic solvents, especially, discrimination of methanol and ethanol with subtle differences in polarities though remains a challenge but is important primarily due to the environmental and health impact of such alcohols. As a result of tremendous research effort, several analytical methods have been developed for measurement of and discrimination among structurally similar alcohols which is clear from a vast majority of literatures as described above. Among the developed methods,

chromatographic method is the most sensitive and accurate, however, suffers from short comings such as high cost, time consuming and laborious. Thus, development of facile and low-cost techniques such as colorimetric, optical and fluorometric sensors for discrimination of methanol-ethanol is attracted current research interest. Several colorimetric, optical and fluorescence-based alcohol sensors have been introduced which found promising in sensing alcohol. However, many of these sensors suffer from various shortcomings as the success of solvatochromic dyes lies with reasonable polarity differences among various analytes. Thus, discrimination of methanol and ethanol with subtle differences in polarities is a difficult task and remains as a challenge. Therefore, design of robust fluorescence sensor of ethanol is highly demanding.

6.5. Objective

In the previous chapter we showed the design and synthesis of triazolyl amino acid scaffold **^{Ar}TAA** (**5.41**) which is in hairpin shape shows optical chirality. This scaffold was primarily designed as nucleator of peptide secondary structures. A study of photophysical property of the scaffold in various organic solvents left us a clue that it can be used for discrimination between methanol and ethanol. Moreover, the axial chirality of the probe scaffold lead us to envisioned that discrimination of methanol and ethanol with subtle differences in polarities could be achieved via differential H-bonding and hydrophobic interactions.

Therefore, we took the task and framed our objective as below:

(a) Synthesis of aromatic triazolo amino acid scaffold **^{Ar}TAA, 5.52** which is already discussed in **Chapter 5**.

(b) As the wavelength of emission for the aromatic triazolo amino acid scaffold **5.52** lies in the UV-region, so we planned to modify the scaffold and prepare its mono pyrenyl amide (**6.13**, **PyAm-^{Ar}TAA**) and bis-pyrenyl-bis-amide (**6.14, Py$_2$Am-^{Ar}TAA**) derivatives.

(c) Study of fluorescence photophysical properties toward fluorimetric discrimination of ethanol and methanol of all the sensors.

(d) Preparation of solid coating of these sensors above glass plate for possible sensing of ethanol vapor with the help of fluorescence spectroscopy.

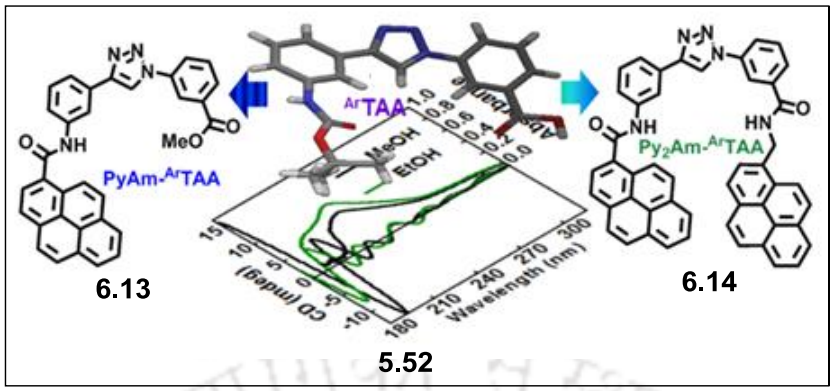

Figure 6.8. Structures of three targeted fluorescent small molecules (**5.52, ^{Ar}TAA**; **6.13**, **PyAm-^{Ar}TAA** and **6.14, Py$_2$Am-^{Ar}TAA**) for possible application in fluorimetric discrimination of ethanol and methanol.

6.6. Results and Discussion

6.6.1. Synthesis of Mono- and Bis-Pyrenylamido Scaffolds 6.13 and 6.14

The synthesis and characterization for aromatic triazolo amino acid scaffold **5.41, ^{Ar}TAA** and its bis-protected form **5.52** were already discussed in **Chapter 5**. Herein the synthesis of mono- and bis-pyrenyl derivatives of the aromatic triazolyl amino acid scaffold is described and presented in **Scheme 6.1**.[30] Thus, N-Boc deprotection of bis-protected scaffold amino acid, **5.52** was first carried out using TFA for about 1 h at room temperature in dry DCM to afford TFA-salt, **6.15.** Next, the neutralization of **6.15** with Et_3N afforded the free amine **6.16** which was undergone coupling with in-situ generated pyrene carboxylic acid chloride ultimately to yield the desired *C*-protected pyrenyl amide scaffold amino acid **6.13** (**PyAm-^{Ar}TAA**). A LiOH mediated hydrolysis of the methyl ester led the *N*-pyrenylamido-aromatic triazolo amino acid scaffold **6.17.** The second round of coupling of **6.17** with pyrenyl methyl amine following a peptide coupling protocol afforded the desired bis-pyrenylamido scaffold **6.14** (**Py$_2$Am-^{Ar}TAA**) in very good yield (**Scheme 6.1**). All the synthesized compounds and the proposed sensors were purified via silica-gel column chromatography and characterized by 1D ^{1}H NMR and mass spectrometry.

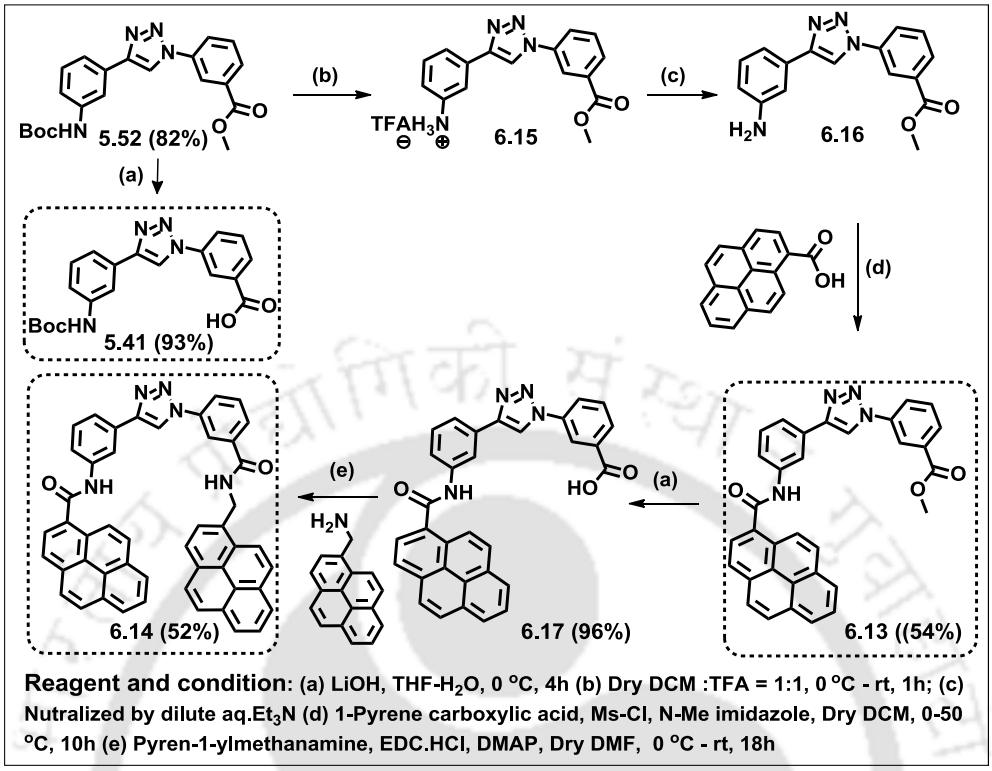

Scheme 6.1. Synthetic scheme of mono and di-pyrene amide derivatives of ^{Ar}**TAA** (**6.13** and **6.14**).

6.6.2. Spectral Characterisation of the Synthesized Scaffold/Peptides

All the synthesized sensors were characterized mainly by NMR spectroscopy. As representative example the structural assignments of sensor **6.13** and **6.14** are shown in **Figure 6.9a** and **6.9b**, respectively. For mono-pyrenyl amide derivative of ^{Ar}**TAA 6.13 (PyAm-^{Ar}TAA),** the triazolyl hydrogen appeared as a singlet at the characteristic position of δ 8.18. The methyl hydrogens of OMe group also resonated as a singlet at δ 3.89. The N-H hydrogens appeared as a singlet at δ 10.35. While the aromatic hydrogens of ^{Ar}**TAA** scaffold at C-2 (N-terminal Ar, Ring A) resonated as singlet at δ 8.20, the C-4, C-5 and C-6 hydrogens appeared as a doublet at δ 7.57, 7.40 and 7.86 with coupling constants J = 8, 7.6 and 8 Hz, respectively. On the other hand, the C-2′ (C-terminal Ar, Ring B) aromatic hydrogens of ^{Ar}**TAA** scaffold appeared as singlet at δ 8.63. The C-4′, C-5′ and C-6′ hydrogens resonated as a doublet, triplet and doublet at δ 8.14, 7.65 and 8.08 with coupling constants J = 8.0, 7.6 and 4.4 Hz, respectively. The pyrenyl hydrogens at C-8, C-9 and C-14 resonated as doublet at δ 8.56, 8.42 and 8.08 with coupling constants J = 9.6, 13.2 and 4.4 Hz, respectively and C-10, C-11, C-15 and C-16 hydrogens resonated as multiplet at δ 8.05. The hydrogens at C-12 and

C-13 appeared as a doublet of a doublet at δ 8.11 with coupling constants J = 8, 4.4 Hz.

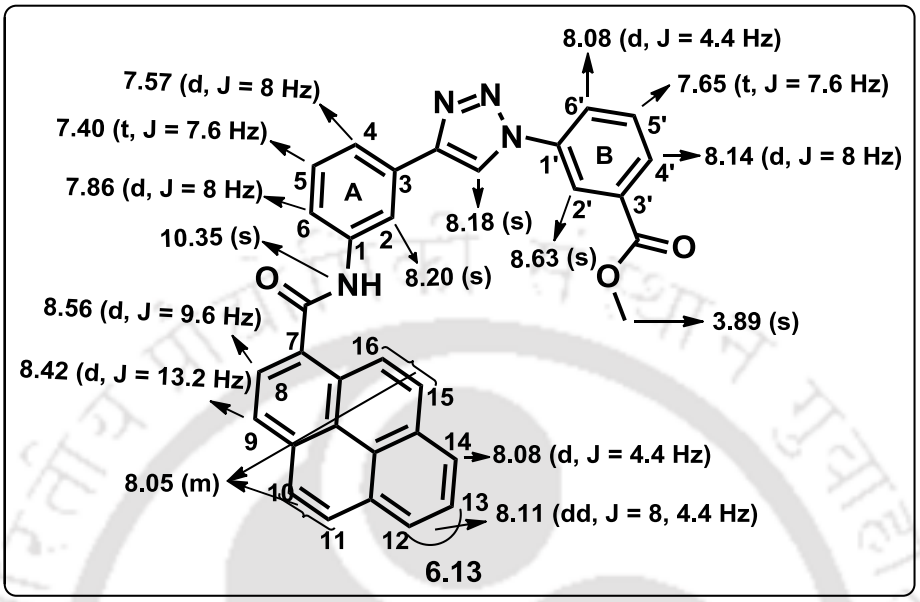

Figure 6.9a. ^{1}H NMR assignment of **PyAm-^{Ar}TAA, 6.13.**

The chemical shift assignment for the sensor **6.14** is shown in **Figure 6.9b**. The detailed assignments of both the sensors including the intermediate compounds are given in the experimental section.

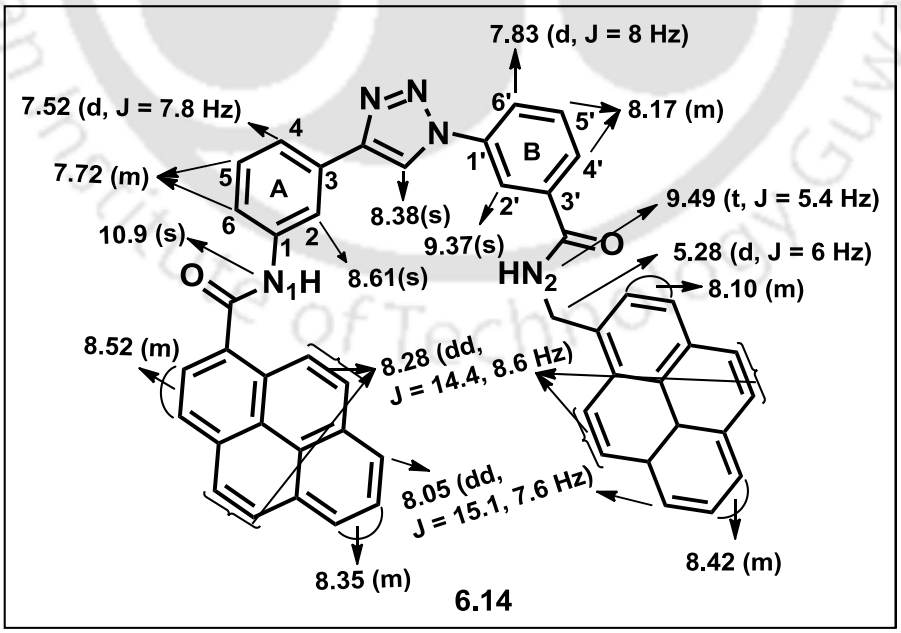

Figure 6.9b. ^{1}H NMR assignment of **Py$_2$Am-^{Ar}TAA 6.14.**

6.6.3. Study of Photophysical Properties

After having all three sensors in pure form, we first studied the photophysical properties in various organic solvents and in alcohols (**Figure 6.10a**). Analysis of UV-visible spectra of the scaffold amino acid **5.41** (^{Ar}**TAA**) revealed highly solvatochromic nature of long wavelength absorption (294 nm) band which experienced a large hyperchromicity along with a bathochromic shift of 8 nm in ethanol compared to methanol. On the other hand, switching from methanol to ethanol did not perturb the wavelength of the absorption at 234 nm though an increased intensity was observed (**Figure 6.10b, Table 6.1**). This observation clearly supported that the out-of-plane aminophenyl unit and in-plane conjugated triazolyl benzoic acid unit of the axially chiral scaffold interacted differently in the ground state with ethanol/methanol.

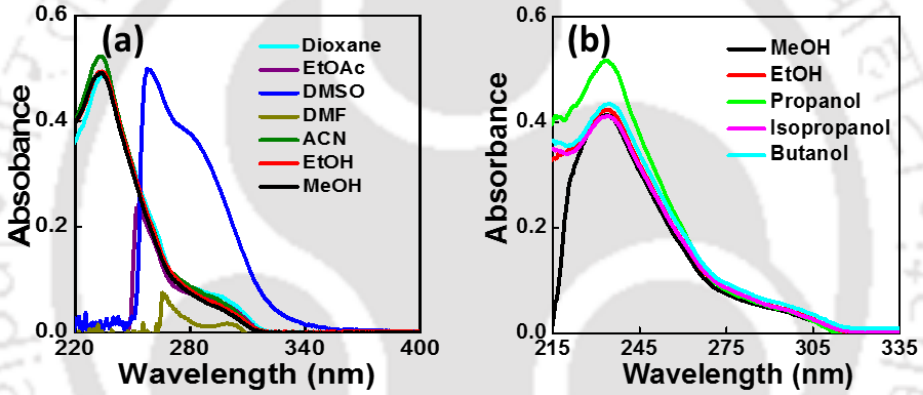

Figure 6.10. The UV-visible spectra of scaffold **5.41** in various (a) organic solvents and (b) alcohols.

This observation clearly supported that the out-of-plane aminophenyl unit and in-plane conjugated triazolyl benzoic acid unit of the axially chiral scaffold interacted differently in the ground state with ethanol/methanol. Excitation spectra monitored at emission maxima exhibits bands at 285 nm and 265 nm in dioxane and in other alcohols like methanol, propanol, isopropanol, butanol with very faint intensity. On the other hand, in ethanol the intensities of both the bands are 3-4 times stronger (**Figure 6.11 a-b**).

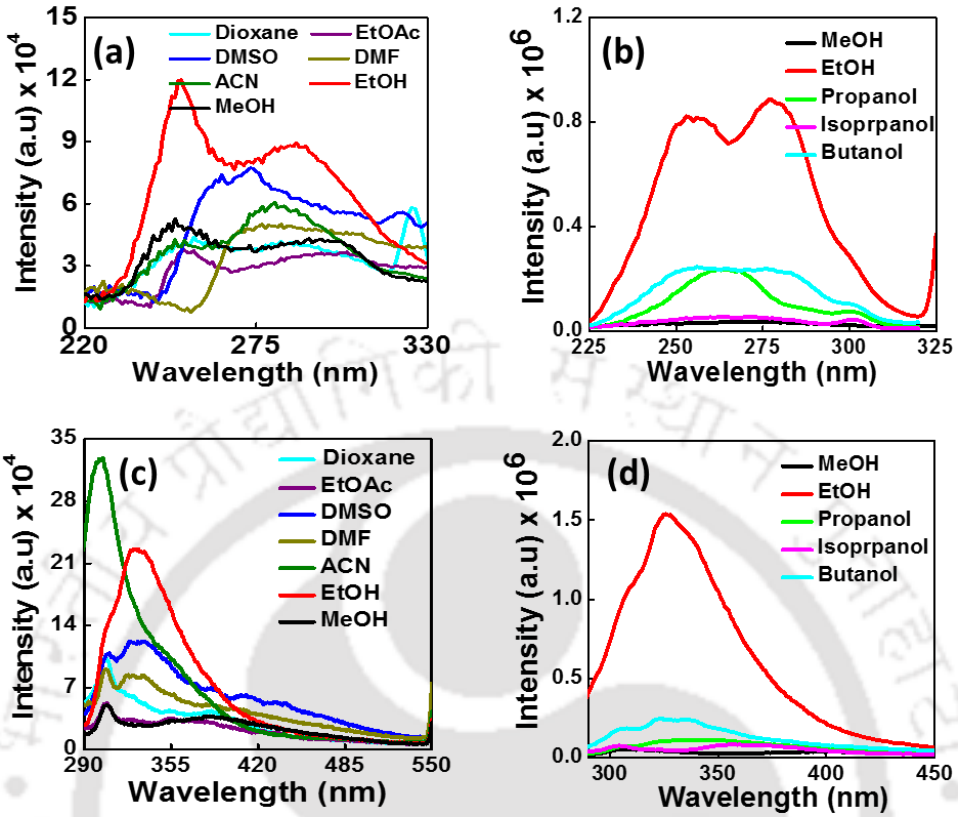

Figure 6.11. The fluorescence excitation spectra of the ^{Ar}**TAA** (**5.41**) in various (a) organic solvents and in (b) alcohols. The emission spectra in various (c) organic solvents and in (d) alcohols.

Upon excitation at 280 nm, very faint emission was observed for methanol, propanol, isopropanol, butanol at around 320-360 nm while a blue shifted strong and broad emission at 330 nm was observed in case of ethanol (**Figure 6.11c-d, Table 6.1**). In summary, the probe **5.41** (^{Ar}**TAA**) shows about 15 fold enhancement in intensity in ethanol compared to methanol. The quantum yield enhancement from methanol to ethanol was found to be 1650% (**Table 6.1**). The methyl ester of scaffold amino acid, **5.52** also behaved exactly in a similar way in respect of interaction between methanol and ethanol and photophysical outcome. It is so possible that ethanol and methanol behaved differently in respect of solvation of the units of axially chiral scaffold through differential H-bonding interaction and ultimately causing differential fluorescence signal generation.[31]

Table 6.1. Summary table of photophysical properties of the **^{Ar}TAA, 5.41.**

Entry	Solvents	Relative polarity	UV-Vis & Fluorescence			
			λ_{max}^{abs} (nm)	ε_{max} x 10^2	λ_{max}^{fl} (nm)	Φ_f
5.41, ^{Ar}TAA	MeOH	0.762	287	63	305	0.004
	EtOH	0.654	289	72.7	326	0.07
	Propanol	0.617	284	69.8	342	0.008
	Isopropanol	0.546	279	73.8	364	0.005
	Butanol	0.586	288	82.1	330	0.012
	% of enhancement intensity from MeOH to EtOH					
	λ_{ex}= 280 nm		λ_{em} = 330 nm		2430	
	% of enhancement Φ_f from MeOH to EtOH					
	λ_{ex}= 280 nm		λ_{em} = 330 nm		1750	

Therefore, the restricted rotation of out-of-plane aminophenyl unit both in ground state and in excited state of scaffold, **5.41** (**^{Ar}TAA**), possibly is responsible for a differential interactions and discrimination of methanol from ethanol. While the time resolved emission followed a single exponential decay in methanol, in ethanol a biexponential fitting gave the best fit with an increase in τ_{av} value from 3.48 ns (in methanol) to 6.21 ns (in ethanol) clearly supporting the differential interaction behaviour of the scaffold in methanol and ethanol (**Figure 6.12, Table 6.2**). The methyl ester of scaffold amino acid, **5.52** also behaved exactly in a similar way in respect of interaction between methanol and ethanol and photophysical outcome. It is so possible that ethanol and methanol behaved differently in respect of solvation of the units of axially chiral scaffold through differential H-bonding interaction and ultimately causing differential fluorescence signal generation.[31]

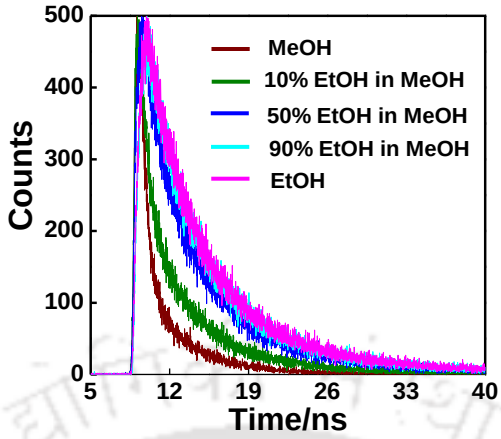

Figure 6.12. Time resolved fluorescence spectra of **5.41, ^{Ar}TAA** in methanol with v/v% increasing ethanol (λ_{ex} = 290 nm; λ_{em} = 330 nm).

Table 6.2. Summary table of fluorescence lifetimes of the **5.41, ^{Ar}TAA** in methanol with v/v% increasing ethanol.

Entry	Solvents	Φ_f	λ [nm]	τ_1 [ns]	τ_2 [ns]	$<\tau>$ [ns]	k_f [$10^8 s^{-1}$]	k_{nr} [$10^8 s^{-1}$]	χ^2
5.41, ^{Ar}TAA	**MeOH**	0.004	330	3.48 (100%)	------	3.48	0.011	2.86	0.93
	10% EtOH	0.005	330	1.14 (31%)	5.01 (69%)	3.8	0.013	2.61	0.95
	50% EtOH	0.008	330	2.0 (24%)	6.44 (75%)	5.39	0.014	1.83	1.04
	90% EtOH	0.02	330	3.59 (50%)	8.59 (50%)	5.92	0.033	1.65	1.02
	Only EtOH	0.07	330	3.65 (49%)	8.85 (51%)	6.21	0.112	1.49	1.03
For lifetimes of the molecule **5.41**, λ_{ex} = 290 nm. Concentration of the compound = 10 μM; $<\tau>$, k_f, and k_{nr} are weighted means from the biexponential fits: $<\tau> = 1/(\alpha_1/\tau_1 + \alpha_2/\tau_2)$, $k_f = \Phi_f/<\tau>$, and $k_{nr} = (1-\Phi_f)/<\tau>$.									

In all above alcohols, both the absorption at 290 nm corresponding to the scaffold as well as at 350 nm corresponding to pyrene appears with very low intensity compared to that in ethanol in case of sensor **6.13** (**PyAm-^{Ar}TAA**) (**Figure 6.13a, Table 6.3**). Upon excitation at 280 nm it shows two emission bands at 320 nm (from scaffold) and at 410 nm (from **Py**) both of which are faint in methanol, propanol, isopropanol, butanol compared to ethanol (**Figure 6.13c, Table 6.3**). The pyrene emission intensity as well as wavelength is also affected and clearly discriminate between methanol and ethanol. Thus, when excited at pyrene absorption of 350 nm,

the intensity and quantum yield are higher in ethanol compared to methanol and other alcohols. However, again the % enhancement of intensity and quantum yield is maximized at the emission wavelength of scaffold at 320nm (**Table 6.4**).The unstructured pyrene emission band at 385 nm in methanol shifted to 430 nm in presence of ethanol. Thus utilising emission from both the scaffold as well as of pyrene allows to discrimate between methanol and ethanol via a drastic enhancement of fluorescence intensity and quantum yield and wavelength shift. Time resolve fluorescence also supported this observation (**Figure 6.14, Table 6.5**).

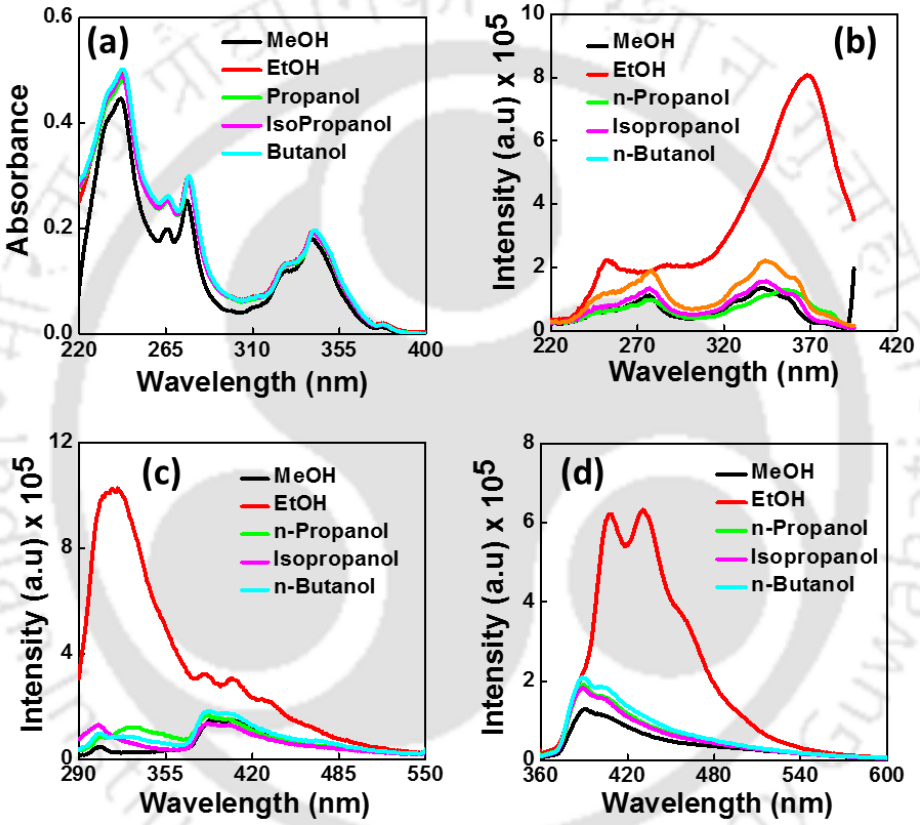

Figure 6.13. (a) UV-Visible (b) excitation (λ_{ex} = 410-430 nm) and fluorescence emission spectra (c) λ_{ex} = 280 nm and (d) λ_{ex} = 350 nm of **6.13** (**PyAm-^{Ar}TAA**) in different alcohol [10 µM, r.t.].

Table 6.3. Summary table of photophysical properties of the sensor **6.13** in different alcohol.

Entry	Solvents	Relative polarity	UV-Vis & Fluorescence			
			λ_{max}^{abs} (nm)	ε_{max} x 10^2	λ_{max}^{fl} (nm)	Φ_f
6.13, $Py^{Ar}TAA$	MeOH	0.762	275, 341	163	305, 401	0.004
	EtOH	0.654	276, 342	180	318, 408, 432	0.030
	Propanol	0.617	276, 341	178	329, 390, 401	0.01
	Isopropanol	0.546	276, 342	179	303, 388, 400	0.009
	Butanol	0.586	276, 341	187	316, 389, 404	0.01

Table 6.4. Summary table of % of enhancement of intensity and quantum yield from MeOH to EtOH of compound **6.13**.

Entry	**% of enhancement intensity from MeOH to EtOH**				
6.13 $Py^{Ar}TAA$	**λ_{ex}= 280 nm**	**λ_{em}**		**λ_{ex}= 350 nm**	**λ_{em}**
		320 nm	430 nm		430 nm
		2260	220		503
% of enhancement Φ_f from MeOH to EtOH					
6.13 $Py^{Ar}TAA$	**λ_{ex}= 280 nm**	1700	300	**λ_{ex}= 350 nm**	350

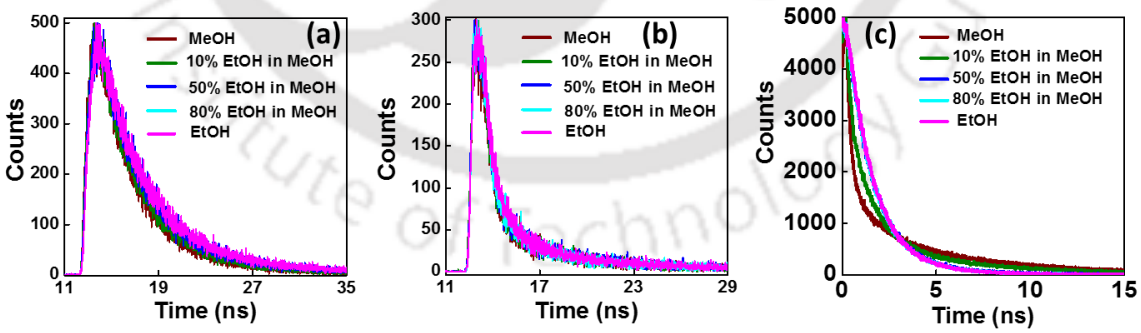

Figure 6.14. Time resolved fluorescence spectra of **$Py^{Ar}TAA$, 6.13** in methanol with v/v% increasing ethanol (a) λ_{ex} = 290 nm; λ_{em} = 330 nm; (b) λ_{ex} = 290 nm; λ_{em} = 410 nm; (c) λ_{ex} = 375 nm; λ_{em} = 410 nm.

Table 6.5. Summary table of fluorescence lifetimes of the **6.13** in methanol with v/v% increasing ethanol.

Entry →	**Py^{Ar}TAA, 6.13**				
Solvents →	**MeOH**	**10% EtOH**	**50%EtOH**	**80% EtOH**	**Only EtOH**
λ_{ex} = 290 nm, λ_{em}= 330 nm					
Φ_f	0.001	0.002	0.009	0.014	0.017
τ_1 [ns]	3.73(100%)	2.25 (19%)	2.98 (44%)	3.22 (49%)	3.38 (55%)
τ_2 [ns]	-----	4.57 (81%)	6.15 (55%)	6.75 (51%)	7.43 (45%)
<τ> [ns]	**3.73**	**4.13**	**4.75**	**5.00**	**5.18**
k_f[$10^8 s^{-1}$]	0.002	0.007	0.040	0.050	0.055
k_{nr} [$10^8 s^1$]	2.67	2.41	2.06	1.94	1.87
χ^2	1.00	0.98	0.99	1.00	1.04
λ_{ex} = 290 nm, λ_{em}= 430 nm					
Φ_f	0.004	0.006	0.009	0.010	0.012
τ_1 [ns]	0.62(30%)	0.71(16%)	0.76(19%)	0.97 (27%)	0.96 (29%)
τ_2 [ns]	4.35 (70%)	4.36 (84%)	4.72 (80%)	5.04 (73%)	5.25 (71%)
<τ> [ns]	**3.22**	**3.74**	**3.96**	**3.94**	**3.99**
k_f[$10^8 s^{-1}$]	0.015	0.018	0.025	0.030	0.032
k_{nr} [$10^8 s^1$]	3.09	2.65	2.50	2.50	2.47
χ^2	0.96	0.95	0.99	1.02	1.00
λ_{ex} = 375 nm, λ_{em}= 430 nm					
Φ_f	0.008	0.010	0.015	0.022	0.028
τ_1 [ns]	0.78 (34%)	1.17 (59%)	1.39 (79%)	1.4 (85%)	1.43 (89%)
τ_2 [ns]	4.51 (66 %)	4.09 (40%)	4.22 (21%)	3.5 (15%)	3.75(11%)
<τ> [ns]	**3.24**	**2.34**	**1.98**	**1.71**	**1.69**
k_f [$10^8 s^{-1}$]	0.024	0.042	0.075	0.122	0.213
k_{nr} [$10^8 s^1$]	3.06	4.23	4.97	5.72	5.70
χ^2	0.98	0.98	0.96	0.93	0.97

For lifetimes of the molecule **6.13** Py^{Ar}TAA, λ_{ex} = 290 nm and 375. Concentration of the compound = 10 μM; <τ> is weighted means from the biexponential fits: <τ> =$1/(\alpha_1/\tau_1+ \alpha_2/\tau_2)$

Next, the third sensor **6.14** (**Py$_2$Am-^{Ar}TAA**) was tested toward detection of ethanol in presence of methanol. Thus, upon excitation at 290 nm the probe shows negligible emission at 300 nm and weak emission at 395 (py-monomer) and a strong emission at 465 nm (py-excimer) in methanol. On the contrary, in ethanol it shows a drastic enhancement of all the emission bands (**Figure 6.15**). However, again the % enhancement of intensity and quantum yield is maximized at the emission wavelength of scaffold at 315 nm (**Table 6.6**). This result indicated that the pyrenyl moiety does not perturb the axial chirality of the scaffold and hence the solvation of pyrenyl

moiety in both methanol and ethanol are almost equal. Therefore, pyrenyl moiety of sensor **6.14** does not play any role in the discrimination process.[31]

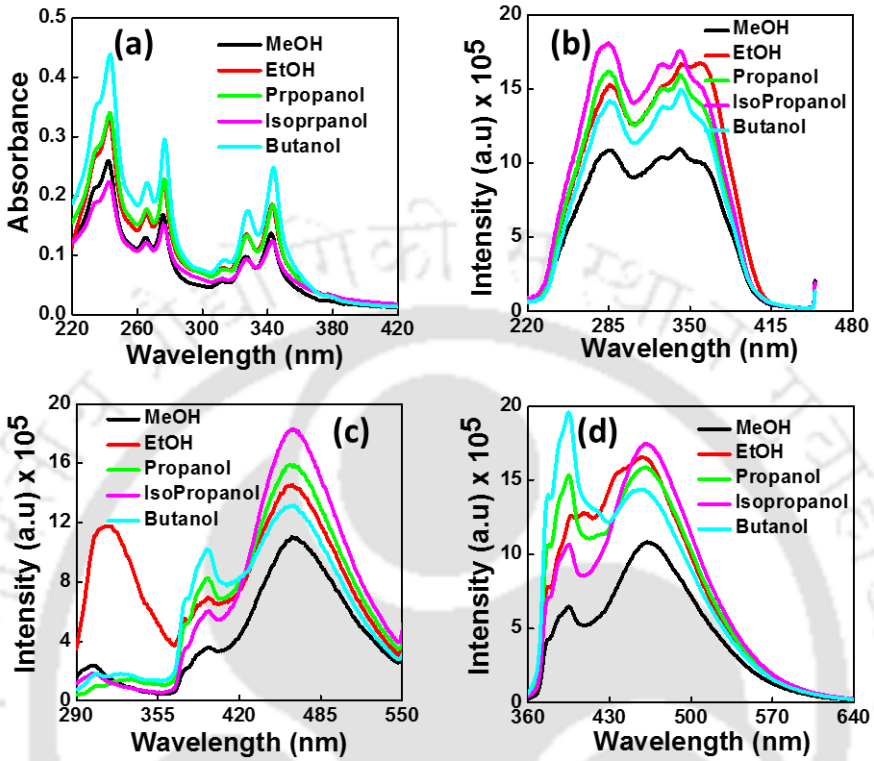

Figure 6.15. (a) UV-Visible (b) excitation (λ_{ex} = 460 nm) and fluorescence emission spectra (c) λ_{ex} = 280 nm and (d) λ_{ex} = 350 nm of **6.14 (Py_2Am-^{Ar}TAA)** in different alcohol [10 µM, r.t.].

Table 6.6. Summary table of photophysical properties of the sensor **6.14** in different alcohol.

Entry	Solvents	Relative polarity	UV-Vis & Fluorescence			
			λ_{max}^{abs} (nm)	ε_{max} x 10^2	λ_{max}^{fl} (nm)	Φ_f
6.14, Py_2^{Ar}TAA	MeOH	0.762	275, 326, 342	109	303, 394, 462	0.06
	EtOH	0.654	276, 326, 342	159	316, 395, 461	0.12
	Propanol	0.617	276, 327, 343	169	330, 394, 462	0.10
	Isopropanol	0.546	276, 327, 343	111	303, 395, 463	0.12
	Butanol	0.586	276, 327, 342	230	326, 394, 462	0.081

Table 6.7. Summary table of % of enhancement of intensity and quantum yield from MeOH to EtOH of compound **6.14**.

Entry	**% of enhancement intensity from MeOH to EtOH**						
6.14 $Py_2^{Ar}TAA$	λ_{ex}= **280 nm**	λ_{em}			λ_{ex}= **350 nm**	λ_{em}	
		330 nm	430 nm	465 nm		430 nm	465 nm
		511	192	133		202	155
% of enhancement Φ_f from MeOH to EtOH							
6.14 $Py_2^{Ar}TAA$	λ_{ex}= **280 nm**	1025	620	153	λ_{ex}= **350 nm**	160	142

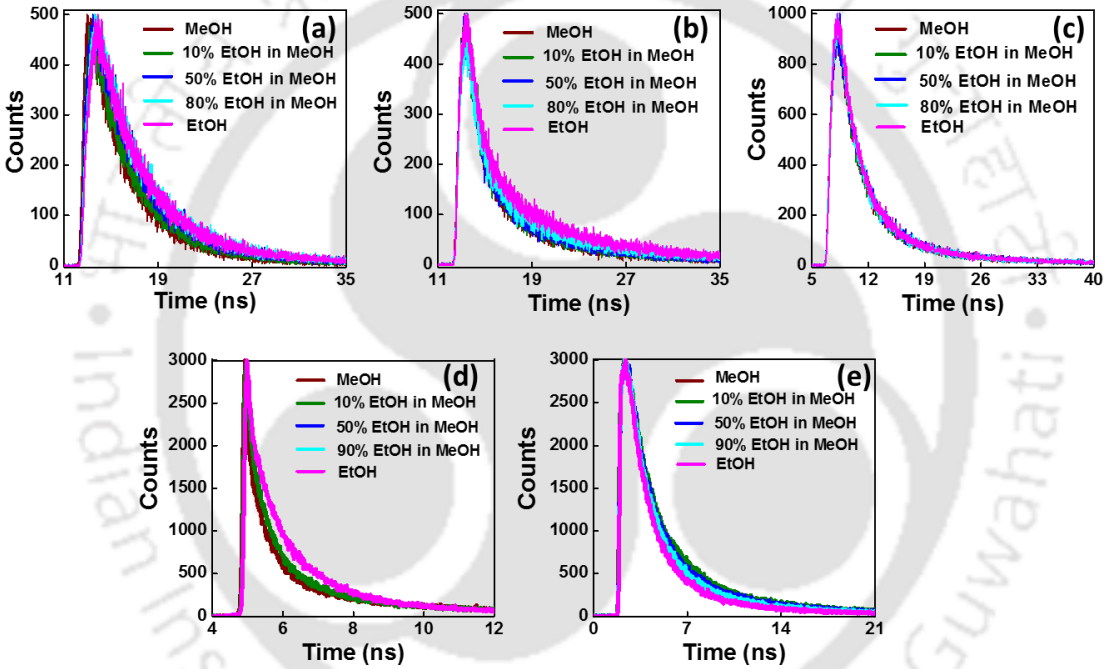

Figure 6.16. Time resolved fluorescence spectra of **$Py_2^{Ar}TAA$, 6.14** in methanol with v/v% increasing ethanol (a) λ_{ex} = 290 nm, λ_{em} = 330 nm; (b) λ_{ex} = 290 nm, λ_{em} = 410 nm; (c) λ_{ex} = 290 nm, λ_{em} = 465 nm; (d) λ_{ex} = 375 nm, λ_{em} = 410 nm; (e) λ_{ex} = 375 nm, λ_{em} = 465 nm.

Table 6.8. Summary table of fluorescence lifetimes of **6.14** in in methanol with v/v% increasing ethanol

Entry →	**$Py_2^{Ar}TAA$, 6.14**				
Solvents →	**MeOH**	**10% EtOH**	**50%EtOH**	**80% EtOH**	**Only EtOH**
λ_{ex} = 290 nm, λ_{em}= 330 nm					
Φ_f	0.004	0.012	0.025	0.030	0.041
τ_1 **[ns]**	1.8 (15%)	2.12(20%)	3.23 (53%)	3.34 (54%)	3.39 (56%)
τ_2 **[ns]**	4.08 (85%)	4.6 (80%)	6.21 (46%)	6.8 (56%)	7.1 (44%)
<τ> [ns]	**3.74**	**4.10**	**4.62**	**4.92**	**4.99**
k_f**[$10^8 s^{-1}$]**	0.013	0.029	0.05	0.06	0.082
k_{nr} **[$10^8 s^1$]**	2.66	2.40	2.11	1.97	1.92
χ^2	0.94	0.95	1.00	1.00	1.02
λ_{ex} = 290 nm, λ_{em}= 410 nm					
Φ_f	0.005	0.011	0.021	0.024	0.031
τ_1 **[ns]**	1.34(33%)	1.38 (32%)	1.31 (29%)	1.37 (25%)	1.36(22%)
τ_2 **[ns]**	6.74 (67%)	7.14 (68%)	7.32 (71%)	7.94 (75%)	8.03(78%)
<τ> [ns]	**4.98**	**5.28**	**5.58**	**6.29**	**6.53**
k_f**[$10^8 s^{-1}$]**	0.012	0.020	0.037	0.038	0.067
k_{nr} **[$10^8 s^1$]**	1.99	1.87	1.75	1.55	1.48
χ^2	1.03	1.06	1.04	1.06	1.05
λ_{ex} = 290 nm, λ_{em}= 465 nm					
Φ_f	0.045	0.060	0.062	0.064	0.069
τ_1 **[ns]**	2.99 (53%)	2.97 (54%)	3.05 (54%)	3.12 (47%)	3.09(52%)
τ_2 **[ns]**	12.56 (47%)	12.73 (46%)	12.74 (46%)	12.93 (53%)	13.30(48%)
<τ> [ns]	**7.48**	**7.48**	**7.49**	**8.24**	**8.03**
k_f**[$10^8 s^{-1}$]**	0.060	0.080	0.082	0.077	0.085
k_{nr} **[$10^8 s^1$]**	1.27	1.25	1.25	1.13	1.15
χ^2	1.01	1.00	1.02	1.00	0.99
λ_{ex} = 375 nm, λ_{em}= 410 nm					
Φ_f	0.005	0.006	0.006	0.007	0.008
τ_1 **[ns]**	1.23 (26%)	1.24 (34%)	1.31 (52%)	1.34 (60%)	1.37 (63%)
τ_2 **[ns]**	6.69 (73%)	6.64 (66%)	6.61 (48%)	6.14 (40%)	6.04 (37%)
<τ> [ns]	**5.25**	**4.82**	**3.97**	**3.25**	**3.12**
k_f**[$10^8 s^{-1}$]**	0.001	0.012	0.015	0.020	0.025
k_{nr} **[$10^8 s^1$]**	1.89	2.06	2.50	2.96	3.17
χ^2	1.05	1.02	1.01	1.02	1.02
λ_{ex} = 375 nm, λ_{em}= 465 nm					
Φ_f	0.073	0.079	0.083	0.103	0.104
τ_1 **[ns]**	3.45 (50%)	3.32 (49%)	3.27 (49%)	3.07 (49%)	2.79 (48%)
τ_2 **[ns]**	15.87 (50%)	15.70 (51%)	15.51 (51%)	14.81(51%)	13.74(52%)
<τ> [ns]	**9.67**	**9.68**	**9.54**	**9.06**	**8.50**
k_f**[$10^8 s^{-1}$]**	0.08	0.081	0.087	0.113	0.164
k_{nr} **[$10^8 s^1$]**	0.953	0.951	0.961	0.99	1.011
χ^2	1.08	1.06	1.04	1.05	1.00
For lifetimes of the molecule **6.14,** λ_{ex} = 290 nm and 375. Concentration of the compound = 10 μM; <τ> is weighted means from the biexponential fits: $<\tau> = 1/(\alpha_1/\tau_1 + \alpha_2/\tau_2)$.					

***Titration Experiment*:** Next we carried out a titration experiment. The simple scaffold sensor **5.41** in methanol exhibited only one unstructured emission band of low intensity at 300 nm when excited at 280 nm. However, an increasing of v/v% of EtOH when added gradually the sensor shows a regular increase in intensity as well as quantum yield with appearance of a structured band centered at 330 nm (**Figure 6.17**). Similar results were observed in case of compound **5.52**. Differential interaction behaviour of the scaffold in methanol and ethanol clearly supported from a time resolved spectroscopic study. In methanol, the decay curve could be fitted as single exponential while with increasing v/v% ethanol life time of the sensor graduly increases and finally it becomes a biexponential fitting gave the best fit with an increase in life time from 3.48 ns (in methanol) to 6.21 ns (in ethanol) (**Figure 6.12 Table 6.2**).

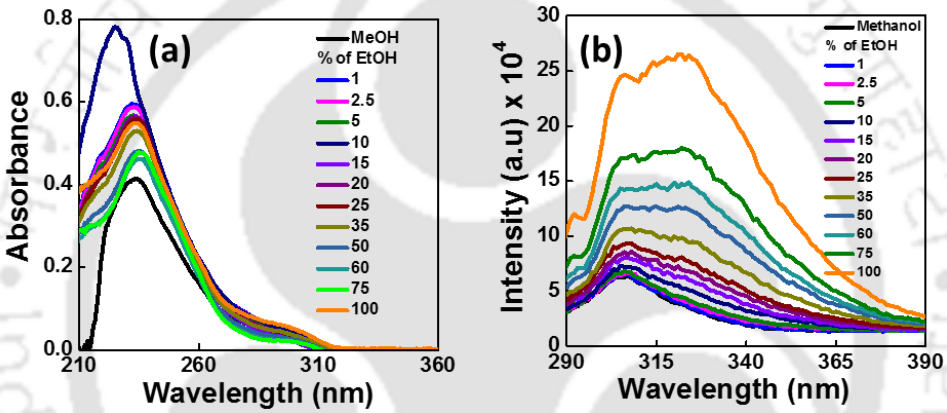

Figure 6.17. (a) UV-Visible and (b) fluorescence emission spectra of the **^{Ar}TAA, 5.41** in methanol with increasing volume of ethanol. [10 μM, r.t.; $\lambda_{ex} = \lambda_{max} \approx 280$ nm in each solvent].

The results of a titration experiment in case of a methanolic solution of mono pyrenyl amide **6.13** (**PyAm-^{Ar}TAA**) were found to be similar to that observed in case of sensor **5.41**. Thus, upon excitation at 290 nm the intensity of both the scaffold (λ_{em} = 320 nm) and pyrene (λ_{em} = 410 nm) emission gradually increases as the v/v % of ethanol increases and reaches maximum at pure ethanol. On the other hand, excitation at pyrene absorption of 350 nm, a regular increase in emission intensity at 410-430 nm was observed (**Figure 6.18c-d**). Addition of 50% ethanol modulated the emission wavelength from 410 to 420 nm which is also supported from time resolve spectra (**Figure 6.14a-b, Table 6.5**). Interestingly, excitation at pyrene at 375 laser the decay curve showed a clear isosbestic point at around 3.5 ns as to be expected for such a binary mixture (**Figure 6.14c**).[32] Thus the sensor is highly efficient in sensing ethanol in presence of methanol, drastically in the region of scaffold and moderately at pyrenyl emission.

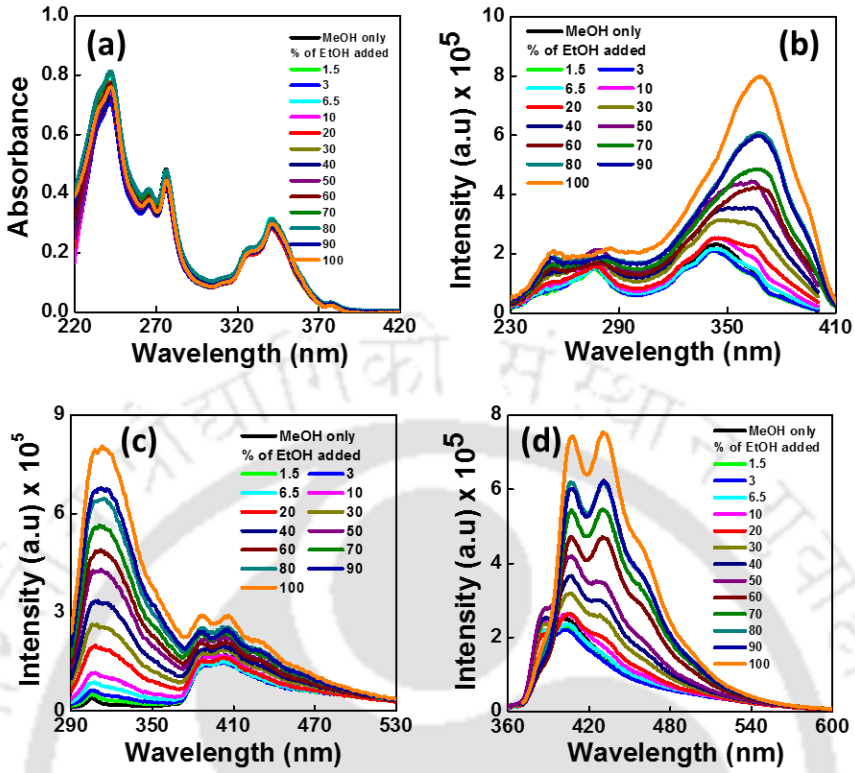

Figure 6.18. (a) UV-Visible (b) excitation (λ_{ex} = 410-430 nm) and fluorescence emission spectra (c) λ_{ex} = 280 nm and (d) λ_{ex} = 350 nm of **613, (PyAm-^{Ar}TAA)** in methanol with increasing volume of ethanol.[10 µM, r.t.].

The bis-pyrenyl bis-amide sensor **6.14**, on the other hand, upon excitation at 290 nm showed negligible emission at 315 nm and strong emission at 395 (py-monomer) and 465 nm (py-excimer) methanol. Addition of an increasing v/v% EtOH to the methanolic solution results in a gradual increase in scaffold intensity similar to the case of other two sensors which was also supported from a time resolve spectra (**Figure 6.19c-d**). Both the pyrenyl monomer emission as well as excimer emission intensity also increases while the changes are less drastic compared to the change in intensity at the scaffold emission wavelength supported further from a time resolve emission study. Thus, sensor **6.14** also follows same trend of excited state decay i.e. the decay time regularly increases from methanol to ethanol when excited at 290 nm and monitored at all the emission wavelength 330, 410 and 465 nm. But excitation at pyrene at 375 nm laser, life time time value remain more or less same. Therefore, fluorescen decay experiment clearly supported the discrimination property of **Py$_2$Am-^{Ar}TAA** (**6.14**) towards methanol-ethanol (**Figure 6.16, Table 6.8**).

All the results of all probes reflected the important role and differential interaction with the axially chiral scaffold.

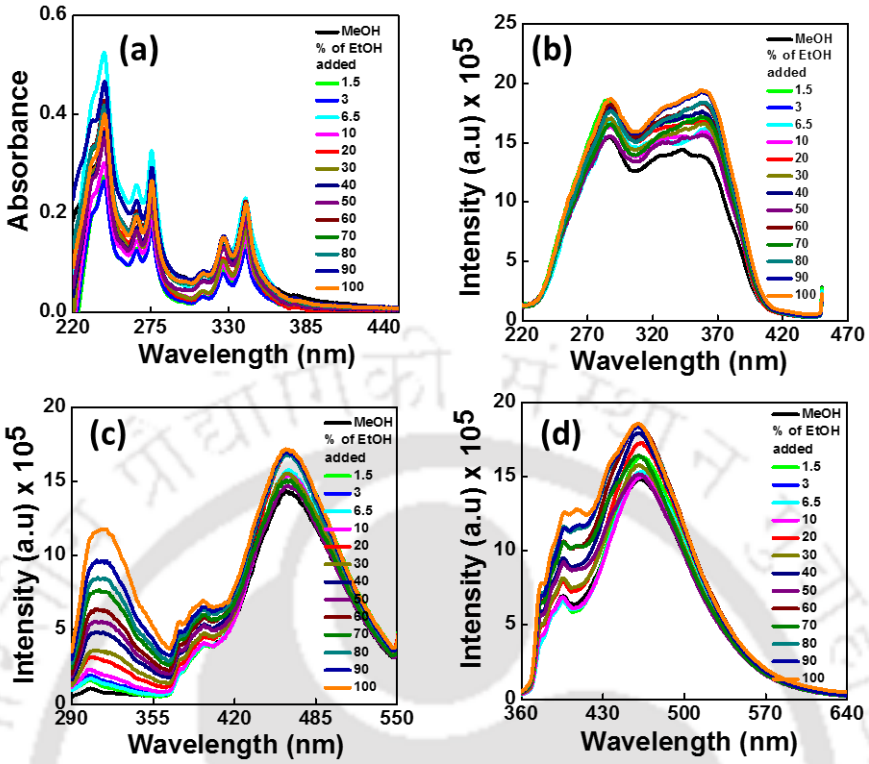

Figure 6.19. (a) UV-Visible (b) excitation (λ_{ex} = 460 nm) and fluorescence emission spectra (c) λ_{ex} = 280 nm and (d) λ_{ex} = 350 nm of **6.14 (Py_2Am-^{Ar}TAA)** in methanol with increasing volume of ethanol. [10 µM, r.t.].

Colour Under Fluorescence Light: The fluorescence color intensity obtained under UV-irradiation (λ_{ex} = 280, 350 nm) of **^{Ar}TAA** gradually became deeper and brighter with increasing v/v% of ethanol. Other two pyrenyl derivartives also showed similar type of result (**Figure 6.20**).

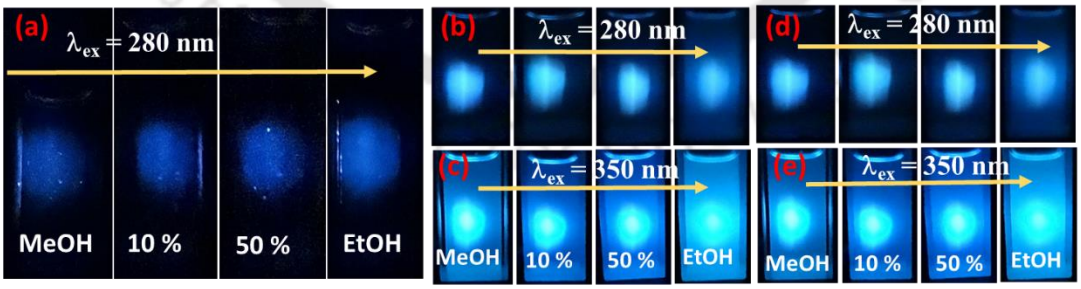

Figure 6.20. Picture under fluorescence light of compound (a) **5.41, ^{Ar}TAA**; (b-c) **6.13, PyAm-^{Ar}TAA**; (d-e) **6.14, Py_2Am-^{Ar}TAA** in MeOH**,** 10% EtOH in MeOH, 50% EtOH in MeOH and EtOH solvents.

All these observations indicated that axial chirality of the hairpin-shaped scaffold **5.41** or **5.52** or scaffold moiety in **6.13-6.14** involve in differential solvation and H-bonding interaction with methanol/ethanol. In methanol both the in-plane and out-of-plane moieties were solvated almost equally while the axial chirality in ethanol remained preserved leading to unequal solvation and H-bonding interactions.[31] These observations are also supported from spectroscopic evidences. Pyrenyl moieties in sensors **6.13-6.14** did not perturbed the chirality of the scaffold unit in the sensors leading to almost similar interaction with both the methanol and ethanol which ultimately resulted in a less drastic change in the emission region of pyrene. Therefore, it can be concluded that the axial chirality leaded differential solvation and H-bonding interaction possibly played a crucial role in discriminating ethanol and methanol of closest boiling points and polarities.

6.6.4. Determination of the Detection Limit

The detection limit was calculated from fluorescence titration experiments for all the probes.[22] Thus, we observed that the simple scaffold sensor **5.41** and other two sensors **6.13-6.14** showed high sensitivity in sensing ethanol in presence of methanol (2-2.6 v/v %). To evaluate the detection limit of ethanol we have plotted $(I_{min} - I)/(I_{min} - I_{max})$ *vs* log of added EtOH volume. The linear fit was drawn by taking the five points (volume of ethanol 20 µl to 700 µl) of the linear region. The extended line where it crossed the coordinate axes is the ethanol detection limit which was found to be 2.6 % (λ_{em} = 320 nm) for **5.41** (**^{Ar}TAA**), 2% (λ_{em} = 320 nm) and 2.2% (λ_{em} = 430 nm) for **6.13 (PyAm-^{Ar}TAA)** and 2.2% (λ_{em} = 320 nm) for **6.14 (Py$_2$Am-^{Ar}TAA).**

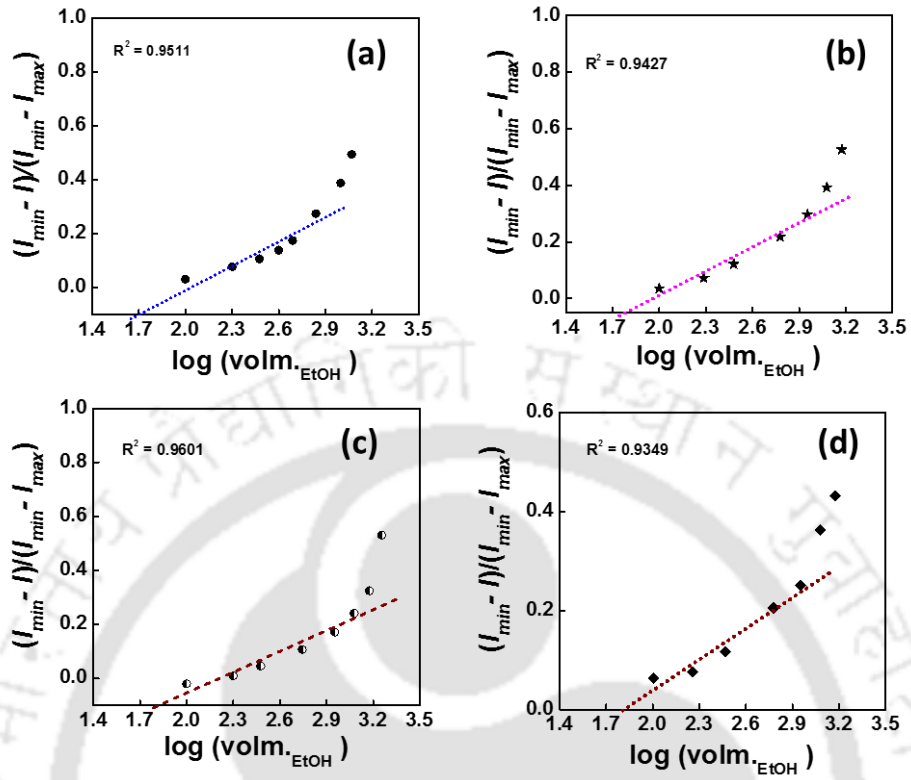

Figure 6.21. Plot of $(I_{min} - I)/(I_{min} - I_{max})$ *vs* log (Volume $_{EtOH}$) of (a) **5.41 ^{Ar}TAA** (λ_{em} = 320); **6.13 PyAm-^{Ar}TAA** (b) λ_{em} = 320, (c) λ_{em} = 430; (d) **6.14 Py$_2$Am-^{Ar}TAA** (λ_{em} = 320).

6.6.5. Study for Ethanol Vapor Sensing

The vapour sensing ability by these sensors was next studied. For that purpose, we prepared solid films of these sensors via a spin coating method for possible sensing of ethanol vapour with the help of fluorescence spectroscopic technique. It was observed that the fluorescence intensity of **^{Ar}TAA** coated solid film increased with increasing the vapour pressure of ethanol in a methanol-ethanol mixture. Other two pyrenyl derivatives also behaved in a similar way to detect ethanol vapour from a mixture of methanol-ethanol (**Figure 6.22-6.24**).[33] Molecular adsorption on the surface of the sensors possibly occurred through H-bonding, dipole-dipole interaction, and dispersion force between the amine/acid functionality of the scaffolds and the ethanol/methanol vapour. The molecular affinity of ethanol vapour to the solid scaffold surface are more compared to methanol which is evident from Hansen polarity parameters which is probably the reason of enhancement of luminescence intensity as the vapour pressure of ethanol gradually increases. [33c-d]

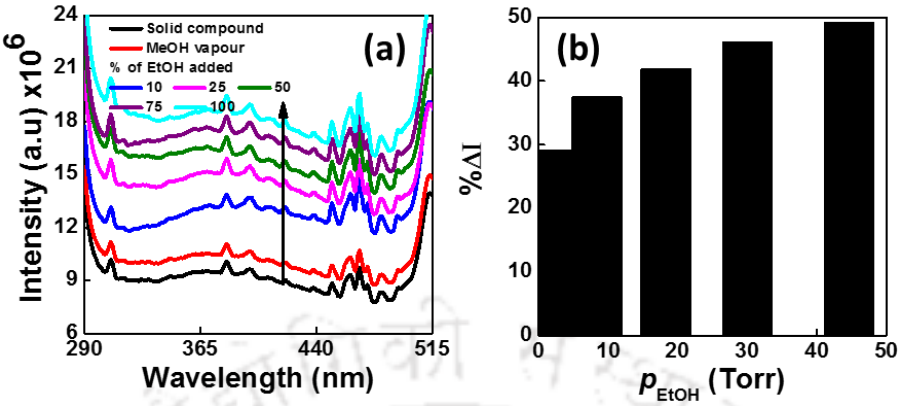

Figure 6.22. (a) Fluorescence emission spectra (λ_{ex} = 280 nm) of the **5.41, ^{Ar}TAA** with increasing the vapor pressure of ethanol in a methanol-ethanol mixture (room temperature). (b) Plot of relative change of the fluorescence intensity, % ΔI with ethanol vapor pressure (λ_{em} = 390 nm).

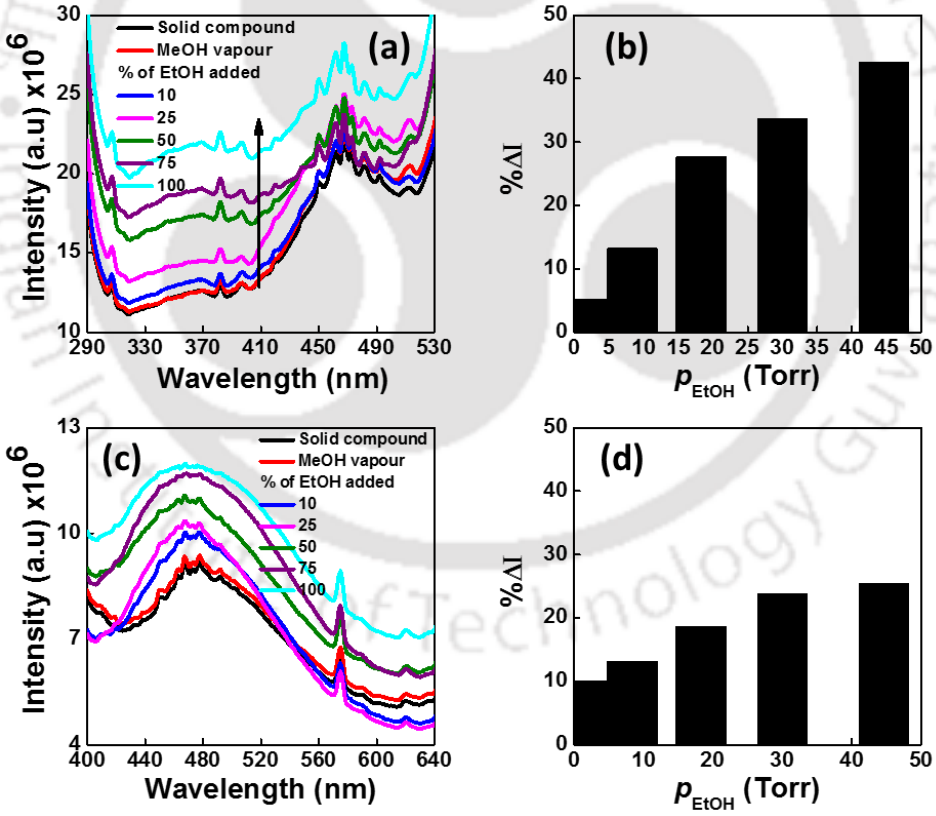

Figure 6.23. Fluorescence emission spectra (a) λ_{ex} = 280 nm; (c) λ_{ex} = 350 nm of the **6.13 (PyAm-^{Ar}TAA)** with increasing the vapor pressure of ethanol in a methanol-ethanol mixture (r.t). (b-d) Plot of % ΔI with ethanol vapor pressure (λ_{em} = 390, 470 nm).

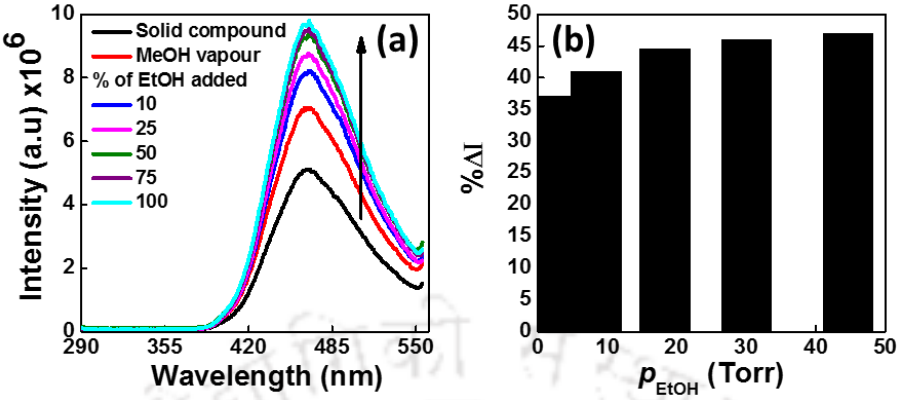

Figure 6.24. (a) Fluorescence emission spectra (λ_{ex} = 280 nm) of the **6.14 (Py_2Am-^{Ar}TAA)** with increasing the vapor pressure of ethanol in a methanol-ethanol mixture (r.t.). (b) Plot of % ΔI with ethanol vapor pressure (λ_{em} = 470 nm).

6.6.6. Mechanistic Interpretation of EtOH Sensing

To support of proposal that the axial chirality of the aromatic triazolo amino acid scaffold **5.41** moiety in all the probes and differential solvation mediated H-bonding and hydrophobic interactions between ethanol/methanol and the scaffold possibly played an important role in fluorimetric discrimination of methanol from ethanol, we next have carried out some spectroscopic experiments like IR, CD, specific rotation, and theoretical study such as Molecular modeling and gaussian 09 optimization with CPCM solvent model.

***Study of IR Spectroscopy*:** The differential H-bonding interaction was evident from IR spectra that showed the major differential perturbation and a noticeable change occurred at ester carbonyl and triazole-N=N stretching frequency, respectively. As a representative example, the ester carbonyl of scaffold **5.41** in solid KBr exhibited stretching frequency at 1719 cm^{-1} and triazole-N=N stretching appeared at 1441/1459 cm^{-1} while the amide I stretching was not observed. However, the sample when soaked with methanol, ethanol or a mixed solvent and recorded the IR we found nice differential stretching frequencies of all the above functional groups.[18, 34] Thus, while ester >C=O absorb at 1713 cm^{-1} along with the appearance of amide-I band at 1668 cm^{-1} in methanol, the scaffold behaved similar to the solid state in ethanol with a stretching frequency at 1715 cm^{-1} corresponding to ester>C=O. The triazole-N=N-stretching also in ethanol (1436/1458 cm^{-1}) was more correlating to a solid state compared to that observed in methanol (1418/1450 cm^{-1}).

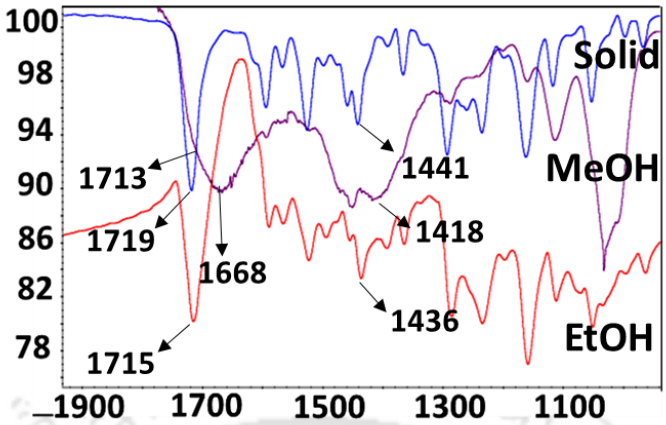

Figure 6.25. IR spectra of **5.41,** ^{Ar}**TAA** under solid and soaked in methanol and ethanol.

Whereas, scaffold **5.52** exhibited acid carbonyl stretching frequency at 1702 cm^{-1} with amide-I band at 1687 cm^{-1} and triazole-N=N stretching appeared at 1440/1463 cm^{-1} in solid KBr. when the sample soaked with methanol acid>C=O absorb at 1699 cm^{-1} and amide-I band at 1668 cm^{-1}. But when scaffold soaked in ethanol acid>C=O absorb at 1700 cm^{-1} with amide-I band at 1674 cm^{-1}. The triazole-N=N-stretching also in ethanol (1430/1454 cm^{-1}) was more correlating to a solid state compared to that observed in methanol (1406/1445 cm^{-1}).

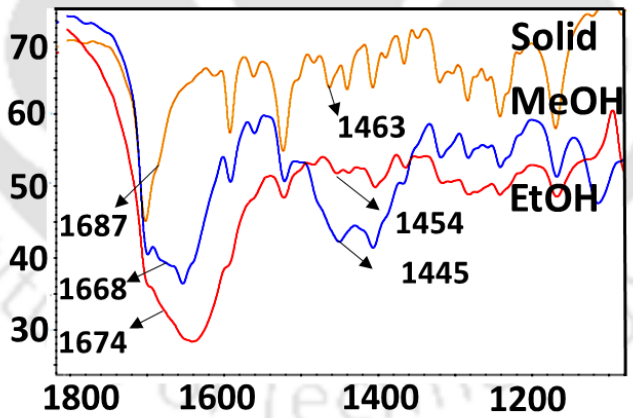

Figure 6.26. IR spectra of **5.52,** ^{Ar}**TAA** under solid and soaked in methanol and ethanol.

Therefore, it is clear that interactions such as H-bonding in methanol and ethanol are very much different and is more in methanol compared to ethanol. Probably, this caused the scaffold to attain more planar geometry in methanol compared to the case in ethanol leading to a drastic quenching of fluorescence in methanol.[34c] The biexponential and monoexponential time resolved fluorescence decay curve,

respectively, in ethanol and methanol also supported the differential interaction through H-bonding.

***Study of Specific Rotation and Circular Dichroism Spectroscopy* (CD):** We further investigated the H-bond mediated conformational switching in both the methanol and ethanol utilising specific rotation in a polarimeter and CD spectrophotometer. Thus, the specific rotation in methanol was found to be +1.5° while a higher rotation with opposite chirality (-8.0 °) was observed in ethanol. The circular dichroism spectra in both the solvents exhibited opposite cotton effect.[35a] In methanol the scaffold **5.41** showed a strong positive and a negative band at 185 and 190 nm, respectively, representing predominant β-sheet with some contribution from turn like structure.[35] Increasing % of ethanol changes the conformation from predominant β-sheet to random coil to α-helix. In pure ethanol the CD spectrum showed a positive band at 190 nm which is characteristic of predominant α-helical conformation (**Figure 6.27a**). Therefore, both the CD and polarimetric study showed a conformational switching in scaffold **5.41** which is most probably the cause of discriminating methanol from ethanol. Other two compounds also shows similar results (**Figure 6.27b-c**).

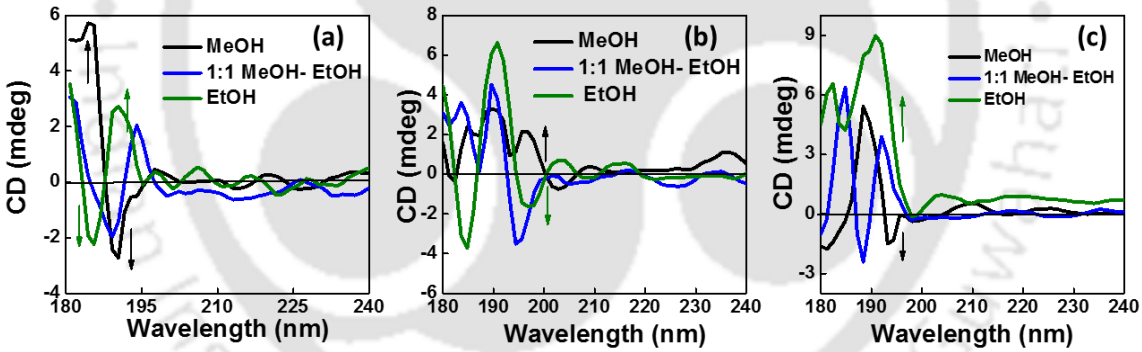

Figure 6.27. CD spectra of scaffolds **5.41,** ^{Ar}**TAA** (a); **6.13, PyAm-**^{Ar}**TAA** (b) and **6.14, Py$_2$Am-**^{Ar}**TAA (c)** in methanol, ethanol and 1:1 mixture of two solvent (*l* = 10 mm, r.t., 100 μM concentration).

Theoretical Study with Maestro vs. 9.1 and Gaussian 09: Finally we tried to get more support from a Molecular modelling study and a theoretical calculation. At first we utilize macromodel study. Thus, a conjugate gradient minimization scheme [PRCG (Polak-Ribiere Conjugate Gradient)] that uses the Polak-Ribiere first derivative method with restarts every 3N iterations was employed for the minimization of the scaffold ^{Ar}**TAA** (**5.52**) using Schrodinger Macromodel (Maestro vs. 9.1) software with Amber* force field in MeOH/EtOH. Next, we carried out conformational search using Amber* force field at respective dielectric in MeOH/EtOH with "large scale low-frequency-mode conformational search" (Mixed

torsional/Large scale low-mode sampling = MCMM/LMCS) method. A total of 500 structures were processed with 500 maximum no. of steps iteration. A global search analysis eliminates redundant conformers using RMS deviation for all compared atoms exceed the threshold Cutoff of 0.5 Å. An optimal minimization method was chosen for minimizing the generating conformers.

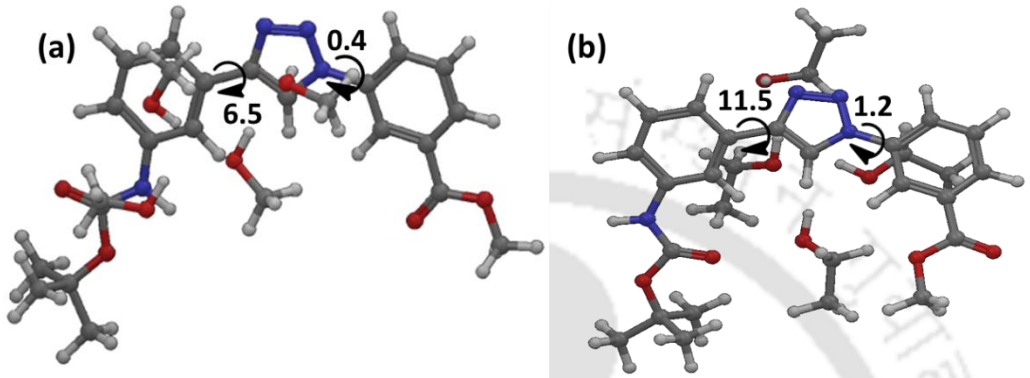

Figure 6.28. The conformer obtained after conformational search, with 1.00 k.cal/mole (4.18 kJ/mole) global minimum. (a) ^{Ar}**TAA, 5.52** with four **MeOH** solvent molecule (b) ^{Ar}**TAA, 5.52** with four **EtOH** solvent molecule.

Thus, Amber* force field conformational search for the scaffold **5.52** in ethanol and/or methanol was carried out which indicated a noticeable change in dihedrals and H-bonding interactions in both the solvents. While in ethanol, the aminophenyl unit remain 12^{o} out-of-plane which is mimicking the geometry in solid state, in methanol the molecule remained almost planar (**Figure 6.28**).[36]

Furthermore, we next optimized the scaffold **5.52** with four molecules of methanol or ethanol using Gaussian 09 programme at B3LYP/6-311G level of theory with CPCM solvent model.[37] The energy minimized geometry revealed that the aminophenyl unit remained almost in plane with triazole ring in both Methanol and ethanol solvent. It is true that the DFT calculation does not mimick the conformation of solid state. However, the differential change in dihedral angles in methanol and ethanol reflected similar observation as was interpreted based on Macromodel study. However, the benzoic acid unit experienced more out-of-planarity (33^{o}) in ethanol compared to that in methanol (20^{o}). We observed a noticeable change in H-bonding interaction pattern by MeOH or EtOH with the various possible sites of the molecule. Thus, one of the EtOH involved in H-bonding through carbamate->C=O…..$H_{Triazole}$, lifting benzoic acid unit more out-of-plane. On the other hand methanol involved in H-bonding through ester >C=O…..$H_{Triazole}$, decreasing the out-of-planarity (20 ^{o}) of the benzoic acid unit (**Figure 6.29**).

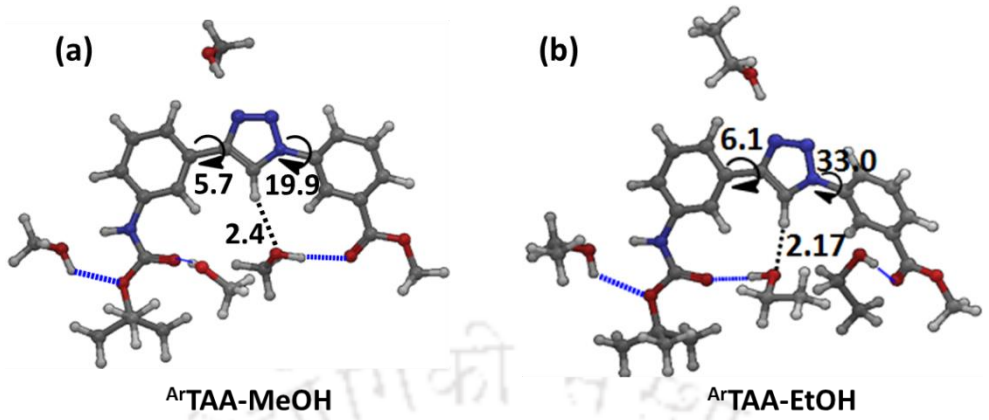

Figure 6.29. B3LYP/6-31G Optimized Structure of (a) **5.52**, **^{Ar}TAA-MeOH** in MeOH solvent (b) **5.52**, **^{Ar}TAA-EtOH** in EtOH solvent.

Whereas, in case of **Py$_2$^{Ar}TAA** (**6.14**) sensor two pyrene moiety come closer in ethanol solvent compare to methanol where two fluorophoric unit are outward (**Figure 6.30**). This observation supported the maximum interaction between two pyrenyl unit leading to stronger excimer emission in ethanol compared to methanol.

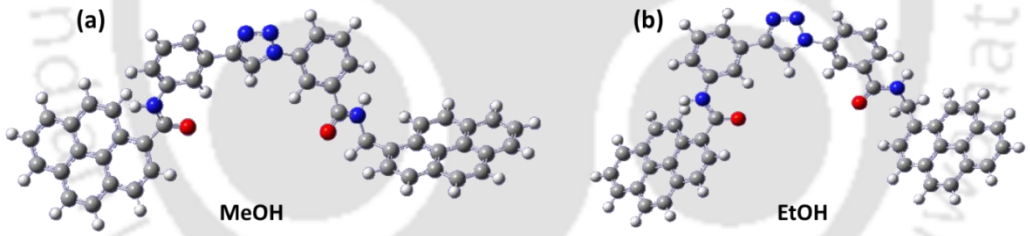

Figure 6.30. B3LYP/6-31G optimized structure of **Py$_2$^{Ar}TAA** (**6.14**) in (a) MeOH and (b) EtOH solvent.

Therefore, it is clear that interactions such as H-bonding in methanol and ethanol are very much different and is more in methanol compared to ethanol. Probably, this caused the scaffold to attain more planar geometry in methanol compared to the case in ethanol leading to a drastic quenching of fluorescence in methanol.

6.7. Conclusion

In conclusion, we have designed three new alcohol sensors involving both solution and solid-state fluorescence emission. The simple scaffold and other two sensors showed high sensitivity in sensing ethanol in presence of methanol (2-2.6 v/v %) which was determined by simple observation of fluorescence. In addition,

combining the ethanol sensors in a solid film enabled detection of ethanol in the vapor phase. The diffential solvation mediated H-bonding interaction played a crucial role in fluorimetric discrimination of methanol from ethanol by the axially chiral scaffold or the scaffold moieties in the sensors. In terms of applicability, we believe that such a simple system would attract to develop system which could estimate ethanol content on-the-spot. We are currently working to develop such practical sensory devices with these small organic molecules.

6.8. Experimental Section

6.8.1. General Experimental

All reaction were carried out under nitrogen atmosphere in flame-dried glassware, using a nitrogen filled balloon. Organic extracts were dreid over anhydrous sodium sulfate. Solvents were removed in a rotary evaporator under reduced pressure. Silica gel (60- 120 mesh size) was used for the column chromatography. Reactions were monitored by TLC on silica gel 60 F254 (0.25). 1H NMR spectra were recorded either at 400MHz or at 600MHz and 13C NMR spectra were recorded either at 100 MHz or at 150 MHz (mentioned accordingly). Coupling constants (J value) were reported in hertz (Hz). The chemical shift were shown in ppm downfield form tetramethylsilane, using residual chloroform (δ = 7.26 in ^{1}H NMR, δ = 77.23 in ^{13}C NMR), DMSO (δ = 2.5 in ^{1}H NMR, δ = 39.5 in ^{13}C NMR), as an internal standard. Mass spectra were recorded with a HR mass spectrometer and data analysed by using built-in software. IR spectra were recorded in KBr on a FT-IR spectrometer.

6.8.2. Synthesis and Characterization

***Synthesis of methyl 3-(4-(3-((tert-butoxycarbonyl)amino)phenyl)-1H-1,2,3-triazol-1-yl)benzoate* (5.52):** The compound **5.52** was synthesized in a similar way as per our earlier protocol discussed in the previous **Chapter 5**.

***Synthesis of 3-(4-(3-((tert-butoxycarbonyl)amino)phenyl)-1H-1,2,3-triazol-1-yl)benzoic acid* (5.41):** To a solution of the starting material **5.52**, (250 mg, 0.65 mmol) in THF : H_2O = 5 : 1, lithium hydroxide (1.5 equivalent) was added at 0 ^{o}C. The reaction mixture was stirred about 3-4 hour until starting material was consumed. Reaction was monitored by TLC. After completion of the reaction, solvent was dried by rotary evaporator. Then water (4-5 ml) was added to the reaction mixture and cooled to 0 ^{o}C. The dilute acetic acid was added to the reaction mixture to adjust pH~ 3 to 4. The reaction mixture was extracted

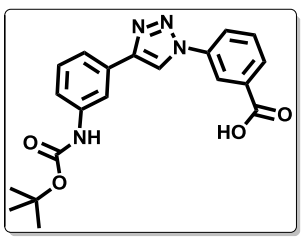

with EtOAc. The combined organic layers were dried over Na_2SO4. Title compound **5.41** (222 mg, 0.58 mmol) was isolated as a white solid material in pure form by column chromatography (Si-gel, PE : EtOAc = 1:2).. Yield 93%. ^{1}H NMR (d_6-DMSO; 400 MHz) δ 1.47 (9H, s); 7.36 (2H, s); 7.51 (1H, s); 7.75 (1H, t, *J* = 7.6 Hz); 8.04 (1H, d, *J* = 6.8 Hz), 8.16 (1H, s); 8.08 (1H, d, *J* = 8.0 Hz); 8.46 (1H, s); 9.33 (1H, s); 9.47 (1H, s); ^{13}C NMR (d_6-DMSO; 100 MHz) δ 28.4, 79.6, 115.3, 118.5, 119.9, 120.1, 120.6, 120.7, 124.4, 129.5, 130.8, 132.9, 137.1, 140.4, 147.9, 153.2, 166.7. HRMS calcd for $C_{20}H_{21}N_4O_4$ $[M + H]^+$ 379.1557, found 379.1558.

Synthesis of methyl 3-(4-(3-aminophenyl)-1H-1,2,3-triazol-1-yl)benzoate **(6.16):** The compound **5.52** was dissolved in dry DCM and cooled to 0 °C then equal amount of TFA (w.r.to solvent) was added and allowed to warm to room temperature. After stirring at room temperature until the starting material was consumed (TLC monitoring). The reaction mixture was evaporated *in vacuo.* The product **6.16** (as a TFA salt) was obtained in quantitative yield. To get free amine, water (4-5 ml) was added to salt and cooled to 0 ^{o}C. Then diluted aq.Et_3N was added to the reaction mixture to neutralized excess TFA and adjust pH~ 8. Then the reaction mixture was extracted with EtOAc. The combined organic layers were dried over Na_2SO_4 and evaporated *in vacuo* to yield the crude product **6.16** in quantitative yield to use for next step.

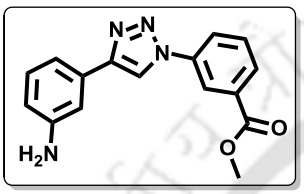

Synthesis of methyl 3-(4-(3-(pyrene-1-carboxamido)phenyl)-1H-1,2,3-triazol-1-yl)benzoate **(6.13):** In a dry R.B, 1-pyrene carboxylic acid 125 mg (0.5 mmol) with dry DCM was cooled 0 ^{o}C in ice bath. Reaction mixture basify with N-methyl imidazole 119 µl (1.5 mmol) and mesyl chloride 38 µl (0.5 mmol) was added under nitrogen atmosphere. After 15 minute ice bath was removed to attain room temperature. The free amine **6.16** (132 mg (0.45 mmol) was dissolved in dry DCM then added to the reaction mixture and reflux at 50 ^{o}C overnight. After consumption of amine solvent was dried by rotary evaporator, then it was partitioned between EtOAc and aqueous $NaHCO_3$ solution (20 ml each). The organic layer was washed with brine solution. Pure product **6.13** (120 mg, 0.229 mmol) was isolated in pure form by column chromatography (Si-gel, PE : EtOAc = 2:1). Yield 54 %. IR (KBr) 3248, 3043, 2952, 2850, 1724, 1655, 1591, 1527, 1248, 1041, 849, 756 cm^{-1}. ^{1}H NMR ($CDCl_3$ and d_6-DMSO mix; 400 MHz) δ 3.89 (3H, s); 7.40 (1H, t, *J* = 7.6 Hz); 7.65 (1H, t, *J* = 7.6 Hz); 7.57 (1H, d, *J* = 8 Hz); 7.86 (1H, d, *J* = 8 Hz); 8.05 (4H, m); 8.08 (2H, d, *J* = 4.4 Hz); 8.11 (1H, d, *J* = 8 Hz); 8.11 (2H, dd, *J* = 8, 4.4 Hz); 8.18 (1H, s); 8.20 (1H, s); 8.42 (1H, d, *J* = 13.2 Hz), 8.56 (1H, d, *J* = 9.6 Hz); 8.63 (1H, s); 10.35 (1H, s); ^{13}C NMR (d_6-DMSO; 100 MHz) δ 52.2, 117.2, 117.9, 119.9, 120.5, 121.1, 123.8, 123.9, 124.1, 124.2, 124.3, 124.9, 125.3, 125.5, 126.1, 126.7, 128.2, 128.3, 129.1, 129.7, 130.2, 130.3, 130.6, 131.3,

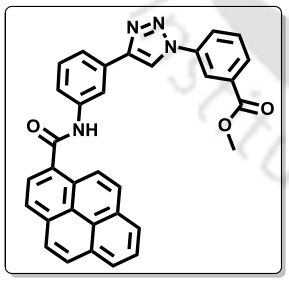

131.4, 132.0, 136.7, 139.6, 148.1, 165.3, 168.2. HRMS calcd for $C_{33}H_{23}N_4O_3$ ([M + H]$^+$) 523.1764, found 523.1742.

***Synthesis of N-(3-(1-(3-((pyren-1-ylmethyl)carbamoyl)phenyl)-1H-1,2,3-triazol-4-yl)phenyl)pyrene-1-carboxamide* (6.14):** In a dry R.B, starting material **6.17** (30 mg, 0.059 mmol) with dry DMF was cooled 0 ^{o}C in ice bath and EDC.HCl (0.088 mmol) and DMAP (0.177 mmol) was added under nitrogen atmosphere. After 15 min. pyren-1-ylmethanamine was added to the reaction mixture and stirrer about half an hour at 0 ^{o}C. Then ice bath was removed and reaction mixture was stirrered about 18 hour. After completion of reaction, it was partitioned between EtOAc and aqueous $NaHCO_3$ solution (10 ml each). The organic layer was washed with brine solution. Pure product **6.14** (22 mg, 0.03 mmol) was isolated in pure form by column chromatography (Si-gel, $CHCl_3$: MeOH = 10 : 1). Yield 52 %. IR (KBr) 3421, 3264, 3042, 2922, 2845, 1724, 1643, 1533, 1482, 1340, 1306, 1036, 845, 709 cm^{-1}. ^{1}H NMR (d_6-DMSO mix; 600 MHz) δ 5.28 (2H, d, J = 6 Hz); 7.52 (1H, t, J = 7.8 Hz); 7.77-7.67 (2H, m); 7.83 (1H, d, J = 8 Hz); 8.05 (2H, dd, J = 15.1, 7.6 Hz); 8.19-8.10 (5H, m); 8.28 (8H, dd, J = 14.4, 8.6 Hz); 8.33-8.43 (2H, m); 8.38 (1H, s); 8.47-8.56 (3H, m); 8.61 (1H, s); 9.37 (1H, s), 9.49 (1H, t, J = 5.4 Hz); 10.9 (1H, s); ^{13}C NMR (d_6-DMSO; 150 MHz) δ 41.3, 116.9, 119.0, 119.9, 121.2, 122.8, 123.2, 123.7, 123.8, 124.0, 124.1, 124.5, 124.8, 125.2, 125.3, 125.5, 125.8, 126.1, 126.3, 126.7, 126.9, 127.1, 127.3, 127.4, 127.7, 127.9, 128.2, 128.6, 129.6, 130.2, 130.3, 130.8, 130.9, 131.7, 131.9, 132.6, 135.9, 136.7, 140.1, 147.5, 165.2, 167.9. HRMS calcd for $C_{49}H_{32}N_5O_2$ ([M + H]$^+$) 722.2550, found 722.2540.

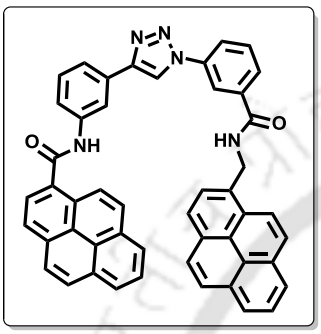

6.8.3. Photophysical Studies of the Sensors

UV-visible measurements: All the *UV* –visible spectra of the sensors (10 µM) were measured in different solvents using a UV-Visible spectrophotometer with a cell of 1 cm path length. The measurements were carried out in absorbance mode. The absorbance values of the sample solutions were measured in the wavelength regime of 200–550 nm. All the sample solutions were prepared just before doing the experiment.

Study of Circular Dichroism Spectroscopy: Circular dichroism spectra were recorded using a CD spectropolarimeter with a cell path length of 10 mm at 25 ^{o}C. All the samples were prepared in spectroscopic grade Ethanol/methanol solvent with 100 µM concentration.

Fluorescence experiments: All the sample solutions were prepared as described in UV measurement experiments. Fluorescence spectra were obtained using a fluorescence spectrophotometer at 25 °C using 1 cm path length cell. The excitation

wavelengths for all the cases were set at the excitation maxima of each sample in each solvents and emission spectra were measured in the wavelength regime of 290–650 nm with an integration time of 0.2 sec. All the sample solutions were prepared just before doing the experiment. Total volume of 1.0 ml from a stock solution of 2 ml of 10 μM concentration for each case was used for fluorescence experiment in 1 ml cell. Fluorescence emissions were collected exciting the samples at the wave length corresponding to their absorption maxima. Steady-state fluorescence emission spectra were recorded at room temperature as an average of five scans using an excitation slit of 3.0 nm, emission slit 3.0 nm, and scan speed of 120 nm/min. The fluorescence quantum yields (Φ_f) were determined using quinine sulphate as a reference with the known Φ_f (0.55) in 0.1 molar solution in sulphuric acid. The following equation was used to calculate the quantum yield,

$$\Phi_S = \Phi_R \frac{Fl_S^{Area}}{Fl_R^{Area}} \frac{Abs_R}{Abs_S} \frac{n_S^2}{n_R^2}$$

where, Φ_R is the quantum yield of standard reference, Fl_S^{Area} (sample) and Fl_R^{Area} (reference) are the integrated emission peak areas, Abs_S (sample) and Abs_R (reference) are the absorbances at the excitation wavelength, and n_S (sample) and n_R (reference) are the refractive indices of the solutions.

The fluorescence lifetime experiment was carried out using a time resolved fluorescence spectrophotometer at 25 °C using 1 cm path length cell. 290 and 375 nm laser was used as excitation light source. The lifetime data were calculated by software with fixed fitting range. The time correlated single photon counting (TCSPC) method was used to calculate the lifetime data. The life time data (Global Analysis) were calculated by the software package with fitting range 205 – 4000 channels.

6.9. ^{1}H and ^{13}C NMR Spectra

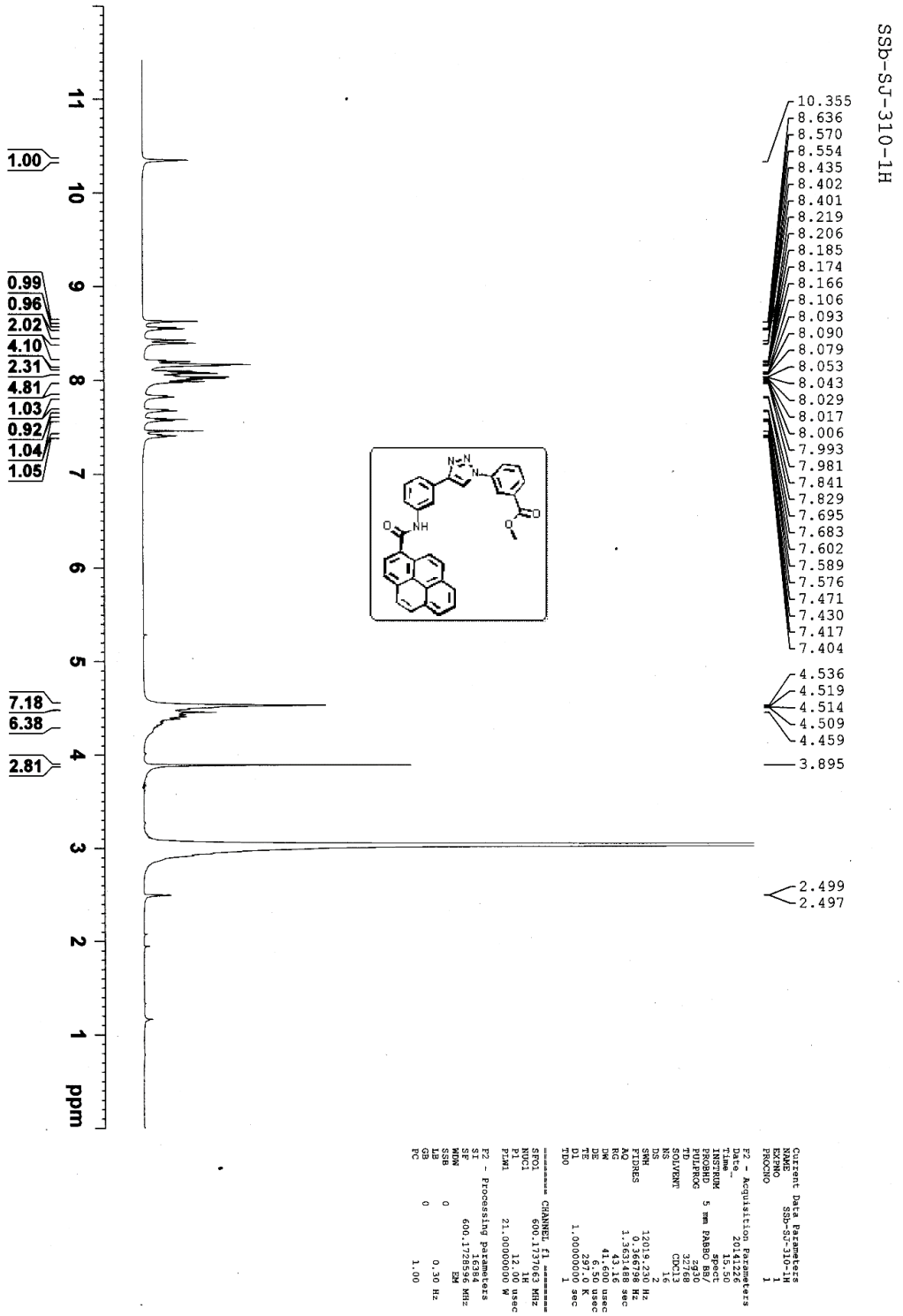

Figure 6.31. ^{1}H NMR spectra of synthesized compound **6.13.**

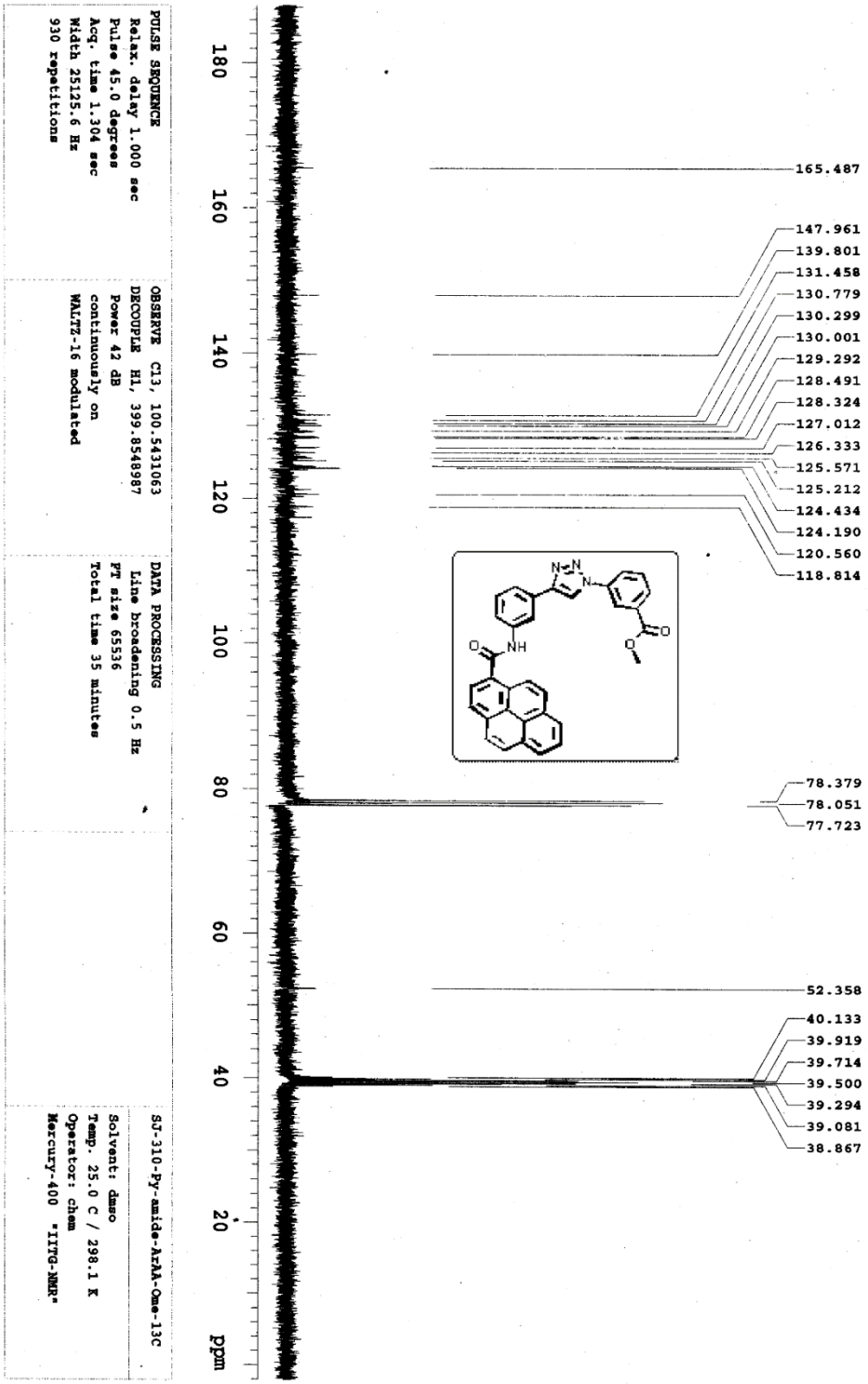

Figure 6.32. ^{13}C NMR spectra of synthesized compound **6.13.**

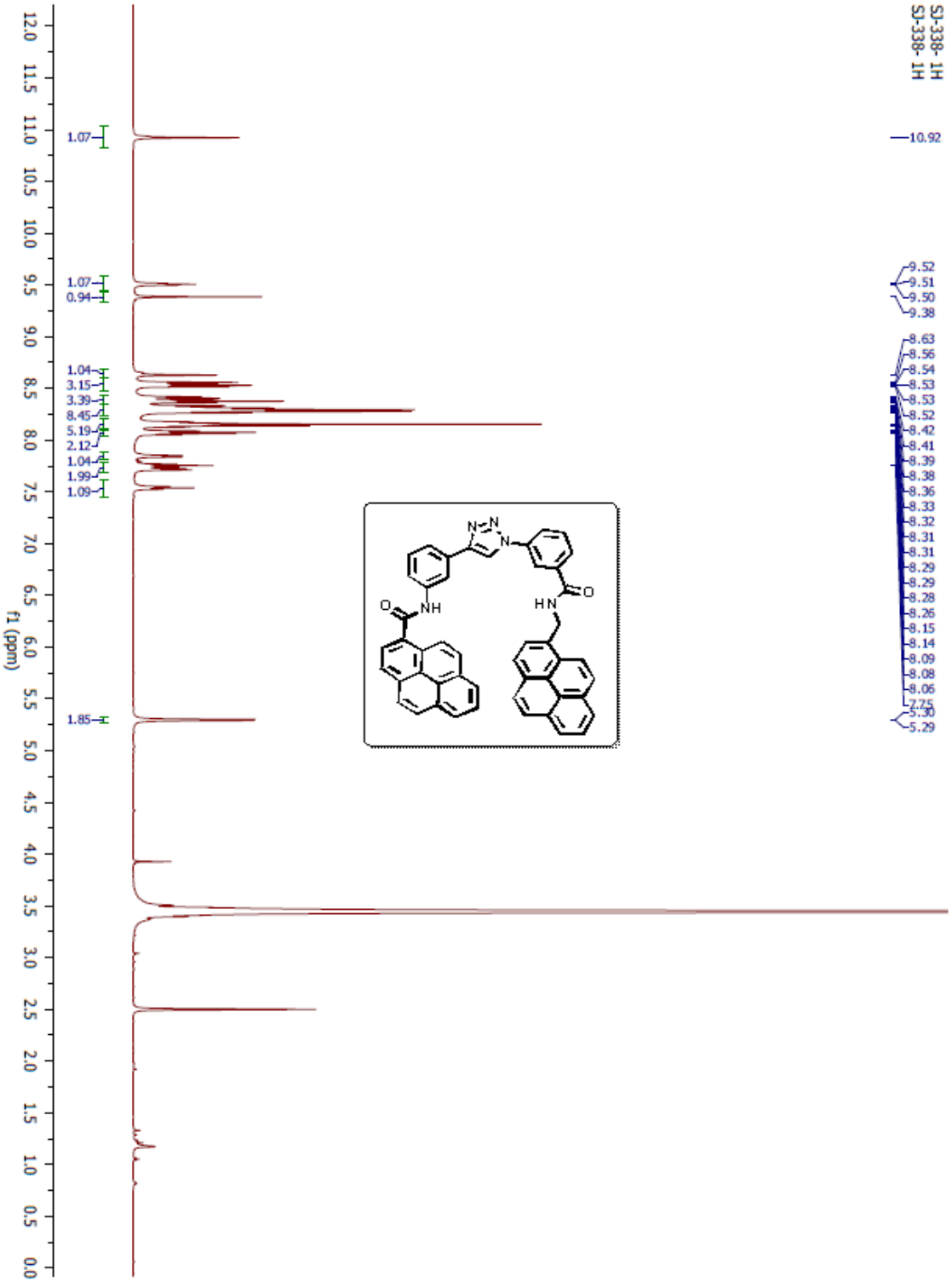

Figure 6.33. ^{1}H NMR spectra of synthesized compound **6.14.**

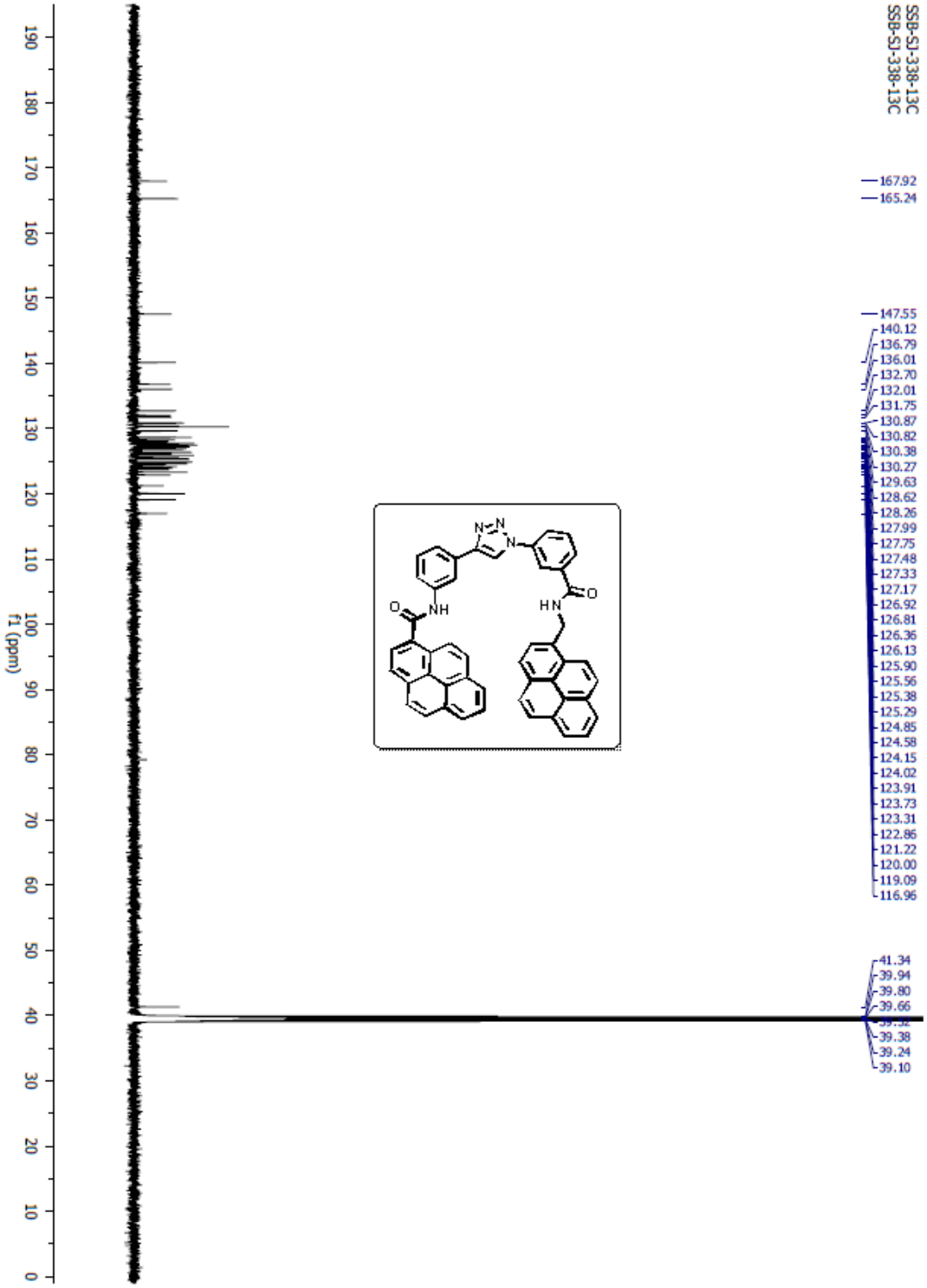

Figure 6.34. ^{13}C NMR spectra of synthesized compound **6.14.**

6.10. References

1. Demirbas, A. *Energy Sources* **2008**, *30*, 529.
2. (a) Petrova, S.; Kostov, Y.; Jeffris, K.; Rao, G. *Chemical & Biosens*. **2007**, *40*, 715. (b) Lachenmeier, D. W.; Godelmann, R.; Steiner, M.; Ansay, B.; Weigel, J.; Krieg, G. *Chem. Cent. J*. **2010**, *4*, 5. (c) Lee, J.; Chang, H. T.; An, H.; Ahn, S.; Shim, J.; Kim, J. -M. *Nat. Commun.* **2013**, *4*, 2461. (d) Zhang, Y.; Li, D.; Li, Y.; Yu, J. *Chem. Sci*, **2014**, *5*, 2710.
3. (a) Kini, M. M.; Cooper, J. R. *Biochem J.* **1962,** *82*, 164. (b) Liesivuori, J.; Savolainen, A. H. *Pharmacology & Toxicology* **1991**, *69*, 157. (c) Rathi, M.; Sakhuja, V.; Jha, V. *Hemodial Int*. **2006**, *10*, 8. (d) LoVecchio, F.; Sawyers, B.; Thole, D. *Hum. Exp. Toxicol*. **2004**, *23*, 473. (e) Sharma, R.; Marasini, S.; Sharma, A. K.; Shrestha, J. K.; Nepal, B. P. *Optom Vis Sci*. **2011**, *28*.
4. Niu, C. G.; Guan, A. L.; Zeng, G. M.; Liu, Y. G.; Wu, L. Z. *Anal. Chim. Acta*. **2006,** *577*, 264
5. (a) Jammalamadaka, D.; Raissi, S. *Am. J. Med. Sci*. **2010**, *339*, 276. (b) Aricò, A. S.; Srinivasan, S.; Antonucci, V. *Fuel Cells* **2001**, *1*, 133.
6. Ragauskas, A. J.; Williams, C. K.; Davison, B. H.; Britovsek, G.; Cairney, J.; Eckert, C. A.; Frederick, W. J.; Hallett, J. P.; Leak, D. J.; Liotta, C. L.; Mielenz, J. R.; Murphy, R.; Templer, R.; Tschaplinski, T. *Science* **2006**, *311*, 484.
7. (a) Ishihara, S.; Iyi, N.; Labuta, J.; Deguchi, K.; Ohki, S.; Tansho, M.; Shimizu, T.; Yamauchi, Y.; Sahoo, P.; Naito, M.; Abe, H.; Hill, J. P.; Ariga, K. *ACS Appl. Mater. Interfaces* **2013**, *5*, 5927. (b) Galpothdeniya, W, I, S.; Regmi, B. P.; McCarter, K. S. de Rooy, S. L. Siraj, N.; Warner, I. M. *Anal. Chem*. **2015**, *87*, 4464.
8. (a) Sun, Z.; Zhang, X.; Na, Na.; Liu, Z.; Han, B.; An, G. *J. Phys. Chem. B* **2006**, *110*, 13410. (b) Sänze, S.; Hess, C. *J. Phys. Chem. C* **2014**, *118*, 25603. (c) Kieser, B.; Dieterle, F.; Gauglitz, G. *Anal. Chem*. **2002**, *74*, 4781.
9. (a) Diban, N.; Voinea, O. C.; Urtiaga. A.; Ortiz, I. *J. Membrane Sci.* **2009,** 326, 64. (b) García-Llobodanin, L.; Ferrando, M.; Güell, C.; López, F *Eur Food Res Technol*. **2008**, *228*, 75. (c) Hernández-Gómez, L. F.; Úbeda-Iranzo, J.; García-Romero, E.; Briones-Pérez, A. *Food Chem* **2005**, *90*, 115. (d) López-Vázquez, C.; Bollaín, M. H.; Berstsch, K.; Orriols, I. *Food Control* **2010,** *21*, 1436. (e) Wang, M. L.; Choong, Y. M.; Su, N. W.; Lee, M. H *J Food Drug Anal* **2003,** *11*, 133.
10. Battiste, D. R.; Fry, S. E.; White, F. T.; Scoggins, M. W.; McWilliams, T. B. *Anal. Chem.* **1981**, *53*, 1096.
11. Coldea, T. E.; Socaciu, C.; Fetea, F.; Ranga, F.; Pop, R. M.; Florea, M. *Not Bot Horti Agrobo* **2013**, *41*, 143.
12. Kessler, M. A.; Gailer, J. G.; Wolfbeis, O. S. *Sens. Actuators, B* **1991**, *3*, 267.

13. Podgorsek, R. P.; Franke, H.; Woods, J.; Morrill, S. *Sens. Actuators, B* **1998,** *51*, 146.
14. Taylor, P.; Petrova, S.; Kostov, Y.; Jeffris, K.; Rao, G. *Anal. Lett*. **2007**, *40*, 715.
15. Petrova, S.; Kostov, Y.; Jeffris, K.; Rao, G. *Anal. Lett*. **2007**, *40*, 715.
16. Kermis, H. R.; Kostov, Y.; Harms, P.; Rao, G. *Biotechnol. Prog*. **2002**, *18*, 1047.
17. Kostov, Y.; Rao, G. *Rev. Sci. Instrum*. **1999**, *70*, 4466.
18. Chang, C.; Bastiaansen, C. W. M.; Broer, D. J.; Kuo, H. *Macromolecules* **2012**, *45* 4550.
19. Ishihara, S.; Iyi, N.; Labuta, J.; Deguchi, K.; Ohki, S.; Tansho, M.; Shimizu, T.; Yamauchi, Y.; Sahoo, P.; Naito, M.; Abe, H.; Hill, J. P.; Ariga, K.; *ACS Appl. Mater. Interfaces* **2013**, *5*, 5927.
20. Akamatsu, M.; Mori, T.; Okamoto, K.; Komatsu, H.; Kumagai, K.; Shiratori, S.; Yamamura, M.; Nabeshima, T.; Sakai, H.; Abe, M.; Hill, J. P.; Ariga, K. *ACS Appl. Mater. Interfaces* **2015**, *7*, 6189.
21. (a) Win, D. T. *Aust. Off. J. Pat*. **2006**, *10*, 75. (b) Matyushov, D. V.; Schmid, R.; Ladanyi, B. M. A. *J. Phys. Chem. B* **1997**, *101*, 1035.
22. Galpothdeniya, W. I. S.; Regmi, B. P.; McCarter, K. S.; de Rooy, S. L.; Siraj, N.; Warner, I. M. *Anal. Chem*. **2015**, *87*, 4464.
23. Guan, L.; Pang, H.; Wang, J.; Lu, Q.; Yin, J.; Gao, F *Chem. Commun*. **2010**, *46*, 7022.
24. Kimmel, H.; Mages, G. R. Anal. Chem. **1988**, *60*, 1377.
25. Kieser, B.; Dieterle, F.; Gauglitz, G.; *Anal. Chem*. **2002**, *74*, 4781.
26. Wang, L.; Fei,T.; Lou, Z.; Zhang, T. *ACS Appl. Mater. Interfaces* **2011**, *3*, 4689.
27. (a) Sänze, S.; Hess, C. *J. Phys. Chem. C* **2014**, *118*, 25603. (b) Singh, V. N.; Metha, B. R.; Joshi, R. K.; Kruis, F. E. J. *Nanosci. Nanotechnol*. **2007**, *7*, 1930. (c) Chu, X. F.; Wang, C. H.; Jiang, D. L.; Zheng, C. M. *Chem. Phys. Lett*. **2004**, *399*, 461.
28. (a) Anglos, D.; Stassinopoulos, A.; Das, R. N.; Zacharakis, G.; Psyllaki, M.; Jakubiak, R.; Vaia, R. A.; Giannelis, E. P.; Anastasiadis, S. H. *J. Opt. Soc. Am. B* **2004**, *21*, 208. (b) Klini, A.; Pissadakis, S.; Das, R. N.; Giannelis, E. P.; Anastasiadis, S. H. Anglos, D. *J. Phys. Chem. C* **2015**, *119*, 623.
29. Park, S.; Kim, S.; Sun, G. –J.; Lee, C. *ACS Appl. Mater. Interfaces* **2015**, *7*, 8138.
30. Bag, S. S.; Jana, S.; Yashmeen, A.; De, S. *Chem. Commun.* **2015**, *51*, 5242.
31. (a) Joshi, R.; Meitei, O. R.; Kumar, H.; Jadhao, M.; Ghosh, S. K. *J. Phys. Chem. A* **2016**, *120*, 1000. (b) Chevreux, S.; Allain, C.; Wilbraham, L.; Nakatani, K.; Jacques, P.; Ciofinic, I.; Lemercier, G. *Faraday Discuss*. **2015**,

185, 285. (c) Homocianu, M.; Airinei, A.; Dorohoi, D. O. *J. Adv. Res. Phys.* **2011**, *2*, 11105.

32. (a) Grabolle, M.; Kapusta, P.; Nann, T.; Shu, X.; Ziegler, J.; Resch-Genger, U. *Anal. Chem.*, **2009**, *81*, 7807. (b) Berezin, M. Y.; Achilefu, S. *Chem. Rev.* **2010**, *110*, 2641.

33. (a) Jiang, X. H.; Man, S. Y.; Sun, A. M.; Xu, X. L.; Li, W. Q.; Wang, T. T.; Jin, W. X.; Luo, J.; Cheng, L.; Mao, Y. Z. *Mater. Lett*. **2015**, *159*, 5. (b) Akamatsu, M.; Mori, T.; Okamoto, K.; Komatsu, H.; Kumagai, K.; Shiratori, S.; Yamamura, M.; Nabeshima, T.; Sakai, H.; Abe, M.; Hill, J. P.; Ariga, K. *ACS Appl. Mater. Interfaces*, **2015**, *7*, 6189. (c) Barton, A. F. M. in *Handbook of Solubility Parameters*, CRC Press, **1983**, pp 153-157. (d) Belmares, M.; Blanco, M.; Goddard, W. A.; Ross, R. B.; Caldwell, G.; Chou, S.-H.; Pham, J.; Olofson, P. M.; Thomas, C. *J. Comput. Chem.* **2004**, *25*, 1814.

34. (a) Fita, P.; Fedoseeva, M.; Vauthey, E. *J. Phys. Chem. A*, **2011**, *115*, 2465. (b) Landis, R. F.; Yazdani, M.; Creran, B.; Yu, X.; Nandwana, V.; Cooke, G.; Rotello, V. M. *Chem. Commun.* **2014**, *50*, 4579. (c) Dereka, B.; Letrun, R.; Svechkarev, D.; Rosspeintne, A.; Vauthey, E. *J. Phys. Chem. B* **2015**, *119*, 2434.

35. (a) Eguchi, T.; Kondo, K.; Kakinuma, K.; Uekusa, H.; Ohashi, Y.; Mizoue, K.; Qiao, Y.-F. *J. Org. Chem.* **1999,** *64*, 5371 and references therein. (b) Knipe ,P. C.; Thompson, S.; Hamilton, A. D. *Chem. Sci.* **2015**, *6*, 1630. (c) Micsonai, A.; Wien, F.; Kernya, L.; Lee, Y.-H.; Goto, Y.; Réfrégiers, M.; Kardos, J. *PNAS* **2015**, E3095.

36. (a) MacroModel, Version 9.9 Schrodinger, LLC, New York, NY, **2012. (**b) Kolossvry, I. W.; Guida, C. *J. Am. Chem. Soc.*, **1996**, *118*, 5011.

37. Frisch, M. J. *et al*. Gaussian, Inc. Wallingford CT, **2009**.

SUMMARY AND OUTLOOK

Summary and Outlook

Major findings and the future outlook of the present investigations described in this dissertation have been summarized below:

This dissertation has a total of six chapters out which two chapters are devoted to the synthesis of unnatural donor-acceptor triazolyl amino acids and incorporation of a donor/acceptor pair in a short peptide *via* "Click" reaction and peptide coupling protocol respectively. Another two chapters describe the synthesis of aliphatic triazolo-β-aza-ε-amino acid (**^{Al}TAA**) and its aromatic analogue (**^{Ar}TAA**) and their applications in a peptide backbone as a conformationally constrained molecular scaffolds to induce desirable secondary structures in small linear peptides. Last chapter describe the synthesis and application of mono and bis-pyrenyl amide derivative of **^{Ar}TAA** for fluorimetric discrimination of ethanol from methanol. The **Chapter 1** is a review chapter focussing on the various applications of unnatural non-fluorescent/fluorescent amino acids, peptides and amino acid scaffolds. Thus, this chapter is a reflection/overview of all the chapters of the present dissertation.

The **Chapter 2** described few conceptually new triazolyl donor and/or acceptor chromophore decorated fluorescent unnatural amino acids via generated via click reaction which showed modulated photophysical properties in various organic solvents. The dipolar interaction mediated resonance energy transfer phenomenon was observed in a donor/acceptor pair of amino acids **^{TPhen}Ala^{Do}** and **^{TCNB}Ala^{Ac}** in acetonitrile solvent wherein **^{TCNB}Ala^{Ac}** acts as FRET donor and **^{TPhen}Ala^{Do}** acts as FRET acceptor. The design concept of such triazolyl-donor-acceptor amino acids is based on the hypothesis that a pair might further be exploited in designing FRET-peptide probe for application in studying interaction events between peptide-protein/peptide-DNA. Moreover, the fluorescent triazolyl perylene amino acid (**^{TPer}Ala^{Do}**) has been exploited for studying interaction with BSA protein with the help of fluorescence spectroscopic technique. It has been observed that the hydrophobic triazolyl perylene amino acid is capable of sensing BSA with a switch-on fluorescence response. The other donor/acceptor aromatic triazolyl amino acids might be useful for sensing the biomolecular microenvironment. Furthermore, the present investigation on the photophysical properties of click chemistry derived triazolyl fluorescent amino acids is of great importance for the development of new pair of donor-acceptor amino acids useable for the design of fluorescent peptide/peptidomimetics which could be utilized as probe for studying interbiomolecular interaction.

The **Chapter 3** is the reflection of designing concept of **Chapter 2**, which deals with a judicious design of donor/acceptor triazolyl unnatural amino acids decorated tripeptide wherein a donor/acceptor pair is placed properly to achieve a photophysical dipolar interaction among them. Based on all the spectroscopic study it has been concluded that the designed tripeptides adopt β-turn conformation stabilized by intra

molecular backbone hydrogen bonding as well as side chain hydrophobic interaction. A Förster resonance energy transfer (FRET) process has been established in the conceptually designed novel unnatural β-turn peptide containing a new class of fluorescent unnatural donor/acceptor amino acids. The FRET process occurs from **TCNB** moiety of ^{TCNB}**Ala**^{Ac} (FRET donor) to **TPhen** unit of ^{TPhen}**Ala**^{Do} (FRET acceptor). The developed FRET pair, ^{TCNB}**Ala**^{Ac} - ^{TPhen}**Ala**^{Do}, wherein both the partners are unnatural amino acid, is conceptually new and novel. As FRET can provide information about peptide/protein conformation, the unnatural amino acid pair (FRET pair) and the FRET peptide might find applications in studying solution conformational distribution of an unstructured peptide and FRET based bioassay. The modulation of FRET emission is also an attractive finding which would find application in FRET-based bioassay to improve the detection sensitivity.

The **Chapter 4** describes the synthetic strategy of easily accessible aliphatic triazolo amino acid scaffold (^{Al}**TAA**), which is uncovered, for the first time, as a β-turn-mimetic constrained molecular scaffold. The structural and conformational analysis of Leu-enkephalin analogue peptide and fluorescent peptide containing such scaffold by various spectroscopic techniques and molecular dynamics (MD) simulation studies establishes well-defined type II β-turn structure induced by the novel β-turn-mimetic constrained molecular scaffold, the triazolo amino acid scaffold ^{Al}**TAA**. Moreover, the FRET process has been established in pentapeptide containing a new class of fluorescent unnatural triazolyl amino acids at the two termini. Exploration of turn mimetics and the sequence specific DNA binding event of tetra-amides of this molecular scaffold might lead to the generation of a new family of distamycin analogue which is an important future outlook of this chapter.

The design concept of **Chapter 4**, has been utilised further to generate more rigid aromatic analogue of triazolo amino acid ^{Ar}**TAA** and a newly designed trichromophoric β-sheet pentapeptide which represents a serendipitous discovery of a "dual door entry system for excimer emission" and is the content of **Chapter 5**. Both the processes of excitation of **TPy** of ^{TPy}**Ala**^{Do}-either energy transfer from excited scaffold amino acid, ^{Ar}**TAA** (FRET) to **TPy** or direct excitation of **TPy**-led to the excimer emission in fluorescent pentapeptide has been uncovered. This study would provide fundamental guidelines to design such conceptual fluorescent probe of dual door entry system to excimer emission. This is the start of a new generation of probes which would find wide applications in the field of chemical biology. Moreover, the novel probe of dual door entry to excimer emission system has been found to be an effective fluorescence light-up probe for detecting and studying protein–peptide interactions in solution. Studying other specific protein–peptide interactions of significant clinical interest utilizing conceptual fluorescent peptide-probe is the future prospect of this chapter in particular.

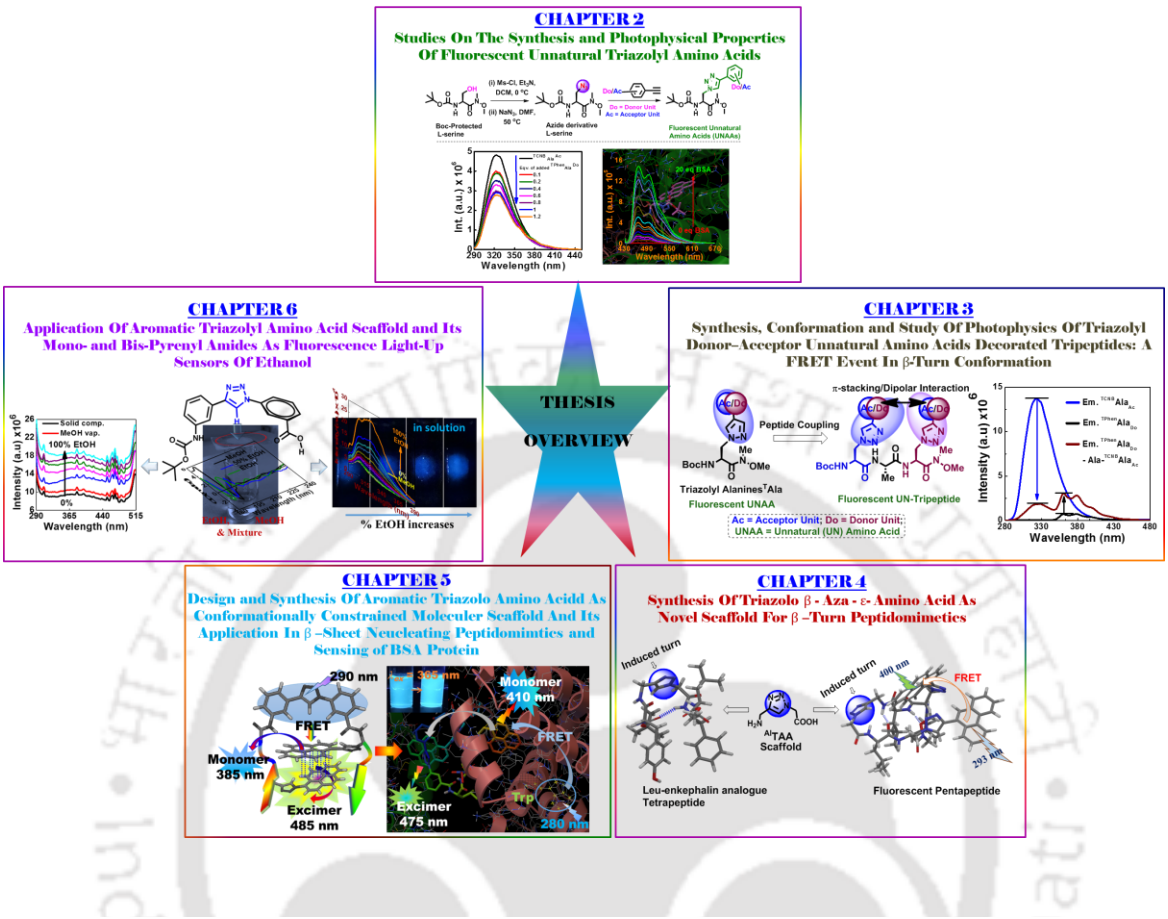

Finally, **Chapter 6** introduced three new and novel alcohol sensors involving both solution and solid-state fluorescence emission. The simple scaffold **^{Ar}TAA** and other two sensors **PyAm-^{Ar}TAA** and **Py$_2$Am-^{Ar}TAA** show high sensitivity in sensing ethanol in presence of methanol (2-2.6 v/v %) which has been demonstrated fluorimetrycally. In addition, the ethanol sensors in a solid film are found to be effective in detection of ethanol in the vapor phase. The differential solvation mediated H-bonding interaction is considered to play a crucial role in fluorimetric discrimination of methanol from ethanol by the axially chiral scaffold or the scaffold moieties in the sensors. In terms of applicability, it is believed that such a simple system would attract to develop a practical sensor which could estimate ethanol content on-the-spot. Development of such practical sensory devices with these small organic molecules is the future focus of this chapter.

Therefore, these novel and important findings presented in this dissertation are expected to further define research to establish and to create more of such conceptually designed amino acid based peptidomimetics system for future applications in chemistry, biology and material sciences. The results presented herein are sufficient enough to advance the on-going examination of such related systems and thus, attract the interest of broad scientific community. The concept of designing

fluorescent triazolyl amino acids and small molecular scaffold probes might find special attention in future in the field of chemical biology. The rapidly growing research toward the expansion of genetic code as well as growing demand of peptide based diagnostics and sensing materials necessitates the design and incorporation of unnatural amino acids with high stability as well as tuned charge transfer/photophysical properties. In this connection, the concept of unnatural donor-acceptor amino acid pair (FRET pair), the FRET peptide, designed peptide conformational impact on the photophysical outcome, predefined conformation to generate predefined photophysics in fluorescent unnatural peptides and the fundamental concept of "Dual door entry to excimer emission" might knock the future chemical biologists to uncover and utilize such type peptide-based probe system for a wide range of applications in chemical biology and in materials sciences.

With the advent of sophisticated synthetic chemistry more complex amino acids are being designed the encoding of which need the evolution of new aaRS/tRNA pairs that may also allow the *in vivo* synthesis of biopolymers with unnatural backbones. The incorporation of unnatural amino acid into protein expectedly would generate protein-based therapeutics that would certainly have an impact on medicine. Furthermore, The peptidomimetic approach has been found to be powerful in addressing the key recognition elements by scaffold-based peptidomimetic architectures that expectedly would afford a wide array of medicinally important molecules displaying different binding affinity and pharmacokinetic profile. With the advancement of knowledge and strategies of chemistry and biology, FUAAs expectedly would continue to be at the forefront in aiding researchers to gain insights into fundamental questions concerning life's essential biological functions involving protein interactions, recognition, and synthesis. Many more advancements in the field of unnatural amino acids/fluorescent peptides are expected in near future.